NOTICE

The quality of this microfiche is heavily dependent upon the quality of the original thesis submitted for microfilming. Every effort has been made to ensure the highest quality of reproduction possible.

If pages are missing, contact the university which granted the degree.

Some pages may have indistinct print especially if the original pages were typed with a poor typewriter ribbon or if the university sent us a poor photocopy.

Previously copyrighted materials (journal articles, published tests, etc.) are not filmed.

Reproduction in full or in part of this film is governed by the Canadian Copyright Act, R.S.C. 1970, c. C-30. Please read the authorization forms which accompany this thesis.

THIS DISSERTATION
HAS BEEN MICROFILMED
EXACTLY AS RECEIVED

AVIS

La qualité de cette microfiche dépend grandement de la qualité de la thèse soumise au microfilmage. Nous avons tout fait pour assurer une qualité supérieure de reproduction.

S'il manque des pages, veuillez communiquer avec l'université qui a conféré le grade.

La qualité d'impression de certaines pages peut laisser à désirer, surtout si les pages originales ont été dactylographiées à l'aide d'un ruban usé ou si l'université nous a fait parvenir une photocopie de mauvaise qualité.

Les documents qui font déjà l'objet d'un droit d'auteur (articles de revue, examens publiés, etc.) ne sont pas microfilmés.

La reproduction, même partielle, de ce microfilm est soumise à la Loi canadienne sur le droit d'auteur, SRC 1970, c. C-30. Veuillez prendre connaissance des formules d'autorisation qui accompagnent cette thèse.

LA THÈSE A ÉTÉ
MICROFILMÉE TELLE QUE
NOUS L'AVONS REÇUE

SUBCOOLED AND LOW QUALITY FILM BOILING OF WATER IN VERTICAL FLOW AT ATMOSPHERIC PRESSURE

BY

KEE-KWONG FUNG

A THESIS SUBMITTED AS A PARTIAL FULFILMENT
OF THE REQUIREMENTS FOR THE DEGREE OF
DOCTORAT EN PHILOSOPHIE
IN THE UNIVERSITY OF OTTAWA

DEPARTMENT OF CHEMICAL ENGINEERING
UNIVERSITY OF OTTAWA

AUGUST 1981

ABSTRACT

Subcooled and low quality film boiling is usually encountered in safety analyses of nuclear reactors. In most of the previous subcooled film boiling studies, cryogenic fluids were used either in a stagnant pool or a forced convective set-up. These data cannot be applied to reactor safety analysis without excessive conservatism or skepticism.

In this study, a unique method is used to establish flow film boiling of water in a vertical tube at atmospheric pressure. The data cover a mass flux range of 50-500 $kg.m^{-2}.s^{-1}$ and an inlet subcooling range of 5-70^{o}C. It is found that the heat transfer coefficient depends on the mass flux, inlet subcooling and the axial distance from the point where film boiling first starts.

A physical model is developed to predict the wall temperature of a tube during inverted annular film boiling. It considers the thermal boundary layers in the subcooled liquid core and in the superheated vapour film. The predicted wall temperatures and void fractions compare well with the measurements.

ACKNOWLEDGEMENTS

One of my more pleasant tasks in putting the finishing touches to this report is to express my gratitude to all those who have helped in the course of this study. I am deeply grateful to Dr. D.C. Groeneveld for his continuous guidance since 1975 when I first came to work at Chalk River Nuclear Laboratories (CRNL) under the National Summer Student Program. Although my subsequent attachments at CRNL were under various sponsorships, he continued to take interest in my work and could always find time, either in the office, in the laboratory, or beside a campfire, to share his expertise in heat transfer with me. I also owe my sincere thanks to Professor S.C. Cheng for his advice and many interesting technical discussions.

The present study was carried out in the heat transfer laboratories of the Advance Engineering Branch at CRNL. I am delighted to take this opportunity to thank Dr. S.Y. Ahmad for his consent to use the facilities to carry out the experiment. Each and every member of the Branch is to be commended for either assisting enthusiastically or tolerating wholeheartedly whenever my experiment intervened with their schedules, or called for extra work beyond their normal duties. In particular, the unfailing effort of J.H. Woodall in perfecting the fabrication of the test section was instrumental in the smooth progress of the project. R.J. Cowhey wrote the program for the on-line computer used for data acquisition.

Mr. V.G. Hulbert of the Electrical, Instrument and Power Branch, devoted much of his time in helping me to set up the instruments for void fraction measurement. His suggestions are very much appreciated.

Dr. S.R.M. Gardiner, who left CRNL in 1977 to join the faculty of the University of Toronto, did the pioneering work in adapting the technique used in the present study. I am very grateful for his efforts.

The present study formed part of the requirements of a degree program offered jointly by the Chemical and Mechanical Engineering Departments of the University of Ottawa. It is said that a man cannot serve two masters. Nevertheless, I want to express my appreciation to Professors S.C. Cheng and F.D. Talbot for their efforts in making such an otherwise formidable task into a fruitful experience for me. Professor Cheng administered the research contract admiringly so that I could concentrate on the study.

This study was sponsored by the United States Nuclear Regulatory Commission. The generous financial support is gratefully acknowledged. Atomic Energy of Canada Limited also contributed financially by providing the laboratory facilities and the support staff.

Miss E. Gehlert typed a large portion of this report. I want to express my admiration for her patience in deciphering the manuscripts. Miss B. Fairbanks completed the typing upon very short notice. I would consider it amiss of me if her mastery over equations typing is left unrecorded.

TABLE OF CONTENTS

LIST OF FIGURES

NOMENCLATURE.

NOTE: The less frequently referenced symbols are defined when they appear in the text

A	Area
Cp	Specific heat
D	Tube diameter
De	Hydraulic equivalent diameter, tube diameter
E	Energy flux
f	Friction factor
F	View factor
g	Acceleration due to gravity
G	Mass flux
h	Enthalpy, heat transfer coefficient
i	Enthalpy
I	Count rate
J	Radiosity
k	Thermal conductivity
L	Length
m	Wave number
M	Momentum flux
Nu	Nusselt number (h D/k)
P	Pressure
Pr	Prandtl number (μ Cp/k)
q	Heat transfer rate
r	Radial distance
R	Radius

Re	Reynolds number
t	Time; thickness
T	Temperature
U,u	Velocity
V	Velocity
v	Velocity normal to solid surface
X	Quality
y	Distance perpendicular to wall
Z	Axial coordinate

GREEK

α	Void fraction, thermal diffusivity
Γ	Evaporation mass flux
δ	Film thickness
ε	Eddy diffusivity, emissivity
η	Dimensionless distance
θ	Angle, dimensionless temperature
μ	Dynamic viscosity
ν	Kinematic viscosity
Φ	Surface heat flux
ρ	Density
σ	Surface tension
σ_{SB}	Stefan-Boltzmann constant
τ	Shear stress
τ_v	Transmissivity
ΔH	Local subcooling, $h_s - h$
$\Delta \dot{m}$	Evaporation mass flux
ΔT	Local subcooling, $T_s - T$

Subscripts

a	Actual value
c	Core, convective, condensation
CHF	Critical heat flux
Cond	Conduction
conv	Convection
e	Equilibrium value, evaporation
E	Empty
f	Saturated liquid
F	Full
fg	Difference between saturated vapor and saturated liquid value
g	Saturated vapor
H	Heat transfer
i	Initial, interface, inner
in	Inlet
ℓ	Liquid
o	Outer
rad	Radiation
s	Saturation
sat	Saturation
T	Turbulent
v	Vapour
w	Wall

I.0 INTRODUCTION

During the normal operation of water-cooled reactors, the fuel sheath temperature is maintained at near saturation temperature. However, during a postulated loss-of-coolant accident (LOCA), the fuel cladding may experience a rapid increase in temperature as a result of a change in heat transfer mode from nucleate boiling to the less efficient film boiling. The subsequent injection of emergency core coolant will result in a return to moderate sheath temperatures by changing the heat transfer mode from film boiling, via transition boiling back to nucleate boiling and forced convection. It is during this phase that film boiling in an inverted annular flow regime is most likely to be encountered.

In most of the previous subcooled film boiling studies, cryogenic fluids were used (see review reports by Groeneveld & Gardiner (1977) and Fung (1978)). One of the reasons why water has not been used more frequently in the investigations is the high heater wall temperature required to maintain film boiling at low qualities in water.

Previously derived correlations are based on data obtained in cryogenic fluids and therefore lack the necessary data base to substantiate their applicability to water reactor safety analysis. At present, one of the correlations recommended to be used in this region is that by Hsu (1977), which is a modified Bromley equation for pool film boiling.

In this investigation, a unique technique is used to establish steady-state film boiling for water during forced convection inside a directly heated tube. It permits the measurement of film boiling at low qualities in which the flow pattern is inverted annular. This has not been possible in the previously reported film boiling studies using a directly heated channel.

II.0 TWO-PHASE FLOW AND HEAT TRANSFER

II.1 Boiling Curve in Pool Boiling Systems

When a heated surface is maintained at a temperature above the saturation temperature of the liquid close to it, a change in phase from liquid to vapour may occur. If we plot the heat flux and the corresponding surface temperature (or more frequently the wall superheat, $T_w - T_s$), we obtain what is referred to as the boiling curve. A typical boiling curve in a pool boiling system is shown in Fig. 1.

If the surface is heat flux controlled, e.g., by resistance heating, the boiling curve follows a path similar to A B C D F G on increasing heat flux and G F E C B A on decreasing heat flux. Initially, up to point B, heat transfer is by forced convection. At point B, the surface attains the minimum superheat for nucleation, and vapour bubbles are formed on the surface. The region from B to D is called nucleate boiling. One of the main characteristics of this mode of boiling which distinguishes it from the others is the continuous contact between the liquid and the heated surface.

At point D, the maximum limit of nucleate boiling is reached. The heat flux at this point is called critical heat flux (CHF). Various other names, such as dryout, burnout, first boiling crisis and departure from nucleate boiling (DNB) are also used.

If the heat flux is increased beyond the CHF, the curve will follow path DF. The transient is usually very fast so that no stable operation can be maintained along DF. Point F lies on the film boiling

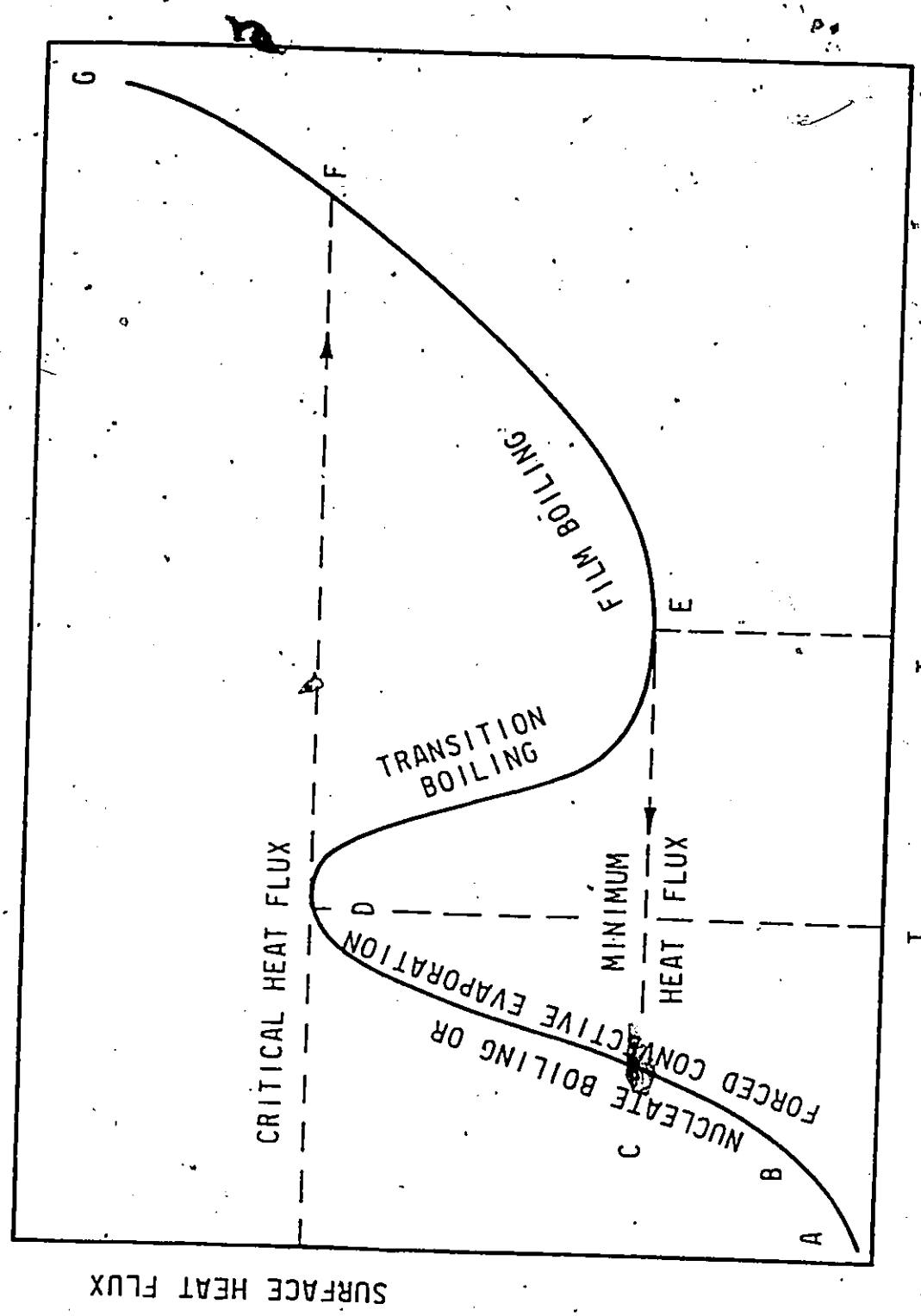

FIGURE 1 POOL BOILING CURVE

region of the boiling curve.

At heat flux above F, the film boiling curve follows path FG. On decreasing the heat flux, the curve traces out GFE instead of returning to D. This hysteresis is typical of pool film boiling. It is due to the fact that once a vapour film is established, it does not collapse suddenly but instead decreases in thickness as the heat flux is lowered.

The minimum wall temperature required to maintain stable film boiling is called the Leidenfrost temperature. It corresponds to point E in Fig. 1. On further reduction in heat flux, the surface temperature will rapidly drop to that corresponding to point C, which is in the nucleate boiling region.

The above discussion applies to a heat flux controlled system. In a temperature controlled system, such as one in which heat is supplied by a condensing vapour, the continuous curve shown in Fig. 1 is obtained. The region DE, which is not attainable in a heat flux controlled system, is called transition or partial film boiling. In this boiling mode, liquid-surface contact is intermittent.

II.2 Forced Convection Boiling

II.2.1 Flow Regimes

Forced convection boiling is commonly investigated in electrically heated channels. The mass quality increases along the heated channel, with corresponding changes in the flow regime. Fig. 2 shows

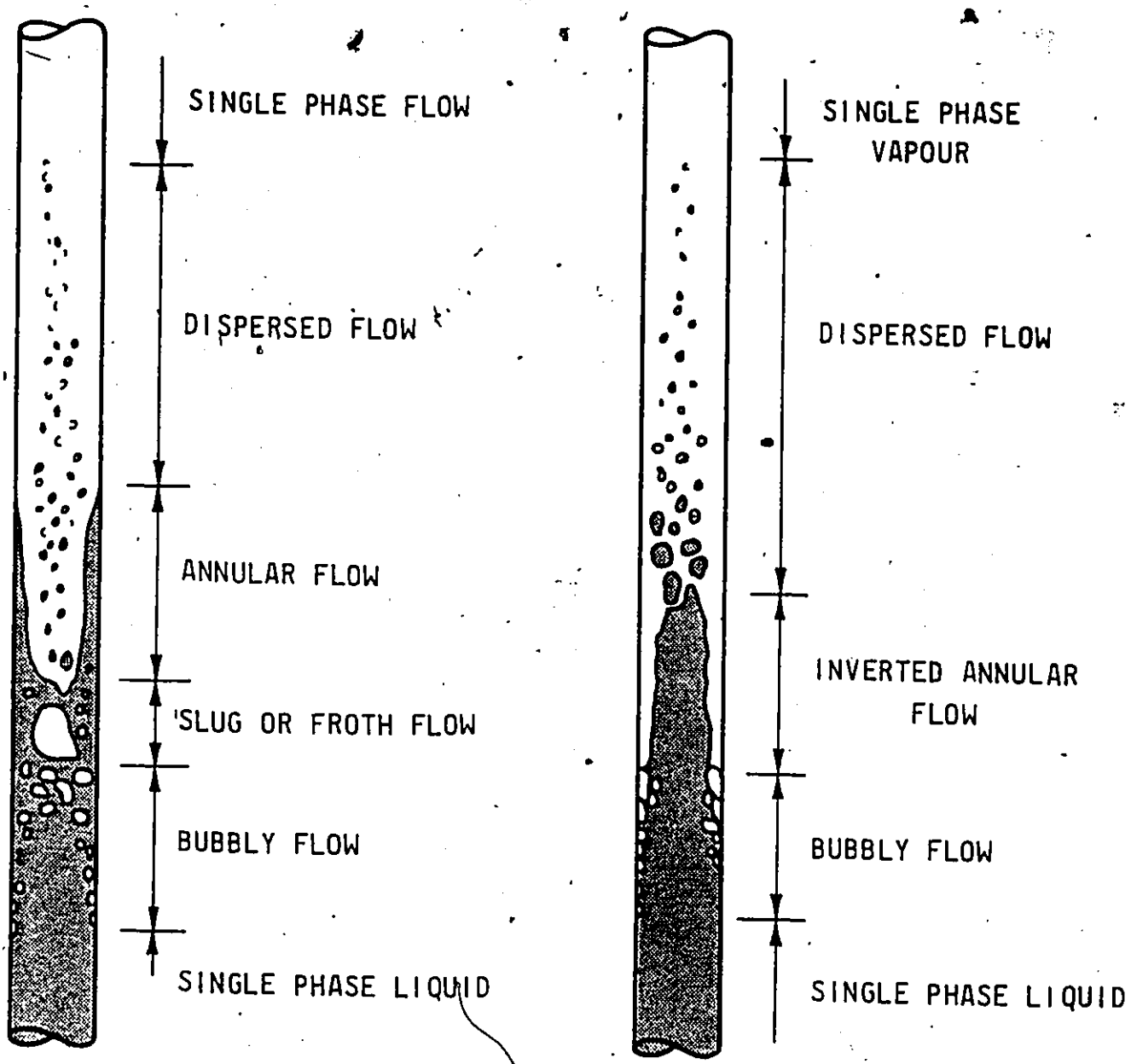

FIGURE 2 FLOW REGIMES IN A DIRECTLY HEATED TUBE

two possible configurations of the flow structures inside a heated channel. Fig. 2(a) is most commonly encountered under low heat flux conditions while Fig. 2(b) is typical of high heat flux conditions.

The flow regimes and heat transfer modes along the channel length can be divided into the following regions:

(a) Single-phase forced convection

(b) Bubbly flow

Here the heated surface attains the minimum superheat for nucleation. Bubbles are formed and remain in the wall region, since the bulk of the liquid is still subcooled.

Further downstream, the liquid becomes saturated. In this fully developed bubbly flow bubbles exist in the core region and coalesce to form larger bubbles.

(c) Slug flow or froth flow

Here nucleate boiling is still the dominating mode of heat transfer. However, the vapour volume is comparable to the liquid volume. At low mass flux, the flow is intermittent, with vapour plugs followed by liquid plugs. At high velocity, the flow structure tends to be the more homogeneously mixed froth flow.

(d) Annular flow

The vapour now occupies the central part of the channel, with liquid droplets entrained in it. A liquid film exists around the heated surface. Often, nucleation is suppressed and heat transfer is

by forced convection across the liquid film and then by evaporation at the vapour-liquid interface.

(e) Dispersed flow

This is the post-CHF region. Heat transfer is by forced convection to vapour, evaporation at the droplet surface and droplet-thermal boundary layer interaction.

(f) Inverted annular flow

Fig. 2(b) represents the situation in which the heat flux is sufficiently high that boiling crisis is encountered by bubble clouding or subcooled dryout (Tong (1972)). Here the post-CHF flow regime is inverted annular, with a vapour film separating the liquid core and the heated surface. It is usually encountered at void fraction below 30%. The transition between this flow regime and the previously discussed annular flow can be represented schematically by a flow regime map, as shown in Fig. 3.

II.2.2 Forced Convection Boiling Curves

A typical boiling curve for forced flow inside a directly heated tube is shown schematically in Fig. 4. The same curve will be traced out on increasing or decreasing heat flux. This is different from the hysteresis behaviour in the film boiling region in the case of pool boiling. The reason why the heat flux does not fall below the CHF along the film boiling section of the boiling curve is that a rewetting front propagates along the channel as the heat flux is reduced.

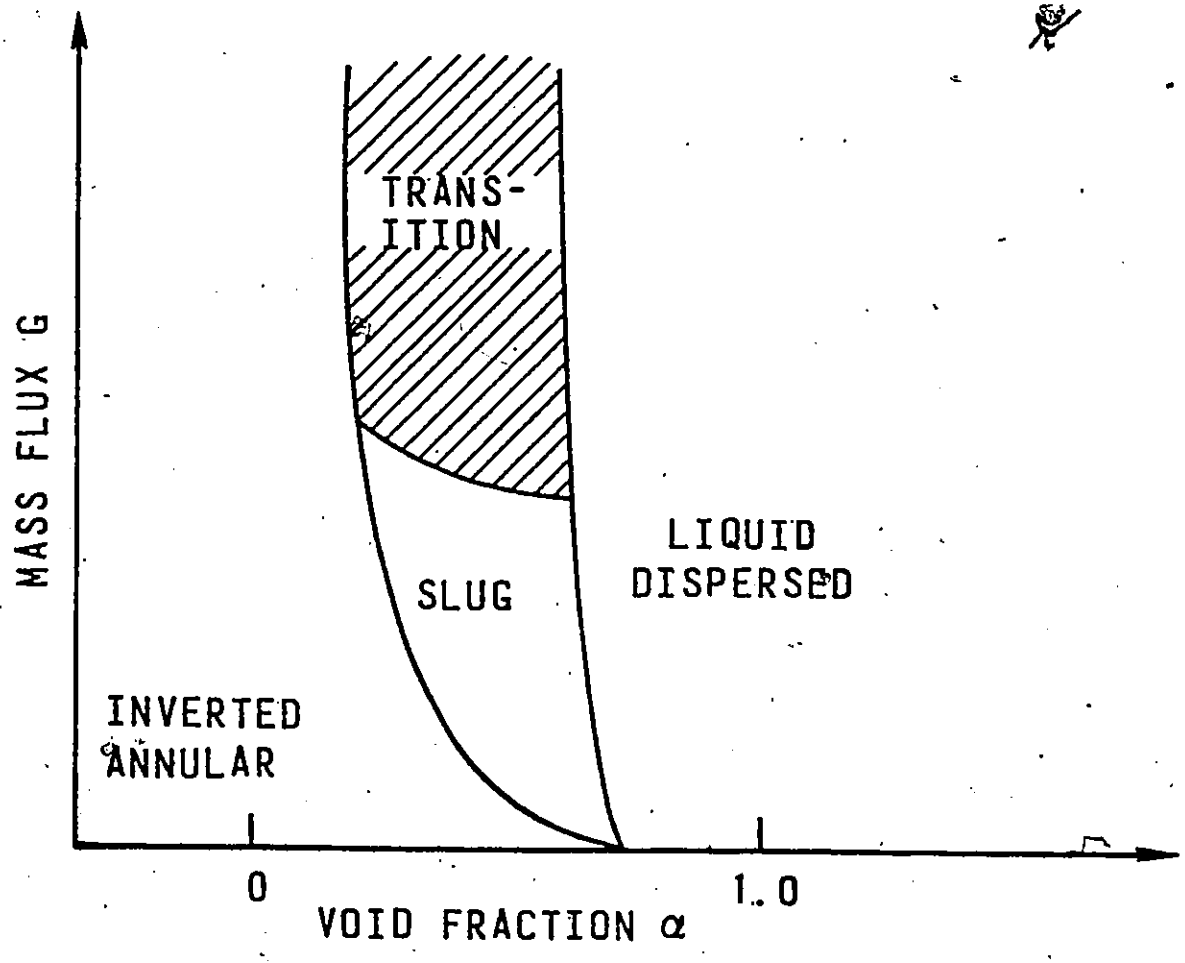

FIGURE 3 SCHEMATIC FLOW REGIME MAP

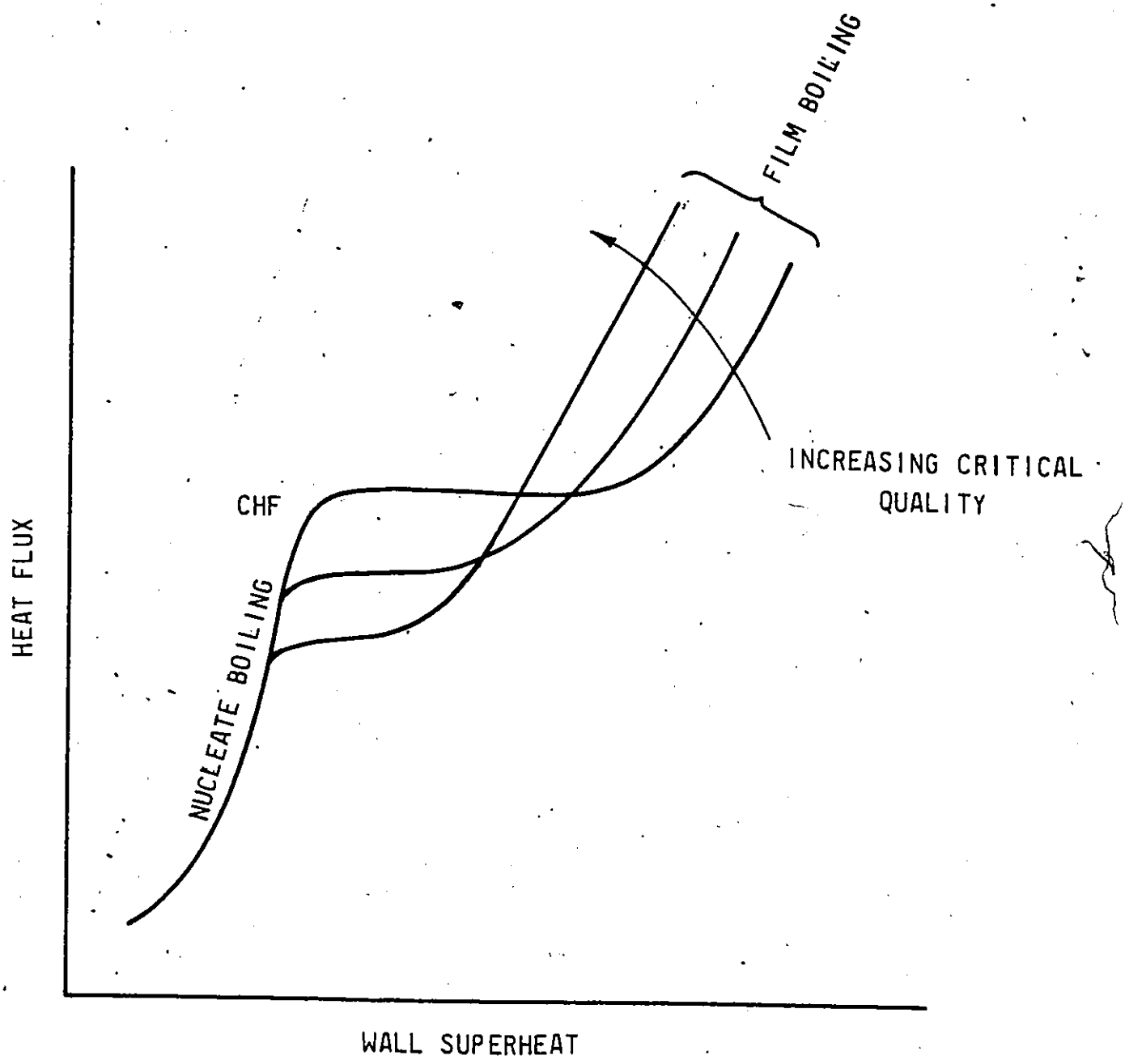

FIGURE 4

FORCED CONVECTION BOILING CURVE IN A DIRECTLY HEATED TUBE

However, if the system is temperature controlled, the film boiling heat flux can fall below the CHF, as in the case of pool boiling. A heater with a high thermal capacity, such as a nuclear fuel bundle, will resemble a temperature controlled system. In most of the previous film boiling studies in directly heated channels, this part of the film boiling curve could not be measured. In this study, a unique technique is used to enable the measurement of this portion of film boiling in a directly heated tube. Instead of approaching film boiling from CHF (which will result in excessive wall temperature), it is established by using a hot patch to stop the propagation of a rewetting front.

It must be mentioned that a temperature controlled system is not generally used because of its relatively high cost and technical difficulties. With water as the test fluid, the choice of the secondary heating liquid is very limited. Only liquid metal will possess the high heat transfer coefficient required in such applications.

II.2.3 Effect of Quality on the Boiling Curve

The forced convection boiling curve depends, among other factors, on the mass flux and the quality. Consider a boiling curve plotted with quality as a parameter. In Fig. 5, a set of curves of different quality in the film boiling region is shown. The film boiling curve has also been extended to below the CHF, since this is the region considered in this study.

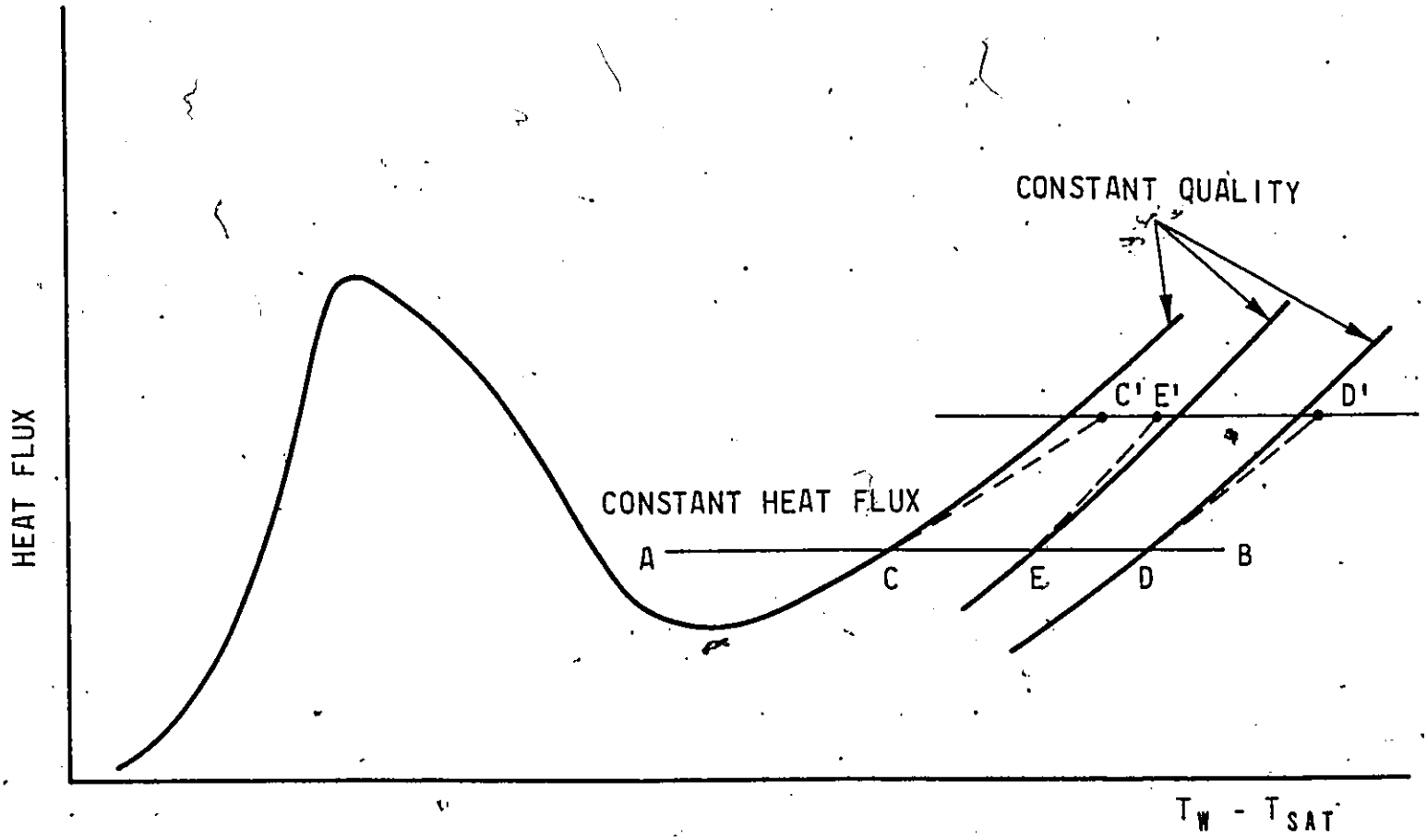

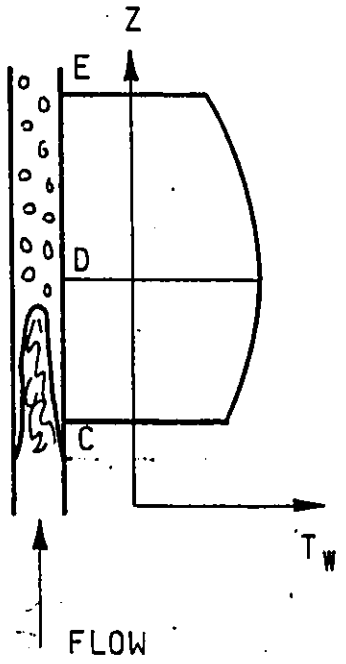

FIGURE 5 EFFECT OF QUALITY ON BOILING CURVE

Consider a point near the beginning of the heated length where inverted annular film boiling has been established. This point is shown as point C on Fig. 5. The wall temperature has been observed to increase initially and then decrease towards the downstream end. Fig. 6 shows an axial temperature variation taken from the report of Dougall and Rohsenow (1963). The same form of temperature distribution has been observed in the present study.

Therefore, point D in Fig. 5 will lie to the right of point C and point E to the left of point D. At higher heat fluxes, all points will be shifted upwards to C', D' and E'. The dotted lines such as CC' will therefore represent a segment of the boiling curve for a fixed point on the heated channel.

Since point E is downstream of point D, the quality is higher at E. Therefore, the constant quality line through E represents a higher quality than that through D. In addition, since the temperature at E is lower than that at D at the same heat flux, the heat transfer coefficient is also higher at E. This improvement in heat transfer is due to the increase in vapour velocity in the dispersed flow regime.

The effect of quality on the boiling curve has been studied by Groeneveld and Fung (1976). The parameter trend is shown schematically in Fig. 7. The lines corresponding to low quality and subcooled film boiling, where inverted annular flow prevails, have been included in this figure. Note the opposite trend of quality in the two different

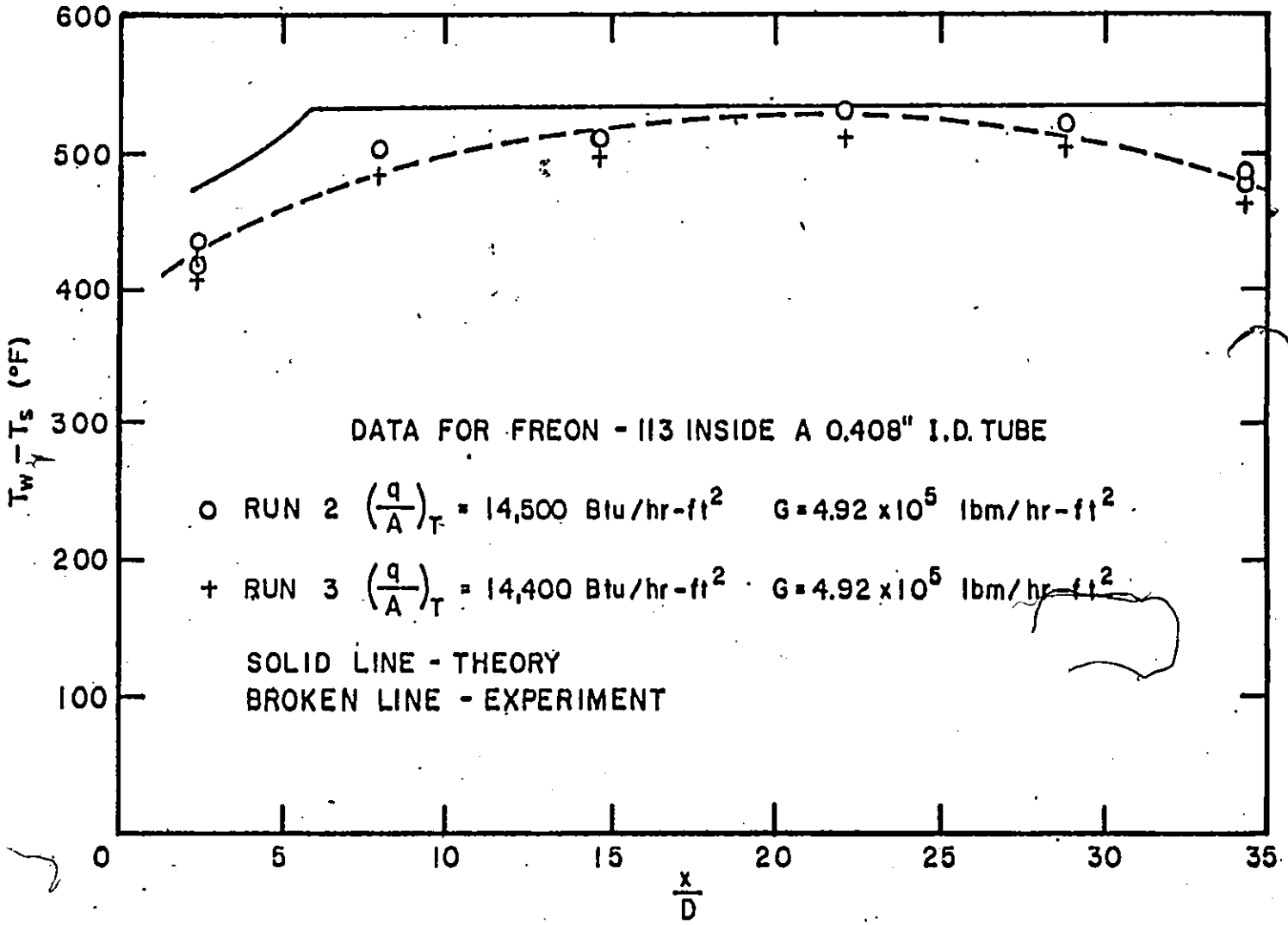

FIGURE 6 TEMPERATURE DISTRIBUTION ALONG 0.408" I.D. TUBE FOR $\left(\frac{q}{A}\right)_T$ = 14,500 Btu/hr - ft^2 FROM DOUGALL AND ROHSENOW (1963)

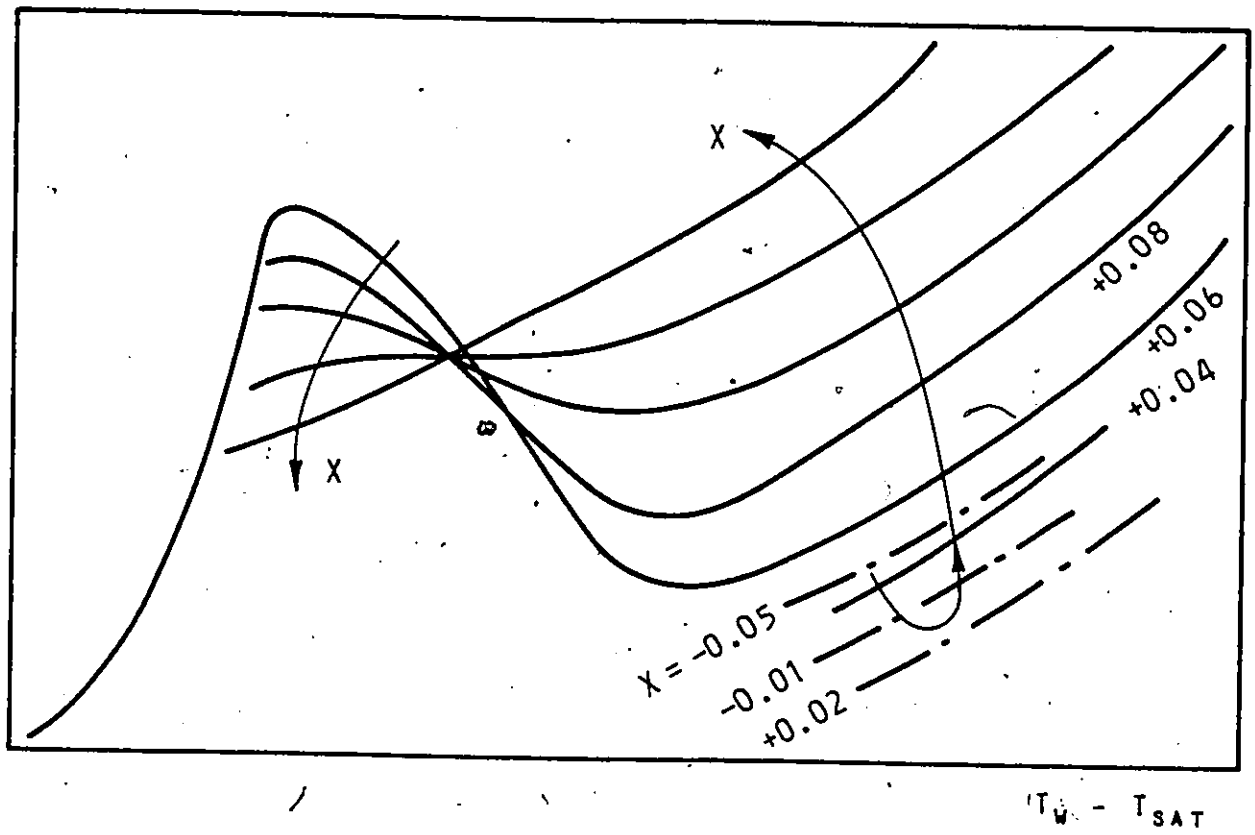

FIGURE 7

SCHEMATIC REPRESENTATION OF THE EFFECT OF QUALITY ON FORCED CONVECTIVE BOILING CURVE

flow regimes. The changeover point would be a suitable criterion for demarcation of inverted annular and dispersed flow. Obviously, the quality at this changeover point will depend on the mass flux.

III.0 LITERATURE REVIEW

III.1 General

Post-CHF heat transfer has been the subject of several review reports (Collier (1975), Groeneveld & Gardiner (1977), Fung (1978) and Mayinger & Langner (1978)). In the present study, we are primarily concerned with convective film boiling of water in low quality and subcooled conditions. Therefore, pool boiling studies will only be mentioned briefly if they are pertinent.

The experimental conditions covered by the available film boiling data have been examined by Groeneveld & Gardiner (1977) and the result is shown schematically in Fig. 8. Most of the previous investigations have concentrated on the high pressure, high mass flux and high quality conditions, which are relevant to boiler tube design. The areas marked "Data available but questionable" are relevant to water reactor accident conditions and interest in it has been enhanced in the last ten years. The present study is part of an integral research program aimed at a better understanding of the post-CHF heat transfer under reactor accident conditions.

III.2 Review of Experimental Studies

III.2.1 Experimental Work

As mentioned earlier, most of the previous studies of low quality film boiling have been carried out with cryogenics and refrigerants, mainly because of the relatively low wall temperatures

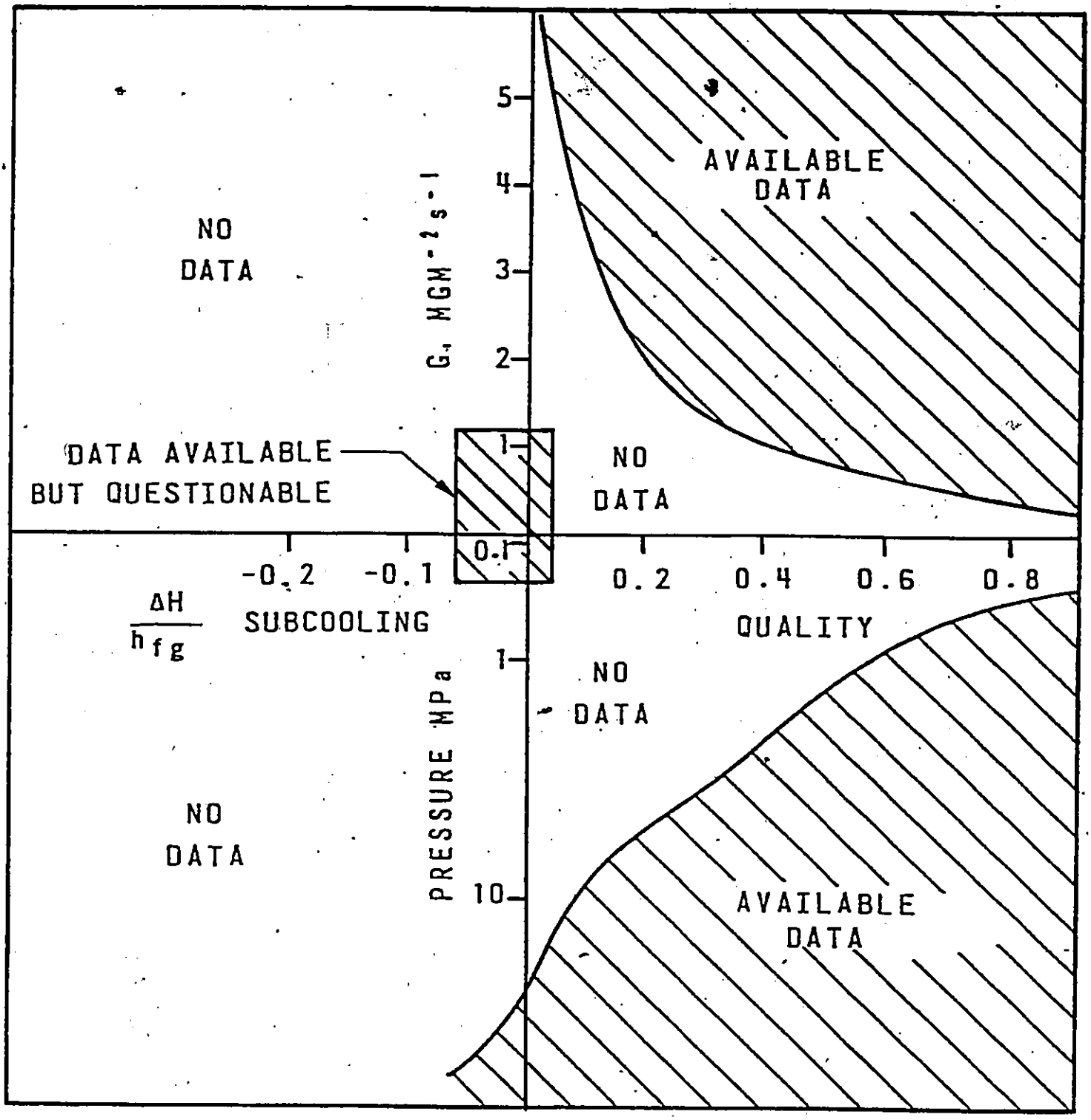

FIGURE 8 RANGE OF AVAILABLE FILM BOILING DATA

required. Recently, because of the interest in LOCA heat transfer, some of these studies have also been carried out in water. Table 1, taken from Groeneveld & Gardiner (1977), summarizes the studies reported in the literature.

The last four entries in Table 1 represent a new approach to obtaining post-CHF heat transfer data in the past five years. It was mentioned earlier that the post-CHF region below the CHF is unattainable for water in a directly heated thin-wall tube due to the propagation of the rewetting front. To circumvent this, these authors used thick copper cylinders in which the flow was passed through a central bore. Heat was either supplied by cartridge heaters embedded in the copper block (Fung, Cheng & Ng, Smith) or by wound-on heaters (Newbold). Due to the high thermal conductivity and thermal capacity of the copper cylinder, this type of test section approaches the situation of a temperature controlled system.

The experiments of Fung and Cheng & Ng were primarily designed to obtain transition boiling data. The limitation of this type of test section in obtaining film boiling data is the melting point of copper. Practically, it is limited to below 750°C. Therefore, the obtainable temperature range in film boiling is relatively narrow. The experiments of Newbold covered the temperature range below 700°C.

The extension to this technique is to incorporate the copper block in a tube. Smith (1976) adopted this method to obtain data in the inverted annular and dispersed flow film boiling regimes, but he was unable to maintain film boiling in his test section using a single block. Instead, he had several copper blocks clamped to the tube. Each of the blocks is independently heated by cartridge heaters and acted as heat source of the tube. Most of the data were obtained in the dispersed flow regime.

III.2.2 Parametric Trends Observed

The overall film boiling heat flux is affected by the mass flux, system pressure, liquid subcooling and some other secondary factors. The parametric trends observed in experimental studies are discussed below:

(a) Effect of mass flux

Bromley (1953) studied film boiling of liquid in upward flow over horizontal tubes. He observed that an increase in mass flux increased the heat transfer coefficient. Kalinin (1969) observed a similar trend in cryogenics. On the other hand, Dougall & Rohsenow (1963), Ellion (1954) and Rankin (1961) found no significant effect of mass flux on the film boiling heat transfer coefficient measured in vertical channels. It is possible that, beyond a certain mass flux, the vapour velocity is more dependent on the

vapour content of the flow than on the velocity of the flow prior to vapour generation.

At low flow, situations are similar to pool boiling and buoyancy force becomes important. For upward flow over horizontal tubes, Bromley (1953) used the Froude number as a criterion for transition between free and convective film boiling. The criterion is as follows:

$U/gD \leq 1.0$ free convection

$U/gD > 2.0$ forced convection

No similar criterion has been proposed for flow inside tube.

Newbold et al. (1975) studied the effect of flow direction on film boiling in internal flow in a short test section using a transient quenching technique. They found that the heat flux increased with increasing mass velocity, although for upflow the increase is small above 400 kg/m^2s. The higher rate of increase near the low flow region is probably due to the relatively higher increase of the inertial force over the buoyancy force. For conditions of higher inlet subcooling and pressure, they observed no significant difference between upflow and downflow. However, with low subcooling the heat transfer in downward flow is significantly lower than for upward flow. They attributed this to the buoyancy force acting in the opposite direction to the interfacial shear, thus increasing the vapour film thickness and reducing the rate of heat transfer.

(b) Effect of subcooling

The effect of subcooling on the film boiling heat transfer coefficient has been investigated experimentally and analytically. Increased heat transfer with increasing subcooling was observed in the pool boiling experiments of Tachibana & Fukui (1960) and Hein (1975), in quenching experiments with spheres by Farahat (1977) and Dhir (1978), and in transient cooling of short cylindrical blocks under internal forced flow conditions by Fung (1976), Cheng (1976) and Lauer & Hufschmidt (1976). Under steady-state conditions, inverted annular film boiling has only been observed in cryogenics and refrigerants. Kalinin's data (1969) for downward flow of nitrogen in a vertical tube and Bromley's data (1953) for vertical cross flow over a horizontal tube showed enhancement of heat transfer with increased subcooling.

Theoretical analyses of forced convective film boiling on flat surfaces were carried out by Cess & Sparrow (1961) and Sparrow & Cess (1962), using a laminar boundary layer approach. They found that the surface heat flux increased with subcooling, and the rate of increase was higher at a lower temperature level.

(c) Effect of pressure

No systematic experimental studies on the effect of pressure have been carried out. Qualitatively, pressure affects the film boiling heat transfer primarily through the changes in fluid

properties. In his theoretical analysis of laminar film boiling, Ellion (1954) derived the following expression for the film thickness

$$\delta^4 = 12\left(\frac{k_v \mu_v}{h_{fg}\ \rho_\ell\ \rho_v}\right) \Delta T_s Z$$

The conductivity and viscosity increase with pressure, whereas the latent heat and liquid density decrease with pressure. Together, they tend to increase the film thickness. However, the most significant change is in the vapour density. For example, for ΔT_s = 500°C and Z = 0.1 m, the calculated film thickness at 0.1 MPa and 10 MPa are 1.6 and 0.42 mm respectively. A thinner film will have a stabilizing effect on film boiling, since the onset of turbulence will be delayed.

With a thinner vapour film, the heat transfer coefficient will be increased. Therefore, at the same wall superheat, the total heat flux will be higher at higher pressure.

(d) Effect of surface property

In film boiling there is no direct liquid-surface contact. Therefore surface roughness and oxide layers are unlikely to have an effect on film boiling if the roughness height is less than the laminar sublayer thickness. If the roughness peaks penetrate

through the sublayer the film boiling heat transfer coefficient will be increased due to the existence of eddies near the asperities.

III.3 Breakup of Liquid Core in Inverted Annular Flow

In experiments carried out inside heated tubes, the mass quality increases along the flow direction. Therefore, starting from an inverted annular flow near the inlet, the liquid core will break up as quality increases until eventually a dispersed flow is formed. Tong (1965) considers the inverted annular flow as a liquid jet discharging into a moving vapour stream. The stability criterion under such conditions is

$$m \cdot \sigma \left(\frac{1}{\rho_c} + \frac{1}{\rho_v} \right) > \left(U_v - U_c \right)^2$$

where m is the wave number. Rankin (1965) included in his analysis a vapour thrust force which exerted on the vapour-liquid interface during dry wall collision and derived the following stability criterion

$$\left[\frac{\sigma \cdot m}{\rho_c} + \frac{2 k_v^2 \, \Delta T^2}{m \, \rho_c \, \rho_v \, h'_{fg} \, t_v^3} \right] \left[1 + \frac{\rho_c}{\rho_v} m t_v \right] > \left(U_v - U_c \right)^2$$

where $\Delta T = T_w - T_{sat}$

$$h'_{fg} = h_{fg}\left[1 + 0.4\,\frac{Cp\ \Delta T}{h_{fg}}\right]^2$$

$$t_v = \frac{f}{3Pr^{2/3}}\,\frac{Cp\ \Delta T\ Z}{h'_{fg}} = \text{vapour film thickness}$$

f = friction factor

Z = distance from dryout location

Both stability criteria depend on the wave number m, which is unknown.

The breakup of the liquid core will result in a slug flow initially. This will increase the vapour-liquid interfacial area and therefore will increase the local heat transfer. Such a situation may lead to rewetting of the surface. If no rewetting takes place, the flow will gradually change to a dispersed flow. If there is a rewetting front, the heated surface will gradually be quenched.

Dougall & Rohsenow (1963) used a different correlation for the heat transfer coefficient in dispersed flow and in inverted annular flow. They suggested that as the vapour film thickened due to increase in quality, the heat transfer coefficient, and hence the Nusselt number, decreased accordingly. The minimum Nusselt number then

corresponds to the transition between inverted annular and dispersed flow. Smith (1976) used the same criterion to compare his data.

Various authors use the void fraction as a criterion for transition from inverted annular flow to dispersed flow. For example, Hughes (1976) uses 0.2 and Kaufman (1976) uses 0.4 as the critical void fraction. This type of criterion is convenient to use but does not describe the mechanism of the transition. In addition, other effects, such as mass flux and pressure, also influence the transition. This is evident from the various flow regime maps suggested (see Collier (1972)).

III.4 Review of Theoretical Analyses

Several theoretical analyses relevant to the present investigation are discussed in this section. In all analyses, the purpose is to predict the wall heat flux, or the temperature, depending on which boundary condition is known. The most commonly adopted strategy is to solve the boundary layer equation for the vapour and/or the liquid. Most of the uncertainties lie in the interface and many assumptions are made for the interfacial shear stress and heat transfer.

III.4.1 Ellion (1953)

In his analysis, Ellion makes the following assumptions

(i) the liquid is at the saturation temperature;

(ii) the interfacial velocity is virtually zero;

(iii) all the heat leaving the tube is used to vaporize the liquid. This assumption also implies that there is no superheat in the vapour and that the rate of vapour generation is constant along the tube;

(iv) the total pressure gradient is equal to the hydrostatic pressure gradient.

By assumptions (i) and (iii) the interaction between the liquid and the vapour is known and consequently no analysis of the liquid core is required.

For the vapour film, Ellion makes the following assumptions

(v) the vapour film flow is laminar, and

(vi) the vapour properties are independent of temperature.

With some additional assumptions which are common to boundary layer analysis, the momentum equation for the vapour film is reduced to

$$\frac{d^2u}{dy^2} + \frac{\rho_\ell}{\mu} = 0$$

subject to the boundary conditions of

$u = 0$ at $y = \delta$ and $y = 0$

Once the velocity distribution across the film is known, the total vapour flow can be obtained by integrating across the vapour film. By assumption (iii), the vapour flow at any location can also be calculated from the power. These two equations for the vapour flow can be solved to give the vapour film thickness. The film boiling heat

transfer coefficient is then calculated by assuming pure conduction across the vapour film and is found to be

$$h_{FB} = \left[\frac{i_{fg}\, \rho_\ell\, \rho_v\, k_v^3}{12\, \Delta T_{sat}\, Z\, \mu_v} \right]^{\frac{1}{4}}$$

It is noted that h_{FB} does not contain any subcooling nor mass flux effect. This is the result of assumptions (i) and (ii).

III.4.2 Rankin (1961)

Rankin considers the separate cases of laminar and turbulent vapour film flow. The analysis of the laminar film is similar to that of Ellion, except that the interfacial velocity and the pressure gradient (which is assumed constant) are unspecified and appeared as parameters in the solution.

For the turbulent film, Rankin assumes that the interfacial velocity is zero. The vapour flow is then considered to be equivalent to that between two parallel stationary plates. The interfacial shear stress is taken to be the same as the wall shear stress. By neglecting the momentum change of the gas, a force balance gives

buoyancy force = frictional force

or $\delta g(\rho_\ell - \rho_v) = 2 \times \frac{1}{2} f \rho_v U_v^2$.

By neglecting the body force of the vapour the film thickness is expressed as

$$\delta = f \frac{\rho_v}{\rho_\ell} \frac{U_v^2}{g} \qquad 4.2.1$$

The momentum and heat transfer at the wall are related by the Colburn 'j' factor as follows:

$$j = \frac{f}{2} = \frac{h}{Cp_v \rho_v U_v} Pr^{2/3}$$

By assuming that all the heat goes into vapour generation, the change in vapour flow can be related to the vapour generation at the interface as follows:

$$\rho_v \, d(U_v \delta) = \left(\frac{\phi}{h'_{fg}} \right) dZ$$

$$= \frac{h . \Delta T_w}{h'_{fg}} dZ$$

$$\therefore \; d(U_v \delta) = \frac{G \, \Delta T_w \, f \, U_v}{2 \, h'_{fg} \, Pr^{2/3}} dZ$$

Substituting δ from Eq. 4.2.1 the following equation is obtained

$$3U_v \frac{dU_v}{dZ} = \frac{Cp\ g\ \Delta T_w\ \rho_\ell}{2h'_{fg}\ \rho_v\ P_r^{2/3}}$$

Direct integration gives the vapour velocity. The final expression for the heat transfer coefficient is

$$h_z = \frac{f}{2\sqrt{3}\,Pr}\left[\frac{g\ Cp_v^3\ \Delta T_w\ \rho_\ell\ \rho_v\ Z}{h'_{fg}}\right]^{1/2}$$

III.4.3 Dougall & Rohsenow (1963)

In this analysis the liquid core is assumed to be at saturation. Rather than solving the boundary layer equation for the vapour film, it is assumed that the universal turbulent velocity distribution holds from the wall to the point of maximum velocity in the film, and its mirror image for the other half of the film. Close to the interface, they consider the following possible situations

(i) the turbulent layer exists up to the interface,

(ii) a buffer zone exists next to the interface, and

(iii) both the laminar sublayer and the buffer layer exist.

The total shear stress and heat flux are then assumed to be given by

$$\frac{\tau}{\rho_v} = \left(\nu_v + \varepsilon_m\right) \frac{du}{dy} \qquad \ldots \quad 4.3.1$$

and

$$\frac{\phi}{\rho_v \, Cp_v} = - \left(\alpha_v + \varepsilon_H\right) \frac{dT}{dy} \qquad \ldots \quad 4.3.2$$

It is further assumed that the Reynolds analogy is valid, i.e., $\varepsilon_m = \varepsilon_H$. The eddy diffusivity is then calculated from Eq. 4.3.1 by using the universal velocity profile. For the case of constant heat flux, Eq. 4.3.2 is integrated to yield the temperature. A typical comparison between the theory and their data is shown in Fig. 6 (p. 14).

III.4.4 Kalinin et al. (1977)

This is a one-dimensional flow model of subcooled film boiling. The liquid is assumed to move in the form of a turbulent jet, which is separated from the pipe wall by a turbulent film. Both vapour and liquid are assumed to move at the same velocity. In addition, the heat transfer from the wall to the vapour and from the vapour into the liquid are assumed to follow the equations:

$$Nu_v = A \, Re_v^m \qquad \ldots \quad 4.4.1$$

$$Nu_\ell = B \, Re_\ell^n \qquad \ldots \quad 4.4.2$$

Since the velocity distribution has been assumed uniform, the momentum equation is not required in the analysis. Then, by combining the continuity and energy equations, a differential equation for the dimensionless vapour film thickness $b = \frac{2\delta}{D}$ is obtained and is shown below

$$\frac{db}{dH} - \psi_1(b) - E\ \psi_2(b) = 0 \qquad \ldots\ 4.4.3$$

H is a function of Nu_v and the axial wall temperature distribution. E is a function of Nu_v and Nu_ℓ. Qualitatively, H contains the prior history of the flow and E is proportional to the fraction of heat that goes into the liquid.

The solution of Eq. 4.4.3 requires that A and B in Eqs. 4.4.1 and 4.4.2 be specified. Once b has been found, the heat flux is obtained from Eq. 4.4.1.

The most questionable assumption is that of the equal and uniform velocity in both liquid core and vapour film. The usual assumption in a one-dimensional two-phase separated flow analysis is to assume a different velocity for each phase. The assumption of equal velocity in the two phases seems more realistic in dispersed flow than in inverted annular flow.

III.4.5 Barnes (1973)

In this analysis, similarity transformation is applied to the governing equations. Analogous to laminar flow, a similarity variable η, a stream function ψ and a dimensionless energy function ϕ are defined. Since the analysis is applicable to turbulent flow, η and ψ are functions of the eddy diffusivity. The latter is assumed to follow an exponential relationship with η, as well as being dependent on the fluid velocity. The general form is

$$\varepsilon = \varepsilon_{\infty}(1 - \exp(-b\eta)) + \nu(\exp(-b\eta))$$

where ε_{∞} is the free stream eddy diffusivity and b is a shape factor.

The momentum and energy equation are then reduced to a set of simultaneous ordinary differential equations of the transformed velocity and temperature. For the solution, the entire fluid domain is divided into three regions, namely the vapour film, the mixture layer and the subcooled liquid. Numerical method is used to solve the coupled ordinary differential equations, using experimentally measured wall temperatures to evaluate the vapour and liquid thermophysical properties.

III.4.6 General Comments

Most of the analyses assume that the liquid is at saturation. This enables the vapour generation rate to be calculated. By further

assuming the velocity at the vapour-liquid interface, the liquid layer or core is decoupled from the vapour film. This seems to be an over-simplification compared with the case of subcooled film boiling where significant thermal non-equilibrium exists.

In most of the analyses (except Barnes'), the vapour-liquid interface has been assumed to be smooth. In the actual situation, it has been observed (Dougall & Rohsenow) to be wavy. The quantitative effect of waves on the interfacial shear and evaporation rate is not amenable to theoretical analysis at the present time, since the prediction of the same quantities in the case of a smooth interface still depends on some correlation parameters based on experimental data. Assumptions must therefore be made concerning the momentum and energy transfer at the interface.

In addition, in the case of a subcooled liquid core, part of the heat transferred at the interface eventually goes into heating up the liquid. This portion of heat transfer diminishes as the liquid temperature approaches the saturation temperature. The situation is quite similar to a thermal-entry-length problem (Kays (1966)) in which the heat transfer coefficient assumes a very high value at the entrance, and gradually decreases along the length. No analysis of film boiling has so far considered this developing thermal boundary layer in the liquid core. This is because in saturated flow the liquid remains at a constant temperature.

III.5 Correlations for Low Quality and Subcooled Film Boiling

Most of the correlations are developed based on cryogenic or refrigerant film boiling data. Their applicability to water has not been established through comparison with water data. The available correlations have been examined by Groeneveld & Gardiner (1977) and are tabulated in Table 2. Basically, they fall into three categories

(i) Correlations based on laminar flow of the vapour film. These correlations have the form

$$h_c = A \left[\frac{k_v^3 \rho_v (\rho_\ell - \rho_v) i_{fg}}{\mu_v \Delta T_{sat} L} \right]^{\frac{1}{4}} + h_{rad}$$

where A depends on the vapour-liquid interfacial velocity and L is a characteristic length.

(ii) Dittus-Boelter type correlations

These correlations assume that all resistance to heat transfer lies in the vapour film. By suitably defining a Reynolds number the correlations have the form

$$Nu = a\, Re^b\, Pr^c\, F$$

where F is incorporated to fit particular sets of data.

(iii) Phenomenological correlation

These are developed, based on physical phenomena, with some empirically correlated parameters. They are less cumbersome to apply than mechanistic models, which require the solution of several simultaneous differential equations.

IV.0 EXPERIMENTAL DESIGN

IV.1 Background

The most widely used system in forced convective boiling studies is a heat flux controlled system where the heat output of an electrically heated element is independently controlled. However, as mentioned previously, such a system does not permit the measurement of flow film boiling data for subcooled water due to the advancing of the rewetting front.

The method used in the present study is the so-called hot patch technique originally used by Groeneveld (1974) to study the effect of flux spikes on CHF in Freon. Fig. 9, taken from the original report by Groeneveld, shows schematically the flow structure downstream of the hot patch. It was noticed that, after steady film boiling was established at the hot patch and the test section power increased gradually, the drypatch propagated downstream into the heated tube. This method was subsequently used in a water flow loop by Groeneveld & Gardiner (1978) to establish stable film boiling.

In the case of water, the vapour film established inside the bore of the hot patch cannot be propagated downstream into the test tube by raising the power. This is due to the much higher latent heat of water compared with Freon. Therefore, both the hot patch and the test tube have to be preheated to above the Leidenfrost temperature before the injection of water. The role of the hot patch is then to

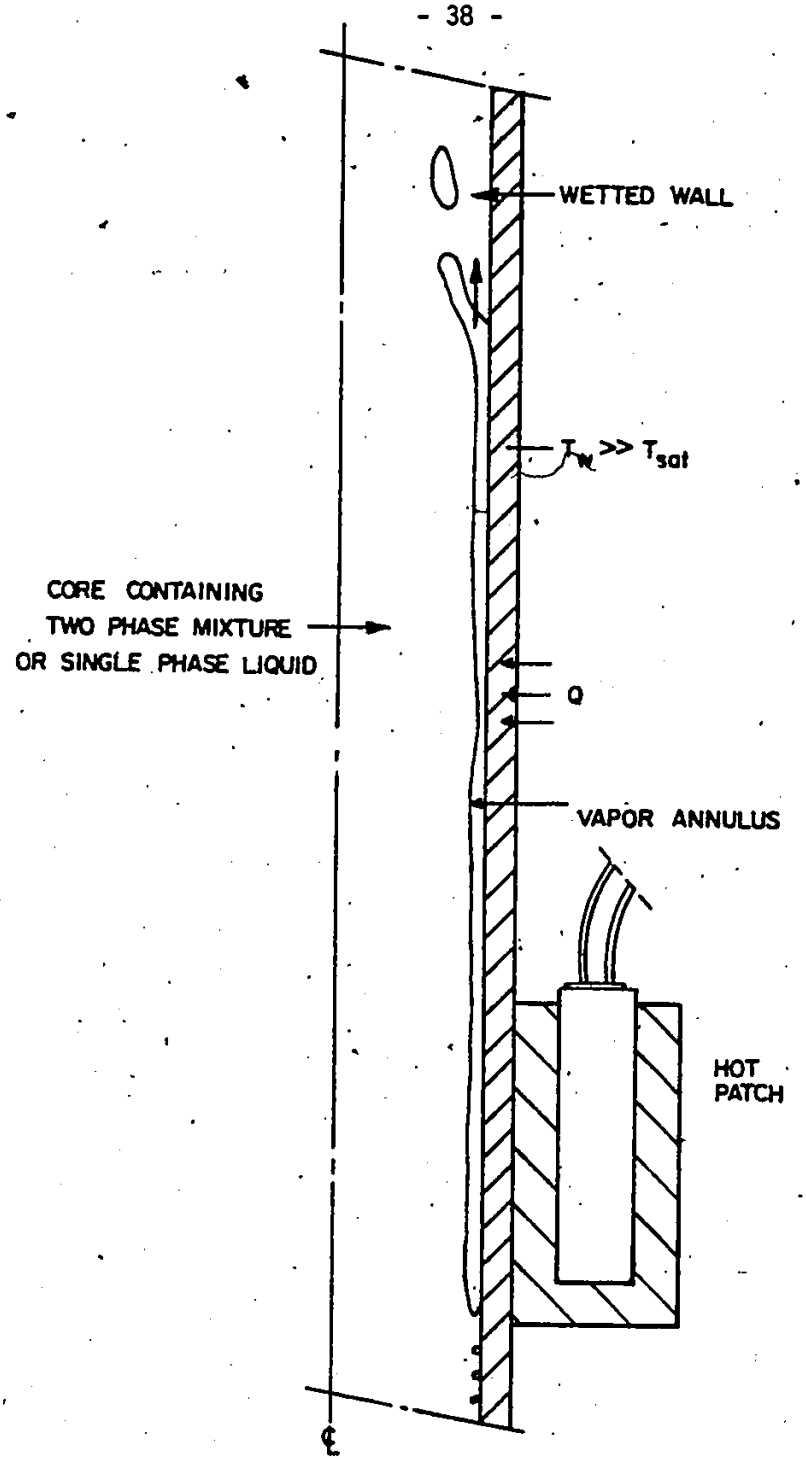

FIGURE 9 SPREADING OF DRY PATCH DOWNSTREAM OF HOT PATCH FROM GROENEVELD (1974)

prevent the rewetting front from propagating into the tube. This slight difference in procedure is imperative in the successful establishment of stable film boiling.

IV.2 Test Section

The test section is shown schematically in Fig. 10. Details of the hot patch clamp are shown in Fig. 11. It was machined from oxygen-free copper and equipped with eight cartridge heaters. The support ring was welded to the test tube and the copper block was then held to it by three bolts prior to brazing.

The copper block was brazed to the Inconel tube in an inert atmosphere using a high temperature silver solder (melting point = 780°C). Two types of test section were made: one with a 6.25 cm long and one with a 2.54 cm long hot patch. A total of four test sections was used in the study. Details of the dimensions of the test sections are presented in Table 3.

The optimum length of the test section was determined experimentally during the initial trial runs. It was desirable to have the heated length as long as possible, so that the effect of length on the heat transfer could be examined. The actual length was finally determined by using the following criteria:

(i) the maximum wall temperature must be below the melting point of the tube, and

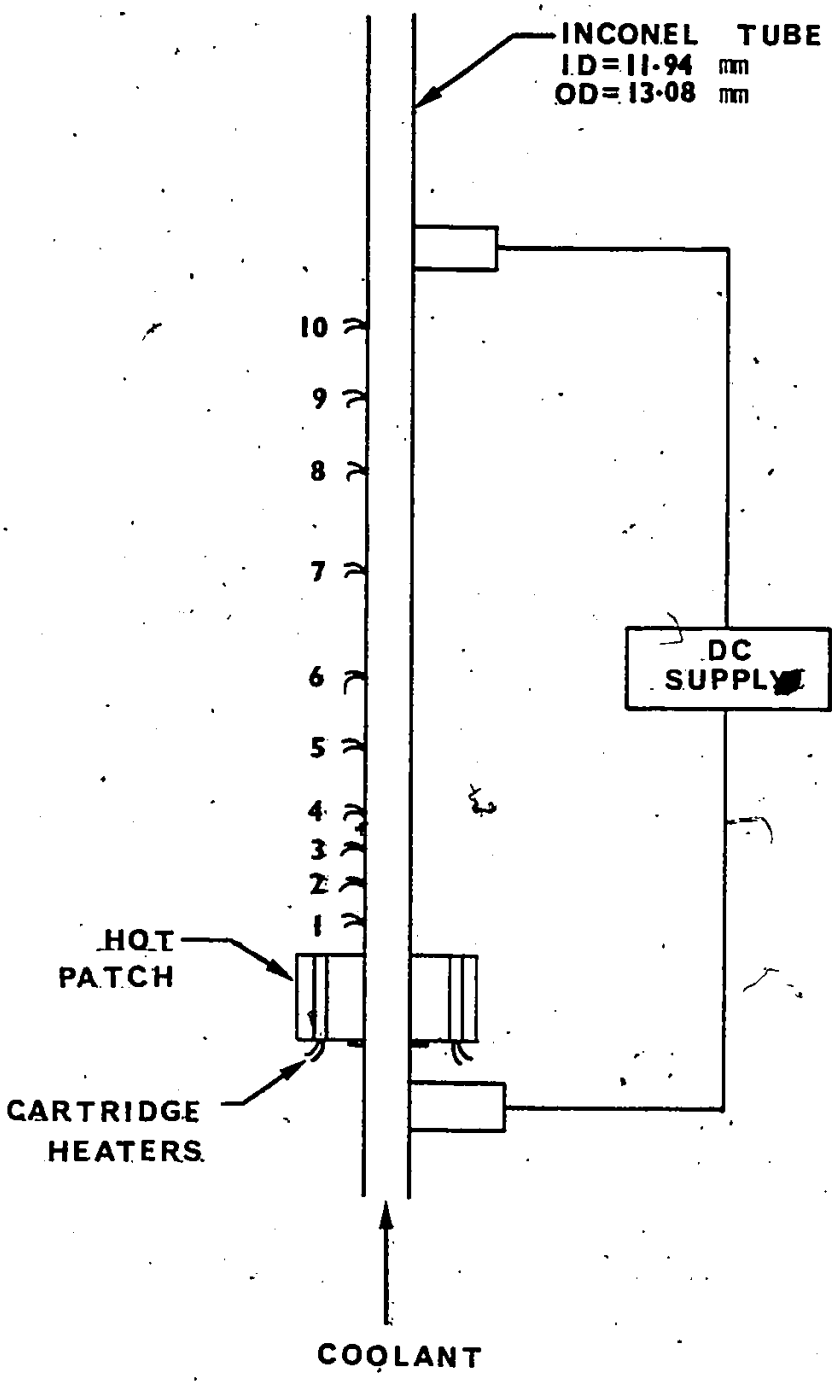

FIGURE 10
SCHEMATIC OF TEST SECTION

T/C	ELE'N (CM) FROM TOP OF HOT PATCH
1	3
2	6
3	9
4	12
5	18
6	24
7	35
8	45
9	50
10	55

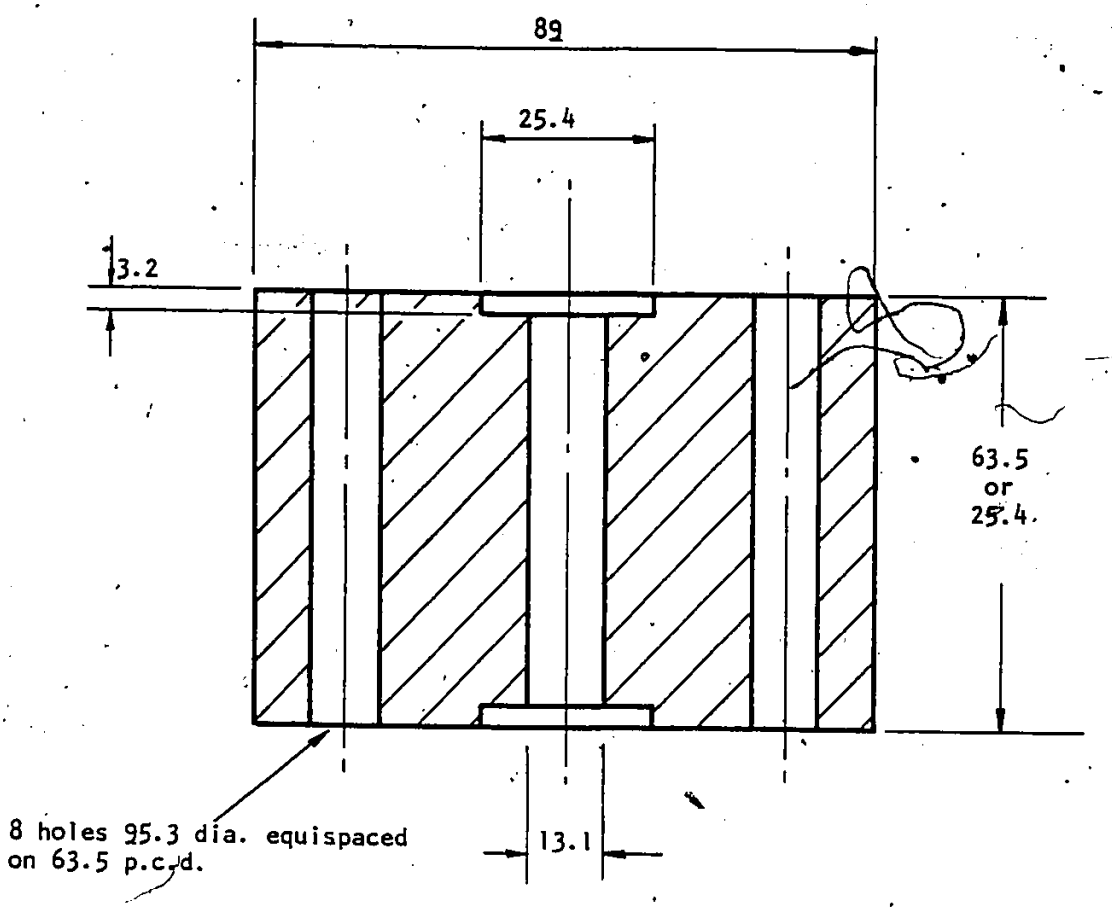

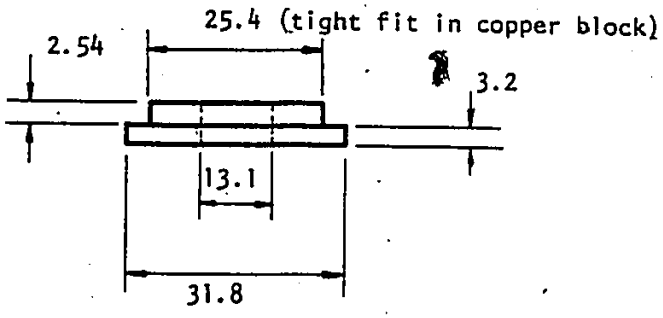

MATERIAL OXYGEN-FREE COPPER (BLOCK)
304 STAINLESS STEEL (SUPPORT RING)

All dimensions in mm

FIGURE 11 DIMENSIONS OF HOT PATCH

(ii) at least a 20% variation in total test section power between the runs at maximum and minimum (before quenching) wall temperature.

The least variation in test section power usually occurred at the lowest flow because the axial temperature variation was then the largest.

Chromel-Alumel thermocouples were spot-welded to the outside surface of the tube at various axial locations to monitor the temperature during the test. All thermocouples were located on the same vertical plane. The locations of the thermocouples are tabulated in Table 3. The entire test section was insulated with a high temperature ceramic fiber and covered on the outside with aluminum tape to reduce radiative heat loss.

IV.3 Flow Loop

The experiments were carried out in a low pressure water loop unofficially referred to as the SOUP LOOP (Subcooled Or Unsaturated Post-CHF). A schematic diagram of the loop is shown in Fig. 12. Part of the flow through the preheater was bypassed back to the tank in order to obtain a more stable control over the coolant temperature at the inlet to the test section. The flow rate was measured by a bank of rotameters, each covering a different range. The bypass leg downstream

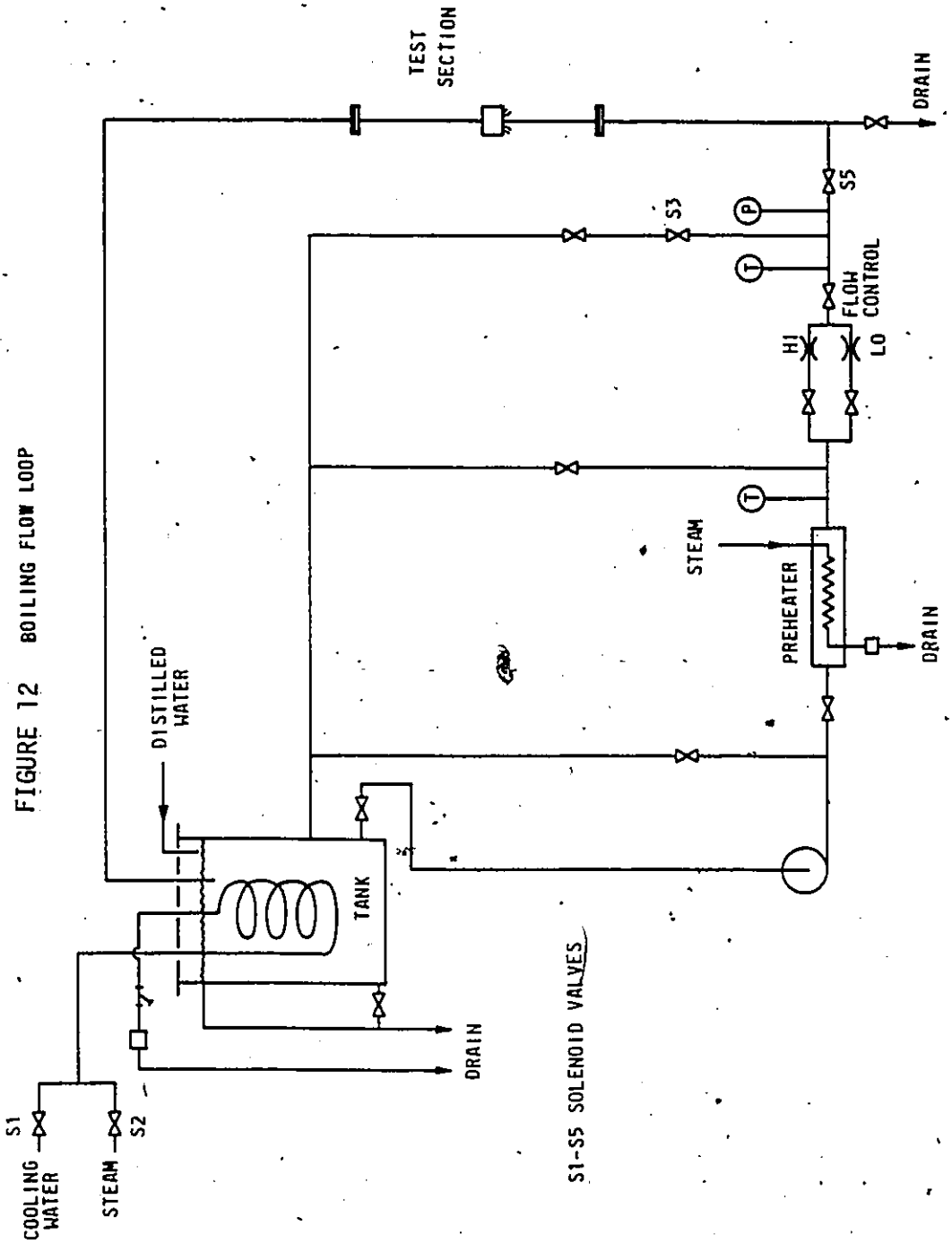

FIGURE 12 BOILING FLOW LOOP

of the flow meter was set to the same flow resistance as the test section leg. During the heat-up of the test section, the flow was directed through the bypass leg to establish the required flow rate and subcooling.

IV.4 Experimental Procedure

The test section formed part of the flow loop through which water was circulated at atmospheric pressure at the test section exit. Initially the test section and hot patch were heated separately, while the desired flow condition was established in the bypass leg. The hot patch thermocouple and selected test section thermocouple signals were displayed on an 8-channel chart recorder. When the hot patch temperature exceeded the minimum temperature required to maintain film boiling (usually in the range of 350-550°C, as determined in previous calibration tests), the test section power was increased to raise the tube temperature rapidly to the 500-800°C range. The flow was then diverted from the bypass to the test section. As soon as the first test section thermocouple showed a decrease in temperature (indicating that water had arrived at that location), the test section power was increased to prevent the test section from being quenched. The presence of the hot patch at the entrance created a vapour annulus around the circumference, which could be maintained downstream in the heated tube under appropriate conditions.

When steady film boiling was established, the test section power was increased and/or decreased in steps of approximately 10%. After each change, conditions were allowed to reach a steady state before the data were recorded. A typical sequence of event is shown in Fig. 13.

For tests at high mass fluxes (typically $G \geq 300$ kg·m^{-2}·s^{-1}) it was necessary to start with a lower mass flux in order to prevent the test section from being quenched when the coolant first reached it. The mass flux and the heat flux were then gradually increased to reach the desired flow rate.

IV.5 Data Acquisition

The test section power and thermocouple signals were scanned at regular intervals (generally set at 20 seconds) and converted to engineering units by means of an on-line computer. The hot patch power was measured separately by a wattmeter and the flow by a rotameter. These values were keyed into the computer through a teletype console by the operator. All information was displayed on a CRT. When conditions were steady, data were recorded on magnetic tape. Further processing of the data was carried out on a CDC Cyber 170.

For each inlet condition, data were recorded at several power levels. The test section power was limited so that the maximum tube wall temperature did not exceed 1100°C. The test was terminated when the tube started to rewet as the heat flux was reduced. The test matrix is given in Table 4.

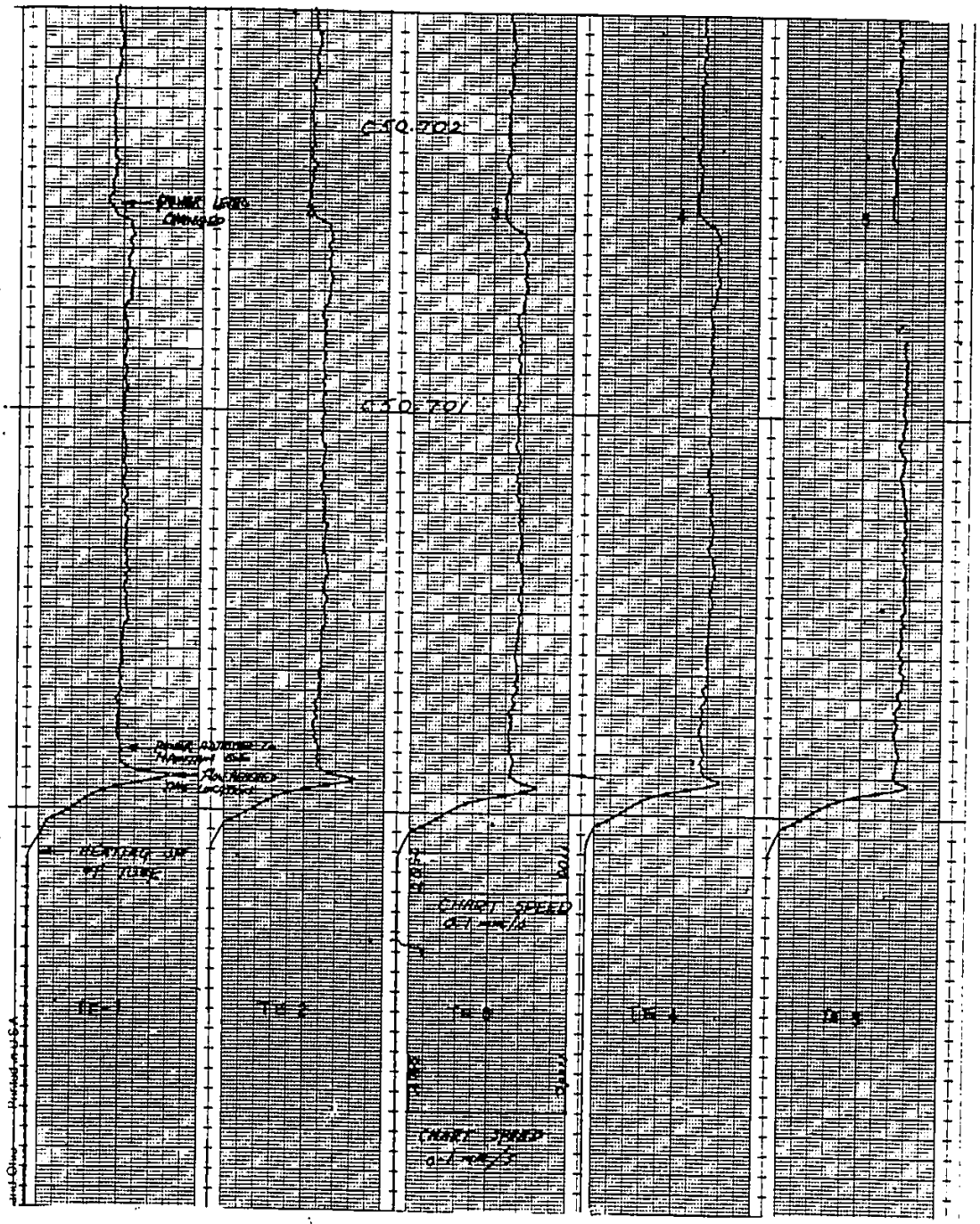

FIGURE 13 TYPICAL TRACE OF TS THERMOCOUPLES DURING TEST

IV.6 Measurement of Void Fraction

A γ-densitometer was used to measure the void fraction for test sections D and E. The relative positions of the radioactive source, test section and detector are shown in Fig. 14. A schematic design of the electronic circuit is shown in Fig. 15. The source (50 mCi Cesium 137) is encased in a collimator which, together with the detector, can be moved parallel to the tube axis to measure the attenuation at different axial locations.

The gamma beam was collimated so that it was just slightly wider than the tube diameter at the measurement region. This ensured a maximum sensitivity and ease of alignment. It is desirable to have a high counting rate in order to reduce the random error for a fixed sampling time. This can be achieved by increasing the height of the collimator windows. For practical reasons, the collimator windows in the present setup were adjusted to give approximately a counting rate of 12,500 c/s and a sampling time of 200 s was used.

The void fraction is deduced from the attenuation of the γ-beam. A detailed description of the calibration and error estimate is given in Appendix A.

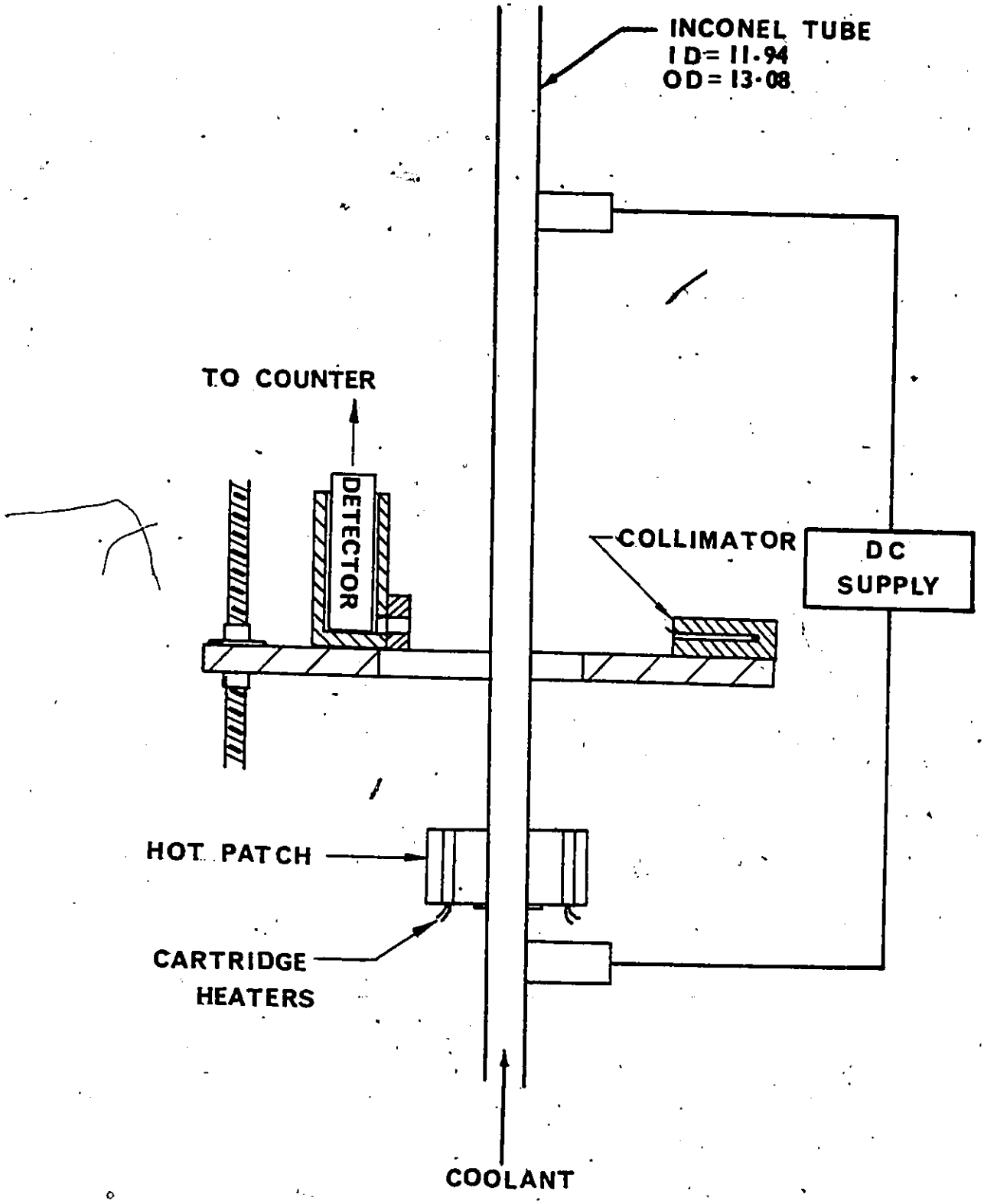

FIGURE 14 SCHEMATIC OF TEST SECTION AND γ-DENSITOMETER

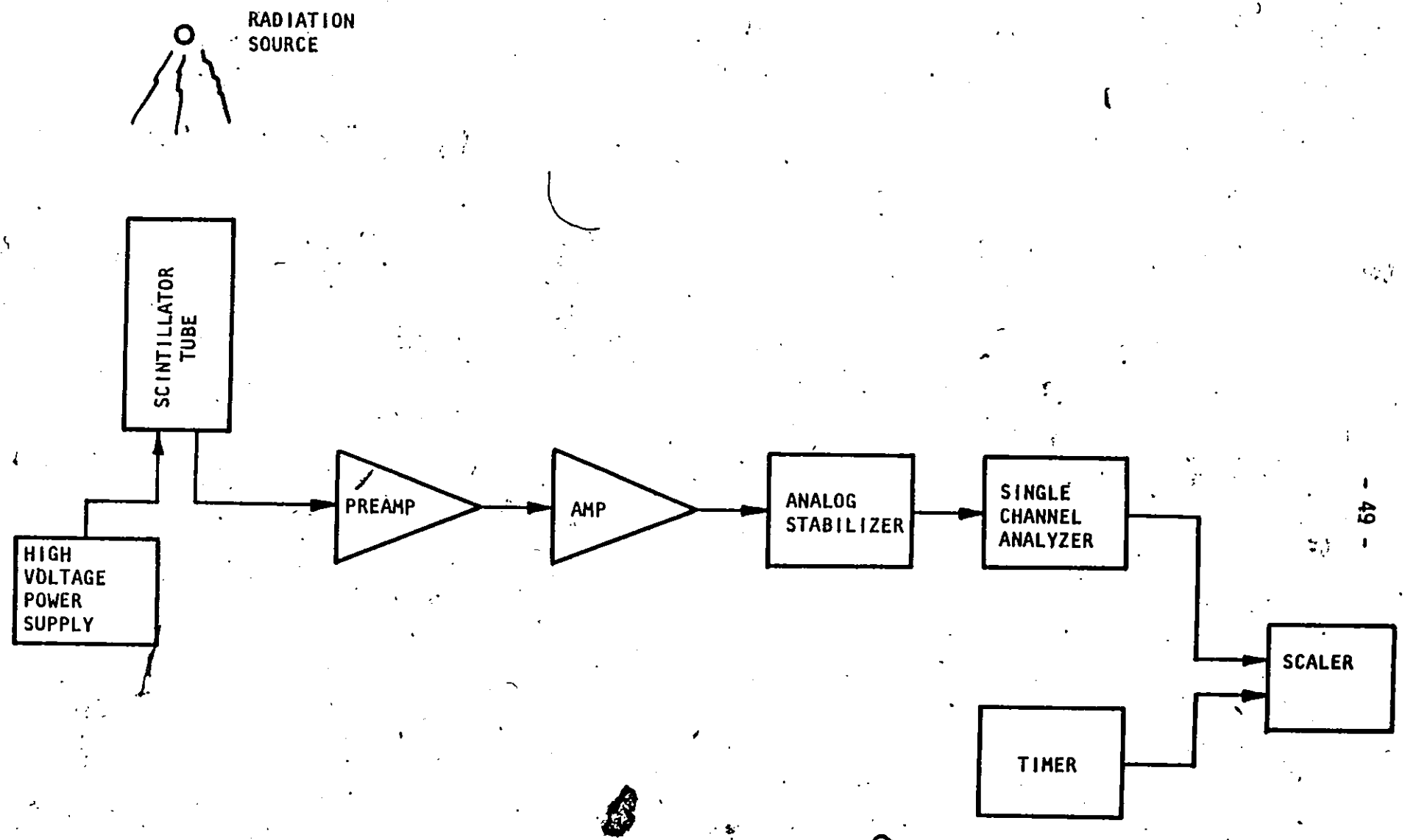

FIG. 15: BLOCK DIAGRAM OF γ-DENSITOMETER

V.0 DATA REDUCTION

V.1 General

For each run the test section current, voltage and thermocouple signals were recorded. The test section power was then calculated based on the current and resistance of the test section. This was used to calculate the local heat flux and heat transfer coefficient (based on wall superheat), taking into account the conduction along and across the tube wall and heat loss to the surroundings. The various corrections are discussed in Appendix B.

V.2 Tabulation of Heat Transfer Data

The thermocouple signals and the test section power fluctuated slightly about their mean values at each steady-state condition. To reduce this random error, the data for each run were recorded on magnetic tape for three times, with approximately 10 seconds between each recording. The total amount of raw data is therefore too large to be tabulated completely. It is decided to examine the data and pick out only one set from each group of three recordings. The criterion used is that the data of the chosen set are approximately the mean among the group of three.

The reason why averaging is not used is that the heat transfer coefficient averaged over the three sets will not be equal to the average heat flux divided by the average wall superheat.

The reduced data are tabulated in Appendix C and shown as boiling curves in Appendix D.

V.3 Void Fraction Data

The densitometer signals were processed as explained in Appendix A. The void fraction data are tabulated and plotted in Appendix E.

VI.0 DISCUSSION OF RESULTS

The results are shown graphically as heat flux versus wall superheat in Appendix D. To this author's knowledge, these are the first non-transient data on subcooled flow film boiling of water obtained over a wide range of mass flux and inlet subcooling. Furthermore, the test conditions are comparable to those that are expected to exist inside reactor core during the initial stage of emergency core coolant injection after a LOCA. The only similar data available are the few points obtained by Ellion (1954) in a short test section (7.6 cm). The reflooding tests of the FLECHT program (Cadek, 1971) also contain some information, but it is difficult to interpret the data due to the transient conditions.

Observations from the data and the parametric effects on the boiling curve are discussed in this chapter. Test section C contains the widest test range and will be used as the reference when comparisons are made with other test sections.

VI.1 Dryout Location Inside the Hot Patch

The location where film boiling starts inside the hot patch was not measured during the experiment. However, such information is important in the theoretical analysis. If it can be ascertained that dryout occurs over a short distance compared to the length of the hot patch, then it can be assumed that the entire block is in film boiling.

To analyze this, the total power over a uniformly heated tube in which CHF occurs at the end is calculated using two correlations: the local conditions form of the Macbeth correlation (1963) applicable to low

pressure and short length and the Menegus (1959) correlation. The correlations are shown in Appendix F. The results are shown as critical heat flux versus critical quality in Fig. 16.

Another independent check can be made from the CHF data reported by Fung (1976) in his transition boiling study. The copper cylinder used in that study was similar to the hot patch of the present experiment. The CHF's deduced from the transient cooling curve are reproduced here in Fig. 17.

For comparison, the average heat flux over the length of the hot patch during film boiling tests for test sections C and E are shown in Fig. 18.. It can be seen that the average heat flux at the hot patch is much lower than any of the predicted CHF's. This means that film boiling with a lower heat transfer coefficient exists over most of the hot patch. Dryout actually occurs near the inlet and the difference in temperature between the wet and the dry side of the surface will cause significant axial conduction along the copper cylinder. This also suggests that the average heat flux of the hot patch is always higher than if pure film boiling occurs on the entire surface.

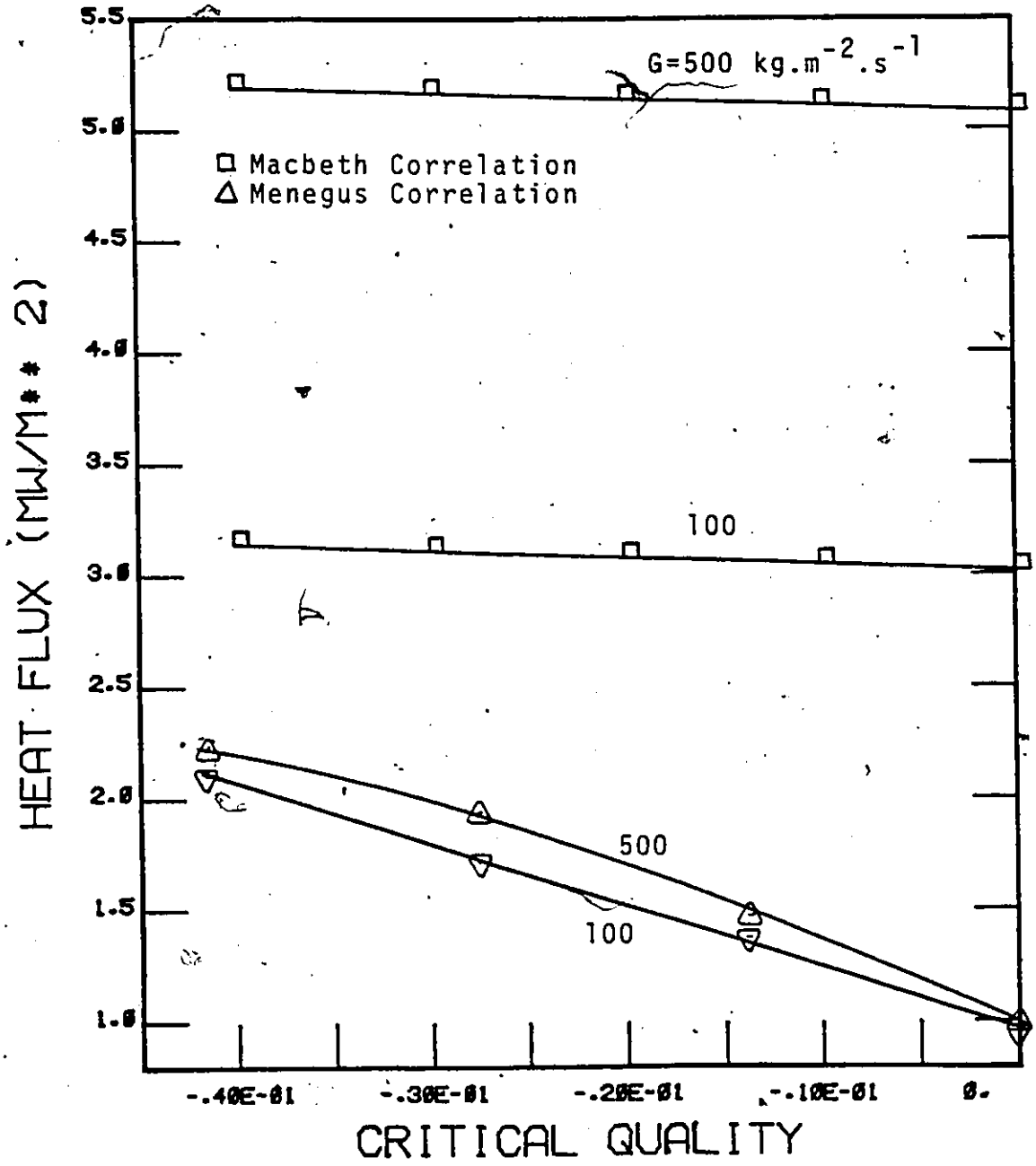

FIGURE 16. PREDICTION OF HOT PATCH HEAT FLUX USING CHF CORRELATIONS

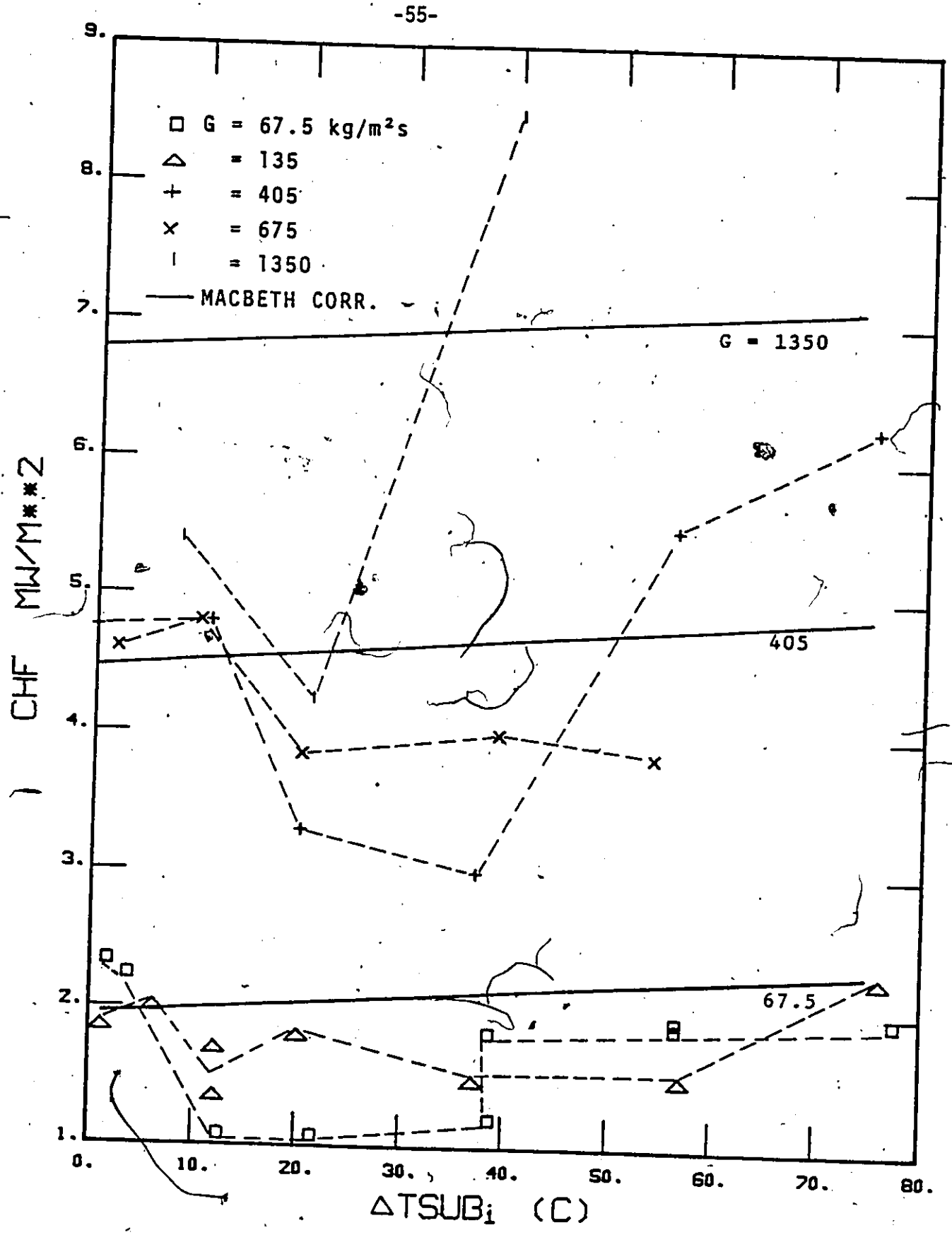

FIGURE 17 THE EFFECT OF (INLET) SUBCOOLING ON CHF FROM FUNG (1976)

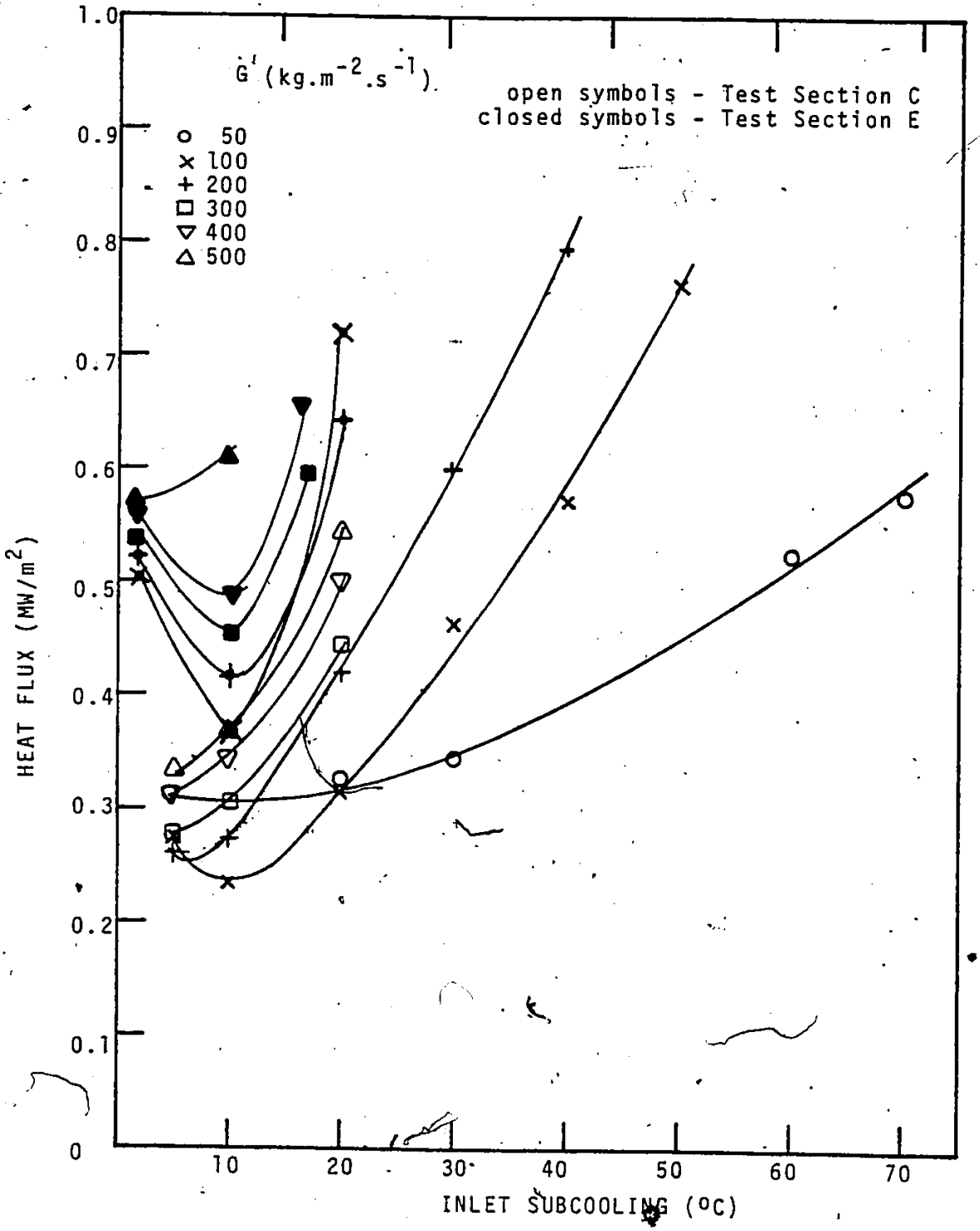

FIGURE 18 HEAT FLUX AT THE HOT PATCH FOR TEST SECTIONS C&E

For the same inlet conditions, test section E has a higher average heat flux. This is because of the larger fraction of its length over which CHF occurs. The increase in the heat flux near the region of saturated inlet condition for test section E can be regarded as the behaviour of CHF around this region. This phenomenon has been observed by Fung (1976) in a transition boiling study and is attributed to the higher turbulence due to vapour generation.

In Fig. 18 the heat fluxes at G = 50 $kg.m^{-2}.s^{-1}$ do not follow the same trend as those at higher mass fluxes. It is conceivable that at such low mass flux, the void fraction increases rapidly over a short distance into the hot patch. In other words, inverted annular flow does not exist over any appreciable length at such low flow in the present setup.

VI.2 Effect of Hot Patch Temperature

Fig. 19 shows two sets of results at virtually identical conditions, except for different hot patch temperatures. No significant effect on the film boiling curve was observed. It was also observed that a change in hot patch temperature of the order of 100°C did not significantly change the power required to keep the block temperature constant. This is in agreement with the results of Cheng et al (1978) and Fung (1976), who observed a constant film boiling heat flux in the region just beyond the minimum film boiling temperature. In both studies, the test sections used were very similar to the hot patch of the present test section. The above observations were valid for all conditions, except at the lowest flow of 50 $kg.m^{-2}.s^{-1}$ where the post-CHF flow regime and the vapour superheat might have changed significantly inside the hot patch.

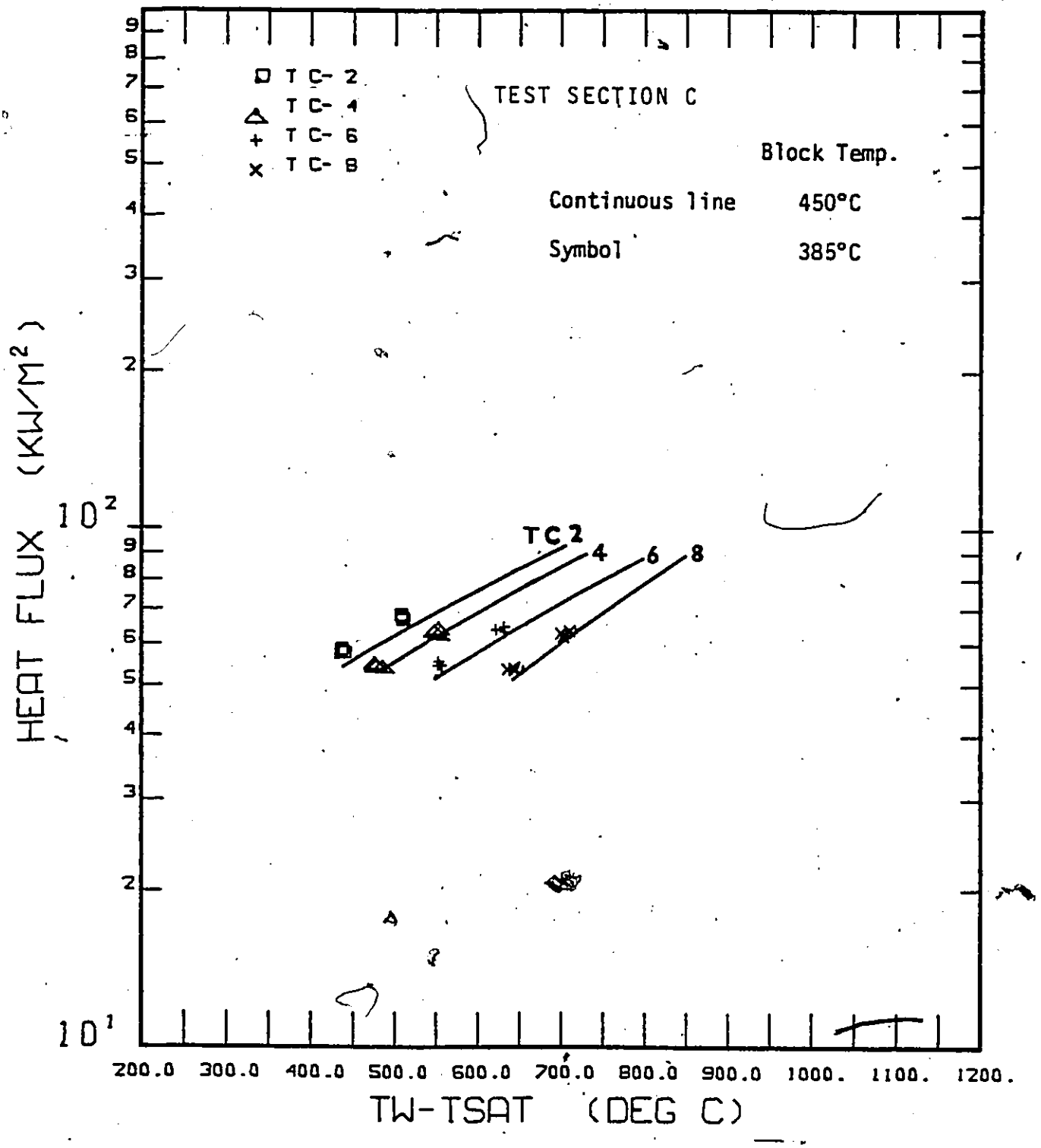

FIGURE 19 COMPARISON OF DATA AT TWO DIFFERENT BLOCK TEMPERATURES. NOMINAL BLOCK POWER = 500W, MASS FLUX = 100 $kg.m^{-2}.s^{-1}$ INLET SUBCOOLING = 10°C

VI.3 Reproducibility of Results

A total of four test sections were used in the experiments. Each differed in some aspects from the others. The exact dimensions of each test section are shown in Table 3.

In addition to the difference in dimensions, there was structural difference in the region of soldering between the hot patch and the tube. Such difference was not intended purposely, but was the result of imperfections in the soldering process. In particular, if the gap between the central core of the hot patch and the outside surface of the tube was not completely filled with solder, then some spots would be rewetted more easily. In such case, a higher average heat flux would be required. A comparison of the average heat flux in the hot patch in test sections A and C is shown in Fig. 20. The difference in power in the hot patch affects the heat transfer coefficient in the film boiling section, because the local enthalpy of the fluid will then be different.

A more suitable basis to compare the data from different test section is the wall temperature versus thermodynamic equilibrium quality. This is not totally satisfactory, because nonequilibrium exists due to vapour superheat. Nevertheless, it is informative to examine such plots.

In each of Figs. 21-24, data from test sections A and C are compared. The nominal inlet subcooling, flow and average heat flux are kept close between the two test sections. For sensitivity comparison, two runs using the same test section are shown for two power levels on each of the graphs.

Fig. 21 shows data at the lowest mass flux and inlet temperature. The wall temperature is most sensitive to changes in inlet temperature under

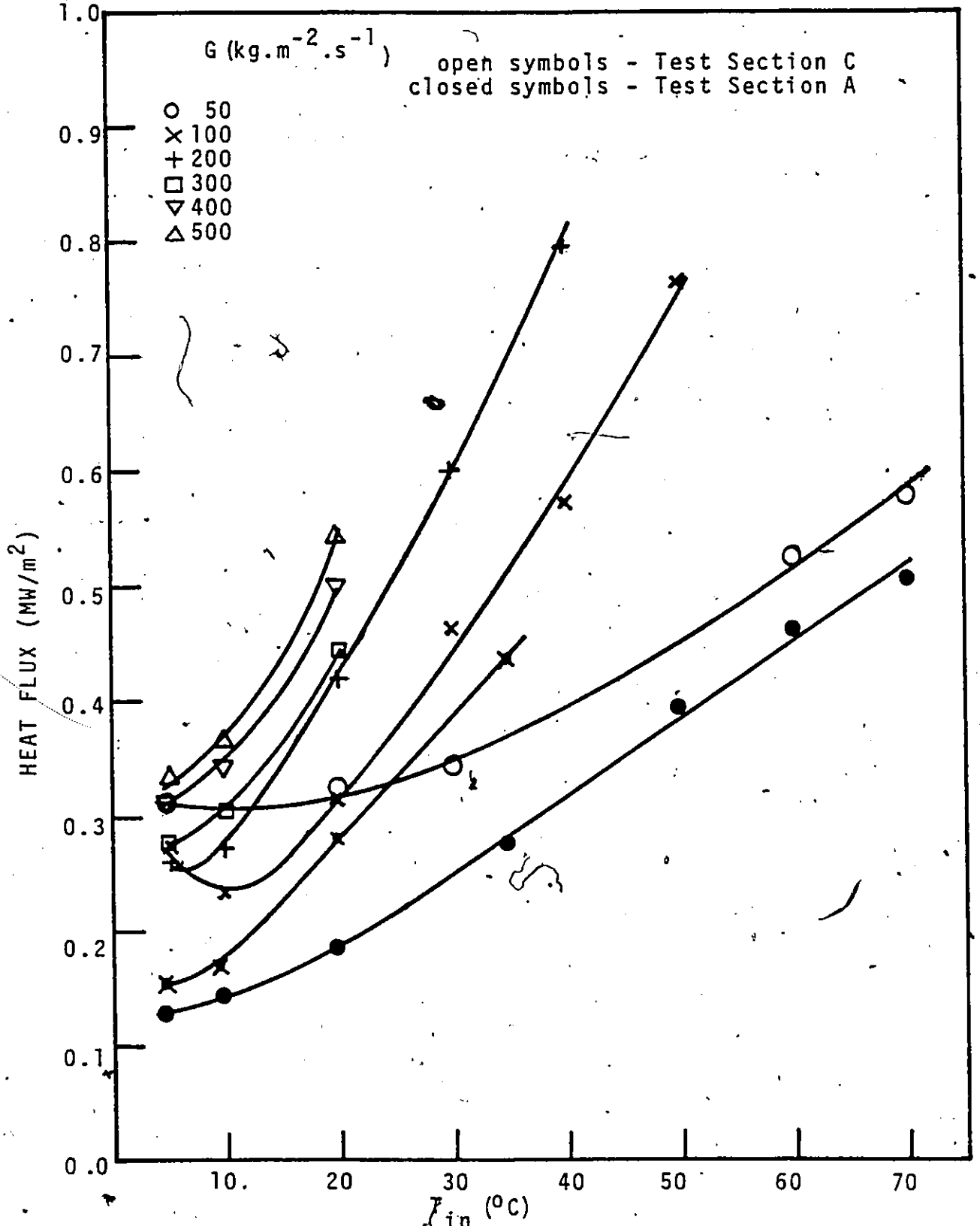

FIGURE 20 HEAT FLUX AT THE HOT PATCH FOR TEST SECTIONS A&C

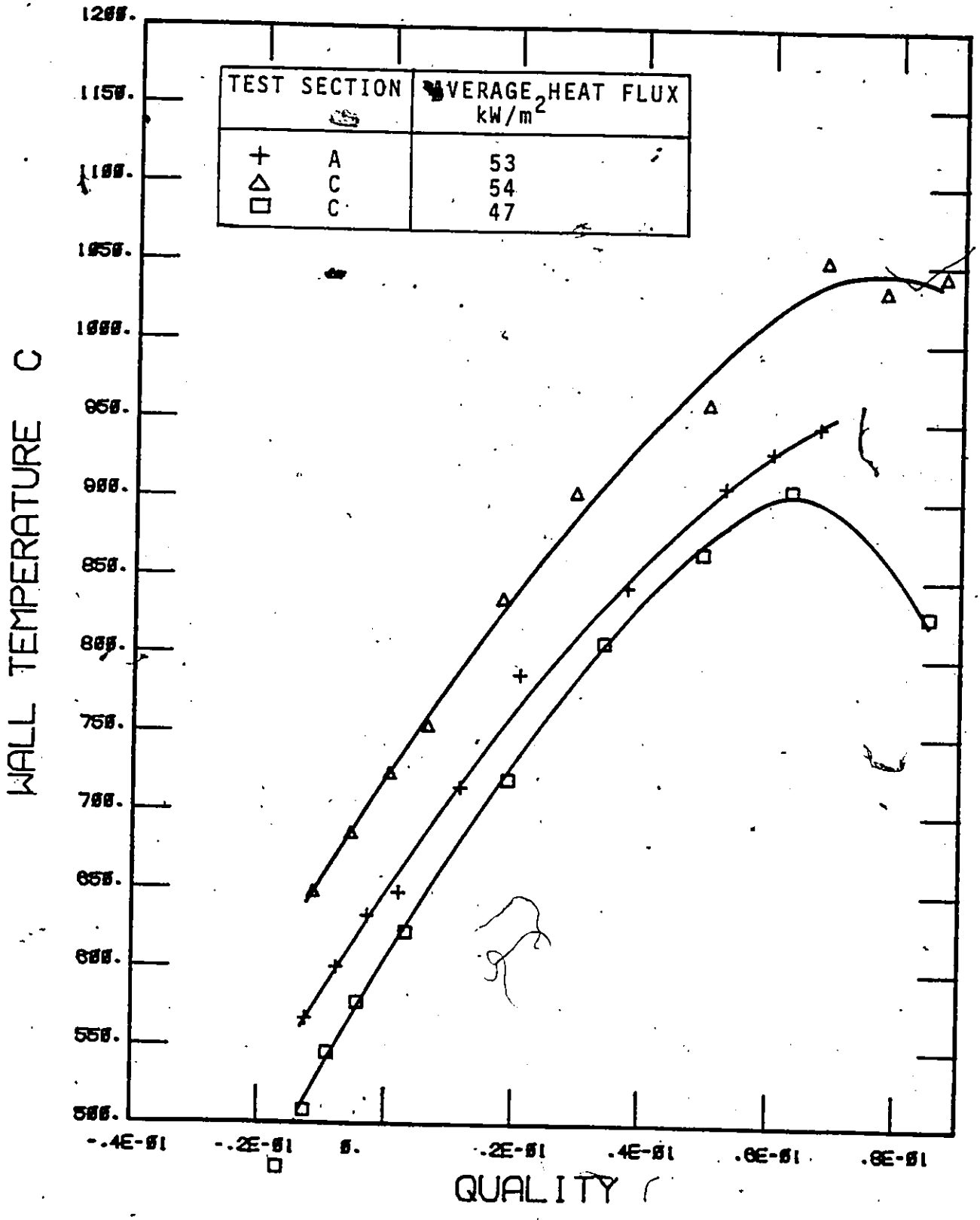

FIGURE 21 TEMPERATURE DISTRIBUTION DURING FILM BOILING
MASS FLUX = 50 $kg.m^{-2}.s^{-1}$, INLET SUBCOOLING = $70^{0}C$

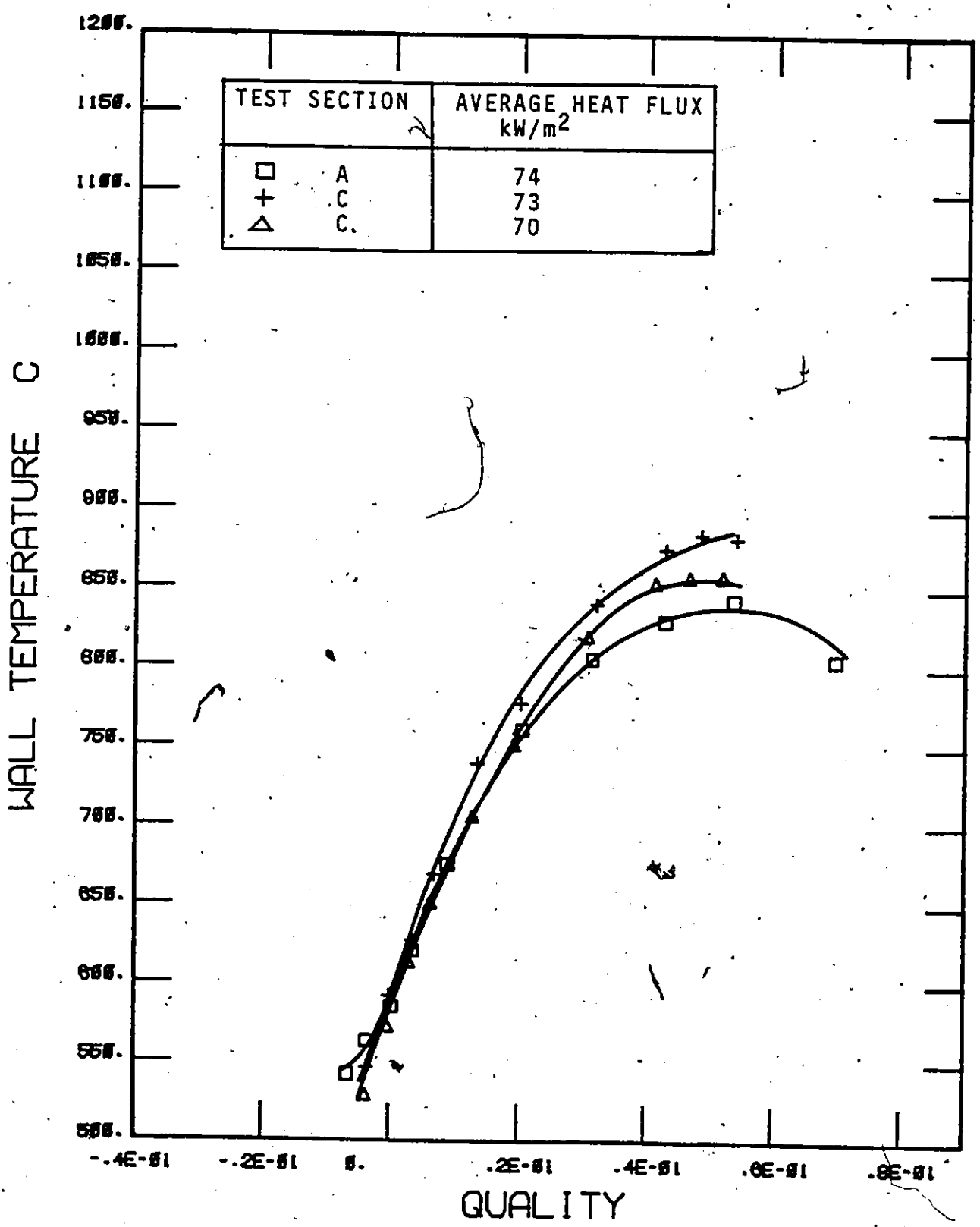

FIGURE 22 TEMPERATURE DISTRIBUTION DURING FILM BOILING
MASS FLUX = 700 $kg.m^{-2}.s^{-1}$,
INLET SUBCOOLING = 70 °C

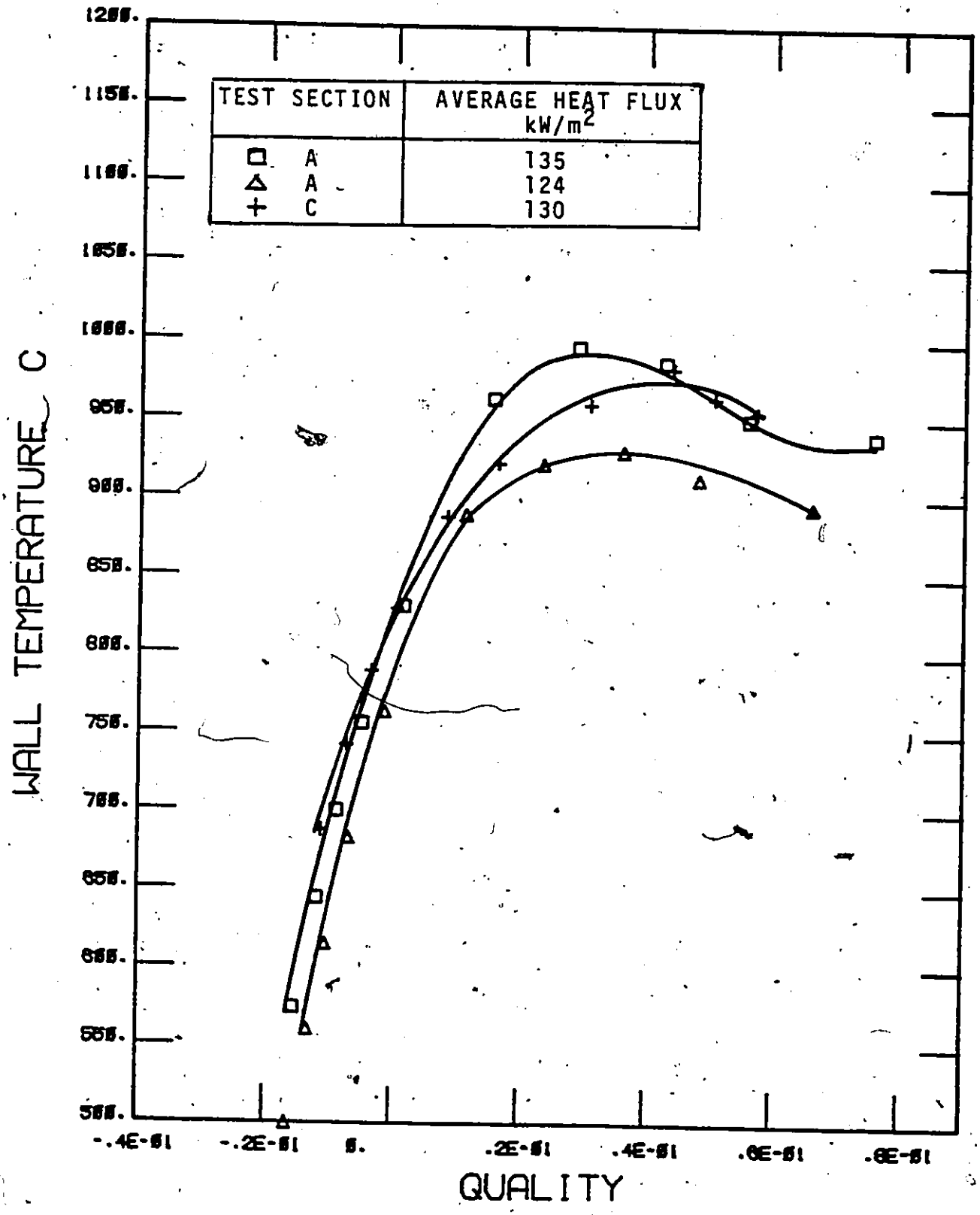

FIGURE 23 TEMPERATURE DISTRIBUTION DURING THE BOILING
MASS FLUX = 150 $kg.m^{-2}.s^{-1}$,
INLET SUBCOOLING = 20°C

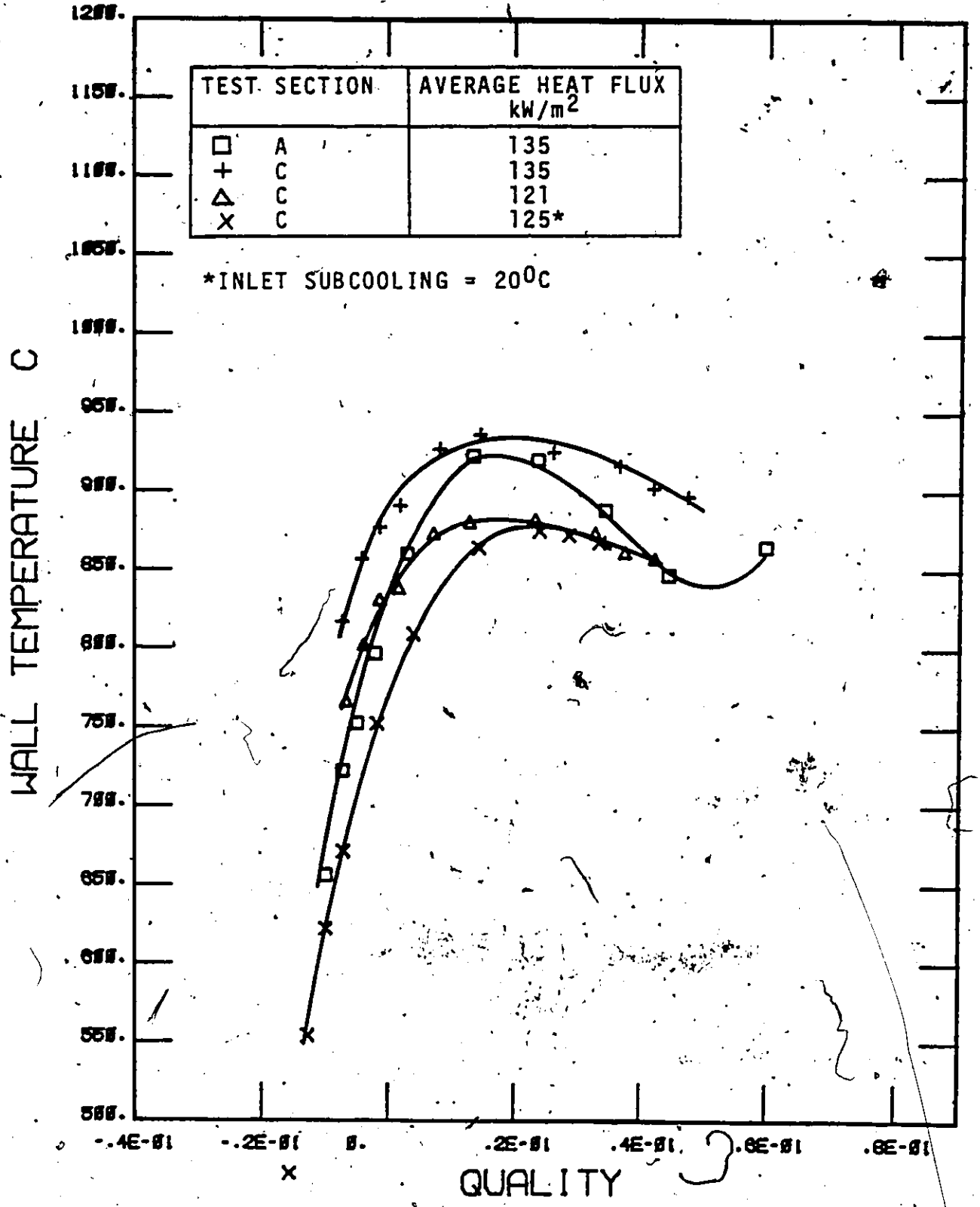

FIGURE 24 TEMPERATURE DISTRIBUTION DURING FILM BOILING
MASS FLUX = 200 $kg.m^{-2}.s^{-1}$
INLET SUBCOOLING = 10°C

these conditions. Fig. 22 shows very close resemblance of the data from the two test sections. It is noted that these runs have the closest matching conditions, including the power at the hot patch. Fig. 23 and 24 present some further comparison.

In drawing any conclusion from these comparisons, it should be reiterated that the basis of comparison (i.e. Tw vs. Xe) is not totally satisfactory. This will be reconsidered after the development of the theoretical model. The slight difference in the construction of the test sections makes it difficult to compare statistically the systematic error in the measured temperature in different test sections. However, qualitative comparisons show that the results are quite reproducible.

VI.4 Temperature Profile Along Film Boiling Section

Fig. 25 and 26 show the temperature profile at a fixed mass flux and a fixed inlet subcooling respectively. It can be seen that at low subcoolings (close to saturation), the axial temperature gradient is rather moderate. A steeper increase is observed for inlet subcooling greater than 20°C. At low inlet subcoolings, the vapour generation rate is high. The corresponding increase in vapour velocity will tend to lower the temperature increase. The heat transfer mechanism can be regarded as convection dominating. At high inlet subcooling, most of the heat input goes to heating up the liquid core. The vapour film gradually thickens and increases in velocity. Most of the resistance to heat transfer lies in the vapour film. The wall temperature is therefore more sensitive to an increase in film thickness.

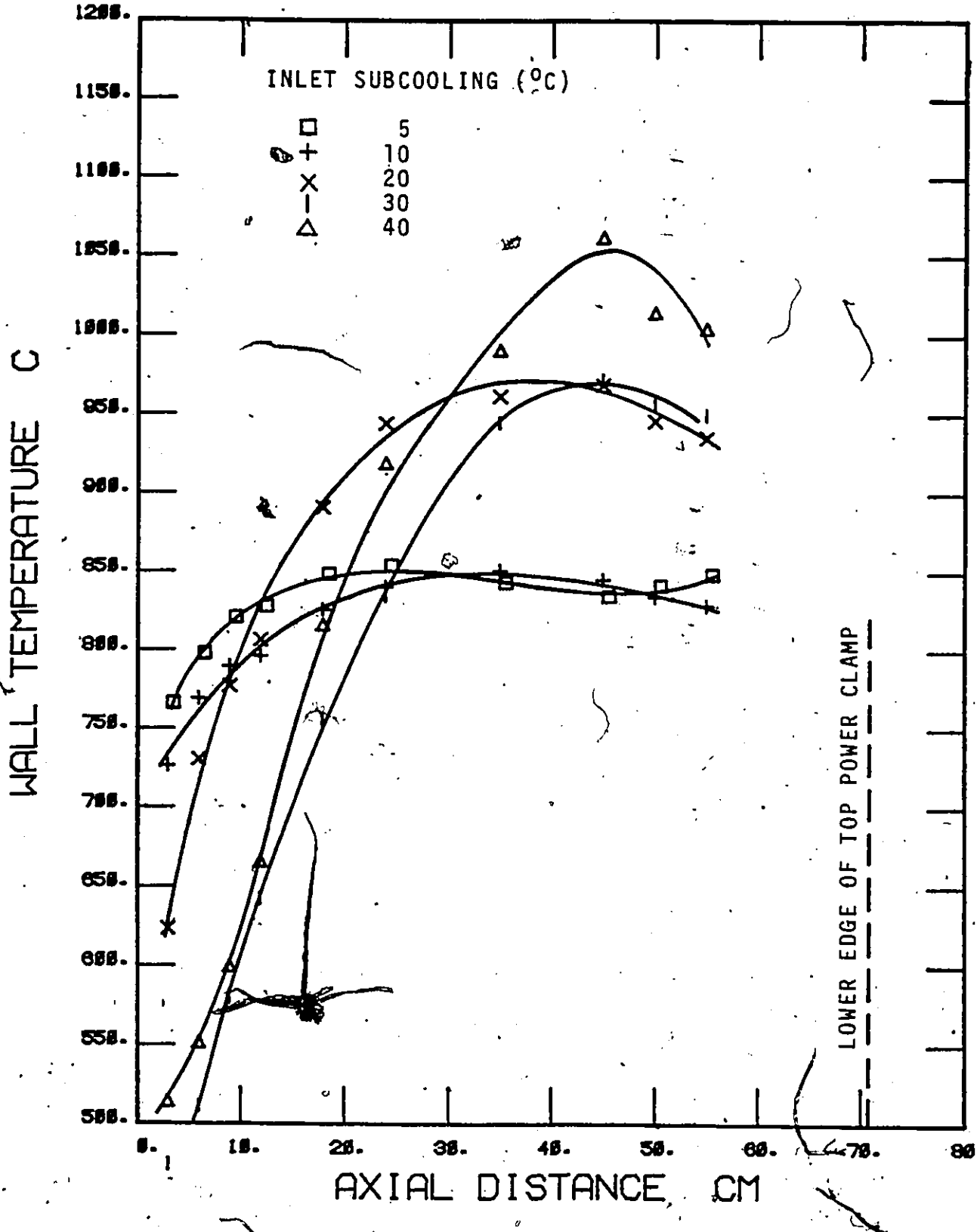

FIGURE 25 TEMPERATURE DISTRIBUTION DURING FILM BOILING
NOMINAL MASS FLUX = 200 $kg.m^{-2}.s^{-1}$

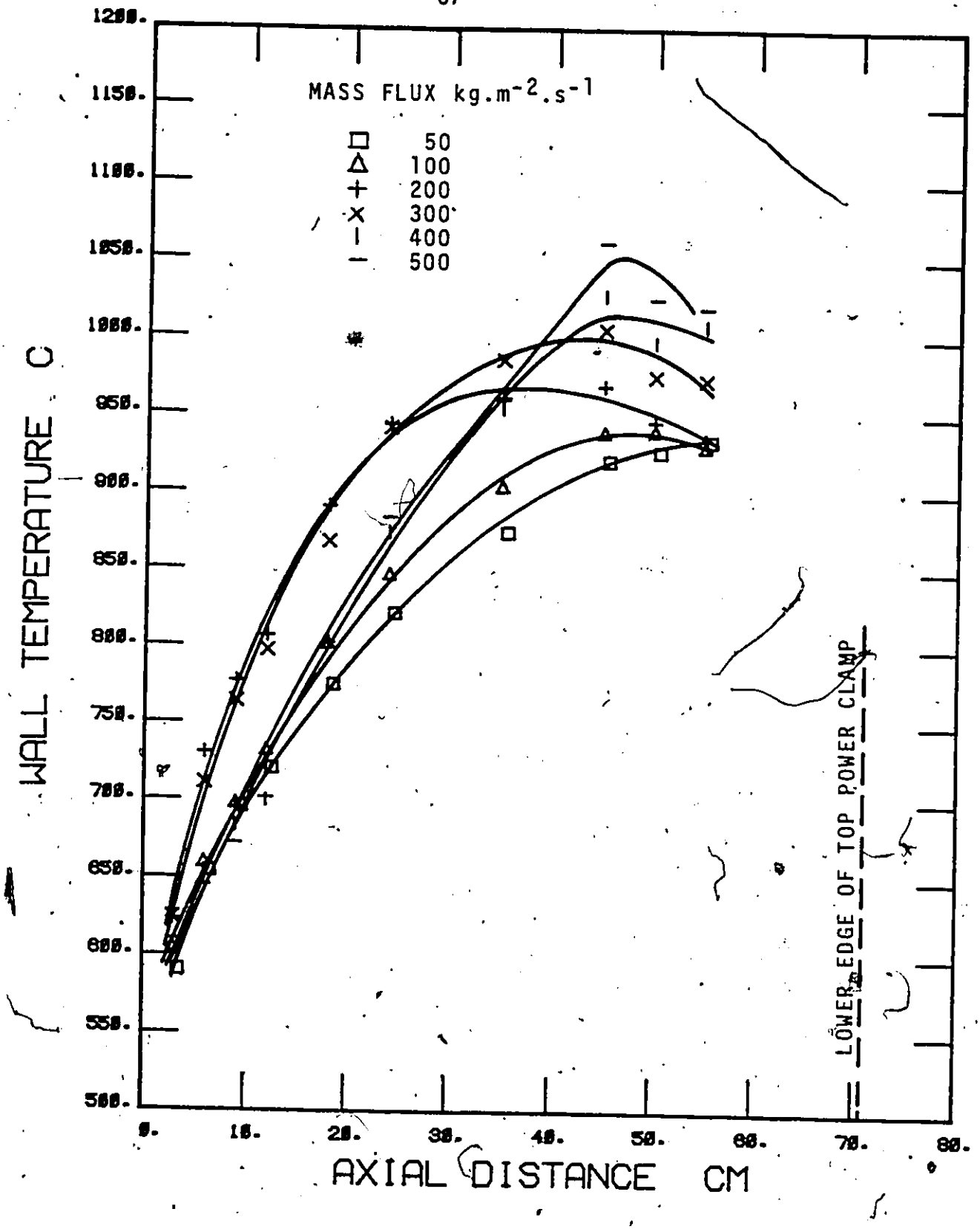

FIGURE 26 TEMPERATURE DISTRIBUTION DURING FILM BOILING
NOMINAL INLET SUBCOOLING = 20°C

It can also be observed from these figures that the wall temperature reaches a maximum at locations quite far away from the power clamp. The subsequent drop in temperature is therefore not likely to be due to end effects. Most likely, it is due to the increase in vapour velocity and liquid-vapour interfacial velocity, which together will improve the heat transfer.

VI.5 Effect of Axial Location

Fig. 27 shows that the axial location has a strong effect on the film boiling temperature. This effect may be more readily seen when the heat transfer coefficient is plotted as a function of axial location. Fig. 28 indicates that the heat transfer coefficient decreases initially, but levels off towards the end and, under certain conditions, it may increase. The observed axial location effect can be attributed to the following:

(a) Entrance effect

Analogous to a single-phase thermal-entry-length problem, the heat transfer coefficient near the entrance is much higher than at a "fully-developed" downstream region. In addition, in the present situation, the creation of a vapour blanket at the hot patch considerably disturbs the flow. The resulting higher heat transfer coefficient at the beginning of the dry patch decays with distance downstream. Fully developed conditions cannot be attained for our two-phase conditions because of the continuous vapour production; however, in analogy with single phase heat transfer in an entrance region, most of the change in heat transfer coefficient due to developing boundary layer would have taken place within 25 diameters from the hot patch.

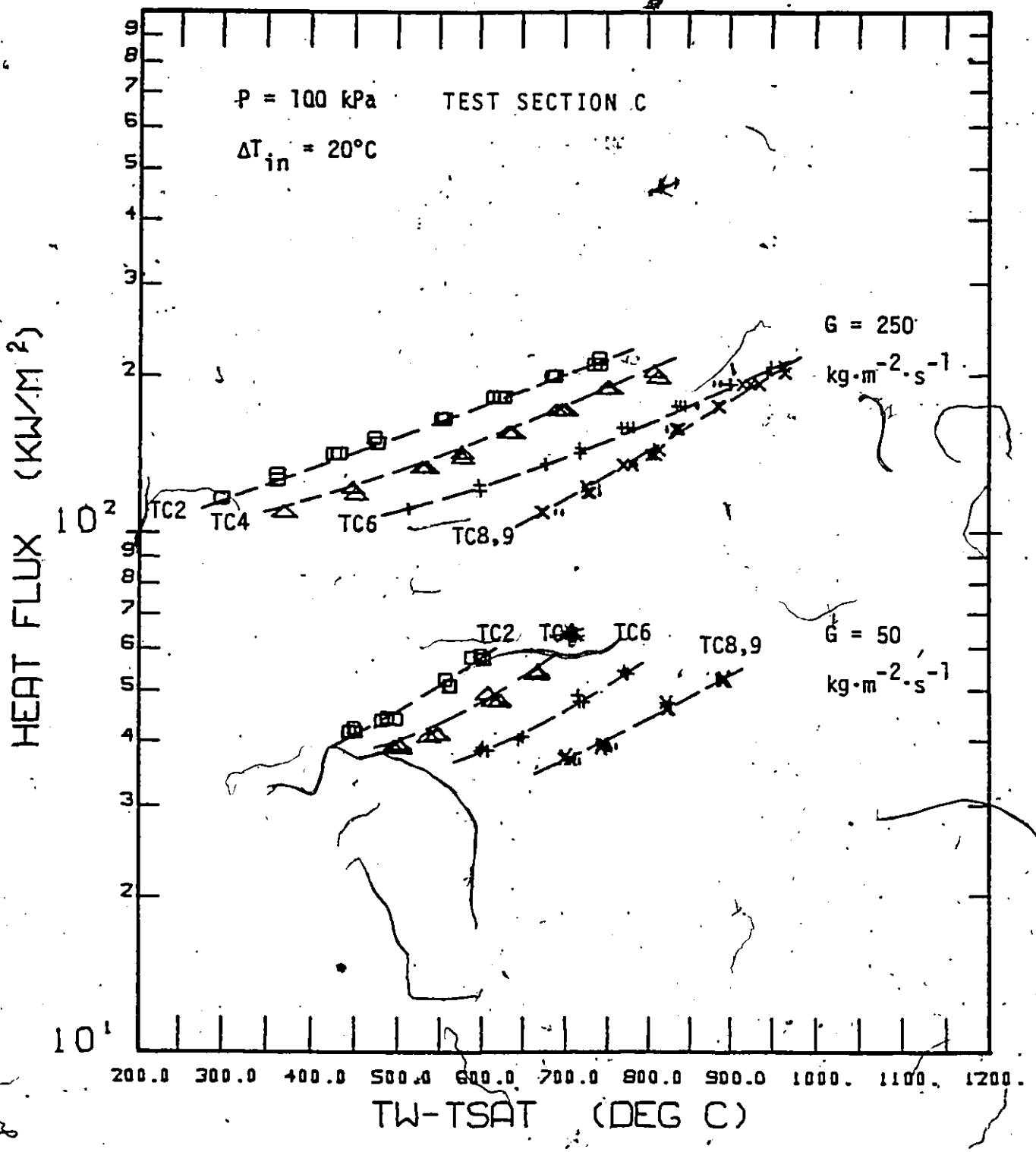

FIGURE 27 TYPICAL RESULTS AT TWO MASS FLUXES

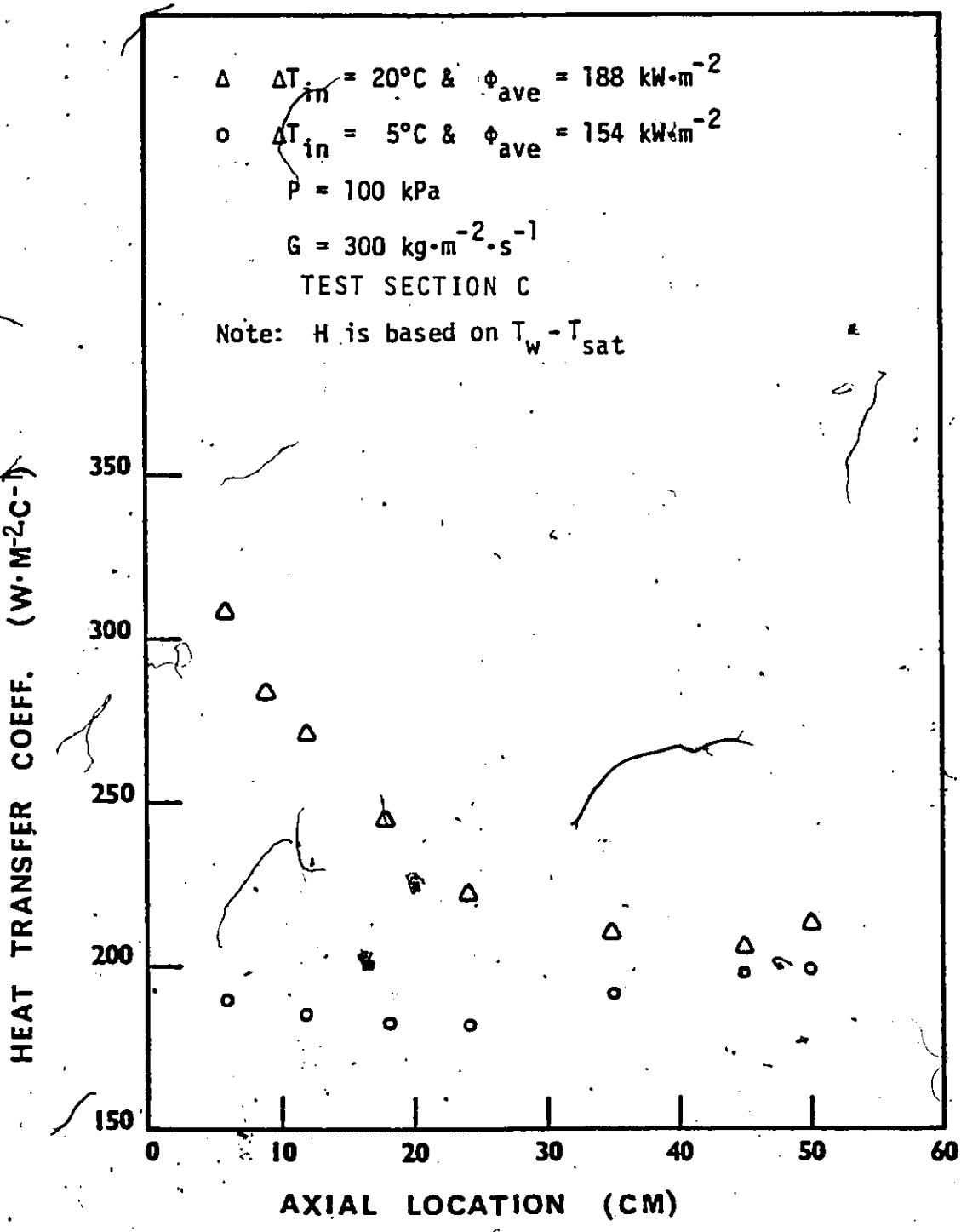

FIGURE 28. VARIATION OF HEAT TRANSFER COEFFICIENT ALONG HEATED LENGTH

(b) Change in Vapour Film Thickness

At axial locations near the beginning of the vapour blanket the vapour film thickness is least due to the higher local subcooling and shorter film boiling length. Here heat transfer across the vapour film is mainly by conduction. At downstream locations the vapour film thickness increases because of increased vapour flow rate. Initially this results in an increased thermal resistance, thus lowering the heat transfer coefficient. At locations further downstream the vapour velocity also increases, especially when the bulk of the coolant reaches saturation. This increases the convective component and the overall heat transfer coefficient will then increase.

(c) Increase in Vapour Superheat

Near the end of the heated length, high void fractions are encountered during the low flow or low subcooling tests. As has been observed in other post-dryout studies, a significant degree of vapour superheat can be expected for these conditions. For such cases, the wall superheat, (T_w-T_{sat}), is no longer a representative temperature difference. The heat transfer coefficient based on this difference, instead of (T_w-T_v), will result in an artifically lower value.

VI.6 Effect of Inlet Subcooling

Fig. 29 compares data at different inlet subcoolings. It can be seen that the effect of inlet subcooling is positive for short film boiling lengths: the film boiling heat flux at TC 2 (L/D=5) increases with an increase in inlet subcooling. However, at TC 8 (L/D=38), the effect is much reduced and the trend is reversed.

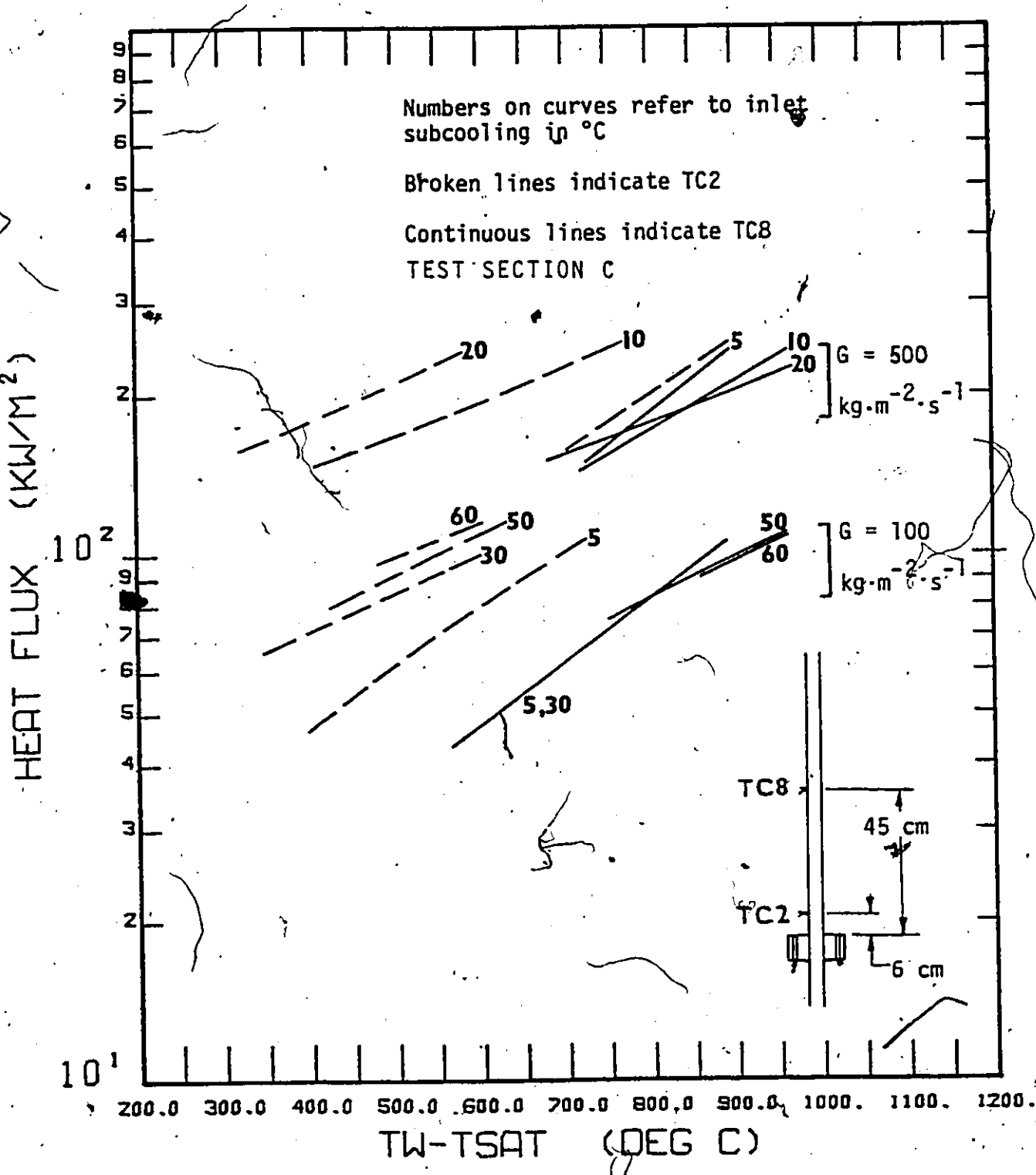

FIGURE 29 EFFECT OF INLET SUBCOOLING

The effect of inlet subcooling can be understood by considering the local subcooling or quality effect. Near the hot patch the void fraction is low and the flow regime is inverted annular. Heat transfer is primarily by conduction through the vapour film. The vapour film thickness depends strongly on the bulk coolant temperature and hence the inlet subcooling, with the thinnest films occurring at the highest subcoolings (Groeneveld and Gardiner (1977)).

It has already been shown that at locations well downstream from the hot patch convective heat transfer becomes more important. This is especially true for lower inlet subcoolings, due to the corresponding higher local void fractions. Consequently, as can be deduced from Fig. 29, the film boiling heat flux is higher for lower inlet subcoolings at TC 8.

VI.7 Effect of Mass Flux

The effect of mass flux at a fixed axial location and inlet subcooling is shown in Fig. 30. The film boiling heat flux increases with mass flux for all axial locations.

In inverted annular flow the vapour layer thins appreciably at high mass velocities, thus decreasing the resistance to heat transfer across the film. This thinning of the film may be sufficient to allow liquid contact with surface asperities and may explain the observed higher rewetting temperatures at higher mass velocities.

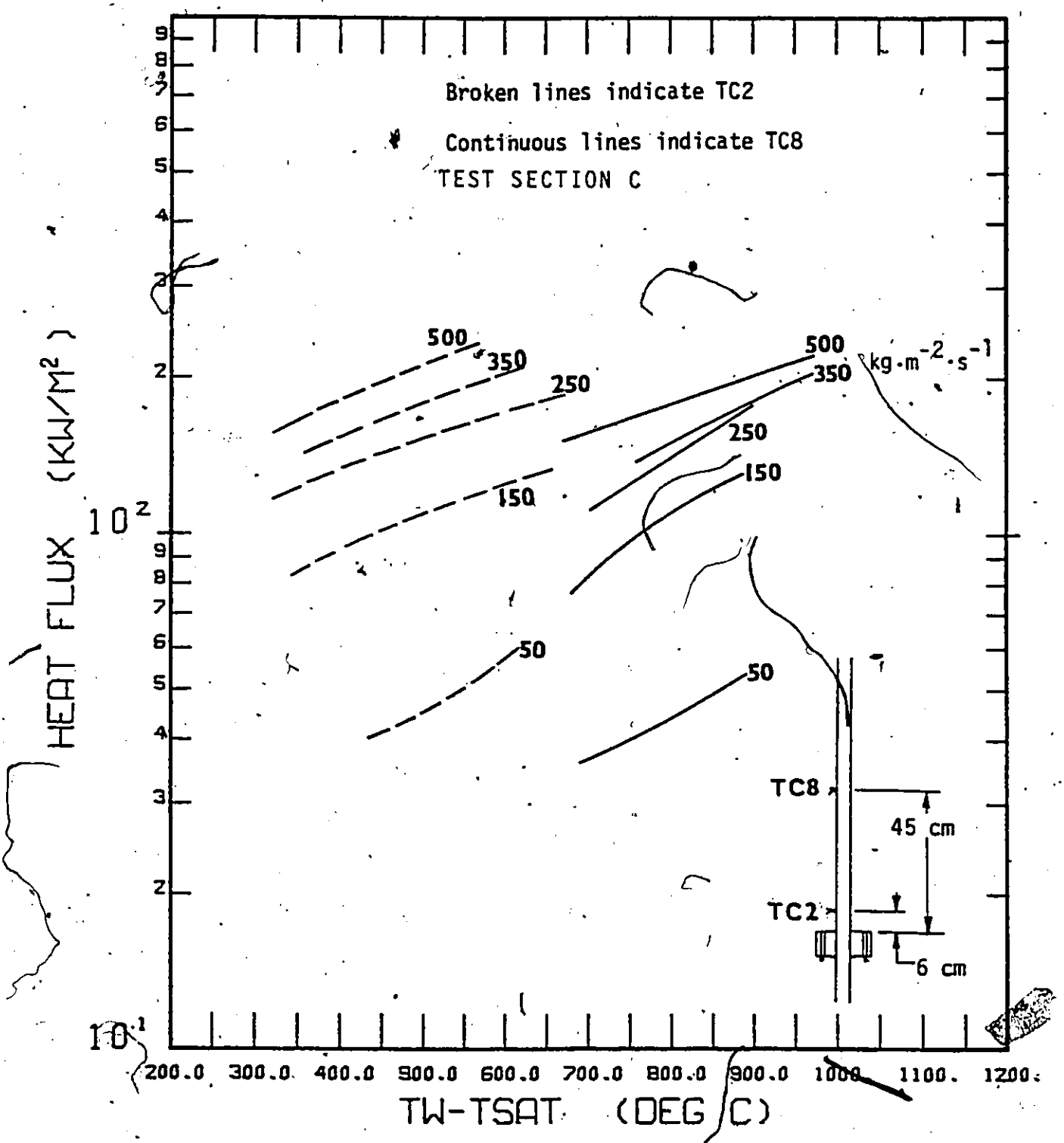

FIGURE 30 EFFECT OF MASS FLUX AT INLET SUBCOOLING OF 20°C

VI.8 Effects of Quality on the Convection Heat Transfer Component

The total heat flux can be considered to consist of a radiation and a convection component. To examine the convection component, the radiation component is first subtracted from the total heat flux. The radiation component is calculated according to Appendix H together with the void fraction correlation of Appendix G. The convection component is then expressed in terms of a Nusselt number. Thus,

$$Nu_{CON} = \frac{(\phi_{TOT} - \phi_{Rad})\ De}{(T_w - T_s)\ k_v}$$

The Nusselt number thus calculated is plotted against the local equilibrium quality in Figs. 31-37. It can be seen that for mass fluxes above 100 $kg.m^{-2}.s^{-1}$, Nu_{CON} decreases initially with increasing Xe. It passes through a minimum before increasing again. To the left of the minimum, the flow regime is primarily inverted annular and a significant fraction of the heat transferred from the wall is needed to heat up the subcooled liquid core. To the right of the minimum, the flow regime is dispersed liquid droplet flow and the wall heat flux is primarily used for evaporation. The increase in Nusselt number with increase in equilibrium quality in this region can be attributed to the increase in vapour velocity.

It can be seen from Fig. 31 that at the lowest flow (50 $kg.m^{-2}.s^{-1}$), there is no prominent component for heating up the liquid core. This is because at such low flow, the liquid core is broken up into slugs and droplets. It is also evident that the Nusselt number decreases with axial location. This again suggests a high vapour superheat at this low flow.

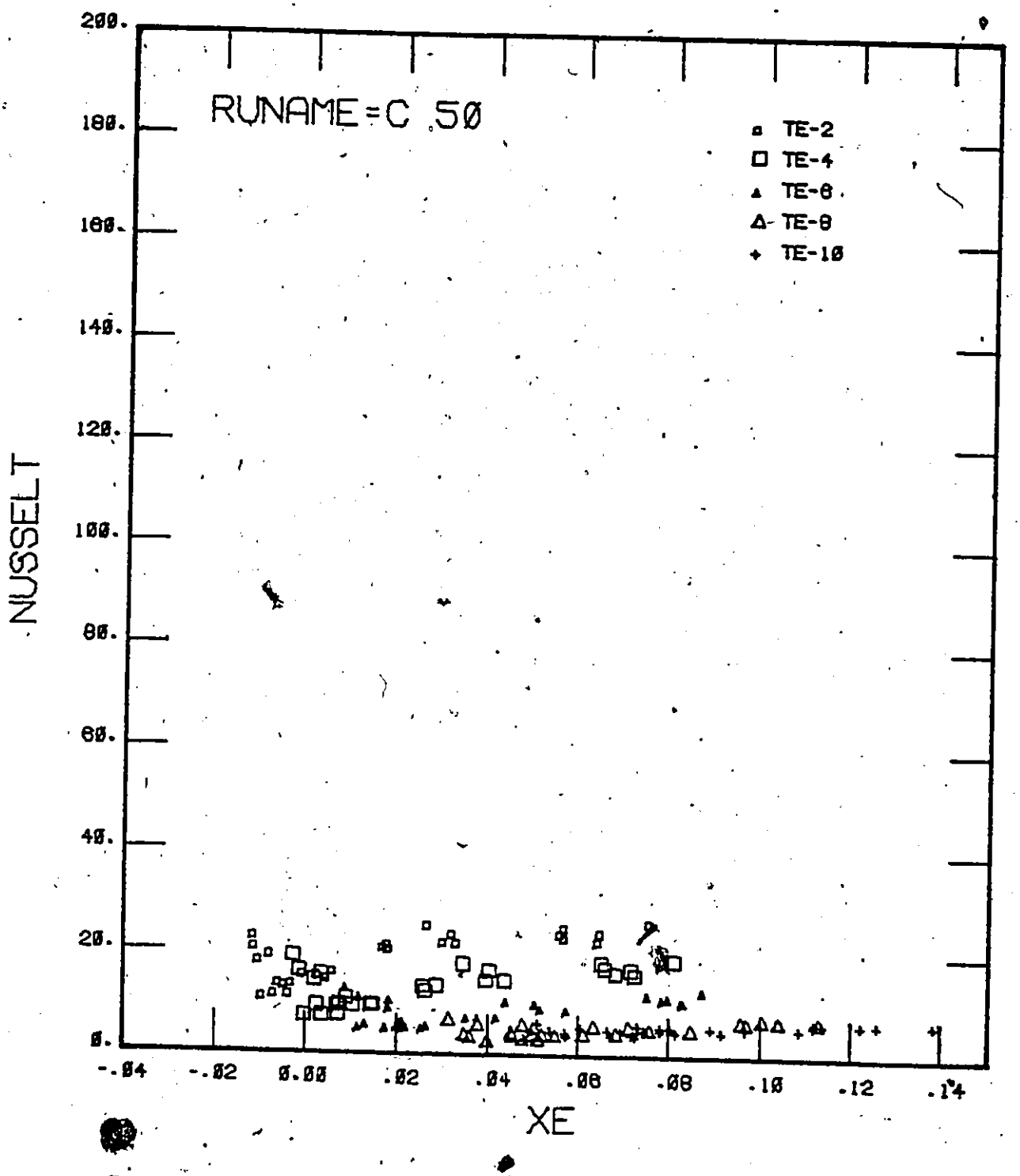

FIGURE 31 NUSSELT NUMBER AS A FUNCTION OF EQUILIBRIUM QUALITY FOR G = 50 $kg.m^{-2}.s^{-1}$

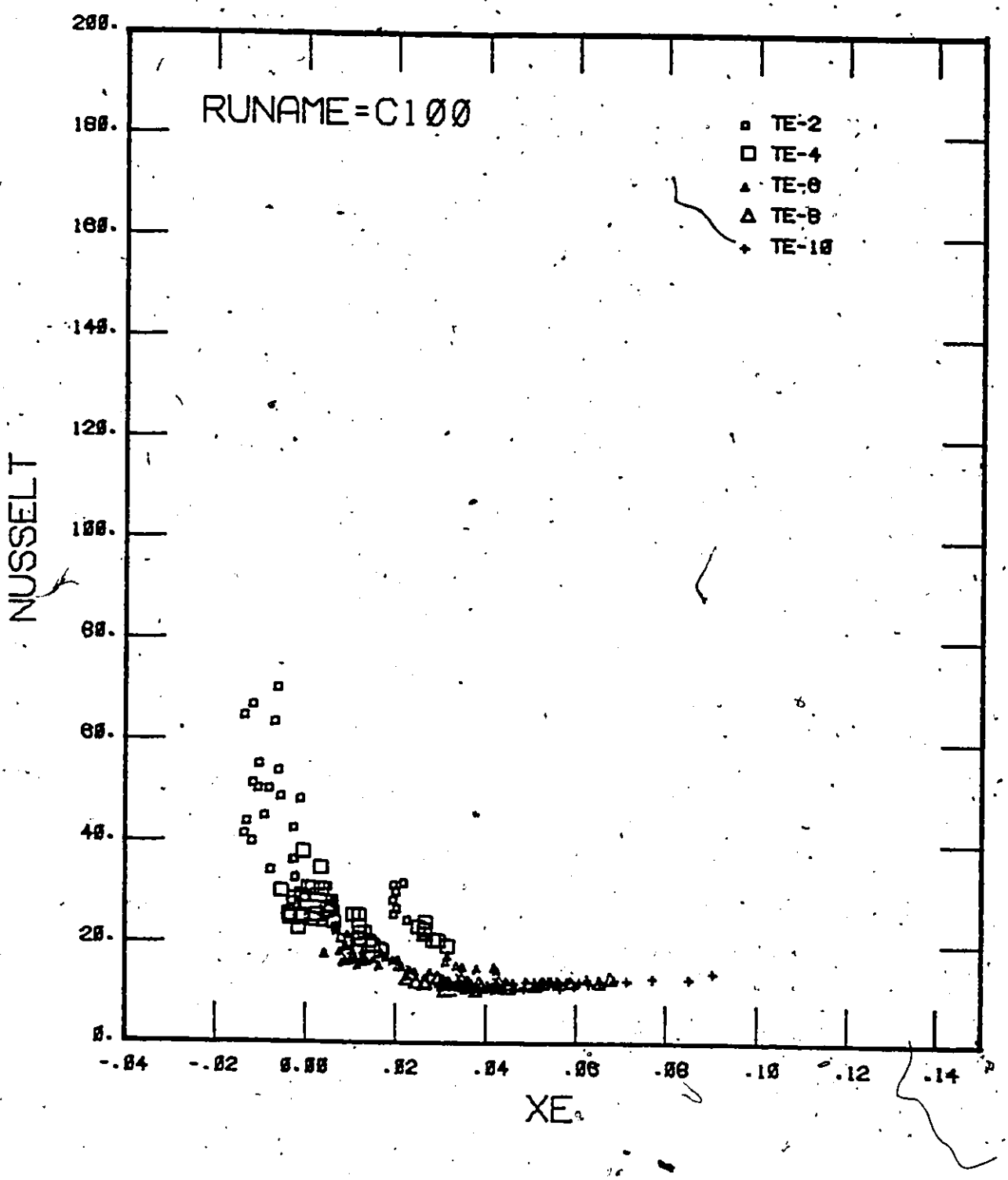

FIGURE 32 NUSSELT NUMBER AS A FUNCTION OF EQUILIBRIUM QUALITY FOR G = 100 $kg.m^{-2}.s^{-1}$

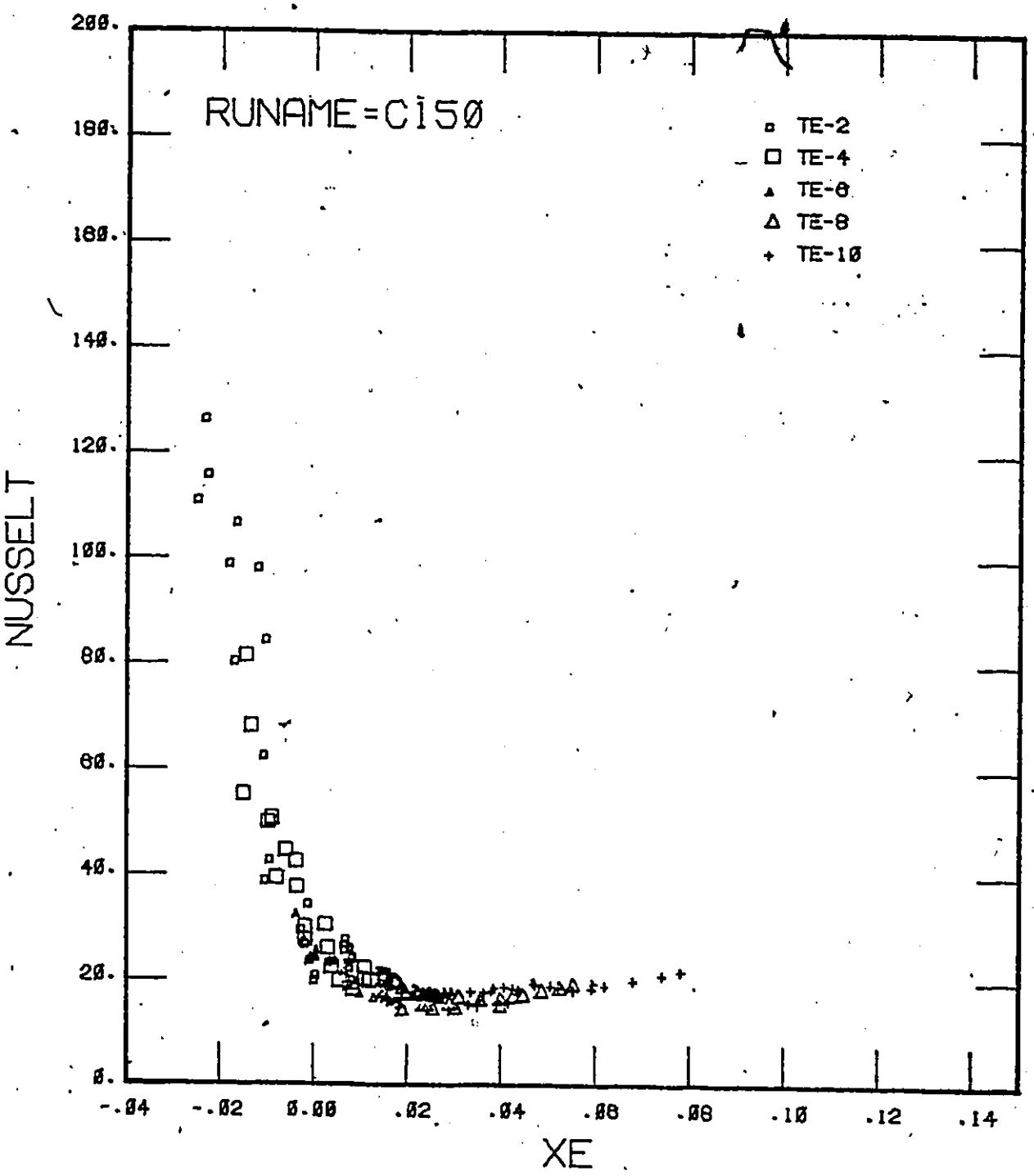

FIGURE 33 NUSSELT NUMBER AS A FUNCTION OF EQUILIBRIUM QUALITY FOR G = 150 kg.m-2.s-1

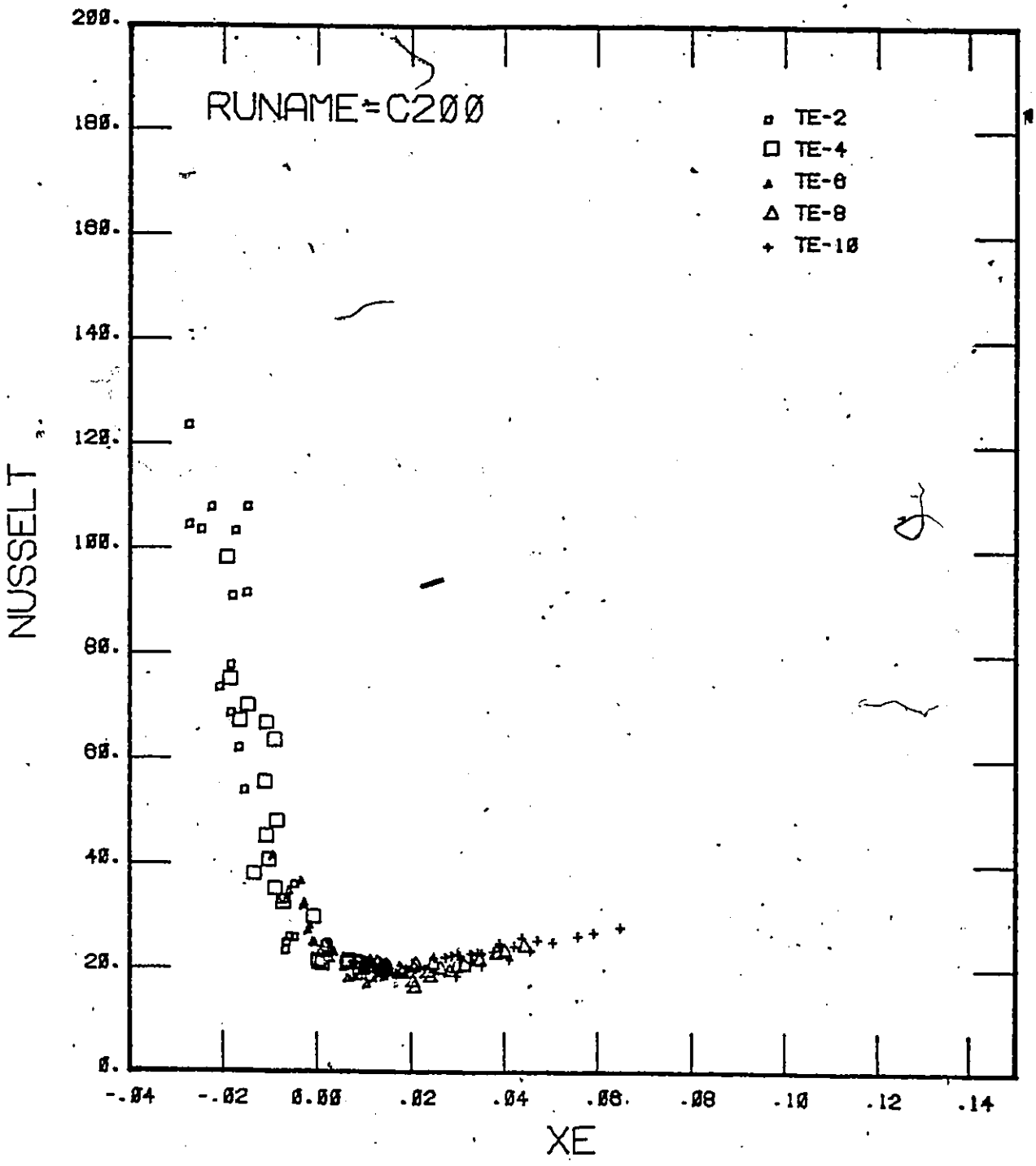

FIGURE 34 NUSSELT NUMBER AS A FUNCTION OF EQUILIBRIUM QUALITY FOR G = 200 $kg.m^{-2}.s^{-1}$

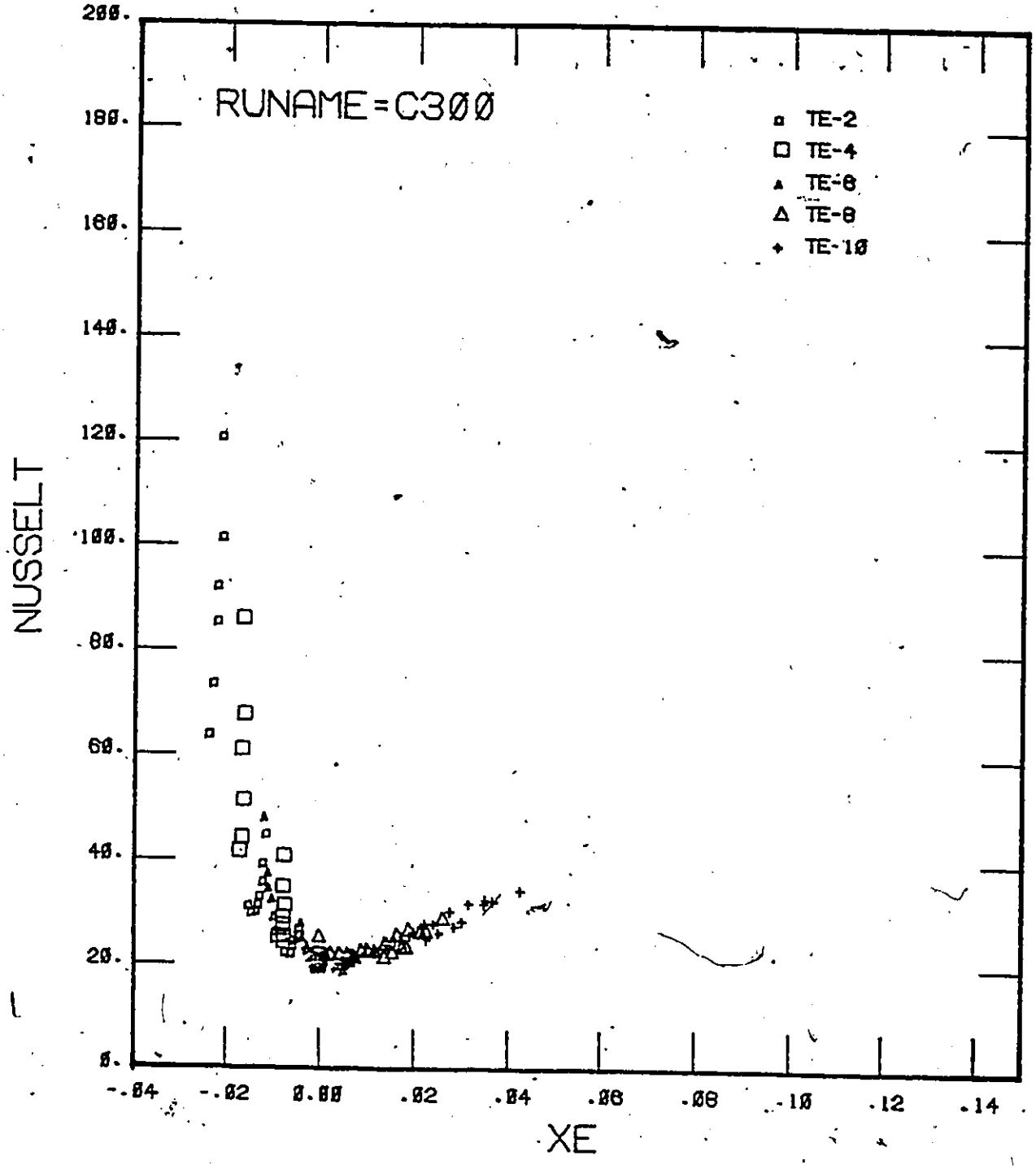

FIGURE 35 NUSSELT NUMBER AS A FUNCTION OF EQUILIBRIUM QUALITY FOR G = 300 $kg.m^{-2}.s^{-1}$

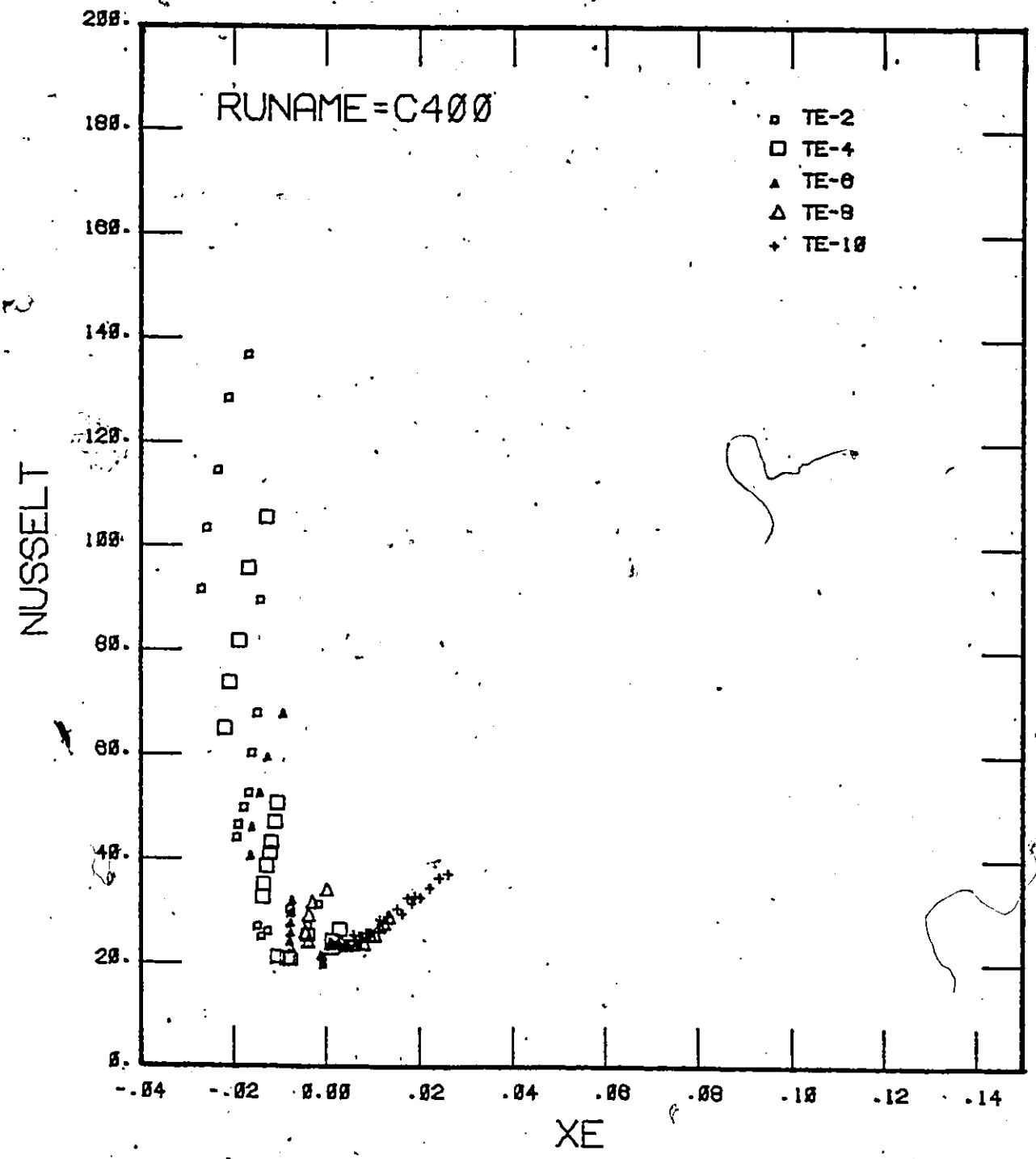

FIGURE 36 · NUSSELT NUMBER AS A FUNCTION OF EQUILIBRIUM QUALITY FOR G = 400 $kg.m^{-2}.s^{-1}$

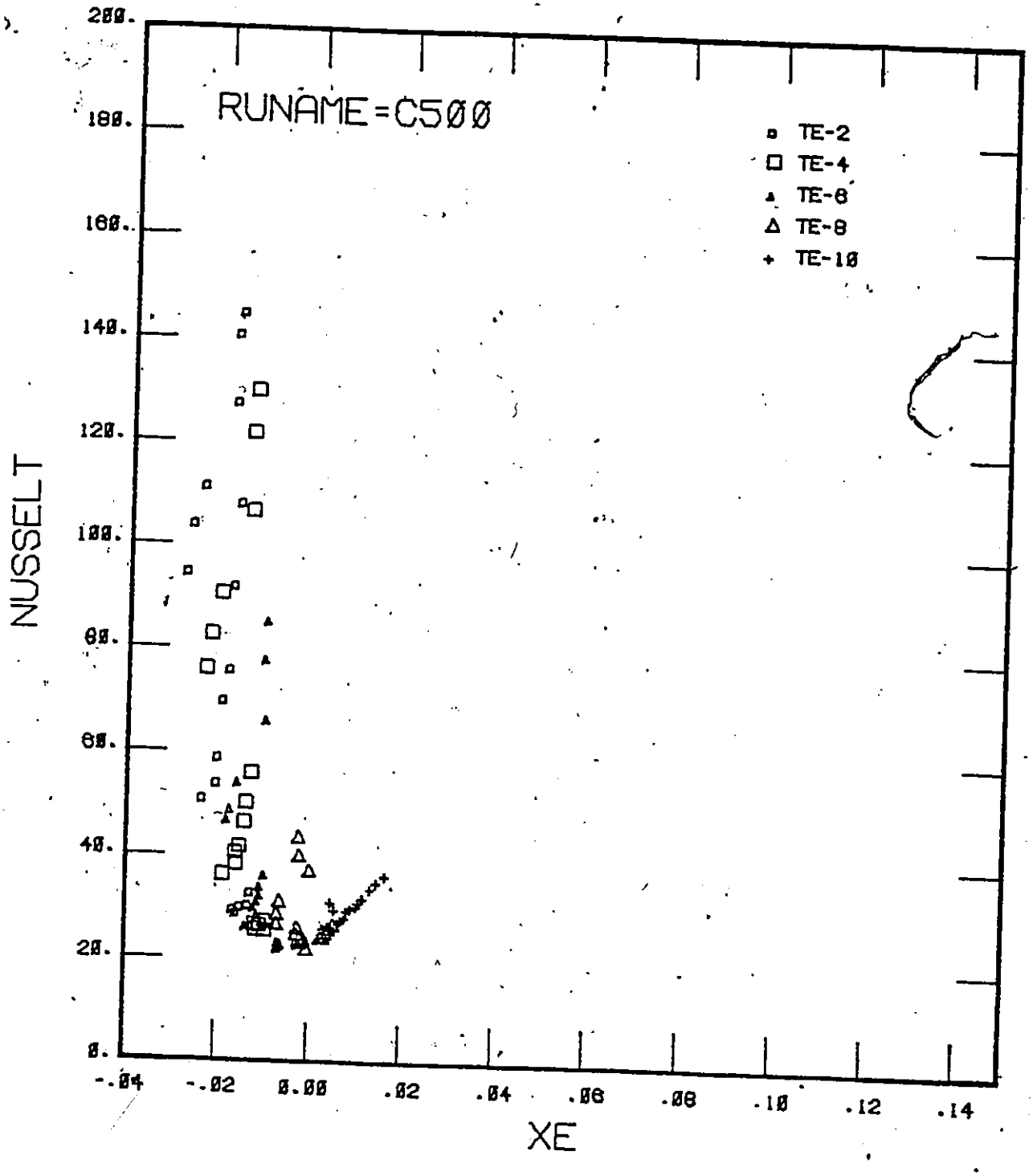

FIGURE 37 NUSSELT NUMBER AS A FUNCTION OF EQUILIBRIUM QUALITY FOR G = 500 $kg.m^{-2}.s^{-1}$

VI.9 Minimum Film Boiling Temperature

In some of the tests, as the power was reduced, the test section started to quench. In most cases quenching started either at the start of the film boiling section, or at the power clamp at the downstream end. This kind of rewetting is due to conduction along the heated surface, and is sometimes referred to as "conduction-controlled rewetting". The measured temperature at the moment of rewetting is not a genuine minimum film boiling temperature, since it is influenced by the conditions nearby.

An examination of the strip chart records of the thermocouple traces shows that in some cases the first thermocouple that indicated rewetting was TC3. Such rewetting occurs when the liquid penetrates through the vapour thermal boundary layer next to the wall. At heat fluxes above the minimum film boiling temperature, the vapour generated at the vapour-liquid interface will create a vapour thrust force. If the force is large enough, it will push the liquid away from the wall, thus preventing liquid-wall contact. If the liquid momentum in the direction towards the wall is greater than this thrust force, the liquid will contact the wall momentarily. Whether the surface will rewet after liquid-wall contact has been initiated will depend on the thermal capacities of the wall and the liquid in the region around the point of contact. Henry (1974) has considered the minimum film boiling temperature to be determined by this transient cooling mechanism. This kind of instantaneous rewetting has also been termed "impulse cooling rewet" (Tan & Griffith (1976)).

Table 5 shows the minimum film boiling temperature extracted from the strip chart records of the present experiments. Since rewetting occurred

during a reduction in test section power, no record of the exact power at rewetting was available. The equilibrium quality shown on this table was calculated at a steady state film boiling condition just prior to the change in power. Usually the change in power was a reduction of 5-10%. A better way of estimating the exact power is to extrapolate the heat flux versus the wall temperature at location 3 to the minimum film boiling temperature. In view of the somewhat qualitative nature of this discussion, we will not pursue it here.

Fig. 38 shows the minimum film boiling temperature plotted against the local equilibrium quality. It shows the asymptotic trend of the minimum film boiling temperature. At high qualities, the minimum film boiling temperature is close to the saturation temperature. This can also be seen from Fig. 4, where the high quality boiling curve changes gradually from CHF to film boiling. At negative qualities (corresponding to subcooling), the minimum film boiling temperature increases rapidly.

VI.10 Void Fraction Measurements

Details of the void fraction measurements are discussed in Appendix A. The 95% confidence interval for the measured void fraction ranges from ±3% to ±6%, depending on whether the void fraction is near the upper (100%) or lower ends (0%). This level of accuracy has been optimized with respect to the sampling time, the radioactive source strength and the information obtained. Furthermore, this interval only contains the random error due to radioactive decay. Other measurement errors have not been included.

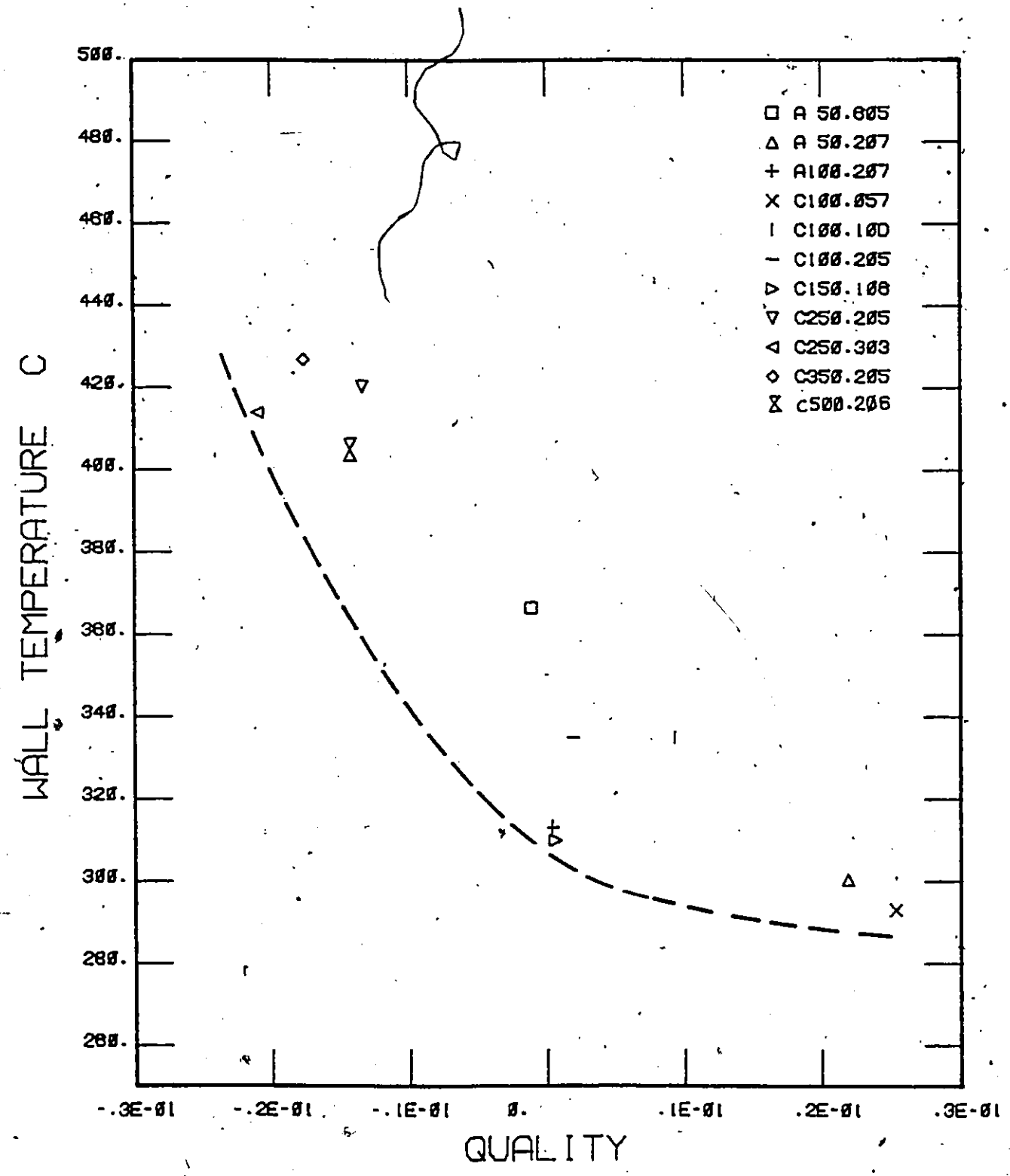

FIGURE 38 MINIMUM FILM BOILING TEMPERATURE

Figs. 39 and 40 show some of the data plotted as measured void fraction versus axial location. It can be seen that the void fraction at a fixed axial location increases with a decrease in inlet subcooling and an increase in heat flux. The increase in void fraction with increase in equilibrium quality is small in the high subcooling region (large negative quality). This implies that most of the heat input goes to heating up the liquid core.

The same data as shown on Figs. 39 and 40 are replotted against the equilibrium quality based on local pressure in Figs. 41 and 42. It can be seen that the data fall fairly closely on the same line. This suggests that the local phase and velocity distribution is primarily a function of equilibrium quality.

Fig. 43 shows all data from test section E plotted together. The mass flux effect is more evident in Fig. 44 in which only the best curve through the data of each mass flux is shown. It can be seen that an increase in mass velocity increases the void fraction at a given equilibrium quality.

Inside the hot patch the flow regime will be inverted annular when film boiling is first established. The distance over which this flow regime is maintained depends on the void fraction. Plummer (1974) suggested that at a void fraction of approximately 40% the inverted annular flow regime changes into dispersed flow. It can be seen from Fig. 43 that the void fraction is in the neighbourhood of 50% at zero equilibrium quality. This would suggest that most of the data in the net equilibrium quality region are in the dispersed flow regime.

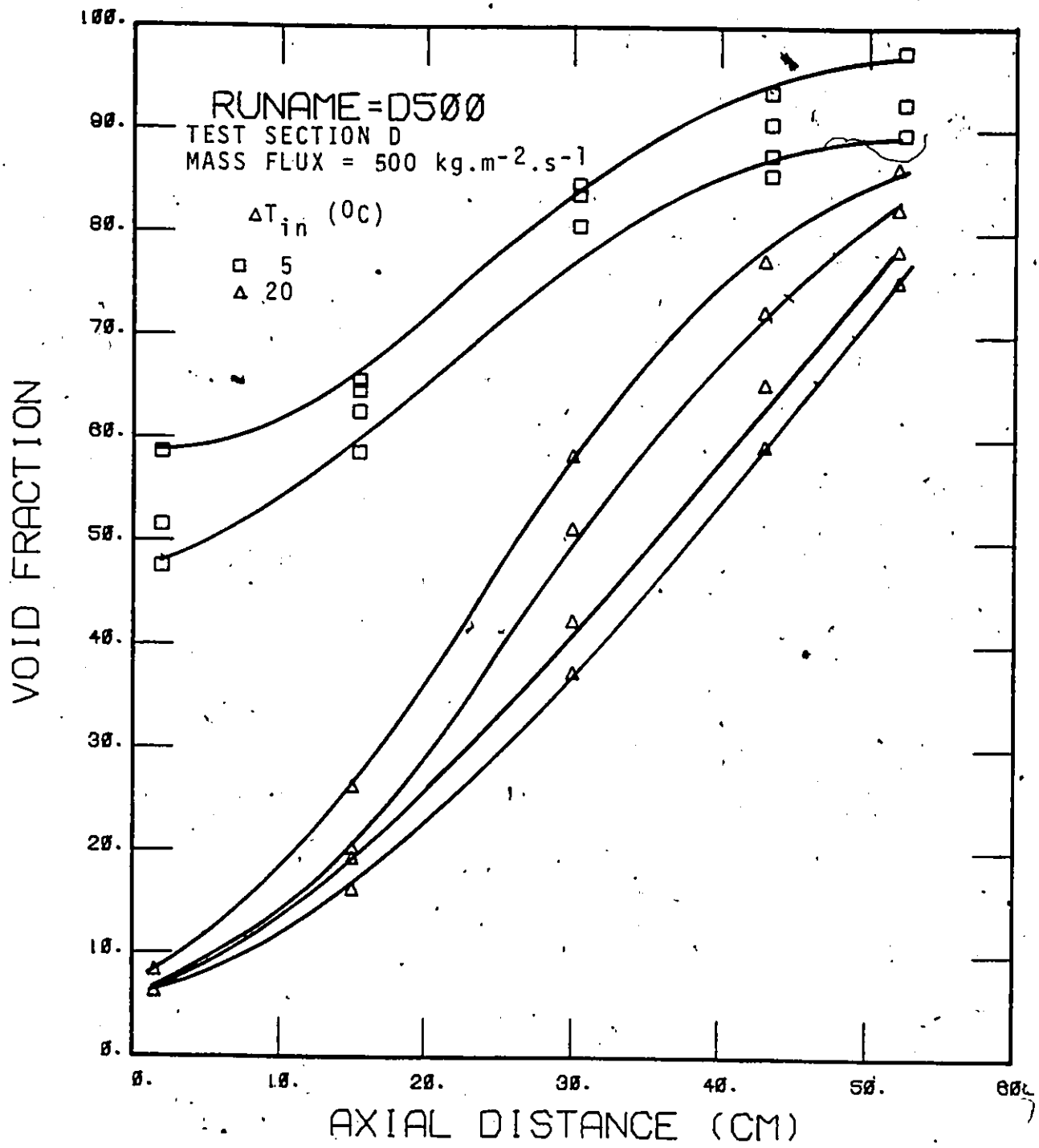

FIGURE 39 AXIAL VARIATION OF VOID FRACTION, MASS FLUX = 500 kg.m^{-2}.s^{-1}

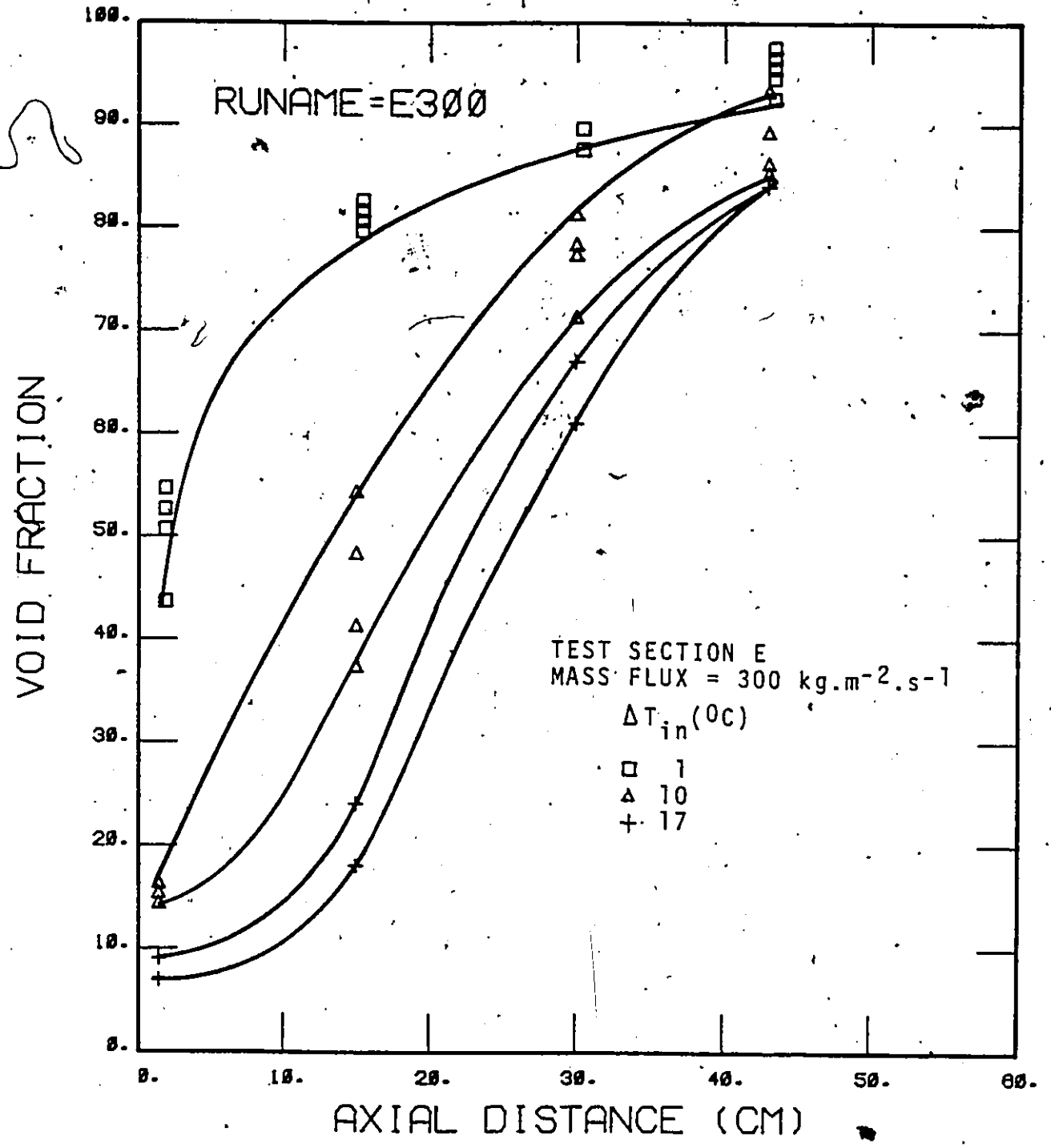

FIGURE 40 AXIAL VARIATION OF VOID FRACTION.
MASS FLUX = 300 kg.m-2.s-1

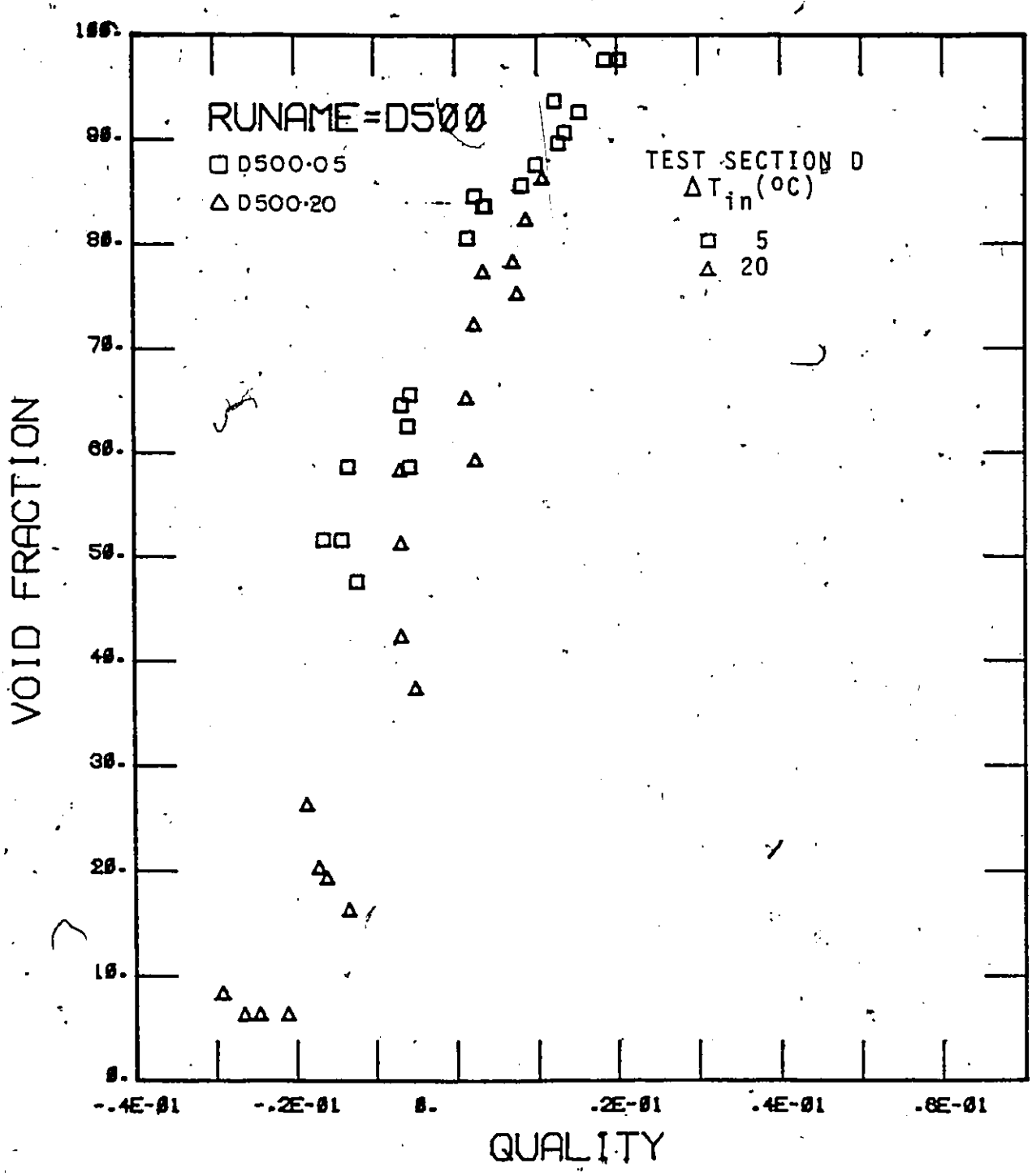

FIGURE 41 VOID FRACTION AS A FUNCTION OF EQUILIBRIUM QUALITY
MASS FLUX = 500 kg.m-2.s-1

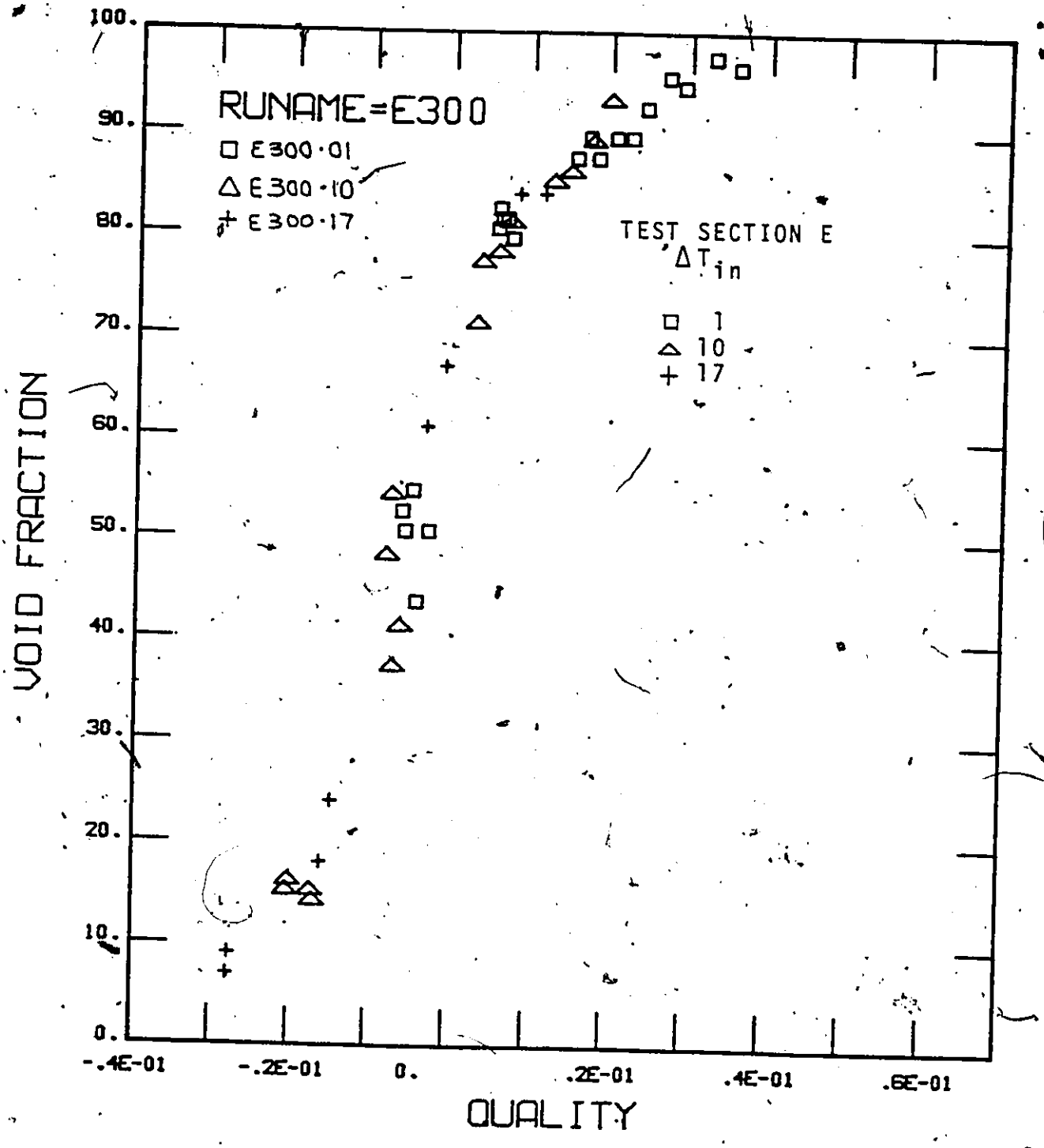

FIGURE 42 VOID FRACTION AS A FUNCTION OF EQUILIBRIUM QUALITY, MASS FLUX = 300 $kg.m^{-2}.s^{-1}$

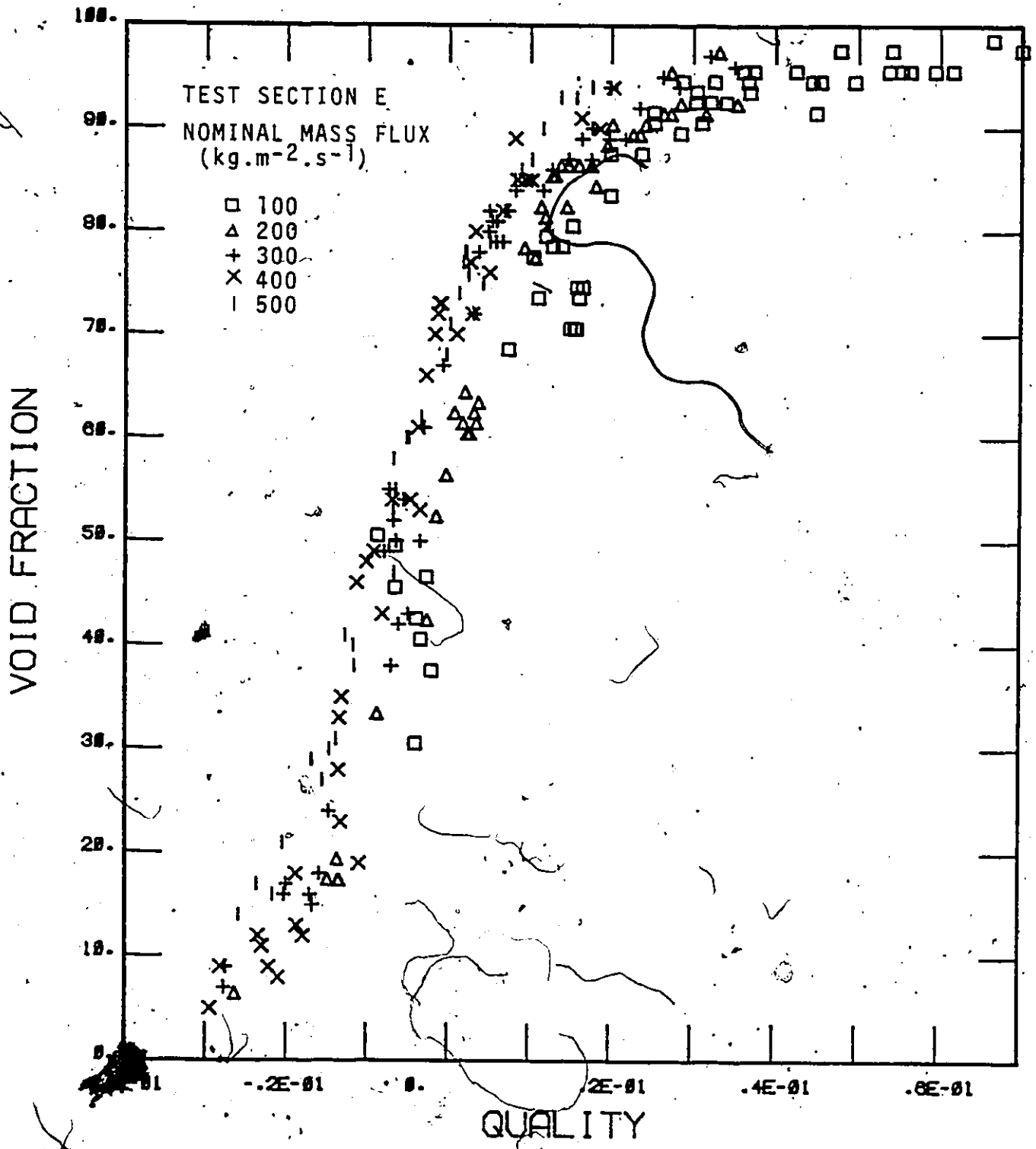

FIGURE 43 VOID FRACTION AS A FUNCTION OF EQUILIBRIUM QUALITY

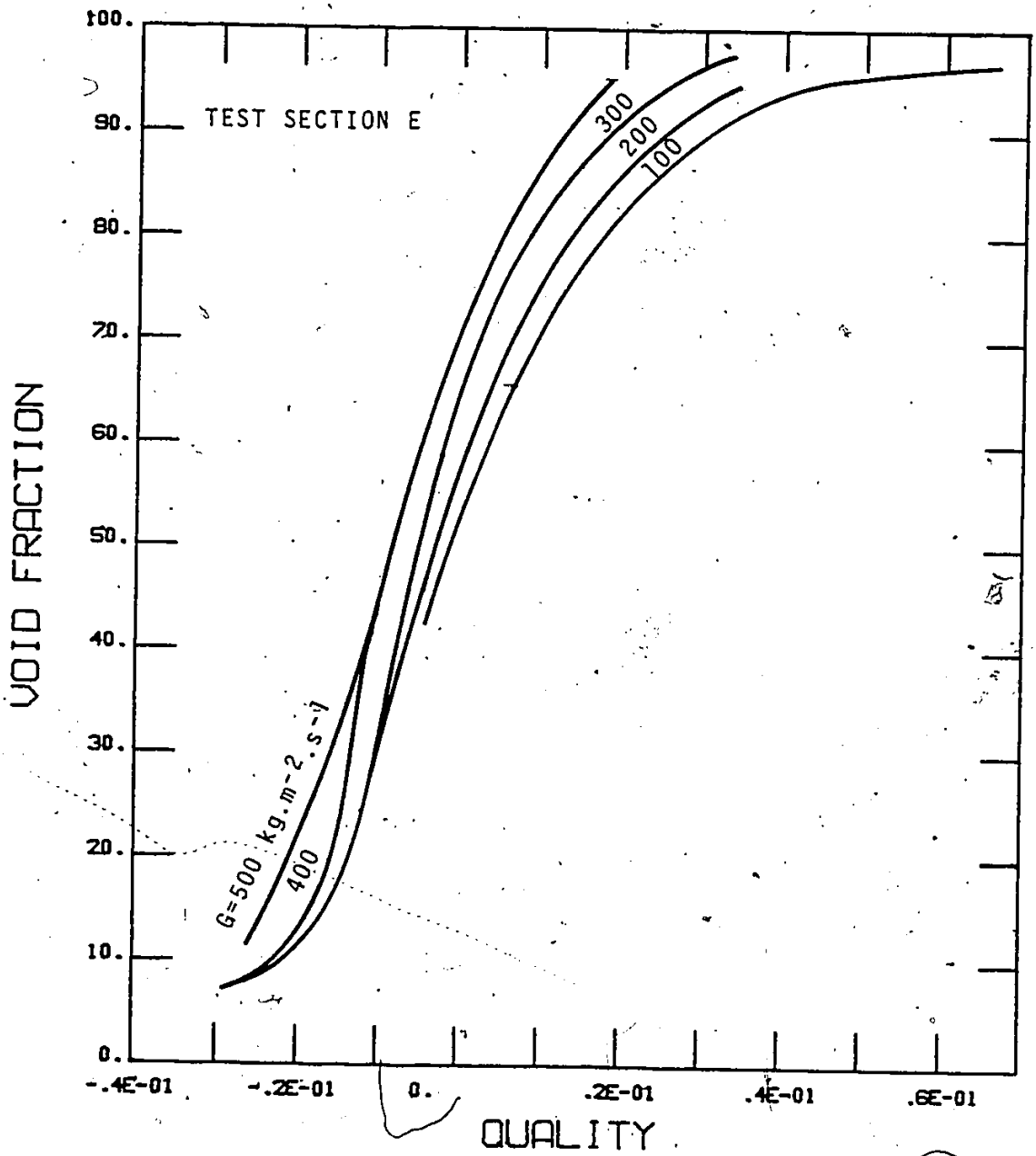

FIGURE 44 EFFECT OF MASS FLUX ON VOID FRACTION

In Fig. 45 the calculated void fraction, $\alpha = X\left[X + \rho_v/\rho_\ell . S.(1-X)\right]$, based on constant slip and either saturated or film temperature for the vapour, is compared to the data measured during a low inlet subcooling test. In calculating the void fraction it is assumed that the liquid has reached saturation before the first measurement station. This assumption is reasonable since the coolant is only slightly subcooled at the test section inlet. The predictions show that high slip ratios tend to lower the predicted void fraction, while higher vapour superheats can affect the void fraction either way through a decrease both in quality and vapour density (the cross section average enthalpy remains constant). For the condition of Fig. 45 an increase in vapour superheat increases the void fraction.

Fig. 45 shows that a no slip assumption results in a large over-prediction of the void fraction just downstream from the hot patch. Hence high slip velocities must have developed inside the hot patch. Also, near the start of the film boiling region the measured axial gradient in void fraction is lower than any of the predictions. This may be explained by (i) an increase in slip ratio, or (ii) a combination of increase in slip ratio and decrease in vapour superheat.

Further downstream the axial void fraction gradient becomes larger than any of the predictions. This is to be expected as the flow regime will be dispersed and the liquid core will have broken up into small droplets. It has been shown (Groeneveld & Delorme (1976)) that smaller droplets are more likely to be accelerated, thus reducing the slip ratio and hence increasing the axial void fraction gradient above the constant slip ratio predictions of Fig. 45.

An empirical correlation of the void fraction data is developed in Appendix G.

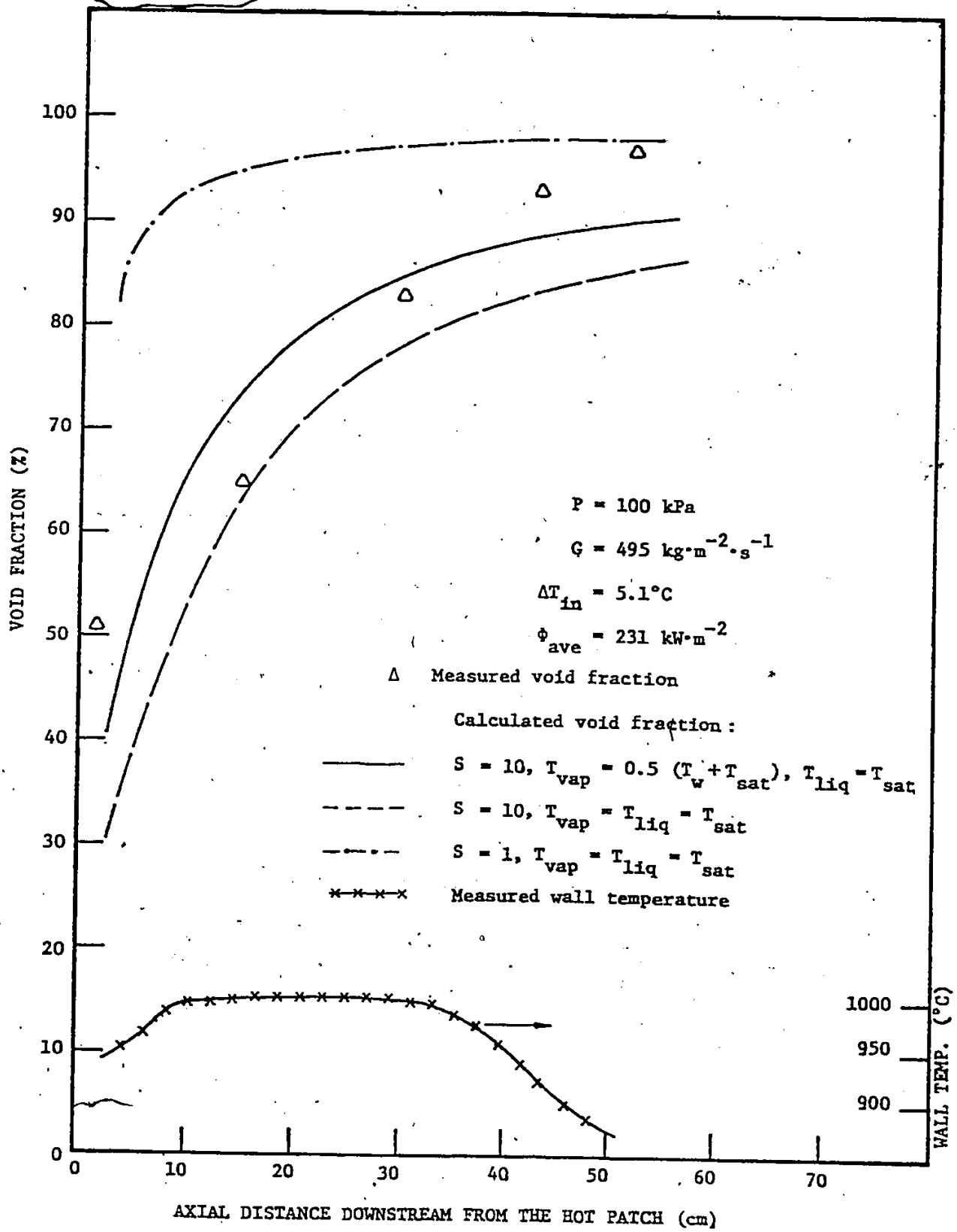

FIGURE 45 COMPARISON OF MEASURED VOID WITH PREDICTIONS

VII.0 PHYSICAL MODEL OF INVERTED ANNULAR FILM BOILING

VII.1 Approach and Assumptions

The present analysis uses the one-dimensional integral technique similar to the analysis of single-phase boundary layers. A similar method was used by Dougall and Rohsenow (1963) to analyse film boiling. The present analysis differs from the analysis of Dougall & Rohsenow in that it considers the initial stage of the vapor film to be in laminar flow. As the vapor film thickens, it changes into turbulent flow. In addition, a subcooled rather than saturated liquid core is considered in the analysis. A sketch of the laminar and turbulent regions are shown in Fig. 46. Note that the designation of the laminar sublayer is slightly different from the usual convention in the laminar film region. The reason for this will be explained later.

In the analysis, the acceleration of the vapor is taken into account. Heat transfer to the subcooled liquid core is analysed by solving the energy equation. The main feature is that the enhancement of the heat transfer coefficient at the start of film boiling (equivalent to the entrance region in single phase flow) is considered in the analysis.

The wall temperature is calculated by assuming pure conduction through the laminar sublayer adjacent to the wall. The radiation component is calculated by assuming radiation exchange between two cylindrical surfaces.

The following assumptions are made in order to obtain a simplified form of the momentum and energy equations:

(1) The change of vapor momentum is negligible in laminar flow. Consequently, the viscous force is balanced by the buoyancy force.

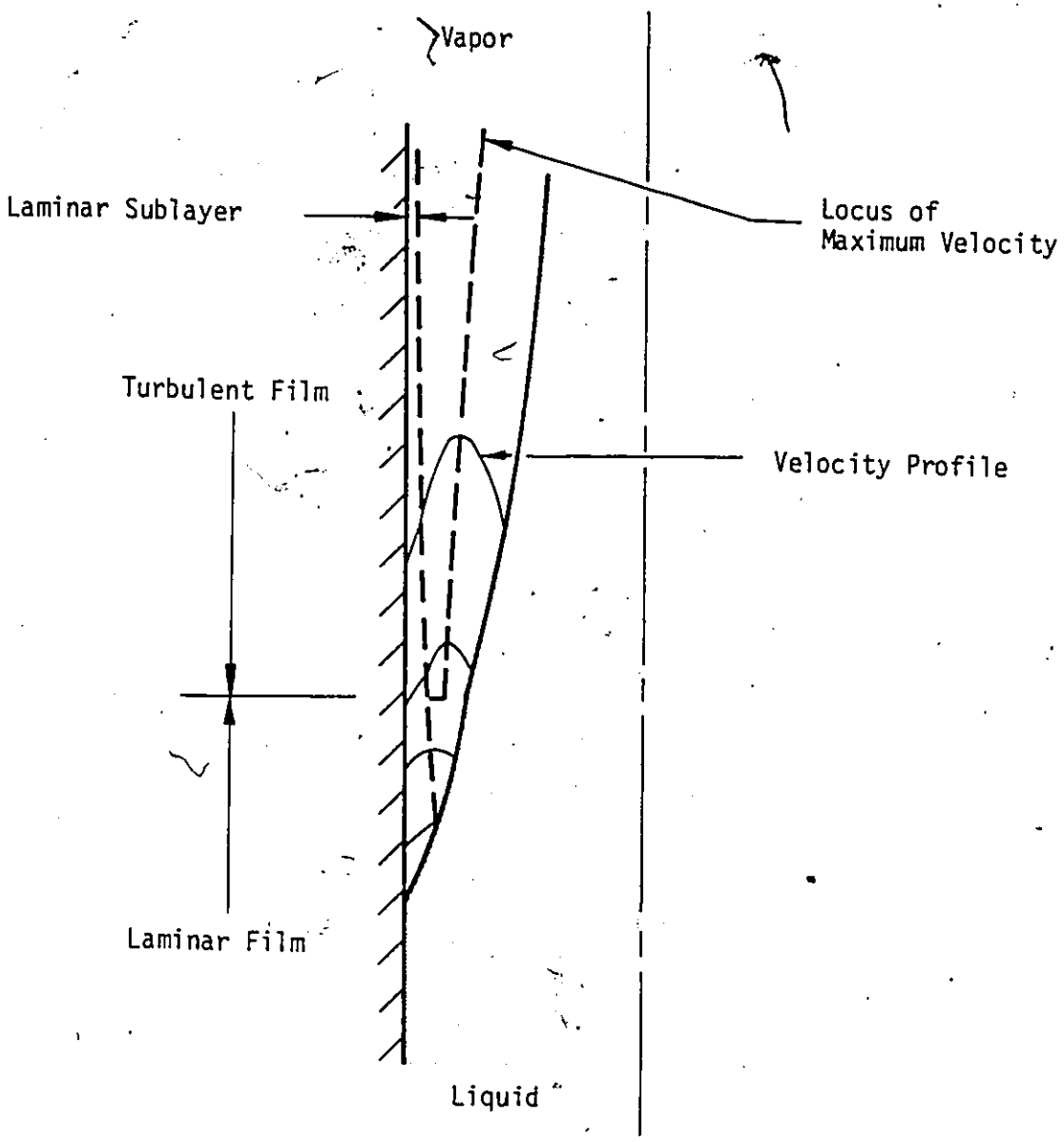

Fig. 46 DEVELOPMENT OF VAPOR FILM

(2) Axial conduction is negligible in the fluid.

(3) Kinetic energy and viscous dissipation are negligible. This is true at low Mach number.

(4) The vapor density is much less than the liquid density, so that $(\rho_\ell - \rho_v) \simeq \rho_\ell$.

(5) The liquid density is constant.

(6) The liquid core is assumed to be in turbulent flow. This is justified since the Reynolds number at G = 100 $kg \cdot m^{-2} s^{-1}$ is 2100. At low Reynolds number, there are two possible situations. The first is that the liquid volume is large, and conditions approach that of pool boiling. The second is that the liquid volume is small, so that transition from inverted annular flow to slug flow takes place over a short distance. The present analysis does not consider these boundary cases.

(7) The velocity profile of the liquid core is assumed uniform. This is reasonable as a consequence of the previous assumption.

(8). The flow is steady.

The momentum and energy equations will be developed based on these assumptions. Further assumptions will be made and justified in order to reduce the complexity of the mathematics.

After the solution of the governing equations has been obtained, a sample calculation is performed to check the validity of the assumptions. This is shown in Appendix J.

VII.2 Momentum Equations

VII.2.1 Laminar vapor film

In the laminar film region, the vapor film is thin. Therefore, we can use Cartesian instead of cylindrical coordinates. A sketch of the region under consideration is shown in Fig. 47. According to assumptions (1) and (4), the momentum equation is simply

$$\mu_v \frac{d^2u}{dy^2} = -g\rho_\ell$$

This is identical to the derivation of Ellion (1953). The solution is

$$u_v = \frac{-g\rho_\ell}{\mu_v}\frac{y^2}{2} + C_1 y + C_2$$

At $y=0$, $u=0$

$\therefore C_2=0$

Assuming an interfacial velocity equal to the liquid average velocity U_ℓ, the constant C_1 can be evaluated. The result is

$$u_v = \frac{g\rho_\ell y\delta}{2\mu_v}\left(1-\frac{y}{\delta}\right) + U_\ell \frac{y}{\delta}$$

This can be substituted into the definition of the vapor mass flux:

$$G_v = \frac{2\pi R}{\pi R^2}\int_0^\delta u_v \rho_v dy$$

$$= \frac{2}{R}\int_0^\delta \rho_v\left[\frac{g\rho_\ell y\delta}{2\mu_v}\left(1-\frac{y}{\delta}\right) + U_\ell\frac{y}{\delta}\right]dy$$

Assuming that the vapor properties can be evaluated at the film temperature, we obtain

$$G_v = \frac{2}{R}\rho_v\left[\frac{g\rho_\ell\delta^3}{12\mu_v} + \frac{U_\ell\delta}{2}\right]$$

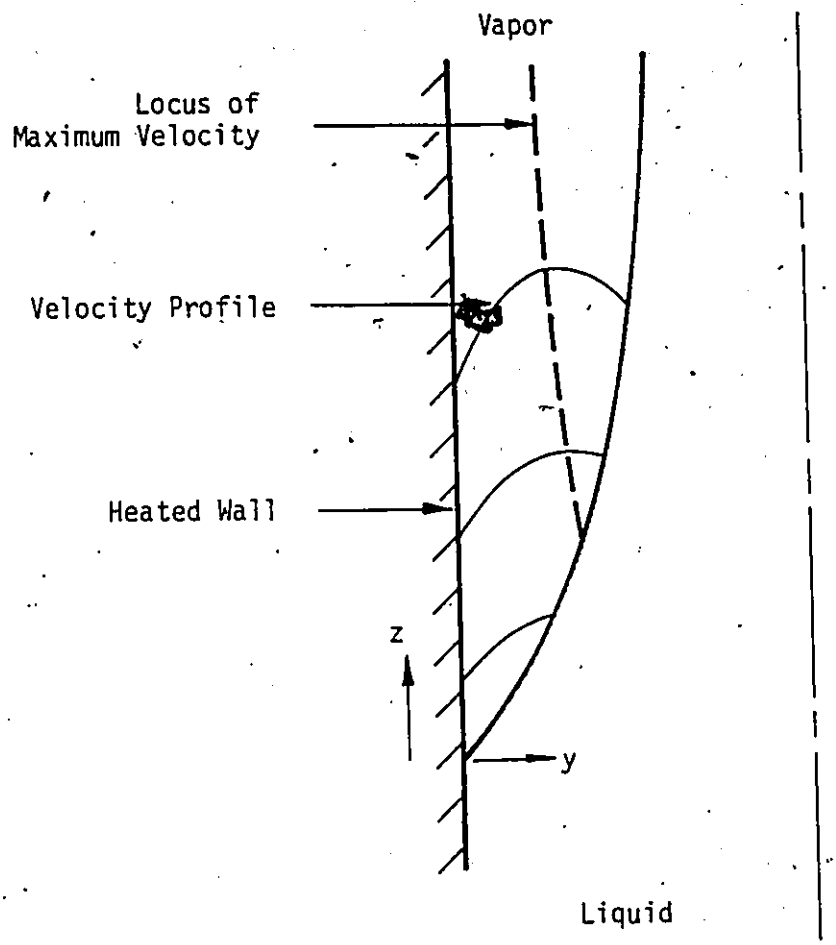

FIG. 47 LAMINAR VAPOR FILM

The energy equation will give another relation for G_v. This will be considered later. Differentiating the above equation with respect to the axial direction Z, and assuming that $\frac{dU_\ell}{dz}$ is negligible in the laminar film region, we obtain

$$\frac{dG_v}{dz} = \frac{2p_v}{R}\left[\frac{g\rho_\ell\delta^2}{4\mu_v} + \frac{U_\ell}{2}\right]\frac{d\delta}{dz} \qquad \text{- - - - -} \qquad 7.1$$

This equation will be used in later analysis.

VII.2.2 Turbulent vapor film

The liquid and vapor control volumes under consideration are shown in Fig. 48. The forces in the Z direction acting on per unit length of the vapor control volume are

(i) Wall shear = $-2\pi R\tau_w$

(ii) interfacial shear = $-\tau_i(2\pi)(R-\delta)\left(\frac{\Delta z}{\cos\theta}\right)\frac{\cos\theta}{\Delta z}$

$= -2\pi(R-\delta)\tau_i$

(iii) pressure force at Z and Z+ΔZ

$$= -\frac{d}{dz}\left[p_v\pi(R^2-(R-\delta)^2)\right]$$

$$= -\pi\delta(2R-\delta)\frac{dp_v}{dz} - 2\pi p_v(R-\delta)\frac{d\delta}{dz}$$

$$= -\pi\delta(2R-\delta)\frac{dp_v}{dz} - 2\pi(R-\delta)p_v\tan\theta$$

(iv) pressure force at liquid-vapor interface

$$= p_\ell\left(\frac{2\pi(R-\delta)\Delta z}{\cos\theta}\right)\frac{\sin\theta}{\Delta z}$$

$$= 2\pi(R-\delta)p_\ell\tan\theta$$

(v) Gravity force - this is assumed to be negligible.

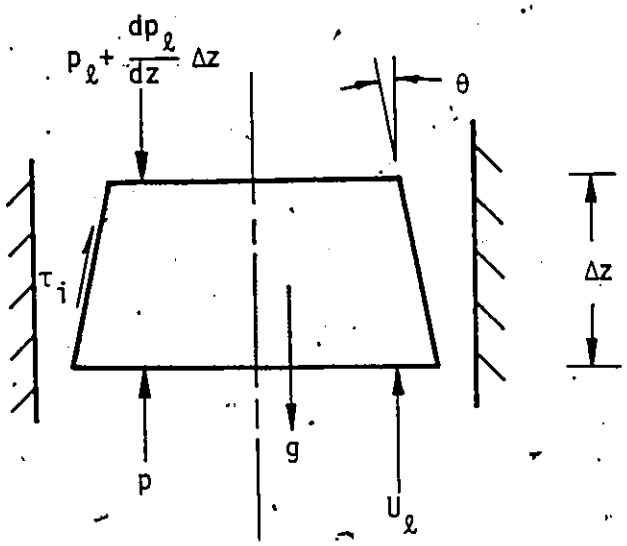

(i) Liquid Control Volume

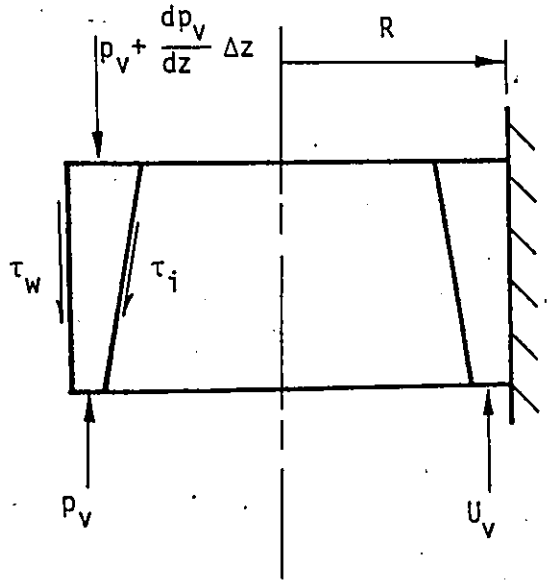

(ii) Vapor Control Volume

FIG. 48 CONTROL VOLUME IN INVERTED ANNULAR FLOW

The changes in momentum are:

(vi) Change in momentum between z and z+Δz

$$= \frac{d}{dz} \int_{R-\delta}^{R} 2\pi \rho_v u_v^2 r dr$$

(vii) momentum crossing the liquid vapor interface

$$= U_\ell \frac{d}{dz} \int_{R-\delta}^{R} 2\pi r \rho_v u_v dr$$

The pressures p_v and p_ℓ at the two sides of the interface are not equal, due to the presence of a vapor thrust force. If the evaporating mass undergoes a change in normal velocity from $V_{\ell N}$ to V_{gN} across the interface, then the difference in pressure is

$$p_v - p_\ell = \Delta \dot{m}_v (V_{gn} - V_{\ell N}) = \Delta \dot{m}_v^2 \left(\frac{1}{\rho_g} - \frac{1}{\rho_\ell}\right).$$

It is shown in Appendix J that this effect is small. Therefore, we assume that the pressures on both sides of the interface are equal. Under this assumption, the second term in (iii) can be equated to (iv). Combining (i) through (vii), the resulting equation is

$$\frac{d}{dz} \int_{R-\delta}^{R} 2\pi \rho_v u_v^2 r dr - U_\ell \frac{d}{dz} \int_{R-\delta}^{R} 2\pi r \rho_v u_v dr$$

$$= -2\pi R \tau_w - 2\pi \tau_i (R-\delta) - \pi \left(\frac{dp}{dz}\right) \delta (2R-\delta) \quad ----- \quad 7.2$$

Similarly, for the liquid core, the forces in the direction of flow are

(i) Interfacial shear = $2\pi(R-\delta)\tau_i$

(ii) pressure force at z and z+Δz

$$= - \frac{d}{dz}\left[p_\ell \pi (R-\delta)^2\right]$$

$$= - \pi(R-\delta)^2 \frac{dp_\ell}{dz} + 2\pi p_\ell (R-\delta) \frac{d\delta}{dz}$$

$$= - \pi(R-\delta)^2 \frac{dp_\ell}{dz} + 2\pi p_\ell (R-\delta)\tan\theta$$

(iii) Pressure force at liquid-vapor interface

$$= -2\pi(R-\delta)p_v \tan\theta$$

(iv) Gravity force $= - g\rho_\ell \pi (R-\delta)^2$

(v) Change in momentum

$$= \rho_\ell \frac{d}{dz} \int_0^{R-\delta} 2\pi U_\ell^2 r dr$$

Combining (i) through (v) and again assuming $p_v = p_\ell$, the liquid momentum equation is

$$\rho_\ell \frac{d}{dz} \int_0^{R-\delta} 2\pi U_\ell^2 r dr = 2\pi\tau_i (R-\delta) - \pi(R-\delta)^2 \left(\frac{dp}{dz}\right) - g\rho_\ell \pi (R-\delta)^2 \quad \text{- - - - - 7.3}$$

Equating the pressure gradient in eqs. 7.2 and 7.3 we obtain*

$$- \frac{dp}{dz} = \frac{2R\tau_w}{\delta(2R-\delta)} + \frac{2\tau_i (R-\delta)}{\delta(2R-\delta)} + \frac{1}{\pi\delta(2R-\delta)} \frac{d}{dz} \int_{R-\delta}^{R} 2\pi\rho_v u_v^2 r dr$$

$$- \frac{U_\ell}{\pi\delta(2R-\delta)} \frac{d}{dz} \int_{R-\delta}^{R} 2\pi\rho_v u_v dr$$

$$= g\rho_\ell - \frac{2\tau_i}{R-\delta} + \frac{1}{\pi(R-\delta)^2} \frac{d}{dz} \int_0^{R-\delta} 2\pi\rho_\ell U_\ell^2 r dr \quad \text{- - - - - 7.4}$$

This equation can be regarded as the relative motion equation since it describes the difference between the rates at which the two phases are gaining kinetic energy.

---

* In the more advanced two-fluid models currently being developed, the pressure gradients in the two phases are considered to be different. This will result in a cross flow component in addition to the evaporation/condensation. In the present analysis, the evaporation component is dominating.

The vapor mass flux can be defined as

$$G_v = \frac{1}{\pi R^2} \int_{R-\delta}^{R} 2\pi r \rho_v u_v dr.$$

Similarly we define the momentum fluxes to be

$$M_v = \frac{1}{\pi R^2} \int_{R-\delta}^{R} 2\pi \rho_v u_v^2 r dr$$

and

$$M_\ell = \frac{1}{\pi R^2} \int_{0}^{R-\delta} 2\pi \rho_\ell U_\ell^2 r dr$$

Equation 7.4 can then be written as

$$\frac{dM_v}{dz} - U_\ell \frac{dG_v}{dz} - \frac{\delta(2R-\delta)}{(R-\delta)^2} \frac{dM_\ell}{dz} = - \frac{2\tau_w}{R} - \frac{2\tau_i}{R-\delta} + \frac{g\rho_\ell (2R-\delta)\delta}{R^2} \quad \text{- - - - -} \quad 7.5$$

VII.3 Energy Equation

VII.3.1 Vapor film

Consider the vapor control volume as shown in Fig. 49. We assume that all condensation and evaporation take place in a narrow region at the liquid-vapor interface. This region has been combined into the vapor control volume under consideration. Therefore, the condensation and evaporation mass fluxes Γ_c and Γ_e (based on interfacial area) will have enthalpy h_f associated with them. According to assumptions (2) and (4), the energy equation for the vapor control volume can be written as

$$\pi D \phi_{TOT} = 2\pi \phi_\ell (R-\delta)\left(\frac{1}{\cos\theta}\right) + 2\pi \frac{d}{dz} \int_{R-\delta}^{R} u_v \rho_v h_v r dr$$

$$+ 2\pi (\Gamma_c - \Gamma_e) h_f (R-\delta)\left(\frac{1}{\cos\theta}\right) \quad \text{- - - - - - - -} \quad 7.6$$

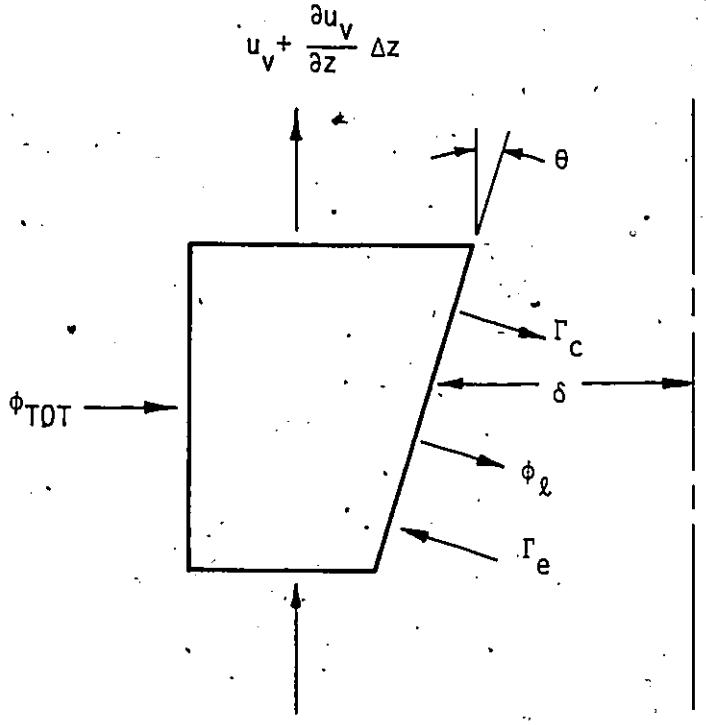

FIG. 49 ENERGY BALANCE FOR VAPOR CONTROL VOLUME

Here ϕ_ℓ is the net heat flux based on interfacial area going into the liquid core. If the liquid core is saturated, this component is zero. The total energy transferred away from the heated wall goes to increasing the total vapor enthalpy.

A mass balance at the interface gives

$$\pi(D-2\delta)(\Gamma_c-\Gamma_e)\frac{1}{\cos\theta} = -\frac{d}{dz}\int_{R-\delta}^{R} 2\pi\rho_v u_v r dr$$

$$= -\pi R^2 \frac{dG_v}{dz}$$

Similar to the definition of the momentum flux, we define the energy flux as

$$E_v = \frac{1}{\pi R^2}\int_{R-\delta}^{R} 2\pi\rho_v u_v h_v r dr$$

Eq. 7.6 can then be written as

$$2R\phi_{TOT} - 2(R-\delta)\phi_\ell \frac{1}{\cos\theta} = R^2 \frac{dE_v}{dz} - R^2 h_f \frac{dG_v}{dz}$$

It is more convenient to consider ϕ_ℓ based on the projection of the interfacial area on the tube wall. Using this modified definition of ϕ_ℓ, the above equation becomes

$$2R\phi_{TOT} - 2(R-\delta)\phi_\ell = R^2 \frac{dE_v}{dz} - R^2 h_f \frac{dG_v}{dz} \quad \text{- - - - - -} \quad 7.7$$

VII.3.2 Liquid Core

So far, the liquid velocity has been assumed uniform across a cross-section. However, the liquid average velocity changes due to evaporation and increases in vapor film thickness. Consider the 2-dimensional continuity and energy equations written for the liquid core:

$$\frac{1}{r}\frac{\partial}{\partial r}rv_\ell + \frac{\partial u_\ell}{\partial z} = 0 \qquad \text{- - - - -} \qquad 7.8$$

and $$u_\ell \frac{\partial T}{\partial z} + v_\ell \frac{\partial T}{\partial r} = \frac{1}{r}\frac{\partial}{\partial r}(\varepsilon_H+\alpha)r\frac{\partial T}{\partial r} \qquad \text{- - - - -} \qquad 7.9$$

Since we assume that u_ℓ is uniform, we can replace the partial derivative w.r.t. z with the ordinary derivative. Thus eq. 7.8 becomes

$$\frac{1}{r}\frac{\partial}{\partial r}rv_\ell + \frac{dU_\ell}{dz} = 0$$

Defining $r^* = \frac{r}{R-\delta}$, the above equation can be written as

$$\frac{1}{(R-\delta)r^*}\frac{\partial r^* v_\ell}{\partial r^*} + \frac{dU_\ell}{dz} = 0$$

Integrating over the cross-section of the core, we obtain

$$v_\ell = \frac{f(z)}{r^*} - (R-\delta)\frac{r^*}{2}\frac{dU_\ell}{dz}$$

Since v_ℓ is finite at $r^* = 0$, $f(z) = 0$.

$$\therefore\ v_\ell = -(R-\delta)\frac{r^*}{2}\frac{dU_\ell}{dz}$$

At the liquid-vapor interface, this velocity v_ℓ can be considered as the rate at which the radius of the liquid core is diminishing. Substituting v_ℓ into equation 7.9 and again using the dimensionless radial distance r^*, we obtain

$$U_\ell\frac{\partial\theta}{\partial z} = \frac{1}{(R-\delta)^2}\ \frac{1}{r^*}\frac{\partial}{\partial r^*}r^*(\varepsilon_H+\alpha)\frac{\partial\theta}{\partial r^*} + \frac{r^*}{2}\frac{dU_\ell}{dz}\frac{\partial\theta}{\partial r^*}$$

where $$\theta = \frac{T_s - T(r^*,z)}{T_s - T_{in}} \qquad \text{- - - - - - -} \qquad 7.10$$

It is interesting to consider a limiting case of eq. 7.10. If δ = constant and $\frac{dU_\ell}{dz} = 0$, Eq. 7.10 reduces to a familiar thermal-entry-length problem (Kays (1966)). However, since ε_H depends on r^* as well as z, the

reduced equation cannot be treated as a Sturm-Liouville problem. Nevertheless, it can be seen that qualitatively the heat transfer at the boundary of the liquid core behaves similarly: an enhanced coefficient near the entrance, gradually diminishing to the steady state value.

The solution of eq. 7.10 will give the temperature gradient. The heat flux ϕ_ℓ at the vapor-liquid interface is therefore

$$\phi_\ell = -\rho_\ell c_{p_\ell} (\varepsilon_H + \alpha) \frac{\partial T}{\partial r}\bigg|_{r=R-\delta}$$

$$= \rho_\ell c_{p_\ell} (\varepsilon_H + \alpha) \frac{\partial \theta}{\partial r^*}\bigg|_{r^*=1} \frac{(T_s - T_{in})}{(R-\delta)} \qquad \text{- - - - - - - -} \qquad 7.11$$

However, equation 7.10 cannot be solved independently, because the vapor film thickness is unknown. It is coupled with the momentum equations 7.1 or 7,5 and the vapor energy equation 7.7.

VII.4 Constitutive Equations

In order to obtain a complete set of equations, the constitutive equations for the interfacial shear and eddy diffusivity has to be specified.

VIII.4.1 Interfacial Shear

The general approach of estimating the interfacial shear in two phase flow with vapor generation is to determine a correction factor for the non-evaporating/non-condensing friction factor. For adiabatic two phase flow, there are at least two approaches of estimating the friction factor. One approach is to express the equivalent roughness of the interface in terms of other system parameters such as phase velocities, void fraction and surface tension. This approach has been used by Cohen & Hanratty (1968)

and Kordyban (1974) with some success. However, as commented by Hughes et al (1976), "the general applicability of the approach has yet to be established due in part to the large number of degrees of freedom associated with the interface flow regime."

Another approach is to use empirical correlation. Wallis (1970) found that, in gas-liquid annular flow, the interfacial friction factor can be correlated by

$$f_i = 0.005\ [1+300\ \delta/D] \qquad \text{- - - - -} \qquad 7.12$$

Moeck (1970) also proposed a similar correlation. Eq. 7.12 has been suggested to be used in inverted annular flow by Hughes et al (1976). In such case, δ is the vapor film thickness. Until more satisfactory correlations become available, eq. 7.12 will be used in the present analysis.

A simple approach to correct the effect of evaporation is to use the Reynolds flux concept. This has been developed by Silver and Wallis (1965). The correction is expressed as follows

$$\frac{f_i^*}{f_i} = e^{-\frac{\phi}{2f_i}} - \frac{\phi}{f_i} \qquad \text{- - - - - - - -} \qquad 7.13$$

where f_i^* and f_i are respectively the friction factors with and without phase changes;

$$\phi = \frac{2\Gamma}{\rho_v \overline{u_v}}$$

and the phase change mass flux is

$$\Gamma = \frac{\pi R^2 \frac{dG_v}{dz}}{2\pi(R-\delta)}$$

$$= \frac{R^2}{2(R-\delta)} \frac{dG_v}{dz}$$

Various similar expressions have been proposed by Mickley (1954) and Spalding (1963), among others. In view of the empirical nature of these expressions, there is no strong reason to reject either one. For the present analysis, we will use eqs. 7.12 and 7.13, together with a factor C_1 to be adjusted later. Thus the interfacial friction factor is

$$f_i^* = C_1 0.005 \left[1+300 \frac{\delta}{D}\right]\left[e^{\frac{\phi}{2f_i}} - \frac{\phi}{f_i}\right] \qquad \text{- - - - - - - 7.14}$$

and the interfacial shear is

$$\tau_i = \frac{1}{2} f_i^* \rho_v |u_v-u_\ell| (u_v-u_\ell)$$

VII.4.2 Eddy Diffusivity in the Liquid Core

The turbulent thermal diffusivity is required in equation 7.10 and also in evaluating ϕ_ℓ from the temperature gradient at the vapor-liquid interface. Two possible sources of information available from literature are pipe flow and jet flow. The absence of a rigid wall in the present situation seems to suggest that conditions are closer to jet flow than pipe flow. In free turbulent jet flow, it has been found that a constant value of ε_m across the main part of the jet is a reasonable assumption (see Hinze (1975)). Using Prandtl mixing length hypothesis, the eddy diffusivity for momentum transfer is given by

$$\varepsilon_m = C_1 b(\bar{u}_{max}-\bar{u}_{min})$$

where b is the mixing zone and C_1 is a proportionality constant.

We intend to use this expression in the present analysis. Since the turbulence in the vapor-interface, and consequently within the liquid core, is expected to increase as the vapor film thickens, the mixing zone will be defined to be half of the vapor film thickness (i.e. from the point of maximum velocity to the interface). In addition, the velocity difference

is assumed to be proportional to the average liquid velocity. Therefore,

$$\varepsilon_m = CU_\ell \left(\frac{1}{2}\delta_T\right)$$

By assuming that Reynold's analogy is valid, the constitutive equation for the eddy diffusity of heat transfer in the present analysis is

$$\varepsilon_H = CU_\ell \left(\frac{1}{2}\delta_T\right) \qquad \text{- - - - - - - 7.15}$$

VII?.5 Solution of the Momentum and Energy Equations

To carry out the analysis further, information about the velocity profile has to be specified in the turbulent film region. We first express G_v, M_v and E_v in terms of dimensionless quantities

Define $$u^+ = \frac{u_v}{\sqrt{\frac{\tau_w}{\rho_v}}}$$

and $$\eta = \frac{y\sqrt{\frac{\tau_w}{\rho_v}}}{\nu_v}$$

We further stipulate that all vapor properties to be evaluated at the film temperature i.e. at $T_v = \frac{1}{2}(T_w+T_s)$. From the definition of G_v

$$G_v = \frac{1}{\pi R^2}\int_{R-\delta}^{R} 2\pi\,\rho_v u_v r dr$$

and on replacing r by (R-y), we obtain

$$G_v = \frac{2}{R^2}\left[\int_0^\delta \rho_v u_v R dy - \int_0^\delta \rho_v u_v y dy\right]$$

$$= \frac{2}{R^2}\left[R\mu_v \int_0^{\delta^+} u_v^+ d\eta - \frac{\rho_v \nu_v^2}{\sqrt{\frac{\tau_w}{\rho_v}}} \int_0^{\delta^+} u_v^+ \eta d\eta\right]$$

Define $\theta_1 = \int_0^{\delta^+} u_v^+ d\eta$ ----- 7.16

and $\theta_2 = \int_0^{\delta^+} u_v^+ \eta d\eta$ ----- 7.17

$\therefore G_v = \frac{2}{R^2}\left[R\mu_v\theta_1 - \frac{\rho_v\nu_v^2}{\sqrt{\frac{\tau_w}{\rho_v}}}\theta_2\right]$ ----- 7.18

$$M_v = \frac{1}{\pi R^2}\int_{R-\delta}^{R} 2\pi\rho_v u_v^2 r dr$$

$$= \frac{2}{R^2}\int_0^{\delta} \rho_v u_v^2 (R-y)dy$$

$$= \frac{2}{R^2}\rho_v\nu_v^2\left[\int_0^{\delta^+} R^+ u_v^{+2} d\eta - \int_0^{\delta^+} u_v^{+2}\eta d\eta\right]$$

Define $\theta_3 = \int_0^{\delta^+} u_v^{+2} d\eta$ ----- 7.19

and $\theta_4 = \int_0^{\delta^+} u_v^{+2}\eta d\eta$ ----- 7.20

$\therefore M_v = \frac{2}{R^2}\rho_v\nu_v^2\left[R\frac{\sqrt{\frac{\tau_w}{\rho_v}}}{\nu_v}\theta_3 - \theta_4\right]$ ----- 7.21

$$E_v = \frac{1}{\pi R^2} \int_{R-\delta}^{R} 2\pi \rho_v u_v h_v r dr$$

$$= h_v \times \frac{1}{\pi R^2} \int_{R-\delta}^{R} 2\pi \rho_v u_v r dr$$

$$= h_v G_v \qquad \text{- - - - -} \qquad 7.22$$

$$M_\ell = \frac{1}{\pi R^2} \int_{0}^{R-\delta} 2\pi \rho_\ell U_\ell^2 r dr$$

$$= \frac{2}{R^2} \rho_\ell U_\ell^2 \frac{(R-\delta)^2}{2}$$

$$= (1-\frac{\delta}{R})^2 \rho_\ell \left[\frac{G_\ell}{\rho_\ell(1-\alpha)}\right]^2$$

$$= (1-\frac{\delta}{R})^2 \frac{1}{\rho_\ell} \left[\frac{(G-G_v)R^2}{(R-\delta)^2}\right]^2$$

$$= \frac{1}{\rho_\ell} \left[\frac{(G-G_v)R}{R-\delta}\right]^2 \qquad \text{- - - - -} \qquad 7.23$$

VII.5.1 Laminar Vapor Film

Substituting eq. 7.22 into eq. 7.7, we obtain

$$R^2 \frac{d}{dz}(h_v-h_f)G_v = 2R\phi_{TOT} - 2(R-\delta)\phi_\ell \qquad \text{- - - - - - - -} \qquad 7.24$$

The liquid heat flux ϕ_ℓ is given by eq. 7.11. Using a numerical method to integrate step by step in the z direction, we can assume that at each step (h_v-h_f) is independent of z. Therefore, eq. 7.24 becomes

$$R^2(h_v-h_f)\frac{dG_v}{dz} = 2R\phi_{TOT} - 2(R-\delta)\phi_\ell.$$

Combining this equation with eq. 7.1, the vapor film thickness can be obtained upon integration.

VII.5.2 Turbulent Vapor Film

For the turbulent vapor film, we assume that it consists of a laminar sublayer and a turbulent layer. This two-layer approach has been used by Hsu (1960) to analyse film boiling on vertical surface. In the present analysis, we assume that in the laminar region

$$u^+ = \eta \qquad 0 < \eta < \eta_s$$

and in the turbulent region the velocity profile is symmetrical about the line of maximum velocity. In each half of this turbulent region, the 1/n-th power law is assumed to hold, i.e.

$$u^+ = C\eta^{\frac{1}{m}} \qquad \eta > \eta_s$$

where $m = 7$

$C = 8.74$

Similar approach was used by Dougall and Rohensow to analyse the vapor film. They used the universal velocity distribution law.

The thickness of the dimensionless laminar sublayer η_s has to be specified. Its lower limit is equal to 5, as has been found in pipe flow. The buffer zone usually lies between $5 < \eta < 26$. However, similar to the analysis of Hsu (1960), the buffer zone is omitted and the laminar and turbulent layers are both extrapolated so that they coincide at the transition point. Hsu chose a value of 10. Therefore, for the present analysis

$$5 < \eta_s < 26$$

Having specified the velocity profile, eqs. 7.16, 7.17, 7.19, 7.20 can be expressed in terms of η.

$$\therefore \theta_1 = \int_0^{\delta^+} C\eta^{\frac{1}{m}} d\eta$$

$$= \int_0^{\eta_s} \eta d\eta + 2 \int_{\eta_s}^{\eta} C\eta^{\frac{1}{m}} d\eta$$

$$= \frac{\eta_s^2}{2} + \frac{2mC}{m+1}\left(\eta^{\frac{m+1}{m}} - \eta_s^{\frac{m+1}{m}} \right) \quad ----- \quad 7.25$$

Similarly

$$\theta_2 = \frac{1}{3}\eta_s^3 + \frac{2mC}{2m+1}\left(\eta^{\frac{2m+1}{m}} - \eta_s^{\frac{2m+1}{m}} \right) ------ \quad 7.26$$

$$\theta_3 = \frac{\eta_s^3}{3} + \frac{2mC^2}{2+m}\left(\eta^{\frac{2+m}{m}} - \eta_s^{\frac{2+m}{m}} \right) ------ \quad 7.27$$

$$\theta_4 = \frac{\eta_s^4}{4} + \frac{mC^2}{m+1}\left(\eta^{\frac{2+2m}{m}} - \eta_s^{\frac{2+2m}{m}} \right) ------ \quad 7.28$$

Integrating the energy equation 7.24, we obtain

$$R^2(h_v - h_f)G_v = \int_0^z [2R\phi_{TOT} - 2(R-\delta)\phi_\ell]dz$$

and after rearranging

$$G_v = \frac{1}{R^2(h_v - h_f)} \int_0^z [2R\phi_{TOT} - 2(R-\delta)\phi_\ell]dz$$

From eq. 7.18

$$G_v = \frac{2}{R^2}\left[R\mu_v\theta_1 - \frac{\rho_v\nu_v^2}{\sqrt{\frac{\tau_w}{\rho_v}}}\theta_2 \right]$$

$$\therefore \quad R\theta_1 - \frac{\nu_v}{\sqrt{\frac{\tau_w}{\rho_v}}}\theta_2 = \frac{1}{2\mu_v(h_v-h_f)} \int_0^z [2R\phi_{TOT} - 2(R-\delta)\phi_\ell]dz \quad ----- \quad 7.29$$

The integral on the R.H.S. can be evaluated since ϕ_{TOT} is specified and ϕ_ℓ is given by eq. 7.11. Let us denote the R.H.S. by Q and substitute eq. 7.25 and 7.26 into 7.29. The result, after rearrangement, is

$$\eta = \left[\frac{Q - \eta_s^2\left(\frac{3R-2\delta_s}{6}\right)+2mc\eta_s^{\frac{m+1}{m}}\left(\frac{R}{m+1} - \frac{\delta_s}{2m+1}\right)}{2mC\left[\frac{(2m+1)R - \frac{\delta_T}{2}(m+1)}{(m+1)(2m+1)}\right]}\right]^{\frac{m}{m+1}} \quad -- \quad 7.30$$

If we assume that inverted annular flow exists at void fraction below 40%, then $(2m+1)\,R >> \frac{\delta_T}{2}(m+1)$ in most situations. The laminar sublayer thickness is also negligible compared to R. Thus eq. 7.30 can be simplified to

$$\eta \approx \left[\frac{\left(Q - \eta_s^2\frac{R}{2} + 2mcR\,\eta_s^{\frac{m+1}{m}}\right)(m+1)}{2mCR}\right]^{\frac{m}{m+1}}$$

Differentiating w.r.t. z, we obtain

$$\frac{d\eta}{dz} = \left(\frac{m}{m+1}\right)\left[\frac{\left(Q - \eta_s^2\frac{R}{2} + 2mcR\,\eta_s^{\frac{m+1}{m}}\right)(m+1)}{2mCR}\right]^{\frac{-1}{m+1}} \frac{m+1}{2mcR}\frac{dQ}{dZ}$$

$$= \frac{1}{2CR}\eta^{\left(\frac{m+1}{m} \times \frac{-1}{m+1}\right)}\frac{dQ}{dZ}$$

$$= \frac{1}{2CR}\eta^{\frac{-1}{m}}\frac{dQ}{dZ} \quad -- \quad 7.31$$

$\frac{dQ}{dz}$ is, except for a factor, equal to the integrand of eq. 7.29.

We can now substitute M_v and M_ℓ into the momentum equation 7.5. Details of the mathematics are given in Appendix I. The result is an ordinary differential equation in the form

$$f_1 \frac{d\delta}{dz} = f_2 \frac{dn}{dz} + f_3 \qquad \text{- - - - -} \qquad 7.32$$

where the f's are functions of n, n_s, δ, G and fluid properties. $\frac{dn}{dz}$ is given by eq. 7.31. Thus eq. 7.32 can be integrated numerically.

At each step of the numerical integration, the film temperature is updated. This is equivalent to evaluating the wall temperature and is considered in the next section.

VII.6 Prediction of Wall Temperature

Assume that the total heat transfer rate at the wall can be divided into a conduction and a radiation component, i.e.

$$q_{TOT} = q_{cond} + q_{rad}$$

It has been shown by Nicholas (1965) that such assumption is justified for optically thin* gas.

(i) Conduction Component

For the conduction component, we assume that most of the resistance to heat transfer lies in the laminar sublayer adjacent to the heated wall. If we denote this sublayer thickness by δ_s, then the conduction component is given by

$$q_{cond} = 2\pi R \frac{k_v(T_w - T_s)}{\delta_s} \Delta z$$

---

* An optically thin gas means either self-absorption is negligible or the dimension of the gas body is small. See Appendix H for detailed discussions.

In the laminar vapor film region, δ_s is taken to be the sum of the distances from the wall to the point of maximum velocity and one half from the point of maximum velocity to the interface. The reason is that from the point of maximum velocity to the vapor-liquid interface, the turbulence induced by the irregularity of the interface results in less resistance for heat transfer. Such assumption also gives a smoother transition from the laminar region to the turbulent region. From section VII.2.1, the maximum velocity occurs at

$$\frac{du}{dy} = \frac{g\rho_\ell \delta}{2\mu_v}\left(1 - \frac{2y}{\delta}\right) + \frac{U_\ell}{\delta} = 0$$

$$\text{or } y = \frac{\delta}{2}\left[1 + \frac{2\mu_v U_\ell}{g\rho_\ell \delta^2}\right]$$

Close to the point where the vapor film is first created, y may be greater than δ. In this case, the maximum velocity occurs at the interface and therefore $y = \delta$.

In the turbulent region δ_s is given by

$$\delta_s = \frac{\eta_s}{2\eta - \eta_s}\,\delta$$

(ii) Radiation Component

The radiation component is evaluated by assuming radiation exchange between the tube wall and the liquid core, with an absorbing medium in between. Details of the calculation are given in Appendix H.

VIII.0 DISCUSSION OF THEORETICAL MODEL

VIII.1 General

The theoretical model developed in the last chapter incorporates the effects of (i) mass flux, (ii) inlet subcooling, (iii) axial location, and (iv) system pressure to predict the surface temperature at a given heat flux and an inlet condition. Most of the uncertainties lie in the value of the thermal diffusivity of the liquid core and the thickness of the dimensionless laminar sublayer n_s. In this chapter, the parametric effects on the predicted wall temperature and heat transfer coefficient are discussed. Unless otherwise stated, the standard run has the following values for the parameters:

D_e = 0.01194 m

n^* = 10

P = 105 kPa

C_1 = 1.5 (This is a factor to adjust the interfacial friction factor, see equation 7.14.)

VIII.2 Effect of Mass Flux

At the same inlet condition, the quality at any axial location depends on the mass and heat fluxes. Therefore, to compare the effect of mass flux on a local condition basis, the inlet temperature is kept identical and the heat flux is set proportional to the mass flux, so that the local equilibrium quality is identical.

The wall temperatures predicted by the model are shown in Figure 50. The discontinuities in the curves are due to the transition from laminar to turbulent film flow. In the theoretical model, laminar flow is assumed to change to turbulent flow when the local Reynolds number n_s is greater than n^*. The neglect of a transition region results in some discontinuity and shows up in the predicted temperature profile. Figure 51 shows schematically the thermal sublayer where all the resistance to heat transfer is assumed to concentrate. By appropriately choosing n^*, the discontinuity in δ_{Th} at the transition point can be minimized. This will be considered in the next chapter.

The overall heat transfer coefficients (based on T_w-T_s) are shown in Figure 52. This 'overall' HTC includes the contribution by thermal radiation, which ranges approximately from 10% at T_w=600°C to 40% at T_w=1000°C. The 'convective' component of the HTC is shown in Figure 53. It can be seen from these two figures that both the overall and convective heat transfer coefficients increase with mass flux. The increase is greater at higher mass flux.

The increase in the convective component is due to the increase in the vapour film velocity. The predicted vapour velocity is shown in Figure 54. It indicates that the vapour velocity increases with mass flux. The vapour velocity reaches a maximum at around 45-50 cm. This will suggest that the actual flow regime will change into a dispersed flow.

VIII.3 Effect of Local Equilibrium Quality

The predicted heat transfer coefficient at the same inlet temperature and mass flux are compared in Figure 55. It can be seen that,

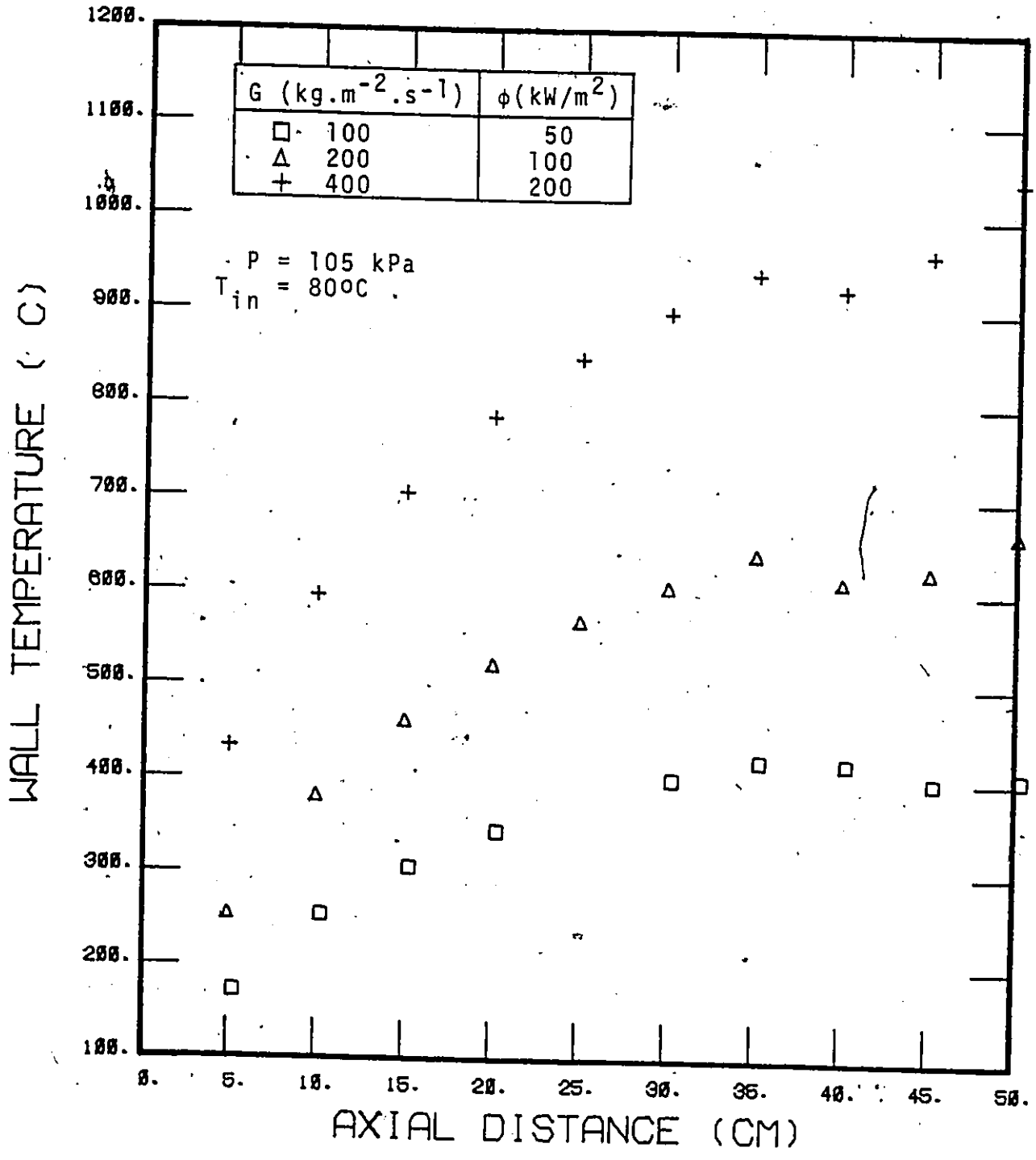

FIGURE 50 PREDICTED WALL TEMPERATURE

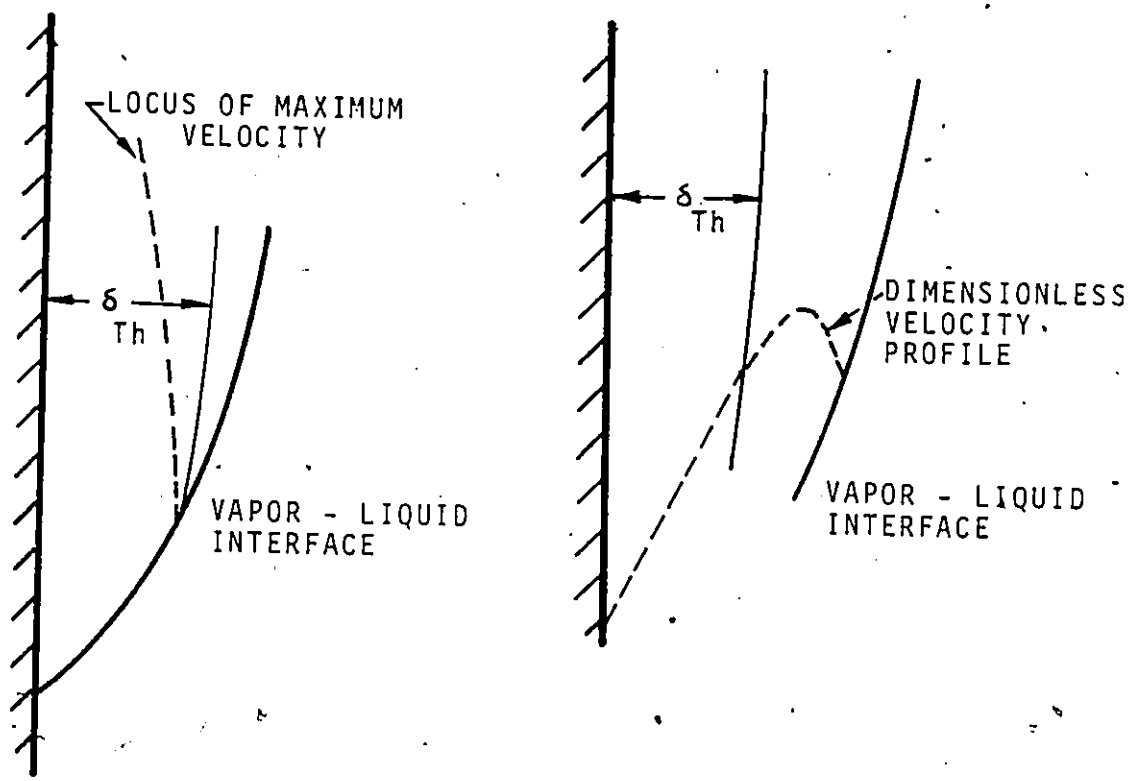

(i) LAMINAR VAPOR FILM

(ii) TURBULENT VAPOR FILM

FIGURE 51 DEFINITION OF THERMAL LAMINAR SUBLAYER

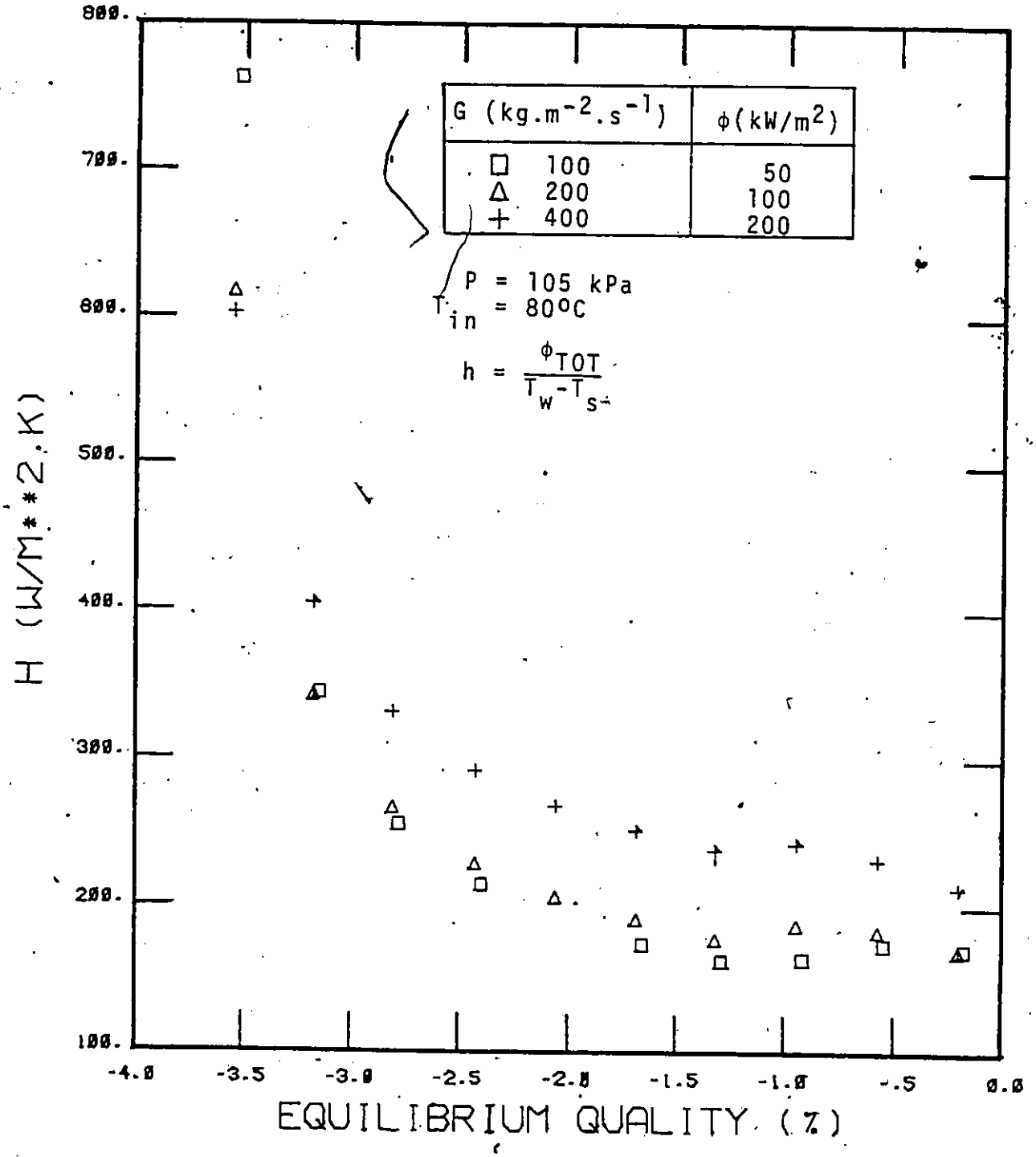

FIGURE 52 HEAT TRANSFER COEFFICIENT AS A FUNCTION OF EQUILIBRIUM QUALITY

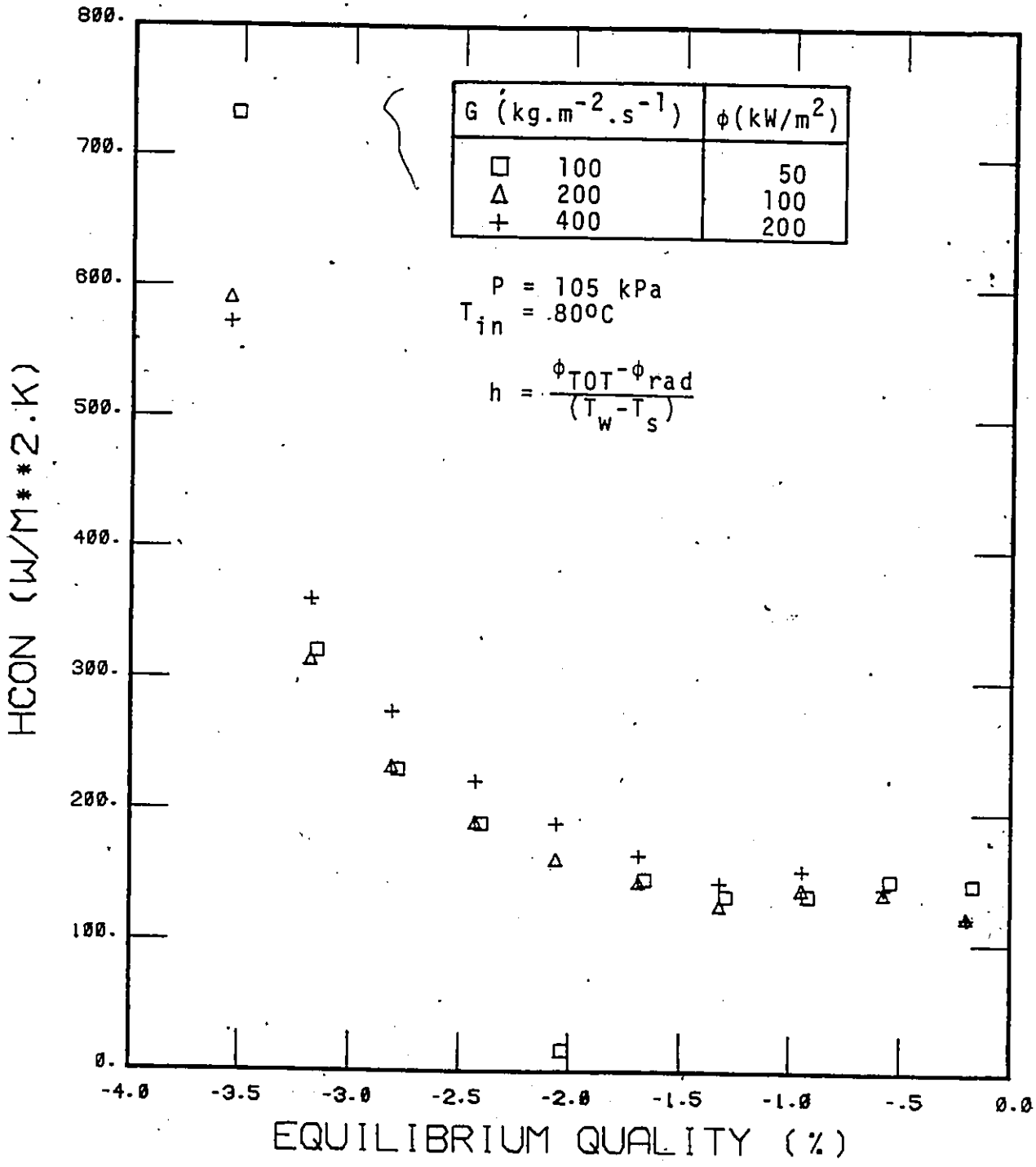

FIGURE 53 CONVECTIVE COMPONENT OF HEAT TRANSFER COEFFICIENT

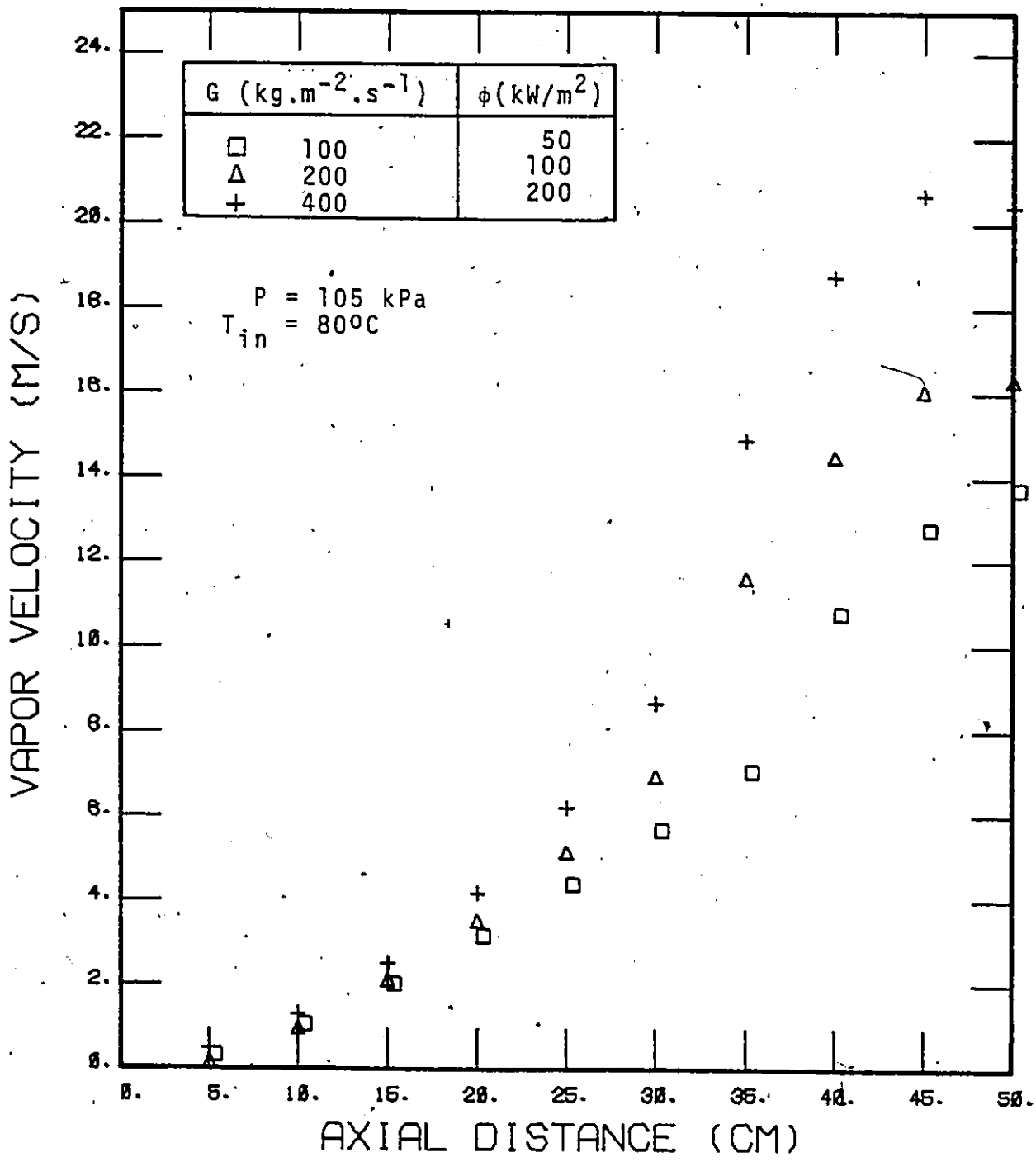

FIGURE 54 PREDICTED VAPOR FILM VELOCITY

at the same inlet condition, the overall heat transfer coefficient decreases with the local equilibrium quality. Figure 56 shows the same effect at a mass flux of 400 $kg.m^{-2}.s^{-1}$.

The increase in the heat transfer coefficient in the subcooled region is due primarily to the increased portion of the total heat flux transferred to the liquid core. This results in less vapour generation and consequently a thinner vapour film.

VIII.4 Effect of Inlet Subcooling

The effect on the heat transfer coefficient of an increase in inlet subcooling at a fixed mass flux is shown in Figure 57. At higher inlet subcoolings, higher heat fluxes are required to maintain the tube in film boiling. Therefore, the comparison shown in this figure is based on the same outlet equilibrium quality at the end of a 60 cm tube. The improved heat transfer is most noticeable near the entrance. Further downstream the heat transfer coefficients for different inlet subcooling approach each other.

The improved heat transfer is due to the higher heat transfer to the liquid core near the entrance. The development of the temperature profile of the liquid core for one typical case is shown in Figure 58. It shows a high temperature gradient at the entrance, which subsequently diminishes as the thermal boundary layer develops. Figure 59 shows the percentage of the total heat flux transferred to the liquid core. At higher inlet subcooling, a higher percentage is used to heat up the liquid core. The increase in the percentage of liquid core heat flux at

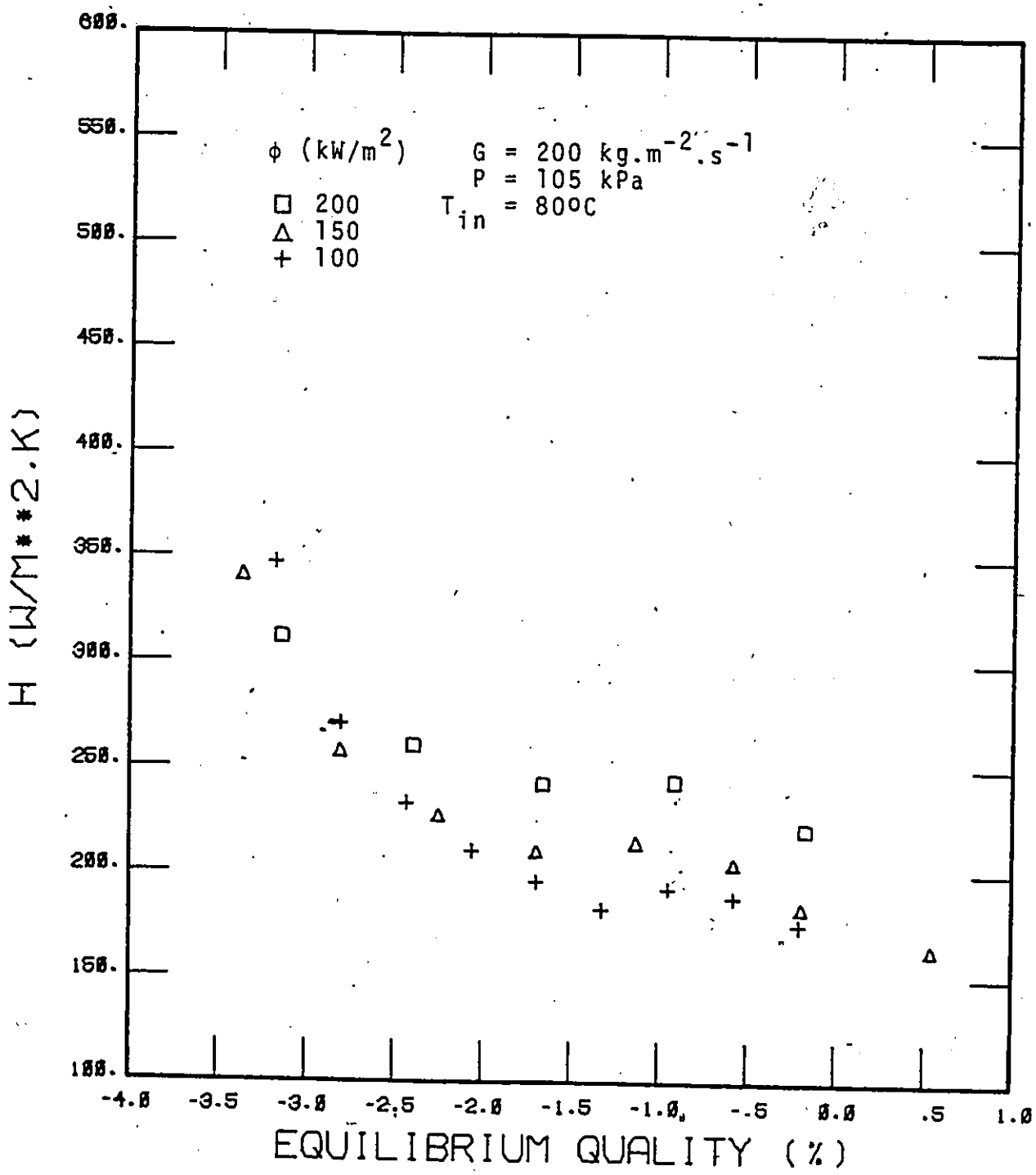

FIGURE 55 EFFECT OF EQUILIBRIUM QUALITY ON THE HEAT TRANSFER COEFFICIENT

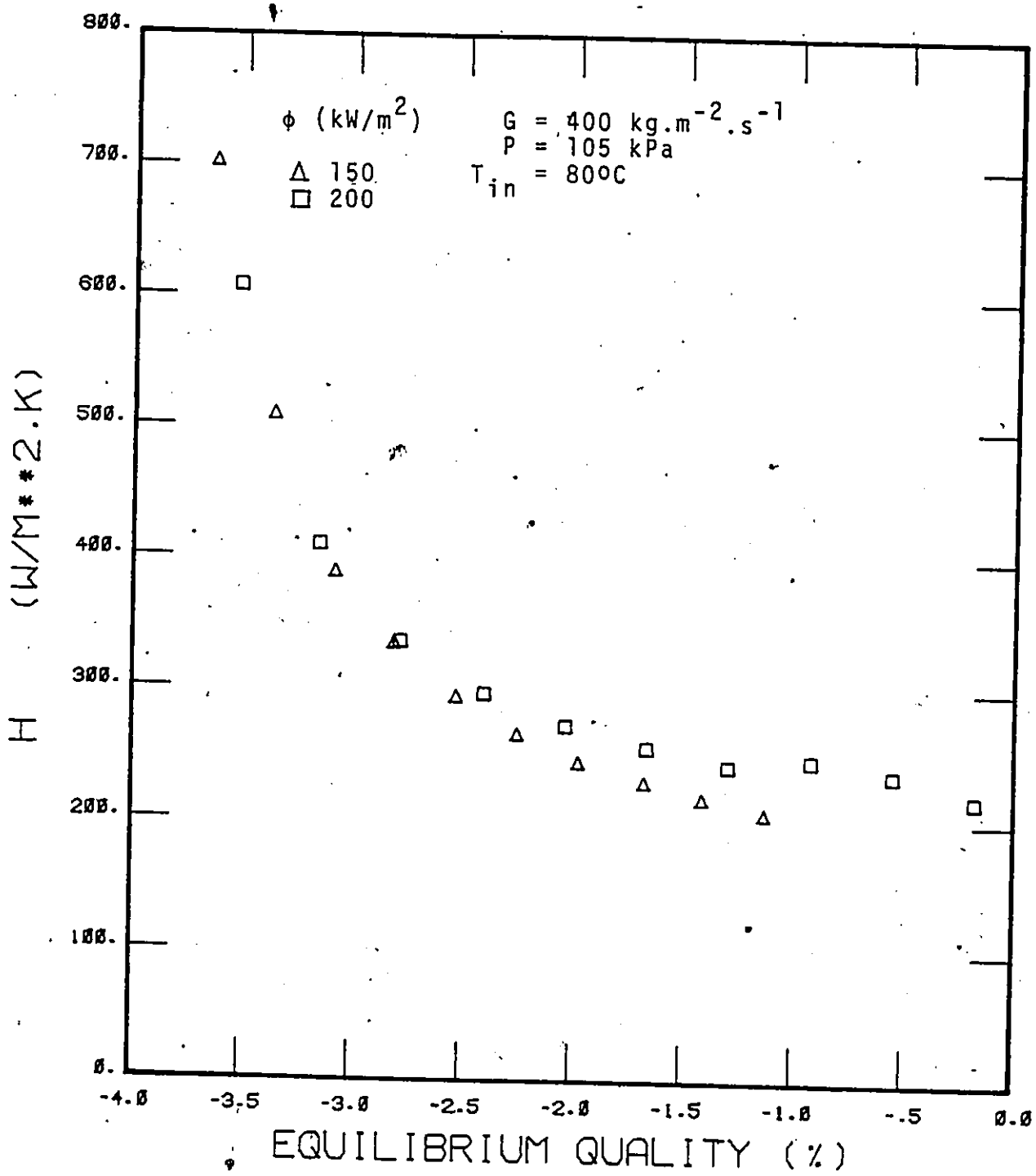

FIGURE 56 EFFECT OF EQUILIBRIUM QUALITY ON THE HEAT TRANSFER COEFFICIENT

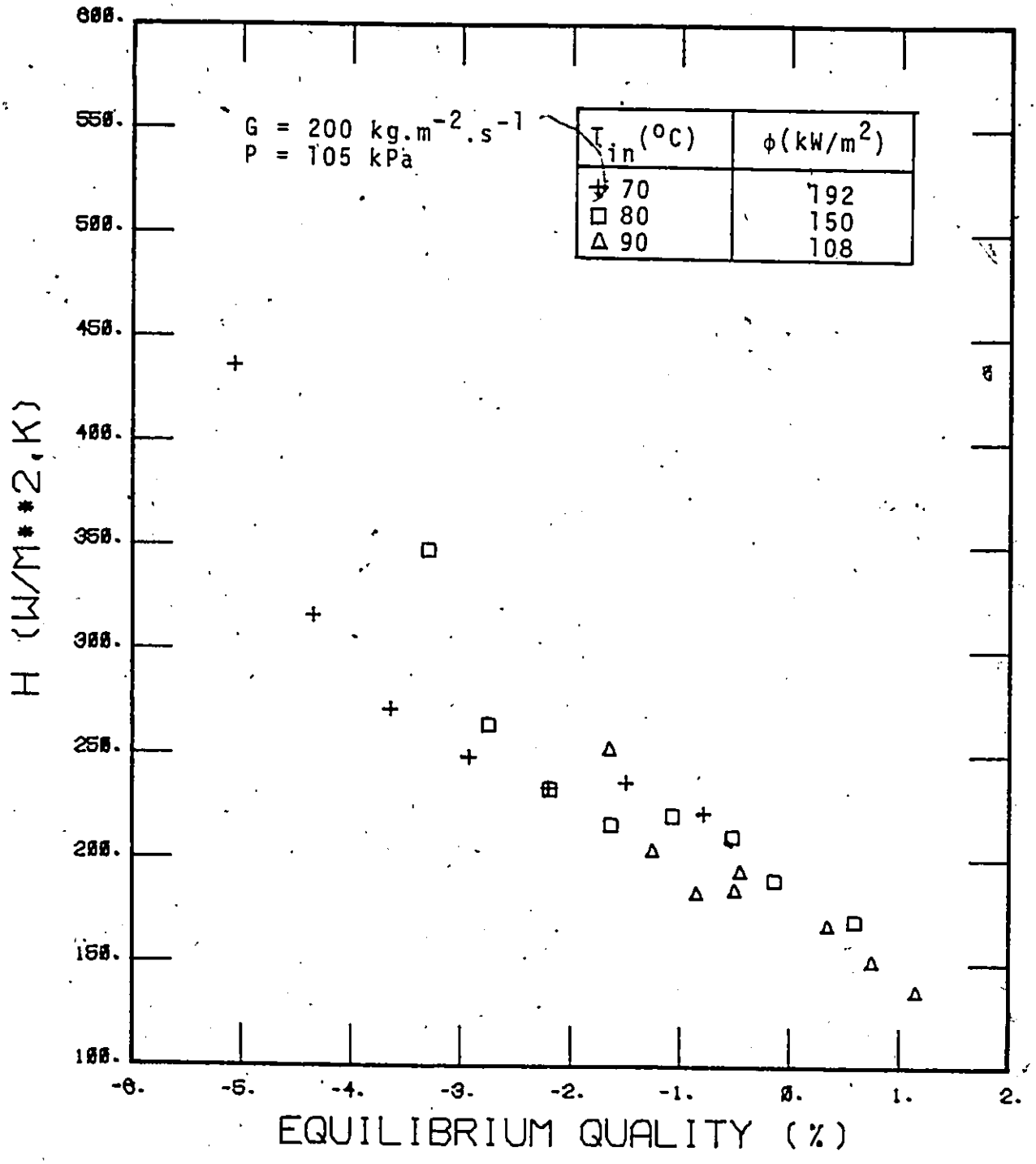

FIGURE 57 EFFECT OF INLET SUBCOOLING ON THE HEAT TRANSFER COEFFICIENT

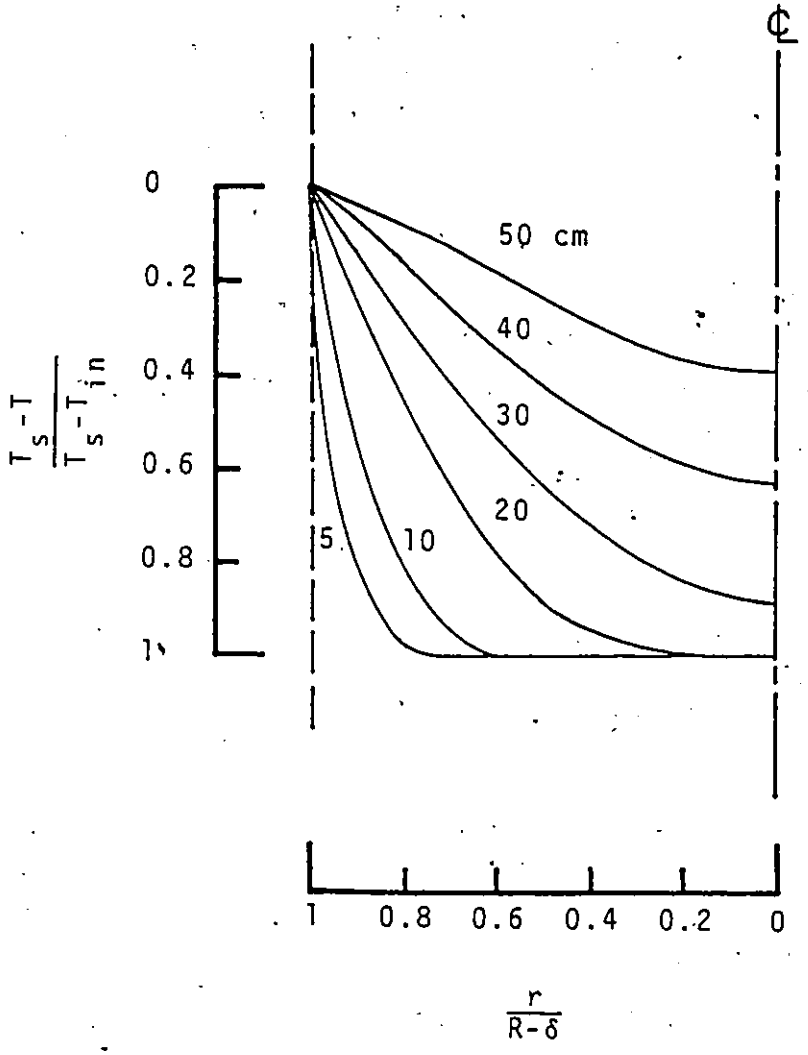

G = 200 kg.m^{-2}.s^{-1}
T_{in} = 80°C
R = 0.00597m
NUMBERS ON CURVES INDICATE AXIAL DISTANCE

FIGURE 58 DEVELOPMENT OF THE TEMPERATURE PROFILE IN THE LIQUID CORE

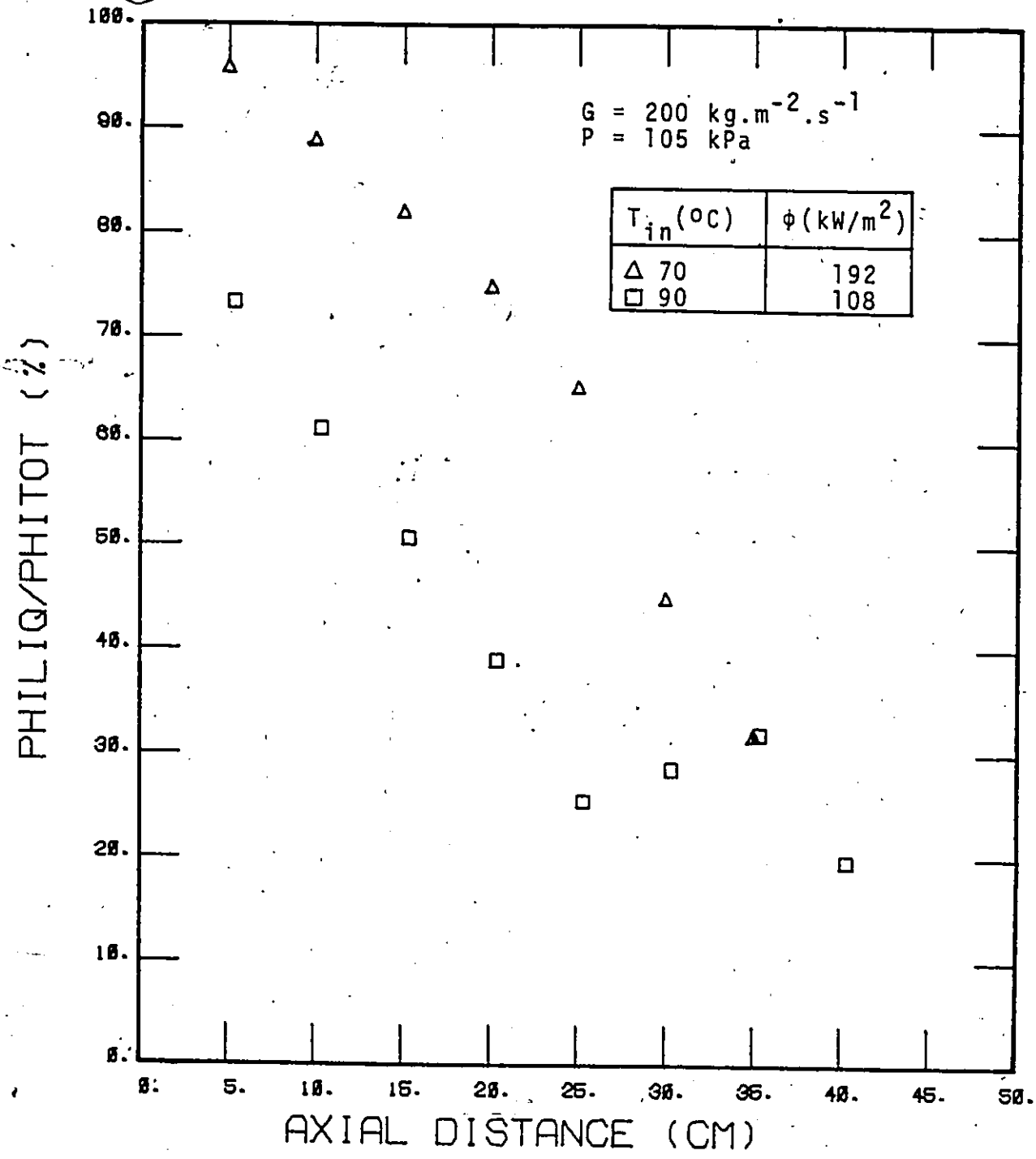

FIGURE 59 FRACTION OF THE TOTAL HEAT FLUX TRANSFERRED TO THE LIQUID CORE

around 25 cm is due to the increase in the turbulent thermal diffusivity. Had this diffusivity remain constant along the boiling length, the heat flux to the liquid core would have decreased monotonically. However, in the model the diffusivity is assumed to increase with the vapour film thickness. Physically, this can be interpreted as the increase in the waviness of the vapour-liquid interface. Consequently the resistance to heat transfer is reduced.

Based on the results of Figure 57, an entrance length* of 6 L/D's is obtained. This is much shorter than in tube flow and can be attributed to the increase in turbulence in the liquid core due to the creation of the vapour film.

In the experimental program of this study, a hot patch was used to establish film boiling at the entrance. As discussed earlier, CHF occurred initially and developed into inverted annular film boiling. It is not certain how the radial temperature profile of the liquid core adjusts under such circumstance. In the theoretical analysis, the liquid core is assumed to be at a uniform temperature at the entrance. This results in the very distinct entrance effect. Referring back to Figures 31-37 where the convective Nusselt number is plotted against the equilibrium quality, the "scatter" can be attributed to this entrance effect, although at a reduced magnitude.

* When a fluid flows into a heated channel, the temperature at the boundary changes instantaneously from its temperature prior to entrance to the temperature of the channel. The heat transfer coefficient is therefore infinite at the entrance. As the thermal boundary layer develops, the heat transfer coefficient diminishes. An entrance length is the length over which the heat transfer coefficient approaches the "fully-developed" HTC.

VIII.5 Actual Quality in Subcooled Film Boiling

In low quality inverted annular film boiling, the vapour is superheated above the saturation temperature, while the liquid remains subcooled. Therefore, the equilibrium quality can be negative. The actual quality, however, is always between 0 and 1. Its value depends on the actual vapour temperature and the slip velocity. In the theoretical model, the vapour film is assumed to be at the "film" temperature ($=0.5*(T_w+T_{sat})$). The velocity distribution across the film is either calculated (for laminar film) or assumed to follow the law of the wall (turbulent film). The vapour mass flux is obtained by integrating across the film. The calculated actual quality ($=G_v/G$) is shown in Figures 60 and 61 for two mass fluxes. It can be seen that, at the same mass flux, the actual quality increases with the heat flux level. This can be explained as follows.

The heat conducted to the liquid core is limited by the temperature gradient in the liquid thermal boundary layer next to the vapour-liquid interface. Figure 62 shows the percentage of the liquid core heat flux (based on tube diameter) at the vapour-liquid interface. At the same mass flux, the thermal boundary layer develops approximately at the same rate (neglecting for the time being the influence due to evaporation). Any increase in the total heat flux will therefore be used for evaporation.

Figures 60 and 61 show that the actual quality depends not only on the equilibrium quality, as is usually observed in higher quality (dispersed flow) film boiling, but also on the heat flux.

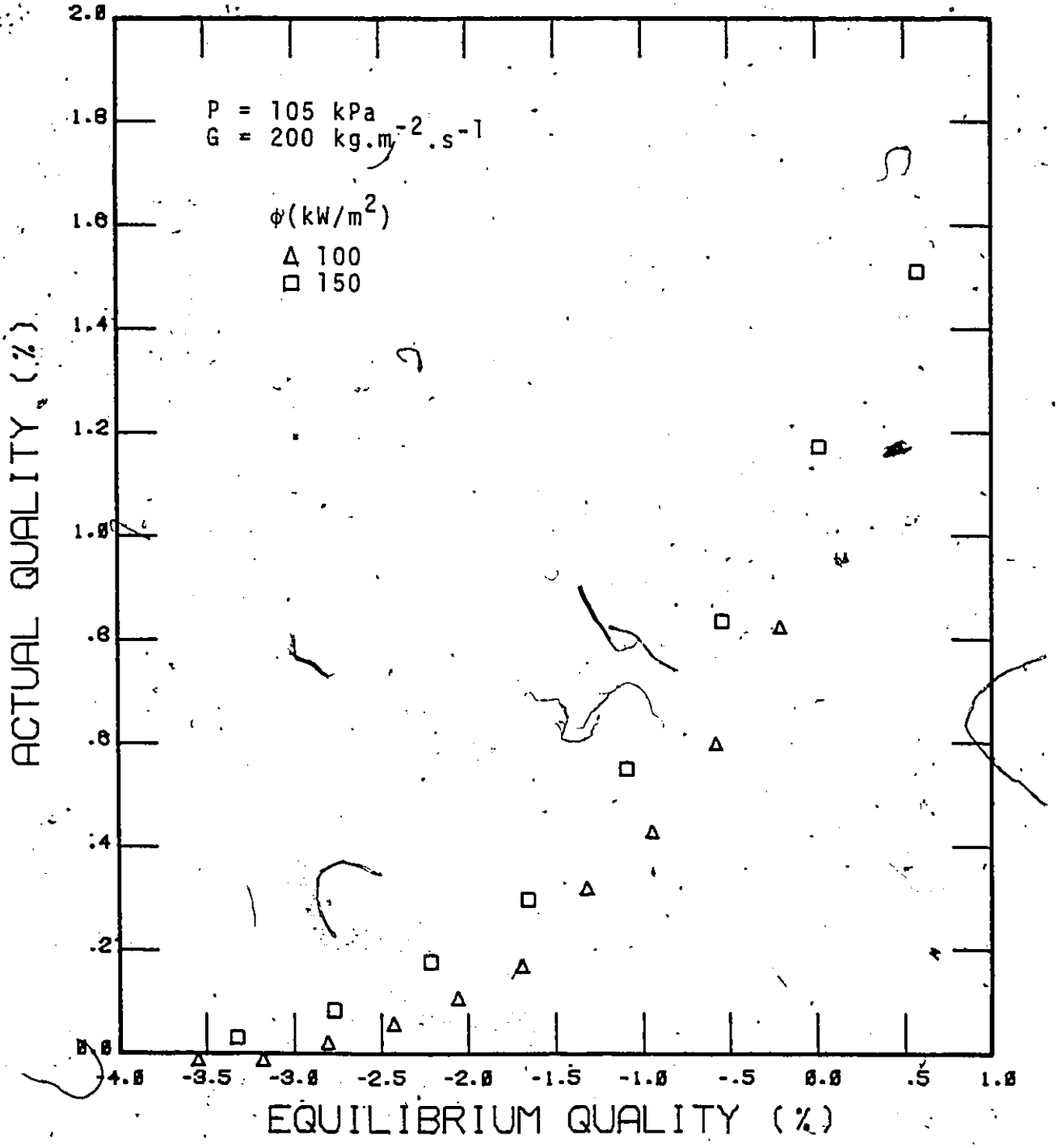

FIGURE 60 PREDICTED ACTUAL QUALITY AT G = 200 kg.m^{-2}.s^{-1}

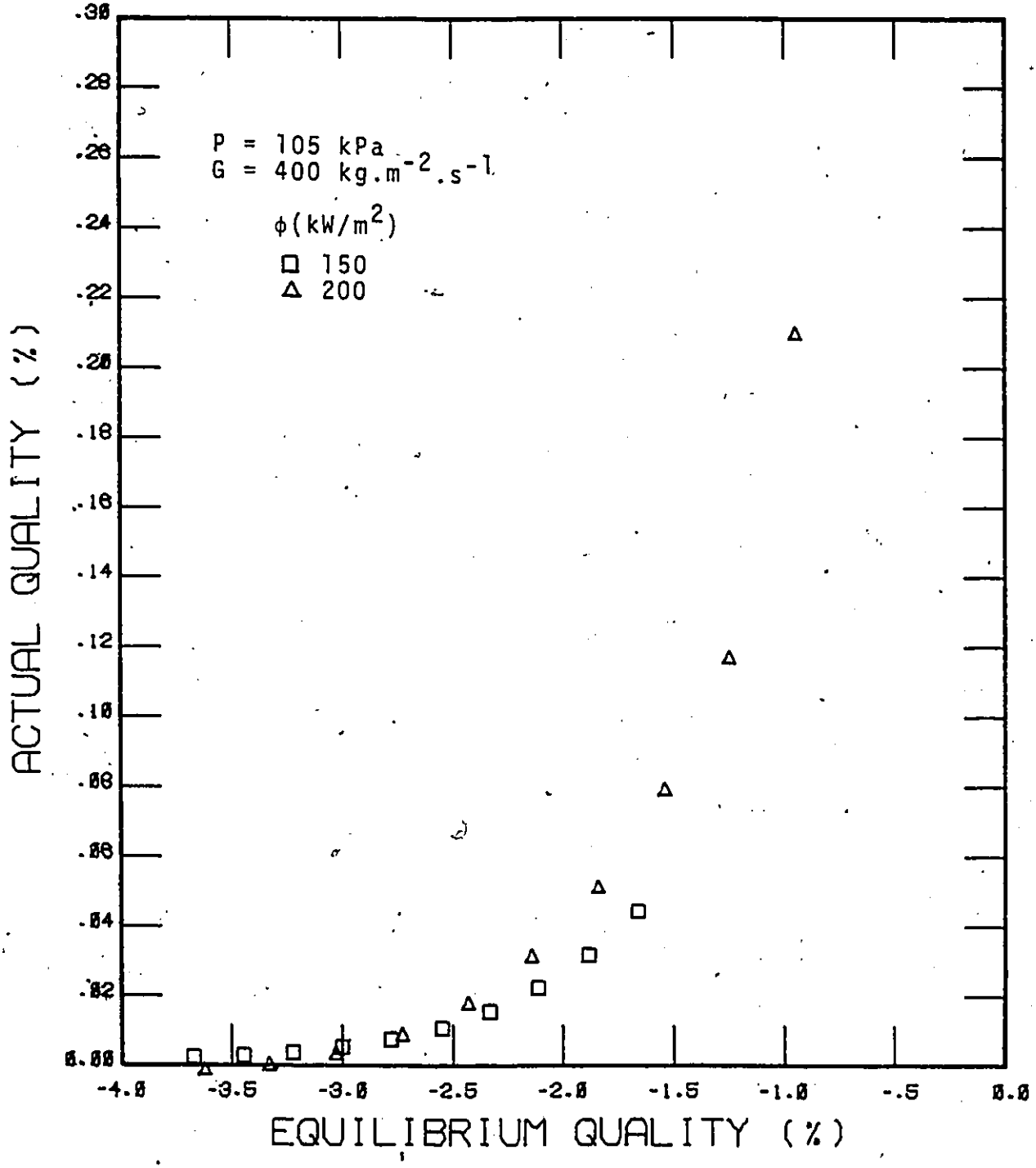

FIGURE 61 PREDICTED ACTUAL QUALITY AT G = 400 $kg.m^{-2}.s^{-1}$

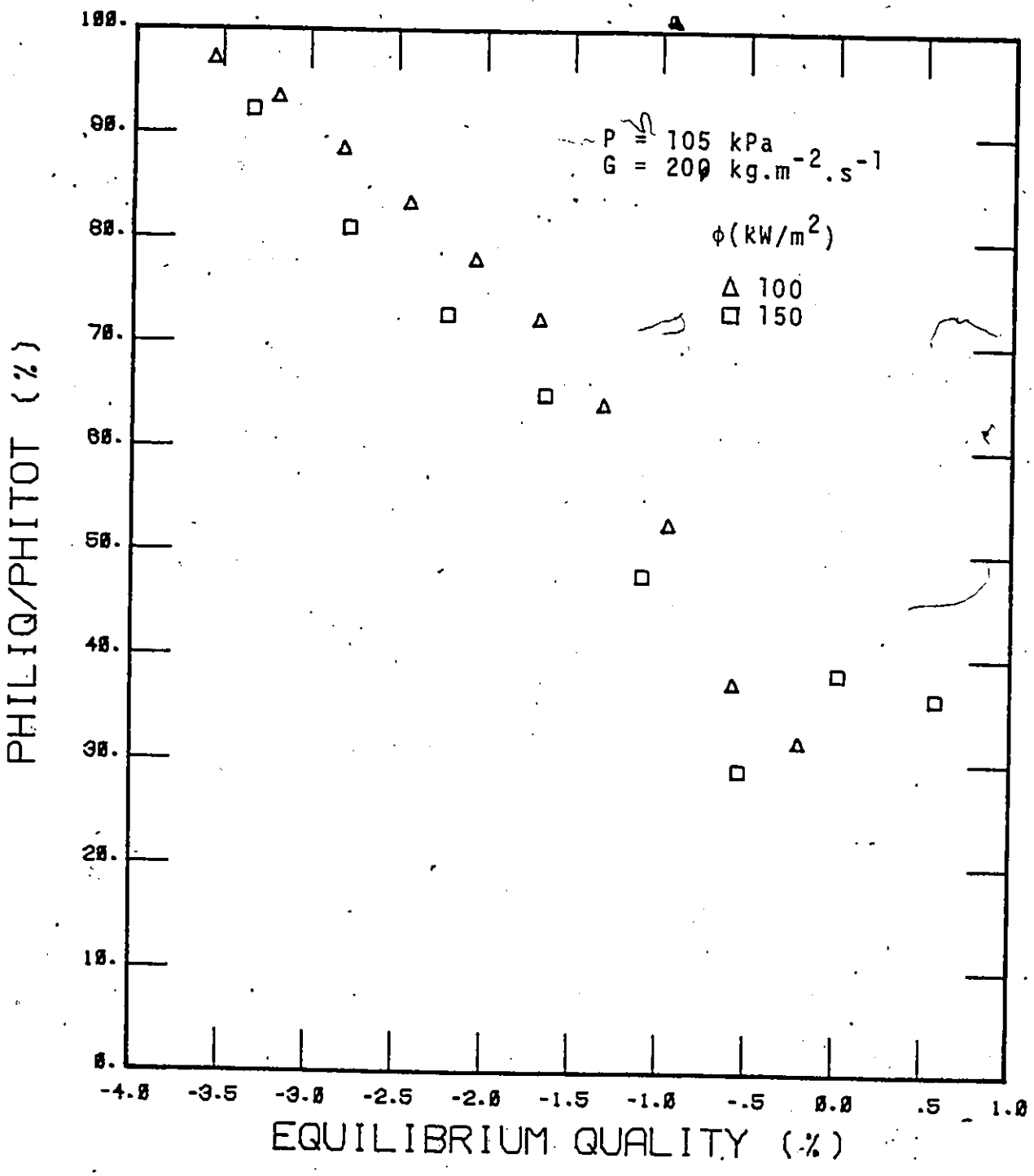

FIGURE 62 PERCENTAGE OF THE TOTAL HEAT FLUX TRANSFERRED TO THE LIQUID CORE

VIII.6 Slip Velocity

In the theoretical model, the velocity of the liquid core is assumed uniform. Nevertheless, it can still vary with the axial distance. The development of the liquid core velocity is shown in Figure 63. The increase is higher for higher initial velocity, i.e., for higher mass flux. This can be explained by considering the hydrodynamics of the vapour film.

The vapour velocities (averaged over the cross-section of the vapour annulus) corresponding to the same conditions as those in Figure 63 have been shown in Figure 54. The vapour film thicknesses are shown in Figure 64. The vapour velocity and the vapour film thickness are primarily determined by the balance between the buoyancy force and the sum of the wall and the interfacial shears. Figure 64 shows that the vapour film is thicker at higher mass flux. A thicker vapour film results in less flow area for the liquid core, and consequently the liquid velocity will increase.

Figure 65 shows the slip under the same system conditions. It indicates that there is less slip at higher mass flux. For higher mass fluxes, the slip reaches a maximum and then gradually decreases. This suggests that the flow is changing to the more homogeneous dispersed flow.

It may seem doubtful whether some of the high slips as shown in this figure actual can exist in inverted annular flow. The high value is actually fictitious. It is due to the neglect of the velocity gradient in both the vapour film and the liquid core in calculating the slip.

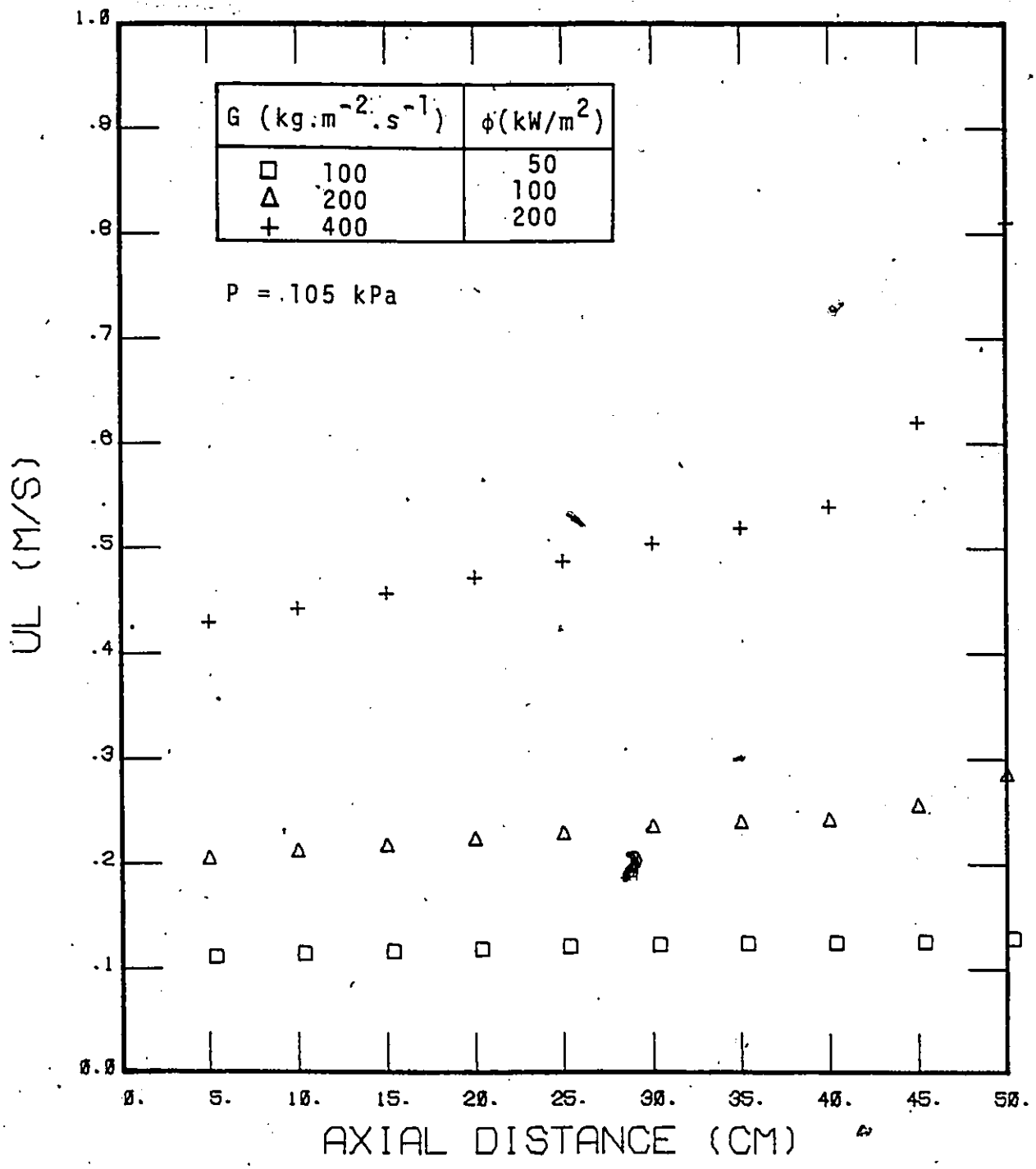

FIGURE 63 PREDICTED LIQUID CORE VELOCITY

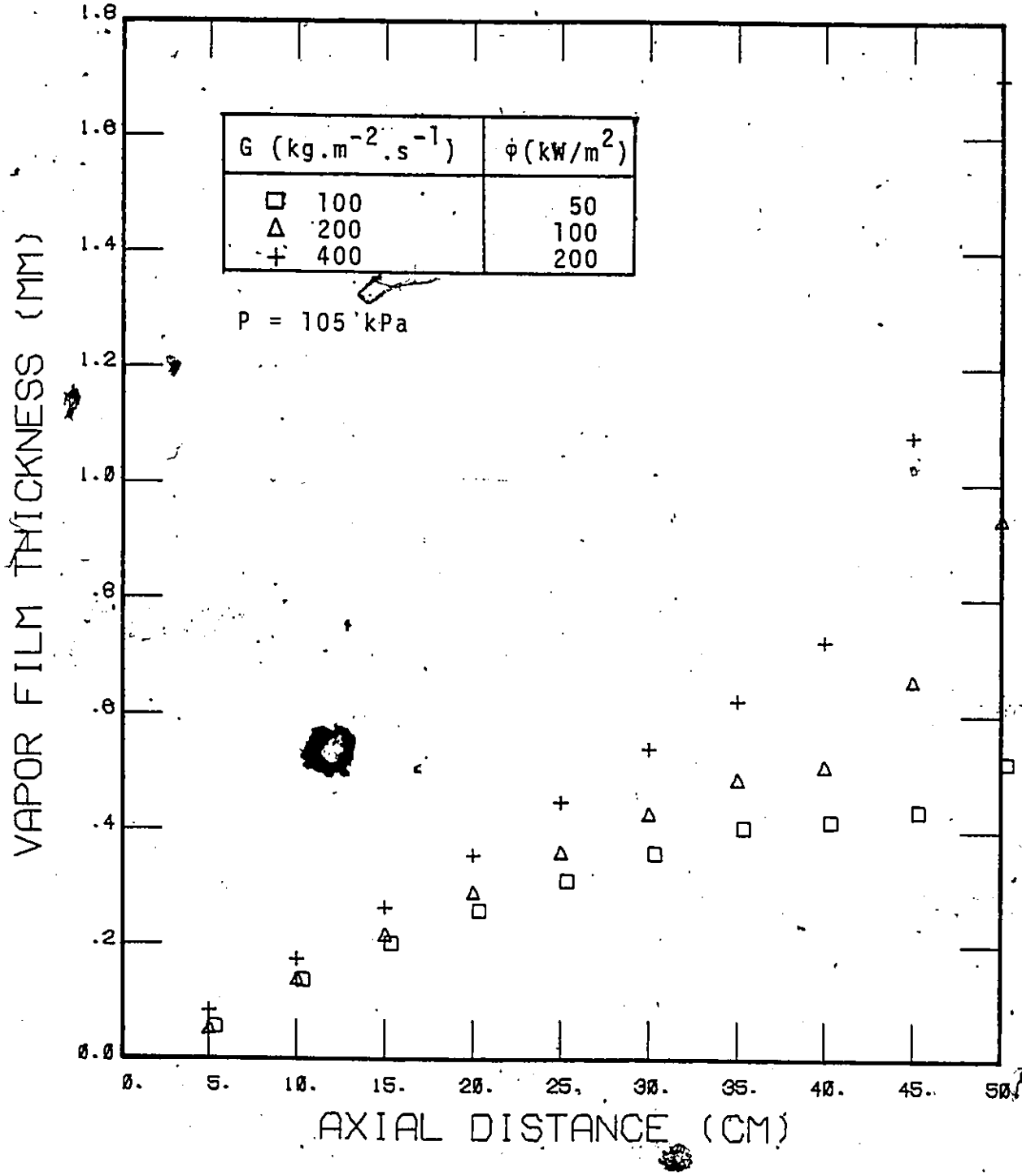

FIGURE 64 PREDICTED VAPOR FILM THICKNESS

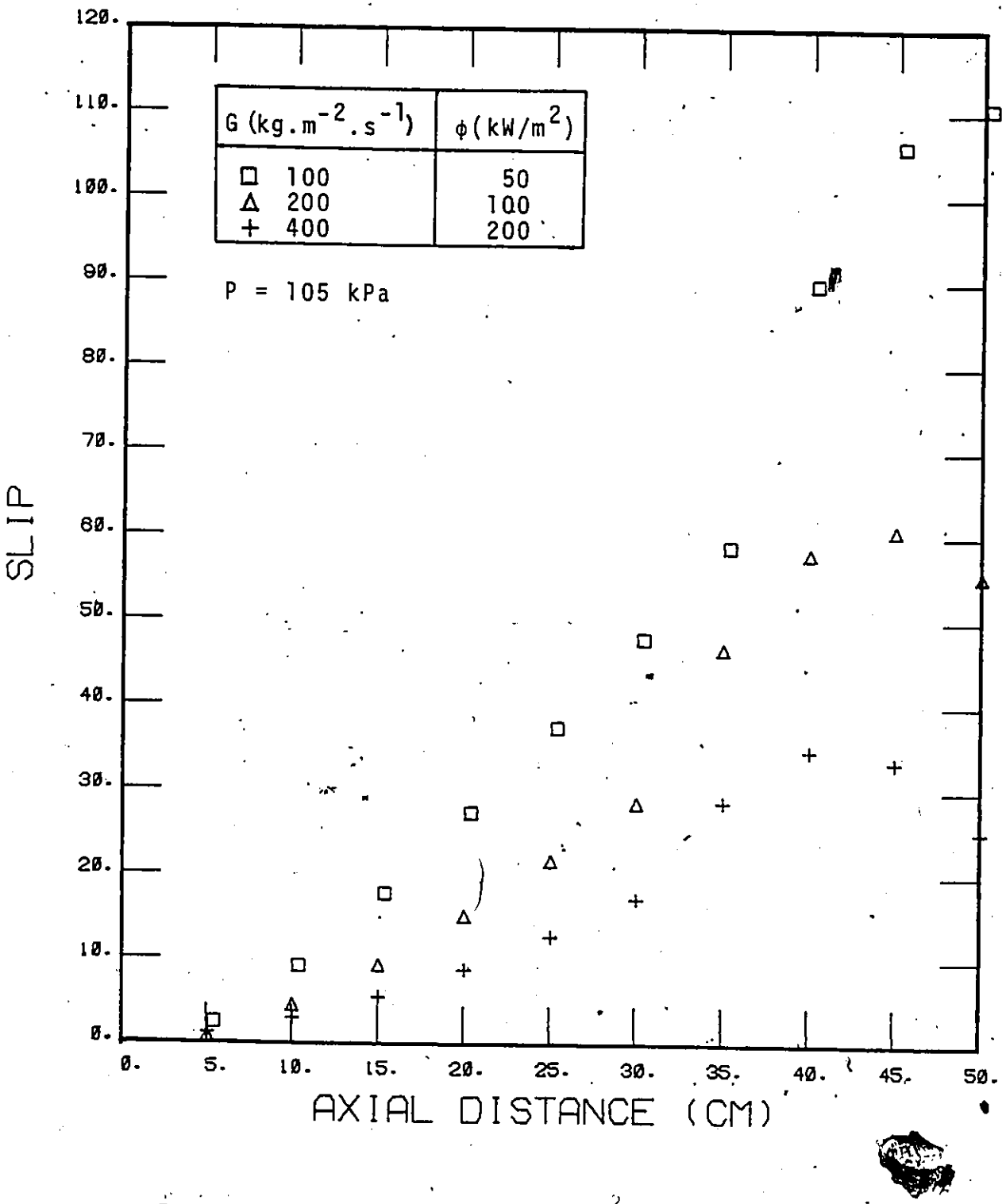

FIGURE 65 PREDICTED SLIP

VIII.7 Effect of System Pressure

Although there is no data obtained at elevated pressure in the present study, the theoretical model is derived for more general situation. Recently, some low quality film boiling data are reported by Groeneveld et al (1981). Figure 66 is reproduced here from this reference. The predictions by the present model are shown for comparison. It seems that there is a shift in the equilibrium quality between the predictions and the experimental data. This is probably due to the exclusion of the "hot patch" region in the theoretical model.

The increases in the heat transfer coefficients with increases in system pressure is due primarily to the increase in vapour density, which results in a thinner vapour film.

VIII.8 Effect of Tube Size

The effect of an increase in the hydraulic diameter on the heat transfer coefficient is shown in Figure 67. It can be seen that, away from the entrance region, the heat transfer coefficients increase with the hydraulic diameter.

Near the entrance, the trend is different. This behaviour can best be explained by considering the vapour film thickness. A thin film means that the heat transfer resistance from the wall to the vapoun-liquid interface is small. On the other hand, the eddy diffusivity of the liquid core is directly proportional to the vapour film thickness. Therefore, as the vapour film grows, the resistance to heat transfer increases in the vapour film but decreases in the liquid core. Depending on which resistance is dominating, the heat transfer coefficient may reach a maximum shortly downstream of the entrance.

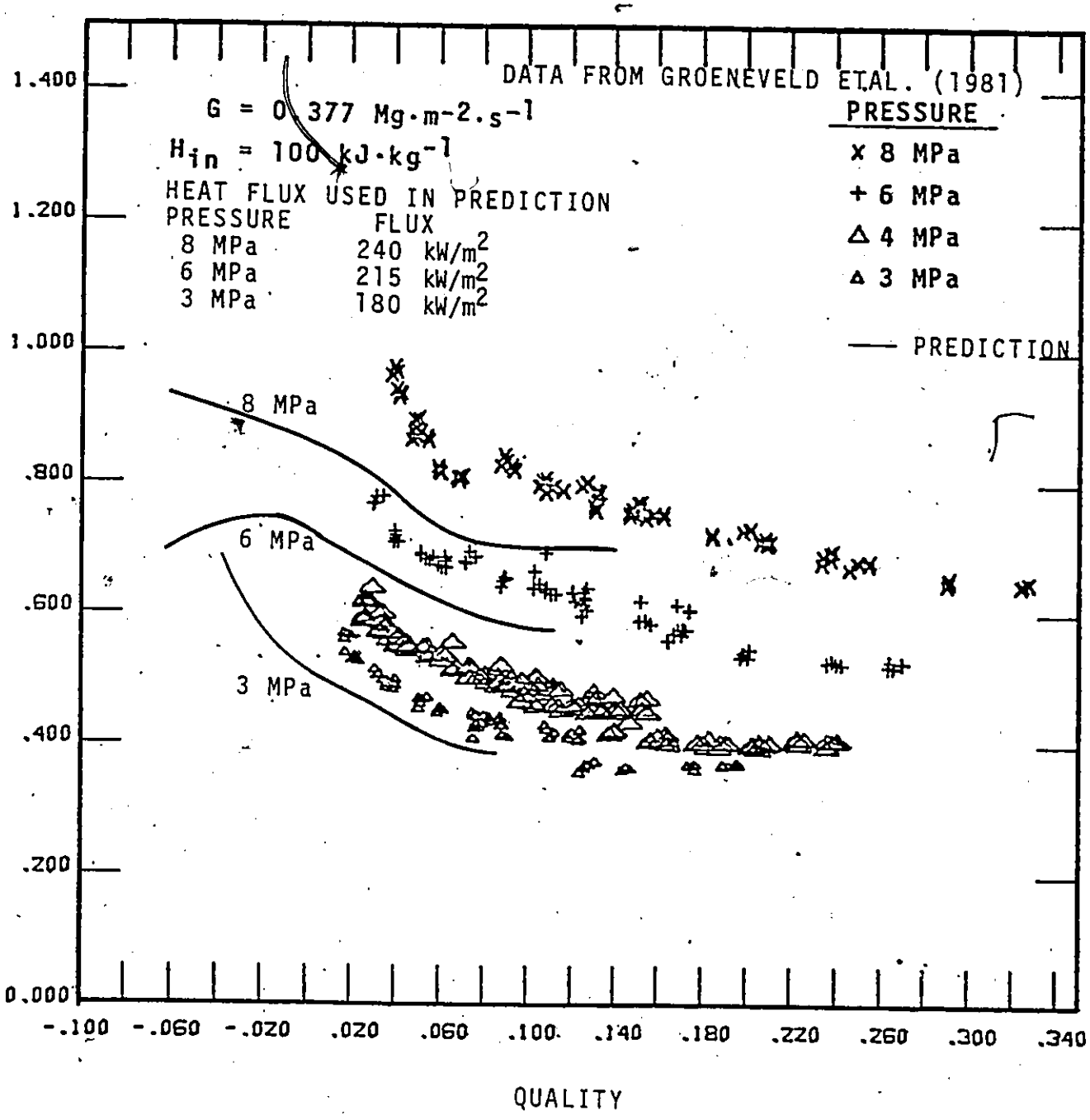

FIGURE 66 THE EFFECT OF PRESSURE ON THE HEAT TRANSFER COEFFICIENT

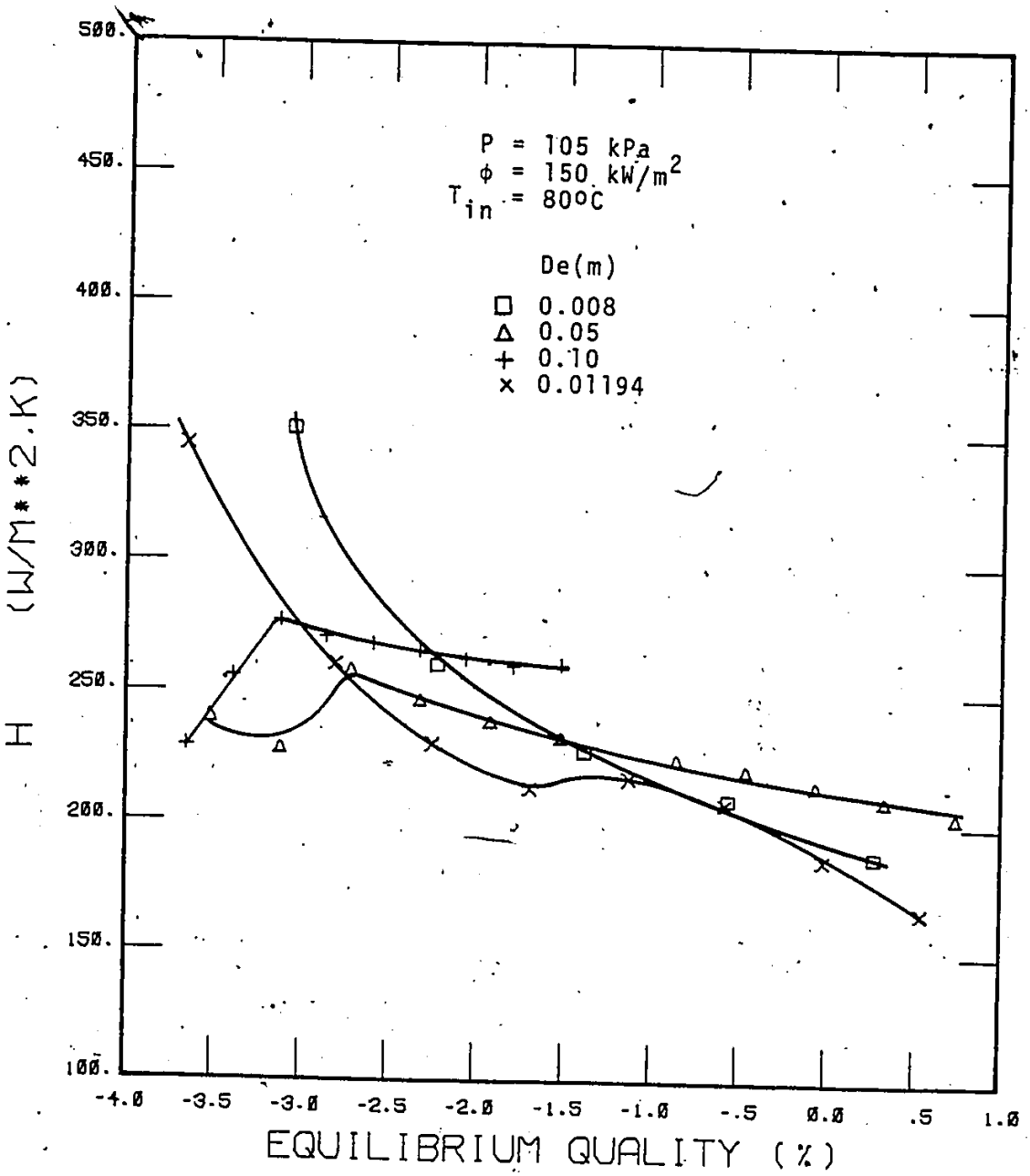

FIGURE 67 EFFECT OF TUBE DIAMETER ON THE FILM BOILING HEAT TRANSFER COEFFICIENT

In a uniformly heated channel, the increase in equilibrium quality is inversely proportional to the hydraulic diameter. In inverted annular film boiling, the heat flux which can be applied to a tube in film boiling is usually limited by the wall temperature at the downstream region where the quality is highest. Therefore, for the same length of tube, the one with a larger diameter can sustain a higher heat flux.

VIII.9 Sensitivity of Model

Most of the uncertainties of the theoretical model lie in the transition between the laminar and turbulent film flow, and in the constitutive equations for the interfacial shear and the liquid eddy diffusivity. Most of the dependence of these quantities on the flow field has been incorporated into the model, leaving only a few factors to be adjusted later. The effects of changes in these factors are discussed in this section.

VIII.9.1 Transition point between laminar and turbulent film

Figure 68 shows the effect of the changeover point from laminar to turbulent. It shows that $n = 12$ gives a smooth transition. A larger n also means that the vapour film is in laminar flow for a longer distance.

VIII.9.2 Interfacial shear

Figure 69 shows the effect of interfacial shear on the predicted temperature. A higher interfacial shear means that the vapour experiences a greater retarding force. This results in a thicker vapour film and consequently higher wall temperatures.

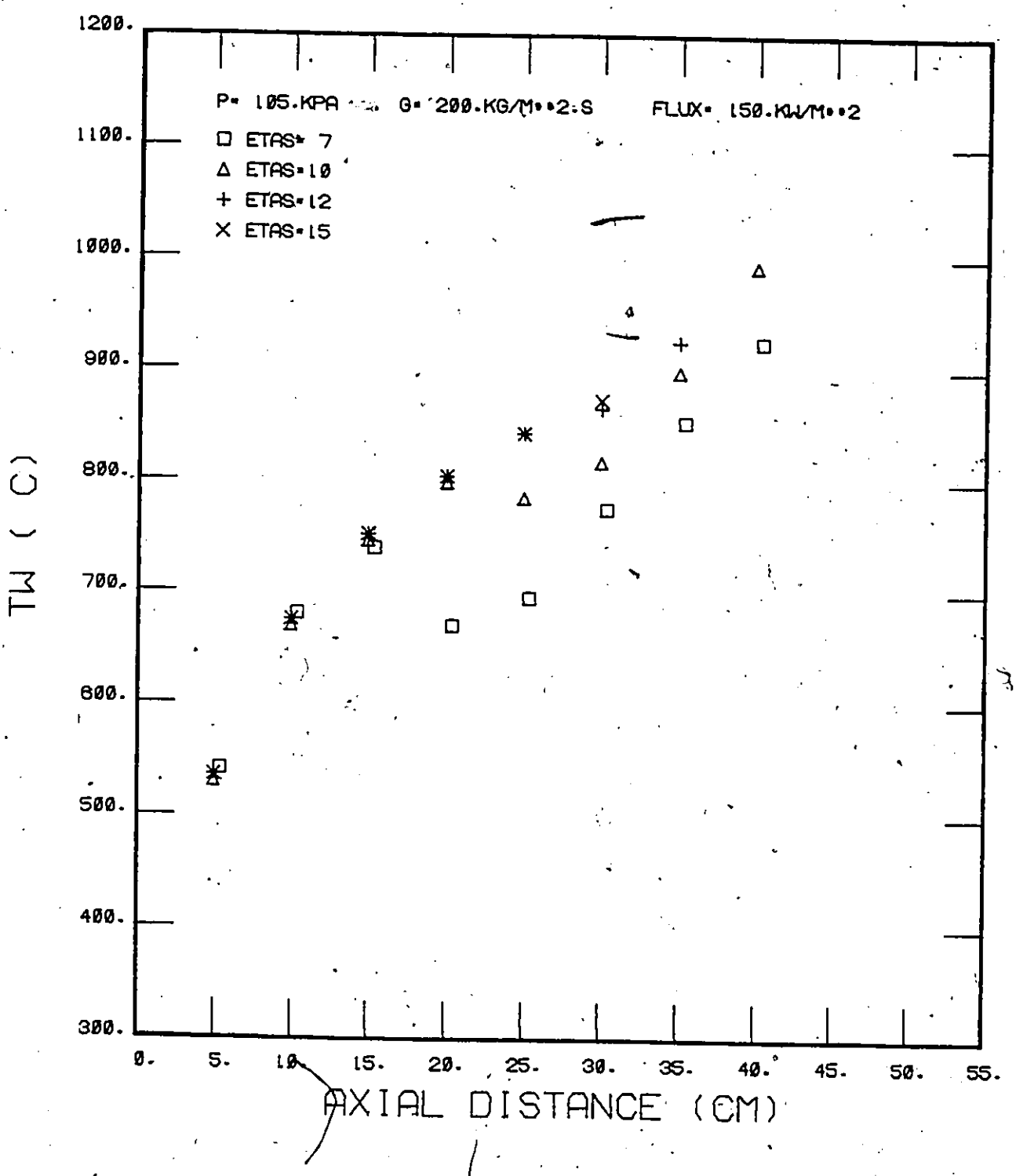

FIGURE 68 EFFECT OF THE TRANSITIONAL POINT BETWEEN LAMINAR AND TURBULENT VAPOR FILM ON THE PREDICTED WALL TEMPERATURES

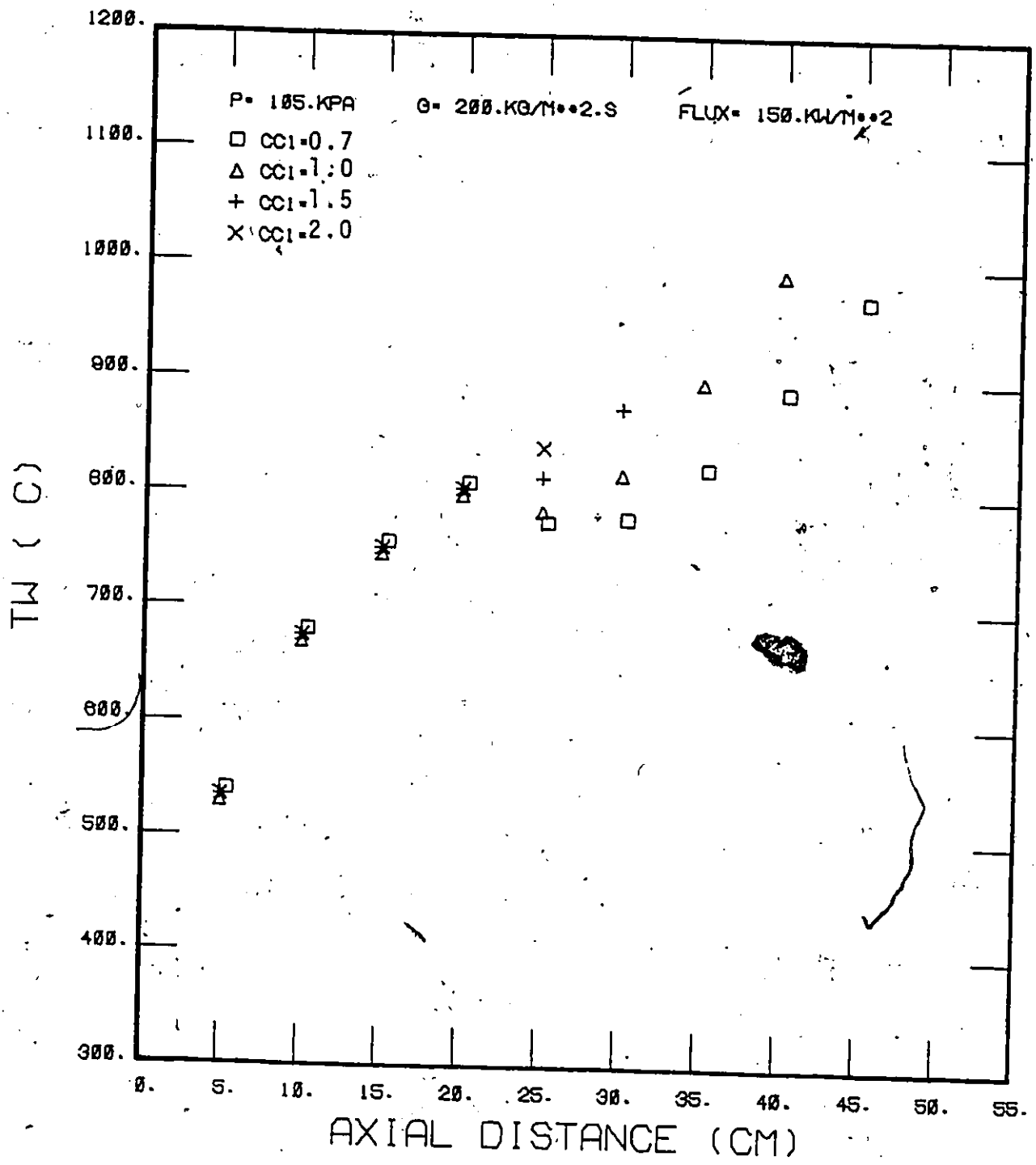

FIGURE 69 EFFECT OF INCREASE IN INTERFACIAL FRICTION ON THE PREDICTED WALL TEMPERATURE

VIII.9.3 Liquid eddy diffusivity

Figure 70 shows the effect of the liquid eddy diffusivity. A higher diffusivity results in a greater fraction of the heat flux conducted to the liquid core and therefore less for vapour generation. Consequently, the vapour film is thinner and the wall temperature is lower.

VIII.9.4 Vapour density

In the development of the model, all of the vapour properties are evaluated at the film temperature. The properties that affect the prediction most significantly are the thermal conductivity and the density. The former affects the prediction of the wall temperatures through its effect on the resistance to heat transfer in the laminar sublayer next to the wall. The latter affects both the predicted wall temperature and void fraction.

Since the laminar sublayer is close to the wall, it seems reasonable to assume that the thermal conductivity can be represented by its value at the film temperature.

The portion of the vapour film beyond the laminar sublayer is assumed not to offer any resistance to heat transfer. This implies that the density of this portion should be evaluated at the saturation temperature. However, in models that contain some simplifying assumptions, it is often found necessary to distort a certain aspect to compensate for it. The ultimate criterion lies in the comparison with the experimental data.

In order to show how the vapour density affects the predicted wall temperature and void fraction, two runs are compared: one with the vapour

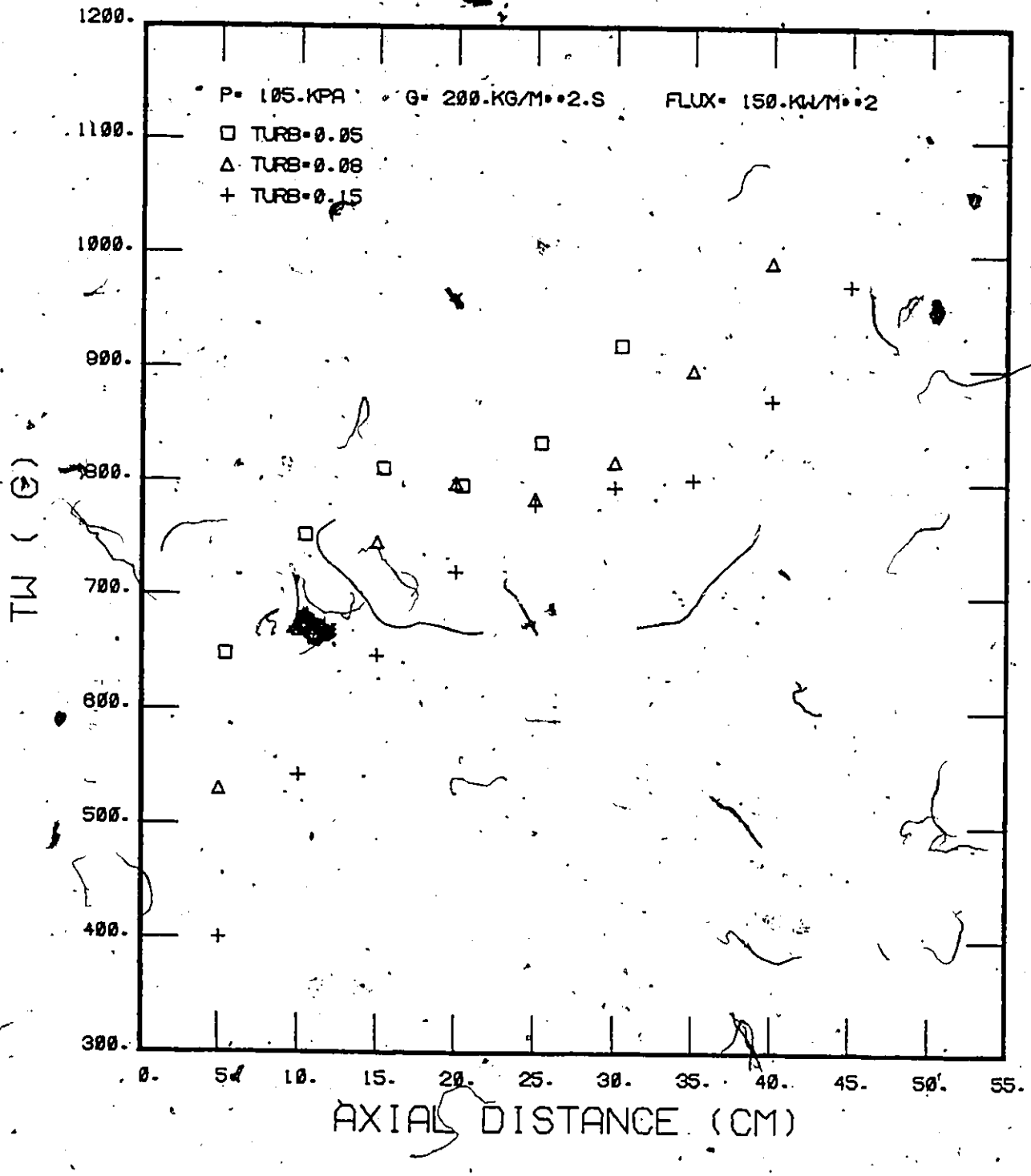

FIGURE 70 EFFECT OF INCREASE IN TURBULENT THERMAL DIFFUSIVITY OF THE LIQUID CORE ON THE PREDICTED WALL TEMPERATURES

density evaluated at the film temperature and the other at the saturation temperature. The results are shown in Figures 71 and 72. It can be seen that the predicted wall temperatures are increased by approximately 100°C when the density is evaluated at the film temperature. The void fraction is also increased.

The measured data favour a higher wall temperatures and void fractions. Therefore, all vapour properties in the model are evaluated at the film temperature.

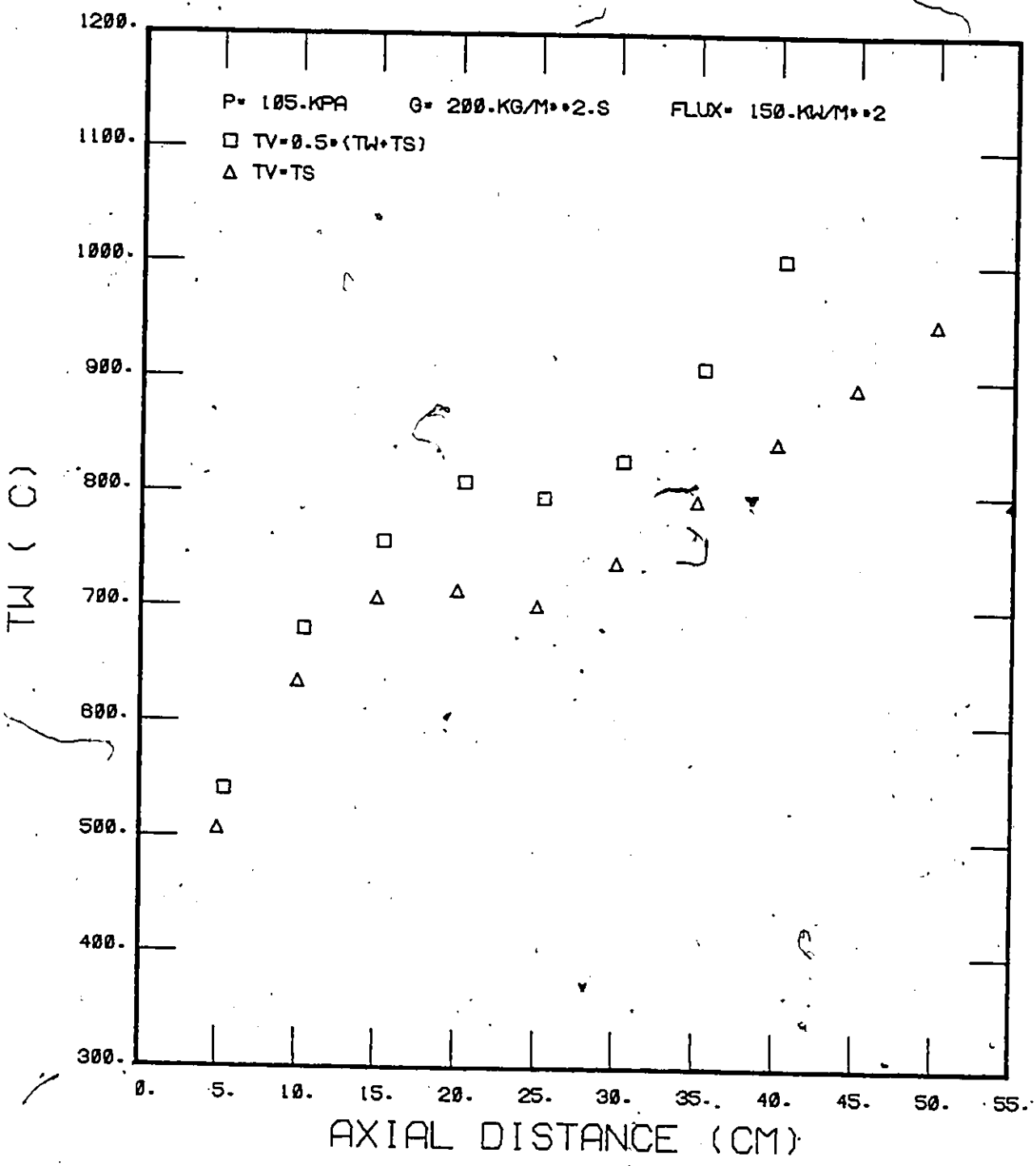

FIGURE 71 EFFECT OF DIFFERENT ASSUMPTIONS OF THE AVERAGE VAPOR TEMPERATURE ON THE PREDICTED WALL TEMPERATURE

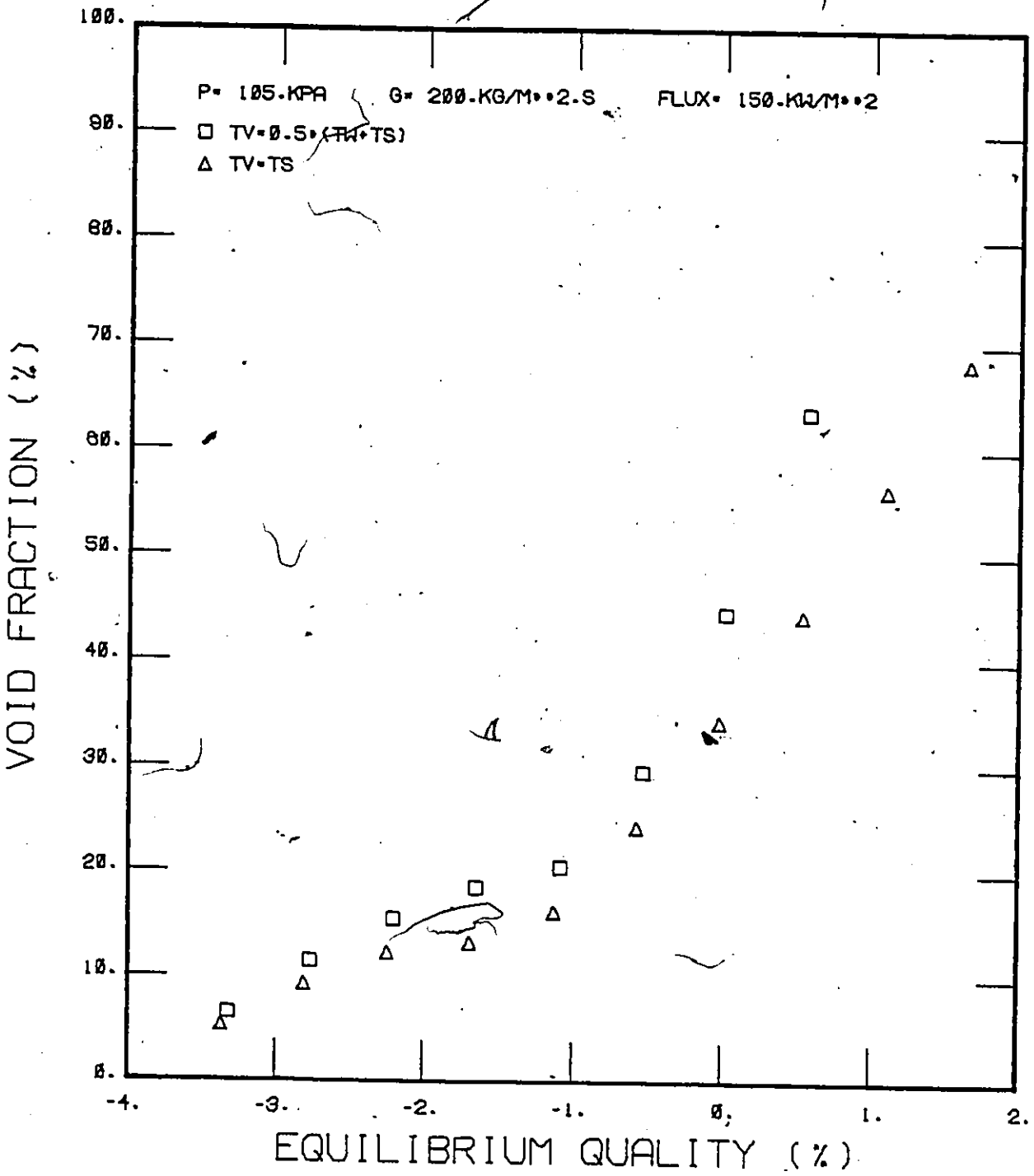

FIGURE 72 PREDICTED VOID FRACTION WITH DIFFERENT ASSUMED VAPOR TEMPERATURES

IX.0 COMPARISON WITH EXPERIMENTAL RESULTS

IX.1 General

The theoretical model is used to predict the experimentally measured wall temperatures. The parameters which are left indeterminate in the model are then chosen to fit the data. To recall briefly, the most sensitive parameters are the interfacial friction and the eddy diffusivity in the liquid core. With the wide range of data in hand, it is possible to use a least squares fit methodology to calculate the best estimates for these parameters. In fact, a preliminary version of FORSIMOPT (Selander 1980)) is available. This computer code will solve the coupled PDE/ODE's and adjust the parameters in the equations to fit the input data. However, the computing time would be prohibitively large, since at present it requires about 100 s computing time on the CDC Cyber 170 to integrate a tube length of 50 cm. In addition, some of the constitutive equations used are only best estimates for the real situation. It does not seem to justify a more precise (in the statistical sense) evaluation of the parameters.

The final method used is to choose various sets of data and compare them with the predictions graphically. For each set of data, the average of the pressures at the inlet and outlet of the film boiling section as calculated in the data reduction is used as the system pressure. In addition, the average heat flux is used as the boundary condition. The initial conditions are the mass flux and the inlet temperature.

The value of the inlet temperature requires some explanation. The theoretical model does not take into consideration the inception of CHF at the start of the test section. It is not certain how this would affect the radial temperature profile of the liquid core. Therefore, in

the theoretical prediction, two initial conditions are considered: in one case the inlet temperature is set equal to the measured inlet temperature, while in the other case an "artificial" inlet temperature is used so as to match the equilibrium quality at the first thermocouple location. For those runs with high mass fluxes, these two values are not very different and the predictions should bound the measured data.

Such "eyeball" fitting produces the following estimates for the parameters

(i) Transition between laminar and turbulent vapour film, $n_s = 12$

(ii) Proportionality constant for interfacial shear, $C_1 = 1.5$

(iii) Proportionality constant for eddy diffusivity, TURB = 0.08

In addition, the theoretical model is only written for inverted annular flow. As the thickness of the vapor film increases, some of the assumptions may break down and will cause the predicted temperature to blow up. There are also uncertainties in the transport properties of superheated steam (Groeneveld et al (1981)). Therefore the computer solution is allowed to proceed up to a film thickness of 0.5R (α = 75%), or a wall temperature of 1600°C, whichever occurs first.

IX.2 Prediction of Wall Temperature

The predictions are shown in Figures 73-86. It can be seen that, in general, the trend and the magnitude of the wall temperatures are correctly predicted. The model performs best at high subcoolings, when it can safely be ascertained that the flow is inverted annular. At close to saturated inlet conditions, the generated vapour will probably be entrained in the liquid core. This effect has not been modelled.

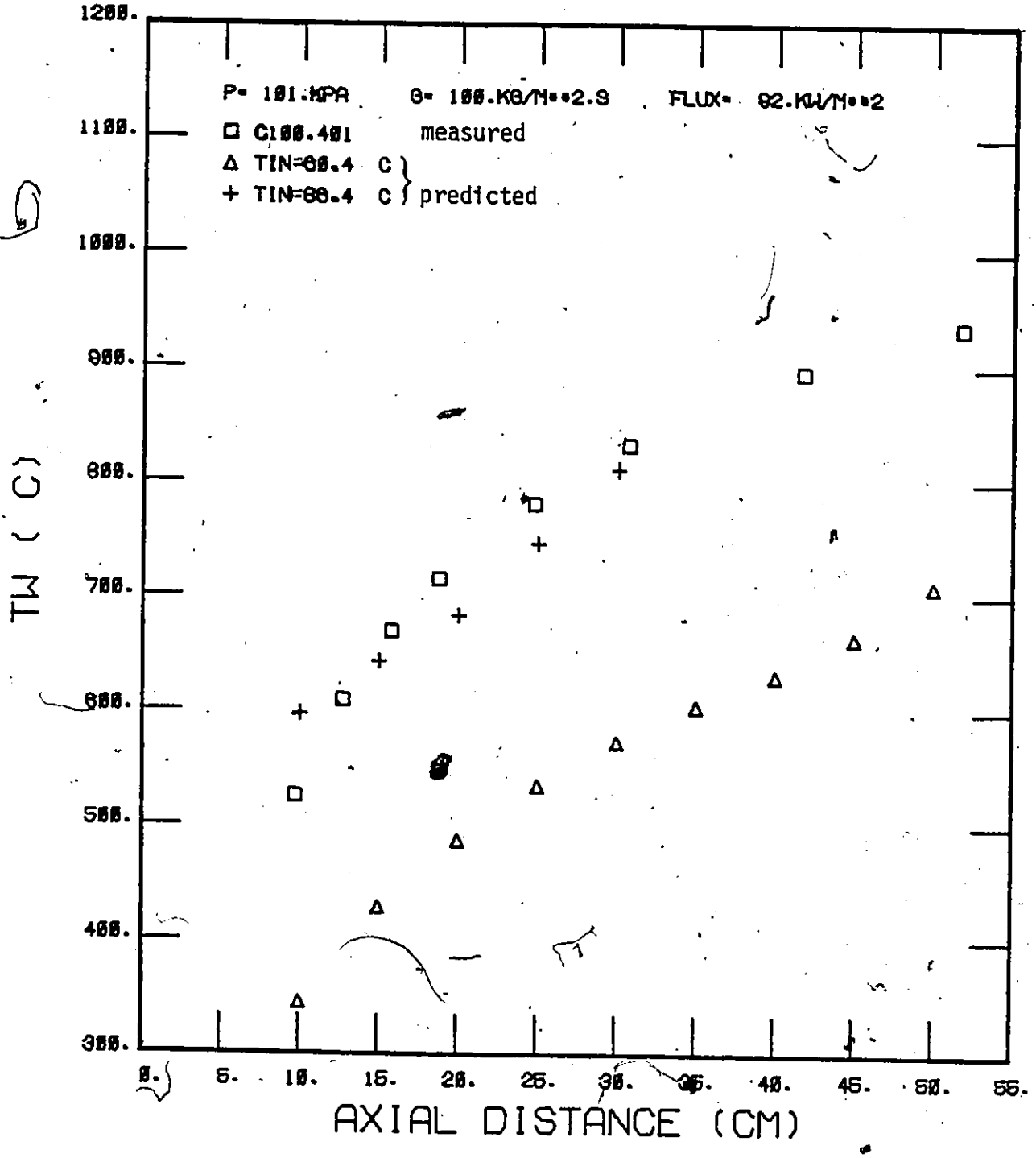

FIGURE 73 COMPARISON OF PREDICTED AND MEASURED WALL TEMPERATURES, G = 100 kg.m-2.s-1, T_{in} = 60°C

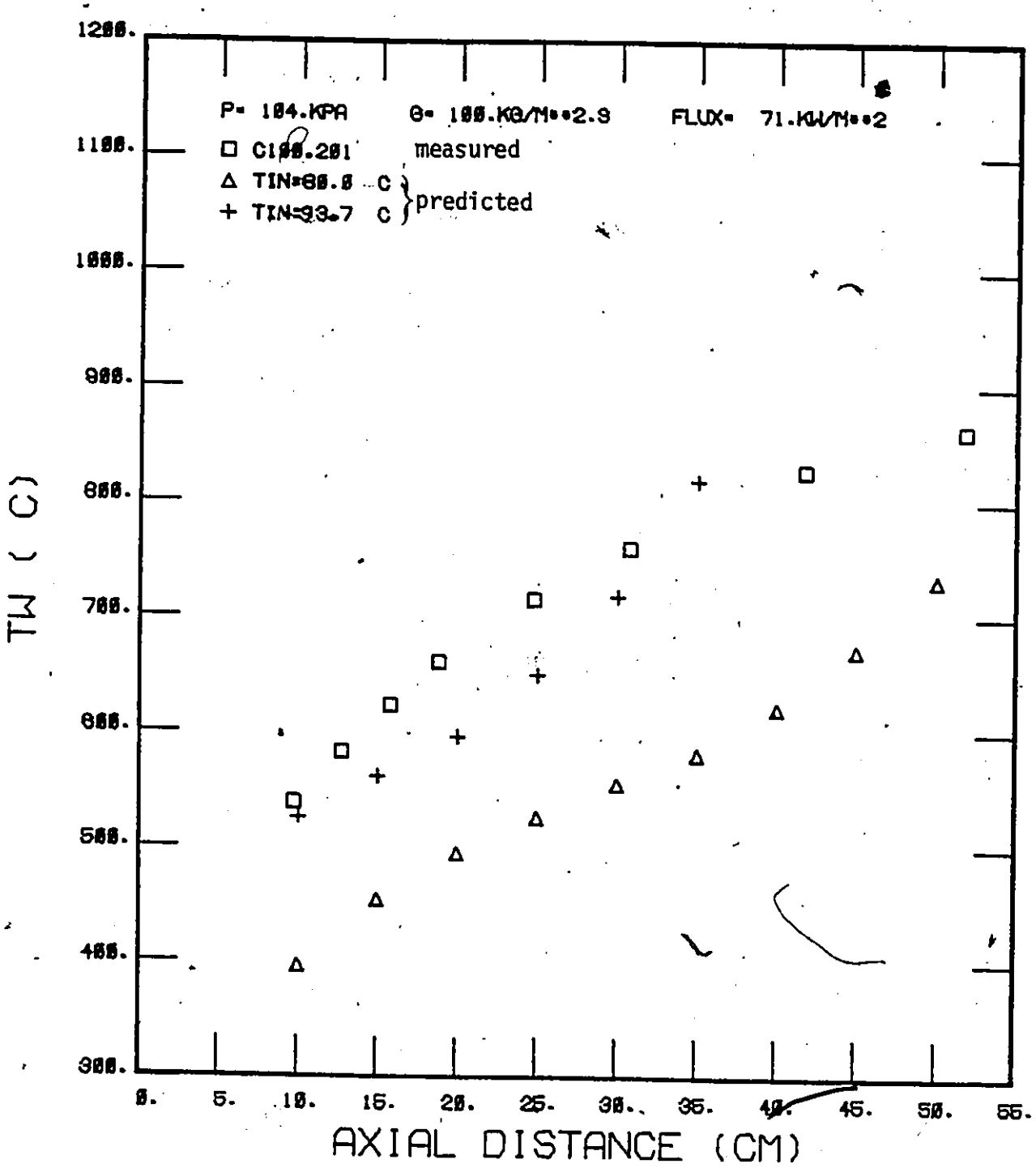

FIGURE 74 COMPARISON OF PREDICTED AND MEASURED WALL TEMPERATURES, G = 100 $kg.m^{-2}.s^{-1}$, T_{in} = 80°C

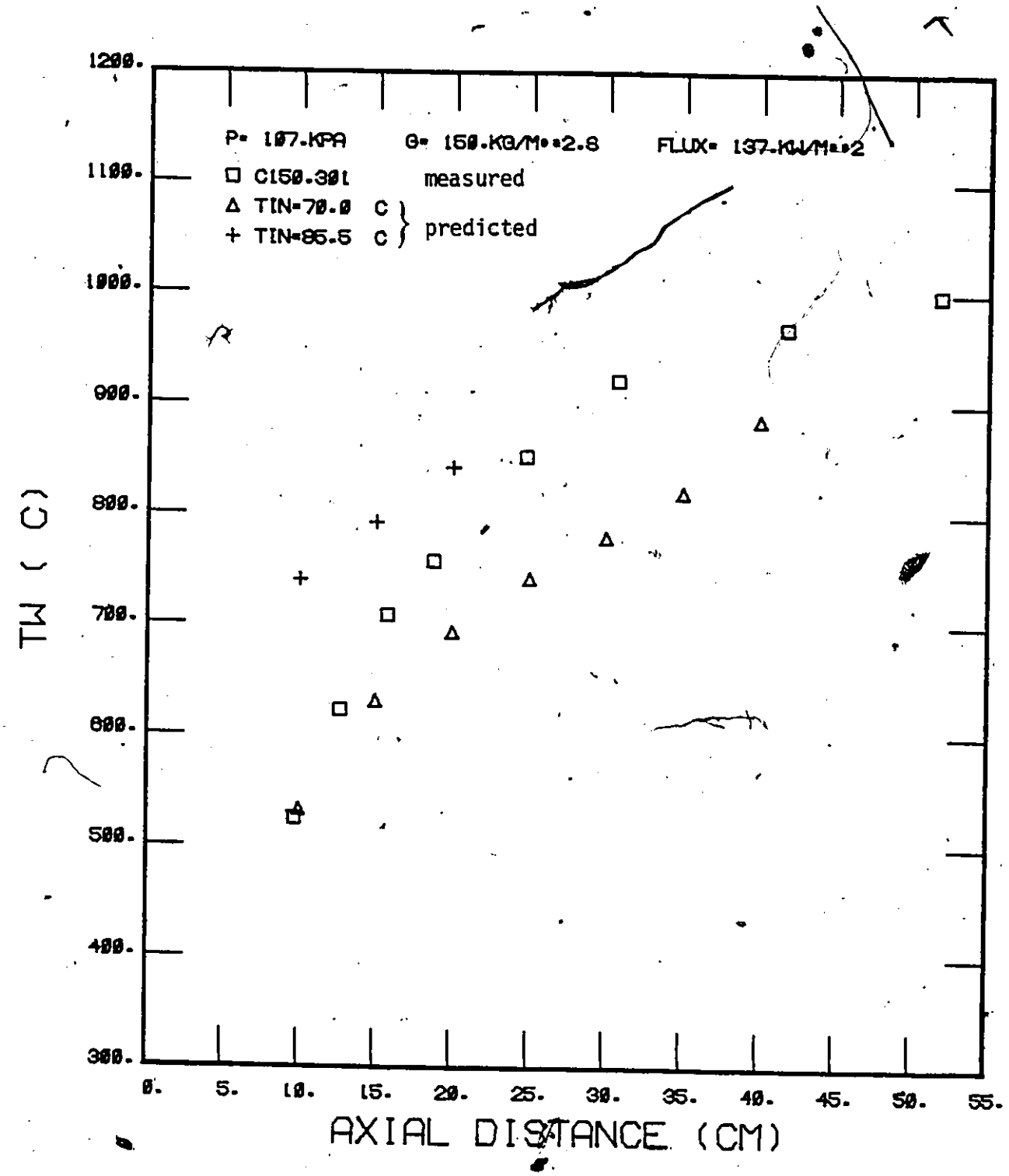

FIGURE 75 COMPARISON OF PREDICTED AND MEASURED WALL TEMPERATURES, G = 150 $kg.m^{-2}.s^{-1}$, T_{in} = 70°C

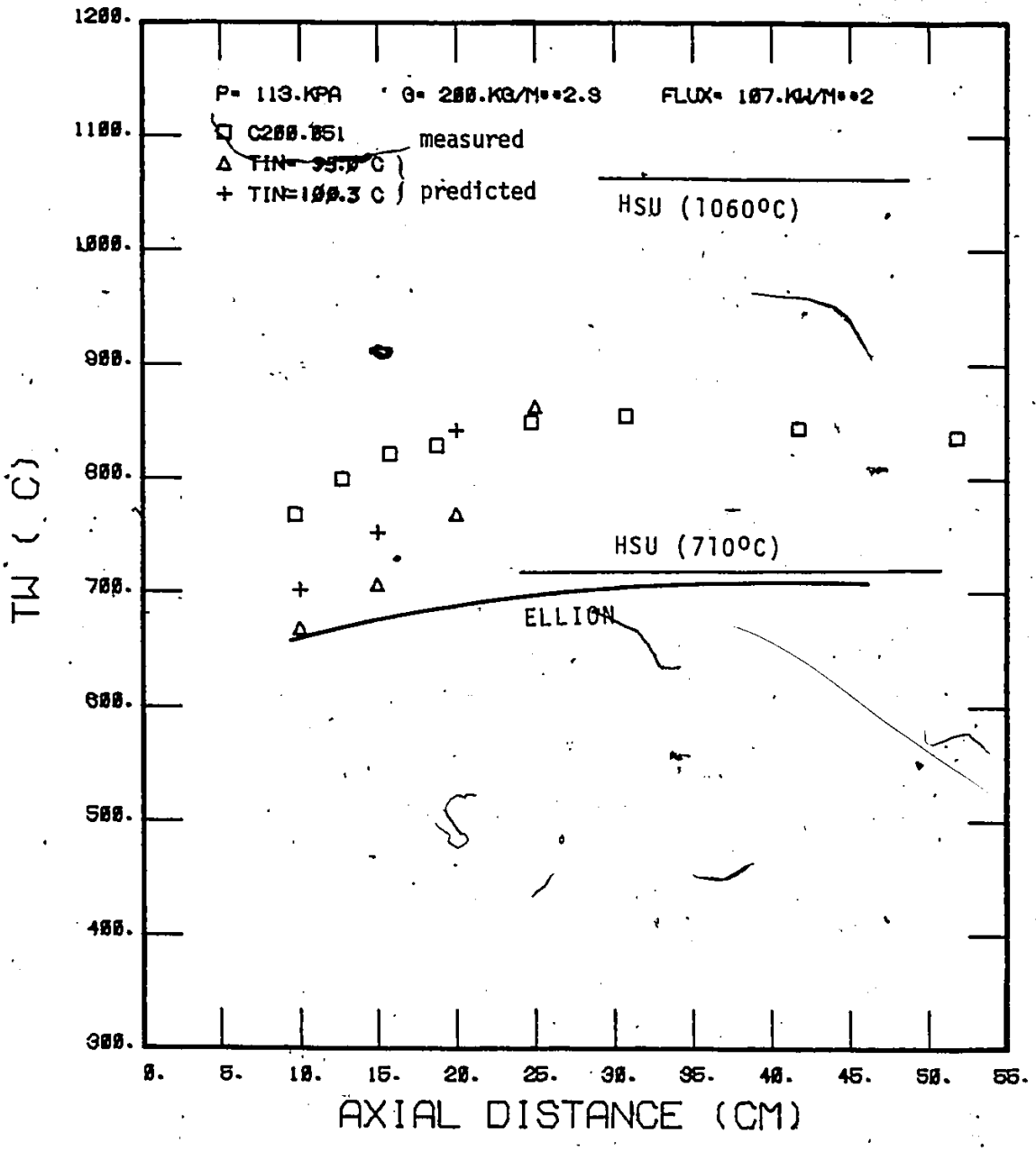

FIGURE 76 COMPARISON OF PREDICTED AND MEASURED WALL TEMPERATURES; G = 200 $kg.m^{-2}.s^{-1}$, T_{in} = 95°C

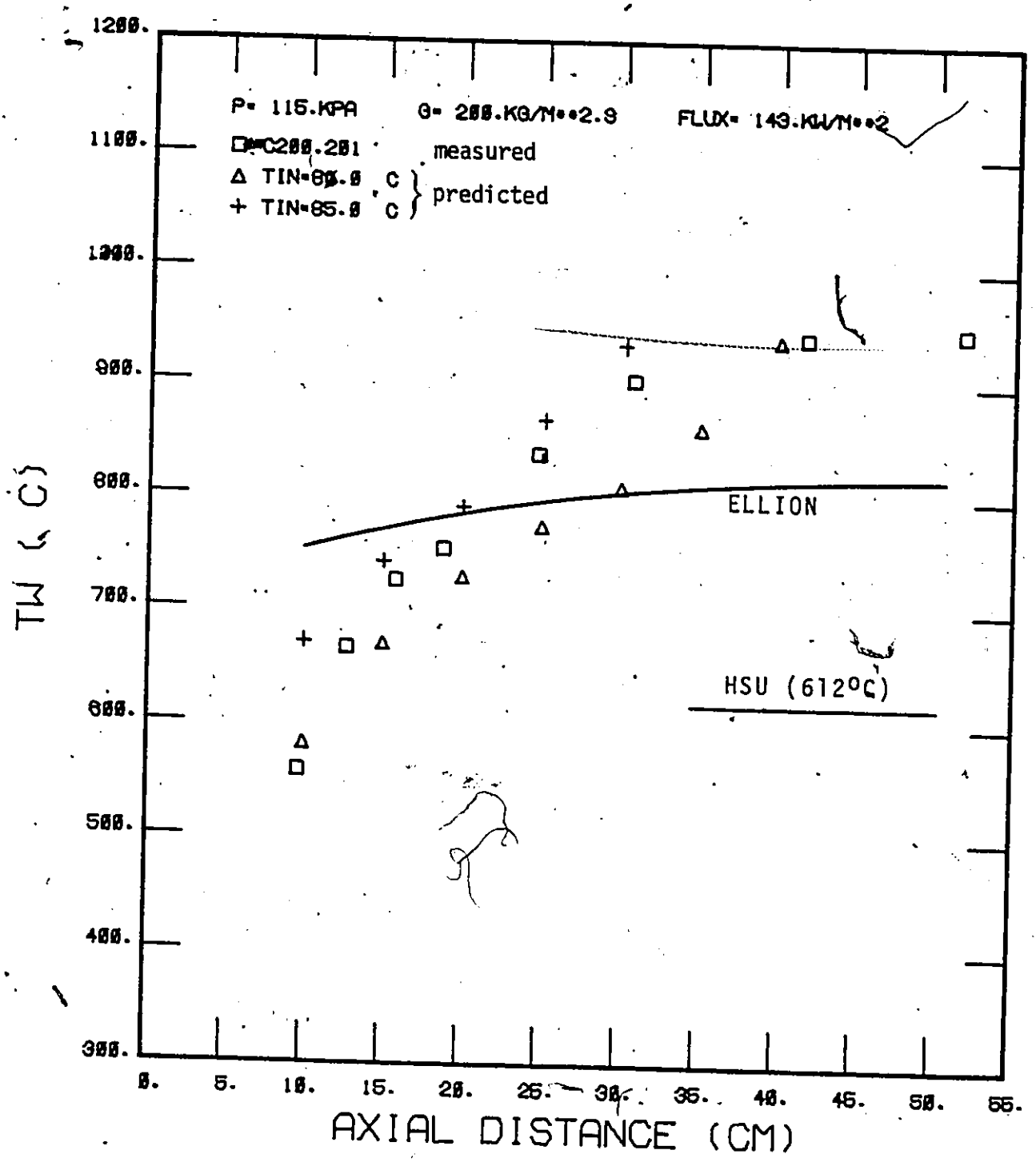

FIGURE 77 COMPARISON OF PREDICTED AND MEASURED WALL TEMPERATURES, G = 200 $kg.m^{-2}.s^{-1}$, T_{in} = 80°C

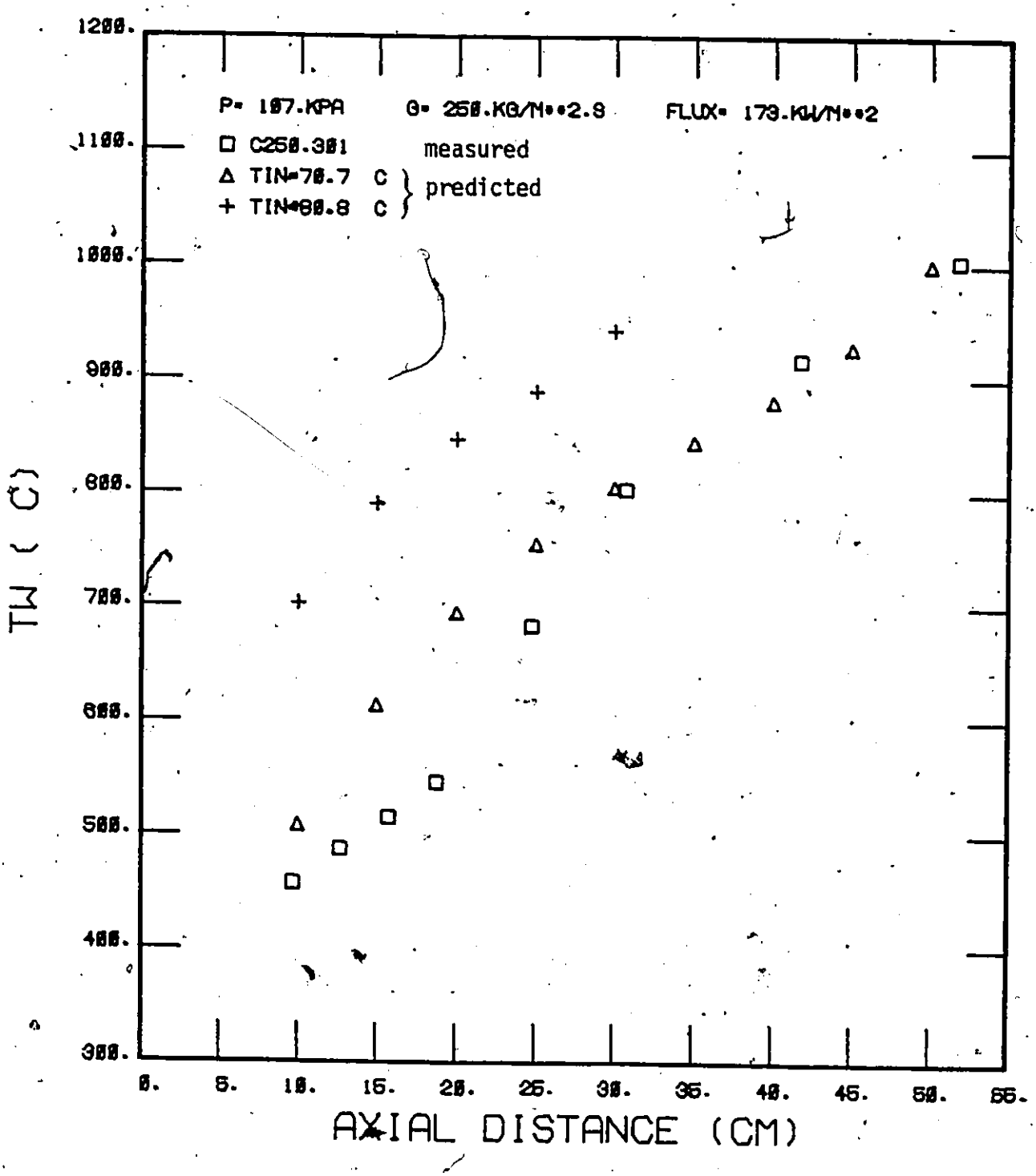

FIGURE 78 COMPARISON OF PREDICTED AND MEASURED WALL TEMPERATURES, G = 250 $kg.m^{-2}.s^{-1}$, T_{in} = 70°C

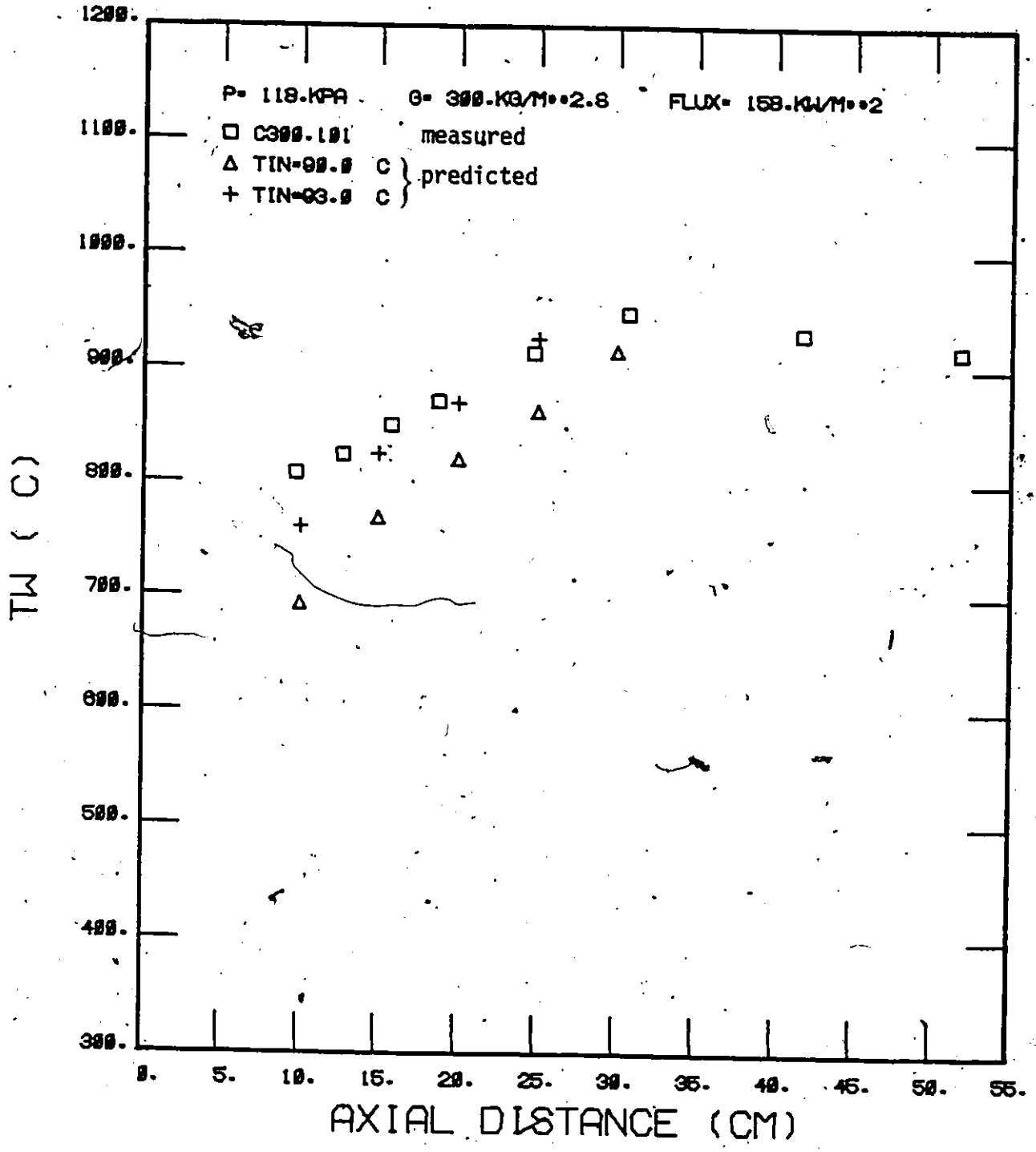

FIGURE 79 COMPARISON OF PREDICTED AND MEASURED WALL TEMPERATURES, G = 300 kg.m-2.s-1, T_{in} = 90°C.

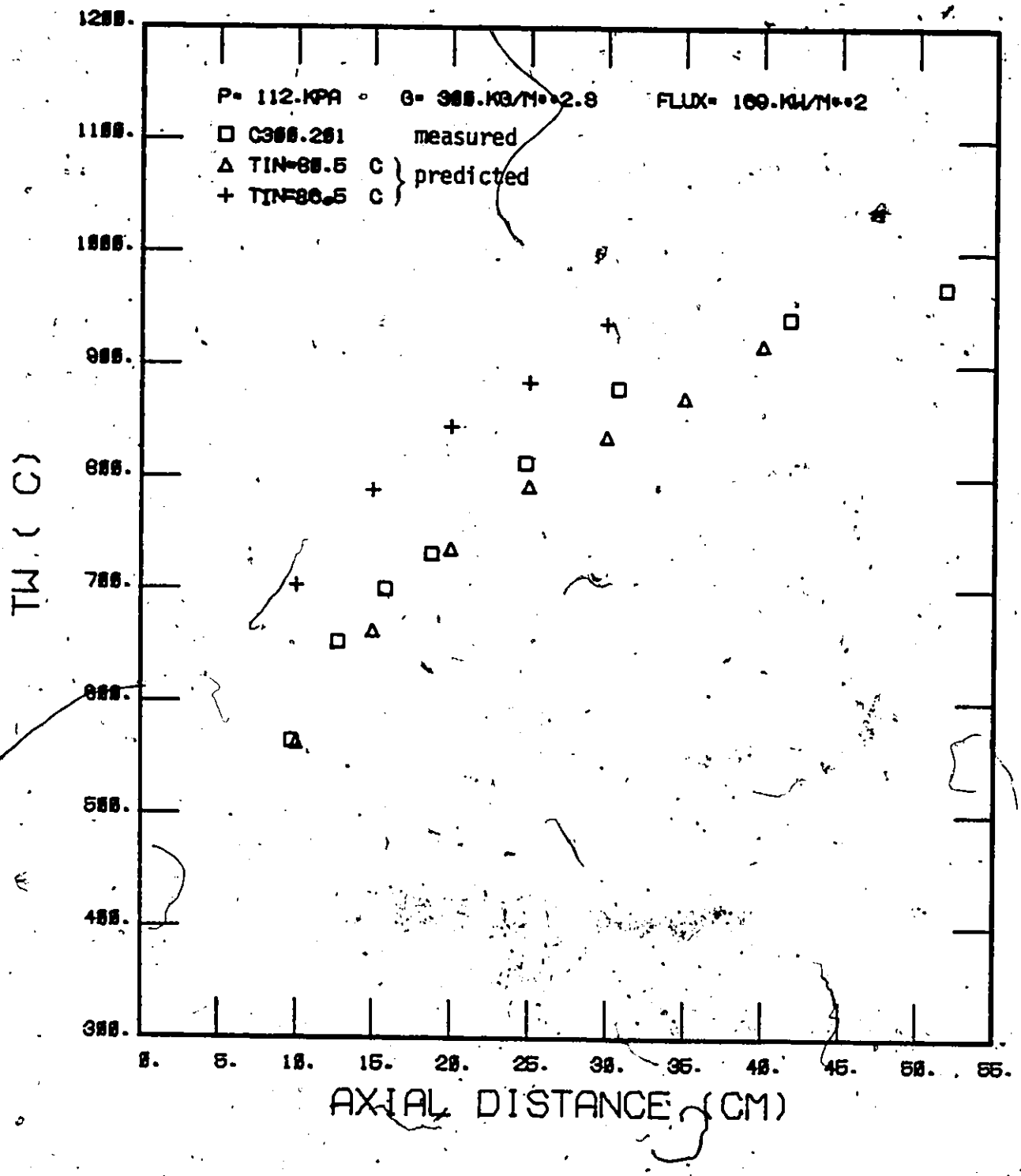

FIGURE 80 COMPARISON OF PREDICTED AND MEASURED WALL TEMPERATURES, G = 300 kg.m^{-2}.s^{-1}, T_{in} = 80.5°C

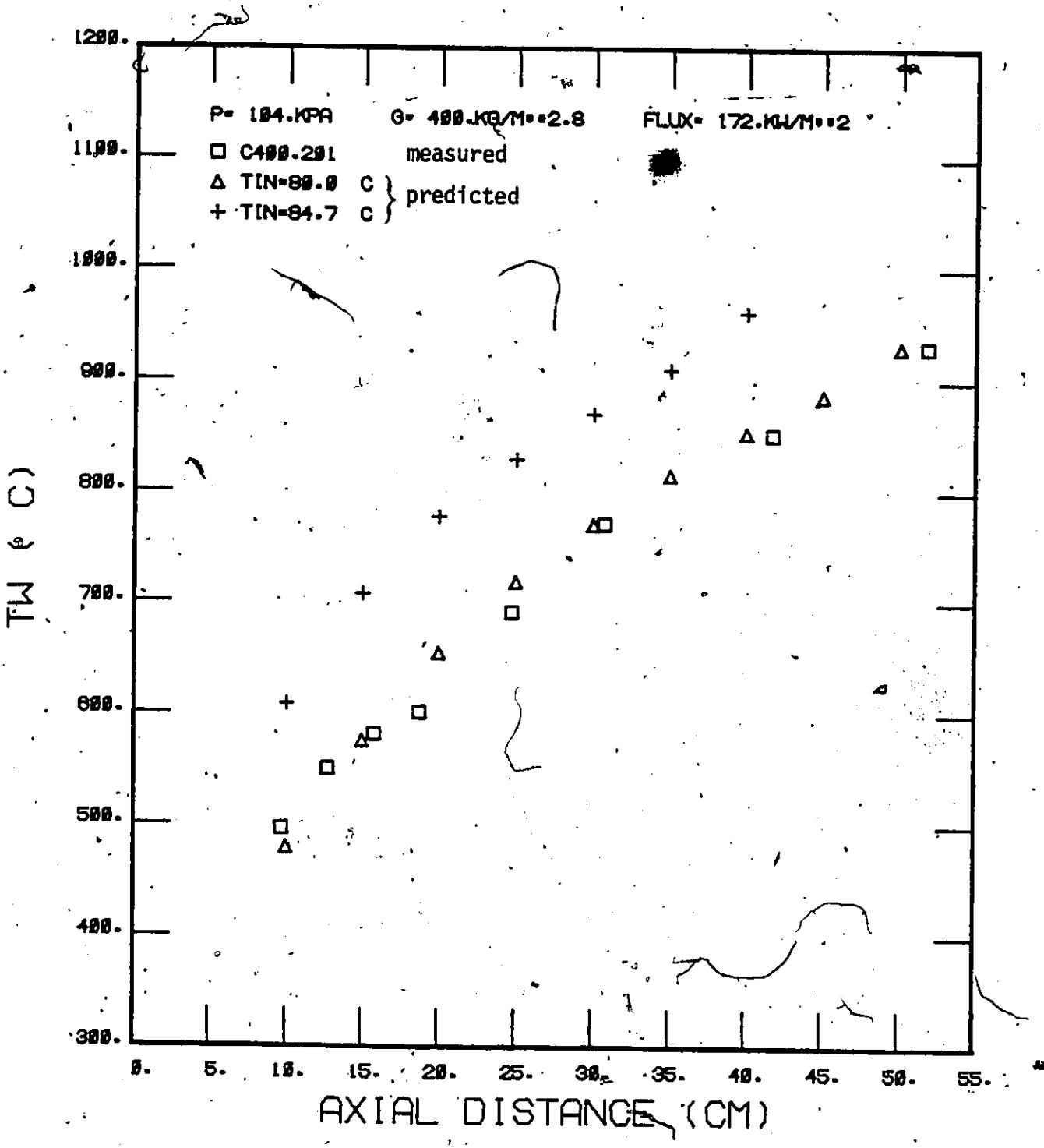

FIGURE 81 COMPARISON OF PREDICTED AND MEASURED WALL TEMPERATURES, G = 400 $kg.m^{-2}.s^{-1}$, T_{in} = 80°C

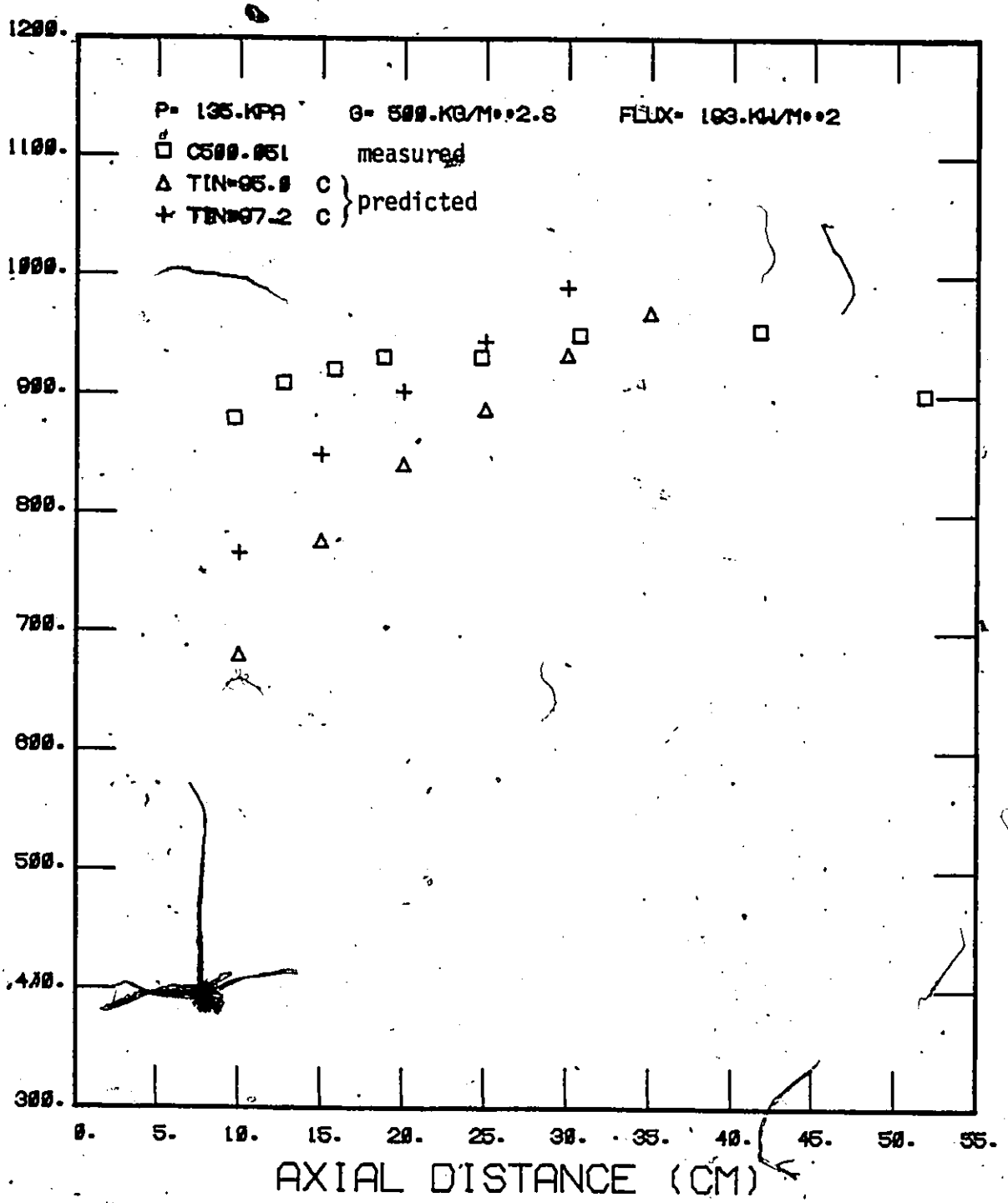

FIGURE 82 COMPARISON OF PREDICTED AND MEASURED WALL TEMPERATURES, G = 500 $kg.m^{-2}.s^{-1}$, T_{in} = 95°C

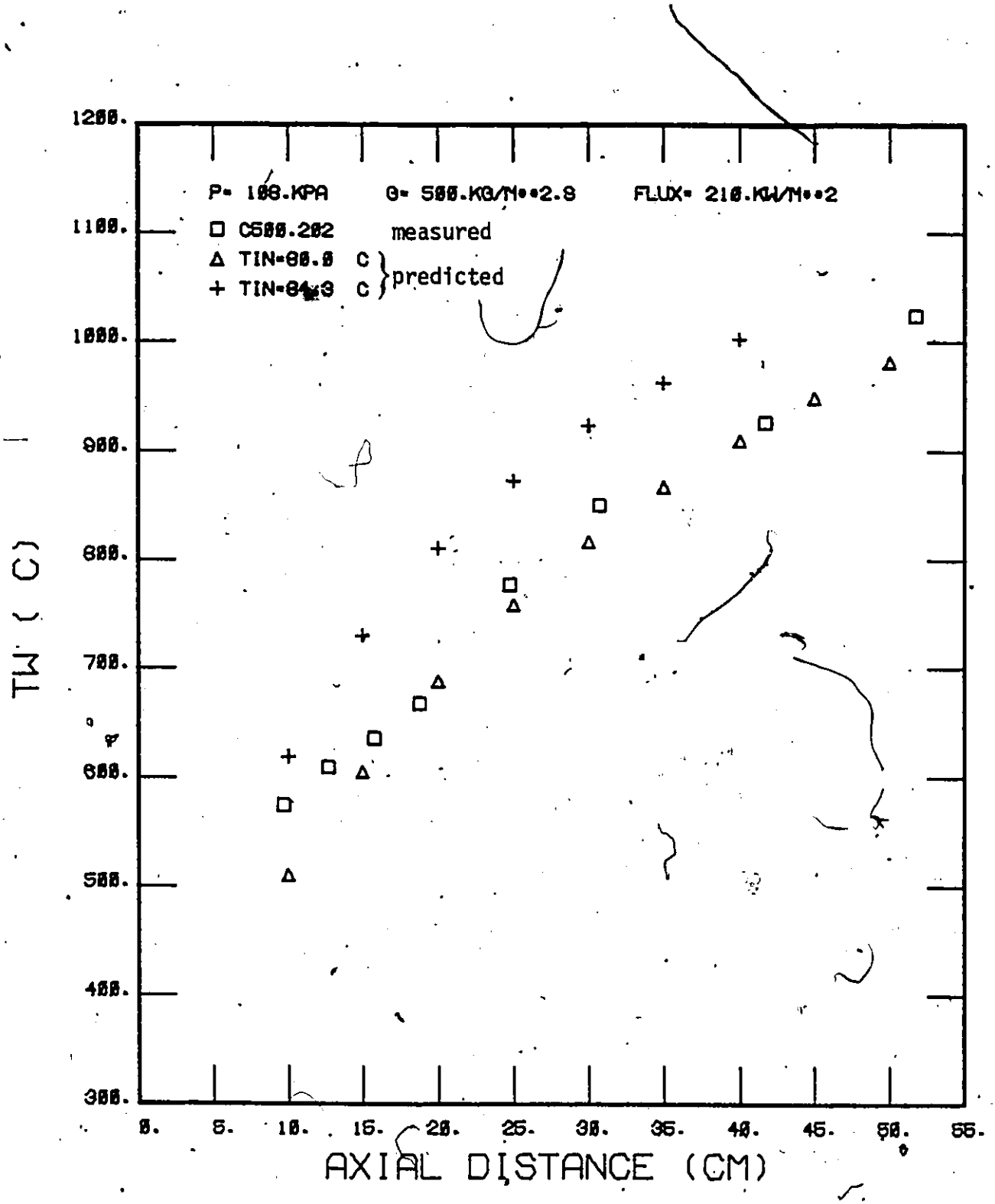

FIGURE 83 COMPARISON OF PREDICTED AND MEASURED WALL TEMPERATURES, G = 500 kg.m^{-2}.s^{-1}, T_{in} = 80°C

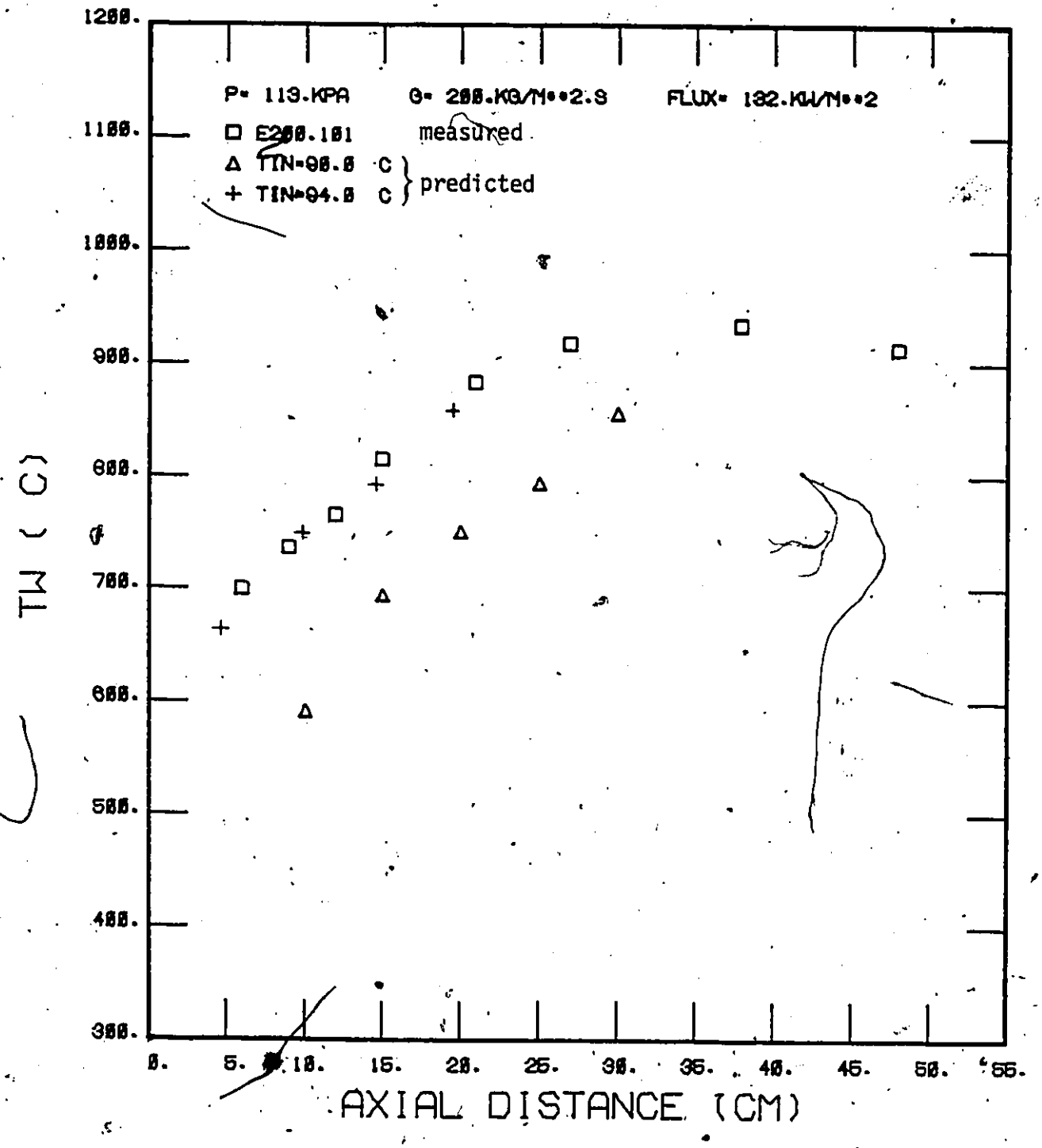

FIGURE 84 COMPARISON OF PREDICTED AND MEASURED WALL TEMPERATURES, G = 200 kg.m^{-2}.s^{-1}, T_{in} = 90°C

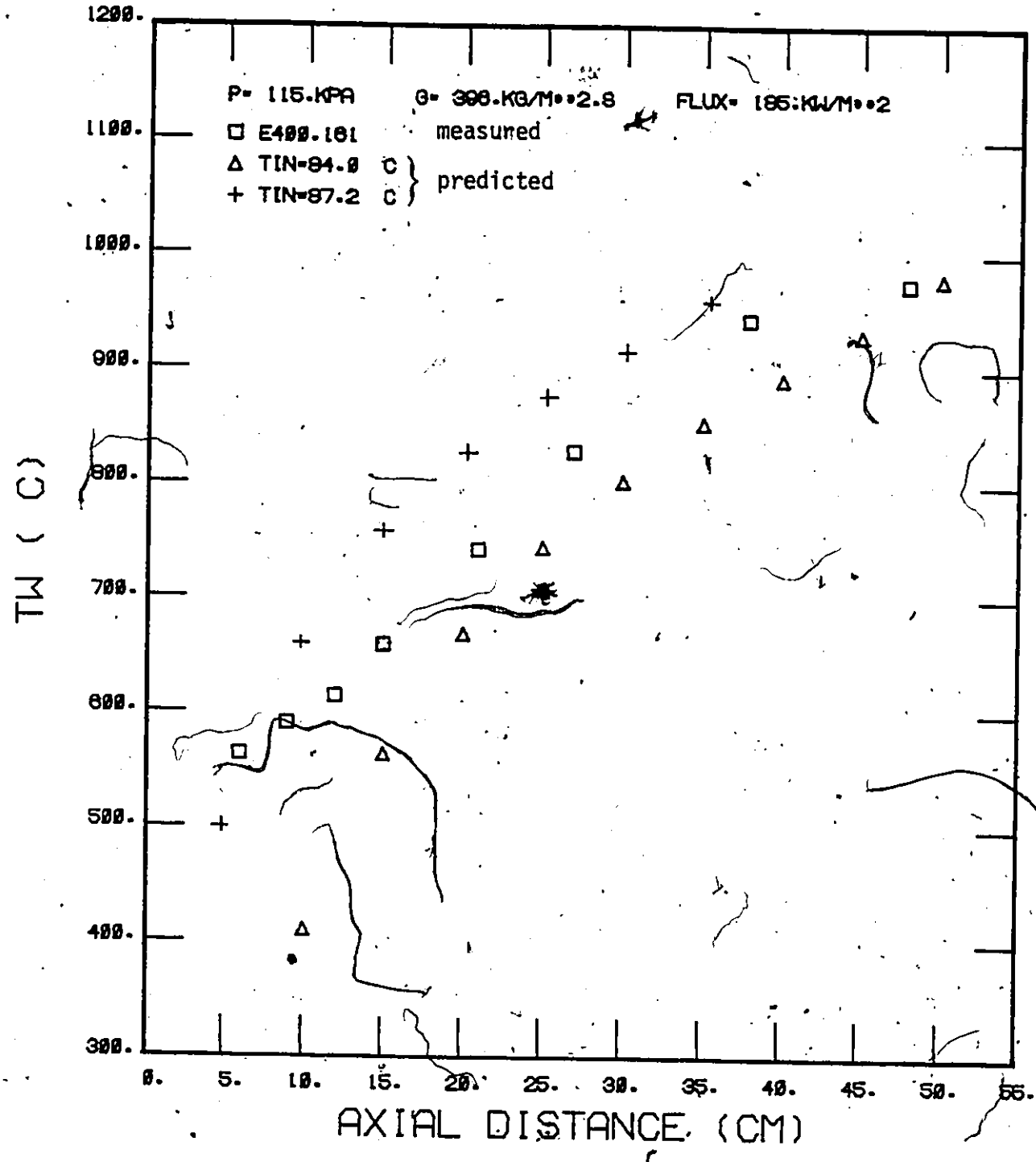

FIGURE 85 COMPARISON OF PREDICTED AND MEASURED WALL TEMPERATURES, G = 396 $kg.m^{-2}.s^{-1}$, T_{in} = 84°C

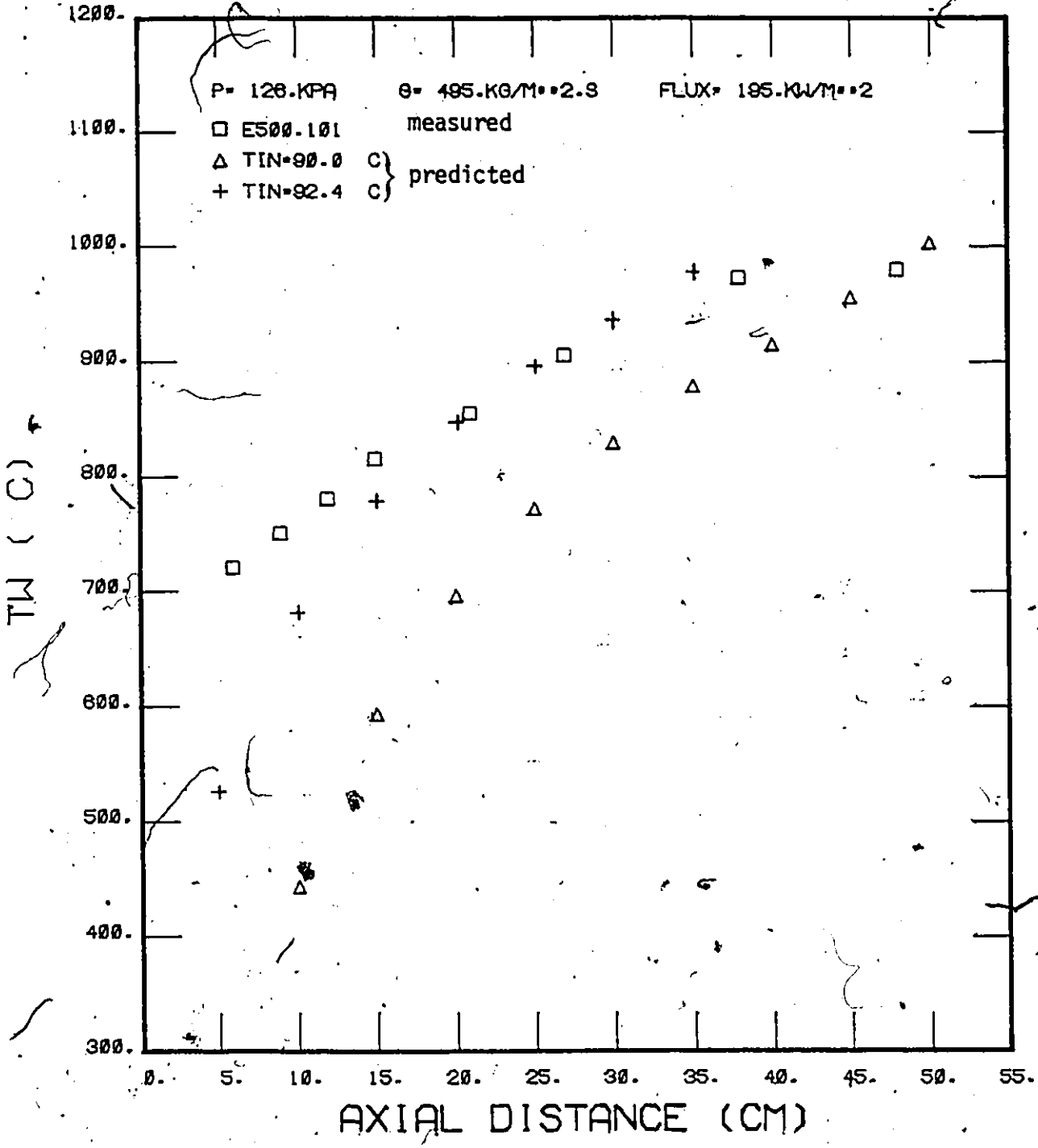

FIGURE 86 COMPARISON OF PREDICTED AND MEASURED WALL TEMPERATURES, G = 495 $kg.m^{-2}.s^{-1}$, T_{in} = 90°C

Figure 74 shows that, at low flow, the predictions are best obtained by using the "equivalent equilibrium temperatures" at the start of the film boiling section (see discussion in last section). This indicates that the temperatures of the liquid core is fairly uniform.

Figures 82 and 86 show greater discrepancies in the predictions. This is probably due to the overestimate of the system pressures. As explained in Appendix B8, the pressure in the film boiling section is estimated by using appropriate correlations. The pressures estimated for the runs shown in Figure 82 and 86 are 135 and 126 kPa respectively. It is felt that these may err on the high side. A higher pressure will result in a higher vapour density and a higher saturation temperature. Both of these will contribute to an underprediction of the wall temperatures.

IX.3 Comparison With Other Correlations

As mentioned earlier, there is no appropriate correlation available to predict the film boiling heat flux under the conditions investigated in this program. None of the correlations considers the effect of subcooling in the liquid core. For saturated conditions, the correlations of Ellion (1954) and Hsu (1977) are the most applicable, although they still lack the effect of mass flux. The correlation of Ellion (1954) was derived analytically based on a laminar flow assumption. The local heat transfer coefficient is expressed in terms of two components:

$$h = h_c + h_{rad}$$

$$= \left[\frac{g h_{fg} \rho_\ell \rho_g k_g^3}{12 \Delta T_{sat} Z \mu_g}\right]^{\frac{1}{4}} + \frac{\sigma_{SB}}{\varepsilon_w + \varepsilon_\ell - 1} \times \frac{(T_w+273)^4 - (T_{sat}+273)^4}{\Delta T_{sat}}$$

The data shown in Figure 76 were obtained under very low inlet subcooling ($T_{in} = 95^{o}C$). Under these conditions, the correlation of Elrion underpredicts the wall temperatures. Figure 77 compares the correlation with the data at a higher inlet subcooling. It can be concluded that the lack of agreement is due to the omission of the subcooling and mass flux effects.

The predictions according to the correlation recommended by Hsu (1977) are also shown on these two figures. This correlation was derived based on post-CHF FLECHT (Cadek, 1971) reflood data. The correlation is reproduced here in SI units:

$$h = h_{Hsu,TB} + h_{mod.Bromley}$$

$$= 2815\, p^{0.558} \exp\left(-0.00481\, p^{0.1733}\, \Delta T_{sat}\right)$$

$$+ 0.62 \left[2\pi \sqrt{\frac{\sigma}{g(\rho_{\ell}-\rho_{g})}}\right]^{-0.25} x \left[\frac{k_g^3\, \rho_g (\rho_{\ell}-\rho_g) h_{fg} g}{\mu_g \Delta T_{sat}}\right]^{0.25}$$

(P is in kPa)

Since the correlation consists of the sum of two components, it predicts two different wall temperatures at the same heat flux. The lower temperature corresponds to the region of transition boiling and the higher temperature the film boiling region. It appears that this correlation does not predict adequately the trend of the data. The discrepancy can also be attributed to the lack of mass flux and subcooling effects in the correlation.

IX.4 Prediction of Void Fraction

The void fractions calculated in the theoretical model for the runs shown in Figures 73-86 are compared with the measured values in Figures 87-91. The calculated values correspond to inlet conditions that give the best agreement between the measured and predicted wall temperatures. The solid curves are the same ones as those shown in Figure 44, which are the eye-ball fit to the measurements in Test Section E.

It can be seen that the measured void fractions are usually higher than the predicted value. This can be due to entrainment of the vapour in the liquid core. The result of entrainment is a thinner vapour film and an increase in the effective eddy diffusivity in the liquid core. The latter was probably included in the proportionality constant for the eddy diffusivity used in the model.

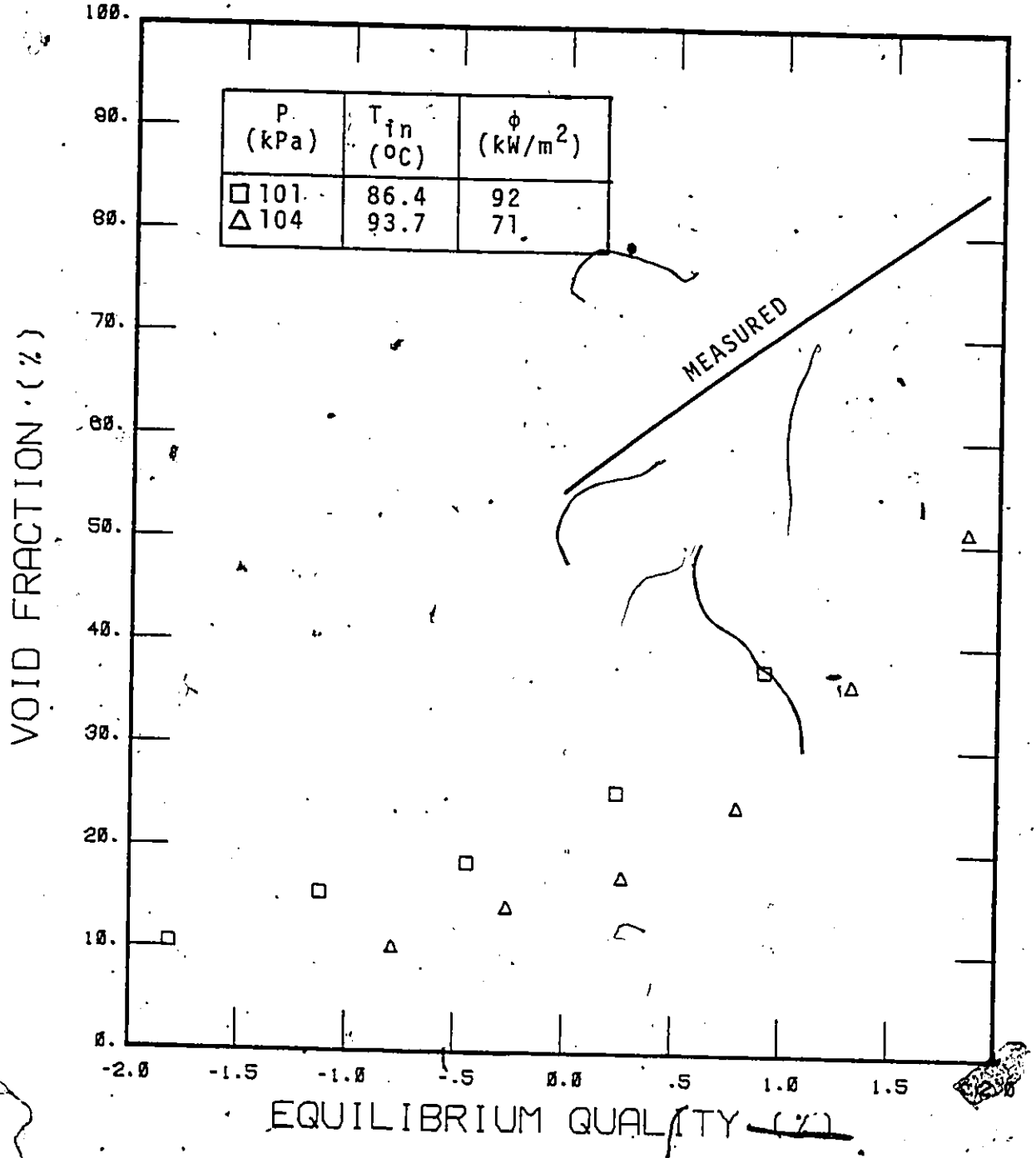

FIGURE 87 COMPARISON OF PREDICTED AND MEASURED VOID FRACTION, G = 100 kg.m^{-2}.s^{-1}

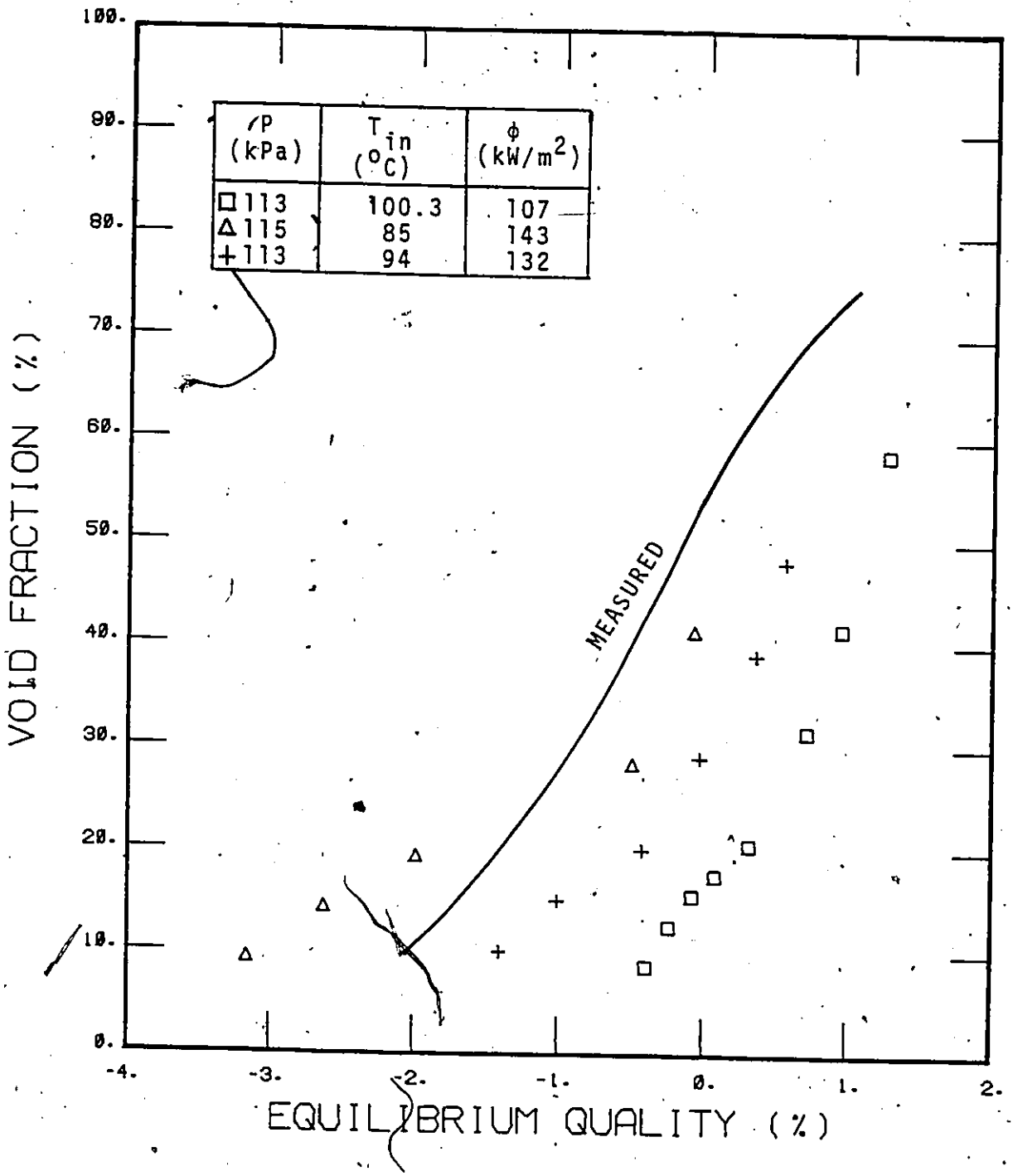

FIGURE 88 COMPARISON OF PREDICTED AND MEASURED VOID FRACTION, G = 200 kg.m-2.s-1

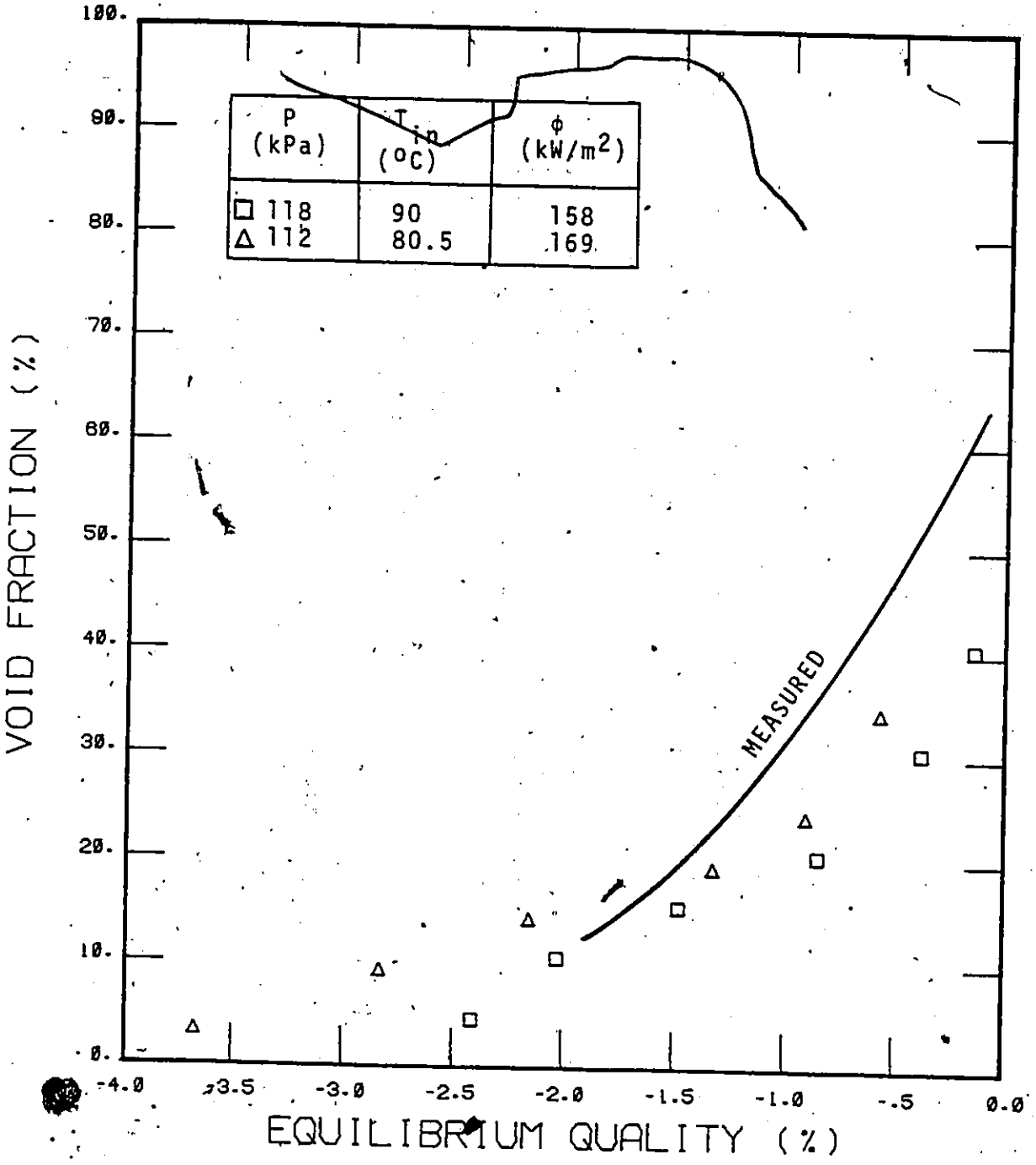

FIGURE 89 COMPARISON OF PREDICTED AND MEASURED VOID FRACTION, G = 300 kg.m-2.s-1

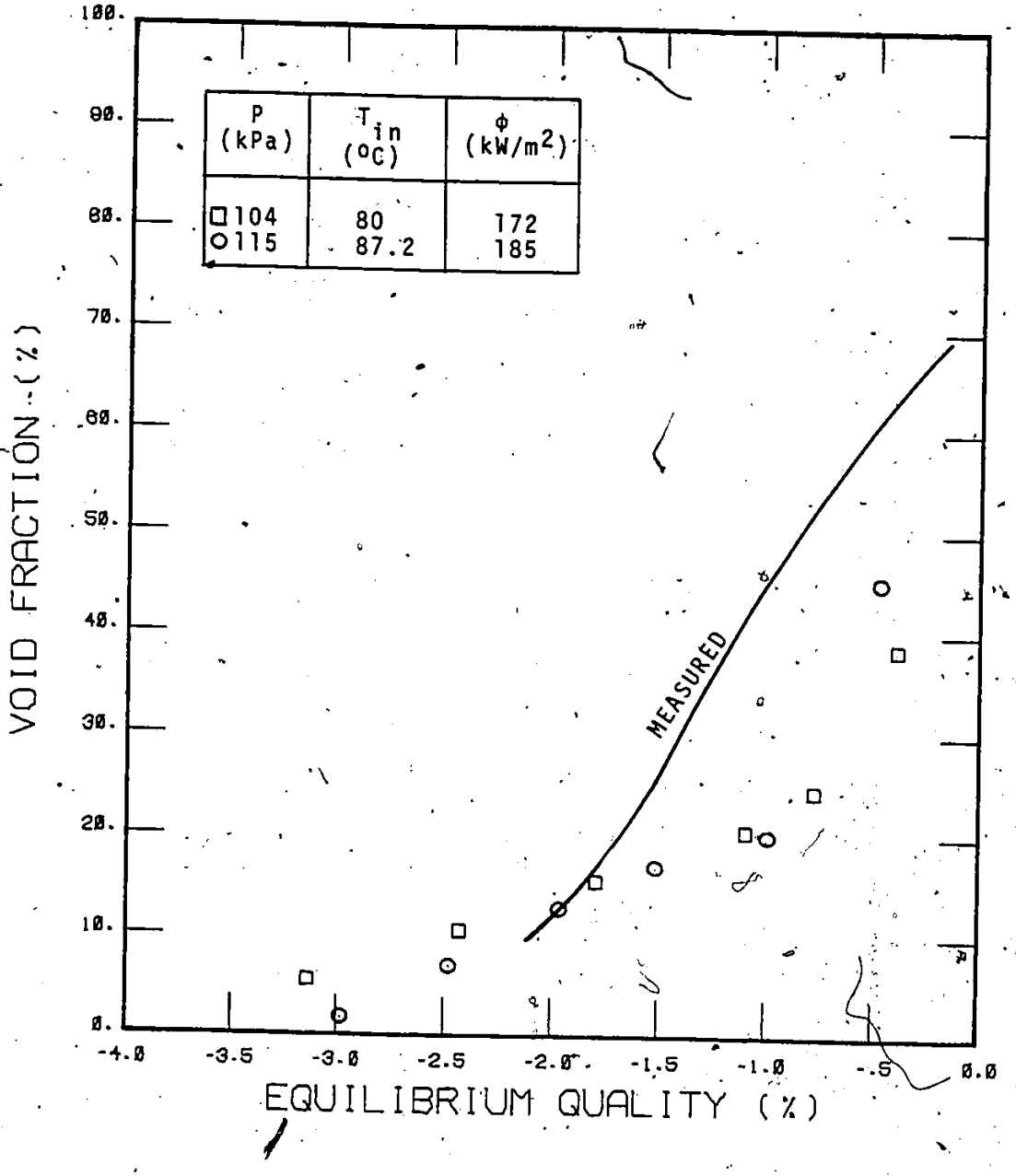

FIGURE 90 COMPARISON OF PREDICTED AND MEASURED VOID FRACTION, G = 400 $kg.m^{-2}.s^{-1}$

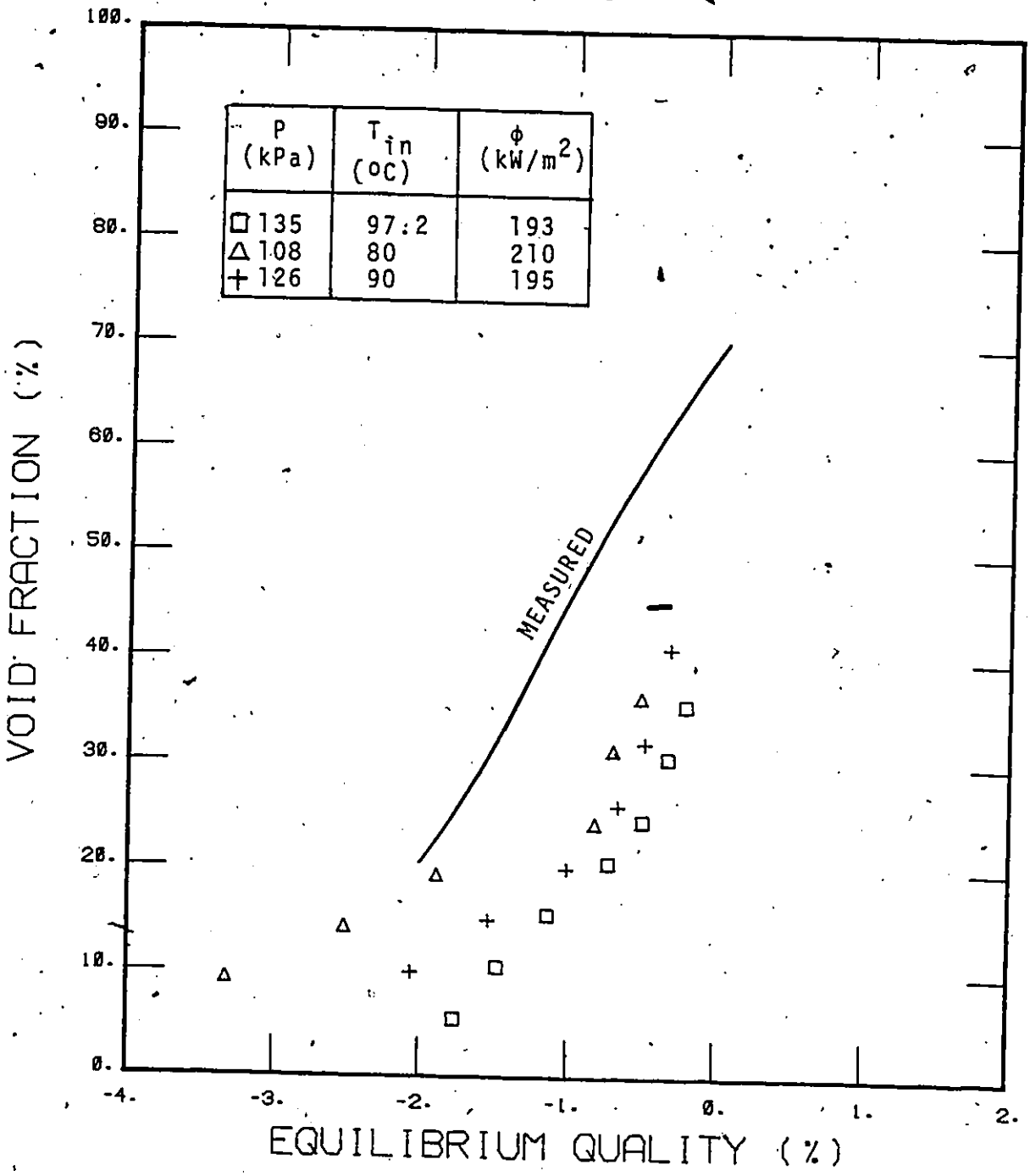

FIGURE 91 COMPARISON OF PREDICTED AND MEASURED VOID FRACTION, G = 500 kg.m^{-2}.s^{-1}

X.0 CONCLUSIONS AND RECOMMENDATIONS

X.1 Summary of Contributions

Subcooled film boiling data were obtained for water under forced flow condition inside a tube. They covered a wide range of mass flux and inlet subcooling similar to those expected to exist in a nuclear fuel channel under accident conditions. Similar data were nonexistent prior to this study. The use of a unique technique to initiate film boiling was instrumental in the success of the experiment.

A theoretical model was developed to predict the surface temperature of a tube during inverted annular film boiling. It incorporates the effects of mass flux, inlet subcooling, pressure, thermal entrance length and hydraulic diameter. The predictions compared well with the experimental data.

Both the theoretical and experimental results indicate that the overall heat transfer coefficient based on $(T_w - T_{sat})$ is a function of the mass flux and local equilibrium quality, except in the thermal entrance region. This region is estimated to be in the order of 6 L/D's from the start of the heated length (which coincides with the start of the film boiling length in the theoretical model). Over this length, the heat transfer coefficient is enhanced by increasing the inlet subcooling. The fully developed heat transfer coefficient decreases with increasing equilibrium quality, until the flow regime changes to dispersed flow. Heat transfer by thermal radiation is an important component at high wall temperature. It may account for about 40% of the overall heat transfer.

The theoretical prediction indicates that the heat transfer coefficient increases with pressure. This is due primarily to the increase in vapour density and consequently decrease in the film thickness, and to the increase in the thermal conductivity.

X.2 Recommendation for Future Work

The theoretical model developed in this thesis gives a skeleton of a mechanistic model of inverted annular film boiling. Most of the uncertainties lie in the interfacial shear and eddy diffusivity. The constitutive equations for them have been under development constantly. It is suggested that such projects be pursued with greater emphasis. This is also consistent with the requirements of the current two-fluid models development.

One of the simplifications adopted in the development of the theoretical model is an assumed uniform velocity in the liquid core. In other words, the velocity boundary layer of the liquid core at the liquid-vapor interface is neglected. This effect can be included in the further development of the model.

The eddy diffusivities of momentum and heat transfer in the liquid core have been assumed equal. There are situations where this assumption is not valid. Therefore, potential users of the model should note this limitation. This is also an area for further investigation.

The theoretical model still needs some data at different pressures and hydraulic diameter to substantiate its applicability. As a theoretical model of such complexity is almost always impossible to put into a large computer code, these additional data will be useful for developing an empirical correlation. The theoretical model may be used to identify the important parameters.

The theoretical model only considers inverted annular film boiling. Each phase is considered to flow separately, without any entrainment of the other phase. The region of low quality dispersed flow has not been included. Such data were almost always obtained in the experimental program. Several models for dispersed flow film boiling at high quality are available in the literature. It would be of academic and practical interests to consider the low quality region.

TABLE 1. LOW QUALITY FILM BOILING EXPERIMENTS

(from Groeneveld & Gardiner (1977))

AUTHORS	GEOMETRY	FLOW CONDITIONS	MAIN OBSERVATIONS
Bromley, LeRoy, and Robbers 1953	Vertical flow over a horizontal cylinder O.D. - 9.8 mm - 12.6 mm - 16.2 mm	N-hexane, CCl_4, benzene, ethyl alcohol were used. Mass fluxes of 0 to 6.56×10^3 $kgm^{-2}s^{-1}$ were tested.	For $U/\sqrt{gD} < 1.0$, h_c is independent of velocity and for $U/\sqrt{gD} > 2.0$, h_c is proportional to $U^{\frac{1}{2}}$.
Murphy, Karmode, and Zahradnik 1970	Horizontal plate	Hexane, benzene, and methanol were used. Mass fluxes of 0.67×10^3 to 4.04×10^3 $kgm^{-2}s^{-1}$ were tested.	Noted a moderate increase in the heat transfer coefficient with velocity.
Rankin 1961	Vertical tube I.D. - 26.9 mm length - 1.22 m	Freon-113 and methanol at mass fluxes of 0.36×10^3 to 4.04×10^3 $kgm^{-2}s^{-1}$	No effect of velocity in film boiling region.
Dougall and Rohsenow 1963	Vertical tube I.D. - 10.2 mm - 4.6 mm length - 386 mm	0.45×10^3 to 1.11×10^3 $kgm^{-2}s^{-1}$ Freon-113	No effect of velocity on film boiling.
Motte and Bromley 1957	Vertical flow over horizontal cylinders O.D. - 9.8 mm - 12.6 mm - 16.2 mm	0 - 6.56×10^3 $kgm^{-2}s^{-1}$ of N-hexane, CCl_4, benzene, and ethyl alcohol with subcoolings of 0 - 45°C	Subcooling increased the heat transfer coefficient by as much as a factor of 4. The effect of subcooling increased with increased velocity.
Kalinin 1969	Downward flow in a vertical tube I.D. - 4 mm to 20 mm length - 100 mm	6.32×10^3 - 18.9×10^3 $kgm^{-2}s^{-1}$ of nitrogen with 0 - 38°C subcoolings in transient tests.	Tenfold increase in heat transfer at highest subcooling over saturated conditions. Threefold increase in heat flux over mass flux range tested.
Ellion 1954	Upward flow in a vertical annulus O.D. - 63.5 mm I.D. - 6.4 mm length - 76.2 mm	0.336×10^3 to 1.53×10^3 $kgm^{-2}s^{-1}$ of water with 28°C to 56°C subcooling.	No effect of subcooling or velocity on film boiling heat transfer.
Fung 1976	Upward flow in a vertical tube I.D. - 12.7 mm length - 101.6 mm	0.068×10^3 to 1.35×10^3 $kgm^{-2}s^{-1}$ of water with 0 - 76°C subcoolings in transient tests.	Heat flux increased fourfold at highest subcooling over saturated conditions. Heat flux increases tenfold at highest flow.
Cheng and Ng 1978	Upward flow in a vertical tube I.D. - 12.7 mm length - 57.15 mm	0.19×10^3 $kgm^{-2}s^{-1}$ of water at subcooling of 0 - 26°C in transient tests.	Heat flux increased sixfold for highest subcooling. Noted a sudden dip in the boiling curve near the minimum film boiling temperature at 26°C subcooling.
Newbold 1976	Vertical tube upward and downward flow. I.D. - 10 mm length - 77 mm	0.016×10^3 to 1.245×10^3 $kgm^{-2}s^{-1}$ of water in transient tests.	Order of magnitude increase in wall heat flux over mass flux range tested.
Smith 1976	Vertical tube I.D. - 12.5 mm length - 1.22 m	0.025×10^3 to 0.132×10^3 $kgm^{-2}s^{-1}$ of water.	Too few data points at the same subcoolings and pressure to draw any conclusions on velocity effect.

TABLE 2. LOW-QUALITY AND SUBCOOLED FILM BOILING CORRELATIONS

(from Groeneveld & Gardiner (1977))

AUTHORS	EQUATION	RANGE OF APPLICABILITY: TEST FLUID	GEOMETRY	PRESSURE MPa	FLOW RATE $kgm^{-2}s^{-1}$	SUBCOOLING °C OR QUALITY	COMMENTS
Bromley 1953	$h = h_{FB} + 3/4\, h_{rad}$ $h_{FB} = 0.62\left[\frac{k_v^3 \varepsilon \rho_v (\rho_l - \rho_v) h'_{fg}}{D \mu_v \Delta T_s}\right]^{1/4}$ $h_{rad} = \frac{5.67 \times 10^{-8} (T_w^4 - T_s^4)}{\left(\frac{1}{\varepsilon_w} + \frac{1}{\varepsilon_l} - 1\right) \Delta T_s}$ $h'_{fg} = h_{fg}\left(1 + \frac{0.4\, C_p\, \Delta T_s}{h_{fg}}\right)^2$	Nitrogen water n-pentane benzene carbon tetrachloride ethyl alcohol	Horizontal carbon cylinders OD = 6.4 mm 9.5 mm 12.7 mm	Not given	Pool boiling	Saturated	Pool film boiling from external surfaces. Laminar theory.
Berenson 1961	$h_{FB} = 0.425\left[\frac{k_v^3 \varepsilon \rho_v (\rho_l - \rho_v) h'_{fg}}{\mu_v \Delta T_s \sqrt{\frac{\sigma}{g(\rho_l - \rho_v)}}}\right]^{1/4}$		Horizontal surface		Pool boiling	Saturated	Theory only.
Sivivour and Ede 1970	$q_{total} = q_v + q_l$ $q_v = 0.613 \frac{k}{D} \Delta T_s \left[\frac{\varepsilon \rho_v (\rho_l - \rho_v) h'_{fg}}{\mu_v k \Delta T_s}\right]^{1/4} + q_{rad}$ $q_l = 0.57 \frac{k}{D} \Delta T_{sub} [Gr\, Pr^2]$ $Gr = g \frac{\beta_l \Delta T_{sub} D^3}{\nu^2}$	Water water plus detergent	Horizontal cylinders OD = 3.2 mm 6.4 mm	0.101	Pool boiling	0 - 98°C	Correlated their data well over the entire range of subcooling.
Anderson et al. 1976	$h_s = C_1\left[\frac{k_v^3 h_{fg}^2 \rho_g^3 (\rho_l - \rho_v)^4 g^4}{\mu_v^4 \Delta T_s^3 \sigma}\right]^{1/12}$ $0.3321 \le C_1 \le 0.5498$				Low flow rates	Saturated	Gives slightly higher heat transfer coefficient than Berenson's equation for $\Delta T_s > 200$°C Theory only.
Elliot 1954	$h = \frac{4}{3}\left[\frac{\varepsilon \rho_l \rho_v k_v^3 h'_{fg}}{12 \Delta T_s L \mu_v}\right]^{1/4} + q_{rad}$	Water	Vertical annulus OD = 63.5 mm ID = 6.4 mm Length = 76.2 mm	0.11 - 0.41	(0.338 - 1.53) $\times 10^3$	28°C - 56°C	
Kolstad et al. 1969	a) Inverted Annular Flow i) entrainment region $Nu = 0.0012\left(\frac{GDe}{\mu_g}\right) Pr^{0.4}\left[1 + 1.22 \exp\left(-0.038 \frac{D}{De}\right)\right]$ ii) non-entrainment region $Nu = 0.0078\left(\frac{\rho_g U_v 2\delta_v}{\mu_g}\right)^{0.75} Pr_g F$ $F = \left[1 + (3 \times 10^{-4})\phi + 1.3 \exp(-4 \times 10^{-4}\phi)\right]$ $\phi = \frac{C_{p_g} \Delta T_{sub}}{h_{fg}}\left(\frac{\rho_g \sigma De}{\mu_g^2}\right)^{0.7}$ b) Slug Flow $St_v = 19\, Re_v^{-0.25}\left[1 + 0.25 \exp\left(-0.05 \frac{D}{De}\right)\right]$ $St_v = \frac{q}{\rho_g U_{tt} C_{p_v} (T_w - T_s)}$ $Re_v = \frac{\rho_g U_{tt} De}{\mu_g}$	Nitrogen	Downward flow in a vertical tube ID = 4 mm to 20 mm length = 100 mm	0.41 - 2.13	(6.32 - 18.9) $\times 10^3$	0 - 18°C	Model required to evaluate the film thickness
Bengali and Schneider 1963	$Nu = \frac{\frac{\rho_v De}{\mu_v}\sqrt{\frac{\tau_w}{\rho_v}}}{\int_0^{\phi^+} \frac{d\phi^+}{1 + Pr \frac{\varepsilon}{\nu}}}$	Freon-113	Vertical tube ID = 10.2 mm and 4.8 mm length = 101.0 mm	0.101	(0.43 - 1.11) $\times 10^3$	Exit quality up to 10%	

TABLE 3

DIMENSIONS OF TEST SECTIONS

	Test Section			
	A	C	D	E
ID (mm)	11.81	←	11.94	→
OD (mm)	12.70	←	13.08	→
Heated length between power clamps (cm)	77.26	75.25	76.73	76.14
Heated length before hot patch (cm)	3.81	3.81	3.786	3.35
Heated length beyond last TS thermocouple	1.39	8.44	9.946	9.79
Hot patch OD (cm)	←	8.89	→	
Hot patch length	←	6.35	→	2.54
Cartridge heaters	←	8 x 250W	→	8 x 150W
Thermocouple location Elevation (cm) from top of hot patch				
TS0			0	
TS1	2.46		3	
TS2	5.08		6	
TS3	7.38		9	
TS4	10.28		12	
TS5	15.08	←	18	→
TS6	25.48		24	
TS7	35.48		35	
TS8	45.88		45	
TS9	55.64		50	
TS10	70.27		55	
TS11	Bottom of downstream power clamp			

TABLE 4 RANGES OF TEST CONDITIONS

T (°C) in (nominal)	Nominal Mass Flux ($kg.m^{-2}.s^{-1}$)								
	50	100	150	200	250	300	350	400	500
1	C	E		E		E		E	E
5	A	A,C	A,C		A,C	C,E	C	C	C
10	A	A,C,E	A,C	A,C,E	C	C,E	C,D	C,D,E	C,E
20	C	A,C,E	A,C	C,E	C	C,E	C,D	C,D,E	C,D
30	A,C	C	C	C	C				
40		C	C	C					
50	C	C							
60	A,C	C							
70	A,C								

Entries in table indicate test section.

TABLE 5 MINIMUM FILM BOILING TEMPERATURE

RUN NAME	T-MIN (C)	QUALITY
A 50.605	365.	-.154800E-02
A 50.104	302.	.218500E-01
A100.207	313.	.390580E-03
C100.057	293.	.252773E-01
C100.10D	335.	.923900E-02
C100.205	335.	.187310E-02
C150.106	310.	.994483E-03
C250.205	419.	-.134619E-01
C250.303	414.	-.214547E-01
C350.205	427.	-.180936E-01
C500.206	405.	-.143072E-01
C500.206	405.	-.143072E-01

APPENDIX A: GAMMA DENSITOMETER

A.1 INTRODUCTION

The radiation attenuation method of density determination is based on the absorption of gamma rays by the intervening material. Theoretically, the attenuation can be predicted and related to the void fraction of the measurement region. In practice, a calibration curve is obtained in a mock-up structure. The method is a well established technique. A comprehensive review of the methodology can be found in Lassahn et al. [1979]. In what follows, the features specific to the present investigation are described.

A.2 DESCRIPTION OF γ-DENSITOMETER ARRANGEMENT AND CALIBRATION

The densitometer consisted of a 50 mCi Cesium 137 source encased in a collimator, a detector and electronic counting devices.

The dimensions of the collimator and detector window are shown in Fig. A.1. The relative positions with respect to the tube are shown in Fig. A.2.

Calibration was carried out by measuring the attenuation through Lucite plugs of various diameter inserted into a mock-up tube to simulate inverted annular flow. The % attenuation is defined as

$$A = \frac{I_E - I}{I_E - I_F}$$

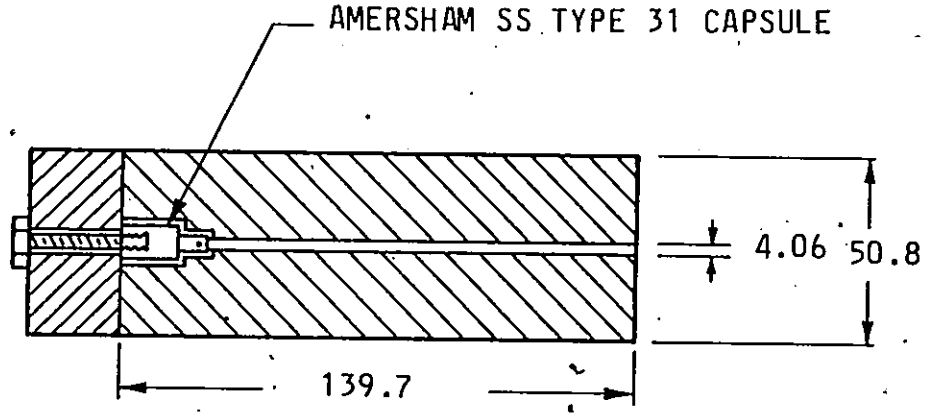

VERTICAL SECTION THROUGH MID - PLANE OF COLLIMATOR

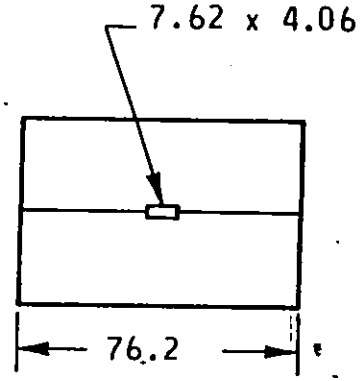

COLLIMATOR (FRONT VIEW)

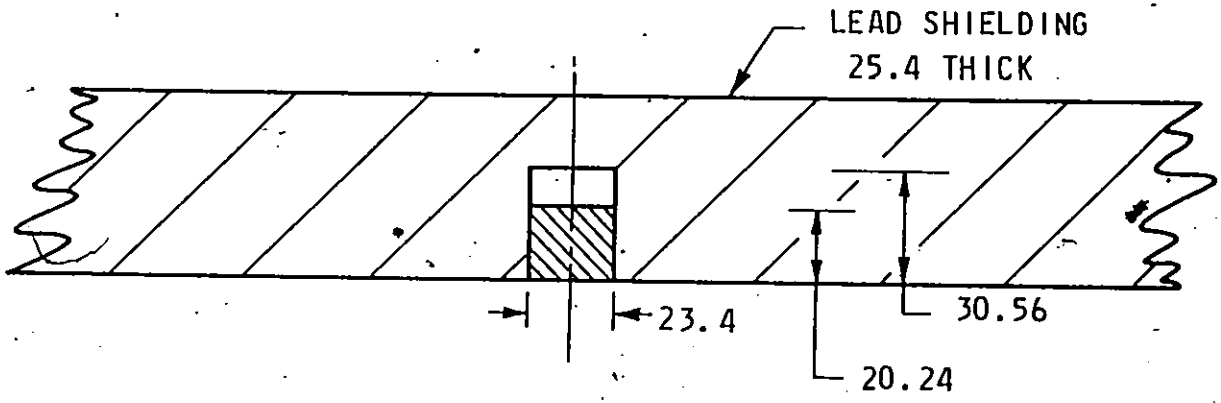

DETECTOR WINDOW (FRONT VIEW)

FIGURE A.1 DIMENSIONS OF COLLIMATORS

(ALL DIMENSIONS IN mm)

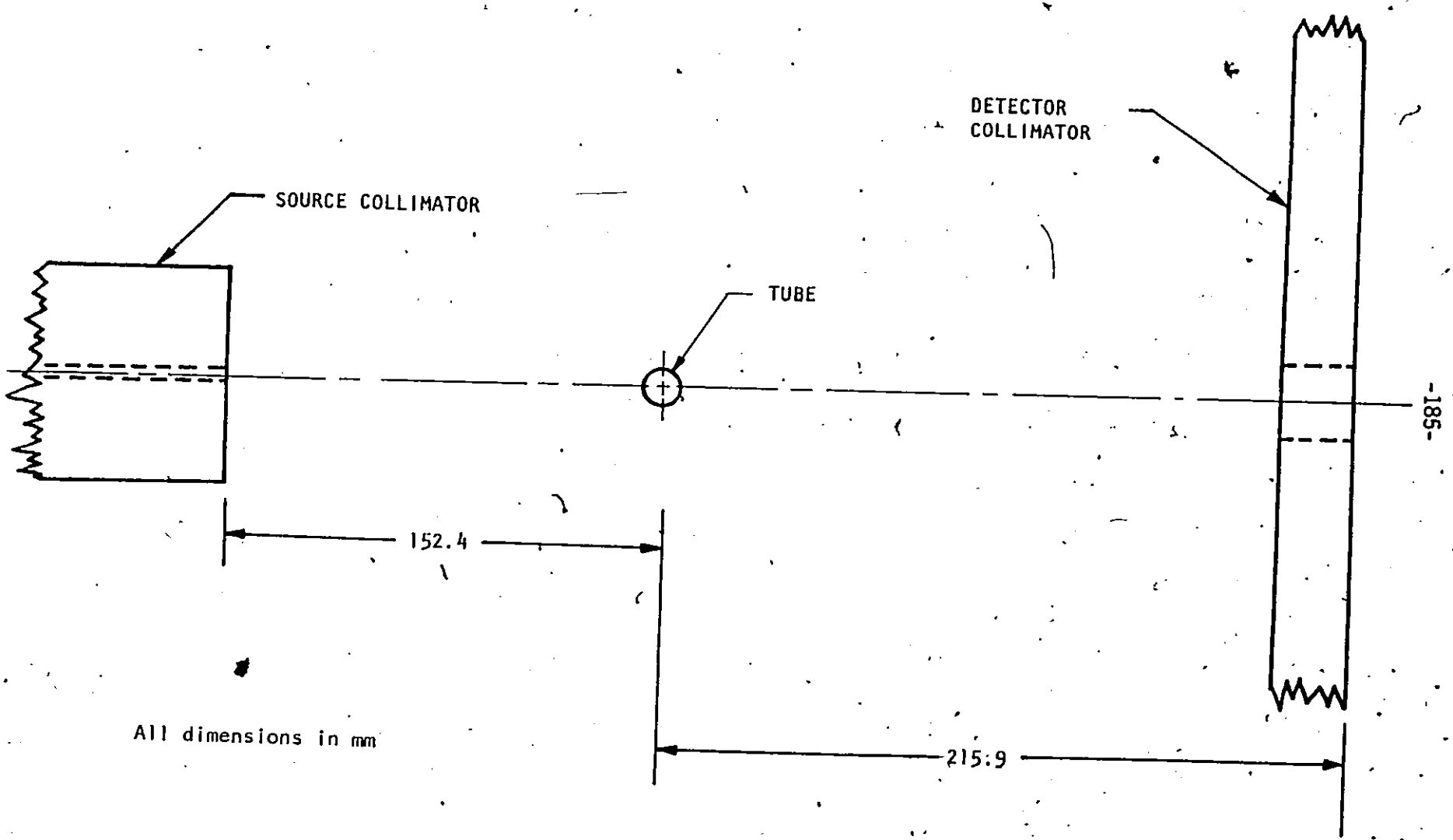

FIG. A.2 PLAN VIEW OF γ-DENSITOMETER ARRANGEMENT

where I_E and I_F are the empty and full count rate respectively.

It can be shown (Chan [1980]) that if I_E/I_F is close to unity, then $A = 1 - \alpha$.

The above method of relating the attenuation to the void fraction is applicable in an arrangement in which the beam is at least as wide as the tube cross section. In such case the void fraction is the average void fraction over the cross section. In order to investigate the effect of preferential void distribution on the measured attenuation, a computer program was written to calculate the attenuation, assuming that the flow was homogeneous in one case and inverted annular in the other. The results are shown in Fig. A.3. It can be seen that the present arrangement does not differentiate between flow regimes.

A.3 ERROR ANALYSIS

Let I_F and I_E be the full and empty count rate averaged over a period of τ s. Since radioactive decay follows Poisson statistics, the associated standard deviations are $\sqrt{I_E/\tau}$ and $\sqrt{I_E/\tau}$ respectively. If during the calibration runs n repeats are taken, then we have

average full count rate = $\bar{I}_F \pm K\sqrt{I_F/n\tau}$

average empty count rate = $\bar{I}_E \pm K\sqrt{I_E/n\tau}$

where K is a function of the confidence level.

For 95% confidence, K = 1.96.

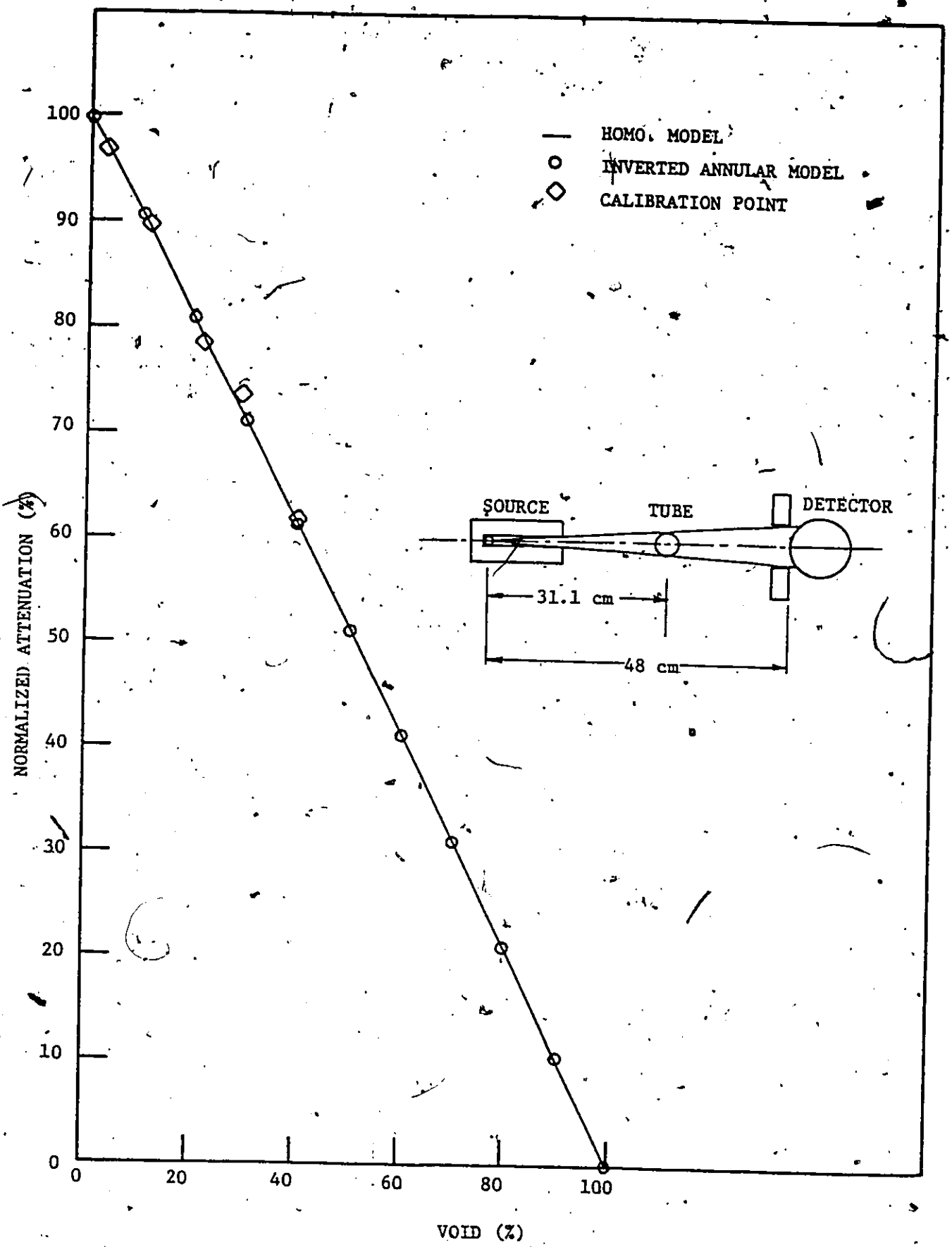

FIGURE A.3 GAMMA DENSITOMETER CALIBRATION CURVE

If we assume that I_E/I_F is close to 1, then the full scale difference can be written as

$$F.S. = (\bar{I}_E - \bar{I}_F) \pm 2K\sqrt{I_E/n\tau}$$

If a count rate of I is obtained over the same period τ during the experiment, then

$$\% \text{ attenuation "a"} = \frac{I_E - I}{I_E - I_F}$$

$$\frac{\Delta a}{a} = \frac{\Delta(I_E - I)}{I_E - I} + \frac{\Delta(I_E - I_F)}{I_E - I_F}$$

$$\Delta a = \frac{\Delta(I_E - I)}{I_E - I_F} + a\,\frac{\Delta(I_E - I_F)}{I_E - I_F}$$

$$= \frac{K}{I_E - I_F}\left[\left(\sqrt{\frac{I_E}{n\tau}} + \sqrt{\frac{I}{\tau}}\right) + 2a\sqrt{\frac{I_E}{n\tau}}\right]$$

$$\approx \frac{K}{I_E - I_F}\left[(1 + \sqrt{n}) + 2a\right]\sqrt{\frac{I_E}{n\tau}}$$

For the densitometer used in this investigation,

$$I_E - I_F \approx 0.05\ I_E$$

$$N_E = 2{,}500{,}000 \text{ for } \tau = 200 \text{ s}$$

$\therefore$ $I_E = 12,500$

$\therefore$ For 95% confidence level

$$\Delta a = 1.96 \left[(1 + \sqrt{5}) + 2a\right] \frac{1}{0.05 \times 12,500} \times \sqrt{\frac{12,500}{200 \times 5}}$$

$$= (3.236 + 2a) \times 0.01108$$

Since $a = 1 - \alpha$

$\therefore$ $\Delta a = \Delta\alpha$

The following table shows the variation of $\Delta\alpha$ at different void fractions

a	α %	$\Delta a = \Delta\alpha$ %
0	100	3.6
0.5	50	4.7
1	0	5.8

The lower $\Delta\alpha$ at large void fraction is due to the slight increase in count rate.

A.4 EFFECT OF THERMAL EXPANSION OF TUBE ON THE ATTENUATION

Consider a small element ΔL along the tube with mass equal to Δm.

Density of tube wall = $\rho \frac{4\Delta m}{\pi D^2 \Delta L}$

$\therefore \frac{d\rho}{\rho} = - \frac{d(\Delta L)}{(\Delta L)}$

The linear absorption coefficient is given by

$$\mu = K\rho(T)$$

where K is a coefficient calculated from the absorption cross section of individual atoms of the tube material.

The change in the absorption coefficient is therefore

$$\Delta\mu = K \frac{d\rho}{dT} \Delta T$$

$$= - K \frac{\rho}{\Delta L} \frac{\alpha(\Delta L)}{dT} \Delta T$$

$$= - K \rho \alpha_L \Delta T$$

$$= - \mu\alpha_L \Delta T$$

$$\therefore \quad \mu = \mu_0(1 - \alpha(T - T_0))$$

For the water inside the tube, the change in temperature is too small to affect the absorption correlation.

A computer program was written to calculate the change in count rate due to expansion of the tube. The results are shown in Table A.1(a).

Measurements were taken by heating up the tube. The results are shown in Table A.1(b). The higher ratio in the measurement was partly due to the lower gas density at higher temperature, and other uncertainties in the insulating material surrounding the tube. It was therefore decided to use the theoretical prediction to correct for the measured count rate. The correction curve is shown in Fig. A.4.

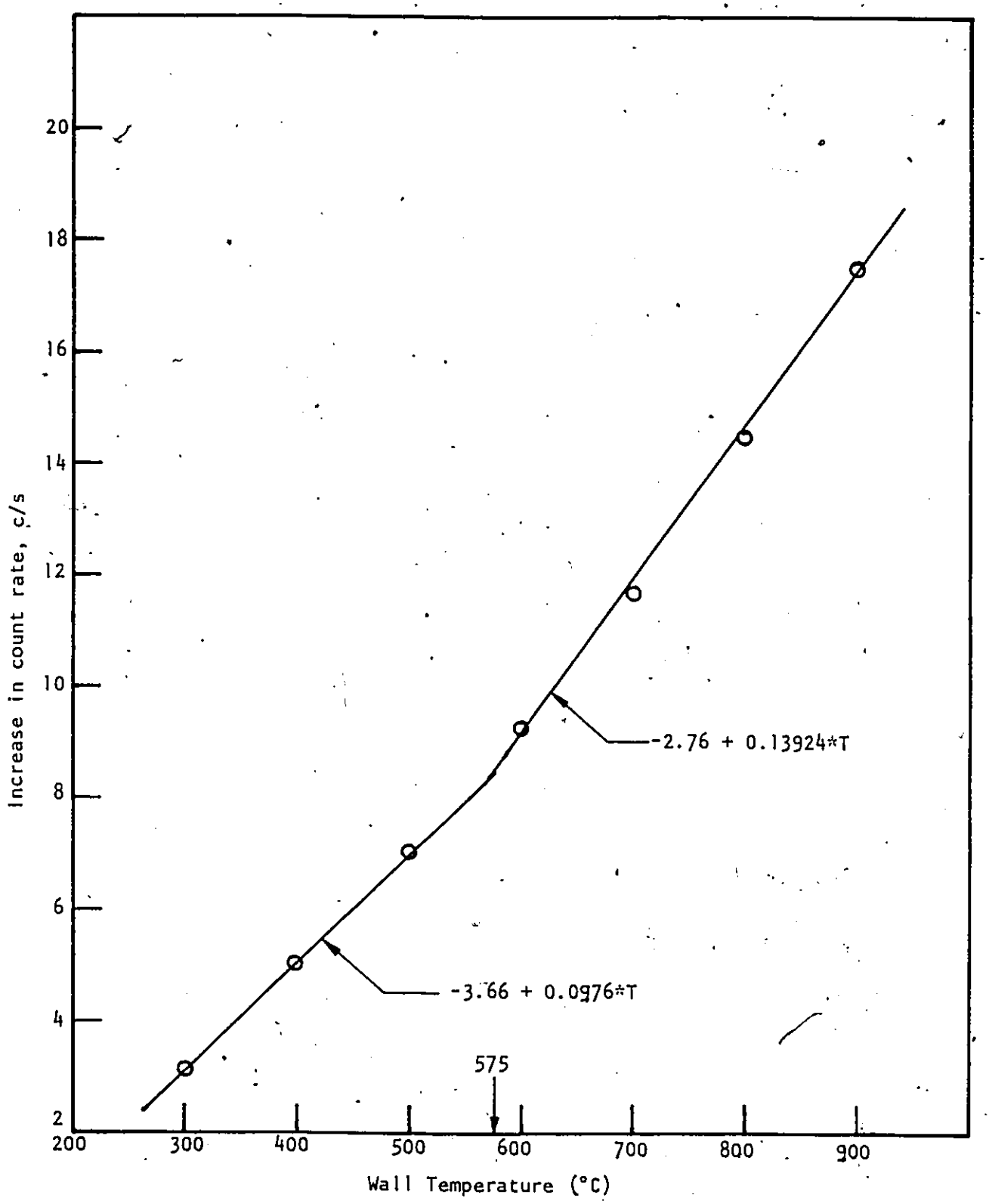

FIG. A.4 TEMPERATURE CORRECTION FOR COUNT RATE

TABLE A.1

TEMPERATURE CORRECTION FOR EMPTY COUNT RATE

(a) Theoretical

T (°C)	Empty count rate ratio I/I_o
20	1
200	1.0003218
300	1.0005145
400	1.0007084
500	1.0009096
600	1.0011290
700	1.0013760
800	1.0016540
900	1.0019530
1000	1.0022470
1100	1.0024830

(b) Experimental

T (°C)	Counts in 200 s	Average over No. of samplings	I/I_o
20	2664271	7	1
400	2665365	8	1.0004106
600	2669760	10	1.0020600
970	2671814	7	1.0028310

APPENDIX B: CORRECTIONS USED IN DATA REDUCTION

B.1 Temperatures on the Inside Surface of the Tube

Since the thermocouples were spot-welded on the outside of the tube, the temperature of the inside surface has to be estimated by solving the steady-state heat conduction equation for the tube wall.

If the axial temperature gradient is assumed to be much smaller than the radial gradient, then the governing equation is

$$\frac{d^2T}{dr^2} + \frac{1}{r}\frac{dT}{dr} + \frac{q'''}{k} = 0$$

where q''' is the heat generation rate in W/m.

The solution in terms of the inside surface heat flux ϕ is

$$T_i = T_o - \frac{\phi R_i}{k}\left[\frac{R_o^2}{R_o^2 - R_i^2}\ \ell n \frac{R_o}{R_i} - \frac{1}{2}\right]$$

For a typical value of ϕ = 200 kW/m^2 and k = 20 W/m^2 (°C/m), $T_o - T_i$ = 2.9°C.

B.2 Electrical Resistivity

For each test section, the electrical resistance per metre of the tube was calculated from the voltage and current measured during a heat balance run in which the maximum wall temperature was about 90°C.

The resistance at other temperatures was then corrected by using the information from the supplier. Table B.1 tabulates the thermal properties of Inconel 718. Assigning a value of 1 to the resistivity at 90°C, the resistivity at other temperatures is given by the following polynomial derived by fitting the data:

$$^{\dagger}RESIST = 0.98372 + (0.162122E\text{-}3)*T - (0.11893E\text{-}6)*T^2 + (0.307604E\text{-}10)*T^3$$

The total power along the tube is calculated using the resistance and the measured current. This is then compared with the product of the measured current and voltage. The difference is generally less than 1%.

B.3 Thermal Conductivity

The normalized thermal conductivity is given by the following correlation:

$$^{\dagger}COND = 0.875672 + (0.120865\text{-}E\text{-}2)*T + (0.174172E\text{-}6)*T^2 - (0.102129E\text{-}9)*T^3$$

---

†T is in °C

B.4 Heat Loss by Axial Conduction

- Consider the heat balance for an elemental length ΔZ

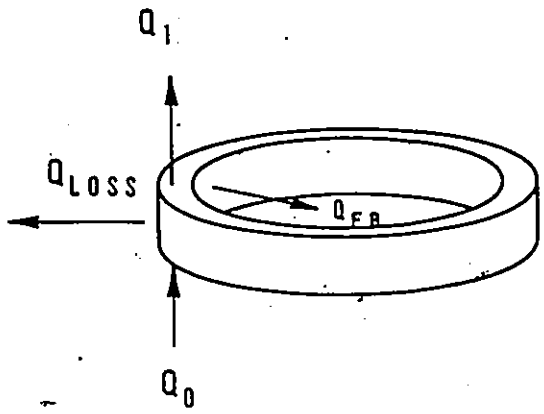

$$Q_{FB} + Q_{LOSS} + Q_1 = Q_0 + q''' \Delta V \qquad \ldots \quad B.4.1$$

where the Q's represent the heat losses from different faces and q''' is the rate of heat generation per unit volume.

In terms of the temperature gradient, Eq. B.4.1 becomes

$$- 2\pi R_i k \Delta Z \left.\frac{\partial T}{\partial R}\right|_{R_i} - 2\pi R_o k \Delta Z \left.\frac{\partial T}{\partial R}\right|_{R_o} - \int_{R_i}^{R_o} 2\pi R \left(k + \frac{\partial k}{\partial Z} \Delta Z\right)\left(\frac{\partial T}{\partial Z} + \frac{\partial}{\partial Z}\left(\frac{\partial T}{\partial Z}\right) \Delta Z\right) dR = - \int_{R_i}^{R_o} 2\pi R k \frac{\partial T}{\partial Z}\, dR + q''' \pi \left(R_o^2 - R_i^2\right) \Delta Z$$

Dividing each side by $2\pi\Delta Z R_i$, we obtain

$$- k \left.\frac{\partial T}{\partial R}\right|_{R_i} - k \frac{R_o}{R_i} \left.\frac{\partial T}{\partial R}\right|_{R_o} - \int_{R_i}^{R_o} \frac{R}{R_i} \frac{\partial}{\partial Z} k \left(\frac{\partial T}{\partial Z}\right) dR = q''' \frac{\left(R_o^2 - R_i^2\right)}{2R_i}$$

$$\because \quad \phi_{FB} = - k \left.\frac{\partial T}{\partial R}\right|_{R_i} \qquad \phi_{LOSS}\Big|_{R_o} = - k \left.\frac{\partial T}{\partial r}\right|_{R_o}$$

$$\therefore \quad \phi_{FB} - \phi_{LOSS}\Big|_{R_o} \frac{R_o}{R_i} - \frac{k}{R_i} \int_{R_i}^{R_o} R \frac{\partial^2 T(R,Z)}{\partial Z^2} dR = q''' \frac{\left(R_o^2 - R_i^2\right)}{2R_i}$$

Since the wall is thin

$$\frac{\partial^2 T}{\partial Z^2}(R,Z) \approx \text{independent of } R \approx \frac{\partial^2 T}{\partial Z^2}(R_o,Z)$$

$$\therefore \quad \phi_{FB} = q''' \frac{\left(R_o^2 - R_i^2\right)}{2R_i} - \phi_{LOSS}\Big|_{R_o} \frac{R_o}{R_i} \frac{R_o^2 + R_i^2}{2R_i} k \frac{\partial^2 T(R_o,Z)}{\partial Z^2}$$

$$q''' = \frac{\text{Power}}{\pi(R_o^2 - R_i^2) \times HL}$$

$$\phi_{FB} = \frac{\text{Power}}{2\pi R_i \times HL} - \phi_{LOSS}\Big|_{R_o} \frac{R_o}{R_i} + \frac{r_o^2 - r_i^2}{2r_i} k \frac{\partial^2 T}{\partial Z^2}(R_o,Z)$$

The second spatial derivative is approximated by first fitting a second order polynomial through three adjacent points and then differentiating the resulting polynomial. Thus, if the temperatures at Z_1, Z_2 and Z_3 are T_1, T_2 and T_3 respectively, then the Lagrange interpolation is

$$T(R_o,Z) = \frac{(Z - Z_2)(Z - Z_3)}{(Z_1 - Z_2)(Z_1 - Z_3)} T_1 + \frac{(Z - Z_1)(Z - Z_3)}{(Z_2 - Z_1)(Z_2 - Z_3)} T_2 + \frac{(Z - Z_1)(Z - Z_2)}{(Z_3 - Z_1)(Z_3 - Z_2)} T_3$$

and

$$\frac{\partial^2 T}{\partial Z^2}(R_o,Z_2) = 2\left[\frac{T_1}{(Z_1 - Z_2)(Z_1 - Z_3)} + \frac{T_2}{(Z_2 - Z_1)(Z_2 - Z_3)} + \frac{T_3}{(Z_3 - Z_1)(Z_3 - Z_2)}\right]$$

For calculating the gradients at the first and last test section thermocouple locations the "zeroth" and "n+1"st thermocouples were used if they were installed in the test section. Otherwise, the temperature at the mid-plane of the hot patch was taken as the "zeroth" temperature; the n+1st temperature was taken to be 450°C below the nth temperature and the location was at the bottom edge of the downstream power clamp. The value 450°C was chosen after an extensive survey of the data in which the n+1st thermocouple was installed.

B.5 Test Section Radial Heat Loss Through Insulations

During the commissioning of a new test section, a dry test was carried out in which the test section was heated up with a slow flow of nitrogen through it instead of water. The heat flux, after being corrected for axial loss, is the radial heat loss. Near the start and end of the heated length, axial conduction was greater than the radial heat loss under dry conditions. Therefore, it was decided to take only the heat loss at the location of zero axial temperature gradient and derive a correlation of heat loss vs. wall temperature. This correlation was then used at other axial locations. For test section A, the correlation is

$$\phi_{LOSS} = 1.23974 - (0.381818E\text{-}2)*T + (0.129243E\text{-}4)*T^2 + (0.194641E\text{-}9)*T^3 \quad kW/m^2 \text{ of tube inside surface}$$

Test sections C, D and E were similar and the heat loss calibration was carried out for test section C only. The correlation is

$$\phi_{LOSS} = 0.22619319E1 - (0.16666573E\text{-}1)*T + (0.46720548E\text{-}4)*T^2 - (0.21880536E\text{-}7)*T^3$$

Another independent estimate can be made by considering the conduction through the insulation.

Consider the situation shown in the following sketch

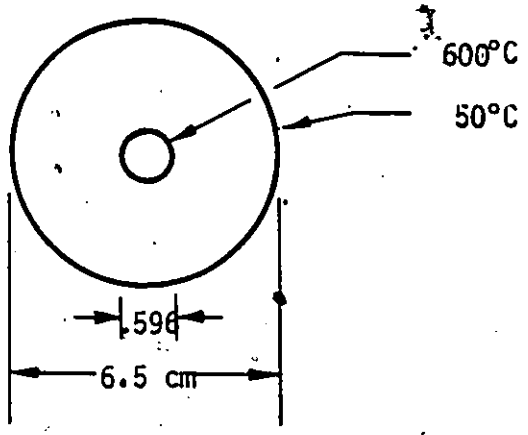

The thermal conductivity of the insulation is assumed to be $0.035\ W \cdot m^{-1} \cdot C^{\circ -1}$.

$\therefore$ Heat loss by conduction through insulation

$$= \frac{k\ \Delta T}{r_i\ \ell n\ (r_o/r_i)}$$

$$= \frac{0.035 \times (600 - 50)}{0.0059 \times \ell n\ (0.065/0.00596)}$$

$$= 1351\ W/m^2 \text{ of tube inside surface.}$$

Using the second correlation expression, the result is $4355\ W/m^2$.

The discrepancies may be due to the following factors;

(i) the insulation close to the tube had been observed to heat up to a glowing red condition. This had the effect of reducing the insulation thickness;

(ii) for a power supply rated at 50 V and 1000 A, it was not possible to measure accurately the actual power at such low levels (a heat flux of 4355 W/m^2 was equivalent to a total power of 114 W for the test section). The empirical correlation will tend to correct for any zero offset.

B.6 Heat Loss in Hot Patch

Dry test similar to those described in B.5 were carried out for the hot patch. The correlation derived is

$$Q = 155.344 - (0.437261)*T + (0.487421E-3)*T^2 \quad W$$

This correction was applied to all test sections. It would appear that test section E should have a different heat loss since the hot patch was shorter. However, the difference was found to be small. This was because the heat loss was more dependent on the area of the exposed insulation surface.

B.7 Linear Expansion

The coefficient of linear expansion is given in Table B.1. The correlation derived by means of least squares fit to these data is

$$\alpha = (12.87195823 + (0.3832677818E\text{-}2)*T + (0.5699454545E\text{-}6)*T^2 + (0.3313636364E\text{-}9)*T^3)*10^{-6}$$

m/m/°C

All dimensions of the Inconel tube are corrected for thermal expansion.

B.8 Pressure Drop Along the Heated Length

The test section pressure at the inlet was measured by means of a pressure gauge. The actual value was not recorded because of its fluctuating nature. Instead, the pressure along the heated length is calculated by using two-phase pressure drop correlations. The calculations are carried out backward from the point where the flow discharges into the reservoir at atmospheric pressure. From this point to the end of the heated length, the Claxton* (1972) correlation for two-phase frictional pressure drop for adiabatic round tubes is used. The calculations are as follows.

* Strictly speaking, this correlation should only be applied to 2ϕ flow in which the wall is wetted. Since there is no correlation available for predicting the pressure drop in inverted annular flow, we will use it as a first approximation. In addition, the correlations quoted in this section are taken from some proprietory report. Therefore, the references will not be given. Luckily, those who work in this field will have no difficulties identifying the sources.

$$Re_g = \frac{G.D}{\mu_g}$$

$$Re_\ell = \frac{G(1 - x)D}{\mu_\ell}$$

Calculate f_ℓ and f_g from the expression

$$f = \begin{cases} 16/Re & \text{if } Re \leq 2000 \\ 0.0014 + 0.125/Re^{0.32} & \text{if } Re > 2000 \end{cases}$$

$$\left(\frac{dP}{dZ}\right)_g = \frac{2f_g G^2 x^2 V_g}{D}$$

$$\left(\frac{dP}{dZ}\right)_\ell = \frac{2f_\ell G^2 (1 - x)^2 v_\ell}{D}$$

$$X = \left[\left(\frac{dP}{dZ}\right)_\ell \Big/ \left(\frac{dP}{dZ}\right)_g\right]^{\frac{1}{2}}$$

$$f_1(G) = 28 - 0.3G^{\frac{1}{2}}$$

$$\Lambda = \frac{\rho_g}{\rho_\ell}\left(\frac{\mu_\ell}{\mu_g}\right)^{0.2}$$

$$T_1 = \exp\left[-\frac{\log_{10}\Lambda + 2.5^2}{2.4 \cdot 10^{-4}\,(G)}\right]$$

$$C = -2 + f_1(G) \cdot T_1$$

$$\phi_\ell^2 = 1 + C/X + 1/X^2$$

$$Re_{\ell o} = \frac{G \cdot D}{\mu_\ell}$$

Calculate $f_{\ell o}$ from $Re_{\ell o}$ as before.

$$T_2 = (1 - x)^2 \frac{f_\ell}{f_{\ell o}}$$

$$\phi_{\ell o}^2 = \phi_\ell^2 \cdot T_2$$

If $\phi_{\ell o}^2 < 1$ put $\phi_{\ell o}^2 = 1$

$$\left(\frac{dP}{dZ}\right) = \frac{2 f_{\ell o} G^2 V_\ell \phi_{\ell o}^2}{D}$$

Along the heated length, Rouhani's (1969) modification of Becker's (1962) correlation is used. The two-phase multiplier is defined as

$$\phi^2 = \frac{(dP/dZ)_{\text{two-phase}}}{(dP/dZ)_{\text{single-phase liquid}}}$$

$$= 1 + 2850\ (X/P) - 8150\ (X/P)^2$$

where X is the vapour weight quality

P is the pressure in bars.

This correlation is applicable in the range $0.001 < X/P < 0.1$. However, it is extrapolated to beyond the upper range for the following reasons:

(a) the length over which the quality is greater than 0.1 in the present study is relatively short, if exists at all.

(b) The overall pressure along the heated length is small.

Therefore, errors introduced due to extrapolation will not significantly affect the pressure drop estimate.

For qualities below 0.001, the value at 0.001 is used.

B.9 Program Listing

A listing of the computer program incorporating all the corrections can be found in the following pages.

TABLE B.1

THERMAL PROPERTIES OF INCONEL 718*

(Ann. 1800°F/h)

Temperature °F	Thermal Conductivity Btu/sq.ft/ht/°F/in.	Electrical Resistivity Ohm/circ.mil/ft.	Mean Linear Expansion in/in/°F x 10^{-6}
200	86	762	7.2
400	98	772	7.8
600	111	775	8.0
800	123	784	8.1
1000	135	798	8.2
1200	147	805	8.6
1400	160	802	9.1
1600	173	799	9.5
1800	185	801	9.8
2000	196	811	10.0

*From International Nickel Company of Canada Ltd. (INCO).

CONVERSION FACTORS

1 Btu/sq.ft/h/F/in. = 0.14423 W/m^2 (°C/m)

1 Ohm/circ.mil/ft = 1.662×10^{-3} $Ohm/mm^2/m$

in/in/°F = 5/9 m/m/°C

```
      PROGRAM BOIL (INPUT,OUTPUT,PUNCH,TAPE5,       TAPE6=OUTPUT,
     *  TAPE7=PUNCH,PLOT)
C
CCCCCCCCCCCCCCCCCCCCCCCCCCCCCCCCCCCCCCCCCCCCCCCCCCCCCCCCCCCCCCCCC
C
C     PROGRAM BOIL CALCULATES LOCAL HEAT FLUX FROM FILM BOILING
C     RAW DATA.  VARIOUS CORRECTIONS ARE INCORPORATED.  SEE
C     APPENDIX B OF THESIS BY K.K.FUNG
C
CCCCCCCCCCCCCCCCCCCCCCCCCCCCCCCCCCCCCCCCCCCCCCCCCCCCCCCCCCCCCCCCC
      REAL STORH(50,10),STORTS(50,10),STORPR(50,10)
      REAL H(12),HLSAT(12),TSAT(12),PP(12)
      COMMON/WATER/RR(13)
      INTEGER RUNAME,PBL
      INTEGER NAME
      REAL TW(12),T(12),R(13),PHI(11),X(12),HTC(11),HT(12)
      REAL TT(8),Z(5)
      REAL STORT(50,10),STORP(50,10)
      REAL TBS(50),PHIS(50)
      COMMON/L120/K(148)
      COMMON /SCALES/ XMIN,XMAX,TICX,FXSCAL,YMIN,YMAX,TICY,FYSCAL
      COMMON /FORMAT/XL,YL, FTITLE(8),FSUBTIT(8),FXAXTIT(8),FYAXTIT(8),
     1NSTVARS,STVARS(10)
      COMMON /SYMEAN/SYMCOD(10),FSYMB1(2),FSYMB2(2),FSYMB3(2),FSYMB4(2),
     1FSYMB5(2),FSYMB6(2),FSYMB7(2),FSYMB8(2),FSYMB9(2),FSYMB10(2)
     1 ,SYMLOCX,SYMLOCY
      COMMON /TITLOC/ TITLOCX,TITLOCY,SUBLOCX,SUBLOCY,XAXLOCX,XAXLOCY,
     1 YAXLOCX,YAXLOCY
      DATA FAREA/1.119316BE-4/
      DATA HT/0.,3.,6.,9.,12.,18.,24.,35.,45.,50.,55.,63./
      DATA Z/1.5,15.,30.,43.,52./
      DATA JOPT1,JOPT2/0,0/
       DATA EQUIL/0./
      DATA JOBPUN/0/
      DATA NOTITL/1/
C
C     JOBPUN=0 MEANS NO PUNCHED CARDS
C     JOPT1=1 NO PLOT
C     DEFAULT IS WITH PLOT AND WITHOUT PUNCHED CARDS
C
C     NOTITLE=0 MEANS NO PLOT HEADING
C
C     DEFAULT IS WITH HEADING
C
      NOTITL=0
      JOPT1=1
C
CCCCCCCCCCCCCCCCCCCCCCCCCCCCCCCCCCCCCCCCCCC
C
C     TEST SECTION GEOMETRY
C
CCCCCCCCCCCCCCCCCCCCCCCCCCCCCCCCCCCCCCCCCCCC
C
C
C
C     NTE  IS TOTAL NUMBER OF T/C MINUS ONE
C     RHO IS ELECTRICAL RESISTANCE PER METER
```



```
C     HLEND  IS HEATED LENGTH BEYOND LAST T/C
C     HLST IS HEATED LENGTH BEFORE HOT PATCH
C     RORI IS (RO**2-RI**2)/RI METER
C     PERIM IS HEATED PERIMETER
C     NEU = NO. OF ADDITIONAL MEASURED POINTS
C     DE = TUBE ID
C     DODO = TUBE OD
C     POUT = OUTLET PRESSURE
C     ADLENG = ADIABATIC LENGTH DOWNSTREAM OF HEATED LENGTH
C     ADHGT = VERTICAL DISTANCE BETWEEN DISCHARGE AND END
C             OF HEATED LENGTH
C
C
CCCCCCCCCCCCCCCCCCCCCCCCCCCCCCCCCCCCCCCCCCCCCCCCCCCCCCCCCCCCCC
C
C     CHANGE THE FOLLOWING VARIABLES FOR DIFFERENT TEST SECTIONS
C     ALSO CHANGE DATA CARD FOR HEATED LENGTH
C     CHANGE FUNCTION TSLOSS
C
C
C     TEST SECTION E
      NTE=11
      RHO=0.055735
      HLEND=0.0979
      HLST=0.0335
      NEU=4
      DE=0.01194
      DODO=0.01308
C
C     END CHANGES
C
CCCCCCCCCCCCCCCCCCCCCCCCCCCCCCCCCCCCCCCCCCCCCCCCCCCCCCCCCCCCCCCCC
C
      POUT=101.3
      ADLENG=4.65
      ADHGT=1.45
      PERIM=3.1416*DE
      RORI=2.*(DODO*DODO-DE*DE)/DE
C     RCOND IS USED IN CORRECTION OF WALL TEMPERATURE
C
      RCOND=0.5*DE*((1./(1.-(DE/DODO)**2))*ALOG(DODO/DE)-0.5)
      CALL PAGE(ISET)
C     READ FIRST GROUP
   39 CONTINUE
      IX=0
      IC=0
   35 READ (5,51) RUNAME,G,PBL
      IF (EOF(5) .NE. 0.) STOP  "EODATA"
      IF (G .EQ. 0.) GO TO 36
      NAME=RUNAME
      IC=IC+1
      PB=FLOAT(PBL)
      READ (5,52)  (T(J),J=2,NTE),TIN,TOUT,TBY,TBL,EI,EE
      IF (NEU .NE. 0) READ (5,52) (TT(I),I=1,NEU)
C
C     IDENTIFY FIRST AND LAST THERMOCOUPLES
C
```

```
      IF (NEU .EQ. 0) GO TO 34
      T(1)=TT(3)
      T0=TT(3)
      T(12)=TT(2)
      GO TO 366
   34 CONTINUE
      T(1)=TBL
      T(12)=T(11)-450.
      T12=110.
      HT1=HT(1)
      HT(1)=-3.18
  366 CONTINUE
C
C     CALCULATE INLET ENTHALPY
C
C
      FTIN=(TIN*1.8)+32.,
      PBRIT=POUT/6.8948
      CALL POLSAN (0.,FTIN,K,R,1)
      HIN=R(2)*2326.
C     CALCULATE FLUID PROPERTIES AT OUTLET (ATM) PRESSURE
C
      CALL POLSAN(PBRIT,0.,K,R,1)
      HFG=(R(8)-R(2))*2326.
      HLOUT=R(2)*2326.
C     CALCULATE POWER AND ENTHALPY UP TO END OF HOT PATCH
C
      PB=PB-BLOSS(TBL)
      POW=HLET*RHO*EI**2
      POW1=PB+POW
      H(1)=HIN+POW1/G/FAREA
C
CCCCCCCCCCCCCCCCCCCCCCCCCCCCCCCCCCCCCCCCCCCCCCCCCCCCCCCCCCCC
C
C     FILM BOILING SECTION
C
CCCCCCCCCCCCCCCCCCCCCCCCCCCCCCCCCCCCCCCCCCCCCCCCCCCCCCCCCCCCC
C      CALCULATE RADIAL HEAT FLUX
C
      DO 11 I=2,NTE
      PHIR=RHO*RESIST(T(I))*EI**2/PERIM/(1.+2.*EXPAN(T(I))*T(I))
C
C
C     CALCULATE AXIAL HEAT CONDUCTION
      DTXX=T(I+1)/((HT(I+1)-HT(I-1))*(HT(I+1)-HT(I)))
     1 +T(I)/((HT(I)-HT(I+1))*(HT(I)-HT(I-1)))
     2 +T(I-1)/((HT(I-1)-HT(I))*(HT(I-1)-HT(I+1)))
   31 CONTINUE
       AXPHI=DTXX*TCOND(T(I))*HORI
C
C     CORRECT RADIAL HEAT FLUX FOR ALL LOSSES
C
      PHI(I)=(PHIR+AXPHI-TBLOSS(T(I))*1000.)/(1.+EXPAN(T(I))*T(I))
      IF (NEU .EQ. 0) HT(1)=HT1
      HL=HT(I)-HT(I-1)
      POW=POW+HL*PHI(I)*0.01*PERIM*(1.+EXPAN(T(I))*T(I))**2
C
```



```
CCCCCCCCCCCCCCCCCCCCCCCCC
C
C     CORRECTED WALL TEMPERATURE
C
CCCCCCCCCCCCCCCCCCCCCCCCCCCCCCCC
C
      TW(I)=T(I)-PHI(I)*RCOND/TCOND(T(I))
C
C
C
      H(I)=HIN+(POW+PB)/(G9FAREA)
      N=I-1
   11 CONTINUE
C
C     CALCULATE TOTAL TEST SECTION POWER
      TNTE=T(NTE+1)
      POWC=POW+RESIST(TNTE)*HLEND*RHO*EI*EI*(1.+EXPAN(TNTE)*TNTE)
     1   /(1.+2.*EXPAN(TNTE)*TNTE)
      HOUT=HIN+POWC/G/FAREA
      POWM=EI*EE
C
CCCCCCCCCCCCCCCCCCCCCCCCCCCCCCCCCCCCCCCCCCCCCCCCCCCC
C
C     ESTIMATE PRESSURE DROP
C
CCCCCCCCCCCCCCCCCCCCCCCCCCCCCCCCCCCCCCCCCCCCCCCCCCCCCC
C
      XOUT=(HOUT-HLOUT)/HFG
      CALL POLSAN(PBRIT,0.,K,RR,1)
C
C     CALCULATE PRESSURE DROP ALONG ADIABATIC SECTION DOWNSTREAM
C     OF HEATED LENGTH
C
      CALL ADPDRO(G,XOUT,DE,DPDZ)
      PD1=-DPDZ*ADLENG
      PBRIT1=PBRIT+PD1/6.8948
      CALL POLSAN (PBRIT1,0.,K,RR,1)
      HFG1=(RR(8)-RR(2))*2326.
      X12=(HOUT-RR(2)*2326)/HFG1
      XAVG=(X12+XOUT)*0.5
      IF(XAVG .LE. 0.) XAVG=0.
      VAVG=((R(1)+RR(1))*0.5*(1.-XAVG)+XAVG*0.5*(R(7)+RR(7)))/16.018
      P12=POUT+PD1-ADHGT*9.81/VAVG/1000.
      PP(NTE+1)=P12
      X(NTE+1)=X12
C
C     CALCULATE PRESSURE DROP ALONG HEATED LENGTH
C
      NTE1=NTE+1
      DO 17 J=2,NTE1
      LL=NTE+2-J
      LL1=LL+1
      CALL DIPDRO (G,X(LL1),PP(LL1),DE,DPDZ)
      PP(LL)=PP(LL1)-DPDZ*(HT(LL1)-HT(LL))*0.01
     1     +0.01*(HT(LL1)-HT(LL))*9.81/1000./((RR(1)*(1.-X(LL1))+
     2      RR(7)*X(LL1))/16.018)
      PBRIT2=PP(LL)/6.8948
```

```
      PROGRAM BOIL      74/74   OPT=1 ROUND=--=*/                    FTN 4.8+498      80-09-03  11.29.29      PAGE    5

                CALL POLSAN (PRINT2,0.,K,RR,1)
                X(LL)=(E(LL)/2326.-RR(2))/(RR(8)-RR(2))
                TSAT(LL)=(RR(13)-32.)/1.8
                HLSAT(LL)=RR(2)*2326.
             17 CONTINUE
                IF (PP(1) .LT. POUT) PP(1)=POUT
      C
      C         DATA TABULATION
      C
                IF (ISET .EQ. 10) CALL PAGE (ISET)
                WRITE (6,67) RUNAME,TIN,G,PB,TBL,PONN,PONC
                WRITE (6,66) PP(1),PP(12),HIN,E(1),TSAT(1),HLSAT(1)
                WRITE(6,691) (TW(II),II=2,NTE)
                WRITE(6,692) (PHI(II),II=2,NTE)
                WRITE(6,693) (E(II),II=2,NTE)
                ISET=ISET+1
                NTE1=NTE-1
      C
      C         STORE DATA FOR PLOT
      C
                DO 12 J=1,NTE1
                STORT(IC,J)=TW(J+1)
                STORP(IC,J)=PHI(J+1)
                STORPH(IC,J)=PP(J+1)
                STORE(IC,J)=E(J+1)
                STORTS(IC,J)=TSAT(J+1)
                PHI(J+1)=PHI(J+1)*0.001
             12 CONTINUE
                IF (JOBFUN .EQ. 0) GO TO 35
                WRITE (7,71) RUNAME,TIN,G,TBL,PB,E(1)
                WRITE (7,72)  (TW(J),J=2,NTE),TW(1),TW(NTE+1)
                WRITE (7,73) (PHI(J),J=2,NTE)
                GO TO 35
      C
             36 CONTINUE
                IF(JOBFUN .NE.0) WRITE (7,74) G
      C
                IF ( JOPT1 .EQ. 1) GO TO 39
      C         PLOT DATA
                XMIN=200.      $ XMAX=1200.
                YMIN=10.      $ YMAX=1.E3
                TICX=50.
                XL=5.6   $YL=6.6
                IF (NOTITL .EQ. 0) GO TO 32
                FTITLE(1)=10H('SUBCOOLE
                FTITLE(2)=10HD FLUX BOI
                FTITLE(3)=10HLING')
                GO TO 33
             32 CONTINUE
                FTITLE(1)=10H(' ')
             33 CONTINUE
                FSUBTIT(1)=10H('RUNAME='
                FSUBTIT(2)=10H,A10)
                NSTVARS=1
                CALL CHAR(0,NAME,7,1,NSTVARS(1))
                FXATTIT(1)=10H('TW-TSAT
                FXATTIT(2)=10H (DEG C)')


      PROGRAM BOIL.     74/74   OPT=1 ROUND=--=*/                    FTN 4.8+498      80-09-03  11.29.29      PAGE    6

                FYATTIT(1)=10H('HEAT FLU
                FYATTIT(2)=10HX   (KW/M**
                FYATTIT(3)=10H2)')
                SYMLOCX=0.75
                SYMLOCY=6.1
                SUBLOCX=3.
                SUBLOCY=6.1
                FSYMB1(1)=10H('T/C- 1')
                FSYMB2(1)=10H('T/C- 2')
                FSYMB3(1)=10H('T/C- 3')
                FSYMB4(1)=10H('T/C- 4')
                FSYMB5(1)=10H('T/C- 5')
                FSYMB6(1)=10H('T/C- 6')
                FSYMB7(1)=10H('T/C- 7')
                FSYMB8(1)=10H('T/C- 8')
                FSYMB9(1)=10H('T/C- 9')
                FSYMB10(1)=10H('T/C-10')
                JOBOPT=1
                NTE1=NTE-1
                DO 14 II=1,NTE3,2
                DO 13 J=1,IC
                TSS(J)=STORT(J,II)-STORTS(J,II)
                PHIS(J)=STORP(J,II)/1000.
             13 CONTINUE
                SYMCOD(II)=II
                CALL SIMPLT(JOBOPT,TSS,PHIS,IC,0,II,2)
                JOBOPT=1
             14 CONTINUE
                II=9
                SYMCOD(II)=16
                DO 15 J=1,IC
                TSS(J)=STORT(J,II)-100.
                PHIS(J)=STORP(J,II)/1000.
             15 CONTINUE
                CALL SIMPLT(JOBOPT,TSS,PHIS,IC,0,16,2)
                GO TO 39
             31 FORMAT (A8,42X,F10.3,I10)
             32 FORMAT( 1X,8F7.2)
             66 FORMAT (1X,16X,10E12.6)
             67 FORMAT (1X,A10,6X,10E12.6)
            691 FORMAT (2X,'T',2X,10E12.6)
            692 FORMAT (2X,'P',2X,10E12.6)
            693 FORMAT (2X,'E',2X,10E12.6,/)
             71 FORMAT (A8,F8.2,2F6.0,F7.0,E10.3)
             72 FORMAT(12F6.0)
             73 FORMAT(10F6.1)
             74 FORMAT (16X,F6.0)
                END
```

```
      SUBROUTINE PAGE (ISET)
      WRITE (6,60)
   60 FORMAT ('1')
      ISET=0
      RETURN
      END


      FUNCTION RESIST (T)
C
C     ELECTRICAL RESISTIVITY OF INCONEL 718 NORMALISED
C
      RESIST=(((0.3076048E-10*T-0.1189308E-6)*T+0.162122E-3)*T+0.98372)
      RETURN
      END


      FUNCTION EXPAN(T)
C
C     LINEAR COEFFICIENT OF EXPANSION
C
      EXPAN=((((.3313636364E-9)*T+.5699454545E-6)*T+.3832677818E-2)
     1     *T+.1287195823E2)*1.E-6
      RETURN
      END


      FUNCTION TCOND(T)
C
C     THERMAL CONDUCTIVITY OF INCONEL 718
C
      TCOND=(((-0.102129E-9*T+0.1741728E-6)*T+0.120865E-2)*T+0.875672)
     1  *12.48
      RETURN
      END


      FUNCTION TSLOSS(T)
C
C     HEAT LOSS CORRECTION FOR TEST SECTION
      TSLOSS=(((-.21880536E-7*T+.46720548E-4)*T-.166665573E-1)*T+
     *.22619319E01)
      IF (T .LT.200.) TSLOSS=0.
      RETURN
      END


      FUNCTION BLOSS(T)
C
C     HEAT LOSS CORRECTION FOR HOT PATCH
C
      BLOSS=(0.487421E-1*T-0.437261)*T+155.344
      IF (T .LT. 200.) BLOSS=0.
      RETURN
      END
```

```
SUBROUTINE ADFDRO     74/74   OPT=1 ROUND=--*/                FTN 4.8+498        80-09-03  11.29.29       PAGE     1

1               SUBROUTINE ADFDRO (G,XE,DE,DFDX)
                COMMON/WATER/RR(13)
              C
              C
5             C
              C
                RHOL=1./RR(1)*16.018
                RHOG=1./RR(7)*16.018
                VISCL=RR(3)*1.4882
                VISCG=RR(9)*1.4882
10              IF (XE .GT. 0.) GO TO 31
                TWOFLO=1
                GO TO 32
             31 REG=G*XE*DE/VISCG
                REL=G*(1.-XE)*DE/VISCL
15              FL=FRICT(REL)
                FG=FRICT(REG)
              C
                DPDZG=2.*FG*((G*XE)**2)/DE/RHOG
                DPDZL=2.*FL*((G*(1.-XE))**2)/DE/RHOL
20            C
                X=SQRT(DPDZL/DPDZG)
                F1=28.-0.3*SQRT(G)
                GAMA=(RHOG/RHOL)*(VISCL/VISCG)**0.2
                T1=EXP(-((ALOG10(GAMA)+2.5)**2)/(3.4-(1.E-4)*G))
25              C=2.*F1*T1
                TWOFL=1.+C/X+1./X/X
             32 CONTINUE
                RELO=G*DE/VISCL
                FLO=FRICT(RELO)
30              IF (XE .LE. 0.) GO TO 33
                T2=((1.-XE)**2)*FL/FLO
                TWOFLO=TWOFL*T2
                IF (TWOFLO .LT. 1.) TWOFLO=1
             33 DPDX=-2.*FLO*G*G*TWOFLO/RHOL/DE
35              DPDX=DPDX/1000.
                RETURN
                END
```

```
SUBROUTINE DIFDRO     74/74   OPT=1 ROUND=--*/                FTN 4.8+498        80-09-03  11.29.29       PAGE     1

1               SUBROUTINE DIFDRO (G,XE,P,DE,DFDX)
                COMMON/WATER/RR(13)
              C
5             C     TWO-PHASE FRICTIONAL PRESSURE DROP FOR HEATED ROUND DUCTS
              C     MOURANI'S MODIFICATION OF BECKER'S CORRELATION
              C
              C     INPUT PRESSURE IS IN KPA
              C
                XA=XE
10              RHOL=1./RR(1)*16.018
                RHOG=1./RR(7)*16.018
                VISCL=RR(3)*1.4882
                VISCG=RR(9)*1.4882
                IF(XA .LT. 0.001) XA=0.001
15              IF(XA .GT. 0.174848) XA=0.174848
                XPBAR=XA/(P/100.)
                TWOFL=1.+2850*XPBAR-8150.*XPBAR*XPBAR
                REL=G*DE/VISCL
                FL=FRICT(REL)
20              DFDX=-2*FL*G*G*TWOFL/RHOL/DE
                DFDX=DFDX/1000.
                RETURN
                END
```

```
1               FUNCTION FRICT (RE)
                FRICT=16./RE
                IF (RE .GT. 2000.) FRICT=0.0014+0.125/(RE**.32)
                RETURN
5               END
```

APPENDIX C : DATA TABULATION

Each run is identified by an eight character alphanumeric run name. The legend is shown below:

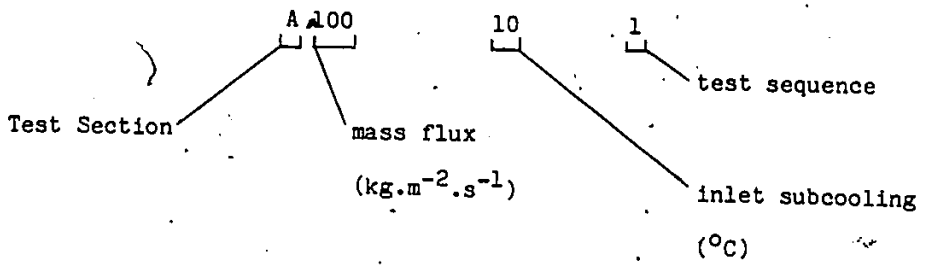

Note that the mass flux and inlet subcooling in the run names are nominal values and should not be used in any actual calculations.

Each set of data consists of five lines. The format is:

First line

Run name

Inlet Temperature (°C)

Mass flux ($kg.m^{-2}.s^{-1}$)

Hot patch power (W)

Hot patch temperature (°C)

Measured power (W)

Corrected power (W)

Second line

Calculated pressure at end of hot patch (kPa)

*Calculated pressure at end of heated length (kPa)

Inlet enthalpy (J/kg)

Enthalpy at end of hot patch (J/kg)

*Saturation temperature at end of hot patch (^{o}C)

*Saturated liquid enthalpy at end of hot patch (J/kg)

Third line

Corrected wall temperature (^{o}C) at 10 locations.

Fourth line

Heat flux (W/m^2) at 10 locations.

Fifth line

Enthalpy (J/kg) at 10 locations.

* In the case where this calculated value is below the atmospheric pressure, the atmospheric pressure is tabulated in its place. The saturation temperature and liquid enthalpy still correspond to the calculated pressure.

The distances in cm of the ten thermocouple locations measured from the top of the hot patch are:

	TEST SECTION	
	A	C, D and E
TS1	2.46	3
TS2	5.08	6
TS3	7.38	9
TS4	10.28	12
TS5	15.08	18
TS6	25.48	24
TS7	35.48	35
TS8	45.88	45
TS9	55.64	50
TS10	70.27	55

```
 A 50.501          .491800E+02 .499600E+02 .936084E+03 .5652402+03 .2157888E+04 .1884488E+04
                   .102701E+03 .1021858+03 .205827E+06 .391678E+06 .1003788+03 .4206598+06
   T   .563701E+03 .617041E+03 .657840E+03 .699398E+03 .735423E+03 .8649608+03 .9570318+03 .1059468E+04 .1119028E+04 .9482568+03
   F   .710046E+05 .7038178+05 .6983408+05 .6913368+05 .6862558+05 .6613528+05 .6401948+05 .6134208+05 .5963528+05 .6423158+05
   E   .403467E+06 .4159388+06 .4268178+06 .4404338+06 .4628108+06 .5097648+06 .5538638+06 .5976378+06 .6378568+06 .7022688+06

 A 50.502          .493600E+02 .499600E+02 .936160E+03 .5645708+03 .1958148+04 .1733858+04
                   .102722E+03 .1021168+03 .206579E+06 .3908158+06 .1003848+03 .4206838+06
   T   .532702E+03 .584829E+03 .6347368+03 .6579078+03 .7023158+03 .8108498+03 .8935238+03 .9564958+03 .1006108+04 .8971358+03
   F   .647693E+05 .6422188+05 .6373578+05 .6318808+05 .6262758+05 .6072448+05 .5900778+05 .5755018+05 .5631288+05 .5892618+05
   E   .401558E+06 .4129238+06 .4228408+06 .4359278+06 .4556668+06 .4986988+06 .5390478+06 .5800878+06 .6178608+06 .6768178+06

 A 50.503          .497300E+02 .499600E+02 .936237E+03 .5638908+03 .1680968+04 .1498558+04
                   .101807E+03 .1015638+03 .208127E+06 .3899688+06 .1001338+03 .4196258+06
   T   .484190E+03 .523686E+03 .5512148+03 .5903788+03 .6373458+03 .7404628+03 .8118058+03 .8707878+03 .9192998+03 .8316088+03
   F   .555114E+05 .5517268+05 .5490388+05 .5447518+05 .5388058+05 .5234238+05 .5094348+05 .4988078+05 .4912488+05 .5067338+05
   E   .399159E+06 .4089028+06 .4174228+06 .4280958+06 .4456028+06 .4825898+06 .5173128+06 .5527498+06 .5853708+06 .6359298+06

 A 50.504          .502900E+02 .499600E+02 .941390E+03 .5625308+03 .1470008+04 .1311838+04
                   .101392E+03 .1010128+03 .210468E+06 .391398E+06 .1000188+03 .4191428+06
   T   .436459E+03 .467728E+03 .4078908+03 .5200898+03 .5603138+03 .6402848+03 .7248168+03 .7885368+03 .8264628+03 .7659558+03
   F   .484888E+05 .4827158+05 .4811748+05 .4781858+05 .4743088+05 .4644058+05 .4524438+05 .4415528+05 .4344538+05 .4455468+05
   E   .399419E+06 .4079228+06 .4153728+06 .4247228+06 .4400908+06 .4728128+06 .5035348+06 .5347968+06 .5637088+06 .6088048+06

 A 50.505          .502900E+02 .499600E+02 .936689E+03 .5598008+03 .1329628+04 .1210288+04
                   .1013008+03 .9943558+02 .2104688+06 .3894058+06 .9961228+02 .4174398+06
   T   .413473E+03 .438347E+03 .4804308+03 .4879458+03 .5127688+03 .5999738+03 .6896858+03 .7370178+03 .7711518+03 .3242478+03
   F   .440012E+05 .4385068+05 .4369928+05 .4344738+05 .4327428+05 .4236158+05 .4116108+05 .4044228+05 .3984638+05 .4434268+05
   E   .396674E+06 .4043958+06 .4111558+06 .4196448+06 .4333698+06 .4634148+06 .4913268+06 .5198868+06 .5463438+06 .5898028+06

 A 50.051          .945700E+02 .499600E+02 .310788E+03 .3587108+03 .1636718+04 .1434538+04
                   .1037748+03 .1030708+03 .396177E+06 .4657548+06 .1006708+03 .4218928+06
   T   .549271E+03 .597980E+03 .6314508+03 .6689008+03 .7128648+03 .7858918+03 .8526118+03 .8604978+03 .8980948+03 .8561658+03
   F   .532368E+05 .5270108+05 .5227868+05 .5177158+05 .5110948+05 .4986618+05 .4910408+05 .4842038+05 .4782338+05 .4850778+05
   E   .474589E+06 .4819208+06 .4920568+06 .5022298+06 .5188808+06 .5541838+06 .5876648+06 .6220488+06 .6538378+06 .7022868+06

 A 50.052          .947500E+02 .499600E+02 .299809E+03 .3622508+03 .2123338+04 .1836508+04
                   .1044218+03 .1036518+03 .396935E+06 .4684648+06 .1008458+03 .4226308+06
   T   .658400E+03 .723243E+03 .7605978+03 .8014218+03 .8543278+03 .9340968+03 .1006038+04 .1054628+04 .1111888+04 .9814618+03
   F   .688735E+05 .6787838+05 .6721698+05 .6648008+05 .6559998+05 .6363848+05 .6183918+05 .6053848+05 .5891008+05 .6246778+05
   E   .480115E+06 .4921918+06 .5027078+06 .5158398+06 .5373258+06 .5826558+06 .6235158+06 .6668528+06 .7082398+06 .7709768+06

 A 50.053          .938500E+02 .499600E+02 .3030328+03 .3615408+03 .1904238+04 .1665778+04
                   .1041148+03 .1033768+03 .393145E+06 .4637098+06 .1007628+03 .4222808+06
   T   .613338E+03 .6744228+03 .7039248+03 .7330618+03 .7910148+03 .8694678+03 .9257458+03 .9614438+03 .1002478+04 .9268468+03
   F   .620595E+05 .6123678+05 .6078368+05 .6023848+05 .5928768+05 .5772108+05 .5647278+05 .5562618+05 .5460768+05 .5644568+05
   E   .474032E+06 .4849048+06 .4941908+06 .5082738+06 .5295698+06 .5666548+06 .6053248+06 .6450028+06 .6816248+06 .7381748+06

 A 50.054          .942100E+02 .499600E+02 .325940E+03 .3495008+03 .1341068+04 .1177648+04
                   .1033418+03 .1026878+03 .394661E+06 .4643818+06 .1005538+03 .4213968+06
   T   .487014E+03 .5374818+03 .5539308+03 .5777528+03 .6028148+03 .7004108+03 .7211608+03 .7573058+03 .7908308+03 .7741238+03
   F   .434949E+05 .4304118+05 .4287508+05 .4281808+05 .4232758+05 .4100008+05 .4067828+05 .4008938+05 .3949748+05 .3979308+05
   E   .471584E+06 .4791888+06 .4858428+06 .4941888+06 .5079218+06 .5368478+06 .5644668+06 .5928138+06 .6190588+06 .6588688+06

 A 50.055          .945700E+02 .499600E+02 .326144E+03 .3518308+03 .1127448+04 .1000668+04
                   .1030568+03 .1024408+03 .396177E+06 .4641368+06 .1004758+03 .4210688+06
   T   .434745E+03 .4678718+03 .4834588+03 .5036788+03 .5358528+03 .6118268+03 .6458808+03 .6761238+03 .7172898+03 .6454708+03
   F   .366568E+05 .3642268+05 .3610008+05 .3612918+05 .3583168+05 .3499038+05 .3455948+05 .3413678+05 .3352228+05 .3455868+05
   E   .470196E+06 .4766158+06 .4822358+06 .4892928+06 .5008898+06 .5254938+06 .5488868+06 .5729488+06 .5951588+06 .6293868+06

 A 50.101          .879000E+02 .499600E+02 .545939E+03 .4886208+03 .1693808+04 .1475898+04
                   .1036438+03 .1029048+03 .368107E+06 .4601548+06 .1006358+03 .4217428+06
   T   .586015E+03 .6215278+03 .6507138+03 .6818408+03 .7142288+03 .8010038+03 .8623338+03 .9119268+03 .9333798+03 .8131098+03
   F   .543255E+05 .5407048+05 .5377028+05 .5336668+05 .5277038+05 .5126778+05 .5005718+05 .4899018+05 .4850468+05 .5101698+05
   E   .489214E+06 .4987978+06 .5071628+06 .5176348+06 .5340268+06 .5711438+06 .6053258+06 .6401928+06 .6728198+06 .7235028+06

 A 50.102          .893500E+02 .499600E+02 .396041E+03 .5227108+03 .1642168+04 .1269428+04
                   .1033128+03 .1026548+03 .374205E+06 .4574188+06 .1005458+03 .4213628+06
   T   .549344E+03 .5850248+03 .5988508+03 .6166708+03 .6438448+03 .7235668+03 .7994388+03 .8401768+03 .8672378+03 .7589098+03
   F   .467681E+05 .4638168+05 .4623008+05 .4600338+05 .4565138+05 .4428328+05 .4317248+05 .4239528+05 .4185018+05 .4389208+05
   E   .465180E+06 .4733888+06 .4805748+06 .4895968+06 .5044298+06 .5357158+06 .5651198+06 .5951998+06 .6210978+06 .6667608+06

 A 50.101          .902500E+02 .499600E+02 .330792E+03 .3856308+03 .2038468+04 .1767418+04
                   .1041398+03 .1034008+03 .3779928+06 .4546618+06 .1007698+03 .4223088+06
   T   .633502E+03 .6952338+03 .7394818+03 .7867958+03 .8087028+03 .9111368+03 .9733908+03 .1032938+04 .1098668+04 .9714808+03
   F   .663864E+05 .6550048+05 .6478178+05 .6426998+05 .6352098+05 .6135698+05 .5987338+05 .5887078+05 .5815068+05 .5951908+05
   E   .465712E+06 .4773528+06 .4874758+06 .5001508+06 .5209248+06 .5643918+06 .6059678+06 .6474278+06 .6853048+06 .7456548+06

 A 50.102          .898900E+01 .499600E+02 .336792E+03 .3856308+03 .1787798+04 .1562948+04
                   .1033978+03 .1030968+03 .376477E+06 .4523348+06 .1006768+03 .4219188+06
   T   .582085E+03 .6234328+03 .6527498+03 .6821668+03 .7311048+03 .8292068+03 .9040328+03 .8728678+03 .9482438+03 .8867158+03
   F   .579993E+05 .5747448+05 .5710978+05 .5668798+05 .5591908+05 .5413898+05 .5324428+05 .5256798+05 .5155558+05 .5290268+05
   E   .461970E+06 .4721578+06 .4810528+06 .4921968+06 .5194278+06 .5488228+06 .5853198+06 .6225978+06 .6570878+06 .7095998+06

 A 50.103          .902500E+02 .499600E+02 .338963E+03 .3884708+03 .1635968+04 .1456288+04
                   .1036398+03 .1029558+03 .377992E+06 .4528168+06 .1006148+03 .4217378+06
   T   .555696E+03 .6069778+03 .6336428+03 .6585668+03 .6935358+03 .7858838+03 .8421458+03 .8729058+03 .9087418+03 .8650618+03
   F   .540135E+05 .5341538+05 .5309778+05 .5276008+05 .5225678+05 .5078678+05 .4986948+05 .4899978+05 .4823578+05 .4916318+05
   E   .461783E+06 .4712478+06 .4795118+06 .4898748+06 .5068808+06 .5437868+06 .5767948+06 .6116068+06 .6431848+06 .6923958+06

 A 50.104          .895300E+02 .499600E+02 .340792E+03 .3856308+03 .1401618+04 .1239128+04
                   .1032508+03 .1026168+03 .374963E+06 .4479078+06 .1005528+03 .4212918+06
   T   .491570E+03 .5298118+03 .5621088+03 .5631398+03 .5980678+03 .6912918+03 .7370048+03 .7775138+03 .8089068+03 .7875478+03
   F   .437413E+05 .4540618+05 .4528038+05 .4506298+05 .4466918+05 .4333868+05 .4270368+05 .4201298+05 .4144198+05 .4183238+05
   E   .455483E+06 .4613508+06 .4705278+06 .4793678+06 .4938378+06 .5244108+06 .5534218+06 .5831538+06 .6107118+06 .6523738+06

 A 50.201          .806600E+02 .499600E+02 .436826E+03 .4914208+03 .2012688+04 .1772958+04
                   .1037928+03 .1030868+03 .337687E+06 .4330878+06 .1006758+03 .4219128+06
   T   .581246E+03 .6292798+03 .6667948+03 .7069408+03 .7533318+03 .8658528+03 .9456148+03 .1010038+04 .1037118+04 .8470028+03
   F   .661006E+05 .6551428+05 .6499818+05 .6439018+05 .6361718+05 .6143428+05 .5963148+05 .5801738+05 .5731178+05 .6182828+05
   E   .444070E+06 .4556838+06 .4658128+06 .4784838+06 .4994218+06 .5426788+06 .5837478+06 .6255228+06 .6637218+06 .7254498+06

 A 50.202          .803000E+02 .499600E+02 .431993E+03 .4872208+03 .1706158+04 .1508298+04
                   .1033508+03 .1026938+03 .336178E+06 .4280578+06 .1005558+03 .4214068+06
   T   .520845E+03 .5702168+03 .6042478+03 .6307838+03 .6818328+03 .7822358+03 .8561428+03 .9031148+03 .9301478+03 .7842978+03
   F   .560468E+05 .5535058+05 .5515848+05 .5482468+05 .5411418+05 .5245918+05 .5102808+05 .5002698+05 .4941918+05 .5242018+05
   E   .437349E+06 .4471758+06 .4557508+06 .4665088+06 .4841168+06 .5212488+06 .5560848+06 .5916758+06 .6247098+06 .6768908+06

 A 50.203          .792100E+02 .499600E+02 .432189E+03 .4816208+03 .1633338+04 .1618008+04
                   .1034908+03 .1028148+03 .331600E+06 .4245968+06 .1005938+03 .4213678+06
   T   .540868E+03 .5887208+03 .6234728+03 .6626968+03 .7047818+03 .8154828+03 .8828678+03 .9477788+03 .9715398+03 .8064688+03
   F   .601956E+05 .5968168+05 .5925838+05 .5872838+05 .5810018+05 .5615888+05 .5477778+05 .5330858+05 .5273728+05 .5631058+05
   E   .434583E+06 .4451468+06 .4542668+06 .4659038+06 .4848268+06 .5246308+06 .5620698+06 .6000708+06 .6353878+06 .6915328+06

 A 50.204          .804800E+02 .499600E+02 .536674E+03 .4949108+03 .1533398+04 .1365218+04
                   .1031438+03 .1024898+03 .328931E+06 .4460868+06 .1004998+03 .4211698+06
   T   .490613E+03 .5227438+03 .5493088+03 .5844488+03 .6261718+03 .7142778+03 .7916348+03 .8435788+03 .8710318+03 .7432618+03
   F   .504968E+05 .5021658+05 .4995758+05 .4958108+05 .4907178+05 .4778118+05 .4649348+05 .4550048+05 .4494118+05 .4733888+05
   E   .454449E+06 .4633178+06 .4710688+06 .4807808+06 .4967158+06 .5304658+06 .5621208+06 .5944088+06 .6243728+06 .6714348+06
```

```
A 50.205          .795800E+02 .499600E+02 .540563E+03 .515090E+03 .140161E+04 .124782E+04
                  .102904E+03 .102281E+03 .333153E+06 .441822E+06 .100434E+03 .420894E+06
  T   .475100E+03 .500725E+03 .518211E+03 .549362E+03 .577727E+03 .669823E+03 .734803E+03 .790628E+03 .825193E+03 .684190E+03
  F   .458729E+05 .456643E+05 .454062E+05 .452070E+05 .449034E+05 .437327E+05 .427396E+05 .417781E+05 .411334E+05 .435236E+05
  E   .449419E+06 .457473E+06 .464513E+06 .473357E+06 .487812E+06 .518731E+06 .547764E+06 .577346E+06 .604717E+06 .647807E+06

A 50.351          .651800E+02 .499600E+02 .526476E+03 .499090E+03 .220592E+04 .195008E+04
                  .103551E+03 .102919E+03 .273779E+06 .385861E+06 .100610E+03 .421636E+06
  T   .551791E+03 .603150E+03 .643590E+03 .693344E+03 .748856E+03 .864943E+03 .959916E+03 .104692E+04 .109201E+04 .890137E+03
  F   .730531E+05 .724782E+05 .719558E+05 .712455E+05 .704531E+05 .680481E+05 .658530E+05 .635837E+05 .623134E+05 .674936E+05
  E   .387986E+06 .410821E+06 .422024E+06 .436037E+06 .459015E+06 .507347E+06 .552509E+06 .598043E+06 .640012E+06 .707522E+06

A 50.352          .646300E+02 .499600E+02 .654966E+03 .487920E+03 .193115E+04 .172445E+04
                  .103078E+03 .102471E+03 .270476E+06 .404558E+06 .100481E+03 .421094E+06
  T   .505142E+03 .552886E+03 .595326E+03 .637253E+03 .676889E+03 .788384E+03 .862055E+03 .930079E+03 .967828E+03 .839703E+03
  F   .641085E+05 .636594E+05 .631898E+05 .626620E+05 .621053E+05 .602448E+05 .587836E+05 .572755E+05 .563742E+05 .592445E+05
  E   .415181E+06 .426435E+06 .436256E+06 .448554E+06 .468759E+06 .511412E+06 .551554E+06 .592350E+06 .630097E+06 .689228E+06

A 50.353          .657300E+02 .499600E+02 .651826E+03 .491420E+03 .206631E+04 .183683E+04
                  .103775E+03 .102674E+03 .275083E+06 .409395E+06 .100670E+03 .421893E+06
  T   .529877E+03 .583948E+03 .630651E+03 .665804E+03 .707752E+03 .831686E+03 .914942E+03 .981827E+03 .102143E+04 .862214E+03
  F   .685040E+05 .679404E+05 .673863E+05 .668817E+05 .662452E+05 .640037E+05 .622045E+05 .605943E+05 .595734E+05 .633693E+05
  E   .420756E+06 .432779E+06 .443263E+06 .456404E+06 .477981E+06 .523377E+06 .565952E+06 .609212E+06 .649201E+06 .712509E+06

A 50.354          .651800E+02 .499600E+02 .651705E+03 .494210E+03 .172501E+04 .154704E+04
                  .102846E+03 .102322E+03 .272779E+06 .404162E+06 .100418E+03 .420826E+06
  T   .467619E+03 .510758E+03 .544750E+03 .578662E+03 .630103E+03 .734692E+03 .800987E+03 .867980E+03 .897204E+03 .788451E+03
  F   .573737E+05 .568911E+05 .566714E+05 .563112E+05 .556875E+05 .541373E+05 .529638E+05 .516312E+05 .510046E+05 .531954E+05
  E   .413651E+06 .423711E+06 .432503E+06 .443531E+06 .461616E+06 .499863E+06 .535938E+06 .572614E+06 .606859E+06 .659640E+06

A 50.355          .648200E+02 .499600E+02 .651705E+03 .494210E+03 .154134E+04 .137733E+04
                  .102291E+03 .102126E+03 .271271E+06 .400996E+06 .100266E+03 .420185E+06
  T   .436429E+03 .470411E+03 .499819E+03 .536511E+03 .584148E+03 .661970E+03 .741080E+03 .799818E+03 .845509E+03 .749855E+03
  F   .508874E+05 .506545E+05 .504201E+05 .500853E+05 .495810E+05 .485908E+05 .473766E+05 .463627E+05 .454618E+05 .472278E+05
  E   .409409E+06 .416331E+06 .423147E+06 .435942E+06 .452017E+06 .486249E+06 .518440E+06 .551266E+06 .581544E+06 .628508E+06

A 50.356          .646300E+02 .499600E+02 .651826E+03 .491420E+03 .140767E+04 .125901E+04
                  .102262E+03 .101754E+03 .270476E+06 .399041E+06 .100258E+03 .420153E+06
  T   .407890E+03 .439249E+03 .469547E+03 .499875E+03 .535754E+03 .605541E+03 .682299E+03 .748930E+03 .790628E+03 .703629E+03
  F   .463118E+05 .461264E+05 .459149E+05 .456715E+05 .454451E+05 .445795E+05 .435527E+05 .425057E+05 .417781E+05 .432318E+05
  E   .406689E+06 .414812E+06 .421916E+06 .430836E+06 .445512E+06 .476853E+06 .506378E+06 .536424E+06 .564185E+06 .607098E+06

A 50.357          .653700E+02 .499600E+02 .651911E+03 .489320E+03 .130323E+04 .116680E+04
                  .102085E+03 .101641E+03 .273575E+06 .401215E+06 .100209E+03 .419947E+06
  T   .388537E+03 .413571E+03 .442038E+03 .460448E+03 .482480E+03 .574136E+03 .646651E+03 .702546E+03 .744904E+03 .609774E+03
  F   .426422E+05 .425167E+05 .423359E+05 .422081E+05 .420399E+05 .411657E+05 .402749E+05 .394769E+05 .388037E+05 .407494E+05
  E   .408254E+06 .415734E+06 .422279E+06 .430511E+06 .444093E+06 .473000E+06 .500267E+06 .528121E+06 .553858E+06 .594164E+06

A 50.701          .294100E+02 .499600E+02 .116321E+04 .588210E+03 .210140E+04 .182597E+04
                  .102870E+03 .101149E+03 .123198E+06 .349193E+06 .100424E+03 .420854E+06
  T   .548141E+03 .605283E+03 .641768E+03 .682056E+03 .731077E+03 .862005E+03 .962639E+03 .106929E+04 .114839E+04 .953585E+03
  F   .692666E+05 .688286E+05 .681581E+05 .675823E+05 .668030E+05 .643102E+05 .620017E+05 .591994E+05 .568940E+05 .632214E+05
  E   .360687E+06 .372842E+06 .383453E+06 .396740E+06 .418519E+06 .464191E+06 .506717E+06 .549156E+06 .587583E+06 .649994E+06

A 50.702          .309100E+02 .499600E+02 .116454E+04 .578120E+03 .182662E+04 .162274E+04
                  .101300E+03 .916634E+02 .129466E+06 .353403E+06 .974042E+02 .408119E+06
  T   .503392E+03 .546522E+03 .583257E+03 .615627E+03 .658504E+03 .763514E+03 .847059E+03 .921696E+03 .962785E+03 .875423E+03
  F   .605400E+05 .601394E+05 .597452E+05 .593578E+05 .587876E+05 .571216E+05 .555101E+05 .539150E+05 .529457E+05 .549360E+05
  E   .363456E+06 .374083E+06 .383365E+06 .395005E+06 .414118E+06 .454519E+06 .492414E+06 .530802E+06 .566248E+06 .621162E+06

A 50.703          .296000E+02 .499600E+02 .120698E+04 .557070E+03 .163737E+04 .144794E+04
                  .101300E+03 .876965E+02 .123992E+06 .353829E+06 .961588E+02 .402870E+06
  T   .468598E+03 .505264E+03 .542017E+03 .574006E+03 .619383E+03 .717116E+03 .804450E+03 .862148E+03 .903136E+03 .824080E+03
  F   .539464E+05 .536534E+05 .533119E+05 .529761E+05 .524387E+05 .510422E+05 .495247E+05 .483863E+05 .475130E+05 .491479E+05
  E   .362757E+06 .372226E+06 .380496E+06 .390869E+06 .407881E+06 .443928E+06 .477665E+06 .512028E+06 .543750E+06 .592771E+06

A 50.704          .296000E+02 .499600E+02 .120748E+04 .552290E+03 .142492E+04 .127229E+04
                  .101300E+03 .876965E+02 .123992E+06 .352114E+06 .964866E+02 .402406E+06
  T   .436428E+03 .464055E+03 .488819E+03 .515494E+03 .550243E+03 .634608E+03 .707973E+03 .768111E+03 .815612E+03 .743300E+03
  F   .489216E+05 .467355E+05 .465441E+05 .463144E+05 .459786E+05 .449939E+05 .439458E+05 .429563E+05 .420912E+05 .433772E+05
  E   .359872E+06 .368108E+06 .375315E+06 .384363E+06 .399254E+06 .430919E+06 .460741E+06 .491129E+06 .519128E+06 .562252E+06

A 50.705          .296000E+02 .499600E+02 .120677E+04 .538580E+03 .132390E+04 .120140E+04
                  .101300E+03 .876965E+02 .123992E+06 .351583E+06 .960919E+02 .402588E+06
  T   .405158E+03 .430983E+03 .451204E+03 .478779E+03 .520142E+03 .596251E+03 .681152E+03 .718378E+03 .771151E+03 .663583E+03
  F   .440467E+05 .438973E+05 .437645E+05 .435607E+05 .432068E+05 .424056E+05 .415712E+05 .407221E+05 .398464E+05 .415360E+05
  E   .358858E+06 .366585E+06 .373353E+06 .381854E+06 .395831E+06 .425633E+06 .453792E+06 .482543E+06 .509000E+06 .550166E+06

A 50.601          .408200E+02 .499600E+02 .109521E+04 .572710E+03 .222007E+04 .195769E+04
                  .102827E+03 .102163E+03 .170879E+06 .385907E+06 .100412E+03 .420804E+06
  T   .570935E+03 .619692E+03 .663264E+03 .704643E+03 .751734E+03 .870618E+03 .964972E+03 .109232E+04 .113828E+04 .971424E+03
  F   .738303E+05 .732514E+05 .726587E+05 .720110E+05 .712412E+05 .688989E+05 .666474E+05 .632672E+05 .619049E+05 .665343E+05
  E   .398170E+06 .411150E+06 .422471E+06 .436844E+06 .459890E+06 .508838E+06 .554560E+06 .599966E+06 .641756E+06 .708547E+06

A 50.602          .406400E+02 .499600E+02 .109496E+04 .574740E+03 .199862E+04 .177373E+04
                  .102130E+03 .101607E+03 .170127E+06 .383217E+06 .100221E+03 .419899E+06
  T   .534432E+03 .578554E+03 .616461E+03 .659549E+03 .706940E+03 .829802E+03 .925714E+03 .992608E+03 .104086E+04 .921642E+03
  F   .665905E+05 .661310E+05 .656789E+05 .651017E+05 .643901E+05 .621801E+05 .601006E+05 .584730E+05 .572110E+05 .601935E+05
  E   .394262E+06 .405963E+06 .416179E+06 .428967E+06 .449940E+06 .494038E+06 .535192E+06 .574960E+06 .613397E+06 .675688E+06

A 50.603          .408200E+02 .499600E+02 .109462E+04 .577440E+03 .171849E+04 .153394E+04
                  .101607E+03 .101016E+03 .170879E+06 .381467E+06 .100078E+03 .419392E+06
  T   .487783E+03 .523667E+03 .560250E+03 .591400E+03 .640188E+03 .739573E+03 .829892E+03 .888730E+03 .930140E+03 .857055E+03
  F   .571842E+05 .568748E+05 .565118E+05 .561654E+05 .555543E+05 .541227E+05 .524067E+05 .511891E+05 .502659E+05 .518569E+05
  E   .390937E+06 .400980E+06 .409752E+06 .420757E+06 .438606E+06 .477044E+06 .512782E+06 .549177E+06 .582777E+06 .634572E+06

A 50.604          .408200E+02 .499600E+02 .109437E+04 .579460E+03 .144216E+04 .128807E+04
                  .101300E+03 .876965E+02 .170879E+06 .378969E+06 .962475E+02 .403244E+06
  T   .439230E+03 .464045E+03 .486869E+03 .525531E+03 .561231E+03 .653839E+03 .744063E+03 .787532E+03 .822358E+03 .763061E+03
  F   .476853E+05 .475150E+05 .473389E+05 .470016E+05 .466441E+05 .455101E+05 .441110E+05 .433896E+05 .427419E+05 .438206E+05
  E   .386853E+06 .395227E+06 .402556E+06 .411744E+06 .426855E+06 .458911E+06 .488889E+06 .519607E+06 .548044E+06 .591645E+06

A 50.605          .406400E+02 .499600E+02 .109358E+04 .585530E+03 .134627E+04 .121640E+04
                  .101300E+03 .876965E+02 .170127E+06 .377307E+06 .961214E+02 .402712E+06
  T   .421738E+03 .441099E+03 .460420E+03 .487936E+03 .526527E+03 .626238E+03 .688767E+03 .733537E+03 .795185E+03 .666057E+03
  F   .447077E+05 .445870E+05 .444540E+05 .442425E+05 .439025E+05 .427925E+05 .419294E+05 .409022E+05 .401713E+05 .422563E+05
  E   .384694E+06 .392546E+06 .399422E+06 .408059E+06 .422264E+06 .452371E+06 .480803E+06 .509721E+06 .538419E+06 .576303E+06

A100.051          .983500E+02 .100130E+03 .363425E+03 .473210E+03 .311162E+04 .286560E+04
                  .110651E+03 .108681E+03 .411106E+06 .457891E+06 .102485E+03 .429551E+06
  T   .790059E+03 .833195E+03 .864650E+03 .889169E+03 .921934E+03 .100513E+04 .103885E+04 .104076E+04 .100576E+04 .916380E+03
  F   .102403E+06 .101587E+06 .100888E+06 .100318E+06 .993204E+05 .973171E+05 .963620E+05 .963064E+05 .973045E+05 .996568E+05
  E   .486655E+06 .475813E+06 .483520E+06 .493443E+06 .509762E+06 .544467E+06 .577561E+06 .611963E+06 .644528E+06 .694321E+06

A100.052          .978100E+02 .100130E+03 .360425E+03 .473210E+03 .276375E+04 .251148E+04
                  .109563E+03 .107735E+03 .409819E+06 .453862E+06 .102204E+03 .428365E+06
  T   .712849E+03 .780818E+03 .806187E+03 .840192E+03 .872925E+03 .942202E+03 .966818E+03 .966818E+03 .952829E+03 .882172E+03
  F   .899219E+05 .892205E+05 .887216E+05 .880153E+05 .872957E+05 .856463E+05 .850198E+05 .850198E+05 .853784E+05 .870839E+05
  E   .461362E+06 .469300E+06 .476236E+06 .484925E+06 .499208E+06 .529663E+06 .558765E+06 .589030E+06 .617535E+06 .660961E+06
```

```
A100.053 -      .978100E+02 .100130E+03 .362458E+03 .471800E+03 .247053E+04 .223507E+04
                .108764E+03 .107040E+03 .409828E+06 .452732E+06 .101996E+03 .427489E+06
  T  .707615E+03 .744512E+03 .770781E+03 .793216E+03 .817803E+03 .882675E+03 .911693E+03 .908501E+03 .903828E+03 .839537E+03
  F  .799740E+05 .793515E+05 .788776E+05 .786538E+05 .779669E+05 .769814E+05 .759142E+05 .759890E+05 .760979E+05 .779177E+05
  E  .459393E+06 .466443E+06 .472601E+06 .480033E+06 .493058E+06 .520218E+06 .546139E+06 .573119E+06 .598470E+06 .637074E+06

A100.054        .974500E+02 .100130E+03 .368504E+03 .469700E+03 .190680E+04 .170628E+04
                .107138E+03 .105645E+03 .408122E+06 .449250E+06 .101570E+03 .425689E+06
  T  .605912E+03 .633540E+03 .658486E+03 .682730E+03 .708566E+03 .768010E+03 .790473E+03 .791523E+03 .793654E+03 .744247E+03
  F  .612540E+05 .609029E+05 .605610E+05 .602705E+05 .598143E+05 .588131E+05 .584035E+05 .583839E+05 .583441E+05 .582265E+05
  E  .454333E+06 .459720E+06 .464428E+06 .470335E+06 .480056E+06 .500815E+06 .520655E+06 .541202E+06 .560629E+06 .590008E+06

A100.055        .970900E+02 .100130E+03 .368545E+03 .467590E+03 .181898E+04 .145978E+04
                .106320E+03 .104953E+03 .406794E+06 .446560E+06 .101353E+03 .424774E+06
  T  .548330E+03 .568592E+03 .586923E+03 .620943E+03 .642675E+03 .688959E+03 .712872E+03 .725439E+03 .736934E+03 .682226E+03
  F  .524190E+05 .522059E+05 .520009E+05 .515693E+05 .513061E+05 .506395E+05 .502812E+05 .500804E+05 .498920E+05 .507476E+05
  E  .450901E+06 .455508E+06 .459539E+06 .464588E+06 .472906E+06 .490725E+06 .507752E+06 .525399E+06 .541905E+06 .567018E+06

A100.056        .983500E+02 .100130E+03 .368624E+03 .462670E+03 .120579E+04 .109682E+04
                .105367E+03 .104126E+03 .412106E+06 .450154E+06 .101099E+03 .423702E+06
  T  .469628E+03 .478842E+03 .486186E+03 .511889E+03 .538472E+03 .589717E+03 .594388E+03 .605613E+03 .615858E+03 .571327E+03
  F  .392252E+05 .391536E+05 .390945E+05 .388734E+05 .386220E+05 .382969E+05 .380177E+05 .378841E+05 .377587E+05 .382780E+05
  E  .453394E+06 .456838E+06 .459858E+06 .463648E+06 .469885E+06 .493301E+06 .496119E+06 .509408E+06 .521842E+06 .540707E+06

A100.057        .972700E+02 .100130E+03 .370659E+03 .459850E+03 .103321E+04 .933009E+03
                .104630E+03 .103509E+03 .407553E+06 .445014E+06 .100901E+03 .422867E+06
  T  .427413E+03 .432956E+03 .439409E+03 .451334E+03 .485339E+03 .515652E+03 .530289E+03 .550397E+03 .561392E+03 .519256E+03
  F  .333274E+05 .332915E+05 .332486E+05 .331658E+05 .329043E+05 .326400E+05 .325019E+05 .323010E+05 .321857E+05 .326054E+05
  E  .447762E+06 .450686E+06 .453250E+06 .456477E+06 .461781E+06 .473194E+06 .484127E+06 .495435E+06 .506013E+06 .522052E+06

A100.101        .907900E+02 .100130E+03 .341932E+03 .408300E+03 .328725E+04 .299409E+04
                .109920E+03 .108112E+03 .380266E+06 .424903E+06 .102297E+03 .428756E+06
  T  .760960E+03 .807411E+03 .846604E+03 .869042E+03 .910765E+03 .100374E+04 .103624E+04 .107730E+04 .102283E+04 .946953E+03
  F  .107732E+06 .106810E+06 .105965E+06 .105455E+06 .104456E+06 .101999E+06 .101068E+06 .998384E+05 .101457E+06 .103536E+06
  E  .433895E+06 .443408E+06 .451707E+06 .462130E+06 .479249E+06 .515621E+06 .550327E+06 .586053E+06 .620036E+06 .671837E+06

A100.102        .906100E+02 .100130E+03 .381987E+03 .409720E+03 .307338E+04 .282041E+04
                .109411E+03 .107657E+03 .379506E+06 .426850E+06 .102165E+03 .428199E+06
  T  .724364E+03 .776429E+03 .801110E+03 .835648E+03 .875789E+03 .942108E+03 .985428E+03 .100995E+04 .981536E+03 .919692E+03
  F  .101408E+06 .100452E+06 .999629E+05 .992385E+05 .983401E+05 .967253E+05 .955851E+05 .949103E+05 .956902E+05 .972874E+05
  E  .435302E+06 .444238E+06 .452051E+06 .461846E+06 .477939E+06 .512331E+06 .545079E+06 .578933E+06 .610922E+06 .659539E+06

A100.103        .906100E+02 .100130E+03 .337932E+03 .408300E+03 .277943E+04 .255828E+04
                .108867E+03 .106998E+03 .379506E+06 .421667E+06 .101976E+03 .427404E+06
  T  .683700E+03 .723012E+03 .751545E+03 .773282E+03 .815174E+03 .888406E+03 .929825E+03 .946045E+03 .940061E+03 .882162E+03
  F  .919924E+05 .913536E+05 .908522E+05 .904495E+05 .896230E+05 .880228E+05 .870323E+05 .866280E+05 .867762E+05 .881652E+05
  E  .429322E+06 .437431E+06 .444516E+06 .453422E+06 .468051E+06 .499277E+06 .529018E+06 .559827E+06 .588781E+06 .632769E+06

A100.104        .891700E+02 .100130E+03 .365564E+03 .398800E+03 .244719E+04 .225606E+04
                .107256E+03 .106056E+03 .373448E+06 .416628E+06 .101601E+03 .425820E+06
  T  .605145E+03 .642365E+03 .668606E+03 .685279E+03 .745723E+03 .824857E+03 .855908E+03 .875340E+03 .875340E+03 .831562E+03
  F  .814344E+05 .809505E+05 .805272E+05 .803266E+05 .793302E+05 .778234E+05 .771710E+05 .767455E+05 .767454E+05 .776839E+05
  E  .423385E+06 .430548E+06 .436813E+06 .444694E+06 .457606E+06 .485139E+06 .511426E+06 .538636E+06 .564717E+06 .602845E+06

A100.105        .904300E+02 .100130E+03 .393676E+03 .406880E+03 .218568E+04 .201988E+04
                .107063E+03 .105599E+03 .378749E+06 .423340E+06 .101550E+03 .425605E+06
  T  .569334E+03 .597766E+03 .622595E+03 .655278E+03 .696417E+03 .766903E+03 .799604E+03 .822117E+03 .829992E+03 .788297E+03
  F  .728678E+05 .725432E+05 .722346E+05 .717934E+05 .711823E+05 .699929E+05 .693813E+05 .689385E+05 .687795E+05 .695956E+05
  E  .429378E+06 .435767E+06 .441394E+06 .448429E+06 .459993E+06 .484697E+06 .508275E+06 .532662E+06 .555503E+06 .590088E+06
```

```
A100.106        .904300E+02 .100130E+03 .394090E+03 .412550E+03 .193115E+04 .177103E+04
                .106320E+03 .104944E+03 .378749E+06 .422195E+06 .101353E+03 .424774E+06
  T  .534463E+03 .555586E+03 .581276E+03 .596026E+03 .633071E+03 .707779E+03 .745900E+03 .773566E+03 .781901E+03 .739516E+03
  F  .634235E+05 .636315E+05 .633525E+05 .631816E+05 .627175E+05 .616326E+05 .610042E+05 .605166E+05 .603644E+05 .611116E+05
  E  .427479E+06 .433091E+06 .438002E+06 .444180E+06 .454344E+06 .476046E+06 .496732E+06 .518097E+06 .538104E+06 .568413E+06

A100.107        .900700E+02 .100130E+03 .394208E+03 .416090E+03 .166811E+04 .154299E+04
                .105667E+03 .104280E+03 .377234E+06 .419602E+06 .101179E+03 .424040E+06
  T  .465778E+03 .485992E+03 .508907E+03 .534563E+03 .573227E+03 .835804E+03 .675927E+03 .697419E+03 .713207E+03 .677808E+03
  F  .556498E+05 .554970E+05 .553058E+05 .550696E+05 .546694E+05 .539109E+05 .533535E+05 .530323E+05 .527864E+05 .533246E+05
  E  .424197E+06 .429080E+06 .433356E+06 .438729E+06 .447569E+06 .466501E+06 .484543E+06 .503210E+06 .520657E+06 .547041E+06

A100.108        .904300E+02 .100130E+03 .398208E+03 .416090E+03 .153520E+04 .141179E+04
                .105118E+03 .103961E+03 .376749E+06 .420857E+06 .101059E+03 .423534E+06
  T  .437339E+03 .450228E+03 .466746E+03 .479616E+03 .526455E+03 .600597E+03 .639028E+03 .656287E+03 .679970E+03 .645732E+03
  F  .508615E+05 .507977E+05 .506813E+05 .505844E+05 .501817E+05 .493888E+05 .489039E+05 .486700E+05 .483327E+05 .488129E+05
  E  .425054E+06 .429519E+06 .433431E+06 .438357E+06 .446459E+06 .463780E+06 .480295E+06 .497399E+06 .513354E+06 .537476E+06

A100.109        .897100E+02 .100130E+03 .398090E+03 .412550E+03 .125226E+04 .117025E+04
                .103888E+03 .103146E+03 .375720E+06 .416667E+06 .100701E+03 .422022E+06
  T  .356998E+03 .362581E+03 .379291E+03 .401484E+03 .435593E+03 .506391E+03 .541980E+03 .559846E+03 .587051E+03 .546741E+03
  F  .420360E+05 .420145E+05 .419440E+05 .418355E+05 .416359E+05 .410958E+05 .407411E+05 .406191E+05 .402768E+05 .407117E+05
  E  .420125E+06 .423808E+06 .427036E+06 .431100E+06 .437801E+06 .452165E+06 .465876E+06 .480099E+06 .493348E+06 .513395E+06

A100.351        .644500E+02 .100130E+03 .103329E+04 .648230E+03 .332244E+04 .305816E+04
                .106456E+03 .105117E+03 .269722E+06 .376194E+06 .101389E+03 .424927E+06
  T  .418117E+03 .517474E+03 .618759E+03 .686508E+03 .781447E+03 .910214E+03 .985361E+03 .109661E+04 .102945E+04 .952647E+03
  F  .112914E+06 .112291E+06 .111196E+06 .110216E+06 .108519E+06 .105647E+06 .103683E+06 .101932E+06 .102436E+06 .104561E+06
  E  .385502E+06 .395394E+06 .404025E+06 .414838E+06 .432527E+06 .470041E+06 .505561E+06 .541982E+06 .576303E+06 .628632E+06

A100.201        .808500E+02 .100130E+03 .659034E+03 .703520E+03 .319153E+04 .289746E+04
                .108355E+03 .106693E+03 .338485E+06 .410979E+06 .101890E+03 .427038E+06
  T  .696074E+03 .742947E+03 .773194E+03 .817632E+03 .875118E+03 .971010E+03 .103626E+04 .109654E+04 .103755E+04 .947953E+03
  F  .105345E+06 .104540E+06 .103970E+06 .103076E+06 .101802E+06 .994035E+05 .975829E+05 .957710E+05 .975456E+05 .100009E+06
  E  .419749E+06 .429036E+06 .437154E+06 .447319E+06 .463678E+06 .499371E+06 .532881E+06 .567183E+06 .599878E+06 .649918E+06

A100.202        .804800E+02 .100130E+03 .659649E+03 .701030E+03 .282639E+04 .259172E+04
                .106592E+03 .105866E+03 .336911E+06 .407933E+06 .101425E+03 .425079E+06
  T  .648088E+03 .680656E+03 .712813E+03 .753046E+03 .793097E+03 .875118E+03 .927954E+03 .949519E+03 .945376E+03 .889268E+03
  F  .936137E+05 .931335E+05 .926183E+05 .919171E+05 .911576E+05 .894152E+05 .881634E+05 .876242E+05 .877290E+05 .890082E+05
  E  .415712E+06 .423966E+06 .431180E+06 .440221E+06 .455087E+06 .486789E+06 .516914E+06 .548082E+06 .577342E+06 .621822E+06

A100.203        .806600E+02 .100130E+03 .670877E+03 .704150E+03 .254494E+04 .234065E+04
                .106099E+03 .105234E+03 .337687E+06 .408494E+06 .101295E+03 .424527E+06
  T  .598556E+03 .625799E+03 .652471E+03 .684166E+03 .739308E+03 .824419E+03 .872631E+03 .891583E+03 .893344E+03 .845293E+03
  F  .846228E+05 .842799E+05 .839164E+05 .834487E+05 .825439E+05 .809261E+05 .798937E+05 .794654E+05 .794249E+05 .804877E+05
  E  .415513E+06 .422967E+06 .429488E+06 .437674E+06 .451106E+06 .479737E+06 .506970E+06 .535164E+06 .561612E+06 .601704E+06

A100.204        .797600E+02 .100130E+03 .674611E+03 .687840E+03 .227813E+04 .210425E+04
                .108149E+03 .104488E+03 .333909E+06 .403931E+06 .101836E+03 .428811E+06
  T  .538046E+03 .559144E+03 .581141E+03 .616988E+03 .671540E+03 .756719E+03 .801844E+03 .826173E+03 .839591E+03 .801848E+03
  F  .761308E+05 .759179E+05 .756778E+05 .752468E+05 .744980E+05 .731093E+05 .722676E+05 .717842E+05 .715087E+05 .722662E+05
  E  .410233E+06 .416930E+06 .422796E+06 .430159E+06 .442250E+06 .468043E+06 .492604E+06 .518002E+06 .541759E+06 .577691E+06

A100.205        .795800E+02 .100130E+03 .730249E+03 .672620E+03 .190423E+04 .175549E+04
                .104898E+03 .103475E+03 .331318E+06 .406479E+06 .100973E+03 .423171E+06
  T  .449160E+03 .466614E+03 .476691E+03 .497766E+03 .565706E+03 .663379E+03 .723316E+03 .748260E+03 .765280E+03 .727258E+03
  F  .636166E+05 .634903E+05 .634251E+05 .631376E+05 .626132E+05 .613906E+05 .604730E+05 .600543E+05 .597566E+05 .604069E+05
  E  .411729E+06 .417313E+06 .422211E+06 .428368E+06 .438490E+06 .466071E+06 .490558E+06 .501739E+06 .521531E+06 .551976E+06
```

```
A100.206        .792100E+02 .100130E+03 .731622E+03 .666240E+03 .173152E+04 .159704E+04
                .103834E+03 .102930E+03 .331600E+06 .404285E+06 .100686E+03 .421960E+06
 T   .396667E+03 .405914E+03 .420675E+03 .451037E+03 .499741E+03 .603327E+03 .656679E+03 .687066E+03 .707866E+03 .681043E+03
 F   .577581E+05 .577135E+05 .576363E+05 .574521E+05 .570861E+05 .560237E+05 .553291E+05 .548895E+05 .545704E+05 .549778E+05
 E   .409643E+06 .414108E+06 .418550E+06 .424140E+06 .433347E+06 .452997E+06 .471894E+06 .491007E+06 .509040E+06 .536245E+06

A100.207        .806600E+02 .100130E+03 .731756E+03 .665610E+03 .152906E+04 .142039E+04
                .101158E+03 .102345E+03 .337687E+06 .409556E+06 .100503E+03 .421166E+06
 T   .375458E+03 .378240E+03 .384724E+03 .410613E+03 .461275E+03 .538574E+03 .610863E+03 .628623E+03 .647493E+03 .624891E+03
 F   .512016E+05 .511898E+05 .511622E+05 .510365E+05 .507211E+05 .498615E+05 .492640E+05 .490402E+05 .487904E+05 .490868E+05
 E   .413771E+06 .418259E+06 .422198E+06 .427157E+06 .435327E+06 .452788E+06 .469407E+06 .486623E+06 .502709E+06 .526948E+06

A150.051        .974500E+02 .150000E+03 .401826E+03 .491420E+03 .411434E+04 .382793E+04
                .117308E+03 .114158E+03 .408312E+06 .444072E+06 .104155E+03 .436602E+06
 T   .861009E+03 .905952E+03 .935740E+03 .956459E+03 .979499E+03 .102763E+04 .102923E+04 .101495E+04 .937952E+03 .919385E+03
 F   .134377E+06 .133258E+06 .132647E+06 .131906E+06 .131253E+06 .129827E+06 .129778E+06 .130211E+06 .132412E+06 .132906E+06
 E   .451591E+06 .459547E+06 .466499E+06 .475235E+06 .489639E+06 .520577E+06 .550317E+06 .581328E+06 .610819E+06 .655154E+06

A150.052        .970900E+02 .150000E+03 .401767E+03 .492810E+03 .388851E+04 .355187E+04
                .116166E+03 .113167E+03 .406794E+06 .441688E+06 .103874E+03 .435417E+06
 T   .824016E+03 .870330E+03 .898606E+03 .920114E+03 .938040E+03 .979585E+03 .982329E+03 .962210E+03 .918863E+03 .891199E+03
 F   .124863E+06 .123796E+06 .123098E+06 .122555E+06 .122084E+06 .120946E+06 .120867E+06 .121430E+06 .122593E+06 .123286E+06
 E   .448663E+06 .456043E+06 .462492E+06 .470596E+06 .483969E+06 .512727E+06 .540364E+06 .569214E+06 .596494E+06 .637569E+06

A150.053        .970900E+02 .150000E+03 .391736E+03 .493510E+03 .344443E+04 .321515E+04
                .114879E+03 .112058E+03 .406794E+06 .440057E+06 .103555E+03 .434068E+06
 T   .783413E+03 .834449E+03 .861213E+03 .877486E+03 .898914E+03 .936944E+03 .941998E+03 .921842E+03 .882370E+03 .857029E+03
 F   .113285E+06 .112212E+06 .111608E+06 .111327E+06 .110710E+06 .109749E+06 .109617E+06 .110137E+06 .111110E+06 .111703E+06
 E   .446375E+06 .453053E+06 .458892E+06 .466233E+06 .478339E+06 .504383E+06 .529402E+06 .555522E+06 .580208E+06 .617369E+06

A150.054        .974500E+02 .150000E+03 .389736E+03 .493510E+03 .297442E+04 .277143E+04
                .113275E+03 .110665E+03 .408312E+06 .440094E+06 .103153E+03 .432371E+06
 T   .726572E+03 .777953E+03 .803273E+03 .818876E+03 .834598E+03 .875179E+03 .882514E+03 .864651E+03 .839372E+03 .808397E+03
 F   .979163E+05 .970100E+05 .963087E+05 .961919E+05 .958549E+05 .949531E+05 .947836E+05 .951929E+05 .957520E+05 .964029E+05
 E   .445542E+06 .451303E+06 .456339E+06 .462672E+06 .473125E+06 .495597E+06 .517174E+06 .539693E+06 .560928E+06 .592934E+06

A150.055        .970900E+02 .150000E+03 .383993E+03 .487220E+03 .241006E+04 .221973E+04
                .110986E+03 .108717E+03 .406794E+06 .436547E+06 .102571E+03 .429914E+06
 T   .652524E+03 .692334E+03 .721505E+03 .744532E+03 .756820E+03 .796867E+03 .808304E+03 .791354E+03 .776654E+03 .744532E+03
 F   .787747E+05 .781842E+05 .777138E+05 .773203E+05 .771025E+05 .763544E+05 .761698E+05 .764608E+05 .767392E+05 .773190E+05
 E   .440918E+06 .445545E+06 .449587E+06 .454662E+06 .463043E+06 .481055E+06 .498339E+06 .516371E+06 .533346E+06 .558949E+06

A150.056        .974500E+02 .150000E+03 .388211E+03 .480920E+03 .206631E+04 .190726E+04
                .109839E+03 .107729E+03 .408312E+06 .437346E+06 .102276E+03 .428667E+06
 T   .599699E+03 .638636E+03 .656098E+03 .675791E+03 .687228E+03 .723262E+03 .740332E+03 .734579E+03 .721620E+03 .697285E+03
 F   .677557E+05 .672574E+05 .670200E+05 .667359E+05 .665636E+05 .659840E+05 .657077E+05 .658054E+05 .660210E+05 .664085E+05
 E   .441098E+06 .445070E+06 .448547E+06 .452916E+06 .460132E+06 .475654E+06 .490524E+06 .506008E+06 .520579E+06 .542529E+06

A150.057        .974500E+02 .150000E+03 .394373E+03 .475310E+03 .174888E+04 .161696E+04
                .108644E+03 .106707E+03 .408312E+06 .436816E+06 .101965E+03 .427357E+06
 T   .543770E+03 .573960E+03 .593212E+03 .615655E+03 .629374E+03 .667926E+03 .674480E+03 .674480E+03 .666886E+03 .640180E+03
 F   .575416E+05 .572239E+05 .570046E+05 .567322E+05 .565571E+05 .560298E+05 .559351E+05 .559351E+05 .560448E+05 .564132E+05
 E   .439996E+06 .443368E+06 .446318E+06 .450024E+06 .456141E+06 .469291E+06 .481917E+06 .495049E+06 .507392E+06 .525898E+06

A150.058        .970900E+02 .150000E+03 .390504E+03 .469700E+03 .136737E+04 .126896E+04
                .107028E+03 .105340E+03 .406794E+06 .433987E+06 .101541E+03 .423566E+06
 T   .470477E+03 .492509E+03 .509029E+03 .524717E+03 .533762E+03 .565909E+03 .584209E+03 .585049E+03 .584209E+03 .551331E+03
 F   .451408E+05 .449661E+05 .448241E+05 .446810E+05 .445947E+05 .442653E+05 .440624E+05 .440928E+05 .440624E+05 .444178E+05
 E   .436476E+06 .439117E+06 .441431E+06 .444340E+06 .449147E+06 .459497E+06 .469409E+06 .479717E+06 .489392E+06 .503994E+06

A150.101        .898900E+02 .150000E+03 .446254E+03 .479520E+03 .438109E+04 .409111E+04
                .115780E+03 .113267E+03 .376477E+06 .415667E+06 .103779E+03 .435013E+06
 T   .807947E+03 .866330E+03 .903248E+03 .941738E+03 .972715E+03 .103593E+04 .105887E+04 .102756E+04 .967120E+03 .949063E+03
 F   .145008E+06 .143647E+06 .142711E+06 .141676E+06 .140799E+06 .138893E+06 .138164E+06 .139155E+06 .140960E+06 .141470E+06
 E   .423762E+06 .433234E+06 .439803E+06 .449180E+06 .464627E+06 .497739E+06 .529444E+06 .562606E+06 .594042E+06 .641296E+06

A150.102        .897100E+02 .150000E+03 .450166E+03 .482320E+03 .396127E+04 .369638E+04
                .114433E+03 .111922E+03 .375720E+06 .413924E+06 .103443E+03 .433598E+06
 T   .764598E+03 .812037E+03 .847472E+03 .881805E+03 .915816E+03 .979542E+03 .100508E+04 .981174E+03 .939718E+03 .916047E+03
 F   .131253E+06 .130268E+06 .129472E+06 .128651E+06 .127790E+06 .126056E+06 .125318E+06 .126010E+06 .127158E+06 .127783E+06
 E   .421238E+06 .428985E+06 .435754E+06 .444246E+06 .458230E+06 .488203E+06 .516888E+06 .546852E+06 .575175E+06 .617794E+06

A150.103        .902500E+02 .150000E+03 .449736E+03 .493510E+03 .348973E+04 .325582E+04
                .112884E+03 .110583E+03 .377992E+06 .414809E+06 .103049E+03 .431932E+06
 T   .717408E+03 .767427E+03 .798356E+03 .836240E+03 .864544E+03 .918759E+03 .932200E+03 .918759E+03 .888194E+03 .870229E+03
 F   .115733E+06 .114815E+06 .114196E+06 .113384E+06 .112741E+06 .111423E+06 .111079E+06 .111423E+06 .112180E+06 .112607E+06
 E   .421247E+06 .428062E+06 .434020E+06 .441490E+06 .453800E+06 .480221E+06 .505562E+06 .531983E+06 .556913E+06 .594396E+06

A150.104        .902500E+02 .150000E+03 .453767E+03 .492810E+03 .304821E+04 .284384E+04
                .111401E+03 .109195E+03 .377992E+06 .413776E+06 .102677E+03 .430363E+06
 T   .658065E+03 .694879E+03 .721243E+03 .762528E+03 .796167E+03 .849449E+03 .867573E+03 .861338E+03 .840502E+03 .821847E+03
 F   .101321E+06 .100757E+06 .100318E+06 .995766E+05 .989229E+05 .977987E+05 .973919E+05 .975332E+05 .979950E+05 .983930E+05
 E   .419399E+06 .425362E+06 .430560E+06 .437121E+06 .447891E+06 .471012E+06 .493168E+06 .516238E+06 .537971E+06 .570656E+06

A150.105        .904300E+02 .150000E+03 .457797E+03 .497110E+03 .272346E+04 .254655E+04
                .110341E+03 .108223E+03 .378749E+06 .413852E+06 .102405E+03 .429216E+06
 T   .607696E+03 .639841E+03 .674134E+03 .703638E+03 .730860E+03 .788124E+03 .812772E+03 .810691E+03 .804096E+03 .783651E+03
 F   .908842E+05 .905185E+05 .899698E+05 .895080E+05 .890520E+05 .880006E+05 .875103E+05 .875526E+05 .876855E+05 .880858E+05
 E   .418886E+06 .424232E+06 .428903E+06 .434768E+06 .444438E+06 .465190E+06 .485052E+06 .505717E+06 .525135E+06 .554350E+06

A150.106        .900700E+02 .150000E+03 .457911E+03 .489320E+03 .244020E+04 .226398E+04
                .108688E+03 .107151E+03 .377234E+06 .411474E+06 .101976E+03 .427405E+06
 T   .553503E+03 .577333E+03 .603975E+03 .643507E+03 .673320E+03 .740779E+03 .769670E+03 .766838E+03 .758582E+03 .739348E+03
 F   .809960E+05 .807404E+05 .804283E+05 .799144E+05 .794875E+05 .783982E+05 .778804E+05 .779127E+05 .780628E+05 .784217E+05
 E   .415953E+06 .420710E+06 .424874E+06 .430099E+06 .438712E+06 .457164E+06 .474805E+06 .493171E+06 .510430E+06 .536393E+06

A150.107        .902500E+02 .150000E+03 .458142E+03 .483020E+03 .210789E+04 .197497E+04
                .107667E+03 .106163E+03 .377992E+06 .411347E+06 .101709E+03 .426277E+06
 T   .476601E+03 .492206E+03 .515214E+03 .560099E+03 .595255E+03 .675772E+03 .695115E+03 .700138E+03 .711395E+03 .692433E+03
 F   .708369E+05 .707176E+05 .705246E+05 .700896E+05 .696960E+05 .686219E+05 .682504E+05 .682504E+05 .680715E+05 .683688E+05
 E   .415253E+06 .419408E+06 .423048E+06 .427617E+06 .435146E+06 .451257E+06 .466692E+06 .482730E+06 .497749E+06 .520342E+06

A150.108        .906100E+02 .150000E+03 .478545E+03 .467590E+03 .179390E+04 .168176E+04
                .106144E+03 .105158E+03 .379506E+06 .413166E+06 .101307E+03 .424577E+06
 T   .416177E+03 .423512E+03 .432856E+03 .484139E+03 .520805E+03 .596755E+03 .616537E+03 .630076E+03 .638931E+03 .627604E+03
 F   .602729E+05 .601654E+05 .600440E+05 .598101E+05 .595076E+05 .587093E+05 .584676E+05 .582942E+05 .581773E+05 .583250E+05
 E   .416485E+06 .420012E+06 .423105E+06 .426994E+06 .433406E+06 .447149E+06 .460318E+06 .473980E+06 .486780E+06 .506007E+06

A150.201        .795800E+02 .150000E+03 .717109E+03 .506060E+03 .442954E+04 .414197E+04
                .113367E+03 .111028E+03 .333153E+06 .388589E+06 .103180E+03 .432484E+06
 T   .624457E+03 .704813E+03 .749688E+03 .807044E+03 .897250E+03 .101938E+04 .104610E+04 .102823E+04 .981042E+03 .970792E+03
 F   .149665E+06 .148417E+06 .147568E+06 .146395E+06 .144229E+06 .140761E+06 .139926E+06 .140487E+06 .141913E+06 .142210E+06
 E   .396884E+06 .405672E+06 .413356E+06 .422991E+06 .438761E+06 .472292E+06 .504383E+06 .537862E+06 .569531E+06 .617079E+06

A150.202        .797600E+02 .150000E+03 .692783E+03 .511620E+03 .408521E+04 .382048E+04
                .112288E+03 .109994E+03 .333909E+06 .386889E+06 .102903E+03 .431116E+06
 T   .570224E+03 .640236E+03 .696584E+03 .752628E+03 .827197E+03 .959372E+03 .992511E+03 .982643E+03 .946721E+03 .935771E+03
 F   .113817E+06 .137297E+06 .136422E+06 .135409E+06 .133848E+06 .130513E+06 .129569E+06 .129855E+06 .130863E+06 .131158E+06
 E   .394533E+06 .402642E+06 .409731E+06 .418622E+06 .433214E+06 .464218E+06 .493858E+06 .524739E+06 .553896E+06 .597679E+06
```

```
A150.203          .795800E+02 .150000E+03 .689031E+03 .507450E+03 .171738E+04 .367664E+04
                  .110076E+03 .108787E+03 .333153E+06 .384840E+06 .102337E+03 .428925E+06
 T   .503560E+03 .963999E+03 .618615E+03 .686712E+03 .767408E+03 .892993E+03 .925141E+03 .93362BE+03 .916123E+03 .899049E+03
 F   .125889E+06 .125333E+06 .124684E+06 .123687E+06 .122243E+06 .119456E+06 .118644E+06 .118423E+06 .118877E+06 .119306E+06
 E   .391788E+06 .399170E+06 .405630E+06 .413731E+06 .427024E+06 .455319E+06 .482377E+06 .510477E+06 .5386927E+06 .576690E+06

A200.101          .891700E+02 .200170E+03 .521939E+03 .488620E+03 .508625E+04 .479493E+04
                  .120924E+03 .117749E+03 .373448E+06 .407696E+06 .105029E+03 .440297E+06
 T   .764759E+03 .833937E+03 .871853E+03 .915713E+03 .979223E+03 .105088E+04 .104023E+04 .991736E+03 .921360E+03 .935475E+03
 F   .170005TE+06 .168504E+06 .167539E+06 .166386E+06 .164540E+06 .161996E+06 .162609E+06 .164156E+06 .166229E+06 .165828E+06
 E   .414798E+06 .422314E+06 .428885E+06 .437128E+06 .450659E+06 .479631E+06 .507569E+06 .536835E+06 .5645599E+06 .606041E+06

A200.102          .891700E+02 .200170E+03 .521993E+03 .487220E+03 .452194E+04 .425038E+04
                  .118566E+03 .113551E+03 .373448E+06 .406453E+06 .104462E+03 .437898E+06
 T   .713817E+03 .777454E+03 .817150E+03 .848034E+03 .920900E+03 .988046E+03 .982520E+03 .939559E+03 .881640E+03 .892751E+03
 F   .151017E+06 .149783E+06 .148921E+06 .148202E+06 .146344E+06 .144438E+06 .144601E+06 .145832E+06 .147173E+06 .147086E+06
 E   .412747E+06 .419612E+06 .425239E+06 .432560E+06 .444563E+06 .470309E+06 .495086E+06 .521023E+06 .545559E+06 .582264E+06

A200.103          .893500E+02 .200170E+03 .521883E+03 .490002E+03 .407518E+04 .385038E+04
                  .116821E+03 .113993E+03 .374205E+06 .406279E+06 .104035E+03 .496098E+06
 T   .651920E+03 .718970E+03 .749004E+03 .792941E+03 .856326E+03 .918585E+03 .916013E+03 .884163E+03 .842782E+03 .861391E+03
 F   .137128E+06 .136014E+06 .135478E+06 .134594E+06 .133174E+06 .131617E+06 .131684E+06 .132497E+06 .133492E+06 .133052E+06
 E   .411981E+06 .418070E+06 .423306E+06 .429940E+06 .440832E+06 .464219E+06 .486716E+06 .510224E+06 .533412E+06 .565588E+06

A200.104          .891700E+02 .200170E+03 .481939E+03 .488620E+03 .360627E+04 .339474E+04
                  .115098E+03 .112047E+03 .373448E+06 .407205E+06 .103609E+03 .434298E+06
 T   .583364E+03 .646747E+03 .683416E+03 .726721E+03 .786991E+03 .844461E+03 .865342E+03 .839319E+03 .814917E+03 .824496E+03
 F   .121372E+06 .120552E+06 .119996E+06 .119266E+06 .118117E+06 .116432E+06 .116401E+06 .116999E+06 .117534E+06 .117325E+06
 E   .407739E+06 .413076E+06 .417746E+06 .423608E+06 .433241E+06 .453880E+06 .473722E+06 .494441E+06 .513953E+06 .543162E+06

A200.105          .889900E+02 .200170E+03 .506070E+03 .485120E+03 .327016E+04 .306541E+04
                  .111151E+03 .110589E+03 .372691E+06 .402273E+06 .102664E+03 .430308E+06
 T   .503745E+03 .580773E+03 .620335E+03 .661357E+03 .720504E+03 .821784E+03 .823565E+03 .800455E+03 .785362E+03 .787955E+03
 F   .110037E+06 .109292E+06 .108808E+06 .108236E+06 .107286E+06 .105331E+06 .105293E+06 .105776E+06 .106081E+06 .106028E+06
 E   .406824E+06 .411651E+06 .415876E+06 .421182E+06 .429909E+06 .448546E+06 .466465E+06 .485166E+06 .502756E+06 .529112E+06

A200.106          .891700E+02 .200170E+03 .502233E+03 .480220E+03 .284308E+04 .266179E+04
                  .110621E+03 .108944E+03 .373448E+06 .401939E+06 .102477E+03 .429518E+06
 T   .433070E+03 .502086E+03 .550766E+03 .592807E+03 .645265E+03 .749423E+03 .767647E+03 .747952E+03 .740646E+03 .742828E+03
 F   .956863E+05 .952337E+05 .947919E+05 .943305E+05 .936531E+05 .919824E+05 .916472E+05 .920094E+05 .921399E+05 .920997E+05
 E   .405887E+06 .410981E+06 .413753E+06 .418366E+06 .425961E+06 .442190E+06 .457749E+06 .473982E+06 .489233E+06 .5120846+06

A250.051          .963700E+02 .250050E+03 .410687E+03 .440130E+03 .513000E+04 .485659E+04
                  .127925E+03 .123762E+03 .403760E+06 .427275E+06 .106663E+03 .447200E+06
 T   .872200E+03 .939377E+03 .966907E+03 .971492E+03 .100211E+04 .102232E+04 .982364E+03 .919725E+03 .842454E+03 .878157E+03
 F   .169017E+06 .167101E+06 .166372E+06 .166235E+06 .165292E+06 .164649E+06 .165905E+06 .167739E+06 .169767E+06 .168861E+06
 E   .432950E+06 .438947E+06 .444192E+06 .450801E+06 .461694E+06 .485226E+06 .507983E+06 .531844E+06 .554433E+06 .588163E+06

A250.052          .970900E+02 .250050E+03 .422635E+03 .435180E+03 .471678E+04 .445244E+04
                  .126723E+03 .122271E+03 .406794E+06 .430015E+06 .106388E+03 .446038E+06
 T   .850253E+03 .914153E+03 .936577E+03 .957468E+03 .986257E+03 .992333E+03 .961952E+03 .905774E+03 .833024E+03 .855209E+03
 F   .155136E+06 .153495E+06 .152878E+06 .152284E+06 .153029E+06 .151253E+06 .152154E+06 .153720E+06 .155549E+06 .155014E+06
 E   .435219E+06 .440719E+06 .445532E+06 .451582E+06 .461585E+06 .483172E+06 .504023E+06 .525877E+06 .546565E+06 .577499E+06

A250.053          .965500E+02 .250050E+03 .426635E+03 .435180E+03 .415386E+04 .392409E+04
                  .122552E+03 .119488E+03 .404519E+06 .426924E+06 .105416E+03 .441930E+06
 T   .789913E+03 .850426E+03 .879405E+03 .897472E+03 .915990E+03 .929683E+03 .915990E+03 .865191E+03 .805740E+03 .815450E+03
 F   .137312E+06 .135962E+06 .135261E+06 .134806E+06 .134326E+06 .133963E+06 .134326E+06 .135609E+06 .136974E+06 .136760E+06
 E   .431519E+06 .436376E+06 .440824E+06 .445966E+06 .454784E+06 .473849E+06 .492219E+06 .511464E+06 .529662E+06 .556907E+06
```

```
A250.054          .967300E+02 .250050E+03 .422615E+03 .433760E+03 .353531E+04 .332739E+04
                  .126967E+03 .116756E+03 .405277E+06 .426455E+06 .108444E+03 .446275E+06
 T   .730589E+03 .783701E+03 .810435E+03 .824516E+03 .839952E+03 .861551E+03 .846528E+03 .810435E+03 .758216E+03 .766464E+03
 F   .116723E+06 .115714E+06 .115162E+06 .114860E+06 .114520E+06 .114038E+06 .114372E+06 .115162E+06 .116213E+06 .116053E+06
 E   .430352E+06 .434475E+06 .438081E+06 .442618E+06 .450111E+06 .466291E+06 .481886E+06 .498191E+06 .513601E+06 .536675E+06

A250.055          .967300E+02 .250050E+03 .422594E+03 .432350E+03 .309659E+04 .280715E+04
                  .119016E+03 .114250E+03 .405277E+06 .425516E+06 .104571E+03 .438359E+06
 T   .669259E+03 .723217E+03 .748389E+03 .763131E+03 .780525E+03 .803273E+03 .796678E+03 .760308E+03 .724298E+03 .724298E+03
 F   .988776E+05 .980088E+05 .975639E+05 .973921E+05 .969603E+05 .965088E+05 .966417E+05 .973449E+05 .979905E+05 .979890E+05
 E   .428809E+06 .432293E+06 .435340E+06 .439174E+06 .445503E+06 .459163E+06 .472113E+06 .486066E+06 .499043E+06 .516493E+06

A250.056          .965500E+02 .250050E+03 .422558E+03 .430230E+03 .268415E+04 .258907E+04
                  .114337E+03 .112685E+03 .404519E+06 .424210E+06 .103419E+03 .433497E+06
 T   .620550E+03 .674156E+03 .707543E+03 .721413E+03 .732212E+03 .756591E+03 .748504E+03 .713888E+03 .681852E+03 .679570E+03
 F   .885659E+05 .878157E+05 .872917E+05 .870616E+05 .868773E+05 .864449E+05 .865908E+05 .871875E+05 .876989E+05 .877324E+05
 E   .427154E+06 .430270E+06 .432992E+06 .436417E+06 .442076E+06 .454289E+06 .466048E+06 .478345E+06 .489939E+06 .507323E+06

A250.057          .965500E+02 .250050E+03 .422504E+03 .427400E+03 .222747E+04 .209057E+04
                  .106066E+03 .110588E+03 .404519E+06 .423446E+06 .101286E+03 .424490E+06
 T   .559165E+03 .603140E+03 .634311E+03 .648303E+03 .653557E+03 .686880E+03 .679725E+03 .658360E+03 .638776E+03 .6225848+03
 F   .739563E+05 .734579E+05 .730603E+05 .728702E+05 .727969E+05 .723080E+05 .724165E+05 .727290E+05 .730005E+05 .732129E+05
 E   .425899E+06 .428499E+06 .430771E+06 .433629E+06 .438357E+06 .448545E+06 .458353E+06 .468589E+06 .478223E+06 .492699E+06

A300.051          .967300E+02 .300800E+03 .426713E+03 .452810E+03 .5405255+04 .510629E+04
                  .132759E+03 .128138E+03 .403277E+06 .425673E+06 .107748E+03 .451790E+06
 T   .892486E+03 .957272E+03 .977324E+03 .999919E+03 .101460E+04 .103823E+04 .981950E+03 .924184E+03 .847760E+03 .915393E+03
 F   .177423E+06 .175572E+06 .174962E+06 .174254E+06 .173783E+06 .173005E+06 .176541E+06 .178592E+06 .176588E+06 .176788E+06
 E   .430630E+06 .435869E+06 .440456E+06 .448223E+06 .455749E+06 .476319E+06 .496252E+06 .517133E+06 .536891E+06 .566294E+06

A300.052          .960100E+02 .300800E+03 .430718E+03 .451400E+03 .489483E+04 .461932E+04
                  .128431E+03 .125011E+03 .402243E+06 .422023E+06 .107005E+03 .448644E+06
 T   .846107E+03 .902161E+03 .931422E+03 .935537E+03 .959142E+03 .980674E+03 .959142E+03 .890878E+03 .825353E+03 .874600E+03
 F   .160941E+06 .159508E+06 .158884E+06 .158590E+06 .157912E+06 .157274E+06 .157912E+06 .159608E+06 .161437E+06 .160229E+06
 E   .426510E+06 .431258E+06 .435416E+06 .440650E+06 .449283E+06 .467932E+06 .485919E+06 .504793E+06 .522637E+06 .549239E+06

A300.053          .961900E+02 .300800E+03 .430713E+03 .444350E+03 .444000E+04 .419223E+04
                  .127022E+03 .122866E+03 .403002E+06 .423140E+06 .106457E+03 .446328E+06
 T   .803550E+03 .856272E+03 .874737E+03 .897390E+03 .915679E+03 .933958E+03 .915909E+03 .866318E+03 .801157E+03 .848059E+03
 F   .144672E+06 .143245E+06 .144802E+06 .144225E+06 .143744E+06 .143095E+06 .143738E+06 .145011E+06 .146524E+06 .145452E+06
 E   .426216E+06 .430532E+06 .434311E+06 .439062E+06 .446906E+06 .463842E+06 .480183E+06 .497291E+06 .513470E+06 .537991E+06

A300.054          .960100E+02 .300800E+03 .438721E+03 .449290E+03 .417158E+04 .393350E+04
                  .125445E+03 .121339E+03 .402243E+06 .421227E+06 .106093E+03 .444791E+06
 T   .780363E+03 .831026E+03 .848144E+03 .875461E+03 .878454E+03 .898914E+03 .882588E+03 .839145E+03 .783186E+03 .833199E+03
 F   .137510E+06 .136411E+06 .136015E+06 .135358E+06 .135384E+06 .134769E+06 .135181E+06 .136225E+06 .137452E+06 .136360E+06
 E   .425051E+06 .429099E+06 .432645E+06 .437100E+06 .444470E+06 .460392E+06 .475731E+06 .491791E+06 .506957E+06 .529557E+06

A300.055          .961900E+02 .300800E+03 .458721E+03 .447170E+03 .373651E+04 .350269E+04
                  .122853E+03 .119144E+03 .403002E+06 .421936E+06 .105487E+03 .442231E+06
 T   .744093E+03 .790429E+03 .803041E+03 .817745E+03 .833019E+03 .847371E+03 .854569E+03 .805884E+03 .752752E+03 .801389E+03
 F   .122688E+06 .121780E+06 .121518E+06 .121203E+06 .120867E+06 .120078E+06 .120377E+06 .121458E+06 .122526E+06 .121551E+06
 E   .425343E+06 .428951E+06 .432113E+06 .436092E+06 .442664E+06 .456831E+06 .470480E+06 .484773E+06 .498275E+06 .518394E+06

A300.056          .963700E+02 .300800E+03 .458721E+03 .449990E+03 .340038E+04 .319998E+04
                  .121091E+03 .117629E+03 .403760E+06 .422237E+06 .105069E+03 .440465E+06
 T   .688966E+03 .749234E+03 .769353E+03 .793165E+03 .801492E+03 .824152E+03 .812562E+03 .773447E+03 .728435E+03 .767461E+03
 F   .112414E+06 .111534E+06 .111152E+06 .110679E+06 .110309E+06 .110030E+06 .110278E+06 .111073E+06 .111911E+06 .111187E+06
 E   .425352E+06 .428651E+06 .431540E+06 .435170E+06 .441171E+06 .454129E+06 .466611E+06 .479664E+06 .491985E+06 .510362E+06

A300.057          .963700E+02 .300800E+03 .458721E+03 .449990E+03 .282639E+04 .266216E+04
                  .117766E+03 .114640E+03 .403760E+06 .421427E+06 .104267E+03 .437075E+06
 T   .633214E+03 .688316E+03 .692126E+03 .712453E+03 .732159E+03 .762603E+03 .749423E+03 .715205E+03 .685150E+03 .705367E+03
 F   .938184E+05 .930953E+05 .929543E+05 .926243E+05 .922890E+05 .917414E+05 .919826E+05 .925784E+05 .930639E+05 .927394E+05
 E   .424021E+06 .426772E+06 .429181E+06 .432209E+06 .437206E+06 .447983E+06 .458367E+06 .468232E+06 .479451E+06 .494742E+06
```

```
C 50.051        .947500E+02 .499700E+02 .723446E+03 .277410E+03 .122167E+04 .106418E+04
                .103171E+03 .102517E+03 .396935E+06 .538009E+06 .100506E+03 .421200E+06
 T   .518989E+03 .567704E+03 .598886E+03 .617218E+03 .669732E+03 .718042E+03 .767089E+03 .807941E+03 .820087E+03 .830172E+03
 F   .435304E+05 .428344E+05 .423558E+05 .420646E+05 .411962E+05 .403730E+05 .395241E+05 .388200E+05 .386127E+05 .384413E+05
 E   .546905E+06 .555673E+06 .564354E+06 .572980E+06 .589910E+06 .606513E+06 .636424E+06 .663159E+06 .676461E+06 .689710E+06

C 50.052        .954700E+02 .499700E+02 .671913E+03 .280230E+03 .149788E+04 .130880E+04
                .103575E+03 .102699E+03 .399966E+06 .534465E+06 .100616E+03 .421664E+06
 T   .586752E+03 .643646E+03 .675800E+03 .694475E+03 .753313E+03 .796991E+03 .845860E+03 .891744E+03 .902690E+03 .905892E+03
 F   .530279E+05 .521136E+05 .515713E+05 .512155E+05 .502217E+05 .494538E+05 .486064E+05 .478358E+05 .476570E+05 .476048E+05
 E   .545327E+06 .556025E+06 .566626E+06 .577159E+06 .597865E+06 .618290E+06 .655170E+06 .688230E+06 .704707E+06 .721167E+06

C 50.053        .956500E+02 .499700E+02 .657853E+03 .273890E+03 .174529E+04 .152730E+04
                .103916E+03 .103205E+03 .400726E+06 .535049E+06 .100709E+03 .422054E+06
 T   .640850E+03 .703762E+03 .744543E+03 .765658E+03 .824889E+03 .862123E+03 .913264E+03 .972566E+03 .971855E+03 .976257E+03
 F   .614599E+05 .603809E+05 .596592E+05 .591827E+05 .582288E+05 .575764E+05 .567157E+05 .557820E+05 .557927E+05 .557265E+05
 E   .547664E+06 .560087E+06 .572361E+06 .584608E+06 .608686E+06 .632532E+06 .675669E+06 .714380E+06 .733729E+06 .753059E+06

C 50.054        .965700E+02 .499700E+02 .845766E+03 .213380E+03 .102913E+04 .881978E+03
                .103135E+03 .102481E+03 .398177E+06 .557176E+06 .100496E+03 .421159E+06
 T   .482429E+03 .534673E+03 .564892E+03 .577730E+03 .621826E+03 .662029E+03 .710595E+03 .748444E+03 .760850E+03 .768134E+03
 F   .362742E+05 .355808E+05 .351421E+05 .349448E+05 .342573E+05 .335940E+05 .327778E+05 .321302E+05 .319177E+05 .317927E+05
 E   .564579E+06 .571854E+06 .579047E+06 .586204E+06 .600257E+06 .614060E+06 .638794E+06 .660868E+06 .671837E+06 .682767E+06

C 50.055        .949300E+02 .499700E+02 .995603E+03 .212670E+03 .795966E+03 .678556E+03
                .102790E+03 .102128E+03 .397693E+06 .583203E+06 .100402E+03 .420763E+06
 T   .408024E+03 .451309E+03 .475232E+03 .487119E+03 .526640E+03 .563270E+03 .609213E+03 .645910E+03 .658236E+03 .665399E+03
 F   .280494E+05 .275948E+05 .273114E+05 .271630E+05 .266360E+05 .261075E+05 .254009E+05 .248097E+05 .246071E+05 .244882E+05
 E   .588914E+06 .594540E+06 .600113E+06 .605658E+06 .616547E+06 .627234E+06 .646328E+06 .663305E+06 .671722E+06 .680113E+06

C 50.056        .951100E+02 .499700E+02 .805280E+03 .211270E+03 .125918E+04 .108983E+04
                .103249E+03 .102566E+03 .398451E+06 .554472E+06 .100527E+03 .421290E+06
 T   .552966E+03 .610817E+03 .641097E+03 .656227E+03 .701676E+03 .734706E+03 .778380E+03 .822284E+03 .835010E+03 .839921E+03
 F   .443073E+05 .434225E+05 .429311E+05 .426800E+05 .419088E+05 .413384E+05 .405807E+05 .398256E+05 .396098E+05 .395364E+05
 E   .563537E+06 .572440E+06 .581252E+06 .590017E+06 .607261E+06 .624292E+06 .654996E+06 .682440E+06 .696094E+06 .709723E+06

C 50.201        .799400E+02 .499700E+02 .712853E+03 .273890E+03 .144029E+04 .124997E+04
                .103087E+03 .102522E+03 .334664E+06 .475967E+06 .100483E+03 .421104E+06
 T   .586760E+03 .650809E+03 .692428E+03 .717005E+03 .771640E+03 .818027E+03 .870706E+03 .918820E+03 .922702E+03 .930056E+03
 F   .509841E+05 .499550E+05 .492444E+05 .488185E+05 .478616E+05 .470521E+05 .461546E+05 .454031E+05 .453103E+05 .451949E+05
 E   .486411E+06 .496668E+06 .506795E+06 .516845E+06 .536592E+06 .556043E+06 .591099E+06 .622513E+06 .638191E+06 .653835E+06

C 50.202        .810300E+02 .499700E+02 .707124E+03 .269660E+03 .162387E+04 .141319E+04
                .103159E+03 .102555E+03 .339241E+06 .481269E+06 .100503E+03 .421187E+06
 T   .622584E+03 .692399E+03 .734730E+03 .763290E+03 .827792E+03 .870628E+03 .922136E+03 .986328E+03 .978685E+03 .985448E+03
 F   .573770E+05 .561994E+05 .554574E+05 .549317E+05 .538132E+05 .530746E+05 .522228E+05 .512639E+05 .512546E+05 .512561E+05
 E   .493038E+06 .504596E+06 .516020E+06 .527353E+06 .549607E+06 .571596E+06 .611350E+06 .648916E+06 .664731E+06 .680517E+06

C 50.203        .808500E+02 .499700E+02 .732248E+03 .270370E+03 .123688E+04 .107194E+04
                .102788E+03 .102265E+03 .338485E+06 .481289E+06 .100402E+03 .420760E+06
 T   .529088E+03 .577613E+03 .615679E+03 .641916E+03 .696401E+03 .745990E+03 .793726E+03 .840110E+03 .849885E+03 .856158E+03
 F   .440148E+05 .433080E+05 .427122E+05 .422852E+05 .413640E+05 .405114E+05 .396850E+05 .388941E+05 .387303E+05 .386255E+05
 E   .490287E+06 .499156E+06 .507914E+06 .516594E+06 .533610E+06 .550308E+06 .580353E+06 .607175E+06 .620534E+06 .633861E+06

C 50.204        .793900E+02 .499700E+02 .706131E+03 .294340E+03 .113657E+04 .100[illegible]E+04
                .102554E+03 .102046E+03 .332356E+06 .469716E+06 .100338E+03 .420490E+06
 T   .493367E+03 .542032E+03 .576955E+03 .598920E+03 .662790E+03 .704045E+03 .760788E+03 .802087E+03 .812812E+03 .807970E+03
 F   .414119E+05 .407539E+05 .402384E+05 .398991E+05 .388600E+05 .381607E+05 .371832E+05 .364732E+05 .362904E+05 .363723E+05
 E   .478172E+06 .486507E+06 .494746E+06 .502923E+06 .518889E+06 .534592E+06 .562705E+06 .587818E+06 .600316E+06 .612841E+06
```

```
C 50.301        .713900E+02 .499700E+02 .749572E+03 .255580E+03 .140748E+04 .121153E+04
                .102589E+03 .102089E+03 .298799E+06 .446127E+06 .100347E+03 .420530E+06
 T   .581275E+03 .639583E+03 .710097E+03 .739526E+03 .790647E+03 .829169E+03 .882437E+03 .930070E+03 .932532E+03 .937894E+03
 F   .497216E+05 .484579E+05 .475932E+05 .470804E+05 .461860E+05 .455188E+05 .446215E+05 .438596E+05 .436216E+05 .437388E+05
 E   .456511E+06 .466464E+06 .476258E+06 .485959E+06 .505029E+06 .523855E+06 .557764E+06 .588127E+06 .603297E+06 .618442E+06

C 50.302        .713900E+02 .499700E+02 .750226E+03 .259100E+03 .158909E+04 .137436E+04
                .102922E+03 .102389E+03 .298799E+06 .448176E+06 .100438E+03 .420914E+06
 T   .621532E+03 .695189E+03 .734548E+03 .769762E+03 .845419E+03 .887313E+03 .927565E+03 .992356E+03 .986463E+03 .988534E+03
 F   .559700E+05 .547282E+05 .540391E+05 .534166E+05 .520898E+05 .513790E+05 .507240E+05 .497503E+05 .498340E+05 .498041E+05
 E   .459656E+06 .470912E+06 .482044E+06 .493063E+06 .514620E+06 .535922E+06 .574545E+06 .609083E+06 .626377E+06 .643662E+06

C 50.303        .706600E+02 .499700E+02 .794433E+03 .254870E+03 .120541E+04 .101675E+04
                .102048E+03 .101580E+03 .285739E+06 .449195E+06 .100199E+03 .419905E+06
 T   .530045E+03 .598903E+03 .641131E+03 .665196E+03 .729043E+03 .773678E+03 .819121E+03 .860511E+03 .871015E+03 .885983E+03
 F   .421447E+05 .411216E+05 .404417E+05 .400415E+05 .389513E+05 .381797E+05 .374007E+05 .367075E+05 .365352E+05 .366169E+05
 E   .457811E+06 .466238E+06 .474539E+06 .482766E+06 .498809E+06 .514561E+06 .542909E+06 .568244E+06 .580858E+06 .593497E+06

C 50.601        .406400E+02 .499700E+02 .123708E+04 .341000E+03 .135907E+04 .115538E+04
                .101300E+03 .876962E+02 .170127E+06 .404319E+06 .961346E+02 .402768E+06
 T   .609564E+03 .678982E+03 .729985E+03 .756871E+03 .820027E+03 .857027E+03 .893365E+03 .931643E+03 .933553E+03 .933964E+03
 F   .472979E+05 .461495E+05 .452693E+05 .448005E+05 .437035E+05 .430748E+05 .424724E+05 .418715E+05 .418576E+05 .418354E+05
 E   .414016E+06 .423502E+06 .432825E+06 .442062E+06 .460129E+06 .477965E+06 .510256E+06 .539245E+06 .553735E+06 .568219E+06

C 50.602        .398900E+02 .499700E+02 .122508E+04 .323310E+03 .150372E+04 .128186E+04
                .101300E+03 .876962E+02 .166993E+06 .400388E+06 .961346E+02 .402768E+06
 T   .633624E+03 .724624E+03 .770925E+03 .793359E+03 .847000E+03 .889513E+03 .931137E+03 .986500E+03 .990902E+03 .986640E+03
 F   .519462E+05 .507254E+05 .499116E+05 .495175E+05 .485869E+05 .478723E+05 .471262E+05 .463792E+05 .463174E+05 .463768E+05
 E   .411055E+06 .421501E+06 .431797E+06 .442021E+06 .462130E+06 .481980E+06 .517877E+06 .550066E+06 .566143E+06 .582237E+06

C 50.603        .404500E+02 .499700E+02 .120973E+04 .320490E+03 .121464E+04 .103874E+04
                .101300E+03 .876962E+02 .169333E+06 .397348E+06 .961462E+02 .402817E+06
 T   .580343E+03 .642655E+03 .692596E+03 .718042E+03 .765899E+03 .803709E+03 .855114E+03 .883357E+03 .882927E+03 .741045E+03
 F   .426426E+05 .416500E+05 .408099E+05 .403730E+05 .395447E+05 .388925E+05 .380235E+05 .375608E+05 .375674E+05 .399749E+05
 E   .406082E+06 .414631E+06 .423024E+06 .431335E+06 .447647E+06 .463715E+06 .492576E+06 .518526E+06 .531503E+06 .545230E+06

C 50.601        .398900E+02 .505400E+02 .119235E+04 .476010E+03 .168166E+04 .144344E+04
                .101300E+03 .971268E+02 .166993E+06 .393554E+06 .990226E+02 .414942E+06
 T   .675718E+03 .727177E+03 .775741E+03 .801378E+03 .854972E+03 .899368E+03 .943622E+03 .995568E+03 .990835E+03 .989135E+03
 F   .579329E+05 .570353E+05 .561735E+05 .557188E+05 .547818E+05 .540296E+05 .531167E+05 .525423E+05 .526096E+05 .526335E+05
 E   .405326E+06 .416939E+06 .428399E+06 .439778E+06 .462303E+06 .484362E+06 .524530E+06 .560601E+06 .578656E+06 .596717E+06

C 50.602        .400800E+02 .505400E+02 .118223E+04 .480220E+03 .181715E+04 .156566E+04
                .101719E+03 .100993E+03 .167787E+06 .393847E+06 .100108E+03 .419522E+06
 T   .697146E+03 .766822E+03 .808572E+03 .839543E+03 .911588E+03 .944497E+03 .984748E+03 .104296E+04 .102214E+04 .102152E+04
 F   .627358E+05 .614976E+05 .607508E+05 .602020E+05 .589676E+05 .584343E+05 .578181E+05 .570145E+05 .572888E+05 .572967E+05
 E   .406605E+06 .419147E+06 .431557E+06 .443871E+06 .468068E+06 .492082E+06 .535723E+06 .574951E+06 .594640E+06 .614331E+06

C 50.603        .395200E+02 .505400E+02 .116233E+04 .477420E+03 .150241E+04 .127355E+04
                .101300E+03 .876967E+02 .165448E+06 .388480E+06 .960882E+02 .402573E+06
 T   .625992E+03 .679802E+03 .721641E+03 .744666E+03 .815430E+03 .843436E+03 .882407E+03 .917495E+03 .927810E+03 .927810E+03
 F   .517192E+05 .508181E+05 .500935E+05 .496901E+05 .484494E+05 .479662E+05 .473093E+05 .467400E+05 .465798E+05 .465789E+05
 E   .398970E+06 .409298E+06 .419496E+06 .429620E+06 .449420E+06 .469046E+06 .504592E+06 .536566E+06 .552506E+06 .568445E+06

C 50.701        .303500E+02 .505400E+02 .128040E+04 .725240E+03 .177885E+04 .153242E+04
                .101300E+03 .876967E+02 .127126E+06 .369983E+06 .961068E+02 .402651E+06
 T   .616319E+03 .649017E+03 .690331E+03 .714550E+03 .777197E+03 .847974E+03 .904088E+03 .974377E+03 .978639E+03 .984772E+03
 F   .616642E+05 .613237E+05 .606157E+05 .601912E+05 .590766E+05 .578238E+05 .568671E+05 .557549E+05 .554915E+05 .556007E+05
 E   .382526E+06 .394975E+06 .407300E+06 .419549E+06 .443655E+06 .467316E+06 .510086E+06 .548329E+06 .567427E+06 .586502E+06
```

```
C 50.702          .292200E+02 .505400E+02 .128040E+04 .725240E+03 .194377E+04 .167248E+04
                  .101300E+03 .876967E+02 .122404E+06 .366769E+06 .969787E+02 .406325E+06
  T    .632450E+03 .690253E+03 .728705E+03 .759180E+03 .840249E+03 .9079442+03 .964647E+03 .105743E+04 .103808E+04 .104775E+04
  F    .673316E+05 .666791E+05 .659961E+05 .654511E+05 .639962E+05 .628243E+05 .619068E+05 .606010E+05 .608493E+05 .607230E+05
  E    .380439E+06 .393997E+06 .407436E+06 .420779E+06 .446960E+06 .472738E+06 .519420E+06 .561145E+06 .582073E+06 .602968E+06

C 50.703          .290300E+02 .505400E+02 .128140E+04 .721540E+03 .1570542+04 .136282E+04
                  .101300E+03 .876967E+02 .121610E+06 .362848E+06 .960914E+02 .402586E+06
  T    .567527E+03 .600374E+03 .633471E+03 .648342E+03 .715452E+03 .787220E+03 .843404E+03 .908090E+03 .930671E+03 .946950E+03
  F    .554084E+05 .549023E+05 .543679E+05 .541212E+05 .529693E+05 .517030E+05 .507242E+05 .496400E+05 .492794E+05 .490261E+05
  E    .374062E+06 .385187E+06 .396218E+06 .407204E+06 .428765E+06 .449870E+06 .487919E+06 .521863E+06 .538729E+06 .555520E+06

C 50.704          .296000E+02 .505400E+02 .128867E+04 .712870E+03 .1350412+04 .117918E+04
                  .101300E+03 .876967E+02 .123992E+06 .364497E+06 .961431E+02 .402804E+06
  T    .511628E+03 .535367E+03 .558455E+03 .573926E+03 .635751E+03 .696552E+03 .758790E+03 .807548E+03 .833942E+03 .765314E+03
  F    .480837E+05 .477585E+05 .474262E+05 .471953E+05 .462167E+05 .451916E+05 .441109E+05 .432635E+05 .428106E+05 .439966E+05
  E    .374210E+06 .383865E+06 .393461E+06 .403016E+06 .421770E+06 .440151E+06 .473125E+06 .502583E+06 .517173E+06 .532126E+06

C 50.701          .311000E+02 .505400E+02 .128244E+04 .472510E+03 .172425E+04 .145530E+04
                  .101300E+03 .876967E+02 .130260E+06 .372927E+06 .961026E+02 .402633E+06
  T    .696384E+03 .761292E+03 .812577E+03 .829048E+03 .885442E+03 .919071E+03 .964735E+03 .101394E+04 .100371E+04 .100168E+04
  F    .583010E+05 .571551E+05 .562444E+05 .559548E+05 .549836E+05 .544278E+05 .537121E+05 .530051E+05 .531458E+05 .531739E+05
  E    .384784E+06 .396437E+06 .407929E+06 .419369E+06 .441906E+06 .464248E+06 .504752E+06 .541172E+06 .559421E+06 .577679E+06

C 50.702          .299700E+02 .505400E+02 .129247E+04 .471100E+03 .150241E+04 .126858E+04
                  .101300E+03 .876967E+02 .125538E+06 .368045E+06 .960863E+02 .402468E+06
  T    .658436E+03 .708522E+03 .749699E+03 .777317E+03 .816140E+03 .855002E+03 .896244E+03 .932502E+03 .945619E+03 .922758E+03
  F    .511807E+05 .503223E+05 .496015E+05 .491160E+05 .484371E+05 .477691E+05 .470818E+05 .465034E+05 .463015E+05 .466552E+05
  E    .378438E+06 .388677E+06 .398786E+06 .408806E+06 .428602E+06 .448156E+06 .483552E+06 .519386E+06 .537244E+06 .547306E+06

C 50.703          .297800E+02 .505400E+02 .135246E+04 .471800E+03 .175216E+04 .148956E+04
                  .101300E+03 .876967E+02 .124744E+06 .380152E+06 .961543E+02 .402851E+06
  T    .712978E+03 .773673E+03 .829951E+03 .855948E+03 .906558E+03 .945519E+03 .964619E+03 .102863E+04 .101185E+04 .101050E+04
  F    .584739E+05 .583963E+05 .573976E+05 .569441E+05 .560865E+05 .554589E+05 .551644E+05 .542549E+05 .544806E+05 .544986E+05
  E    .392255E+06 .404168E+06 .415903E+06 .427559E+06 .450569E+06 .473361E+06 .514960E+06 .552264E+06 .570979E+06 .589699E+06

C 50.704          .309100E+02 .505400E+02 .133247E+04 .471100E+03 .133451E+04 .113407E+04
                  .101300E+03 .876967E+02 .129466E+06 .377554E+06 .961116E+02 .402671E+06
  T    .601355E+03 .652741E+03 .690006E+03 .712810E+03 .765852E+03 .790687E+03 .834980E+03 .869508E+03 .878002E+03 .865926E+03
  F    .461229E+05 .452874E+05 .446367E+05 .442641E+05 .433415E+05 .429097E+05 .421483E+05 .415690E+05 .414291E+05 .416275E+05
  E    .386901E+06 .396096E+06 .405175E+06 .414103E+06 .431859E+06 .449377E+06 .480982E+06 .509360E+06 .523506E+06 .537713E+06

C100.051          .963700E+02 .100430E+03 .579497E+03 .367210E+03 .253130E+04 .230223E+04
                  .108540E+03 .106969E+03 .403760E+06 .467415E+06 .101938E+03 .427242E+06
  T    .734299E+03 .780365E+03 .812195E+03 .829591E+03 .867444E+03 .895798E+03 .916364E+03 .944276E+03 .942644E+03 .945186E+03
  F    .900882E+05 .893312E+05 .886346E+05 .883094E+05 .876077E+05 .870914E+05 .867240E+05 .862373E+05 .862654E+05 .862213E+05
  E    .476648E+06 .485811E+06 .494924E+06 .504010E+06 .522068E+06 .540040E+06 .572881E+06 .602605E+06 .617471E+06 .632330E+06

C100.052          .965700E+02 .100430E+03 .563599E+03 .356580E+03 .284193E+04 .260130E+04
                  .109105E+03 .107501E+03 .396177E+06 .459918E+06 .102085E+03 .427864E+06
  T    .759999E+03 .806469E+03 .839832E+03 .861443E+03 .905323E+03 .933348E+03 .952894E+03 .983098E+03 .970258E+03 .972320E+03
  F    .101572E+06 .100679E+06 .100050E+06 .996397E+05 .988204E+05 .983111E+05 .979644E+05 .974451E+05 .976633E+05 .976275E+05
  E    .470339E+06 .480688E+06 .490987E+06 .501253E+06 .521655E+06 .541976E+06 .579134E+06 .612780E+06 .629631E+06 .646478E+06

C100.053          .952900E+02 .100430E+03 .583144E+03 .351630E+03 .229098E+04 .209068E+04
                  .107776E+03 .106310E+03 .399210E+06 .462094E+06 .101738E+03 .426398E+06
  T    .676451E+03 .724909E+03 .758340E+03 .780690E+03 .823597E+03 .848458E+03 .875019E+03 .901209E+03 .899007E+03 .901209E+03
  F    .823927E+05 .815257E+05 .809135E+05 .805012E+05 .797093E+05 .792540E+05 .787735E+05 .783082E+05 .783469E+05 .783079E+05
  E    .470520E+06 .478873E+06 .487174E+06 .495440E+06 .511839E+06 .528161E+06 .557937E+06 .584877E+06 .598352E+06 .611822E+06
```

```
C100.054          .951100E+02 .100430E+03 .587733E+03 .347380E+03 .198675E+04 .181227E+04
                  .106940E+03 .105540E+03 .398451E+06 .460298E+06 .101518E+03 .425468E+06
  T    .616183E+03 .657823E+03 .693215E+03 .712843E+03 .763115E+03 .788125E+03 .815196E+03 .839454E+03 .840204E+03 .840604E+03
  F    .718619E+05 .711709E+05 .705703E+05 .702044E+05 .692996E+05 .688461E+05 .683562E+05 .679203E+05 .679069E+05 .678996E+05
  E    .467630E+06 .474903E+06 .482125E+06 .489314E+06 .503536E+06 .517679E+06 .543452E+06 .566757E+06 .578407E+06 .590056E+06

C100.055          .951100E+02 .100430E+03 .621784E+03 .338170E+03 .174529E+04 .157152E+04
                  .106245E+03 .104954E+03 .398451E+06 .462076E+06 .101333E+03 .424690E+06
  T    .561809E+03 .600275E+03 .638108E+03 .660777E+03 .707645E+03 .731924E+03 .763237E+03 .785653E+03 .783498E+03 .799142E+03
  F    .627091E+05 .621204E+05 .615060E+05 .611247E+05 .603128E+05 .598837E+05 .593259E+05 .589257E+05 .587858E+05 .586850E+05
  E    .466462E+06 .474797E+06 .483078E+06 .487325E+06 .499675E+06 .511949E+06 .534270E+06 .554444E+06 .564509E+06 .574560E+06

C100.056          .951100E+02 .100430E+03 .621239E+03 .333220E+03 .152059E+04 .136589E+04
                  .105614E+03 .104406E+03 .398451E+06 .460950E+06 .101165E+03 .423981E+06
  T    .514201E+03 .553635E+03 .589374E+03 .610682E+03 .650572E+03 .676842E+03 .712717E+03 .736774E+03 .744649E+03 .748712E+03
  F    .547654E+05 .542156E+05 .536777E+05 .533413E+05 .526873E+05 .522624E+05 .516219E+05 .512005E+05 .510820E+05 .509902E+05
  E    .466518E+06 .472037E+06 .477509E+06 .482950E+06 .493716E+06 .504401E+06 .523784E+06 .541278E+06 .550004E+06 .558720E+06

C100.057          .954700E+02 .100430E+03 .676707E+03 .337460E+03 .127482E+04 .114600E+04
                  .105015E+03 .103846E+03 .398968E+06 .466239E+06 .101005E+03 .423304E+06
  T    .468532E+03 .500577E+03 .533613E+03 .550115E+03 .586872E+03 .617193E+03 .647423E+03 .672219E+03 .681045E+03 .687409E+03
  F    .460563E+05 .456615E+05 .452162E+05 .449810E+05 .444302E+05 .439519E+05 .434577E+05 .430421E+05 .428924E+05 .427836E+05
  E    .470914E+06 .475554E+06 .480154E+06 .484733E+06 .493790E+06 .502759E+06 .519036E+06 .533706E+06 .541018E+06 .548313E+06

C100.101          .897500E+02 .984300E+02 .498716E+03 .445760E+03 .211147E+04 .192331E+04
                  .106288E+03 .105128E+03 .374205E+06 .429848E+06 .101345E+03 .424738E+06
  T    .669281E+03 .694925E+03 .717836E+03 .736493E+03 .785475E+03 .815139E+03 .850816E+03 .878837E+03 .887083E+03 .886532E+03
  F    .758178E+05 .753684E+05 .749593E+05 .746225E+05 .737294E+05 .731880E+05 .725424E+05 .720437E+05 .718989E+05 .719079E+05
  E    .437757E+06 .445627E+06 .453461E+06 .461265E+06 .476718E+06 .492075E+06 .520024E+06 .545288E+06 .557899E+06 .570511E+06

C100.102          .895300E+02 .984300E+02 .510702E+03 .442240E+03 .177449E+04 .162348E+04
                  .105423E+03 .104367E+03 .374983E+06 .430084E+06 .101114E+03 .423765E+06
  T    .588473E+03 .615388E+03 .642362E+03 .657725E+03 .694996E+03 .727112E+03 .776639E+03 .806290E+03 .812525E+03 .812865E+03
  F    .645471E+05 .641205E+05 .636764E+05 .634174E+05 .627740E+05 .622072E+05 .613219E+05 .607915E+05 .606804E+05 .606739E+05
  E    .436797E+06 .443472E+06 .450108E+06 .456720E+06 .469830E+06 .482837E+06 .506390E+06 .527643E+06 .538252E+06 .548861E+06

C100.103          .893300E+02 .984300E+02 .526675E+03 .438710E+03 .149906E+04 .136260E+04
                  .104589E+03 .103630E+03 .374205E+06 .429391E+06 .100890E+03 .422820E+06
  T    .524430E+03 .536290E+03 .558359E+03 .583940E+03 .628256E+03 .651083E+03 .702280E+03 .745860E+03 .756797E+03 .748712E+03
  F    .546277E+05 .544638E+05 .541465E+05 .537614E+05 .530404E+05 .526787E+05 .518036E+05 .510407E+05 .508480E+05 .509898E+05
  E    .435059E+06 .440713E+06 .446338E+06 .451929E+06 .462978E+06 .473960E+06 .493799E+06 .511600E+06 .520470E+06 .529362E+06

C100.104          .891700E+02 .984300E+02 .514315E+03 .477420E+03 .253110E+04 .230065E+04
                  .107359E+03 .106060E+03 .373448E+06 .432480E+06 .101628E+03 .425935E+06
  T    .755020E+03 .792887E+03 .808242E+03 .819502E+03 .861779E+03 .889983E+03 .922319E+03 .944276E+03 .943275E+03 .942644E+03
  F    .897040E+05 .889964E+05 .887087E+05 .884980E+05 .877119E+05 .871964E+05 .866189E+05 .862373E+05 .862545E+05 .862648E+05
  E    .441869E+06 .451198E+06 .460502E+06 .469789E+06 .488231E+06 .506586E+06 .540062E+06 .570390E+06 .585556E+06 .600724E+06

C100.105          .893500E+02 .984300E+02 .502489E+03 .470400E+03 .222189E+04 .202477E+04
                  .106585E+03 .105387E+03 .374205E+06 .430721E+06 .101424E+03 .425071E+06
  T    .694872E+03 .724941E+03 .746851E+03 .760283E+03 .810496E+03 .838249E+03 .875798E+03 .901237E+03 .901887E+03 .902017E+03
  F    .795220E+05 .789821E+05 .785830E+05 .783370E+05 .774135E+05 .769036E+05 .762285E+05 .757794E+05 .757680E+05 .757653E+05
  E    .439025E+06 .447282E+06 .455504E+06 .463704E+06 .479944E+06 .496099E+06 .525499E+06 .552099E+06 .565397E+06 .578695E+06

C100.10A          .891700E+02 .984300E+02 .421004E+03 .389180E+03 .226056E+04 .207067E+04
                  .106675E+03 .105482E+03 .373448E+06 .422784E+06 .101448E+03 .425172E+06
  T    .678524E+03 .709985E+03 .734218E+03 .756579E+03 .796635E+03 .829452E+03 .867553E+03 .899017E+03 .899017E+03 .896785E+03
  F    .814988E+05 .809392E+05 .804996E+05 .800900E+05 .793515E+05 .787476E+05 .780549E+05 .774950E+05 .774950E+05 .775332E+05
  E    .431288E+06 .439745E+06 .448163E+06 .456546E+06 .473184E+06 .489719E+06 .519813E+06 .547012E+06 .560611E+06 .574216E+06
```

```
C100.10B        .891700E+02 .984300E+02 .468660E+03 .383510E+03 .200613E+04 .182989E+04
                .105978E+03 .104865E+03 .373448E+06 .425844E+06 .101262E+03 .424190E+06
 T   .618955E+01 .651517E+03 .679513E+03 .702033E+03 .750245E+03 .780992E+03 .826025E+03 .856737E+03 .860149E+03 .860149E+03
 F   .726137E+05 .720716E+05 .715889E+05 .711930E+05 .709278E+05 .697162E+05 .689545E+05 .684052E+05 .683447E+05 .683443E+05
 E   .433406E+06 .440919E+06 .448390E+06 .455825E+06 .470544E+06 .485154E+06 .511693E+06 .535658E+06 .547632E+06 .559606E+06

C100.10C        .891700E+02 .984300E+02 .492749E+03 .384930E+03 .179280E+04 .164358E+04
                .105426E+03 .104376E+03 .373448E+06 .427037E+06 .101115E+03 .423769E+06
 T   .572908E+03 .599533E+03 .631532E+03 .651620E+03 .690139E+03 .730945E+03 .787358E+03 .810084E+03 .818140E+03 .818840E+03
 F   .655411E+05 .651298E+05 .646119E+05 .642762E+05 .634737E+05 .628933E+05 .618830E+05 .614765E+05 .613329E+05 .613200E+05
 E   .433849E+06 .440626E+06 .447356E+06 .454056E+06 .467313E+06 .480466E+06 .504245E+06 .525741E+06 .536467E+06 .547191E+06

C100.10D        .891700E+02 .984300E+02 .500792E+03 .385630E+03 .151590E+04 .138107E+04
                .104614E+03 .103659E+03 .373448E+06 .426373E+06 .100897E+03 .422849E+06
 T   .5067Z5E+03 .532637E+03 .560971E+03 .584771E+03 .625986E+03 .656087E+03 .710347E+03 .743320E+03 .751785E+03 .755718E+03
 F   .555311E+05 .552083E+05 .548015E+05 .544421E+05 .537876E+05 .532678E+05 .523558E+05 .517774E+05 .516282E+05 .515583E+05
 E   .432132E+06 .437862E+06 .443556E+06 .449218E+06 .460421E+06 .471533E+06 .491589E+06 .509645E+06 .518649E+06 .527643E+06

C100.201        .799400E+02 .984300E+02 .694210E+03 .416790E+03 .196747E+04 .179336E+04
                .104891E+03 .103616E+03 .334664E+06 .407333E+06 .100971E+03 .423163E+06
 T   .533218E+03 .576514E+03 .617725E+03 .653091E+03 .710110E+03 .755278E+03 .823741E+03 .857756E+03 .861809E+03 .862019E+03
 F   .723236E+05 .718944E+05 .710447E+05 .704216E+05 .694613E+05 .686506E+05 .674128E+05 .668063E+05 .667348E+05 .667305E+05
 E   .416860E+06 .422293E+06 .429690E+06 .437032E+06 .451546E+06 .465916E+06 .491859E+06 .515265E+06 .526958E+06 .538649E+06

C100.202        .804800E+02 .100430E+03 .674408E+03 .423140E+03 .237477E+04 .217481E+04
                .105831E+03 .104721E+03 .336931E+06 .408365E+06 .101223E+03 .424225E+06
 T   .609021E+03 .663592E+03 .701853E+03 .736367E+03 .806022E+03 .851071E+03 .907736E+03 .942701E+03 .944252E+03 .934546E+03
 F   .869781E+05 .860607E+05 .853830E+05 .847549E+05 .836465E+05 .826324E+05 .816120E+05 .810074E+05 .809811E+05 .811457E+05
 E   .417238E+06 .426034E+06 .434775E+06 .443462E+06 .460621E+06 .477641E+06 .508534E+06 .538453E+06 .550409E+06 .564388E+06

C100.203        .806600E+02 .100430E+03 .678390E+03 .422450E+03 .206262E+04 .189148E+04
                .105119E+03 .103974E+03 .337687E+06 .408001E+06 .101033E+03 .423422E+06
 T   .546875E+03 .592014E+03 .627211E+03 .669302E+03 .739206E+03 .777038E+03 .840167E+03 .875223E+03 .884539E+03 .882148E+03
 F   .761443E+05 .754679E+05 .749012E+05 .741878E+05 .729452E+05 .722573E+05 .711111E+05 .704866E+05 .703232E+05 .703644E+05
 E   .415751E+06 .423445E+06 .431090E+06 .438675E+06 .453631E+06 .468468E+06 .495308E+06 .519529E+06 .531617E+06 .543710E+06

C100.204        .804800E+02 .100430E+03 .690065E+03 .411840E+03 .176476E+04 .161465E+04
                .103390E+03 .103141E+03 .336931E+06 .406817E+06 .100566E+03 .421451E+06
 T   .473729E+03 .523371E+03 .552680E+03 .583799E+03 .638088E+03 .695096E+03 .755603E+03 .788227E+03 .798704E+03 .800765E+03
 F   .653704E+05 .647450E+05 .643340E+05 .638682E+05 .629966E+05 .620218E+05 .609491E+05 .603654E+05 .601782E+05 .601408E+05
 E   .413453E+06 .420038E+06 .426587E+06 .433096E+06 .445962E+06 .458656E+06 .481581E+06 .502249E+06 .512555E+06 .522856E+06

C100.205        .803000E+02 .100430E+03 .722013E+03 .410420E+03 .153093E+04 .140817E+04
                .101300E+03 .102155E+03 .336176E+06 .407814E+06 .997577E+02 .418043E+06
 T   .418619E+03 .452702E+03 .489487E+03 .520666E+03 .581949E+03 .629958E+03 .678885E+03 .727190E+03 .744172E+03 .750466E+03
 F   .572511E+05 .569075E+05 .564797E+05 .560759E+05 .551891E+05 .544258E+05 .536034E+05 .527634E+05 .524645E+05 .523529E+05
 E   .413615E+06 .419389E+06 .425126E+06 .430828E+06 .442076E+06 .453188E+06 .473290E+06 .491311E+06 .500277E+06 .509225E+06

C100.301        .693900E+02 .100430E+03 .100229E+04 .418920E+03 .232294E+04 .214781E+04
                .103950E+03 .103173E+03 .290416E+06 .398081E+06 .100718E+03 .422093E+06
 T   .527547E+03 .590824E+03 .635234E+03 .677259E+03 .737880E+03 .793221E+03 .856595E+03 .897617E+03 .902411E+03 .906294E+03
 F   .864632E+05 .855372E+05 .848159E+05 .840921E+05 .829999E+05 .819778E+05 .808104E+05 .800730E+05 .799883E+05 .799196E+05
 E   .399596E+06 .408316E+06 .416976E+06 .425576E+06 .442592E+06 .459437E+06 .489959E+06 .517501E+06 .531261E+06 .545011E+06

C100.302        .695700E+02 .100430E+03 .102199E+04 .409720E+03 .253283E+04 .233380E+04
                .105030E+03 .103747E+03 .291171E+06 .394300E+06 .101009E+03 .423321E+06
 T   .611820E+03 .662800E+03 .708000E+03 .742597E+03 .810053E+03 .857015E+03 .912922E+03 .954013E+03 .954013E+03 .956629E+03
 F   .931350E+05 .922733E+05 .914666E+05 .908302E+05 .895620E+05 .886912E+05 .876742E+05 .869589E+05 .869589E+05 .869141E+05
 E   .403802E+06 .413251E+06 .422599E+06 .431911E+06 .450327E+06 .468599E+06 .501795E+06 .531781E+06 .546773E+06 .561761E+06
```

```
C100.303        .695700E+02 .100430E+03 .108196E+04 .409010E+03 .193651E+04 .180675E+04
                .101300E+03 .101803E+03 .291171E+06 .396883E+06 .999368E+02 .418798E+06
 T   .469897E+03 .525970E+03 .577215E+03 .612120E+03 .674589E+03 .723312E+03 .787124E+03 .819748E+03 .831487E+03 .836491E+03
 F   .731226E+05 .724231E+05 .716836E+05 .711356E+05 .700863E+05 .692261E+05 .680740E+05 .674846E+05 .672738E+05 .671839E+05
 E   .404306E+06 .411672E+06 .418976E+06 .426233E+06 .440566E+06 .454751E+06 .480388E+06 .503524E+06 .515061E+06 .526585E+06

C100.304        .693900E+02 .100430E+03 .108204E+04 .411130E+03 .173815E+04 .160690E+04
                .101498E+03 .100830E+03 .290416E+06 .395077E+06 .100045E+03 .419255E+06
 T   .391701E+03 .441536E+03 .498537E+03 .541700E+03 .603978E+03 .657745E+03 .731914E+03 .767841E+03 .780720E+03 .784073E+03
 F   .654210E+05 .649749E+05 .643228E+05 .637440E+05 .628049E+05 .619190E+05 .606257E+05 .599848E+05 .597546E+05 .596943E+05
 E   .401701E+06 .408290E+06 .414826E+06 .421313E+06 .434124E+06 .446779E+06 .469560E+06 .490081E+06 .500308E+06 .510525E+06

C100.401        .604200E+02 .100430E+03 .130767E+04 .438000E+03 .253283E+04 .234313E+04
                .101362E+03 .102151E+03 .252849E+06 .381392E+06 .100010E+03 .419106E+06
 T   .520101E+03 .603560E+03 .663511E+03 .709852E+03 .775329E+03 .827379E+03 .891294E+03 .931146E+03 .939542E+03 .943265E+03
 F   .944951E+05 .932689E+05 .922614E+05 .914329E+05 .902192E+05 .892430E+05 .880628E+05 .873529E+05 .872069E+05 .871422E+05
 E   .391001E+06 .400513E+06 .409944E+06 .419306E+06 .437831E+06 .456194E+06 .489505E+06 .519596E+06 .534622E+06 .549639E+06

C100.402        .607800E+02 .100430E+03 .126269E+04 .440820E+03 .277459E+04 .256474E+04
                .104776E+03 .103208E+03 .254356E+06 .380050E+06 .100941E+03 .423033E+06
 T   .592609E+03 .671460E+03 .716353E+03 .762845E+03 .833298E+03 .882684E+03 .939443E+03 .980052E+03 .985860E+03 .986120E+03
 F   .102653E+06 .101322E+06 .100508E+06 .996362E+05 .982953E+05 .973650E+05 .961315E+05 .954959E+05 .955324E+05 .955276E+05
 E   .390515E+06 .400875E+06 .411170E+06 .421393E+06 .441624E+06 .461706E+06 .498222E+06 .531203E+06 .547698E+06 .564192E+06

C100.403        .596800E+02 .100430E+03 .132244E+04 .424570E+03 .226056E+04 .208632E+04
                .101690E+03 .101021E+03 .249752E+06 .378295E+06 .100100E+03 .419488E+06
 T   .443079E+03 .550633E+03 .612874E+03 .657482E+03 .732056E+03 .781511E+03 .840081E+03 .890090E+03 .901999E+03 .907703E+03
 F   .848854E+05 .835688E+05 .826134E+05 .818660E+05 .805390E+05 .796306E+05 .785532E+05 .776534E+05 .774426E+05 .773412E+05
 E   .386904E+06 .395410E+06 .403839E+06 .412205E+06 .428713E+06 .445067E+06 .474716E+06 .501417E+06 .514739E+06 .528046E+06

C100.404        .596800E+02 .100430E+03 .132268E+04 .457740E+03 .276228E+04 .254074E+04
                .104169E+03 .102972E+03 .249752E+06 .380664E+06 .100777E+03 .423343E+06
 T   .576790E+03 .660259E+03 .720310E+03 .760034E+03 .836141E+03 .886258E+03 .944097E+03 .986130E+03 .978234E+03 .978234E+03
 F   .101950E+06 .100575E+06 .994810E+05 .987460E+05 .973001E+05 .963592E+05 .951123E+05 .945929E+05 .947250E+05 .947245E+05
 E   .391051E+06 .401331E+06 .411522E+06 .421654E+06 .441682E+06 .461559E+06 .497696E+06 .530363E+06 .546713E+06 .563062E+06

C100.501        .506600E+02 .100430E+03 .177827E+04 .544080E+03 .265802E+04 .240660E+04
                .101300E+03 .995145E+02 .212016E+06 .382762E+06 .997455E+02 .418008E+06
 T   .532859E+03 .640398E+03 .709508E+03 .745338E+03 .815626E+03 .854502E+03 .901853E+03 .965213E+03 .952483E+03 .964252E+03
 F   .970381E+05 .953729E+05 .941493E+05 .934875E+05 .921656E+05 .914365E+05 .905658E+05 .894555E+05 .896724E+05 .894718E+05
 E   .392634E+06 .402374E+06 .412015E+06 .421601E+06 .440556E+06 .459392E+06 .493666E+06 .524528E+06 .539988E+06 .555421E+06

C100.502        .506600E+02 .100430E+03 .173795E+04 .547500E+03 .302378E+04 .275041E+04
                .102943E+03 .102010E+03 .212016E+06 .380946E+06 .100444E+03 .420938E+06
 T   .621874E+03 .713384E+03 .773084E+03 .805750E+03 .883168E+03 .933285E+03 .978134E+03 .103692E+04 .101342E+04 .102813E+04
 F   .109835E+06 .108211E+06 .107079E+06 .106450E+06 .104983E+06 .104032E+06 .103237E+06 .101967E+06 .102645E+06 .102408E+06
 E   .392155E+06 .403237E+06 .414230E+06 .425172E+06 .446824E+06 .468328E+06 .507530E+06 .542860E+06 .560606E+06 .578324E+06

C100.503        .506600E+02 .100430E+03 .173844E+04 .542020E+03 .245459E+04 .223335E+04
                .101300E+03 .877536E+02 .212016E+06 .378325E+06 .962678E+02 .403330E+06
 T   .500871E+03 .596162E+03 .656091E+03 .693181E+03 .773341E+03 .821755E+03 .872388E+03 .912970E+03 .923516E+03 .939590E+03
 F   .902944E+05 .889386E+05 .879445E+05 .872914E+05 .858213E+05 .849197E+05 .839875E+05 .832607E+05 .830761E+05 .827984E+05
 E   .387300E+06 .396569E+06 .405955E+06 .414488E+06 .432108E+06 .449577E+06 .481321E+06 .509979E+06 .524283E+06 .538549E+06

C100.504        .506600E+02 .100430E+03 .177056E+04 .515090E+03 .213932E+04 .194509E+04
                .101300E+03 .877536E+02 .212016E+06 .379691E+06 .963274E+02 .403581E+06
 T   .413658E+03 .513854E+03 .602213E+03 .645227E+03 .717836E+03 .762576E+03 .808424E+03 .846723E+03 .858539E+03 .887083E+03
 F   .793170E+05 .782274E+05 .769380E+05 .762307E+05 .749593E+05 .741479E+05 .733104E+05 .726160E+05 .722259E+05 .718986E+05
 E   .387727E+06 .395680E+06 .403527E+06 .411313E+06 .426669E+06 .441886E+06 .469519E+06 .494442E+06 .506848E+06 .519208E+06
```

C100.601	.415700E+02	.100430E+03	.202616E+04	.564570E+03	.280466E+04	.254112E+04		
	.101300E+03	.877536E+02	.174014E+06	.367506E+06	.962665E+02	.403326E+06		
T	.527310E+03	.646662E+03	.726647E+03	.762276E+03	.835421E+03	.898899E+03	.943176E+03	.995127E+03	.990394E+03	.991474E+03
F	.102660E+06	.100811E+06	.993722E+05	.987037E+05	.973138E+05	.961259E+05	.953285E+05	.944447E+05	.945224E+05	.945043E+05
E	.377948E+06	.388246E+06	.398428E+06	.408556E+06	.428587E+06	.448426E+06	.484568E+06	.517197E+06	.533521E+06	.549643E+06
C100.602	.417500E+02	.100430E+03	.202504E+04	.574060E+03	.301094E+04	.272618E+04		
	.101300E+03	.877536E+02	.174766E+06	.369114E+06	.955846E+02	.400451E+06		
T	.568591E+03	.680205E+03	.756256E+03	.802918E+03	.875202E+03	.930083E+03	.988412E+03	.103692E+04	.102814E+04	.102912E+04
F	.109709E+06	.107850E+06	.106433E+06	.105537E+06	.104150E+06	.103128E+06	.102101E+06	.101011E+06	.101451E+06	.101435E+06
E	.380289E+06	.391320E+06	.402239E+06	.413066E+06	.434560E+06	.455874E+06	.494663E+06	.529662E+06	.547214E+06	.564763E+06
C100.603	.417500E+02	.100430E+03	.201646E+04	.561850E+03	.258369E+04	.233756E+04		
	.101300E+03	.877536E+02	.174014E+06	.363610E+06	.963266E+02	.403577E+06		
T	.464082E+03	.588821E+03	.675274E+03	.722766E+03	.808231E+03	.866603E+03	.912922E+03	.965031E+03	.971306E+03	.972237E+03
F	.951650E+05	.935021E+05	.920543E+05	.911966E+05	.896018E+05	.885141E+05	.876742E+05	.867733E+05	.866867E+05	.866510E+05
E	.375268E+06	.384799E+06	.394213E+06	.403556E+06	.421978E+06	.440222E+06	.473417E+06	.503354E+06	.518308E+06	.533261E+06
C150.051	.949300E+02	.150310E+03	.566987E+03	.409720E+03	.306243E+04	.283961E+04		
	.112248E+03	.110055E+03	.395419E+06	.438937E+06	.102893E+03	.431273E+06		
T	.767232E+03	.817578E+03	.839301E+03	.849082E+03	.874798E+03	.888842E+03	.897310E+03	.897450E+03	.887971E+03	.888842E+03
F	.110128E+06	.109156E+06	.108733E+06	.108544E+06	.108050E+06	.107782E+06	.107622E+06	.107619E+06	.107799E+06	.107782E+06
E	.446489E+06	.453990E+06	.461468E+06	.468936E+06	.483821E+06	.498678E+06	.525806E+06	.550619E+06	.563001E+06	.575382E+06
C150.052	.949300E+02	.150310E+03	.567674E+03	.458450E+03	.282779E+04	.257492E+04		
	.111398E+03	.109301E+03	.397693E+06	.440366E+06	.102676E+03	.430359E+06		
T	.751042E+03	.785169E+03	.812417E+03	.821596E+03	.850524E+03	.867330E+03	.884387E+03	.865288E+03	.870123E+03	.884235E+03
F	.998584E+05	.992121E+05	.986927E+05	.985180E+05	.979687E+05	.976520E+05	.977073E+05	.976904E+05	.975997E+05	.973358E+05
E	.447209E+06	.454017E+06	.460797E+06	.467568E+06	.481050E+06	.494498E+06	.519164E+06	.541585E+06	.552787E+06	.563965E+06
C150.053	.949300E+02	.150310E+03	.542643E+03	.461260E+03	.323783E+04	.296144E+04		
	.112846E+03	.110585E+03	.397693E+06	.440182E+06	.103045E+03	.431914E+06		
T	.803554E+03	.844710E+03	.874742E+03	.882079E+03	.903471E+03	.912650E+03	.910998E+03	.915252E+03	.915252E+03	.924651E+03
F	.114394E+06	.113590E+06	.113006E+06	.112845E+06	.112455E+06	.112281E+06	.112313E+06	.112232E+06	.112232E+06	.112056E+06
E	.448038E+06	.455852E+06	.463636E+06	.471412E+06	.486923E+06	.502417E+06	.530827E+06	.556641E+06	.569548E+06	.582440E+06
C150.054	.947500E+02	.150310E+03	.542667E+03	.458150E+03	.213776E+04	.192466E+04		
	.108776E+03	.107044E+03	.396935E+06	.435916E+06	.101999E+03	.427502E+06		
T	.640663E+03	.678610E+03	.714373E+03	.728596E+03	.749404E+03	.764958E+03	.776497E+03	.780561E+03	.790148E+03	.798976E+03
F	.754898E+05	.748388E+05	.742049E+05	.739491E+05	.735721E+05	.732689E+05	.730783E+05	.730041E+05	.728291E+05	.726678E+05
E	.441068E+06	.446162E+06	.451259E+06	.456322E+06	.466405E+06	.476455E+06	.494836E+06	.511532E+06	.519863E+06	.528179E+06
C150.055	.947500E+02	.150310E+03	.542692E+03	.456330E+03	.175216E+04	.156539E+04		
	.107306E+03	.105766E+03	.396935E+06	.434683E+06	.101614E+03	.425875E+06		
T	.573721E+03	.616960E+03	.645024E+03	.649027E+03	.671516E+03	.689810E+03	.703301E+03	.713999E+03	.724517E+03	.729811E+03
F	.617859E+05	.611079E+05	.606454E+05	.605784E+05	.601963E+05	.598802E+05	.596446E+05	.594566E+05	.592709E+05	.591768E+05
E	.438868E+06	.443055E+06	.447193E+06	.451328E+06	.459553E+06	.467740E+06	.482699E+06	.496260E+06	.503023E+06	.509775E+06
C150.056	.949300E+02	.150310E+03	.542721E+03	.449290E+03	.160512E+04	.144288E+04		
	.106848E+03	.105366E+03	.397693E+06	.435019E+06	.101493E+03	.425365E+06		
T	.542745E+03	.570029E+03	.597773E+03	.612325E+03	.637165E+03	.651046E+03	.665767E+03	.678867E+03	.688484E+03	.672062E+03
F	.571770E+05	.567780E+05	.563510E+05	.561196E+05	.557144E+05	.554830E+05	.552342E+05	.550103E+05	.548445E+05	.551264E+05
E	.438907E+06	.442771E+06	.446611E+06	.450436E+06	.458038E+06	.465613E+06	.479446E+06	.491976E+06	.498224E+06	.504501E+06
C150.057	.949300E+02	.150310E+03	.542713E+03	.452810E+03	.355907E+04	.327042E+04		
	.114003E+03	.111601E+03	.397693E+06	.441222E+06	.103336E+03	.433144E+06		
T	.839101E+03	.881530E+03	.915117E+03	.921904E+03	.944668E+03	.949613E+03	.944778E+03	.949613E+03	.942866E+03	.952115E+03
F	.126025E+06	.125182E+06	.124523E+06	.124392E+06	.123957E+06	.123863E+06	.123955E+06	.123863E+06	.123991E+06	.123816E+06
E	.449889E+06	.458514E+06	.467106E+06	.475692E+06	.492821E+06	.509941E+06	.541343E+06	.569876E+06	.584153E+06	.598415E+06
C150.058	.949300E+02	.150310E+03	.497697E+03	.455630E+03	.395298E+04	.365024E+04		
	.115373E+03	.112841E+03	.397693E+06	.439817E+06	.103678E+03	.434587E+06		
T	.889160E+03	.936005E+03	.963826E+03	.971884E+03	.987601E+03	.994669E+03	.984520E+03	.991015E+03	.977761E+03	.988092E+03
F	.140128E+06	.139189E+06	.138645E+06	.138490E+06	.138191E+06	.138059E+06	.138249E+06	.138127E+06	.138378E+06	.138182E+06
E	.449475E+06	.459088E+06	.468676E+06	.478256E+06	.497389E+06	.516510E+06	.551598E+06	.583476E+06	.599435E+06	.615378E+06
C150.059	.949300E+02	.150310E+03	.497706E+03	.454220E+03	.418208E+04	.384860E+04		
	.116100E+03	.113486E+03	.397693E+06	.440479E+06	.103858E+03	.435348E+06		
T	.921652E+03	.970830E+03	.993465E+03	.994236E+03	.100862E+04	.101090E+04	.998631E+03	.101864E+04	.991343E+03	.100304E+04
F	.147323E+06	.146342E+06	.145904E+06	.145890E+06	.145618E+06	.145575E+06	.145810E+06	.145432E+06	.145945E+06	.145722E+06
E	.450648E+06	.460771E+06	.470874E+06	.480977E+06	.501158E+06	.521333E+06	.558365E+06	.591973E+06	.608815E+06	.625640E+06
C150.101	.904300E+02	.150310E+03	.552532E+03	.468290E+03	.308448E+04	.285948E+04		
	.111912E+03	.109187E+03	.378749E+06	.421491E+06	.102807E+03	.430913E+06		
T	.805704E+03	.830991E+03	.850762E+03	.864106E+03	.897299E+03	.903515E+03	.906948E+03	.917808E+03	.905977E+03	.902093E+03
F	.110367E+06	.109477E+06	.109494E+06	.109233E+06	.108802E+06	.108485E+06	.108420E+06	.108217E+06	.108439E+06	.108511E+06
E	.429071E+06	.436625E+06	.444159E+06	.451680E+06	.466656E+06	.481619E+06	.509040E+06	.533933E+06	.546399E+06	.558870E+06
C150.102	.902500E+02	.150310E+03	.542532E+03	.468290E+03	.350048E+04	.323635E+04		
	.136157E+03	.110398E+03	.377992E+06	.421421E+06	.108492E+03	.454916E+06		
T	.855172E+03	.892654E+03	.910874E+03	.929864E+03	.954819E+03	.975549E+03	.978232E+03	.985839E+03	.959043E+03	.953628E+03
F	.124656E+06	.123916E+06	.123561E+06	.123194E+06	.122732E+06	.122339E+06	.122290E+06	.122152E+06	.122643E+06	.122744E+06
E	.430000E+06	.438542E+06	.447066E+06	.455573E+06	.472538E+06	.489467E+06	.520495E+06	.548680E+06	.562812E+06	.576952E+06
C150.103	.900700E+02	.150310E+03	.542604E+03	.464070E+03	.264160E+04	.243784E+04		
	.109228E+03	.107673E+03	.377234E+06	.417951E+06	.102117E+03	.427998E+06		
T	.717585E+03	.751111E+03	.780311E+03	.786978E+03	.817487E+03	.829268E+03	.844953E+03	.856463E+03	.854592E+03	.849267E+03
F	.949121E+05	.942904E+05	.937414E+05	.936158E+05	.930396E+05	.928172E+05	.925230E+05	.923077E+05	.923427E+05	.924419E+05
E	.424446E+06	.430908E+06	.437339E+06	.443764E+06	.456550E+06	.469312E+06	.492649E+06	.513826E+06	.524418E+06	.535019E+06
C150.104	.897100E+02	.150310E+03	.542667E+03	.459150E+03	.223141E+04	.205214E+04		
	.107916E+03	.106235E+03	.375720E+06	.415117E+06	.101775E+03	.426555E+06		
T	.634000E+03	.668414E+03	.689557E+03	.696113E+03	.739995E+03	.756600E+03	.781532E+03	.796655E+03	.801119E+03	.798496E+03
F	.805756E+05	.800212E+05	.796170E+05	.795006E+05	.787083E+05	.784065E+05	.779463E+05	.776680E+05	.775859E+05	.776338E+05
E	.420614E+06	.426080E+06	.431523E+06	.436959E+06	.447742E+06	.458490E+06	.478099E+06	.495873E+06	.504752E+06	.513636E+06
C150.105	.893500E+02	.150310E+03	.572716E+03	.452110E+03	.186221E+04	.169881E+04		
	.107882E+03	.104836E+03	.374205E+06	.414178E+06	.101766E+03	.426515E+06		
T	.558172E+03	.583757E+03	.597630E+03	.613095E+03	.659356E+03	.686780E+03	.724451E+03	.750332E+03	.756637E+03	.756777E+03
F	.672909E+05	.669062E+05	.666900E+05	.664432E+05	.656742E+05	.652011E+05	.645364E+05	.640738E+05	.639604E+05	.639576E+05
E	.418756E+06	.423312E+06	.427856E+06	.432385E+06	.441354E+06	.450268E+06	.466466E+06	.481102E+06	.488409E+06	.495715E+06
C150.106	.893500E+02	.150310E+03	.577722E+03	.448580E+03	.159837E+04	.147167E+04		
	.103941E+03	.103927E+03	.374205E+06	.413671E+06	.100715E+03	.422082E+06		
T	.492158E+03	.512607E+03	.524378E+03	.542735E+03	.585813E+03	.613226E+03	.637155E+03	.666729E+03	.678858E+03	.629929E+03
F	.585633E+05	.583035E+05	.581431E+05	.578874E+05	.572475E+05	.568152E+05	.564244E+05	.559275E+05	.557198E+05	.565432E+05
E	.417646E+06	.421606E+06	.425557E+06	.429493E+06	.437290E+06	.445036E+06	.459151E+06	.471885E+06	.478231E+06	.484659E+06
C150.201	.793900E+02	.150310E+03	.856442E+03	.499790E+03	.286671E+04	.268981E+04		
	.107025E+03	.105904E+03	.332156E+06	.392509E+06	.101540E+03	.425562E+06		
T	.509824E+03	.586868E+03	.635174E+03	.673684E+03	.751146E+03	.799028E+03	.845248E+03	.874874E+03	.874764E+03	.875515E+03
F	.107625E+06	.106533E+06	.105741E+06	.105073E+06	.103641E+06	.102727E+06	.101841E+06	.101279E+06	.101281E+06	.101267E+06
E	.399819E+06	.407074E+06	.414288E+06	.421467E+06	.435672E+06	.449778E+06	.475467E+06	.498721E+06	.510348E+06	.521973E+06
C150.202	.808500E+02	.150310E+03	.811148E+03	.505360E+03	.315463E+04	.292451E+04		
	.108661E+03	.107101E+03	.338485E+06	.396764E+06	.101969E+03	.427375E+06		
T	.622935E+03	.674978E+03	.720839E+03	.756172E+03	.823850E+03	.861511E+03	.897417E+03	.916105E+03	.912442E+03	.905195E+03
F	.115744E+06	.114830E+06	.113983E+06	.113310E+06	.111994E+06	.111262E+06	.110573E+06	.110220E+06	.110289E+06	.110425E+06
E	.404657E+06	.412503E+06	.420305E+06	.428071E+06	.443467E+06	.458785E+06	.486739E+06	.512091E+06	.524773E+06	.537446E+06

C150.203	.799400E+02	.150310E+03	.816031E+03	.507450E+03	.357971E+04	.335944E+04			
	.110053E+03	.108373E+03	.334664E+06	.394704E+06	.102331E+03	.428901E+06			
T .687489E+03	.742098E+03	.789462E+03	.829112E+03	.887742E+03	.921869E+03	.958998E+03	.982472E+03	.963953E+03	.954774E+03
F .132173E+06	.131130E+06	.130192E+06	.129397E+06	.128223E+06	.127592E+06	.126841E+06	.126405E+06	.126748E+06	.126920E+06
E .403740E+06	.412721E+06	.421658E+06	.430554E+06	.446228E+06	.465836E+06	.497990E+06	.527152E+06	.541760E+06	.556382E+06
C150.204	.799400E+02	.150310E+03	.846610E+03	.496300E+03	.259720E+04	.241569E+04			
	.106091E+03	.105033E+03	.334664E+06	.393298E+06	.101392E+03	.424517E+06			
T .420737E+03	.903159E+03	.375249E+03	.427865E+03	.712192E+03	.764727E+03	.798330E+03	.825796E+03	.833383E+03	.836216E+03
F .973801E+05	.965113E+05	.955165E+05	.946758E+05	.931928E+05	.922181E+05	.915863E+05	.910695E+05	.909272E+05	.908738E+05
E .399692E+06	.406445E+06	.412947E+06	.419405E+06	.432158E+06	.444804E+06	.467860E+06	.488727E+06	.499147E+06	.509562E+06
C150.205	.790300E+02	.150310E+03	.851674E+03	.494910E+03	.233269E+04	.217691E+04			
	.105047E+03	.103824E+03	.330845E+06	.388965E+06	.101013E+03	.423340E+06			
T .370939E+03	.457725E+03	.533935E+03	.575386E+03	.665387E+03	.709642E+03	.756548E+03	.791089E+03	.803200E+03	.807093E+03
F .880171E+05	.873055E+05	.863760E+05	.857754E+05	.842999E+05	.835141E+05	.826565E+05	.820173E+05	.817929E+05	.817205E+05
E .394915E+06	.400834E+06	.406705E+06	.412545E+06	.424060E+06	.435487E+06	.456261E+06	.475026E+06	.484387E+06	.493742E+06
C150.301	.703000E+02	.150310E+03	.119047E+04	.516480E+03	.371997E+04	.350537E+04			
	.107979E+03	.106527E+03	.294230E+06	.376977E+06	.101791E+03	.426622E+06			
T .519428E+03	.616805E+03	.702784E+03	.752256E+03	.847092E+03	.915854E+03	.963896E+03	.993616E+03	.971754E+03	.970963E+03
F .140274E+06	.138826E+06	.137282E+06	.136330E+06	.134408E+06	.133027E+06	.132095E+06	.131540E+06	.131946E+06	.131960E+06
E .386508E+06	.395973E+06	.405363E+06	.414705E+06	.433200E+06	.451555E+06	.485052E+06	.515414E+06	.530627E+06	.545840E+06
C150.302	.692000E+02	.150310E+03	.123111E+04	.506060E+03	.343917E+04	.324317E+04			
	.106824E+03	.105295E+03	.289620E+06	.373888E+06	.101487E+03	.425339E+06			
T .453371E+03	.522421E+03	.616049E+03	.684453E+03	.787453E+03	.864995E+03	.921366E+03	.957323E+03	.941702E+03	.942888E+03
F .130315E+06	.129537E+06	.128140E+06	.126936E+06	.124952E+06	.123410E+06	.122308E+06	.121628E+06	.122106E+06	.121898E+06
E .382722E+06	.391524E+06	.400260E+06	.408936E+06	.426087E+06	.443081E+06	.474034E+06	.502061E+06	.516092E+06	.530128E+06
C150.303	.692000E+02	.150310E+03	.130244E+04	.472510E+03	.313031E+04	.291193E+04			
	.105500E+03	.103999E+03	.289620E+06	.377018E+06	.101135E+03	.423852E+06			
T .413965E+03	.492235E+03	.582299E+03	.655745E+03	.756044E+03	.823211E+03	.878409E+03	.915285E+03	.915285E+03	.906937E+03
F .117382E+06	.116628E+06	.115396E+06	.114178E+06	.112319E+06	.111015E+06	.109947E+06	.109248E+06	.109248E+06	.109404E+06
E .384964E+06	.392881E+06	.400738E+06	.408534E+06	.423931E+06	.439191E+06	.466964E+06	.492091E+06	.504655E+06	.517232E+06
C150.401	.602300E+02	.150310E+03	.160393E+04	.582830E+03	.365135E+04	.341168E+04			
	.104444E+03	.103427E+03	.252054E+06	.359015E+06	.100851E+03	.422656E+06			
T .412726E+03	.452390E+03	.510324E+03	.594847E+03	.737268E+03	.847142E+03	.921858E+03	.971800E+03	.971029E+03	.984012E+03
F .137014E+06	.136694E+06	.136066E+06	.134863E+06	.132302E+06	.130108E+06	.128823E+06	.127669E+06	.127684E+06	.127444E+06
E .368290E+06	.377556E+06	.386798E+06	.395985E+06	.414108E+06	.432011E+06	.464563E+06	.494002E+06	.508723E+06	.523424E+06
C150.402	.604200E+02	.150310E+03	.161445E+04	.578790E+03	.389650E+04	.359636E+04			
	.105235E+03	.104268E+03	.252849E+06	.361072E+06	.101084E+03	.423553E+06			
T .443071E+03	.492796E+03	.568123E+03	.663670E+03	.797770E+03	.895244E+03	.958906E+03	.102592E+04	.998157E+03	.100527E+04
F .144386E+06	.143889E+06	.142893E+06	.141298E+06	.138691E+06	.136708E+06	.135451E+06	.134211E+06	.134712E+06	.134581E+06
E .370856E+06	.380624E+06	.390149E+06	.399999E+06	.419044E+06	.437893E+06	.472230E+06	.503256E+06	.518806E+06	.534346E+06
C150.403	.604200E+02	.150310E+03	.161496E+04	.574740E+03	.415406E+04	.384512E+04			
	.111089E+03	.105233E+03	.252849E+06	.361946E+06	.102597E+03	.430025E+06			
T .467729E+03	.537629E+03	.639825E+03	.728675E+03	.860527E+03	.945901E+03	.997581E+03	.107063E+04	.102004E+04	.102770E+04
F .154248E+06	.153427E+06	.151825E+06	.150153E+06	.147451E+06	.145705E+06	.144699E+06	.143390E+06	.144281E+06	.144140E+06
E .372408E+06	.382836E+06	.393198E+06	.403479E+06	.423780E+06	.443916E+06	.480662E+06	.513880E+06	.530552E+06	.547214E+06
C200.051	.951100E+02	.200200E+03	.576939E+03	.488620E+03	.305599E+04	.280270E+04			
	.114357E+03	.111767E+03	.398451E+06	.431446E+06	.103424E+03	.433518E+06			
T .762740E+03	.794276E+03	.817261E+03	.824318E+03	.844690E+03	.850425E+03	.839324E+03	.831025E+03	.837903E+03	.844690E+03
F .108249E+06	.107643E+06	.107139E+06	.107062E+06	.106669E+06	.106558E+06	.106772E+06	.106932E+06	.106799E+06	.106668E+06
E .437018E+06	.442566E+06	.448096E+06	.453621E+06	.464640E+06	.475649E+06	.495865E+06	.514264E+06	.523455E+06	.532637E+06
C200.052	.949300E+02	.200200E+03	.577019E+03	.486520E+03	.343361E+04	.315556E+04			
	.115925E+03	.113136E+03	.397693E+06	.431577E+06	.103814E+03	.435165E+06			
T .806964E+03	.844628E+03	.861407E+03	.868613E+03	.882430E+03	.886544E+03	.869866E+03	.861206E+03	.864130E+03	.871978E+03
F .121452E+06	.120707E+06	.120376E+06	.120234E+06	.119963E+06	.119883E+06	.120209E+06	.120380E+06	.120322E+06	.120167E+06
E .437840E+06	.444074E+06	.450296E+06	.456512E+06	.468924E+06	.481330E+06	.504119E+06	.524859E+06	.535225E+06	.545581E+06
C200.053	.949300E+02	.200200E+03	.577019E+03	.486520E+03	.379086E+04	.350122E+04			
	.117510E+03	.114530E+03	.397693E+06	.432444E+06	.104204E+03	.436811E+06			
T .847091E+03	.887681E+03	.905702E+03	.910768E+03	.910650E+03	.929099E+03	.901247E+03	.888552E+03	.888552E+03	.895280E+03
F .134407E+06	.133588E+06	.133228E+06	.133128E+06	.132756E+06	.132767E+06	.133117E+06	.133571E+06	.133571E+06	.133436E+06
E .439387E+06	.446299E+06	.453199E+06	.460094E+06	.473857E+06	.487621E+06	.512931E+06	.535970E+06	.547490E+06	.559001E+06
C200.054	.951100E+02	.200200E+03	.576911E+03	.489320E+03	.416914E+04	.386516E+04			
	.119229E+03	.116054E+03	.398451E+06	.434110E+06	.104622E+03	.438576E+06			
T .889302E+03	.938893E+03	.960899E+03	.960899E+03	.970830E+03	.963742E+03	.929602E+03	.917377E+03	.917377E+03	.932816E+03
F .147987E+06	.146976E+06	.146537E+06	.146537E+06	.146342E+06	.146401E+06	.147163E+06	.147412E+06	.147412E+06	.147098E+06
E .441768E+06	.449390E+06	.456997E+06	.464604E+06	.479805E+06	.495016E+06	.522988E+06	.548647E+06	.561177E+06	.573888E+06
C200.055	.947500E+02	.200200E+03	.551966E+03	.487910E+03	.450682E+04	.418815E+04			
	.120583E+03	.117203E+03	.396935E+06	.432286E+06	.104948E+03	.439953E+06			
T .920952E+03	.964257E+03	.977843E+03	.985192E+03	.995084E+03	.994453E+03	.960672E+03	.949178E+03	.944282E+03	.953233E+03
F .160070E+06	.159177E+06	.158903E+06	.158756E+06	.158560E+06	.158573E+06	.159246E+06	.159486E+06	.159587E+06	.159402E+06
E .440581E+06	.448846E+06	.457101E+06	.465352E+06	.481840E+06	.498329E+06	.528641E+06	.556224E+06	.570022E+06	.583809E+06
C200.056	.951100E+02	.200200E+03	.552045E+03	.489820E+03	.488845E+04	.455489E+04			
	.122312E+03	.118791E+03	.398451E+06	.434721E+06	.105139E+03	.441691E+06			
T .958495E+03	.998647E+03	.102552E+04	.102709E+04	.103552E+04	.102122E+04	.985160E+03	.965040E+03	.970601E+03	.983197E+03
F .173723E+06	.172891E+06	.172351E+06	.172320E+06	.172135E+06	.172436E+06	.173168E+06	.173170E+06	.173470E+06	.173208E+06
E .443739E+06	.452729E+06	.461703E+06	.470674E+06	.488612E+06	.506568E+06	.539564E+06	.569563E+06	.584579E+06	.599580E+06
C200.057	.947500E+02	.200200E+03	.567233E+03	.480220E+03	.267865E+04	.242774E+04			
	.112441E+03	.110074E+03	.396935E+06	.428547E+06	.102942E+03	.431480E+06			
T .712181E+03	.744125E+03	.760101E+03	.769247E+03	.793094E+03	.798320E+03	.794456E+03	.765247E+03	.796478E+03	.806968E+03
F .940999E+05	.935100E+05	.932112E+05	.931148E+05	.929505E+05	.924819E+05	.925648E+05	.927385E+05	.925267E+05	.923286E+05
E .433381E+06	.438190E+06	.442988E+06	.447782E+06	.457325E+06	.466861E+06	.484354E+06	.500281E+06	.508230E+06	.516165E+06
C200.058	.949300E+02	.200200E+03	.567391E+03	.474610E+03	.227306E+04	.200739E+04			
	.110467E+03	.108359E+03	.397693E+06	.428271E+06	.102437E+03	.429351E+06			
T .651430E+03	.685084E+03	.704172E+03	.714332E+03	.737953E+03	.749364E+03	.732987E+03	.747892E+03	.755179E+03	.756620E+03
F .786089E+05	.780250E+05	.776824E+05	.775037E+05	.770741E+05	.768681E+05	.768019E+05	.766950E+05	.767619E+05	.767348E+05
E .432300E+06	.436304E+06	.440294E+06	.444275E+06	.452202E+06	.460112E+06	.474602E+06	.487787E+06	.494371E+06	.500952E+06
C200.401	.607800E+02	.200200E+03	.190453E+04	.641740E+03	.447774E+04	.416775E+04			
	.103793E+03	.102749E+03	.254356E+06	.349991E+06	.100675E+03	.421913E+06			
T .462972E+03	.487821E+03	.518191E+03	.563040E+03	.735398E+03	.833603E+03	.954687E+03	.998810E+03	.983693E+03	.982141E+03
F .167078E+06	.166827E+06	.166474E+06	.165863E+06	.162789E+06	.160743E+06	.158196E+06	.157315E+06	.157613E+06	.157643E+06
E .358498E+06	.366999E+06	.375490E+06	.383964E+06	.400705E+06	.417303E+06	.447407E+06	.474676E+06	.488327E+06	.501980E+06
C200.402	.606000E+02	.200200E+03	.193110E+04	.602930E+03	.478103E+04	.445673E+04			
	.104896E+03	.104747E+03	.253602E+06	.351104E+06	.100973E+03	.423170E+06			
T .518032E+03	.555580E+03	.601606E+03	.670021E+03	.820177E+03	.922569E+03	.994002E+03	.106603E+04	.101841E+04	.100839E+04
F .177309E+06	.176807E+06	.176067E+06	.174691E+06	.171615E+06	.169405E+06	.168115E+06	.166723E+06	.167628E+06	.167826E+06
E .360148E+06	.369179E+06	.378187E+06	.387157E+06	.404888E+06	.422467E+06	.454516E+06	.483508E+06	.498050E+06	.512603E+06
C200.101	.898900E+02	.200200E+03	.612687E+03	.440120E+03	.299997E+04	.275375E+04			
	.110754E+03	.109517E+03	.376477E+06	.411837E+06	.102511E+03	.429662E+06			
T .726552E+03	.769121E+03	.789934E+03	.796321E+03	.825612E+03	.840177E+03	.850448E+03	.844712E+03	.834251E+03	.828475E+03
F .106995E+06	.106187E+06	.105787E+06	.105664E+06	.105099E+06	.104819E+06	.104622E+06	.104732E+06	.104933E+06	.105044E+06
E .417336E+06	.422804E+06	.428255E+06	.433702E+06	.444550E+06	.455375E+06	.475193E+06	.493224E+06	.502253E+06	.511289E+06

C200.102

	.898900E+02	.200200E+03	.587716E+03	.445060E+03	.338849E+04	.3181998+06			
	.113036E+03	.111302E+03	.376477E+06	.410903E+06	.103092E+03	.432114E+06			
T .770726E+03	.804611E+03	.835113E+03	.842564E+03	.877102E+03	.884701E+03	.8[illegible]2E+03	.877102E+03	.865019E+03	.861395E+03
P .123201E+06	.122493E+06	.121927E+06	.1217798+06	.121098E+06	.120949E+06	.12[illegible]E+06	.121098E+06	.121339E+06	.121407E+06
E .417247E+06	.423563E+06	.429858E+06	.436147E+06	.448674E+06	.461189E+06	.484130E+06	.505007E+06	.515461E+06	.525919E+06

C200.103

	.899300E+02	.200200E+03	.587702E+03	.442240E+03	.378960E+04	.3555168+04			
	.114399E+03	.112690E+03	.374963E+06	.410328E+06	.103485E+03	.433773E+06			
T .816968E+03	.856960E+03	.876934E+03	.890761E+03	.926642E+03	.936052E+03	.924399E+03	.915830E+03	.901393E+03	.896137E+03
P .137204E+06	.136391E+06	.135986E+06	.1357078+06	.134991E+06	.134806E+06	.135015E+06	.135205E+06	.135494E+06	.135598E+06
E .417406E+06	.424455E+06	.431488E+06	.438511E+06	.452505E+06	.466485E+06	.492147E+06	.515496E+06	.527188E+06	.538886E+06

C200.104

	.897100E+02	.200200E+03	.587681E+03	.439410E+03	.417124E+04	.3891868+04			
	.117195E+03	.114121E+03	.375720E+06	.411931E+06	.104127E+03	.436486E+06			
T .863846E+03	.901565E+03	.921079E+03	.942605E+03	.963630E+03	.973401E+03	.960997E+03	.951856E+03	.926496E+03	.921570E+03
P .149643E+06	.148872E+06	.148472E+06	.1480338+06	.147616E+06	.147424E+06	.147666E+06	.147850E+06	.148361E+06	.148461E+06
E .419666E+06	.427374E+06	.435066E+06	.442747E+06	.458075E+06	.473190E+06	.501498E+06	.527072E+06	.539888E+06	.552711E+06

C200.105

	.897100E+02	.200200E+03	.647532E+03	.428820E+03	.218911E+04	.2008398+04			
	.107769E+03	.106158E+03	.375720E+06	.409822E+06	.101736E+03	.426390E+06			
T .556970E+03	.584431E+03	.606474E+03	.619408E+03	.657537E+03	.680600E+03	.707436E+03	.721309E+03	.724972E+03	.724972E+03
P .792847E+05	.788722E+05	.785249E+05	.7831538+05	.776751E+05	.772745E+05	.767985E+05	.765491E+05	.764830E+05	.764825E+05
E .413871E+06	.417904E+06	.421922E+06	.425931E+06	.433895E+06	.441825E+06	.456288E+06	.469401E+06	.475952E+06	.482504E+06

C200.201

	.792100E+02	.200200E+03	.967532E+03	.468290E+03	.391516E+04	.3682598+04			
	.120417E+03	.109192E+03	.331600E+06	.384153E+06	.104908E+03	.439764E+06			
T .552316E+03	.659679E+03	.719756E+03	.747576E+03	.832478E+03	.896949E+03	.936856E+03	.942072E+03	.922900E+03	.912347E+03
P .146446E+06	.144694E+06	.143563E+06	.1430158+06	.141290E+06	.139972E+06	.139172E+06	.139069E+06	.139449E+06	.139681E+06
E .391672E+06	.399091E+06	.406468E+06	.413825E+06	.428413E+06	.442905E+06	.469367E+06	.493411E+06	.505456E+06	.517513E+06

C200.202

	.797600E+02	.200200E+03	.907518E+03	.468990E+03	.429941E+04	.4059968+04			
	.113163E+03	.110964E+03	.333909E+06	.384756E+06	.103125E+03	.432251E+06			
T .622246E+03	.730698E+03	.777313E+03	.806548E+03	.890546E+03	.943924E+03	.960935E+03	.968454E+03	.945817E+03	.934873E+03
P .160188E+06	.158179E+06	.157230E+06	.1566218+06	.154854E+06	.153750E+06	.153406E+06	.153255E+06	.153712E+06	.153933E+06
E .392958E+06	.401090E+06	.409189E+06	.417265E+06	.433293E+06	.449244E+06	.478444E+06	.504973E+06	.518263E+06	.531566E+06

C200.203

	.801200E+02	.200200E+03	.937545E+03	.467590E+03	.458331E+04	.4319338+04			
	.114385E+03	.112193E+03	.335420E+06	.388279E+06	.103431E+03	.433547E+06			
T .679402E+03	.776844E+03	.822577E+03	.850675E+03	.943429E+03	.985142E+03	.991158E+03	.995034E+03	.963455E+03	.960711E+03
P .169864E+06	.167903E+06	.166893E+06	.1661158+06	.164355E+06	.163499E+06	.163378E+06	.163300E+06	.163940E+06	.163996E+06
E .396994E+06	.405642E+06	.414256E+06	.422842E+06	.439893E+06	.456887E+06	.488029E+06	.516331E+06	.530517E+06	.544706E+06

C200.204

	.801200E+02	.200200E+03	.937545E+03	.467590E+03	.341202E+04	.3204048+04			
	.108591E+03	.107489E+03	.335420E+06	.385457E+06	.101951E+03	.427299E+06			
T .466338E+03	.553605E+03	.621656E+03	.671151E+03	.752413E+03	.809364E+03	.864168E+03	.874539E+03	.871967E+03	.867061E+03
P .128103E+06	.127023E+06	.125960E+06	.1250958+06	.123560E+06	.122438E+06	.121352E+06	.121146E+06	.121199E+06	.121295E+06
E .391980E+06	.398467E+06	.404916E+06	.411332E+06	.424048E+06	.436677E+06	.459677E+06	.480561E+06	.491006E+06	.501457E+06

C200.205

	.797600E+02	.200200E+03	.967643E+03	.461260E+03	.309488E+04	.2905368+04			
	.107147E+03	.105971E+03	.333909E+06	.384524E+06	.101572E+03	.425699E+06			
T .409372E+03	.467457E+03	.526226E+03	.595112E+03	.681375E+03	.748938E+03	.818267E+03	.835996E+03	.832842E+03	.829089E+03
P .116425E+06	.115911E+06	.115212E+06	.1142048+06	.112696E+06	.111666E+06	.110124E+06	.109780E+06	.109841E+06	.109914E+06
E .390441E+06	.396343E+06	.402221E+06	.408062E+06	.419628E+06	.431098E+06	.451930E+06	.470823E+06	.480274E+06	.489729E+06

C200.301

	.704800E+02	.200200E+03	.137865E+04	.539980E+03	.409283E+04	.3863888+04			
	.107956E+03	.106375E+03	.294984E+06	.366349E+06	.101785E+03	.426597E+06			
T .474224E+03	.510994E+03	.579834E+03	.642330E+03	.755387E+03	.834832E+03	.944632E+03	.971613E+03	.955995E+03	.949327E+03
P .154183E+06	.153770E+06	.152815E+06	.1517788+06	.149615E+06	.147985E+06	.145733E+06	.145198E+06	.145505E+06	.145637E+06
E .374202E+06	.382044E+06	.389855E+06	.397632E+06	.413031E+06	.428311E+06	.458031E+06	.486168E+06	.499755E+06	.506349E+06

C200.302

	.695700E+02	.200200E+03	.135746E+04	.562020E+03	.442411E+04	.4184368+04			
	.109155E+03	.107439E+03	.291171E+06	.362214E+06	.102098E+03	.427919E+06			
T .503408E+03	.539198E+03	.613013E+03	.682515E+03	.795656E+03	.884265E+03	.971478E+03	.100761E+04	.982141E+03	.971478E+03
P .166652E+06	.164201E+06	.163076E+06	.1636288+06	.161545E+06	.159667E+06	.157858E+06	.157144E+06	.157644E+06	.157857E+06
E .370711E+06	.379195E+06	.387644E+06	.396051E+06	.412704E+06	.429226E+06	.459288E+06	.486539E+06	.500192E+06	.513856E+06

C200.303

	.699300E+02	.200200E+03	.165009E+04	.522020E+03	.345103E+04	.3263078+04			
	.103819E+03	.102554E+03	.292679E+06	.374645E+06	.100682E+03	.421944E+06			
T .444203E+03	.478239E+03	.546113E+03	.600224E+03	.691493E+03	.764323E+03	.856616E+03	.889583E+03	.882395E+03	.878260E+03
P .130398E+06	.130063E+06	.129216E+06	.1283998+06	.126806E+06	.125409E+06	.123576E+06	.122935E+06	.123067E+06	.123148E+06
E .381280E+06	.387905E+06	.394502E+06	.401071E+06	.414089E+06	.427001E+06	.450416E+06	.471620E+06	.482231E+06	.492847E+06

C200.304

	.701200E+02	.200200E+03	.162047E+04	.516480E+03	.375897E+04	.3553988+04			
	.106036E+03	.104899E+03	.293476E+06	.374860E+06	.101278E+03	.424456E+06			
T .492829E+03	.535032E+03	.615258E+03	.670970E+03	.754666E+03	.830689E+03	.898472E+03	.918194E+03	.915011E+03	.907773E+03
P .141695E+06	.141169E+06	.139952E+06	.1389758+06	.137370E+06	.135836E+06	.134465E+06	.134072E+06	.134135E+06	.134279E+06
E .382082E+06	.389287E+06	.396450E+06	.403578E+06	.417716E+06	.431740E+06	.457264E+06	.480419E+06	.492001E+06	.503592E+06

C200.305

	.697500E+02	.200200E+03	.164099E+04	.508150E+03	.415025E+04	.3912498+04			
	.107648E+03	.106282E+03	.291925E+06	.379140E+06	.101706E+03	.426255E+06			
T .555884E+03	.611891E+03	.698868E+03	.749240E+03	.832693E+03	.898220E+03	.954549E+03	.975303E+03	.953358E+03	.943987E+03
P .155457E+06	.154586E+06	.153016E+06	.1520238+06	.150304E+06	.148941E+06	.147796E+06	.147387E+06	.147820E+06	.148007E+06
E .383080E+06	.390992E+06	.398849E+06	.406670E+06	.422189E+06	.437610E+06	.465734E+06	.491259E+06	.504040E+06	.516836E+06

C200.306

	.695700E+02	.200200E+03	.164141E+04	.500490E+03	.449550E+04	.4233088+04			
	.108360E+03	.107655E+03	.291171E+06	.375213E+06	.101891E+03	.427043E+06			
T .609914E+03	.679449E+03	.754100E+03	.799533E+03	.886071E+03	.953220E+03	.985300E+03	.100848E+04	.974797E+03	.970682E+03
P .167504E+06	.166381E+06	.164779E+06	.1638318+06	.161988E+06	.160581E+06	.159913E+06	.159473E+06	.160142E+06	.160224E+06
E .383785E+06	.392316E+06	.400795E+06	.409241E+06	.426005E+06	.442671E+06	.473148E+06	.500804E+06	.514668E+06	.528537E+06

C250.051

	.956500E+02	.250090E+03	.629008E+03	.535830E+03	.454026E+04	.4290028+04			
	.124025E+03	.120446E+03	.400726E+06	.431958E+06	.105762E+03	.443394E+06			
T .896679E+03	.935742E+03	.954386E+03	.960834E+03	.970717E+03	.960724E+03	.928763E+03	.901396E+03	.883481E+03	.876611E+03
P .164138E+06	.163314E+06	.162927E+06	.1627948+06	.162591E+06	.162796E+06	.161461E+06	.164039E+06	.164431E+06	.164568E+06
E .438759E+06	.445538E+06	.452307E+06	.459072E+06	.472592E+06	.486122E+06	.510994E+06	.533657E+06	.545006E+06	.556362E+06

C250.052

	.960100E+02	.250090E+03	.622352E+03	.531690E+03	.489237E+04	.4629758+04			
	.123947E+03	.122214E+03	.402243E+06	.433914E+06	.106209E+03	.445282E+06			
T .941665E+03	.981150E+03	.993154E+03	.994906E+03	.997260E+03	.989540E+03	.952050E+03	.917721E+03	.900106E+03	.901247E+03
P .176542E+06	.175690E+06	.175457E+06	.1754218+06	.175373E+06	.175532E+06	.176321E+06	.177061E+06	.177444E+06	.177419E+06
E .441244E+06	.448552E+06	.455854E+06	.463156E+06	.477756E+06	.492364E+06	.519221E+06	.543701E+06	.555958E+06	.568214E+06

C250.053

	.958300E+02	.250090E+03	.623332E+03	.518560E+03	.399713E+04	.3761648+04			
	.121262E+03	.118084E+03	.401485E+06	.431460E+06	.105110E+03	.440627E+06			
T .844755E+03	.896912E+03	.906563E+03	.906563E+03	.915735E+03	.912310E+03	.893067E+03	.866804E+03	.855870E+03	.850362E+03
P .144389E+06	.143117E+06	.143121E+06	.1431218+06	.142935E+06	.143004E+06	.143396E+06	.143935E+06	.144160E+06	.144274E+06
E .437429E+06	.443368E+06	.449302E+06	.455235E+06	.467091E+06	.478950E+06	.500735E+06	.520590E+06	.530529E+06	.540474E+06

C250.054

	.958300E+02	.250090E+03	.625428E+03	.517170E+03	.359180E+04	.3376278+04			
	.119049E+03	.116273E+03	.401485E+06	.430761E+06	.104579E+03	.438393E+06			
T .798704E+03	.844431E+03	.861311E+03	.867899E+03	.879152E+03	.874456E+03	.860740E+03	.832617E+03	.823646E+03	.820672E+03
P .130007E+06	.129088E+06	.128750E+06	.1286188+06	.128394E+06	.128487E+06	.128762E+06	.129326E+06	.129507E+06	.129566E+06
E .436126E+06	.441463E+06	.446790E+06	.452113E+06	.462746E+06	.473385E+06	.492918E+06	.510733E+06	.519649E+06	.528569E+06

C250.055

	.951100E+02	.250090E+03	.625825E+03	.510930E+03	.313204E+04	.2935788+04			
	.116599E+03	.113770E+03	.398451E+06	.426858E+06	.103988E+03	.435867E+06			
T .716008E+03	.780301E+03	.800704E+03	.809484E+03	.825552E+03	.834172E+03	.823850E+03	.806731E+03	.798912E+03	.792605E+03
P .113695E+06	.112863E+06	.112445E+06	.1123758+06	.111961E+06	.111793E+06	.111994E+06	.112328E+06	.112481E+06	.112603E+06
E .431538E+06	.436192E+06	.440832E+06	.445468E+06	.454718E+06	.463959E+06	.480932E+06	.496379E+06	.504115E+06	.511857E+06

C250.056	.956500E+02	.250090E+03	.626148E+03	.505360E+03	.258693E+04	.240981E+04			
	.115765E+03	.111518E+03	.400726E+06	.428091E+06	.103770E+03	.434977E+06			
T	.656009E+03	.694693E+03	.722743E+03	.730572E+03	.746679E+03	.756429E+03	.758200E+03	.747700E+03	.742815E+03	.724746E+03
F	.941993E+03	.935109E+03	.929991E+03	.928547E+05	.925556E+05	.923736E+05	.923404E+05	.925366E+05	.926275E+05	.929614E+05
E	.431956E+06	.435799E+06	.439635E+06	.443448E+06	.451069E+06	.458680E+06	.472629E+06	.485332E+06	.491688E+06	.498063E+06
C250.101	.898900E+02	.250090E+03	.684408E+03	.531000E+03	.373230E+04	.351136E+04				
	.115793E+03	.113579E+03	.376477E+06	.408132E+06	.103782E+03	.435027E+06				
T	.781096E+03	.809905E+03	.838682E+03	.846011E+03	.875147E+03	.890785E+03	.885839E+03	.872183E+03	.856494E+03	.848784E+03
F	.135744E+06	.135163E+06	.134579E+06	.134430E+06	.133841E+06	.133526E+06	.133626E+06	.133900E+06	.134218E+06	.134374E+06
E	.413730E+06	.419310E+06	.424873E+06	.430431E+06	.441513E+06	.452576E+06	.472870E+06	.491346E+06	.500599E+06	.509861E+06
C250.102	.895300E+02	.250090E+03	.684785E+03	.526170E+03	.414527E+04	.390708E+04				
	.117686E+03	.115270E+03	.374963E+06	.407419E+06	.104247E+03	.436993E+06				
T	.803121E+03	.844189E+03	.886862E+03	.874690E+03	.912018E+03	.921079E+03	.910596E+03	.896989E+03	.877964E+03	.874970E+03
F	.150918E+06	.150064E+06	.149716E+06	.149428E+06	.148657E+06	.148472E+06	.148606E+06	.148966E+06	.149360E+06	.149422E+06
E	.413648E+06	.419852E+06	.426047E+06	.432233E+06	.444561E+06	.456879E+06	.479485E+06	.500061E+06	.510368E+06	.520678E+06
C250.103	.895300E+02	.250090E+03	.685041E+03	.522710E+03	.456967E+04	.432082E+04				
	.119786E+03	.117225E+03	.374963E+06	.408256E+06	.104756E+03	.439144E+06				
T	.855617E+03	.896806E+03	.910415E+03	.915502E+03	.954624E+03	.963455E+03	.949177E+03	.926750E+03	.901463E+03	.896806E+03
F	.166223E+06	.165341E+06	.165051E+06	.164943E+06	.164123E+06	.163940E+06	.164236E+06	.164663E+06	.165242E+06	.165341E+06
E	.415132E+06	.421984E+06	.428827E+06	.435668E+06	.449305E+06	.462932E+06	.487945E+06	.510722E+06	.522136E+06	.533556E+06
C250.104	.897100E+02	.250090E+03	.685090E+03	.522020E+03	.508481E+04	.478647E+04				
	.108188E+03	.119500E+03	.375720E+06	.409948E+06	.101844E+03	.426654E+06				
T	.910211E+03	.951982E+03	.960624E+03	.968145E+03	.100382E+04	.100825E+04	.987772E+03	.971419E+03	.943150E+03	.929210E+03
F	.183466E+06	.182554E+06	.182367E+06	.182206E+06	.181454E+06	.181362E+06	.181789E+06	.182136E+06	.182746E+06	.183050E+06
E	.417555E+06	.425138E+06	.432717E+06	.440291E+06	.455403E+06	.470509E+06	.498244E+06	.523486E+06	.536133E+06	.548794E+06
C250.105	.897100E+02	.250090E+03	.686371E+03	.501190E+03	.330262E+04	.309175E+04				
	.113475E+03	.111429E+03	.375720E+06	.406595E+06	.103203E+03	.432584E+06				
T	.723756E+03	.754687E+03	.762506E+03	.772939E+03	.805609E+03	.823149E+03	.838877E+03	.833070E+03	.819154E+03	.812186E+03
F	.119987E+06	.119389E+06	.119242E+06	.119036E+06	.118196E+06	.118051E+06	.117741E+06	.117855E+06	.118130E+06	.118267E+06
E	.421931E+06	.416449E+06	.421363E+06	.426270E+06	.436045E+06	.445798E+06	.463643E+06	.479878E+06	.488009E+06	.496144E+06
C250.106	.900700E+02	.250090E+03	.721224E+03	.503970E+03	.285432E+04	.267802E+04				
	.111359E+03	.109563E+03	.377234E+06	.408510E+06	.102666E+03	.430317E+06				
T	.658847E+03	.678232E+03	.689776E+03	.697625E+03	.731385E+03	.756163E+03	.775184E+03	.772902E+03	.770289E+03	.767276E+03
F	.104382E+06	.104038E+06	.103830E+06	.103687E+06	.103061E+06	.102594E+06	.102232E+06	.102275E+06	.102325E+06	.102382E+06
E	.412793E+06	.417066E+06	.421332E+06	.425594E+06	.434077E+06	.442530E+06	.457904E+06	.472038E+06	.479067E+06	.486100E+06
C250.201	.817500E+02	.250090E+03	.963588E+03	.540640E+03	.481574E+04	.456545E+04				
	.116037E+03	.113947E+03	.342264E+06	.385938E+06	.103842E+03	.435282E+06				
T	.650103E+03	.735207E+03	.789092E+03	.816645E+03	.888099E+03	.936776E+03	.987674E+03	.989578E+03	.951589E+03	.935627E+03
F	.178951E+06	.177293E+06	.176161E+06	.175612E+06	.174013E+06	.172538E+06	.171894E+06	.171855E+06	.172647E+06	.172966E+06
E	.393280E+06	.400578E+06	.407845E+06	.415097E+06	.429513E+06	.443851E+06	.470075E+06	.493912E+06	.505865E+06	.517833E+06
C250.202	.804800E+02	.250090E+03	.944182E+03	.533760E+03	.431261E+04	.406909E+04				
	.113655E+03	.110890E+03	.336931E+06	.378945E+06	.103240E+03	.432775E+06				
T	.566894E+03	.619319E+03	.670224E+03	.715623E+03	.793688E+03	.868216E+03	.929527E+03	.943924E+03	.922738E+03	.907549E+03
F	.161093E+06	.160256E+06	.159349E+06	.158479E+06	.156890E+06	.155323E+06	.154065E+06	.153750E+06	.154185E+06	.154499E+06
E	.385534E+06	.392102E+06	.398645E+06	.405163E+06	.418109E+06	.430966E+06	.454404E+06	.475687E+06	.486344E+06	.497023E+06
C250.203	.817500E+02	.250090E+03	.954352E+03	.531690E+03	.390255E+04	.369768E+04				
	.111727E+03	.109771E+03	.342264E+06	.383895E+06	.102760E+03	.430713E+06				
T	.512838E+03	.579928E+03	.614847E+03	.674594E+03	.758234E+03	.822875E+03	.889390E+03	.901665E+03	.888479E+03	.882201E+03
F	.146973E+06	.146037E+06	.145135E+06	.144421E+06	.142802E+06	.141487E+06	.140125E+06	.139876E+06	.140144E+06	.140271E+06
E	.389895E+06	.395871E+06	.401822E+06	.407753E+06	.419520E+06	.431209E+06	.452493E+06	.471818E+06	.481491E+06	.491175E+06
C250.204	.804800E+02	.250090E+03	.954239E+03	.533070E+03	.364105E+04	.345590E+04				
	.108681E+03	.107725E+03	.336931E+06	.378042E+06	.102027E+03	.427617E+06				
T	.470771E+03	.514927E+03	.553469E+03	.591947E+03	.691138E+03	.742340E+03	.830514E+03	.874432E+03	.871859E+03	.864010E+03
F	.137588E+06	.137083E+06	.136564E+06	.135983E+06	.134253E+06	.132880E+06	.131109E+06	.130628E+06	.130679E+06	.130837E+06
E	.383671E+06	.389268E+06	.394851E+06	.400418E+06	.411452E+06	.422403E+06	.442284E+06	.460310E+06	.469325E+06	.478349E+06
C250.205	.812100E+02	.250090E+03	.954888E+03	.524790E+03	.313204E+04	.296974E+04				
	.106455E+03	.105436E+03	.339996E+06	.380159E+06	.101389E+03	.424925E+06				
T	.389903E+03	.421348E+03	.451749E+03	.478426E+03	.584989E+03	.657395E+03	.770159E+03	.807963E+03	.807963E+03	.805680E+03
F	.118535E+06	.118319E+06	.118054E+06	.117779E+06	.116350E+06	.115141E+06	.113039E+06	.112304E+06	.112304E+06	.112348E+06
E	.384978E+06	.389794E+06	.394603E+06	.399406E+06	.408930E+06	.418380E+06	.435465E+06	.450919E+06	.458646E+06	.466375E+06
C250.201	.806500E+02	.250090E+03	.957949E+03	.547500E+03	.431819E+04	.400882E+04				
	.112947E+03	.110806E+03	.338485E+06	.380873E+06	.103070E+03	.432021E+06				
T	.587919E+03	.647743E+03	.695949E+03	.736977E+03	.809680E+03	.881630E+03	.932763E+03	.932766E+03	.921602E+03	.917327E+03
F	.158444E+06	.157434E+06	.156538E+06	.155731E+06	.154238E+06	.152730E+06	.151877E+06	.151672E+06	.151901E+06	.151988E+06
E	.387359E+06	.393818E+06	.400251E+06	.406662E+06	.419398E+06	.432047E+06	.455150E+06	.476134E+06	.486636E+06	.497143E+06
C250.202	.806600E+02	.250090E+03	.948080E+03	.546130E+03	.475107E+06	.442259E+04				
	.114831E+03	.112734E+03	.337667E+06	.380584E+06	.103543E+03	.434018E+06				
T	.651040E+03	.713940E+03	.759891E+03	.799448E+03	.871780E+03	.932586E+03	.971277E+03	.982360E+03	.960192E+03	.970606E+03
F	.174024E+06	.172820E+06	.171881E+06	.171045E+06	.169487E+06	.168183E+06	.167372E+06	.167147E+06	.167604E+06	.167387E+06
E	.387700E+06	.394808E+06	.401890E+06	.408949E+06	.422980E+06	.436941E+06	.462457E+06	.485633E+06	.497241E+06	.508840E+06
C250.203	.806600E+02	.250090E+03	.938145E+03	.545450E+03	.521558E+04	.485912E+04				
	.117079E+03	.114835E+03	.337687E+06	.381083E+06	.104099E+03	.436365E+06				
T	.721525E+03	.780196E+03	.823373E+03	.853504E+03	.941570E+03	.997168E+03	.101051E+04	.103168E+04	.987114E+03	.987605E+03
F	.190118E+06	.188878E+06	.187932E+06	.187263E+06	.185309E+06	.184114E+06	.183036E+06	.183402E+06	.184327E+06	.184316E+06
E	.388905E+06	.396694E+06	.404457E+06	.412203E+06	.427591E+06	.442919E+06	.470996E+06	.496485E+06	.509267E+06	.522049E+06
C250.204	.808500E+02	.250090E+03	.958210E+03	.544760E+03	.555465E+04	.511575E+04				
	.118476E+03	.116159E+03	.338485E+06	.381116E+06	.104440E+03	.437806E+06				
T	.772087E+03	.833170E+03	.873880E+03	.910070E+03	.987437E+03	.104156E+04	.104539E+04	.106092E+04	.100018E+04	.100722E+04
F	.199368E+06	.198010E+06	.197092E+06	.196266E+06	.194545E+06	.193399E+06	.193321E+06	.193007E+06	.194269E+06	.194118E+06
E	.391336E+06	.399519E+06	.407679E+06	.415817E+06	.432006E+06	.448140E+06	.477714E+06	.504575E+06	.518055E+06	.531529E+06
C250.205	.803000E+02	.250090E+03	.958273E+03	.544080E+03	.391914E+04	.358443E+04				
	.109479E+03	.108299E+03	.336176E+06	.377724E+06	.102182E+03	.426273E+06				
T	.521230E+03	.566305E+03	.623507E+03	.675703E+03	.754653E+03	.816948E+03	.881820E+03	.907140E+03	.907140E+03	.910744E+03
F	.142446E+06	.141821E+06	.140909E+06	.139982E+06	.138463E+06	.137206E+06	.135887E+06	.135378E+06	.135378E+06	.135300E+06
E	.383541E+06	.389342E+06	.395117E+06	.400866E+06	.412274E+06	.423606E+06	.444240E+06	.462948E+06	.472302E+06	.481652E+06
C250.206	.806600E+02	.250090E+03	.958926E+03	.541330E+03	.369991E+04	.342606E+04				
	.108803E+03	.107678E+03	.337687E+06	.378917E+06	.102007E+03	.427531E+06				
T	.479054E+03	.532327E+03	.577387E+03	.631381E+03	.709018E+03	.777624E+03	.848834E+03	.879140E+03	.883875E+03	.893226E+03
F	.136428E+06	.135915E+06	.135135E+06	.134225E+06	.132846E+06	.131505E+06	.130074E+06	.129466E+06	.129372E+06	.129186E+06
E	.384460E+06	.390031E+06	.395560E+06	.401064E+06	.411989E+06	.422833E+06	.442556E+06	.460425E+06	.469355E+06	.478276E+06
C250.207	.804800E+02	.250090E+03	.958771E+03	.538580E+03	.332834E+04	.304072E+04				
	.106400E+03	.105245E+03	.336931E+06	.377384E+06	.101374E+03	.424864E+06				
T	.423108E+03	.455153E+03	.498606E+03	.550893E+03	.629765E+03	.698591E+03	.777812E+03	.829281E+03	.840063E+03	.859624E+03
F	.121321E+06	.121054E+06	.120587E+06	.119880E+06	.118642E+06	.117416E+06	.115903E+06	.114895E+06	.114684E+06	.114301E+06
E	.382322E+06	.387254E+06	.392174E+06	.397074E+06	.406802E+06	.416454E+06	.433977E+06	.449801E+06	.457702E+06	.465584E+06
C250.208	.803000E+02	.250090E+03	.989182E+03	.533760E+03	.302190E+04	.280275E+04				
	.104037E+03	.103040E+03	.336176E+06	.377217E+06	.100741E+03	.422192E+06				
T	.371472E+03	.389105E+03	.426051E+03	.467533E+03	.532667E+03	.612514E+03	.707048E+03	.770933E+03	.787482E+03	.798163E+03
F	.111764E+06	.111667E+06	.111401E+06	.111010E+06	.110221E+06	.109019E+06	.107359E+06	.106152E+06	.105831E+06	.105628E+06
E	.381758E+06	.386298E+06	.390833E+06	.395358E+06	.404363E+06	.413296E+06	.429482E+06	.444067E+06	.451342E+06	.458607E+06

C250.301 .706600E+02 .250090E+03 .137867E+04 .584850E+03 .467774E+04 .438378E+04
.107814E+03 .106474E+03 .295739E+06 .353872E+06 .101740E+03 .426439E+06
T .451803E+03 .482209E+03 .589746E+03 .541049E+03 .678244E+03 .797814E+03 .912144E+03 .998736E+03 .983617E+03 .975097E+03
F .174359E+06 .174072E+06 .173765E+06 .173364E+06 .171092E+06 .168662E+06 .166212E+06 .164418E+06 .164722E+06 .164895E+06
E .360975E+06 .368075E+06 .375168E+06 .382253E+06 .396307E+06 .410227E+06 .435499E+06 .458314E+06 .469735E+06 .481163E+06

C250.302 .706600E+02 .250090E+03 .137393E+04 .582830E+03 .504926E+04 .472037E+04
.109810E+03 .108320E+03 .295739E+06 .354305E+06 .102268E+03 .426635E+06
T .489283E+03 .523310E+03 .555438E+03 .594138E+03 .750018E+03 .856450E+03 .971259E+03 .105831E+04 .100496E+04 .994880E+03
F .187562E+06 .187166E+06 .186734E+06 .186146E+06 .183204E+06 .180898E+06 .178398E+06 .176636E+06 .177696E+06 .177903E+06
E .362036E+06 .369680E+06 .377315E+06 .384936E+06 .400028E+06 .414994E+06 .442191E+06 .466771E+06 .479103E+06 .491444E+06

C250.303 .706600E+02 .250090E+03 .142537E+04 .571150E+03 .392575E+04 .369468E+04
.102538E+03 .101272E+03 .295739E+06 .354140E+06 .100333E+03 .420471E+06
T .388521E+03 .412568E+03 .430098E+03 .449451E+03 .541471E+03 .647151E+03 .789332E+03 .876897E+03 .898423E+03 .903179E+03
F .146961E+06 .146823E+06 .146698E+06 .146538E+06 .145487E+06 .143808E+06 .141065E+06 .139275E+06 .138838E+06 .138742E+06
E .360115E+06 .366089E+06 .372061E+06 .378031E+06 .389922E+06 .401720E+06 .423957E+06 .443279E+06 .451868E+06 .461453E+06

C300.051 .952900E+02 .301660E+03 .621911E+03 .489320E+03 .350828E+04 .320458E+04
.119223E+03 .116616E+03 .399210E+06 .423113E+06 .104621E+03 .438571E+06
T .779946E+03 .811785E+03 .830839E+03 .842572E+03 .856117E+03 .857118E+03 .837716E+03 .819094E+03 .823719E+03 .821307E+03
F .124058E+06 .123427E+06 .123048E+06 .122815E+06 .122547E+06 .122527E+06 .122912E+06 .123282E+06 .123190E+06 .123237E+06
E .427354E+06 .431579E+06 .435794E+06 .440004E+06 .448409E+06 .456813E+06 .472257E+06 .488328E+06 .493359E+06 .500393E+06

C300.052 .954700E+02 .301660E+03 .621826E+03 .491420E+03 .388403E+04 .359389E+04
.121583E+03 .118865E+03 .399968E+06 .424695E+06 .105186E+03 .440968E+06
T .817937E+03 .863986E+03 .884521E+03 .889427E+03 .900560E+03 .901341E+03 .872146E+03 .847786E+03 .854074E+03 .866879E+03
F .138279E+06 .137341E+06 .136924E+06 .136825E+06 .136601E+06 .136585E+06 .137175E+06 .137671E+06 .137543E+06 .137282E+06
E .429230E+06 .433941E+06 .438643E+06 .443342E+06 .452729E+06 .462115E+06 .479377E+06 .495109E+06 .502970E+06 .510820E+06

C300.053 .951100E+02 .301660E+03 .606797E+03 .493110E+03 .427187E+04 .390337E+04
.123440E+03 .120251E+03 .398451E+06 .423049E+06 .105625E+03 .442815E+06
T .863796E+03 .906991E+03 .921570E+03 .931392E+03 .943987E+03 .942605E+03 .904768E+03 .878816E+03 .877964E+03 .893004E+03
F .149454E+06 .148760E+06 .148462E+06 .148262E+06 .148008E+06 .148035E+06 .148806E+06 .149341E+06 .149340E+06 .149044E+06
E .428183E+06 .433294E+06 .438402E+06 .443503E+06 .453694E+06 .463866E+06 .482637E+06 .499725E+06 .508270E+06 .516803E+06

C300.054 .952900E+02 .301660E+03 .606861E+03 .490020E+03 .478103E+04 .444506E+04
.126687E+03 .123265E+03 .399210E+06 .424699E+06 .106379E+03 .446002E+06
T .900969E+03 .945650E+03 .968290E+03 .973174E+03 .974708E+03 .975078E+03 .930249E+03 .898074E+03 .898074E+03 .915088E+03
F .170067E+06 .169115E+06 .168642E+06 .168541E+06 .168509E+06 .168502E+06 .169441E+06 .170130E+06 .170130E+06 .169765E+06
E .430543E+06 .436365E+06 .442177E+06 .447987E+06 .459606E+06 .471224E+06 .492800E+06 .512083E+06 .521825E+06 .531553E+06

C300.055 .954700E+02 .301660E+03 .601911E+03 .489320E+03 .507507E+04 .466213E+04
.128032E+03 .124546E+03 .399968E+06 .425671E+06 .106687E+03 .447304E+06
T .943664E+03 .985261E+03 .998606E+03 .998608E+03 .100271E+04 .999269E+03 .948531E+03 .912530E+03 .912530E+03 .933583E+03
F .177746E+06 .176865E+06 .176589E+06 .176505E+06 .176575E+06 .177643E+06 .178422E+06 .178422E+06 .177921E+06
E .431791E+06 .437891E+06 .443985E+06 .450080E+06 .462265E+06 .474454E+06 .496882E+06 .517329E+06 .527552E+06 .537757E+06

C300.056 .952900E+02 .301660E+03 .601883E+03 .490020E+03 .577139E+04 .536588E+04
.133121E+03 .128208E+03 .399210E+06 .426102E+06 .107607E+03 .451192E+06
T .993966E+03 .102708E+04 .104629E+04 .104606E+04 .105725E+04 .104400E+04 .984962E+03 .956419E+03 .954175E+03 .974687E+03
F .204898E+06 .204175E+06 .203767E+06 .203772E+06 .203539E+06 .203815E+06 .205098E+06 .205741E+06 .205792E+06 .205328E+06
E .433172E+06 .440228E+06 .447276E+06 .454325E+06 .468413E+06 .482511E+06 .508450E+06 .532073E+06 .543886E+06 .555684E+06

C300.058 .949300E+02 .301660E+03 .627119E+03 .483720E+03 .320173E+04 .295051E+04
.117593E+03 .114937E+03 .397693E+06 .421324E+06 .104225E+03 .436897E+06
T .739550E+03 .776535E+03 .801173E+03 .809473E+03 .824249E+03 .830957E+03 .815379E+03 .801173E+03 .805668E+03 .775043E+03
F .114625E+06 .113913E+06 .113433E+06 .113271E+06 .112982E+06 .112851E+06 .113155E+06 .113433E+06 .113345E+06 .113941E+06
E .425236E+06 .429130E+06 .433011E+06 .436888E+06 .444627E+06 .452359E+06 .466563E+06 .479500E+06 .485965E+06 .492456E+06

C300.101 .893500E+02 .301660E+03 .682558E+03 .466890E+03 .441972E+04 .411485E+04
.119185E+03 .116976E+03 .374205E+06 .401386E+06 .104612E+03 .438532E+06
T .802284E+03 .817697E+03 .844096E+03 .864605E+03 .907523E+03 .943439E+03 .926407E+03 .910507E+03 .900844E+03 .914762E+03
F .159043E+06 .158720E+06 .158162E+06 .157729E+06 .156835E+06 .156081E+06 .156432E+06 .156761E+06 .156962E+06 .156674E+06
E .406828E+06 .412263E+06 .417684E+06 .423095E+06 .433876E+06 .444622E+06 .464353E+06 .482315E+06 .491304E+06 .500282E+06

C300.102 .893300E+02 .301660E+03 .667545E+03 .467590E+03 .487162E+04 .454016E+04
.121581E+03 .119413E+03 .374963E+06 .403402E+06 .105186E+03 .440958E+06
T .846626E+03 .881820E+03 .900798E+03 .911743E+03 .963444E+03 .975040E+03 .954282E+03 .932533E+03 .916059E+03 .936488E+03
F .174916E+06 .174150E+06 .173737E+06 .173500E+06 .172397E+06 .172155E+06 .172559E+06 .173053E+06 .173407E+06 .172968E+06
E .408399E+06 .414378E+06 .420348E+06 .426312E+06 .438193E+06 .450063E+06 .471859E+06 .491707E+06 .501645E+06 .511566E+06

C300.103 .897100E+02 .301660E+03 .662558E+03 .466890E+03 .532723E+04 .498857E+04
.127055E+03 .121943E+03 .375720E+06 .403750E+06 .106444E+03 .446360E+06
T .871165E+03 .910127E+03 .934574E+03 .940433E+03 .997114E+03 .100482E+04 .977517E+03 .956587E+03 .942146E+03 .960543E+03
F .191980E+06 .191106E+06 .190561E+06 .189990E+06 .189198E+06 .189035E+06 .189619E+06 .190075E+06 .190393E+06 .189988E+06
E .410338E+06 .416907E+06 .423465E+06 .430011E+06 .443069E+06 .456121E+06 .480093E+06 .501918E+06 .512841E+06 .523750E+06

C300.104 .898900E+02 .301660E+03 .672504E+03 .469700E+03 .575610E+04 .538720E+04
.127772E+03 .124187E+03 .376477E+06 .405460E+06 .106623E+03 .447053E+06
T .911606E+03 .953925E+03 .977051E+03 .987346E+03 .103520E+04 .104973E+04 .100285E+04 .987386E+03 .970200E+03 .984702E+03
F .206767E+06 .205797E+06 .205275E+06 .205044E+06 .204002E+06 .203695E+06 .204702E+06 .205044E+06 .205429E+06 .205104E+06
E .412569E+06 .419657E+06 .426714E+06 .433807E+06 .447913E+06 .462007E+06 .487916E+06 .511493E+06 .523294E+06 .535084E+06

C300.105 .893500E+02 .301660E+03 .677489E+03 .470400E+03 .408538E+04 .378929E+04
.117369E+03 .115245E+03 .374205E+06 .400707E+06 .104170E+03 .436665E+06
T .762165E+03 .780703E+03 .802434E+03 .817145E+03 .860913E+03 .890661E+03 .869340E+03 .874741E+03 .872058E+03 .881720E+03
F .147208E+06 .146832E+06 .146387E+06 .146083E+06 .145178E+06 .144565E+06 .144592E+06 .144892E+06 .144948E+06 .144749E+06
E .405736E+06 .411755E+06 .417764E+06 .423766E+06 .435726E+06 .447652E+06 .464884E+06 .475441E+06 .483731E+06 .492014E+06

C300.106 .895300E+02 .301660E+03 .677518E+03 .468990E+03 .372636E+04 .344078E+04
.115384E+03 .113387E+03 .374963E+06 .400867E+06 .103680E+03 .434599E+06
T .710376E+03 .727851E+03 .750784E+03 .765955E+03 .814449E+03 .855099E+03 .848822E+03 .844907E+03 .848822E+03 .860716E+03
F .133893E+06 .133557E+06 .133109E+06 .132809E+06 .131816E+06 .131016E+06 .131143E+06 .131122E+06 .131143E+06 .130903E+06
E .405431E+06 .409998E+06 .414533E+06 .419070E+06 .428097E+06 .437083E+06 .453568E+06 .468562E+06 .476055E+06 .483539E+06

C300.107 .893500E+02 .301660E+03 .667545E+03 .467590E+03 .335762E+04 .310091E+04
.113513E+03 .111395E+03 .374205E+06 .399345E+06 .103213E+03 .432624E+06
T .655652E+03 .661711E+03 .689960E+03 .707635E+03 .762506E+03 .798010E+03 .817132E+03 .817472E+03 .825482E+03
F .121241E+06 .121134E+06 .120623E+06 .120293E+06 .119242E+06 .118546E+06 .118169E+06 .118169E+06 .118163E+06 .118004E+06
E .403389E+06 .407491E+06 .411600E+06 .415701E+06 .423848E+06 .431959E+06 .446794E+06 .460280E+06 .467023E+06 .473759E+06

C300.108 .895300E+02 .301660E+03 .672582E+03 .465480E+03 .304306E+04 .278530E+04
.112315E+03 .109633E+03 .374963E+06 .399651E+06 .102910E+03 .431344E+06
T .594486E+03 .590480E+03 .621874E+03 .642883E+03 .703982E+03 .750948E+03 .775126E+03 .776618E+03 .788819E+03 .794287E+03
F .110280E+06 .110344E+06 .109835E+06 .109479E+06 .108385E+06 .107503E+06 .107040E+06 .107011E+06 .106815E+06 .106670E+06
E .403395E+06 .407140E+06 .410872E+06 .414594E+06 .421982E+06 .429324E+06 .442739E+06 .454931E+06 .461019E+06 .467100E+06

C300.201 .804800E+02 .301660E+03 .101119E+04 .504670E+03 .463446E+04 .434045E+04
.112630E+03 .111184E+03 .336931E+06 .374183E+06 .103040E+03 .431896E+06
T .560259E+03 .647571E+03 .694961E+03 .725777E+03 .807313E+03 .874144E+03 .935729E+03 .964436E+03 .953182E+03 .964487E+03
F .171887E+06 .170455E+06 .169565E+06 .168955E+06 .167258E+06 .165826E+06 .164517E+06 .163920E+06 .164153E+06 .163910E+06
E .380020E+06 .385817E+06 .391595E+06 .397358E+06 .408807E+06 .420190E+06 .440949E+06 .459777E+06 .469200E+06 .478613E+06

C300.202 .803000E+02 .301660E+03 .101611E+04 .506060E+03 .508013E+04 .473976E+04
.115153E+03 .113327E+03 .336176E+06 .374251E+06 .103623E+03 .434356E+06
T .624168E+03 .711028E+03 .764138E+03 .797237E+03 .879314E+03 .941625E+03 .985235E+03 .100493E+04 .974941E+03 .973058E+03
F .186899E+06 .185261E+06 .184159E+06 .183447E+06 .181895E+06 .180277E+06 .179346E+06 .178937E+06 .179563E+06 .179603E+06
E .380602E+06 .386918E+06 .393210E+06 .399486E+06 .411968E+06 .424380E+06 .447061E+06 .467652E+06 .477969E+06 .488288E+06

```
C300.203          .803000E+02 .301660E+03 .991224E+03 .503970E+03 .547804E+04 .509233E+04
                  .117278E+03 .115294E+03 .336176E+06 .374102E+06 .104146E+03 .436572E+06
 T   .605045E+03 .761061E+03 .806067E+03 .838715E+03 .921062E+03 .987450E+03 .102101E+04 .105090E+04 .990435E+03 .999097E+03
 F   .199879E+06 .198305E+06 .197317E+06 .196585E+06 .194723E+06 .193253E+06 .193538E+06 .191922E+06 .193189E+06 .193002E+06
 E   .380909E+06 .387684E+06 .394437E+06 .401174E+06 .414568E+06 .427900E+06 .452290E+06 .474424E+06 .485532E+06 .496634E+06

C300.204          .803000E+02 .301660E+03 .991407E+03 .500490E+03 .433359E+04 .404627E+04
                  .110797E+03 .109274E+03 .336176E+06 .372357E+06 .102522E+03 .429709E+06
 T   .321964E+03 .589797E+03 .626999E+03 .669518E+03 .766621E+03 .826611E+03 .901594E+03 .930430E+03 .921029E+03 .931341E+03
 F   .160548E+06 .159575E+06 .158960E+06 .158198E+06 .156288E+06 .155040E+06 .153467E+06 .152871E+06 .153064E+06 .152852E+06
 E   .377793E+06 .383209E+06 .388611E+06 .393996E+06 .404676E+06 .415297E+06 .434632E+06 .452164E+06 .460938E+06 .469703E+06

C300.205          .803000E+02 .301660E+03 .101148E+04 .499090E+03 .392144E+04 .362088E+04
                  .108054E+03 .106530E+03 .336176E+06 .372243E+06 .101811E+03 .426706E+06
 T   .471612E+03 .531353E+03 .568123E+03 .607614E+03 .708931E+03 .776230E+03 .856456E+03 .888516E+03 .895244E+03 .906637E+03
 F   .144112E+06 .143412E+06 .142893E+06 .142273E+06 .140455E+06 .139127E+06 .137494E+06 .136844E+06 .136708E+06 .136479E+06
 E   .377114E+06 .381971E+06 .386617E+06 .391648E+06 .401224E+06 .410735E+06 .428025E+06 .443890E+06 .451517E+06 .459335E+06

C300.206          .801200E+02 .301660E+03 .101661E+04 .496300E+03 .360900E+04 .335966E+04
                  .107066E+03 .104359E+03 .335420E+06 .371188E+06 .101551E+03 .425608E+06
 T   .416486E+03 .461628E+03 .491035E+03 .525971E+03 .623638E+03 .696290E+03 .789648E+03 .832962E+03 .850192E+03 .861135E+03
 F   .133786E+06 .133402E+06 .133089E+06 .132660E+06 .131182E+06 .129861E+06 .128067E+06 .127201E+06 .126857E+06 .126638E+06
 E   .375702E+06 .380209E+06 .384710E+06 .389202E+06 .398117E+06 .406968E+06 .423028E+06 .437555E+06 .444803E+06 .452043E+06

C350.051          .954700E+02 .349280E+03 .651642E+03 .495610E+03 .352429E+04 .326308E+04
                  .120940E+03 .118271E+03 .399968E+06 .421448E+06 .105033E+03 .440313E+06
 T   .754798E+03 .798344E+03 .815235E+03 .825397E+03 .842547E+03 .855172E+03 .863819E+03 .814524E+03 .817047E+03 .734520E+03
 F   .126651E+06 .125790E+06 .125454E+06 .125251E+06 .124909E+06 .124657E+06 .125043E+06 .125468E+06 .125418E+06 .127046E+06
 E   .425184E+06 .428901E+06 .432610E+06 .436315E+06 .443710E+06 .451094E+06 .464662E+06 .477028E+06 .483209E+06 .489450E+06

C350.052          .956500E+02 .349280E+03 .656577E+03 .497000E+03 .393616E+04 .361041E+04
                  .123379E+03 .120540E+03 .400726E+06 .422838E+06 .105611E+03 .442754E+06
 T   .800861E+03 .842386E+03 .867788E+03 .874817E+03 .887632E+03 .898345E+03 .866036E+03 .839382E+03 .837930E+03 .820558E+03
 F   .139726E+06 .138879E+06 .138360E+06 .138217E+06 .137957E+06 .137741E+06 .138196E+06 .138941E+06 .138978E+06 .139325E+06
 E   .426967E+06 .431078E+06 .435178E+06 .439275E+06 .447459E+06 .455633E+06 .470869E+06 .484377E+06 .491232E+06 .498100E+06

C350.053          .958300E+02 .349280E+03 .646476E+03 .499090E+03 .443525E+04 .412633E+04
                  .126907E+03 .123776E+03 .401485E+06 .424079E+06 .106430E+03 .446216E+06
 T   .844583E+03 .867403E+03 .917263E+03 .921468E+03 .943506E+03 .941874E+03 .904666E+03 .867555E+03 .864591E+03 .867556E+03
 F   .159322E+06 .158417E+06 .157790E+06 .157703E+06 .157247E+06 .157280E+06 .158054E+06 .158837E+06 .158900E+06 .158836E+06
 E   .428796E+06 .433494E+06 .438180E+06 .442864E+06 .452215E+06 .461567E+06 .478768E+06 .494435E+06 .502304E+06 .510149E+06

C350.054          .960100E+02 .349280E+03 .646407E+03 .500490E+03 .481123E+04 .447885E+04
                  .129284E+03 .126018E+03 .402345E+06 .425313E+06 .106972E+03 .448505E+06
 T   .888126E+03 .936515E+03 .952115E+03 .960647E+03 .973143E+03 .969488E+03 .928884E+03 .888126E+03 .887255E+03 .900955E+03
 F   .171569E+06 .170531E+06 .170201E+06 .170022E+06 .169762E+06 .169838E+06 .170698E+06 .171570E+06 .171589E+06 .171293E+06
 E   .430402E+06 .435470E+06 .440533E+06 .445592E+06 .455700E+06 .465811E+06 .484408E+06 .501371E+06 .509852E+06 .518325E+06

C350.055          .954700E+02 .349280E+03 .646407E+03 .500480E+03 .588212E+04 .549290E+04
                  .135336E+03 .131390E+03 .399968E+06 .424478E+06 .108312E+03 .454173E+06
 T   .974644E+03 .101232E+04 .103605E+04 .103605E+04 .104946E+04 .103414E+04 .981395E+03 .943315E+03 .932126E+03 .955304E+03
 F   .209326E+06 .208485E+06 .207969E+06 .207969E+06 .207683E+06 .208010E+06 .209170E+06 .210044E+06 .210303E+06 .209768E+06
 E   .430711E+06 .436929E+06 .443139E+06 .449349E+06 .461759E+06 .474180E+06 .497024E+06 .517841E+06 .528257E+06 .538658E+06

C350.056          .954700E+02 .349280E+03 .646476E+03 .499090E+03 .537110E+04 .498503E+04
                  .132144E+03 .128472E+03 .399968E+06 .423765E+06 .107612E+03 .451214E+06
 T   .930929E+03 .970427E+03 .994761E+03 .994761E+03 .100817E+04 .100805E+04 .959952E+03 .921174E+03 .912390E+03 .930929E+03
 F   .190640E+06 .189772E+06 .189246E+06 .189246E+06 .188964E+06 .188967E+06 .190001E+06 .190859E+06 .191056E+06 .190642E+06
 E   .429430E+06 .435879E+06 .440719E+06 .446359E+06 .457629E+06 .468899E+06 .489628E+06 .508525E+06 .517980E+06 .527422E+06

C350.057          .952900E+02 .349280E+03 .671767E+03 .492810E+03 .318852E+04 .293559E+04
                  .118543E+03 .116085E+03 .399210E+06 .420725E+06 .104456E+03 .437875E+06
 T   .718876E+03 .756173E+03 .780301E+03 .787599E+03 .806731E+03 .817203E+03 .805680E+03 .786588E+03 .781112E+03 .793102E+03
 F   .114019E+06 .113309E+06 .112843E+06 .112701E+06 .112328E+06 .112124E+06 .112349E+06 .112721E+06 .112826E+06 .113144E+06
 E   .424083E+06 .427425E+06 .430757E+06 .434086E+06 .440726E+06 .447357E+06 .459532E+06 .470639E+06 .476181E+06 .481890E+06

C350.101          .900700E+02 .349280E+03 .671911E+03 .489320E+03 .473729E+04 .442498E+04
                  .123239E+03 .119918E+03 .377234E+06 .400886E+06 .105578E+03 .442615E+06
 T   .772062E+03 .800009E+03 .822535E+03 .844459E+03 .904547E+03 .942389E+03 .932586E+03 .915462E+03 .900852E+03 .897998E+03
 F   .171625E+06 .171033E+06 .170550E+06 .170077E+06 .168781E+06 .167976E+06 .168183E+06 .168548E+06 .168860E+06 .168922E+06
 E   .405934E+06 .410988E+06 .416032E+06 .421067E+06 .431087E+06 .441075E+06 .459401E+06 .476084E+06 .484436E+06 .492790E+06

C350.102          .898900E+02 .349280E+03 .702119E+03 .483720E+03 .534185E+04 .499366E+04
                  .126095E+03 .123127E+03 .376477E+06 .401697E+06 .106243E+03 .445426E+06
 T   .806112E+03 .838760E+03 .883174E+03 .906521E+03 .963177E+03 .993009E+03 .984867E+03 .959952E+03 .932341E+03 .942146E+03
 F   .193436E+06 .192710E+06 .191711E+06 .191187E+06 .189930E+06 .189286E+06 .189460E+06 .190001E+06 .190611E+06 .190393E+06
 E   .407415E+06 .413119E+06 .418804E+06 .424479E+06 .435783E+06 .447064E+06 .467758E+06 .486602E+06 .496043E+06 .505477E+06

C350.103          .900700E+02 .349280E+03 .712142E+03 .483020E+03 .578907E+04 .542774E+04
                  .128960E+03 .125850E+03 .377234E+06 .403328E+06 .106898E+03 .448195E+06
 T   .833032E+03 .880588E+03 .911391E+03 .938235E+03 .100357E+04 .103518E+04 .100465E+04 .987512E+03 .958137E+03 .970186E+03
 F   .209919E+06 .208820E+06 .208101E+06 .207487E+06 .206013E+06 .205326E+06 .205989E+06 .206369E+06 .207032E+06 .206758E+06
 E   .409540E+06 .415732E+06 .421911E+06 .428078E+06 .440362E+06 .452624E+06 .475144E+06 .495638E+06 .505904E+06 .516162E+06

C350.104          .897100E+02 .349280E+03 .711966E+03 .487920E+03 .444861E+04 .415482E+04
                  .112293E+03 .117929E+03 .375720E+06 .399989E+06 .102904E+03 .431321E+06
 T   .731880E+03 .745830E+03 .775969E+03 .800617E+03 .863740E+03 .911916E+03 .913146E+03 .892269E+03 .888955E+03 .892900E+03
 F   .161870E+06 .161388E+06 .160768E+06 .160253E+06 .158918E+06 .157902E+06 .157897E+06 .158314E+06 .158384E+06 .158301E+06
 E   .404798E+06 .409516E+06 .414262E+06 .418998E+06 .428415E+06 .437791E+06 .454981E+06 .470635E+06 .478465E+06 .486292E+06

C350.105          .898900E+02 .349280E+03 .711966E+03 .487920E+03 .400342E+04 .369320E+04
                  .116518E+03 .115271E+03 .376477E+06 .400085E+06 .103961E+03 .435783E+06
 T   .680874E+03 .688727E+03 .715810E+03 .734369E+03 .811910E+03 .860604E+03 .871748E+03 .860964E+03 .863948E+03 .874792E+03
 F   .144304E+06 .144158E+06 .143640E+06 .142879E+06 .141712E+06 .140713E+06 .140485E+06 .140706E+06 .140645E+06 .140422E+06
 E   .404329E+06 .408570E+06 .412801E+06 .417015E+06 .425394E+06 .433731E+06 .448998E+06 .462893E+06 .469838E+06 .476776E+06

C350.106          .897100E+02 .349280E+03 .716939E+03 .488620E+03 .367563E+04 .341055E+04
                  .114753E+03 .113300E+03 .375720E+06 .399062E+06 .103523E+03 .433935E+06
 T   .611254E+03 .604724E+03 .644459E+03 .688387E+03 .761872E+03 .805460E+03 .830752E+03 .828849E+03 .832604E+03 .837630E+03
 F   .134596E+06 .134704E+06 .134031E+06 .133215E+06 .131818E+06 .130947E+06 .130438E+06 .130476E+06 .130401E+06 .130299E+06
 E   .403010E+06 .406960E+06 .410897E+06 .414817E+06 .422595E+06 .430335E+06 .444466E+06 .457253E+06 .463784E+06 .470211E+06

C350.201          .801200E+02 .349280E+03 .105227E+04 .478830E+03 .476720E+04 .447136E+04
                  .104818E+03 .109895E+03 .335420E+06 .368827E+06 .100952E+03 .423080E+06
 T   .545426E+03 .598705E+03 .632726E+03 .670021E+03 .769433E+03 .842011E+03 .915449E+03 .964385E+03 .953130E+03 .958547E+03
 F   .176950E+06 .176147E+06 .175570E+06 .174891E+06 .172897E+06 .171343E+06 .169757E+06 .168723E+06 .168958E+06 .168844E+06
 E   .374005E+06 .379170E+06 .384324E+06 .389466E+06 .399672E+06 .409816E+06 .428299E+06 .445017E+06 .453413E+06 .461765E+06

C350.202          .797600E+02 .349280E+03 .108235E+04 .474010E+03 .523249E+04 .490815E+04
                  .114576E+03 .112417E+03 .333909E+06 .368715E+06 .103479E+03 .433749E+06
 T   .606031E+03 .662197E+03 .701619E+03 .737741E+03 .832343E+03 .900775E+03 .974523E+03 .102020E+04 .983065E+03 .982164E+03
 F   .193563E+06 .192564E+06 .191797E+06 .191057E+06 .189007E+06 .187477E+06 .185858E+06 .184896E+06 .185675E+06 .185694E+06
 E   .374393E+06 .380052E+06 .385698E+06 .391329E+06 .402515E+06 .413642E+06 .433933E+06 .452322E+06 .461539E+06 .470757E+06

C350.203          .797600E+02 .349280E+03 .106237E+04 .475310E+03 .546948E+04 .513421E+06
                  .115922E+03 .113868E+03 .333909E+06 .368531E+06 .103814E+03 .435162E+06
 T   .633663E+03 .693316E+03 .730174E+03 .771726E+03 .858675E+03 .935390E+03 .100018E+04 .1056B9E+04 .997531E+03 .998422E+03
 F   .202152E+06 .201020E+06 .200166E+06 .199376E+06 .197433E+06 .195696E+06 .194269E+06 .193088E+06 .194326E+06 .194307E+06
 E   .374466E+06 .380381E+06 .386282E+06 .392167E+06 .403864E+06 .415497E+06 .436731E+06 .453968E+06 .465622E+06 .475275E+06
```

C350.204		.799400E+02	.349280E+03	.107239E+04	.474610E+03	.429532E+04	.402809E+04			
		.107008E+03	.106387E+03	.334464E+06	.367943E+06	.101536E+03	.425544E+06			
T	.475940E+03	.520981E+03	.553149E+03	.590065E+03	.691111E+03	.774547E+03	.963793E+03	.907574E+03	.910558E+03	.917327E+03
F	.159916E+06	.159399E+06	.158966E+06	.158397E+06	.156631E+06	.154967E+06	.151313E+06	.152190E+06	.152128E+06	.151980E+06
E	.372611E+06	.377272E+06	.381925E+06	.386549E+06	.395785E+06	.404934E+06	.421583E+06	.436642E+06	.444170E+06	.451692E+06
C350.205		.799400E+02	.349280E+03	.107739E+04	.474610E+03	.387156E+04	.361516E+04			
		.102969E+03	.102260E+03	.334664E+06	.367500E+06	.100451E+03	.420968E+06			
T	.422736E+03	.459657E+03	.485351E+03	.520302E+03	.619565E+03	.700418E+03	.787185E+03	.861012E+03	.874829E+03	.888516E+03
F	.144546E+06	.144235E+06	.143972E+06	.143557E+06	.142074E+06	.140617E+06	.138984E+06	.137402E+06	.137121E+06	.136843E+06
E	.371713E+06	.375921E+06	.380126E+06	.384323E+06	.392661E+06	.400939E+06	.415901E+06	.429549E+06	.436323E+06	.443088E+06
C400.051		.960100E+02	.408980E+03	.695041E+03	.522710E+03	.421234E+04	.392819E+04			
		.112814E+03	.124657E+03	.402243E+06	.422349E+06	.102986E+03	.431665E+06			
T	.809016E+03	.850284E+03	.869721E+03	.878903E+03	.900411E+03	.907600E+03	.874317E+03	.839239E+03	.839239E+03	.800233E+03
F	.151940E+06	.151079E+06	.150673E+06	.150482E+06	.150036E+06	.149888E+06	.150578E+06	.151310E+06	.151310E+06	.152123E+06
E	.426185E+06	.430006E+06	.433819E+06	.437630E+06	.445234E+06	.452834E+06	.466811E+06	.479560E+06	.485935E+06	.492333E+06
C400.052		.960100E+02	.408980E+03	.695140E+03	.521330E+03	.463446E+04	.431006E+04			
		.144219E+03	.127171E+03	.402243E+06	.422823E+06	.110197E+03	.462190E+06			
T	.850109E+03	.892190E+03	.915502E+03	.917055E+03	.938703E+03	.944340E+03	.907431E+03	.867474E+03	.863609E+03	.866553E+03
F	.166341E+06	.165439E+06	.164943E+06	.164893E+06	.164434E+06	.164336E+06	.165115E+06	.165969E+06	.166052E+06	.165988E+06
E	.427029E+06	.431221E+06	.435404E+06	.439586E+06	.447936E+06	.456282E+06	.471630E+06	.485631E+06	.492634E+06	.499635E+06
C400.053		.960100E+02	.408980E+03	.690140E+03	.521330E+03	.509681E+04	.474480E+04			
		.139422E+03	.130006E+03	.402243E+06	.423245E+06	.109192E+03	.457898E+06			
T	.896475E+03	.938517E+03	.963372E+03	.960047E+03	.984080E+03	.977311E+03	.933449E+03	.896615E+03	.887130E+03	.901192E+03
F	.182514E+06	.181593E+06	.181057E+06	.181128E+06	.180617E+06	.180760E+06	.181704E+06	.182512E+06	.182722E+06	.182411E+06
E	.427870E+06	.432480E+06	.437081E+06	.441684E+06	.450873E+06	.460067E+06	.476977E+06	.492393E+06	.500107E+06	.507812E+06
C400.054		.958300E+02	.408980E+03	.695090E+03	.522020E+03	.557754E+04	.522374E+04			
		.119614E+03	.132880E+03	.401485E+06	.423151E+06	.104715E+03	.438969E+06			
T	.943049E+03	.974737E+03	.998381E+03	.999042E+03	.100808E+04	.100796E+04	.970270E+03	.922236E+03	.910037E+03	.929918E+03
F	.199440E+06	.198733E+06	.198214E+06	.198200E+06	.198005E+06	.198008E+06	.198832E+06	.199913E+06	.200191E+06	.199738E+06
E	.428215E+06	.433269E+06	.438315E+06	.443360E+06	.453446E+06	.463531E+06	.482066E+06	.498971E+06	.507431E+06	.515878E+06
C400.055		.958300E+02	.408980E+03	.694888E+03	.524790E+03	.594904E+04	.556416E+04			
		.144082E+03	.135071E+03	.401485E+06	.423560E+06	.110169E+03	.462031E+06			
T	.963688E+03	.100235E+04	.102082E+04	.102639E+04	.104216E+04	.103595E+04	.981887E+03	.941903E+03	.928220E+03	.948153E+03
F	.212275E+06	.211399E+06	.210990E+06	.210868E+06	.210526E+06	.210660E+06	.211861E+06	.212779E+06	.213097E+06	.212634E+06
E	.428955E+06	.434337E+06	.439714E+06	.445089E+06	.455829E+06	.466573E+06	.486333E+06	.504342E+06	.513354E+06	.522355E+06
C400.056		.956500E+02	.408980E+03	.695041E+03	.522710E+03	.389861E+04	.361623E+04			
		.124073E+03	.122118E+03	.400726E+06	.420451E+06	.105774E+03	.443442E+06			
T	.770519E+03	.809162E+03	.826796E+03	.839783E+03	.860990E+03	.879042E+03	.856444E+03	.825234E+03	.825234E+03	.828748E+03
F	.140341E+06	.139558E+06	.139198E+06	.138932E+06	.138499E+06	.138131E+06	.138592E+06	.139230E+06	.139230E+06	.139157E+06
E	.423988E+06	.427511E+06	.431028E+06	.434540E+06	.441548E+06	.448543E+06	.461397E+06	.473122E+06	.478984E+06	.484844E+06
C400.101		.895300E+02	.408980E+03	.769939E+03	.524100E+03	.475107E+04	.443273E+04			
		.121799E+03	.119666E+03	.374963E+06	.397288E+06	.105238E+03	.441178E+06			
T	.692079E+03	.709882E+03	.761965E+03	.797384E+03	.856577E+03	.902845E+03	.917815E+03	.912638E+03	.901343E+03	.901423E+03
F	.173250E+06	.172901E+06	.171837E+06	.171009E+06	.169816E+06	.168818E+06	.168497E+06	.168608E+06	.168850E+06	.168848E+06
E	.401641E+06	.405989E+06	.410319E+06	.414636E+06	.423228E+06	.431785E+06	.447455E+06	.461707E+06	.468839E+06	.475972E+06
C400.102		.895300E+02	.408980E+03	.774990E+03	.523410E+03	.524697E+04	.490192E+04			
		.125173E+03	.122829E+03	.374963E+06	.397974E+06	.106030E+03	.444525E+06			
T	.739174E+03	.775082E+03	.814483E+03	.847199E+03	.911592E+03	.964690E+03	.970408E+03	.952943E+03	.930971E+03	.943109E+03
F	.191026E+06	.190262E+06	.189400E+06	.188674E+06	.187237E+06	.186070E+06	.185947E+06	.186325E+06	.186808E+06	.186540E+06
E	.402783E+06	.407580E+06	.412363E+06	.417134E+06	.426639E+06	.436088E+06	.453421E+06	.469199E+06	.477100E+06	.484994E+06

C400.103		.895300E+02	.408980E+03	.765140E+03	.521330E+03	.577129E+04	.539846E+04			
		.128685E+03	.126118E+03	.374963E+06	.398364E+06	.106836E+03	.447931E+06			
T	.791448E+03	.825984E+03	.874032E+03	.911376E+03	.963760E+03	.100242E+04	.100285E+04	.982859E+03	.954175E+03	.953925E+03
F	.209527E+06	.208744E+06	.207637E+06	.206774E+06	.205575E+06	.204711E+06	.204702E+06	.205145E+06	.205792E+06	.205797E+06
E	.403650E+06	.408924E+06	.414180E+06	.419423E+06	.429873E+06	.440297E+06	.459408E+06	.476803E+06	.485516E+06	.494230E+06
C400.104		.897100E+02	.408980E+03	.760332E+03	.518560E+03	.609260E+04	.566975E+04			
		.130812E+03	.128123E+03	.375720E+06	.399350E+06	.107315E+03	.449959E+06			
T	.823002E+03	.865955E+03	.911577E+03	.941859E+03	.996838E+03	.104212E+04	.103407E+04	.101988E+04	.972669E+03	.983076E+03
F	.219638E+06	.218633E+06	.217557E+06	.216846E+06	.215570E+06	.214572E+06	.214748E+06	.215061E+06	.216131E+06	.215891E+06
E	.404899E+06	.410432E+06	.415948E+06	.421454E+06	.432429E+06	.443376E+06	.463454E+06	.481721E+06	.490880E+06	.500033E+06
C400.105		.895300E+02	.408980E+03	.765472E+03	.516480E+03	.441972E+04	.413348E+04			
		.119620E+03	.117609E+03	.374963E+06	.396822E+06	.104717E+03	.438975E+06			
T	.634196E+03	.650327E+03	.725041E+03	.762111E+03	.814843E+03	.864609E+03	.892913E+03	.885574E+03	.878824E+03	.881168E+03
F	.162343E+06	.162056E+06	.160615E+06	.159880E+06	.158780E+06	.157728E+06	.157131E+06	.157286E+06	.157428E+06	.157378E+06
E	.400892E+06	.404958E+06	.409000E+06	.413028E+06	.421047E+06	.429030E+06	.443627E+06	.456905E+06	.463549E+06	.470191E+06
C400.106		.895300E+02	.408980E+03	.770518E+03	.515790E+03	.396119E+04	.364312E+04			
		.116000E+03	.114136E+03	.374963E+06	.396336E+06	.103833E+03	.435243E+06			
T	.568799E+03	.573427E+03	.663855E+03	.706614E+03	.769828E+03	.816883E+03	.850426E+03	.853961E+03	.854061E+03	.860990E+03
F	.143986E+06	.143917E+06	.142400E+06	.141601E+06	.140356E+06	.139401E+06	.138715E+06	.138642E+06	.138640E+06	.138498E+06
E	.399937E+06	.403538E+06	.407112E+06	.410672E+06	.417748E+06	.424788E+06	.437651E+06	.449340E+06	.455184E+06	.461024E+06
C400.107		.897100E+02	.408980E+03	.755739E+03	.512330E+03	.368352E+04	.339009E+04			
		.114359E+03	.112528E+03	.375720E+06	.396469E+06	.103425E+03	.433520E+06			
T	.485483E+03	.512114E+03	.623610E+03	.672407E+03	.728910E+03	.779869E+03	.815185E+03	.824056E+03	.825348E+03	.800496E+03
F	.135279E+06	.134965E+06	.133310E+06	.132491E+06	.131387E+06	.130184E+06	.129677E+06	.129498E+06	.129472E+06	.129971E+06
E	.398843E+06	.403212E+06	.406553E+06	.409879E+06	.416491E+06	.423067E+06	.435074E+06	.445978E+06	.451429E+06	.456896E+06
C400.201		.797600E+02	.408980E+03	.114099E+04	.508150E+03	.467774E+04	.439177E+04			
		.104895E+03	.103811E+03	.333909E+06	.364265E+06	.100972E+03	.423168E+06			
T	.491372E+03	.545479E+03	.575796E+03	.596170E+03	.685798E+03	.765310E+03	.847441E+03	.926303E+03	.943336E+03	.949114E+03
F	.173975E+06	.173304E+06	.172862E+06	.172543E+06	.170949E+06	.169344E+06	.167600E+06	.165911E+06	.165553E+06	.165432E+06
E	.368605E+06	.372936E+06	.377261E+06	.381582E+06	.390171E+06	.398706E+06	.414246E+06	.428278E+06	.435284E+06	.442287E+06
C400.202		.795800E+02	.408980E+03	.109595E+04	.508840E+03	.504924E+04	.472749E+04			
		.108716E+03	.107596E+03	.333153E+06	.362942E+06	.101984E+03	.427438E+06			
T	.539259E+03	.594138E+03	.624185E+03	.643777E+03	.744227E+03	.823036E+03	.904424E+03	.985248E+03	.971259E+03	.983145E+03
F	.187012E+06	.186145E+06	.185642E+06	.185295E+06	.183325E+06	.181633E+06	.179842E+06	.178104E+06	.178398E+06	.178147E+06
E	.367615E+06	.372275E+06	.376928E+06	.381576E+06	.390808E+06	.399985E+06	.416700E+06	.431803E+06	.439363E+06	.446915E+06
C400.203		.795800E+02	.408980E+03	.109599E+04	.508150E+03	.549220E+04	.511091E+04			
		.111969E+03	.110787E+03	.333153E+06	.363416E+06	.102822E+03	.430974E+06			
T	.588172E+03	.649126E+03	.683512E+03	.699667E+03	.804674E+03	.873695E+03	.954052E+03	.102688E+04	.997074E+03	.100813E+04
F	.201615E+06	.200565E+06	.199910E+06	.199589E+06	.197348E+06	.195794E+06	.193986E+06	.192415E+06	.193046E+06	.192809E+06
E	.368462E+06	.373494E+06	.378516E+06	.383533E+06	.393496E+06	.403409E+06	.421478E+06	.437827E+06	.446017E+06	.454201E+06
C400.204		.795800E+02	.408980E+03	.113115E+04	.505360E+03	.432371E+04	.406821E+04			
		.101300E+03	.971424E+02	.333153E+06	.362893E+06	.993260E+02	.416225E+06			
T	.446473E+03	.490616E+03	.515512E+03	.534753E+03	.630265E+03	.710078E+03	.802325E+03	.874167E+03	.898259E+03	.922751E+03
F	.161350E+06	.160920E+06	.160629E+06	.160381E+06	.158903E+06	.157424E+06	.155948E+06	.154040E+06	.153536E+06	.153028E+06
E	.366912E+06	.370926E+06	.374937E+06	.378943E+06	.386911E+06	.394828E+06	.409223E+06	.422221E+06	.428706E+06	.435176E+06
C400.205		.795800E+02	.408980E+03	.114119E+04	.504670E+03	.398856E+04	.369871E+04			
		.101300E+03	.886090E+02	.333153E+06	.362657E+06	.969243E+02	.406096E+06			
T	.411656E+03	.448559E+03	.468773E+03	.488132E+03	.570667E+03	.660585E+03	.755684E+03	.828986E+03	.863911E+03	.888491E+03
F	.146829E+06	.146546E+06	.146355E+06	.146151E+06	.145066E+06	.143567E+06	.141744E+06	.140255E+06	.139540E+06	.139039E+06
E	.366310E+06	.369961E+06	.373609E+06	.377255E+06	.384512E+06	.391719E+06	.404011E+06	.416624E+06	.422509E+06	.428378E+06

C500.051

	.949300E+02	.497360E+03	.724785E+03	.526170E+03	.540548E+04	.506161E+04	
	.136229E+03	.133539E+03	.397693E+06	.815877E+06	.106508E+03	.455002E+06	
T	.881876E+03	.911521E+03	.922388E+03	.929988E+03	.940405E+03	.974456E+03	.956559E+03	.923760E+03	.907114E+03	.915838E+03
F	.194269E+06	.193646E+06	.193404E+06	.193232E+06	.192556E+06	.192248E+06	.192641E+06	.193171E+06	.193745E+06	.193549E+06
E	.419923E+06	.423961E+06	.427995E+06	.432027E+06	.440075E+06	.448114E+06	.482872E+06	.487631E+06	.483068E+06	.489778E+06

C500.052

	.949300E+02	.497360E+03	.732879E+03	.527550E+03	.583360E+04	.546424E+04	
	.139375E+03	.136317E+03	.397693E+06	.816421E+06	.109183E+03	.457856E+06	
T	.920972E+03	.941947E+03	.958123E+03	.964453E+03	.989201E+03	.100005E+04	.981930E+03	.955318E+03	.928926E+03	.930729E+03
F	.209219E+06	.208737E+06	.208366E+06	.208222E+06	.207663E+06	.207422E+06	.207826E+06	.208430E+06	.209037E+06	.208995E+06
E	.420785E+06	.425144E+06	.429497E+06	.433849E+06	.442539E+06	.451224E+06	.467163E+06	.481678E+06	.488948E+06	.496217E+06

C500.053

	.952900E+02	.497360E+03	.724732E+03	.526860E+03	.626614E+04	.588797E+04	
	.143236E+03	.140210E+03	.399210E+06	.818212E+06	.109994E+03	.461788E+06	
T	.943683E+03	.962805E+03	.977149E+03	.984501E+03	.100761E+04	.104180E+04	.100692E+04	.982989E+03	.948521E+03	.955142E+03
F	.225057E+06	.224606E+06	.224269E+06	.224097E+06	.223558E+06	.223292E+06	.223579E+06	.224132E+06	.224943E+06	.224786E+06
E	.422912E+06	.427606E+06	.432296E+06	.436984E+06	.446347E+06	.455693E+06	.472861E+06	.488489E+06	.496319E+06	.504145E+06

C500.054

	.951100E+02	.497360E+03	.729732E+03	.526860E+03	.486938E+04	.448660E+04	
	.132010E+03	.129559E+03	.398451E+06	.816149E+06	.107592E+03	.451088E+06	
T	.838241E+03	.869479E+03	.888807E+03	.889038E+03	.912091E+03	.931147E+03	.917118E+03	.887255E+03	.873966E+03	.871392E+03
F	.172652E+06	.171975E+06	.171555E+06	.171551E+06	.171053E+06	.170645E+06	.170945E+06	.171589E+06	.171877E+06	.171933E+06
E	.419738E+06	.423317E+06	.426891E+06	.430464E+06	.437597E+06	.444719E+06	.457792E+06	.469705E+06	.475668E+06	.481632E+06

C500.055

	.947500E+02	.497360E+03	.729637E+03	.525480E+03	.446433E+04	.416812E+04	
	.128811E+03	.126492E+03	.396915E+06	.814330E+06	.106865E+03	.448053E+06	
T	.799656E+03	.832251E+03	.847523E+03	.848485E+03	.881141E+03	.898872E+03	.888374E+03	.866578E+03	.860752E+03	.853813E+03
F	.161544E+06	.160772E+06	.160447E+06	.160427E+06	.159733E+06	.159401E+06	.159568E+06	.160085E+06	.160166E+06	.160313E+06
E	.417682E+06	.421022E+06	.424359E+06	.427694E+06	.434367E+06	.440981E+06	.453177E+06	.464280E+06	.469834E+06	.475391E+06

C500.101

	.891700E+02	.497360E+03	.790041E+03	.522710E+03	.551276E+04	.516806E+04	
	.125291E+03	.124146E+03	.373448E+06	.382903E+06	.106057E+03	.444640E+06	
T	.711178E+03	.774957E+03	.818198E+03	.845267E+03	.887828E+03	.942997E+03	.971270E+03	.992942E+03	.964580E+03	.948325E+03
F	.201968E+06	.200612E+06	.199651E+06	.199040E+06	.198072E+06	.196823E+06	.196194E+06	.195720E+06	.196342E+06	.196704E+06
E	.397080E+06	.401239E+06	.405385E+06	.409523E+06	.417775E+06	.425994E+06	.441034E+06	.454687E+06	.461526E+06	.468373E+06

C500.102

	.891700E+02	.497360E+03	.825237E+03	.519940E+03	.594904E+04	.557348E+04	
	.126939E+03	.127252E+03	.373448E+06	.393942E+06	.106437E+03	.446247E+06	
T	.761315E+03	.816327E+03	.860130E+03	.880938E+03	.930684E+03	.974616E+03	.997741E+03	.102078E+04	.981367E+03	.969037E+03
F	.218948E+06	.215706E+06	.214689E+06	.214203E+06	.213039E+06	.212026E+06	.211503E+06	.210991E+06	.211868E+06	.212153E+06
E	.398437E+06	.402917E+06	.407383E+06	.411843E+06	.420735E+06	.429602E+06	.445835E+06	.460572E+06	.467958E+06	.475350E+06

C500.103

	.893500E+02	.497360E+03	.817990E+03	.523410E+03	.638577E+04	.599117E+04	
	.135479E+03	.130721E+03	.374205E+06	.394990E+06	.108345E+03	.454313E+06	
T	.802152E+03	.862867E+03	.900740E+03	.920185E+03	.974440E+03	.102476E+04	.104899E+04	.107134E+04	.100189E+04	.999832E+03
F	.232633E+06	.231193E+06	.230280E+06	.229812E+06	.228514E+06	.227344E+06	.226798E+06	.226308E+06	.227871E+06	.227918E+06
E	.399818E+06	.404629E+06	.409428E+06	.414222E+06	.423778E+06	.433308E+06	.450757E+06	.466602E+06	.474553E+06	.482506E+06

C500.104

	.891700E+02	.497360E+03	.819837E+03	.525480E+03	.518439E+04	.484409E+04	
	.122739E+03	.121620E+03	.373448E+06	.393112E+06	.105460E+03	.442117E+06	
T	.644742E+03	.737162E+03	.786703E+03	.811036E+03	.855902E+03	.900803E+03	.938489E+03	.960611E+03	.942215E+03	.952970E+03
F	.190338E+06	.188731E+06	.187468E+06	.186937E+06	.185944E+06	.184945E+06	.184115E+06	.183634E+06	.184034E+06	.183789E+06
E	.397038E+06	.400943E+06	.404831E+06	.408713E+06	.416448E+06	.424157E+06	.438250E+06	.451041E+06	.457445E+06	.463844E+06

C500.105

	.895300E+02	.497360E+03	.809679E+03	.527550E+03	.481123E+04	.450094E+04	
	.120620E+03	.119564E+03	.374963E+06	.394096E+06	.104957E+03	.439990E+06	
T	.601494E+03	.670486E+03	.733244E+03	.768296E+03	.820162E+03	.866615E+03	.904520E+03	.922555E+03	.914604E+03	.912611E+03
F	.177335E+06	.176115E+06	.174879E+06	.174151E+06	.173044E+06	.172147E+06	.171216E+06	.170829E+06	.170999E+06	.171042E+06
E	.397748E+06	.401385E+06	.405004E+06	.408613E+06	.415801E+06	.422965E+06	.436051E+06	.447929E+06	.453872E+06	.459817E+06

C500.106

	.891700E+02	.497360E+03	.794732E+03	.526860E+03	.441744E+04	.410931E+04	
	.116812E+03	.115654E+03	.373448E+06	.391919E+06	.104033E+03	.436088E+06	
T	.527354E+03	.614063E+03	.682941E+03	.716540E+03	.775997E+03	.814145E+03	.860793E+03	.885587E+03	.885587E+03	.885587E+03
F	.162814E+06	.161514E+06	.160279E+06	.159628E+06	.158423E+06	.157626E+06	.156642E+06	.156120E+06	.156120E+06	.156119E+06
E	.395263E+06	.398591E+06	.401902E+06	.405203E+06	.411772E+06	.418318E+06	.430267E+06	.441105E+06	.446524E+06	.451943E+06

C500.107

	.893500E+02	.497360E+03	.809785E+03	.526170E+03	.412601E+04	.383600E+04	
	.114734E+03	.111662E+03	.374205E+06	.392684E+06	.103919E+03	.433916E+06	
T	.473309E+03	.564269E+03	.634772E+03	.673571E+03	.738265E+03	.779878E+03	.826705E+03	.856355E+03	.859258E+03	.858845E+03
F	.153047E+06	.151904E+06	.150765E+06	.150029E+06	.148818E+06	.147978E+06	.147013E+06	.146398E+06	.146338E+06	.146387E+06
E	.395822E+06	.398946E+06	.402054E+06	.405152E+06	.411313E+06	.417450E+06	.428649E+06	.438799E+06	.443873E+06	.448948E+06

C500.201

	.799400E+02	.497360E+03	.124122E+04	.503970E+03	.521307E+04	.486662E+04	
	.103877E+03	.986592E+02	.334664E+06	.361898E+06	.100698E+03	.422009E+06	
T	.523100E+03	.554454E+03	.579294E+03	.611398E+03	.712363E+03	.782516E+03	.866329E+03	.945489E+03	.960020E+03	.971406E+03
F	.192205E+06	.191611E+06	.191442E+06	.190923E+06	.189034E+06	.187958E+06	.189712E+06	.189362E+06	.189647E+06	.189402E+06
E	.365845E+06	.369788E+06	.373726E+06	.377661E+06	.385479E+06	.393258E+06	.407428E+06	.420233E+06	.426629E+06	.433020E+06

C500.202

	.799400E+02	.497360E+03	.122119E+04	.504670E+03	.570538E+04	.535526E+04	
	.109124E+03	.106911E+03	.334664E+06	.362032E+06	.102090E+03	.427884E+06	
T	.568771E+03	.603883E+03	.631381E+03	.662976E+03	.771871E+03	.845191E+03	.920961E+03	.101944E+04	.998340E+03	.997839E+03
F	.211157E+06	.210605E+06	.210127E+06	.209543E+06	.207285E+06	.205632E+06	.203809E+06	.201689E+06	.202148E+06	.202159E+06
E	.366375E+06	.370712E+06	.375045E+06	.379370E+06	.387963E+06	.396514E+06	.412108E+06	.426195E+06	.433247E+06	.440300E+06

C500.203

	.803000E+02	.497360E+03	.118615E+04	.505360E+03	.601617E+04	.565974E+04	
	.112926E+03	.110985E+03	.336176E+06	.363221E+06	.103065E+03	.431998E+06	
T	.610053E+03	.645053E+03	.672169E+03	.701719E+03	.802317E+03	.883623E+03	.959683E+03	.106072E+04	.102490E+04	.101932E+04
F	.222888E+06	.222063E+06	.221546E+06	.220952E+06	.218749E+06	.216854E+06	.215073E+06	.212822E+06	.213596E+06	.213719E+06
E	.367809E+06	.372389E+06	.376964E+06	.381531E+06	.390611E+06	.399644E+06	.416122E+06	.431015E+06	.438476E+06	.445940E+06

C500.204

	.801200E+02	.497360E+03	.128148E+04	.499090E+03	.478103E+04	.449670E+04	
	.101300E+03	.889909E+02	.335420E+06	.362998E+06	.973496E+02	.407888E+06	
T	.472008E+03	.495848E+03	.516157E+03	.548223E+03	.635562E+03	.720088E+03	.802869E+03	.881861E+03	.905295E+03	.921337E+03
F	.177818E+06	.177570E+06	.177332E+06	.176911E+06	.175520E+06	.173914E+06	.172187E+06	.170480E+06	.169975E+06	.169631E+06
E	.366643E+06	.370286E+06	.373927E+06	.377563E+06	.384801E+06	.391998E+06	.405100E+06	.416933E+06	.422838E+06	.428736E+06

C500.205

	.799400E+02	.497360E+03	.122130E+04	.502580E+03	.446197E+04	.419843E+04	
	.101300E+03	.889909E+02	.334664E+06	.360857E+06	.967353E+02	.405289E+06	
T	.423477E+03	.451933E+03	.466689E+03	.492470E+03	.572276E+03	.663586E+03	.751950E+03	.828509E+03	.866634E+03	.885560E+03
F	.166134E+06	.165985E+06	.165851E+06	.165585E+06	.164534E+06	.162991E+06	.161243E+06	.159664E+06	.158856E+06	.158456E+06
E	.364258E+06	.367659E+06	.371058E+06	.374455E+06	.381224E+06	.387953E+06	.400200E+06	.411257E+06	.416767E+06	.422267E+06

C500.206

	.804800E+02	.497360E+03	.124119E+04	.504670E+03	.412601E+04	.388326E+04	
	.101300E+03	.889909E+02	.336931E+06	.363159E+06	.967298E+02	.405276E+06	
T	.409702E+03	.425593E+03	.433679E+03	.454868E+03	.527505E+03	.614204E+03	.700304E+03	.783012E+03	.820466E+03	.838861E+03
F	.153569E+06	.153484E+06	.153402E+06	.153224E+06	.152415E+06	.151116E+06	.149561E+06	.147914E+06	.147142E+06	.146760E+06
E	.366301E+06	.369442E+06	.372583E+06	.375722E+06	.381983E+06	.388210E+06	.399545E+06	.409769E+06	.414863E+06	.419947E+06

```
D350.101          .902500E+02 .366080E+03 .106147E+04 .516480E+03 .336134E+04 .3211578+04
                  .114357E+03 .112476E+03 .377992E+06 .408281E+06 .103475E+03 .4337308+06
  T   .739461E+03 .758496E+03 .781014E+03 .794120E+03 .800608E+03 .818148E+03 .836853E+03 .817108E+03 .806976E+03 .798816E+03
  F   .121745E+06 .121377E+06 .120936E+06 .120678E+06 .120550E+06 .120203E+06 .119793E+06 .120223E+06 .120424E+06 .120584E+06
  E   .411705E+06 .415121E+06 .418528E+06 .421930E+06 .428727E+06 .435510E+06 .447914E+06 .459220E+06 .464880E+06 .470546E+06

D350.102          .902500E+02 .366080E+03 .106433E+04 .518560E+03 .383916E+04 .3706828+06
                  .118022E+03 .115741E+03 .377992E+06 .409008E+06 .104329E+03 .4373398+06
  T  1.783106E+03 .806409E+03 .830651E+03 .844319E+03 .854644E+03 .874456E+03 .887632E+03 .853961E+03 .838771E+03 .825234E+03
  F   .140088E+06 .139614E+06 .139119E+06 .138840E+06 .138592E+06 .138232E+06 .137957E+06 .138642E+06 .138853E+06 .139229E+06
  E   .412956E+06 .416892E+06 .420819E+06 .424741E+06 .432574E+06 .440392E+06 .454706E+06 .467765E+06 .474305E+06 .480854E+06

D350.103          .906100E+02 .366080E+03 .108778E+04 .511620E+03 .427102E+04 .4113778+04
                  .120904E+03 .118723E+03 .379506E+06 .411637E+06 .105025E+03 .4402768+06
  T   .834753E+03 .860819E+03 .889007E+03 .901514E+03 .914801E+03 .924203E+03 .926445E+03 .878864E+03 .863743E+03 .844236E+03
  F   .154868E+06 .154320E+06 .153729E+06 .153468E+06 .153193E+06 .152999E+06 .152953E+06 .153942E+06 .154259E+06 .154466E+06
  E   .416010E+06 .420372E+06 .424722E+06 .429068E+06 .437748E+06 .446421E+06 .462318E+06 .476833E+06 .484101E+06 .4913638+06

D350.104          .906100E+02 .366080E+03 .110619E+04 .504670E+03 .481574E+04 .4639198+04
                  .123391E+03 .121986E+03 .379506E+06 .412782E+06 .105614E+03 .4427668+06
  T   .898034E+03 .926657E+03 .953091E+03 .964115E+03 .970394E+03 .975020E+03 .970554E+03 .906716E+03 .885385E+03 .863512E+03
  F   .173796E+06 .173136E+06 .172615E+06 .172383E+06 .172252E+06 .172136E+06 .172249E+06 .173609E+06 .174072E+06 .174546E+06
  E   .417703E+06 .422611E+06 .427510E+06 .432405E+06 .442189E+06 .451971E+06 .469909E+06 .486299E+06 .494508E+06 .5027318+06

D350.105          .902500E+02 .366080E+03 .116107E+04 .485120E+03 .538629E+04 .5127618+04
                  .132028E+03 .124594E+03 .377992E+06 .413255E+06 .107586E+03 .4511058+06
  T   .948882E+03 .970413E+03 .987678E+03 .100909E+04 .102661E+04 .104146E+04 .101251E+04 .945407E+03 .923322E+03 .899937E+03
  F   .191525E+06 .191053E+06 .190679E+06 .190222E+06 .189856E+06 .189549E+06 .190150E+06 .191602E+06 .192116E+06 .1926188+06
  E   .418690E+06 .424116E+06 .429536E+06 .434949E+06 .445762E+06 .456565E+06 .476406E+06 .494525E+06 .503600E+06 .5126908+06

D350.201          .804800E+02 .366080E+03 .162643E+04 .517170E+03 .518429E+04 .4946148+04
                  .114687E+03 .112827E+03 .336931E+06 .383289E+06 .103557E+03 .4340778+06
  T   .683645E+03 .730318E+03 .766286E+03 .795149E+03 .853518E+03 .917639E+03 .993847E+03 .981870E+03 .970495E+03 .948914E+03
  F   .189604E+06 .188666E+06 .187908E+06 .187280E+06 .185997E+06 .184573E+06 .182926E+06 .183179E+06 .183422E+06 .1838678+06
  E   .388610E+06 .393915E+06 .399205E+06 .404484E+06 .414996E+06 .425456E+06 .444527E+06 .461678E+06 .470561E+06 .4792578+06

D350.202          .806600E+02 .366080E+03 .160404E+04 .522710E+03 .577866E+04 .5624738+06
                  .119821E+03 .117444E+03 .337687E+06 .384395E+06 .104765E+03 .4391808+06
  T   .710382E+03 .748516E+03 .834083E+03 .860362E+03 .914998E+03 .981595E+03 .104918E+04 .101025E+04 .990268E+03 .963717E+03
  F   .214898E+06 .213600E+06 .212582E+06 .211972E+06 .210700E+06 .209170E+06 .207689E+06 .208313E+06 .208975E+06 .2095768+06
  E   .390437E+06 .396457E+06 .402459E+06 .408450E+06 .420390E+06 .432278E+06 .453987E+06 .473766E+06 .483667E+06 .4935658+06

D350.203          .799400E+02 .366080E+03 .162922E+04 .503970E+03 .635885E+04 .6198978+06
                  .122874E+03 .120270E+03 .334664E+06 .382745E+06 .105492E+03 .4422528+06
  T   .734523E+03 .829537E+03 .889667E+03 .921878E+03 .974040E+03 .103491E+04 .109321E+04 .104501E+04 .101002E+04 .9816838+03
  F   .236549E+06 .234807E+06 .233359E+06 .232579E+06 .231325E+06 .229905E+06 .228624E+06 .229677E+06 .230478E+06 .2311438+06
  E   .389402E+06 .396031E+06 .402635E+06 .409227E+06 .422369E+06 .435469E+06 .459417E+06 .481238E+06 .492168E+06 .5031168+06

D350.204          .801200E+02 .366080E+03 .161978E+04 .511620E+03 .521164E+04 .5081748+06
                  .115414E+03 .113320E+03 .835420E+06 .381790E+06 .103688E+03 .4346308+06
  T   .631104E+03 .693309E+03 .763499E+03 .794797E+03 .847169E+03 .910141E+03 .999161E+03 .984881E+03 .970381E+03 .945435E+03
  F   .195698E+06 .194527E+06 .193071E+06 .192391E+06 .191227E+06 .189815E+06 .187870E+06 .188174E+06 .188487E+06 .1890328+06
  E   .387271E+06 .392733E+06 .398168E+06 .403591E+06 .414396E+06 .425149E+06 .444740E+06 .462567E+06 .471490E+06 .4806428+06

D350.205          .803000E+02 .366080E+03 .160952E+04 .515790E+03 .460253E+04 .4378068+06
                  .110379E+03 .108588E+03 .336176E+06 .381362E+06 .102415E+03 .4392558+06
  T   .555683E+03 .615499E+03 .680575E+03 .716450E+03 .775381E+03 .839090E+03 .930328E+03 .943375E+03 .935755E+03 .926082E+03
  F   .169541E+06 .168605E+06 .167431E+06 .166734E+06 .165529E+06 .164179E+06 .162240E+06 .161968E+06 .162136E+06 .1623298+06
  E   .386097E+06 .390817E+06 .395515E+06 .400201E+06 .409525E+06 .418798E+06 .435663E+06 .450979E+06 .458641E+06 .4663108+06

D350.206          .801200E+02 .366080E+03 .158233E+04 .518560E+03 .431464E+04 .4205568+06
                  .108700E+03 .106998E+03 .335420E+06 .379700E+06 .101980E+03 .4274168+06
  T   .494330E+03 .549501E+03 .603803E+03 .639522E+03 .711331E+03 .774503E+03 .874251E+03 .898233E+03 .901488E+03 .901488E+03
  F   .163213E+06 .162514E+06 .161685E+06 .161076E+06 .159731E+06 .158454E+06 .156358E+06 .155855E+06 .155786E+06 .1557868+06
  E   .384249E+06 .388788E+06 .393312E+06 .397825E+06 .406799E+06 .415725E+06 .431939E+06 .446647E+06 .453999E+06 .4611518+06

D400.101          .888900E+02 .396840E+03 .107830E+04 .502580E+03 .467183E+04 .4519028+06
                  .124459E+03 .120681E+03 .376477E+06 .406392E+06 .105864E+03 .4438238+06
  T   .818538E+03 .827713E+03 .853603E+03 .884158E+03 .901343E+03 .925997E+03 .948637E+03 .900201E+03 .885440E+03 .860633E+03
  F   .170636E+06 .170439E+06 .169880E+06 .169220E+06 .168850E+06 .168323E+06 .167845E+06 .168874E+06 .169192E+06 .1697278+06
  E   .410833E+06 .415271E+06 .419699E+06 .424116E+06 .432937E+06 .441739E+06 .457846E+06 .472551E+06 .479911E+06 .4872878+06

D400.102          .900700E+02 .396840E+03 .110074E+04 .493510E+03 .556500E+04 .5374828+06
                  .129756E+03 .126464E+03 .377234E+06 .408695E+06 .107078E+03 .4489558+06
  T   .899835E+03 .904182E+03 .930816E+03 .940734E+03 .961693E+03 .100013E+04 .100472E+04 .942955E+03 .915100E+03 .887785E+03
  F   .201735E+06 .201463E+06 .201029E+06 .200624E+06 .199888E+06 .199483E+06 .199384E+06 .200754E+06 .201387E+06 .2020128+06
  E   .413965E+06 .419232E+06 .424490E+06 .429741E+06 .440221E+06 .450689E+06 .469874E+06 .487386E+06 .496158E+06 .5049478+06

D400.103          .900900E+02 .396840E+03 .114277E+04 .492810E+03 .623714E+04 .6048838+06
                  .134316E+03 .130762E+03 .377234E+06 .410499E+06 .108091E+03 .4532408+06
  T   .925616E+03 .953955E+03 .972567E+03 .994363E+03 .103259E+04 .104930E+04 .104179E+04 .964263E+03 .938028E+03 .913985E+03
  F   .226089E+06 .226214E+06 .225774E+06 .225264E+06 .224390E+06 .224018E+06 .224165E+06 .225970E+06 .226393E+06 .2271688+06
  E   .416391E+06 .422114E+06 .427830E+06 .434139E+06 .445932E+06 .457714E+06 .479324E+06 .499054E+06 .508935E+06 .5188308+06

D400.104          .898900E+02 .396840E+03 .108730E+04 .502580E+03 .400988E+04 .3854628+06
                  .113378E+03 .111615E+03 .376477E+06 .405782E+06 .103179E+03 .4324808+06
  T   .766746E+03 .768638E+03 .789278E+03 .797700E+03 .828934E+03 .861137E+03 .886279E+03 .855870E+03 .838887E+03 .823877E+03
  F   .145990E+06 .145953E+06 .145532E+06 .145340E+06 .144717E+06 .144052E+06 .143535E+06 .144160E+06 .144511E+06 .1448208+06
  E   .409574E+06 .413365E+06 .417148E+06 .420928E+06 .428465E+06 .435977E+06 .449719E+06 .462242E+06 .468516E+06 .4748008+06

D400.201          .808500E+02 .396840E+03 .152404E+04 .512710E+03 .542732E+04 .5284878+06
                  .116574E+03 .114427E+03 .338485E+06 .379351E+06 .103975E+03 .4358428+06
  T   .658914E+03 .712200E+03 .758537E+03 .797049E+03 .858660E+03 .920542E+03 .100017E+04 .987423E+03 .977148E+03 .956458E+03
  F   .203998E+06 .201947E+06 .200984E+06 .200124E+06 .198736E+06 .197329E+06 .195564E+06 .195840E+06 .196065E+06 .1965228+06
  E   .384602E+06 .389836E+06 .395051E+06 .400258E+06 .410621E+06 .420938E+06 .439722E+06 .456869E+06 .465434E+06 .4740108+06

D400.202          .806600E+02 .396840E+03 .156665E+04 .513700E+03 .617260E+04 .5988138+06
                  .121701E+03 .118961E+03 .337687E+06 .380364E+06 .105143E+03 .4407788+06
  T   .718684E+03 .779731E+03 .837621E+03 .875925E+03 .931977E+03 .992695E+03 .106301E+04 .103129E+04 .100694E+04 .983003E+03
  F   .228893E+06 .227545E+06 .226199E+06 .225289E+06 .223952E+06 .222527E+06 .220952E+06 .221648E+06 .222199E+06 .2227508+06
  E   .386300E+06 .392213E+06 .398106E+06 .403984E+06 .415700E+06 .427372E+06 .448692E+06 .468105E+06 .477824E+06 .4875578+06

D400.203          .804800E+02 .396840E+03 .158678E+04 .511620E+03 .664869E+04 .6440058+06
                  .124554E+03 .121894E+03 .336931E+06 .380644E+06 .105886E+03 .4439168+06
  T   .771520E+03 .841166E+03 .895938E+03 .931777E+03 .982810E+03 .104570E+04 .110689E+04 .105767E+04 .102839E+04 .987007E+03
  F   .246201E+06 .244544E+06 .243200E+06 .242316E+06 .241068E+06 .239580E+06 .238220E+06 .239305E+06 .240029E+06 .2409668+06
  E   .387042E+06 .393414E+06 .399765E+06 .406103E+06 .418743E+06 .431342E+06 .454377E+06 .475363E+06 .485672E+06 .4964038+06

D400.204          .806600E+02 .396840E+03 .157561E+04 .514400E+03 .493117E+04 .4760088+06
                  .113237E+03 .110327E+03 .337687E+06 .379069E+06 .102913E+03 .4213588+06
  T   .563793E+03 .626574E+03 .706858E+03 .744258E+03 .789418E+03 .847114E+03 .943297E+03 .953051E+03 .943668E+03 .936448E+03
  F   .184102E+06 .183088E+06 .181981E+06 .180818E+06 .179862E+06 .178602E+06 .176508E+06 .176300E+06 .176500E+06 .1766558+06
  E   .383814E+06 .388544E+06 .393249E+06 .397942E+06 .407293E+06 .416602E+06 .433539E+06 .448924E+06 .456832E+06 .4643248+06

D400.205          .801200E+02 .396840E+03 .156530E+04 .502580E+03 .443301E+04 .4325758+06
                  .108221E+03 .105744E+03 .335420E+06 .376031E+06 .101855E+03 .4268908+06
  T   .504372E+03 .575179E+03 .639459E+03 .670147E+03 .716480E+03 .782831E+03 .881949E+03 .914723E+03 .920952E+03 .916205E+03
  F   .167826E+06 .166868E+06 .165805E+06 .165246E+06 .164352E+06 .162996E+06 .160894E+06 .160202E+06 .160072E+06 .1601718+06
  E   .380350E+06 .384652E+06 .388938E+06 .393214E+06 .401734E+06 .410207E+06 .425603E+06 .439560E+06 .446534E+06 .4535128+06
```

D400.206

	.801200E+02	.396840E+03	.156117E+04	.501190E+03	.398438E+04	.388637E+06		
	.101300E+03	.986655E+02	.335420E+06	.375398E+06	.999489E+02	.418649E+06		
T .442034E+03	.501855E+03	.362168E+03	.384940E+03	.630404E+03	.704619E+03	.806143E+03	.854948E+03	.871710E+03	.874283E+03
F .151077E+06	.150473E+06	.149670E+06	.149335E+06	.148580E+06	.147225E+06	.145182E+06	.144179E+06	.143834E+06	.143780E+06
E .379279E+06	.383145E+06	.387003E+06	.390855E+06	.398532E+06	.406161E+06	.420010E+06	.432538E+06	.438792E+06	.445043E+06

D500.051

	.949300E+02	.495290E+03	.100061E+04	.514400E+03	.493704E+04	.477274E+04		
	.132805E+03	.130384E+03	.395419E+06	.418235E+06	.107759E+03	.451833E+06		
T .873992E+03	.904438E+03	.916005E+03	.926170E+03	.926170E+03	.944085E+03	.949033E+03	.894774E+03	.871668E+03	.847300E+03
F .179267E+06	.176599E+06	.178346E+06	.178125E+06	.178125E+06	.177738E+06	.177632E+06	.178811E+06	.179318E+06	.179854E+06
E .421982E+06	.425721E+06	.429456E+06	.433187E+06	.440651E+06	.448105E+06	.461765E+06	.474235E+06	.480492E+06	.486741E+06

D500.052

	.949300E+02	.495290E+03	.100861E+04	.514400E+03	.568016E+04	.551261E+04		
	.138572E+03	.136804E+03	.397693E+06	.421374E+06	.109012E+03	.457133E+06		
T .938250E+03	.958151E+03	.972784E+03	.983831E+03	.981958E+03	.996950E+03	.993966E+03	.929846E+03	.900427E+03	.869073E+03
F .206154E+06	.205702E+06	.205371E+06	.205123E+06	.205165E+06	.204832E+06	.204898E+06	.206348E+06	.207027E+06	.207752E+06
E .425695E+06	.430011E+06	.434323E+06	.438632E+06	.447250E+06	.455861E+06	.471650E+06	.486063E+06	.493284E+06	.500521E+06

D500.053

	.949300E+02	.495290E+03	.104271E+04	.494210E+03	.628986E+04	.612406E+04		
	.142952E+03	.140356E+03	.395419E+06	.420305E+06	.109934E+03	.461038E+06		
T .968861E+03	.974070E+03	.987142E+03	.997569E+03	.101779E+04	.103585E+04	.102783E+04	.953675E+03	.923605E+03	.895079E+03
F .228645E+06	.228523E+06	.228315E+06	.227971E+06	.227504E+06	.227093E+06	.227274E+06	.229008E+06	.229681E+06	.230417E+06
E .425105E+06	.429903E+06	.434698E+06	.439490E+06	.449063E+06	.458626E+06	.476168E+06	.492181E+06	.500201E+06	.508236E+06

D500.054

	.938500E+02	.495290E+03	.999476E+03	.499090E+03	.439091E+04	.416621E+04		
	.127087E+03	.124952E+03	.393145E+06	.415359E+06	.106471E+03	.446391E+06		
T .823319E+03	.842176E+03	.856236E+03	.867717E+03	.869655E+03	.886137E+03	.904693E+03	.863717E+03	.848525E+03	.818692E+03
F .157433E+06	.157035E+06	.156738E+06	.156581E+06	.156455E+06	.156108E+06	.155720E+06	.156581E+06	.156901E+06	.157530E+06
E .418643E+06	.421921E+06	.425195E+06	.428467E+06	.435007E+06	.441536E+06	.453487E+06	.464393E+06	.469853E+06	.475329E+06

D500.201

	.808500E+02	.495290E+03	.161095E+04	.508840E+03	.608892E+04	.592265E+04		
	.116110E+03	.114638E+03	.338485E+06	.373409E+06	.103860E+03	.435358E+06		
T .673521E+03	.723099E+03	.759249E+03	.788884E+03	.838405E+03	.914046E+03	.100269E+04	.101926E+04	.102485E+04	.100785E+04
F .227041E+06	.226021E+06	.225232E+06	.224563E+06	.223413E+06	.221619E+06	.219548E+06	.219174E+06	.219048E+06	.219430E+06
E .378117E+06	.382813E+06	.387499E+06	.392178E+06	.401503E+06	.410784E+06	.427709E+06	.443081E+06	.450764E+06	.458455E+06

D500.202

	.803000E+02	.495290E+03	.166130E+04	.502580E+03	.691131E+04	.673716E+04		
	.121921E+03	.120275E+03	.336176E+06	.372840E+06	.105267E+03	.441300E+06		
T .727336E+03	.775777E+03	.819199E+03	.854607E+03	.916887E+03	.981470E+03	.107800E+04	.107295E+04	.106871E+04	.104582E+04
F .257438E+06	.256329E+06	.255287E+06	.254415E+06	.252855E+06	.251242E+06	.248935E+06	.249051E+06	.249148E+06	.249682E+06
E .378189E+06	.383526E+06	.388850E+06	.394164E+06	.404755E+06	.415310E+06	.434569E+06	.452081E+06	.460839E+06	.469606E+06

D500.203

	.801200E+02	.495290E+03	.161974E+04	.493510E+03	.550419E+04	.533577E+04		
	.108814E+03	.107388E+03	.335420E+06	.369923E+06	.102010E+03	.427544E+06		
T .567234E+03	.611214E+03	.662043E+03	.709498E+03	.781494E+03	.834943E+03	.929041E+03	.964075E+03	.977134E+03	.982953E+03
F .205880E+06	.205179E+06	.204264E+06	.203326E+06	.202228E+06	.200593E+06	.198451E+06	.197665E+06	.197376E+06	.197248E+06
E .374175E+06	.378420E+06	.382653E+06	.386875E+06	.395290E+06	.403663E+06	.418910E+06	.432738E+06	.439648E+06	.446551E+06

D500.204

	.801200E+02	.495290E+03	.162456E+04	.515090E+03	.496402E+04	.484071E+04		
	.101342E+03	.984331E+02	.335420E+06	.369523E+06	.100004E+03	.419083E+06		
T .536201E+03	.572829E+03	.619776E+03	.663308E+03	.711044E+03	.775704E+03	.871294E+03	.914509E+03	.936421E+03	.943641E+03
F .186999E+06	.186479E+06	.185719E+06	.184935E+06	.184006E+06	.182659E+06	.180571E+06	.179621E+06	.179145E+06	.178988E+06
E .373381E+06	.377233E+06	.381076E+06	.384909E+06	.392551E+06	.400157E+06	.413995E+06	.426533E+06	.432791E+06	.439046E+06

```
E100.021        .979900E+02 .101510E+03 .418739E+03 .512320E+03 .215943E+04 .197279E+04
                .107773E+03 .106374E+03 .410588E+06 .456379E+06 .101737E+03 .426395E+06
  T   .642163E+03 .701971E+03 .724312E+03 .755429E+03 .796694E+03 .829511E+03 .866779E+03 .872513E+03 .867610E+03 .875836E+03
  F   .771036E+05 .760639E+05 .756433E+05 .750980E+05 .743433E+05 .737449E+05 .730741E+05 .729721E+05 .730593E+05 .729128E+05
  E   .464170E+06 .471873E+06 .479543E+06 .487164E+06 .502279E+06 .517293E+06 .544611E+06 .569417E+06 .581833E+06 .594227E+06

E100.022        .979900E+02 .101510E+03 .415563E+03 .515090E+03 .252958E+04 .231333E+04
                .108750E+03 .107234E+03 .410588E+06 .457594E+06 .101993E+03 .427473E+06
  T   .591906E+03 .762399E+03 .783729E+03 .821724E+03 .861589E+03 .897689E+03 .926902E+03 .929614E+03 .918065E+03 .924941E+03
  F   .899631E+05 .886694E+05 .882713E+05 .875604E+05 .868209E+05 .861640E+05 .856463E+05 .855990E+05 .858014E+05 .856601E+05
  E   .466701E+06 .475703E+06 .484672E+06 .493582E+06 .511282E+06 .528876E+06 .560978E+06 .590149E+06 .604762E+06 .619358E+06

E100.023        .979900E+02 .101510E+03 .414518E+03 .529620E+03 .287145E+04 .263595E+04
                .109659E+03 .108039E+03 .410588E+06 .458903E+06 .102229E+03 .428470E+06
  T   .749057E+03 .812054E+03 .833276E+03 .870101E+03 .913411E+03 .944517E+03 .975462E+03 .973931E+03 .964263E+03 .971189E+03
  F   .101780E+06 .100588E+06 .100175E+06 .994725E+05 .986721E+05 .981120E+05 .975743E+05 .976004E+05 .977665E+05 .976467E+05
  E   .469232E+06 .479463E+06 .489663E+06 .499806E+06 .519968E+06 .540042E+06 .576695E+06 .610023E+06 .626708E+06 .643377E+06

E100.024        .979900E+02 .101510E+03 .428332E+03 .518560E+03 .181715E+04 .164282E+04
                .106808E+03 .105527E+03 .410588E+06 .455761E+06 .101483E+03 .425322E+06
  T   .576612E+03 .635516E+03 .660748E+03 .696327E+03 .739341E+03 .765631E+03 .796854E+03 .806290E+03 .806290E+03 .812865E+03
  F   .647299E+05 .637904E+05 .633661E+05 .627507E+05 .619894E+05 .615191E+05 .609600E+05 .607915E+05 .607915E+05 .606733E+05
  E   .462286E+06 .468730E+06 .475138E+06 .481492E+06 .494066E+06 .506558E+06 .529281E+06 .549888E+06 .560192E+06 .570479E+06

E100.025        .979900E+02 .101510E+03 .422510E+03 .490400E+03 .144658E+04 .129637E+04
                .105751E+03 .104611E+03 .410588E+06 .453696E+06 .101202E+03 .424135E+06
  T   .505123E+03 .551101E+03 .573880E+03 .609527E+03 .649177E+03 .676886E+03 .712761E+03 .728921E+03 .734625E+03 .740949E+03
  F   .514751E+05 .508411E+05 .505037E+05 .499488E+05 .493006E+05 .488330E+05 .482148E+05 .479332E+05 .478335E+05 .477224E+05
  E   .458872E+06 .463992E+06 .469083E+06 .474124E+06 .484089E+06 .493971E+06 .511883E+06 .528081E+06 .536165E+06 .544233E+06

E100.026        .983500E+02 .101510E+03 .427904E+03 .407590E+03 .114186E+04 .104411E+04
                .105016E+03 .103963E+03 .412106E+06 .454511E+06 .101005E+03 .423305E+06
  T   .419811E+03 .460321E+03 .485110E+03 .512670E+03 .545663E+03 .574032E+03 .613478E+03 .633680E+03 .641155E+03 .647394E+03
  F   .416413E+05 .412105E+05 .409141E+05 .405580E+05 .400995E+05 .396804E+05 .390661E+05 .387396E+05 .386169E+05 .400743E+05
  E   .458686E+06 .462823E+06 .466935E+06 .471014E+06 .479089E+06 .487088E+06 .501546E+06 .514590E+06 .521051E+06 .527819E+06

E100.101        .893500E+02 .101510E+03 .292837E+03 .525480E+03 .263124E+04 .246101E+04
                .107734E+03 .106544E+03 .374205E+06 .411000E+06 .101727E+03 .426351E+06
  T   .657847E+03 .697733E+03 .730549E+03 .776777E+03 .825775E+03 .861518E+03 .912882E+03 .931107E+03 .931107E+03 .934439E+03
  F   .959649E+05 .952756E+05 .946737E+05 .938081E+05 .928834E+05 .922136E+05 .912729E+05 .909486E+05 .909486E+05 .908484E+05
  E   .420705E+06 .430352E+06 .439951E+06 .449480E+06 .468388E+06 .487187E+06 .521377E+06 .552373E+06 .567872E+06 .583362E+06

E100.102        .898900E+02 .101510E+03 .279626E+03 .528240E+03 .313204E+04 .293523E+04
                .108678E+03 .107819E+03 .376477E+06 .414194E+06 .101974E+03 .427395E+06
  T   .762580E+03 .814680E+03 .832820E+03 .884084E+03 .917787E+03 .971286E+03 .100555E+04 .100567E+04 .100385E+04 .100567E+04
  F   .113185E+06 .112173E+06 .111820E+06 .110827E+06 .110189E+06 .109213E+06 .108621E+06 .108619E+06 .108649E+06 .108618E+06
  E   .425685E+06 .437097E+06 .448481E+06 .459789E+06 .482309E+06 .504682E+06 .545541E+06 .582686E+06 .601261E+06 .619834E+06

E100.103        .898900E+02 .101510E+03 .296518E+03 .515790E+03 .223854E+04 .206869E+04
                .106677E+03 .105626E+03 .376477E+06 .411873E+06 .101448E+03 .425174E+06
  T   .593676E+03 .634000E+03 .664872E+03 .709696E+03 .755158E+03 .793022E+03 .840501E+03 .861907E+03 .869113E+03 .875158E+03
  F   .812310E+03 .805761E+05 .800536E+05 .792574E+05 .784309E+05 .777248E+05 .768648E+05 .764773E+05 .763480E+05 .762394E+05
  E   .420067E+06 .428206E+06 .436302E+06 .444332E+06 .460251E+06 .476054E+06 .504757E+06 .530743E+06 .543718E+06 .556678E+06

E100.104        .906800E+02 .101510E+03 .306783E+03 .511620E+03 .187644E+04 .166914E+04
                .105443E+03 .104673E+03 .379801E+06 .414358E+06 .101120E+03 .423788E+06
  T   .532478E+03 .568243E+03 .603947E+03 .655506E+03 .683807E+03 .717755E+03 .764046E+03 .812516E+03 .832039E+03 .837563E+03
  F   .661275E+05 .656117E+05 .650597E+05 .645461E+05 .637240E+05 .631277E+05 .619424E+05 .614331E+05 .610863E+05 .609882E+05
  E   .421014E+06 .427626E+06 .434190E+06 .440711E+06 .453809E+06 .466404E+06 .489480E+06 .510311E+06 .520674E+06 .531027E+06

E100.105        .900700E+02 .101510E+03 .285706E+03 .454220E+03 .160512E+04 .146602E+04
                .104492E+03 .104036E+03 .377234E+06 .408978E+06 .100864E+03 .422711E+06
  T   .437045E+03 .465353E+03 .507853E+03 .543596E+03 .595230E+03 .634331E+03 .698252E+03 .727172E+03 .743054E+03 .755692E+03
  F   .584778E+05 .581710E+05 .576534E+05 .571651E+05 .563909E+05 .557612E+05 .546759E+05 .541891E+05 .538890E+05 .536652E+05
  E   .414845E+06 .420686E+06 .426484E+06 .432239E+06 .443616E+06 .454881E+06 .475181E+06 .493486E+06 .502597E+06 .511674E+06

E100.201        .803000E+02 .101510E+03 .624779E+03 .317870E+03 .295063E+04 .268429E+04
                .110444E+03 .106032E+03 .316176E+06 .403170E+06 .102432E+03 .429326E+06
  T   .624610E+03 .712411E+03 .748063E+03 .800878E+03 .903801E+03 .975813E+03 .102817E+04 .102171E+04 .100565E+04 .100577E+04
  F   .105923E+06 .104367E+06 .103700E+06 .102553E+06 .100742E+06 .994520E+05 .985939E+05 .986955E+05 .989536E+05 .989510E+05
  E   .413866E+06 .424440E+06 .434962E+06 .445392E+06 .465966E+06 .486346E+06 .523472E+06 .557249E+06 .574168E+06 .591087E+06

E100.202        .803000E+02 .101510E+03 .638739E+03 .312320E+03 .261346E+04 .238697E+04
                .106010E+03 .105262E+03 .336176E+06 .403117E+06 .101271E+03 .424426E+06
  T   .565839E+03 .647821E+03 .691871E+03 .740403E+03 .825777E+03 .882777E+03 .949500E+03 .961059E+03 .954004E+03 .959418E+03
  F   .947535E+05 .934332E+05 .926581E+05 .917696E+05 .901693E+05 .891121E+05 .879276E+05 .877311E+05 .878507E+05 .877583E+05
  E   .412665E+06 .422108E+06 .431488E+06 .440796E+06 .459152E+06 .477335E+06 .510326E+06 .540266E+06 .555251E+06 .570225E+06

E100.203        .803000E+02 .101510E+03 .648826E+03 .491420E+03 .238144E+04 .216291E+04
                .105501E+03 .104668E+03 .336176E+06 .403043E+06 .101113E+03 .423853E+06
  T   .507421E+03 .591875E+03 .637807E+03 .681293E+03 .783492E+03 .850730E+03 .927249E+03 .933553E+03 .935007E+03 .927249E+03
  F   .867278E+05 .855207E+05 .847726E+05 .840210E+05 .821580E+05 .809176E+05 .795559E+05 .794480E+05 .795945E+05 .795552E+05
  E   .411764E+06 .420390E+06 .428955E+06 .437457E+06 .454152E+06 .470641E+06 .500461E+06 .527541E+06 .541100E+06 .554654E+06

E200.011        .985300E+02 .201540E+03 .427125E+03 .534450E+03 .338488E+04 .317174E+04
                .117529E+03 .114635E+03 .412845E+06 .438846E+06 .104209E+03 .436831E+06
  T   .764904E+03 .817108E+03 .828972E+03 .861218E+03 .886005E+03 .889629E+03 .883993E+03 .850656E+03 .835159E+03 .833044E+03
  F   .121251E+06 .120223E+06 .119989E+06 .119352E+06 .118867E+06 .118797E+06 .118906E+06 .119560E+06 .119866E+06 .119908E+06
  E   .445047E+06 .451208E+06 .457360E+06 .463488E+06 .475706E+06 .487920E+06 .510326E+06 .530778E+06 .541024E+06 .551272E+06

E200.012        .985300E+02 .201540E+03 .427067E+03 .535140E+03 .381775E+04 .357550E+04
                .119362E+03 .116257E+03 .412865E+06 .439719E+06 .104654E+03 .438713E+06
  T   .815109E+03 .869698E+03 .891668E+03 .917534E+03 .936915E+03 .953972E+03 .918194E+03 .889451E+03 .868446E+03 .863961E+03
  F   .136152E+06 .135044E+06 .134571E+06 .134085E+06 .133704E+06 .133762E+06 .134072E+06 .134644E+06 .135070E+06 .135160E+06
  E   .446695E+06 .453631E+06 .460550E+06 .467451E+06 .481226E+06 .495004E+06 .520306E+06 .543377E+06 .554939E+06 .566506E+06

E200.013        .985300E+02 .201540E+03 .426588E+03 .540640E+03 .432371E+04 .406477E+04
                .121557E+03 .118209E+03 .412865E+06 .440790E+06 .105180E+03 .440935E+06
  T   .863793E+03 .930430E+03 .949303E+03 .975234E+03 .985526E+03 .985266E+03 .960367E+03 .921029E+03 .901163E+03 .896938E+03
  F   .154257E+06 .152871E+06 .152487E+06 .151968E+06 .151765E+06 .151771E+06 .152284E+06 .153064E+06 .153476E+06 .153563E+06
  E   .448671E+06 .456544E+06 .464401E+06 .472244E+06 .487914E+06 .503585E+06 .533274E+06 .558628E+06 .571793E+06 .584954E+06

E200.014        .985300E+02 .201540E+03 .426949E+03 .536520E+03 .310427E+04 .288834E+04
                .116227E+03 .113488E+03 .412865E+06 .438220E+06 .103889E+03 .435480E+06
  T   .738738E+03 .786784E+03 .805715E+03 .834206E+03 .861344E+03 .865166E+03 .864317E+03 .835287E+03 .821472E+03 .817258E+03
  F   .110674E+06 .109752E+06 .109385E+06 .108832E+06 .108304E+06 .108214E+06 .108251E+06 .108811E+06 .109079E+06 .109160E+06
  E   .443883E+06 .449501E+06 .455104E+06 .460665E+06 .471806E+06 .482922E+06 .503503E+06 .521904E+06 .531223E+06 .540546E+06

E200.015        .985300E+02 .201540E+03 .444296E+03 .533380E+03 .273788E+04 .255312E+04
                .114687E+03 .112118E+03 .412865E+06 .438263E+06 .103507E+03 .433866E+06
  T   .677073E+03 .734889E+03 .760056E+03 .789867E+03 .803031E+03 .812450E+03 .810368E+03 .792800E+03 .781309E+03 .780278E+03
  F   .964158E+05 .973590E+05 .968873E+05 .963223E+05 .960735E+05 .958948E+05 .959343E+05 .962677E+05 .964856E+05 .965046E+05
  E   .443279E+06 .448251E+06 .453205E+06 .458136E+06 .467977E+06 .477803E+06 .495825E+06 .512253E+06 .520481E+06 .528711E+06

E200.016        .987100E+02 .201540E+03 .446785E+03 .526170E+03 .244465E+04 .228266E+04
                .113505E+03 .111072E+03 .413624E+06 .438338E+06 .103211E+03 .432615E+06
  T   .624846E+03 .677214E+03 .701422E+03 .734143E+03 .763011E+03 .773101E+03 .775383E+03 .756365E+03 .745424E+03 .744213E+03
  F   .884738E+05 .875754E+05 .871073E+05 .865471E+05 .860133E+05 .858258E+05 .857833E+05 .861367E+05 .863392E+05 .863611E+05
  E   .443036E+06 .447501E+06 .451945E+06 .456365E+06 .465161E+06 .473942E+06 .490033E+06 .504711E+06 .512063E+06 .519418E+06
```

```
E200.017        .983500E+02 .201540E+03 .447426E+03 .517170E+03 .214678E+04 .200119E+04
                .111986E+03 .109749E+03 .412106E+06 .436441E+06 .102826E+06 .430993E+06
  T   .591980E+03 .636678E+03 .658098E+03 .679470E+03 .710049E+03 .726944E+03 .776483E+03 .724982E+03 .715163E+03 .711110E+03
  F   .779216E+05 .771928E+05 .768328E+05 .764620E+05 .759197E+05 .756157E+05 .754429E+05 .756511E+05 .758280E+05 .759002E+05
  E   .440399E+06 .444327E+06 .448240E+06 .452137E+06 .459885E+06 .467607E+06 .481736E+06 .494611E+06 .501061E+06 .507516E+06

E200.101        .902500E+02 .204670E+03 .325371E+03 .571350E+03 .364105E+04 .347148E+04
                .114667E+03 .112731E+03 .377992E+06 .399761E+06 .103502E+03 .433845E+06
  T   .694172E+03 .731398E+03 .760367E+03 .809853E+03 .878187E+03 .912455E+03 .929134E+03 .907820E+03 .898520E+03 .888589E+03
  F   .134200E+06 .133488E+06 .132919E+06 .131929E+06 .130953E+06 .129872E+06 .129544E+06 .129964E+06 .130148E+06 .130345E+06
  E   .406500E+06 .413211E+06 .419905E+06 .426560E+06 .439770E+06 .452931E+06 .477017E+06 .498963E+06 .509947E+06 .520943E+06

E200.102        .898900E+02 .204670E+03 .316709E+03 .576760E+03 .423151E+04 .406802E+04
                .117208E+03 .115036E+03 .376477E+06 .399139E+06 .104130E+03 .436499E+06
  T   .772610E+03 .817738E+03 .845778E+03 .901594E+03 .960837E+03 .977617E+03 .983754E+03 .958725E+03 .944357E+03 .930430E+03
  F   .156164E+06 .155226E+06 .154637E+06 .153467E+06 .152254E+06 .151921E+06 .151800E+06 .152297E+06 .152567E+06 .152870E+06
  E   .407006E+06 .414839E+06 .422652E+06 .430425E+06 .445867E+06 .461328E+06 .489621E+06 .515396E+06 .528300E+06 .541220E+06

E200.103        .900700E+02 .204670E+03 .335313E+03 .563210E+03 .329105E+04 .312876E+04
                .113071E+03 .111231E+03 .377234E+06 .398699E+06 .103101E+03 .432154E+06
  T   .622463E+03 .678885E+03 .710549E+03 .747367E+03 .817132E+03 .861232E+03 .882034E+03 .870101E+03 .861442E+03 .856176E+03
  F   .121814E+06 .120824E+06 .120238E+06 .119535E+06 .118169E+06 .117302E+06 .116898E+06 .117128E+06 .117298E+06 .117400E+06
  E   .404600E+06 .410863E+06 .416905E+06 .422920E+06 .434847E+06 .446707E+06 .468396E+06 .488142E+06 .498026E+06 .507916E+06

E200.104        .900700E+02 .204670E+03 .336689E+03 .559800E+03 .289008E+04 .275780E+04
                .111759E+03 .109657E+03 .377234E+06 .397955E+06 .102768E+03 .430748E+06
  T   .549210E+03 .597069E+03 .633161E+03 .682617E+03 .742665E+03 .795854E+03 .824363E+03 .825655E+03 .821541E+03 .815494E+03
  F   .108062E+06 .107339E+06 .106708E+06 .106236E+06 .104746E+06 .103751E+06 .103203E+06 .103178E+06 .103257E+06 .103373E+06
  E   .403353E+06 .408723E+06 .414070E+06 .419398E+06 .429940E+06 .440402E+06 .459503E+06 .476865E+06 .485551E+06 .494244E+06

E200.201        .804800E+02 .204670E+03 .552540E+03 .561160E+03 .471410E+04 .453896E+04
                .115109E+03 .113255E+03 .334931E+06 .370857E+06 .103612E+03 .434310E+06
  T   .634423E+03 .693641E+03 .745667E+03 .807242E+03 .895737E+03 .974695E+03 .102745E+04 .100503E+04 .993218E+03 .985198E+03
  F   .176774E+06 .175671E+06 .174623E+06 .173322E+06 .171406E+06 .169730E+06 .168668E+06 .169112E+06 .169350E+06 .169513E+06
  E   .379714E+06 .388536E+06 .397322E+06 .406065E+06 .423423E+06 .440671E+06 .472177E+06 .500859E+06 .515209E+06 .529571E+06

E300.011        .985300E+02 .304550E+03 .459182E+03 .533746OE+03 .407784E+04 .387491E+04
                .128263E+03 .122828E+03 .412865E+06 .431982E+06 .106282E+03 .445590E+06
  T   .782702E+03 .847683E+03 .874729E+03 .907650E+03 .913559E+03 .912896E+03 .885703E+03 .838541E+03 .809761E+03 .799727E+03
  F   .147920E+06 .146578E+06 .146018E+06 .145341E+06 .145185E+06 .145235E+06 .145792E+06 .146767E+06 .147363E+06 .147570E+06
  E   .436992E+06 .441969E+06 .446893E+06 .451881E+06 .461770E+06 .471661E+06 .489843E+06 .506449E+06 .514776E+06 .523111E+06

E300.012        .985300E+02 .304550E+03 .459000E+03 .533831OE+03 .443525E+04 .419877E+04
                .128227E+03 .124550E+03 .412865E+06 .432440E+06 .106732E+03 .447491E+06
  T   .828509E+03 .895003E+03 .912757E+03 .943506E+03 .953258E+03 .948753E+03 .912146E+03 .860766E+03 .832265E+03 .820878E+03
  F   .159664E+06 .158256E+06 .157684E+06 .157247E+06 .157047E+06 .157139E+06 .157897E+06 .158981E+06 .159585E+06 .159825E+06
  E   .437857E+06 .443242E+06 .448618E+06 .453980E+06 .464695E+06 .475414E+06 .495128E+06 .513133E+06 .522159E+06 .531195E+06

E300.013        .985300E+02 .304550E+03 .459125E+03 .534450E+03 .500663E+04 .476085E+04
                .131564E+03 .127520E+03 .412865E+06 .433239E+06 .107483E+03 .450669E+06
  T   .885866E+03 .954466E+03 .964280E+03 .990595E+03 .1003866E+04 .987811E+03 .945544E+03 .885315E+03 .853476E+03 .844331E+03
  F   .180249E+06 .178755E+06 .178546E+06 .177992E+06 .177571E+06 .178050E+06 .178947E+06 .180262E+06 .180964E+06 .181165E+06
  E   .439370E+06 .445469E+06 .451563E+06 .457645E+06 .469798E+06 .481966E+06 .504342E+06 .524779E+06 .535023E+06 .545275E+06

E300.014        .987100E+02 .304550E+03 .458526E+03 .541[illegible]E+03 .546948E+04 .518850E+04
                .134162E+03 .129905E+03 .413624E+06 .434586E+06 .108057E+03 .453097E+06
  T   .920557E+03 .984933E+03 .1003469E+04 .1031619E+04 .1044410E+04 .1026878E+04 .970372E+03 .902538E+03 .873680E+03 .863253E+03
  F   .196028E+06 .194599E+06 .1941948E+06 .193510E+06 .193147E+06 .193703E+06 .194918E+06 .196437E+06 .197092E+06 .197328E+06
  E   .441264E+06 .447912E+06 .454552E+06 .461179E+06 .474426E+06 .487687E+06 .512088E+06 .534375E+06 .545542E+06 .556718E+06

E300.015        .987100E+02 .304550E+03 .458337E+03 .543390E+03 .357300E+04 .336073E+04
                .122717E+03 .120213E+03 .413624E+06 .431999E+06 .105455E+03 .442096E+06
  T   .737318E+03 .786413E+03 .809303E+03 .842523E+03 .888544E+03 .871907E+03 .844556E+03 .806890E+03 .780926E+03 .766956E+03
  F   .129099E+06 .128132E+06 .127675E+06 .127010E+06 .126490E+06 .126423E+06 .126969E+06 .127724E+06 .128242E+06 .128518E+06
  E   .436383E+06 .440703E+06 .445031E+06 .449343E+06 .457941E+06 .466536E+06 .482341E+06 .496775E+06 .504013E+06 .511282E+06

E300.101        .900700E+02 .299840E+03 .358398E+03 .586870E+03 .516369E+04 .495724E+04
                .124665E+03 .122001E+03 .377234E+06 .395208E+06 .105912E+03 .444025E+06
  T   .794628E+03 .848160E+03 .867841E+03 .911592E+03 .972991E+03 .1010049E+04 .1008089E+04 .964199E+03 .930971E+03 .912633E+03
  F   .188832E+06 .188652E+06 .188213E+06 .187237E+06 .185891E+06 .185097E+06 .185147E+06 .186081E+06 .186808E+06 .187218E+06
  E   .401741E+06 .408248E+06 .414745E+06 .421221E+06 .434115E+06 .446976E+06 .470558E+06 .492061E+06 .502838E+06 .513631E+06

E300.102        .898900E+02 .299840E+03 .366538E+03 .578120E+03 .483188E+04 .463547E+04
                .122826E+03 .120160E+03 .376477E+06 .394229E+06 .105481E+03 .442204E+06
  T   .738759E+03 .800417E+03 .817485E+03 .865611E+03 .923967E+03 .985300E+03 .994932E+03 .952076E+03 .920793E+03 .900784E+03
  F   .178453E+06 .177150E+06 .176781E+06 .175731E+06 .174462E+06 .173165E+06 .172966E+06 .173861E+06 .174531E+06 .174964E+06
  E   .400356E+06 .406454E+06 .412544E+06 .418610E+06 .430684E+06 .442702E+06 .464719E+06 .484799E+06 .494863E+06 .504944E+06

E300.103        .898900E+02 .299840E+03 .366453E+03 .578790E+03 .435648E+04 .417524E+04
                .115453E+03 .117694E+03 .376477E+06 .393558E+06 .103698E+03 .434671E+06
  T   .674371E+03 .734105E+03 .764435E+03 .809625E+03 .865816E+03 .926127E+03 .954462E+03 .912159E+03 .887416E+03 .871915E+03
  F   .161614E+06 .160450E+06 .159832E+06 .158890E+06 .157703E+06 .156438E+06 .155856E+06 .156728E+06 .157247E+06 .157574E+06
  E   .399093E+06 .404602E+06 .410096E+06 .415567E+06 .426454E+06 .437282E+06 .457053E+06 .475153E+06 .484308E+06 .493275E+06

E300.104        .[illegible]41000E+02 .299840E+03 .373709E+03 .576760E+03 .385352E+04 .371145E+04
                .[illegible]40356E+03 .115567E+03 .378749E+06 .395371E+06 .103921E+03 .435614E+06
  T   .617983E+03 .661128E+03 .704476E+03 .748863E+03 .800848E+03 .864812E+03 .901757E+03 .879030E+03 .860617E+03 .844806E+03
  F   .144312E+06 .143539E+06 .142748E+06 .141888E+06 .140831E+06 .139522E+06 .138771E+06 .139232E+06 .139608E+06 .139931E+06
  E   .400304E+06 .405218E+06 .410113E+06 .414987E+06 .424682E+06 .434314E+06 .451904E+06 .467933E+06 .475962E+06 .484005E+06

E300.171        .837400E+02 .299840E+03 .502844E+03 .590900E+03 .502533E+04 .483714E+04
                .118427E+03 .116579E+03 .350623E+06 .372712E+06 .104428E+03 .437756E+06
  T   .617917E+03 .656641E+03 .703918E+03 .769974E+03 .858836E+03 .932438E+03 .1011128E+04 .997678E+03 .970301E+03 .948942E+03
  F   .188268E+06 .187576E+06 .186663E+06 .185292E+06 .183348E+06 .181726E+06 .180051E+06 .180332E+06 .180909E+06 .181367E+06
  E   .379147E+06 .385568E+06 .391969E+06 .398339E+06 .410993E+06 .423575E+06 .446511E+06 .467382E+06 .477838E+06 .488309E+06

E300.172        .832000E+02 .299840E+03 .499900E+03 .557760E+03 .459903E+04 .443156E+04
                .115675E+03 .113929E+03 .340354E+06 .368764E+06 .103753E+03 .434903E+06
  T   .540117E+03 .577850E+03 .617604E+03 .674247E+03 .780696E+03 .866287E+03 .963442E+03 .969540E+03 .948663E+03 .934845E+03
  F   .173377E+06 .172831E+06 .172187E+06 .171168E+06 .169025E+06 .167311E+06 .165135E+06 .165010E+06 .165442E+06 .165731E+06
  E   .375673E+06 .381572E+06 .387457E+06 .393320E+06 .404947E+06 .416495E+06 .437485E+06 .456557E+06 .466110E+06 .475673E+06

E400.011        .985300E+02 .396840E+03 .473090E+03 .522020E+03 .528335E+04 .503788E+04
                .138361E+03 .134173E+03 .412865E+06 .429135E+06 .108966E+03 .456942E+06
  T   .891898E+03 .948848E+03 .964649E+03 .994130E+03 .1011188E+04 .1007298E+04 .970427E+03 .897838E+03 .855829E+03 .830025E+03
  F   .191514E+06 .190245E+06 .189898E+06 .189242E+06 .188901E+06 .188983E+06 .189772E+06 .191382E+06 .192327E+06 .192905E+06
  E   .434135E+06 .439115E+06 .444069E+06 .449054E+06 .458971E+06 .468891E+06 .487122E+06 .503783E+06 .512140E+06 .520512E+06

E400.012        .987100E+02 .396840E+03 .479990E+03 .523410E+03 .585411E+04 .558188E+04
                .142249E+03 .137999E+03 .413624E+06 .430640E+06 .109788E+03 .460418E+06
  T   .943290E+03 .987470E+03 .1002778E+04 .1030695E+04 .1050728E+04 .1041408E+04 .987270E+03 .911637E+03 .873610E+03 .859775E+03
  F   .211398E+06 .210390E+06 .2100466E+06 .209306E+06 .2090003E+06 .209202E+06 .210394E+06 .212135E+06 .213023E+06 .213345E+06
  E   .436173E+06 .441689E+06 .447201E+06 .452702E+06 .463695E+06 .474694E+06 .494923E+06 .513401E+06 .522664E+06 .531935E+06

E400.013        .987100E+02 .396840E+03 .480332E+03 .518560E+03 .482971E+04 .458894E+04
                .135482E+03 .131741E+03 .413624E+06 .429564E+06 .108346E+03 .454316E+06
  T   .845544E+03 .900147E+03 .917101E+03 .954282E+03 .977703E+03 .975040E+03 .938611E+03 .874409E+03 .835238E+03 .817499E+03
  F   .174940E+06 .173751E+06 .173385E+06 .172890E+06 .172100E+06 .172155E+06 .172923E+06 .174311E+06 .175165E+06 .175549E+06
  E   .434123E+06 .438861E+06 .443193E+06 .447[illegible]E+06 .456733E+06 .465756E+06 .482345E+06 .497504E+06 .505104E+06 .512723E+06
```

```
E400.014
                .985300E+02 .396840E+03 .480653E+03 .513700E+03 .428419E+04 .406905E+04
                .131719E+03 .128237E+03 .412865E+06 .428244E+06 .107516E+07 .450814E+06
  T  .792340E+03 .850254E+03 .871594E+03 .896938E+03 .917324E+03 .928878E+03 .901914E+03 .844637E+03 .808975E+03 .786231E+03
  F  .155756E+06 .154542E+06 .154094E+06 .153564E+06 .153141E+06 .152901E+06 .153468E+06 .154661E+06 .155409E+06 .155883E+06
  E  .432294E+06 .436322E+06 .440341E+06 .444352E+06 .452357E+06 .460355E+06 .475053E+06 .488486E+06 .495225E+06 .501978E+06

E400.101
                .898900E+02 .396840E+03 .410367E+03 .579470E+03 .542904E+04 .519634E+04
                .127436E+03 .125099E+03 .376477E+06 .391480E+06 .106551E+07 .446729E+06
  T  .788639E+03 .811241E+03 .819866E+03 .860328E+03 .907085E+03 .964101E+03 .101040E+04 .987006E+03 .958264E+03 .932285E+03
  F  .199004E+06 .198502E+06 .198309E+06 .197395E+06 .196334E+06 .195056E+06 .194051E+06 .194554E+06 .195185E+06 .195765E+06
  E  .396653E+06 .401818E+06 .406980E+06 .412127E+06 .422387E+06 .432605E+06 .451282E+06 .468287E+06 .476805E+06 .485339E+06

E400.102
                .897100E+02 .396840E+03 .403843E+03 .583510E+03 .499463E+04 .480403E+04
                .124623E+03 .122332E+03 .375720E+06 .390146E+06 .105902E+07 .443984E+06
  T  .727210E+03 .751666E+03 .763607E+03 .798069E+03 .860132E+03 .911982E+03 .977324E+03 .970315E+03 .941635E+03 .914966E+03
  F  .184931E+06 .184423E+06 .184171E+06 .183429E+06 .182064E+06 .180923E+06 .179513E+06 .179661E+06 .180277E+06 .180857E+06
  E  .394942E+06 .399729E+06 .404512E+06 .409283E+06 .418777E+06 .428233E+06 .445484E+06 .461175E+06 .469037E+06 .476915E+06

E400.103
                .897100E+02 .396840E+03 .406960E+03 .574740E+03 .449754E+04 .433541E+04
                .122298E+03 .119239E+03 .375720E+06 .389703E+06 .105356E+07 .441677E+06
  T  .665367E+03 .688961E+03 .704168E+03 .744439E+03 .805058E+03 .860712E+03 .934884E+03 .931239E+03 .906346E+03 .892217E+03
  F  .167720E+06 .167272E+06 .166977E+06 .166169E+06 .164904E+06 .163717E+06 .162144E+06 .162221E+06 .162745E+06 .163044E+06
  E  .394042E+06 .398173E+06 .402700E+06 .407012E+06 .415591E+06 .424129E+06 .439681E+06 .453824E+06 .460910E+06 .468005E+06

E400.104
                .889900E+02 .396840E+03 .410043E+03 .574060E+03 .403931E+04 .389618E+04
                .116159E+03 .115341E+03 .372691E+06 .386256E+06 .103672E+07 .435409E+06
  T  .551424E+03 .583427E+03 .614214E+03 .666537E+03 .725985E+03 .780948E+03 .866778E+03 .889097E+03 .874258E+03 .867699E+03
  F  .152089E+06 .151613E+06 .151116E+06 .150196E+06 .149062E+06 .147956E+06 .146182E+06 .145722E+06 .146028E+06 .146163E+06
  E  .390174E+06 .394085E+06 .397987E+06 .401871E+06 .409603E+06 .417294E+06 .431273E+06 .443954E+06 .450303E+06 .456657E+06

E400.105
                .902500E+02 .396840E+03 .415332E+03 .518560E+03 .364105E+04 .349228E+04
                .114194E+03 .114161E+03 .377992E+06 .391244E+06 .103384E+07 .433146E+06
  T  .512984E+03 .563457E+03 .599260E+03 .656784E+03 .694082E+03 .733760E+03 .809943E+03 .839040E+03 .832592E+03 .822990E+03
  F  .137108E+06 .136419E+06 .135867E+06 .134886E+06 .134202E+06 .133442E+06 .131927E+06 .131340E+06 .131470E+06 .131663E+06
  E  .394772E+06 .398288E+06 .401794E+06 .405283E+06 .412234E+06 .419157E+06 .431743E+06 .443147E+06 .448854E+06 .454567E+06

E400.161
                .839300E+02 .396840E+03 .574837E+03 .525480E+03 .496402E+04 .478809E+04
                .116181E+03 .114973E+03 .351421E+06 .369662E+06 .103878E+07 .435432E+06
  T  .558225E+03 .584897E+03 .608671E+03 .653576E+03 .713664E+03 .823036E+03 .938544E+03 .970328E+03 .964049E+03 .963298E+03
  F  .186684E+06 .186292E+06 .185904E+06 .185116E+06 .183483E+06 .181633E+06 .179099E+06 .178418E+06 .178551E+06 .178567E+06
  E  .374473E+06 .379278E+06 .384078E+06 .388865E+06 .398385E+06 .407842E+06 .425023E+06 .440605E+06 .448400E+06 .456195E+06

E400.162
                .841100E+02 .396840E+03 .572532E+03 .570000E+03 .559741E+04 .537824E+04
                .120519E+03 .119219E+03 .352177E+06 .371014E+06 .104933E+07 .439888E+06
  T  .640431E+03 .667554E+03 .694475E+03 .751396E+03 .829888E+03 .904929E+03 .100217E+04 .101516E+04 .996992E+03 .977093E+03
  F  .206633E+06 .208125E+06 .207595E+06 .206405E+06 .204657E+06 .202916E+06 .200749E+06 .200468E+06 .200863E+06 .201301E+06
  E  .376407E+06 .381792E+06 .387169E+06 .392527E+06 .403186E+06 .413789E+06 .433103E+06 .450648E+06 .459430E+06 .468223E+06

E500.011
                .988900E+02 .495290E+03 .459296E+03 .532380E+03 .448200E+04 .428469E+04
                .135543E+03 .134578E+03 .414383E+06 .426504E+06 .108359E+07 .454372E+06
  T  .802969E+03 .838493E+03 .857785E+03 .888915E+03 .908932E+03 .906850E+03 .895845E+03 .855658E+03 .820276E+03 .782817E+03
  F  .163758E+06 .163004E+06 .162677E+06 .161929E+06 .161174E+06 .161549E+06 .161782E+06 .162637E+06 .163392E+06 .164162E+06
  E  .429917E+06 .433319E+06 .436717E+06 .440104E+06 .446871E+06 .453634E+06 .466046E+06 .477369E+06 .483049E+06 .488747E+06

E500.012
                .987100E+02 .495290E+03 .485408E+03 .531000E+03 .505392E+04 .481424E+04
                .138737E+03 .138160E+03 .413628E+06 .426682E+06 .109047E+07 .457281E+06
  T  .865526E+03 .901192E+03 .907241E+03 .934671E+03 .948942E+03 .964744E+03 .943614E+03 .884005E+03 .844302E+03 .820032E+03
  F  .183199E+06 .182411E+06 .182278E+06 .181677E+06 .181367E+06 .181027E+06 .181483E+06 .182791E+06 .183670E+06 .184204E+06
  E  .430510E+06 .434328E+06 .438144E+06 .441952E+06 .449559E+06 .457158E+06 .471110E+06 .483852E+06 .490243E+06 .496646E+06

E500.013
                .967100E+02 .495290E+03 .486518E+03 .529620E+03 .564501E+04 .537703E+04
                .136942E+03 .142265E+03 .413624E+06 .427195E+06 .108662E+07 .455653E+06
  T  .905886E+03 .954204E+03 .953953E+03 .983859E+03 .999011E+03 .100803E+04 .982897E+03 .914711E+03 .873701E+03 .849288E+03
  F  .204234E+06 .203132E+06 .201138E+06 .202467E+06 .202133E+06 .201936E+06 .202689E+06 .204032E+06 .204976E+06 .205537E+06
  E  .431470E+06 .435732E+06 .439993E+06 .444246E+06 .452744E+06 .461237E+06 .476833E+06 .491075E+06 .498216E+06 .505369E+06

E500.101
                .900700E+02 .495290E+03 .513949E+03 .547590E+03 .530026E+04 .510295E+04
                .128751E+03 .125271E+03 .377234E+06 .391036E+06 .106394E+07 .446065E+06
  T  .716304E+03 .746424E+03 .775551E+03 .811287E+03 .849804E+03 .901078E+03 .968050E+03 .974840E+03 .958306E+03 .941501E+03
  F  .196653E+06 .196024E+06 .195398E+06 .194611E+06 .193748E+06 .192593E+06 .191104E+06 .190956E+06 .191318E+06 .191669E+06
  E  .395120E+06 .399197E+06 .403264E+06 .407322E+06 .415414E+06 .423475E+06 .438163E+06 .451549E+06 .458239E+06 .464937E+06

E500.102
                .895300E+02 .495290E+03 .515273E+03 .544080E+03 .592668E+04 .568058E+04
                .130300E+03 .128697E+03 .374963E+06 .389294E+06 .107200E+07 .449473E+06
  T  .776240E+03 .828094E+03 .837873E+03 .868781E+03 .904795E+03 .[illegible]045E+03 .102492E+04 .101094E+04 .984737E+03 .967811E+03
  F  .217976E+06 .216792E+06 .216563E+06 .215843E+06 .214998E+06 .[illegible]756E+06 .212246E+06 .212555E+06 .213144E+06 .213531E+06
  E  .393832E+06 .398355E+06 .402875E+06 .407386E+06 .416367E+06 .425356E+06 .441735E+06 .456637E+06 .464100E+06 .471570E+06

E500.103
                .900700E+02 .495290E+03 .516067E+03 .535140E+03 .489594E+04 .449626E+04
                .121968E+03 .120355E+03 .377234E+06 .390541E+06 .105278E+07 .441347E+06
  T  .643515E+03 .663454E+03 .706316E+03 .750305E+03 .789521E+03 .827713E+03 .900452E+03 .917155E+03 .905308E+03 .901343E+03
  F  .174160E+06 .173795E+06 .172973E+06 .172080E+06 .171257E+06 .170439E+06 .168860E+06 .168851E+06 .168765E+06 .168849E+06
  E  .394148E+06 .397750E+06 .401341E+06 .404920E+06 .412054E+06 .419166E+06 .432124E+06 .443887E+06 .449775E+06 .455664E+06

E500.104
                .902500E+02 .495290E+03 .508067E+03 .535140E+03 .428419E+04 .408769E+04
                .119051E+03 .117609E+03 .377992E+06 .390826E+06 .104579E+07 .438394E+06
  T  .610919E+03 .609235E+03 .654701E+03 .706412E+03 .750345E+03 .789155E+03 .863743E+03 .892952E+03 .881207E+03 .874918E+03
  F  .159232E+06 .159260E+06 .158470E+06 .157495E+06 .156620E+06 .155823E+06 .154259E+06 .153647E+06 .153892E+06 .154023E+06
  E  .394120E+06 .397414E+06 .400698E+06 .403968E+06 .410482E+06 .416973E+06 .428792E+06 .439506E+06 .444869E+06 .450235E+06

GRVIEW - PROCESSING COMPLETE
```

APPENDIX D : BOILING CURVES

The boiling curves shown in this appendix corresponds to the data tabulated in Appendix C.

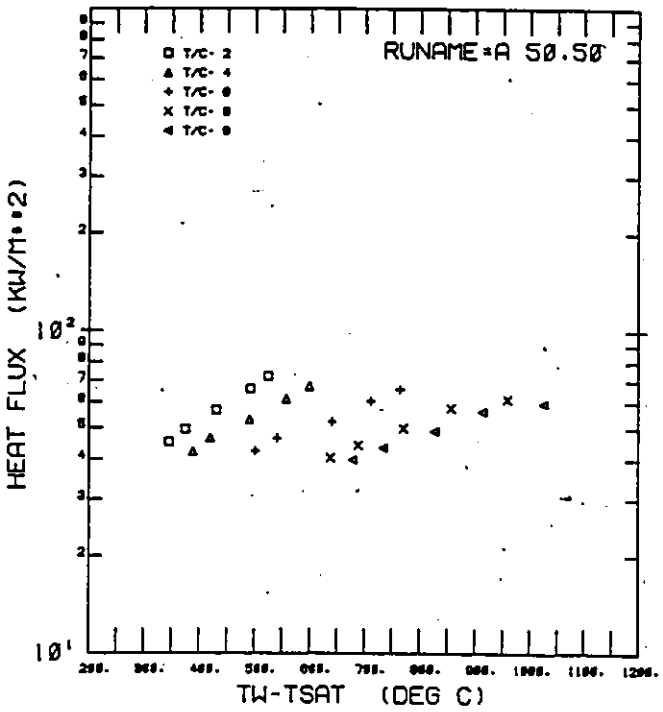
RUNAME=A 50.50
T/C- 2
T/C- 4
T/C- 6
T/C- 8
T/C- 9
HEAT FLUX (KW/M**2)
TW-TSAT (DEG C)

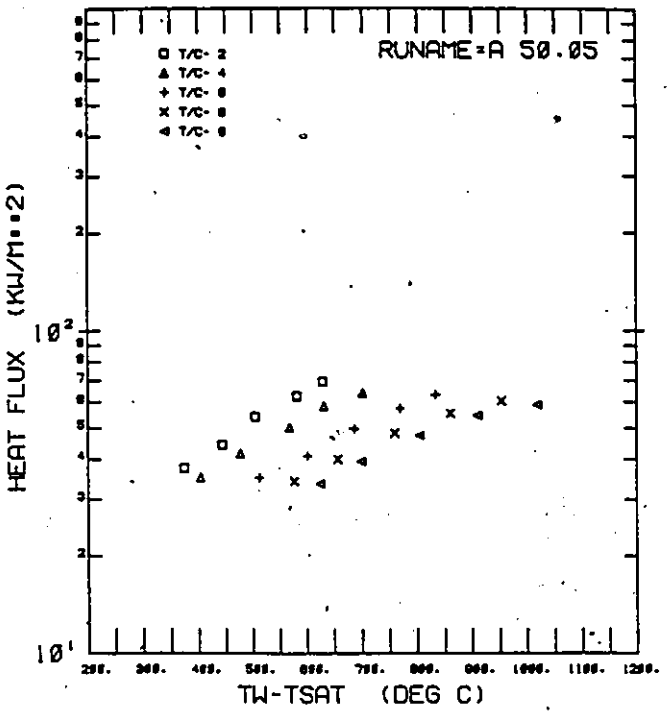
RUNAME=A 50.05
T/C- 2
T/C- 4
T/C- 6
T/C- 8
T/C- 9
HEAT FLUX (KW/M**2)
TW-TSAT (DEG C)

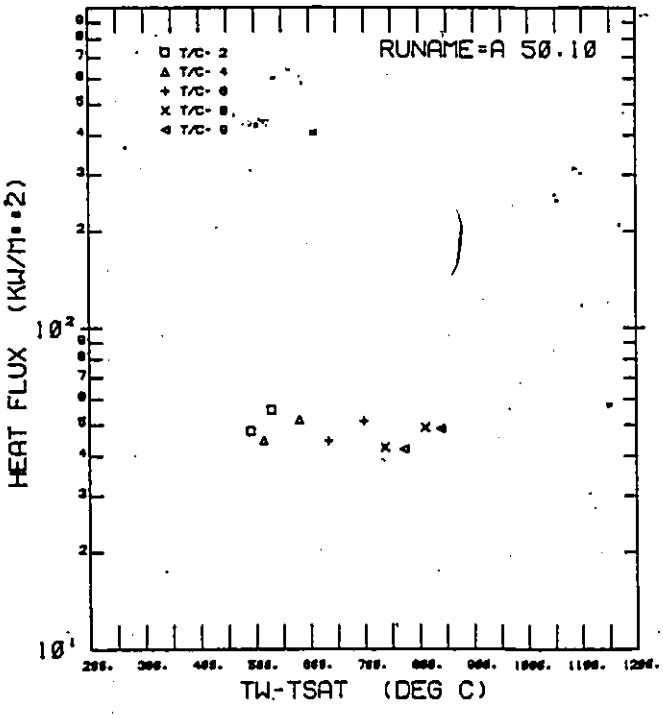
RUNAME=A 50.10
T/C- 2
T/C- 4
T/C- 6
T/C- 8
T/C- 9
HEAT FLUX (KW/M**2)
TW-TSAT (DEG C)

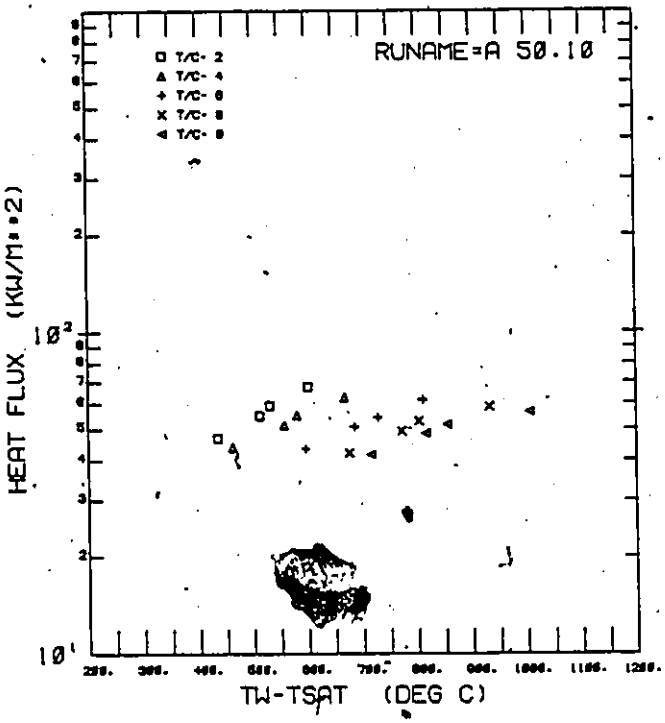
RUNAME=A 50.10
T/C- 2
T/C- 4
T/C- 6
T/C- 8
T/C- 9
HEAT FLUX (KW/M**2)
TW-TSAT (DEG C)

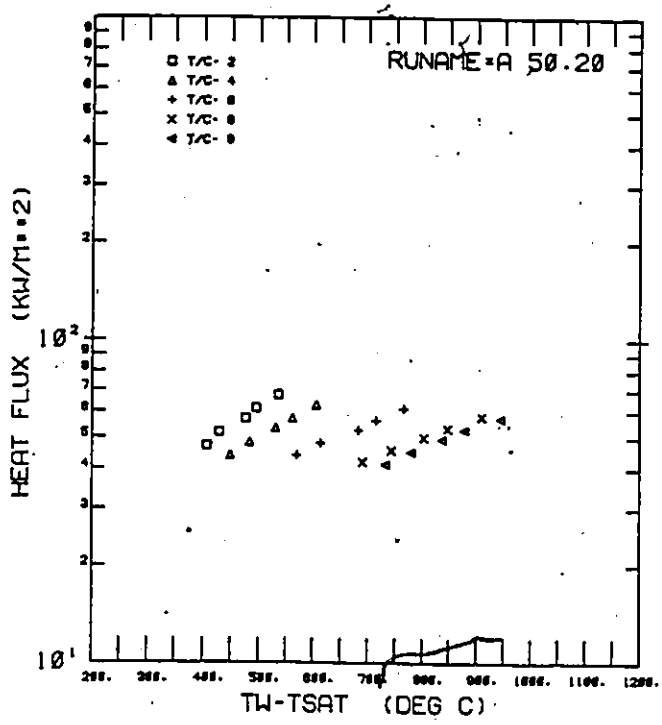
RUNAME=A 50.20
T/C- 2
T/C- 4
T/C- 6
T/C- 8
T/C- 9
HEAT FLUX (KW/M**2)
TW-TSAT (DEG C)

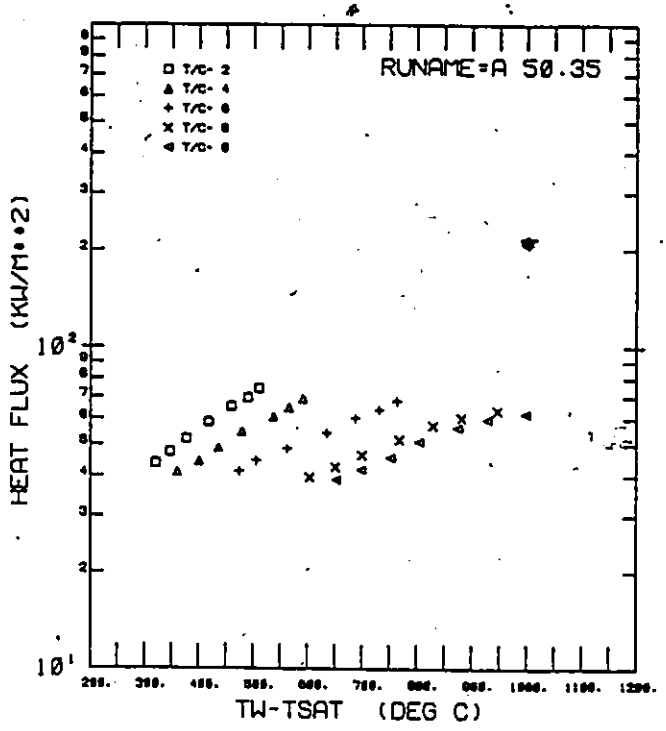
RUNAME=A 50.35
T/C- 2
T/C- 4
T/C- 6
T/C- 8
T/C- 9
HEAT FLUX (KW/M**2)
TW-TSAT (DEG C)

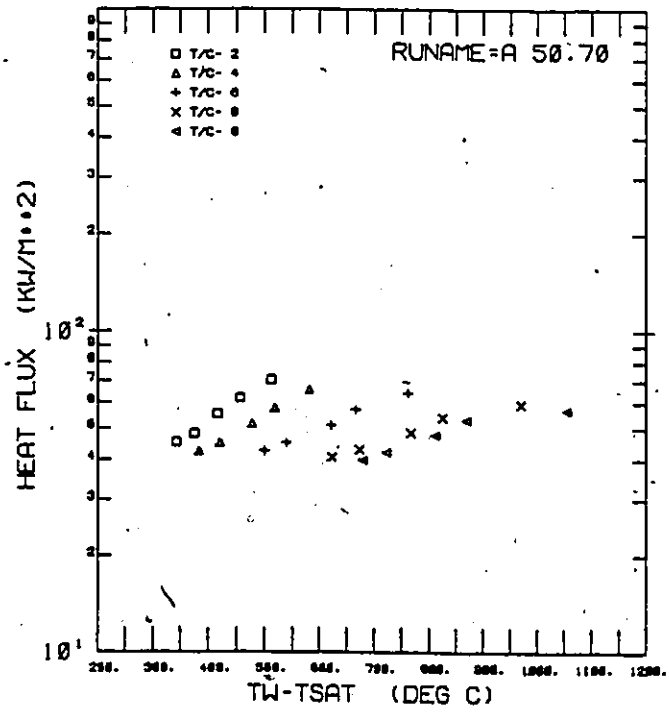
RUNAME=A 50.70
T/C- 2
T/C- 4
T/C- 6
T/C- 8
T/C- 9
HEAT FLUX (KW/M**2)
TW-TSAT (DEG C)

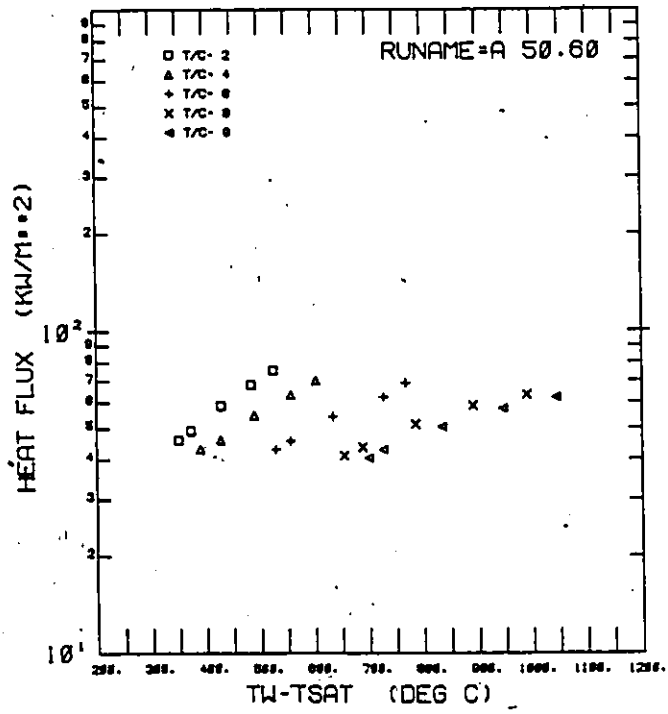
RUNAME=A 50.60
T/C- 2
T/C- 4
T/C- 6
T/C- 8
T/C- 9
HEAT FLUX (KW/M**2)
TW-TSAT (DEG C)

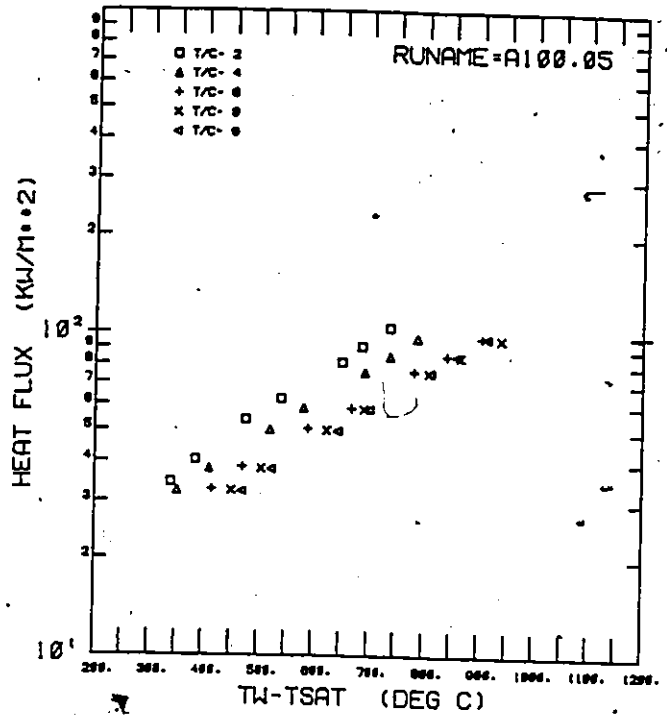
RUNAME=A100.05
T/C- 2
T/C- 4
T/C- 6
T/C- 8
T/C- 9
HEAT FLUX (KW/M**2)
TW-TSAT (DEG C)

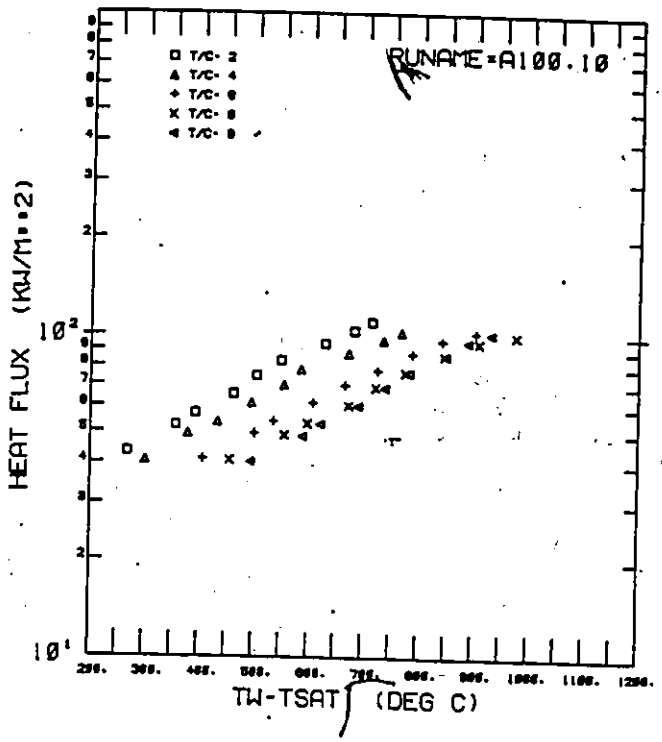
RUNAME=A100.10
T/C- 2
T/C- 4
T/C- 6
T/C- 8
T/C- 9
HEAT FLUX (KW/M**2)
TW-TSAT (DEG C)

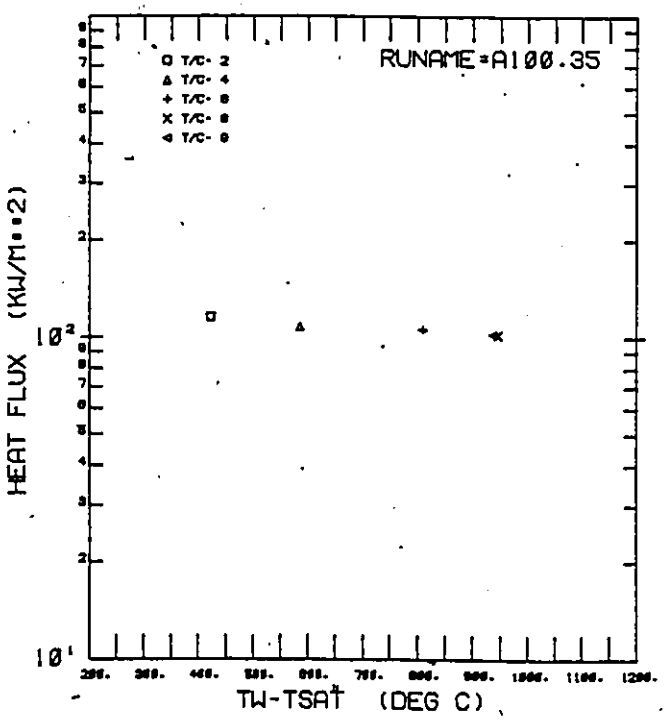
RUNAME=A100.35
T/C- 2
T/C- 4
T/C- 6
T/C- 8
T/C- 9
HEAT FLUX (KW/M**2)
TW-TSAT (DEG C)

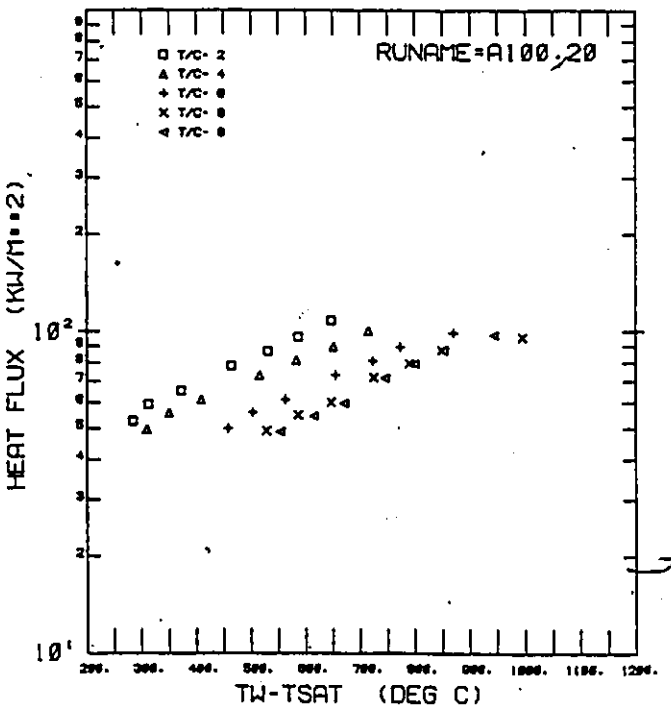
RUNAME=A100.20
T/C- 2
T/C- 4
T/C- 6
T/C- 8
T/C- 9
HEAT FLUX (KW/M**2)
TW-TSAT (DEG C)

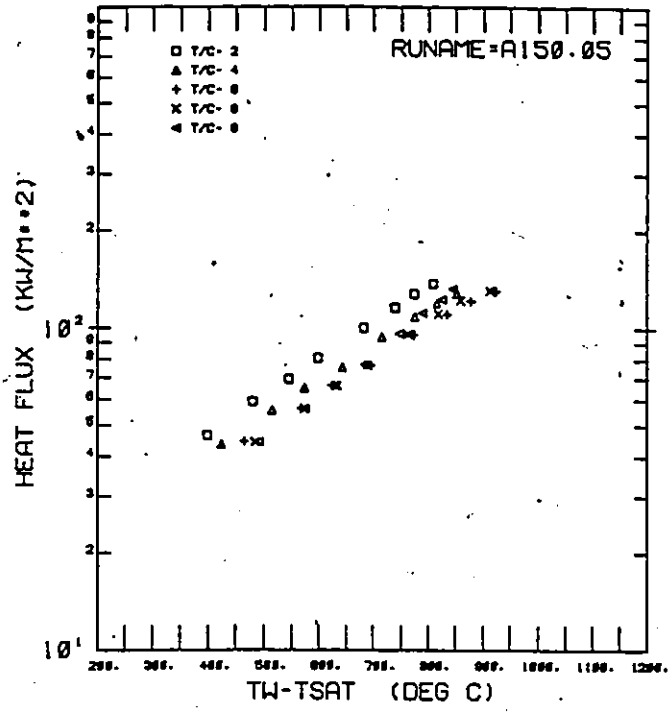
RUNAME=A150.05
T/C- 2
T/C- 4
T/C- 6
T/C- 8
T/C- 9
HEAT FLUX (KW/M**2)
TW-TSAT (DEG C)

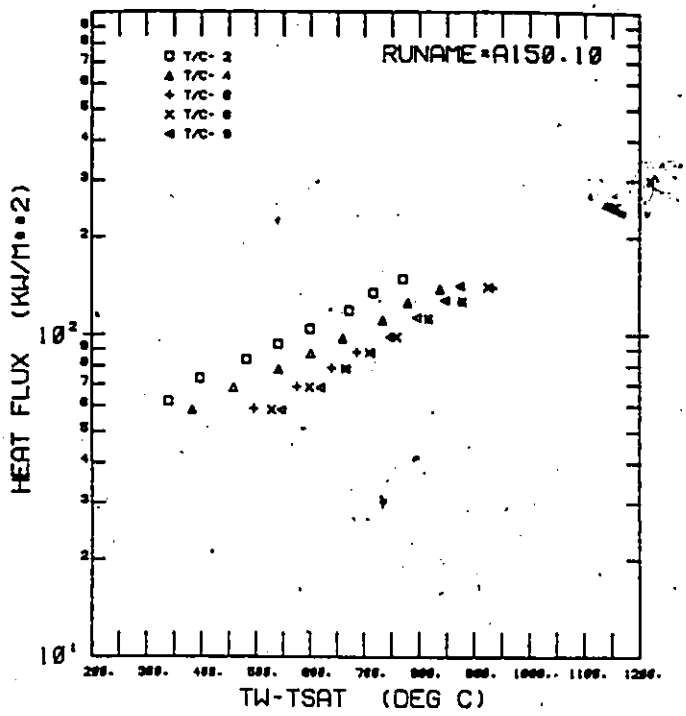
RUNAME=A150.10
T/C- 2
T/C- 4
T/C- 6
T/C- 8
T/C- 9
HEAT FLUX (KW/M**2)
TW-TSAT (DEG C)

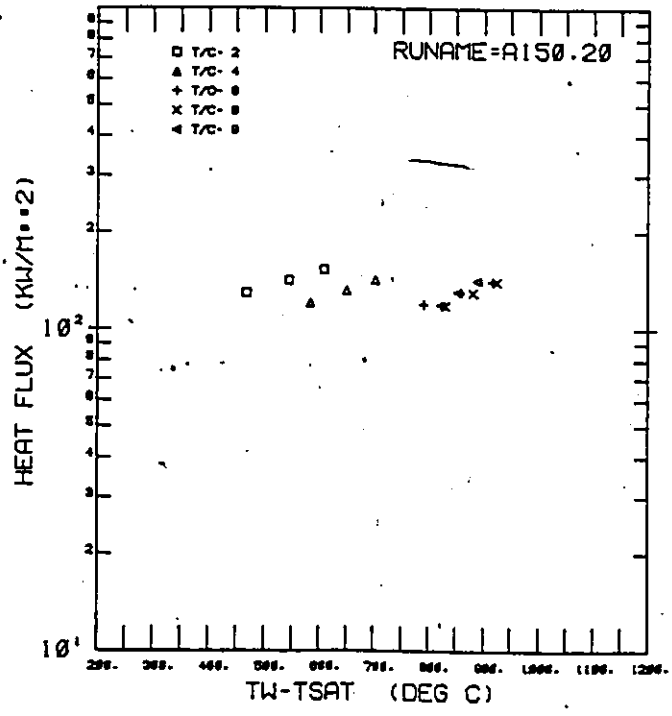
RUNAME=A150.20
T/C- 2
T/C- 4
T/C- 6
T/C- 8
T/C- 9
HEAT FLUX (KW/M**2)
TW-TSAT (DEG C)

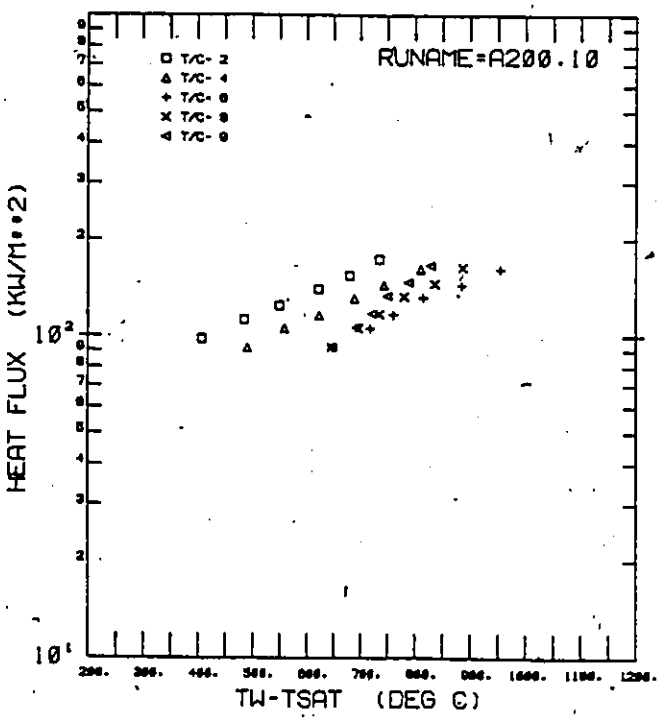
RUNAME=A200.10
T/C- 2
T/C- 4
T/C- 6
T/C- 8
T/C- 9
HEAT FLUX (KW/M**2)
TW-TSAT (DEG C)

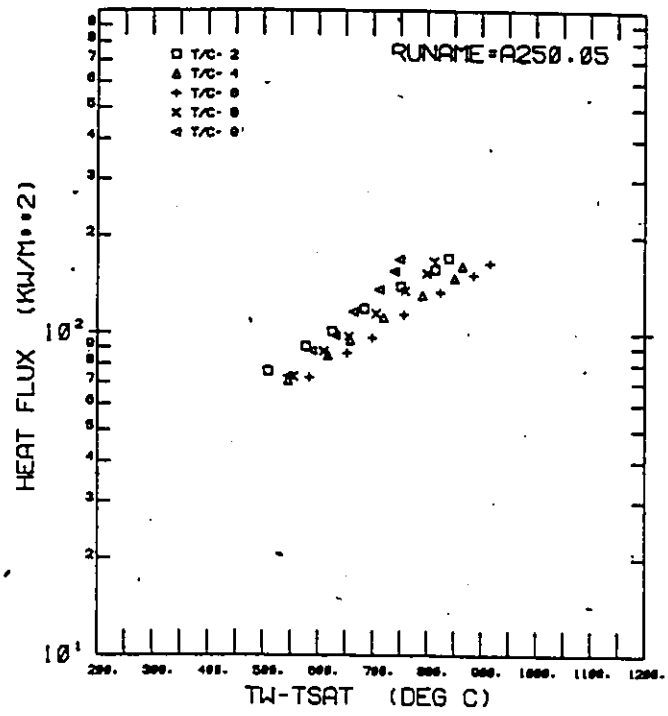
RUNAME=A250.05
T/C- 2
T/C- 4
T/C- 6
T/C- 8
T/C- 9
HEAT FLUX (KW/M**2)
TW-TSAT (DEG C)

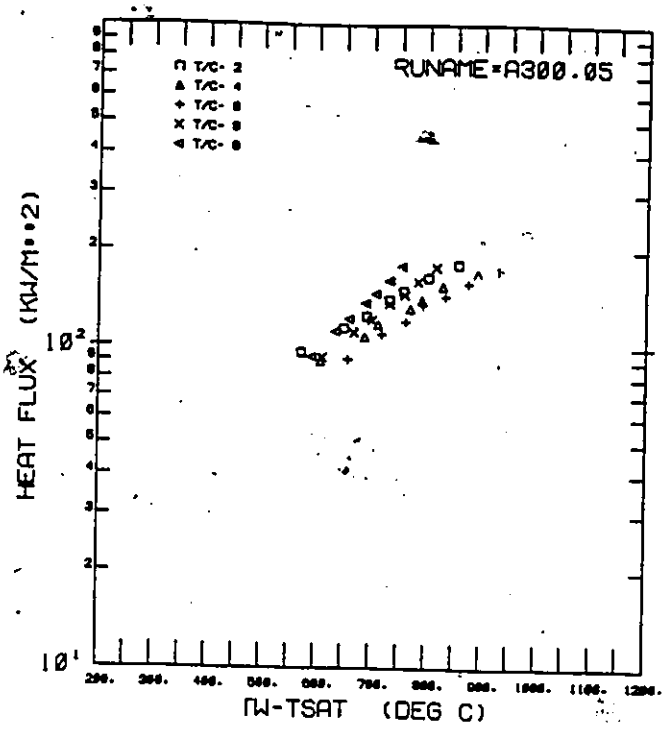
RUNAME=A300.05
T/C- 2
T/C- 4
T/C- 6
T/C- 8
T/C- 9
HEAT FLUX (KW/M**2)
TW-TSAT (DEG C)

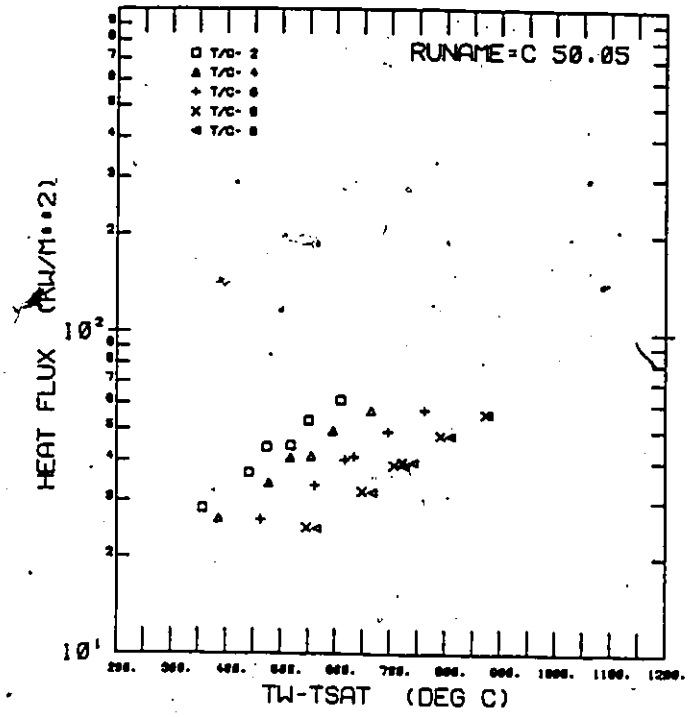
RUNAME=C 50.05
T/C- 2
T/C- 4
T/C- 6
T/C- 8
T/C- 9
HEAT FLUX (KW/M**2)
TW-TSAT (DEG C)

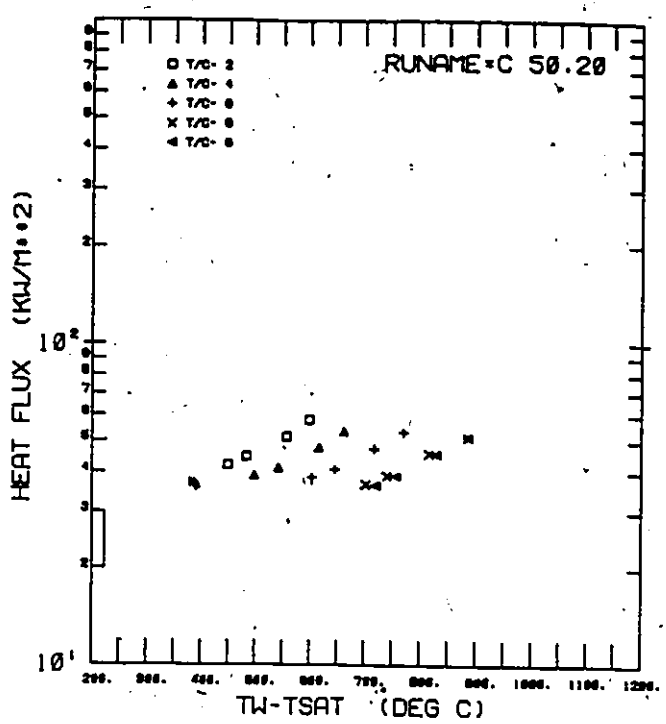
RUNAME=C 50.20
T/C- 2
T/C- 4
T/C- 6
T/C- 8
T/C- 9
HEAT FLUX (KW/M**2)
TW-TSAT (DEG C)

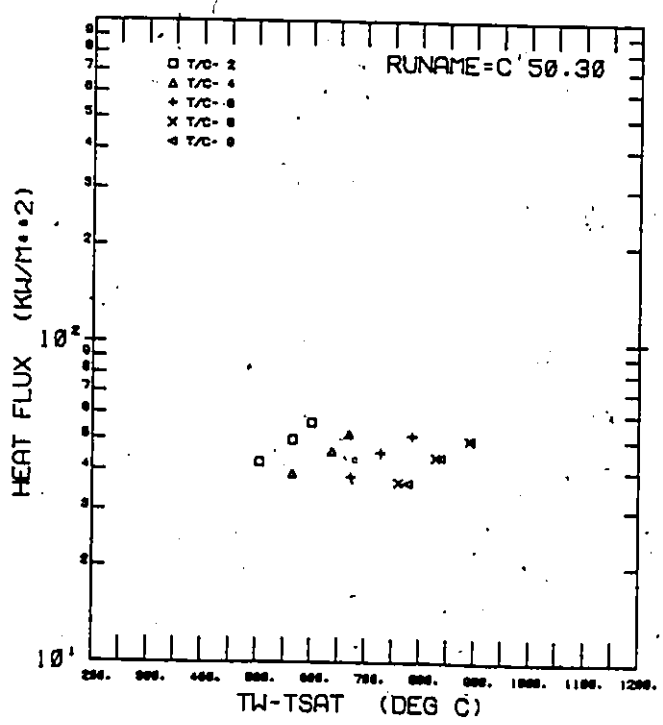
RUNAME=C 50.30
T/C- 2
T/C- 4
T/C- 6
T/C- 8
T/C- 9
HEAT FLUX (KW/M**2)
TW-TSAT (DEG C)

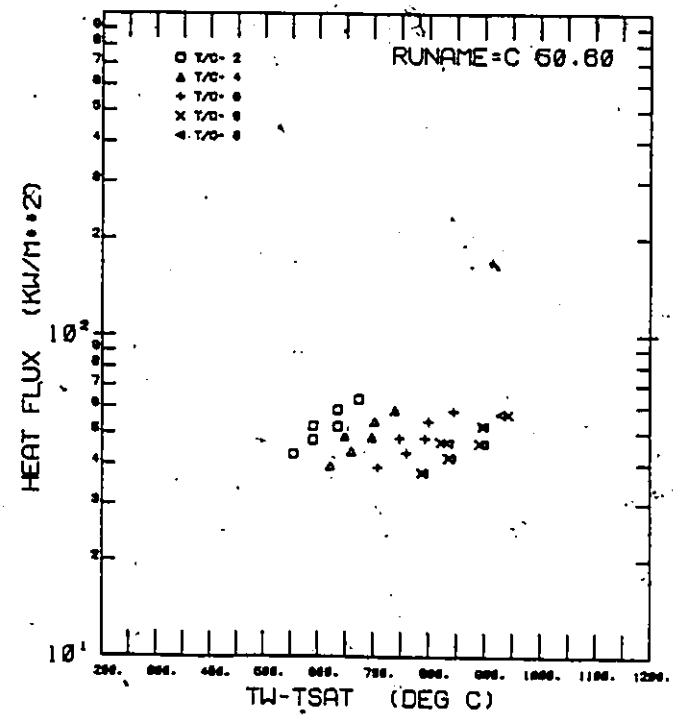
RUNAME=C 50.60
T/C- 2
T/C- 4
T/C- 6
T/C- 8
T/C- 9
HEAT FLUX (KW/M**2)
TW-TSAT (DEG C)

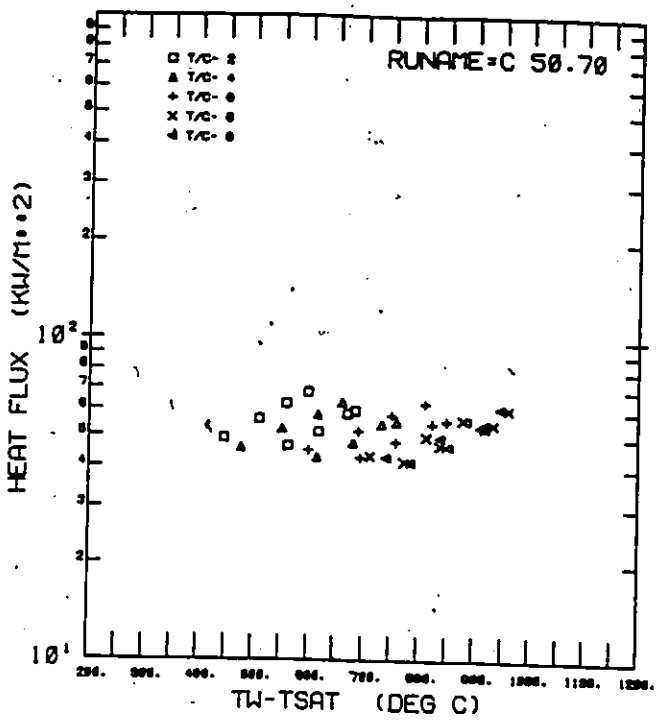
RUNAME=C 50.70
T/C- 2
T/C- 4
T/C- 6
T/C- 8
T/C- 9
HEAT FLUX (KW/M**2)
TW-TSAT (DEG C)

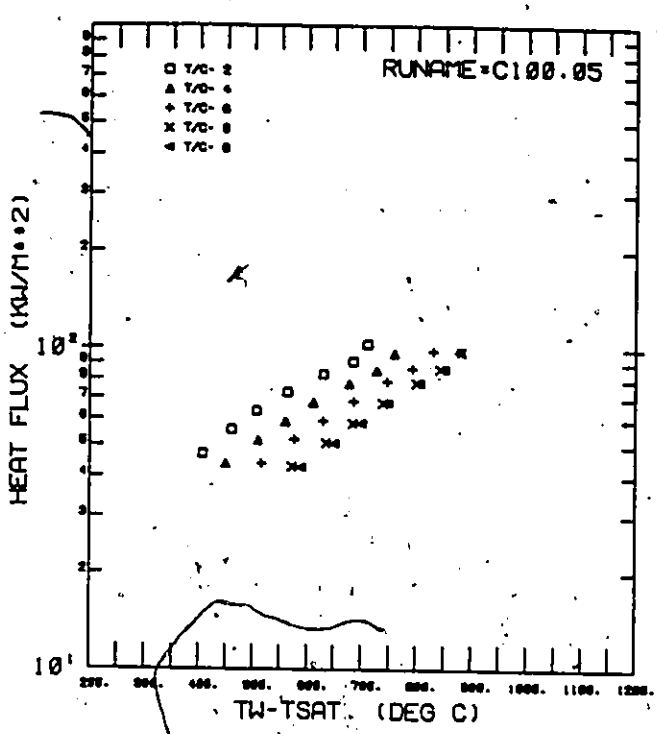
RUNAME=C100.05
T/C- 2
T/C- 4
T/C- 6
T/C- 8
T/C- 9
HEAT FLUX (KW/M**2)
TW-TSAT (DEG C)

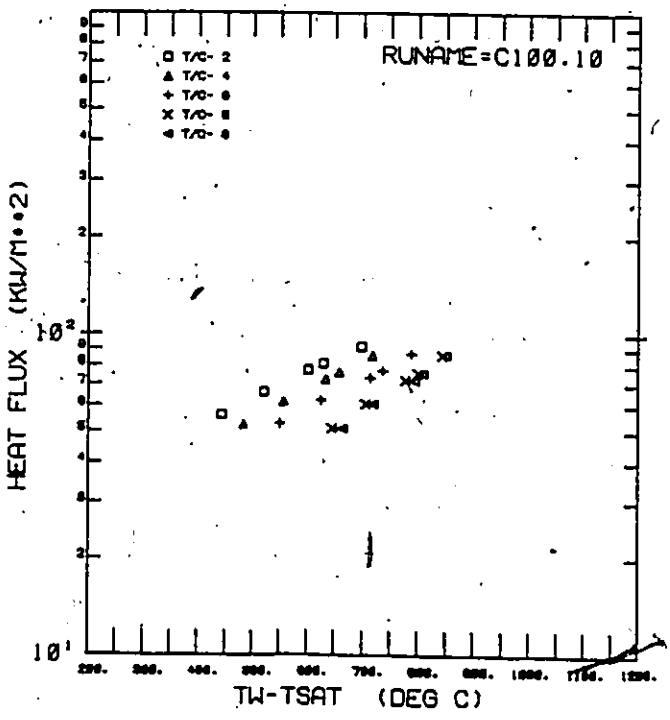
RUNAME=C100.10
T/C- 2
T/C- 4
T/C- 6
T/C- 8
T/C- 9
HEAT FLUX (KW/M**2)
TW-TSAT (DEG C)

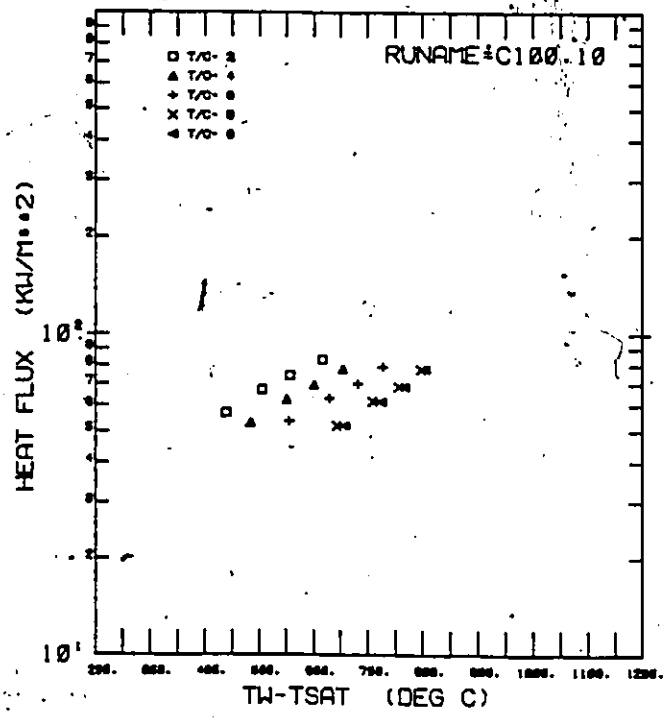
RUNAME=C100.10
T/C- 2
T/C- 4
T/C- 6
T/C- 8
T/C- 9
HEAT FLUX (KW/M**2)
TW-TSAT (DEG C)

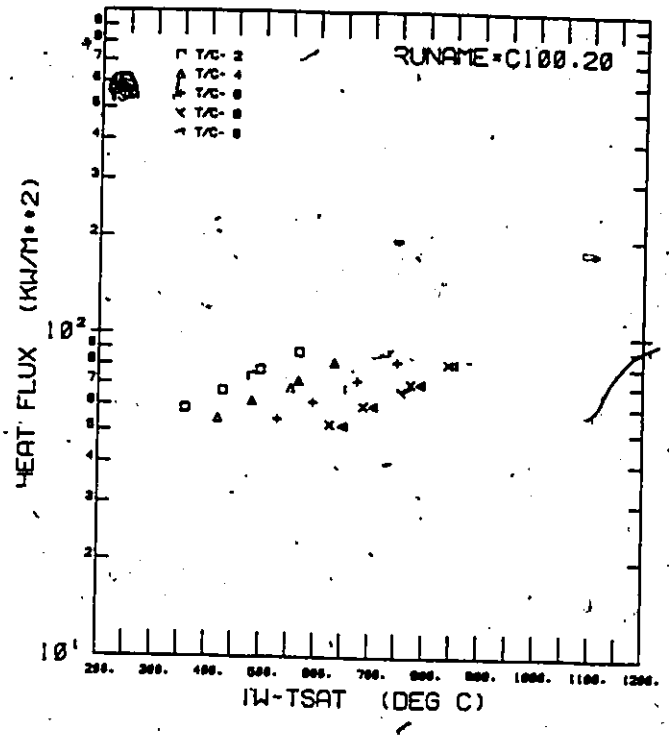
RUNAME=C100.20
T/C- 2
T/C- 4
T/C- 6
T/C- 8
T/C- 9
HEAT FLUX (KW/M**2)
TW-TSAT (DEG C)

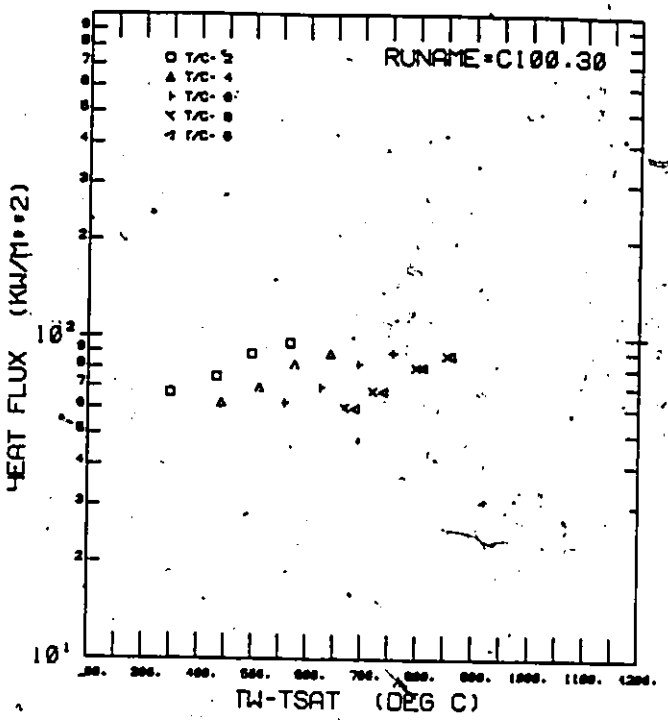
RUNAME=C100.30
T/C- 2
T/C- 4
T/C- 6
T/C- 8
T/C- 9
HEAT FLUX (KW/M**2)
TW-TSAT (DEG C)

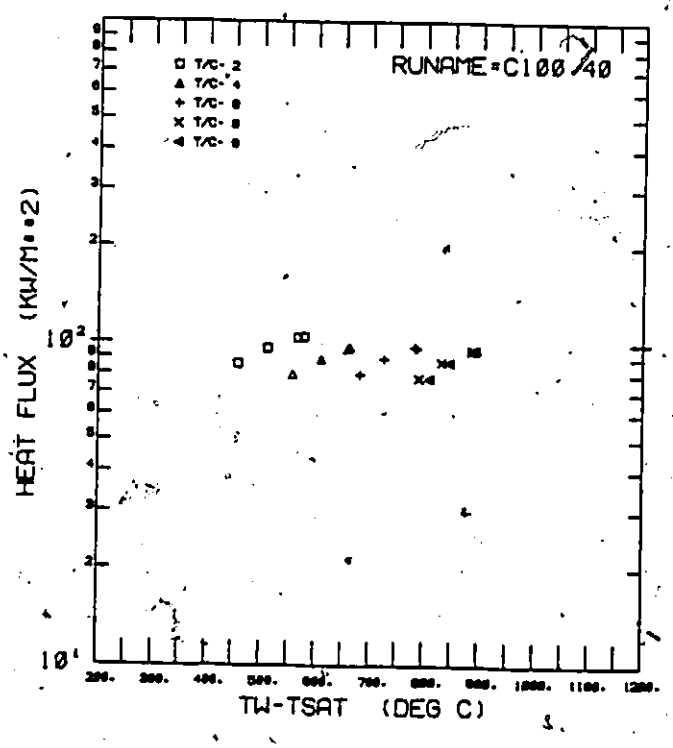
RUNAME=C100.40
T/C- 2
T/C- 4
T/C- 6
T/C- 8
T/C- 9
HEAT FLUX (KW/M**2)
TW-TSAT (DEG C)

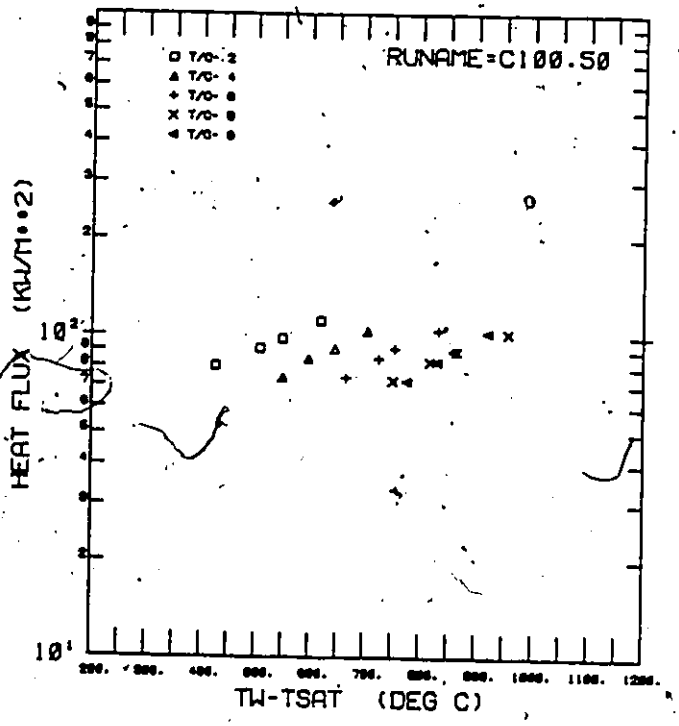
RUNAME=C100.50
T/C- 2
T/C- 4
T/C- 6
T/C- 8
T/C- 9
HEAT FLUX (KW/M**2)
TW-TSAT (DEG C)

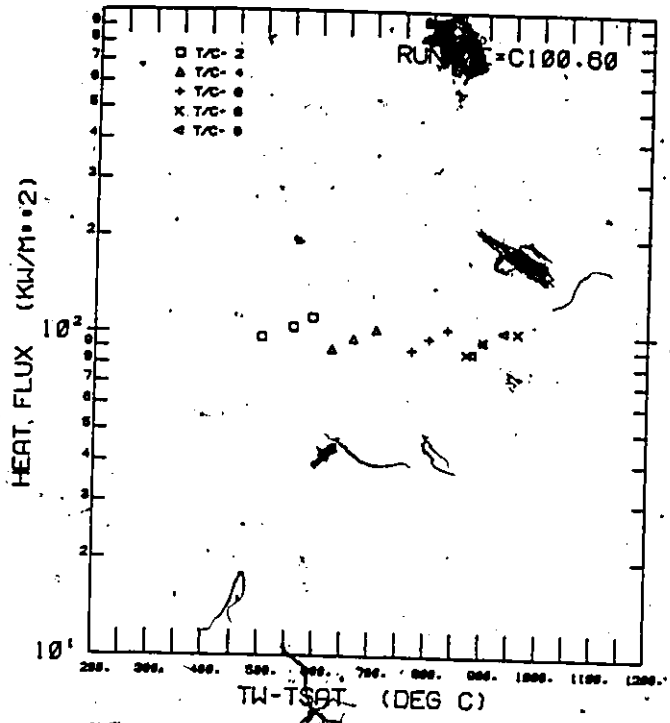
T/C- 2
T/C- 4
T/C- 6
T/C- 8
T/C- 9
RUNAME=C100.60
HEAT FLUX (KW/M**2)
TW-TSAT (DEG C)

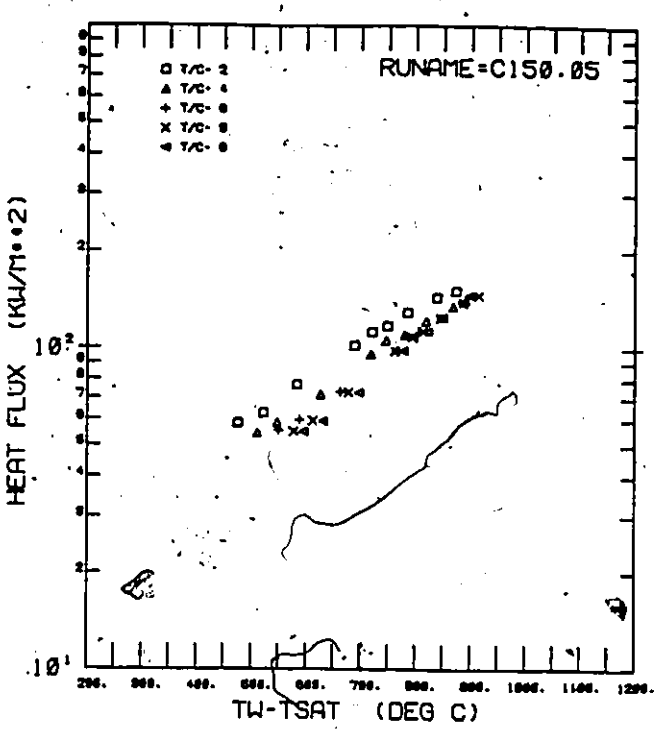
T/C- 2
T/C- 4
T/C- 6
T/C- 8
T/C- 9
RUNAME=C150.05
HEAT FLUX (KW/M**2)
TW-TSAT (DEG C)

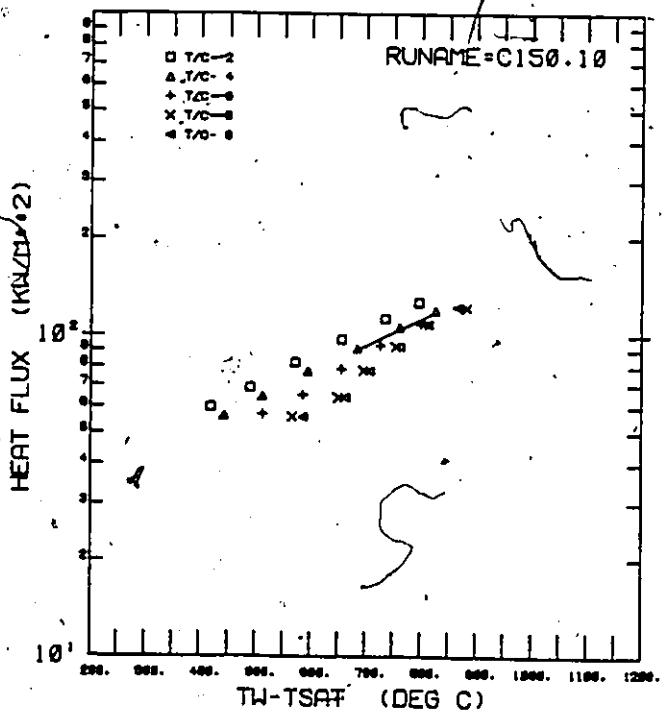
T/C-2
T/C- 4
T/C-6
T/C-8
T/C- 9
RUNAME=C150.10
HEAT FLUX (KW/M**2)
TW-TSAT (DEG C)

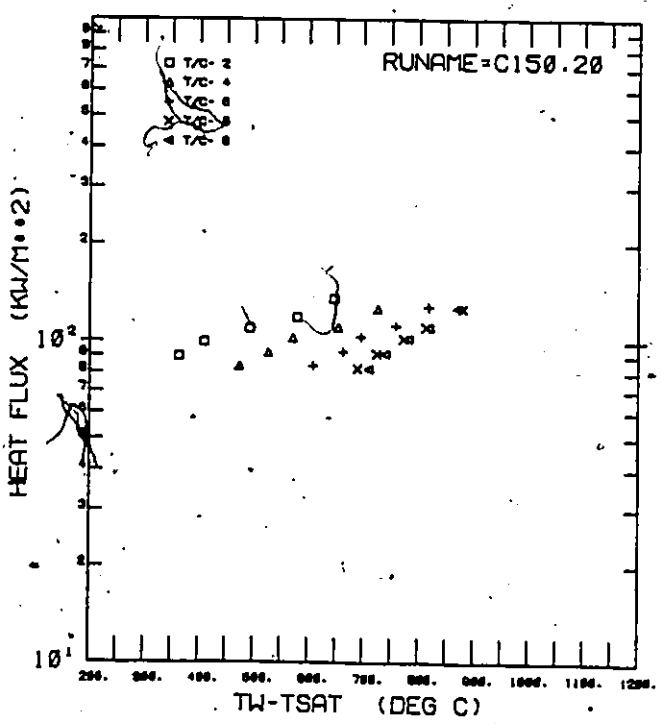
T/C- 2
T/C- 4
T/C- 6
T/C- 8
T/C- 9
RUNAME=C150.20
HEAT FLUX (KW/M**2)
TW-TSAT (DEG C)

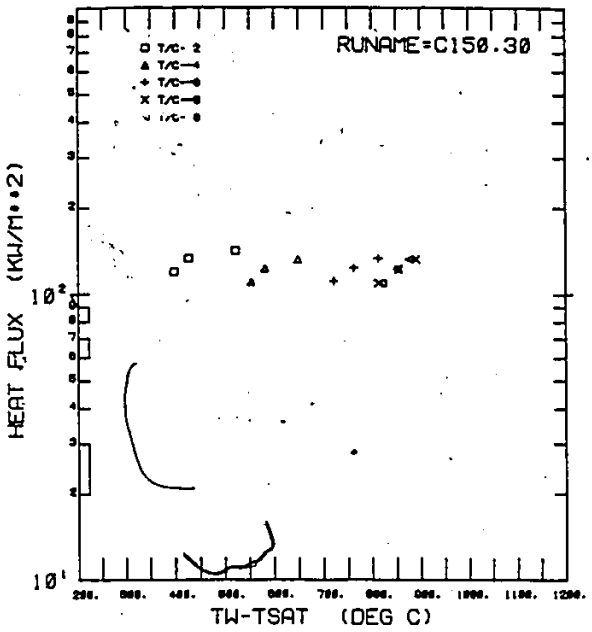
RUNAME=C150.30
HEAT FLUX (KW/M**2)
TW-TSAT (DEG C)

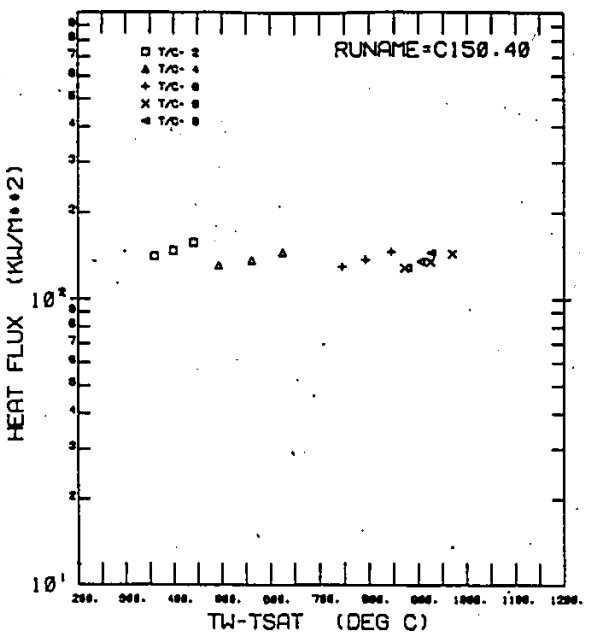
RUNAME=C150.40
HEAT FLUX (KW/M**2)
TW-TSAT (DEG C)

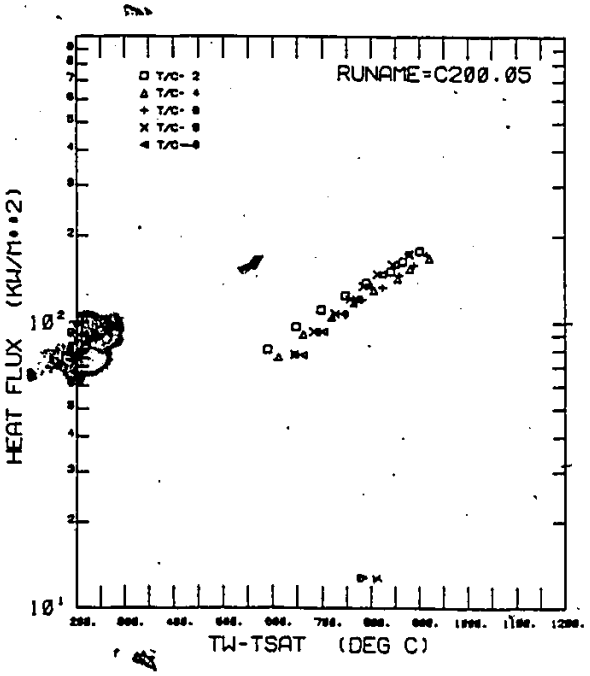
RUNAME=C200.05
HEAT FLUX (KW/M**2)
TW-TSAT (DEG C)

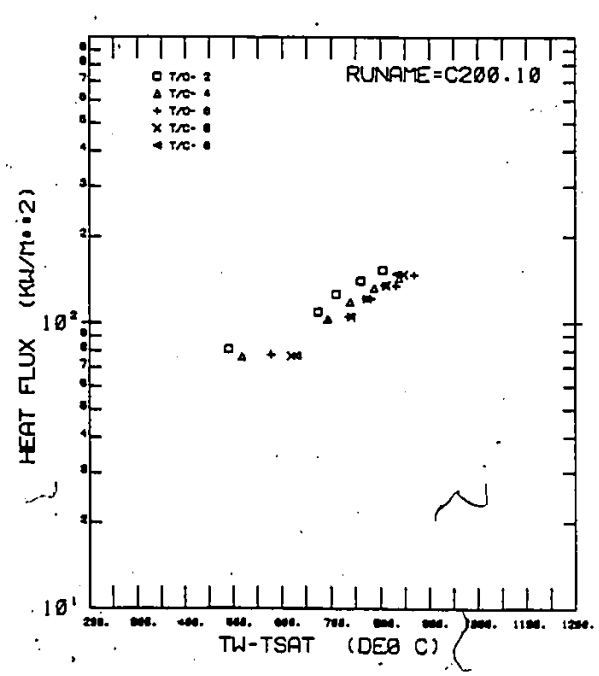
RUNAME=C200.10
HEAT FLUX (KW/M**2)
TW-TSAT (DEG C)

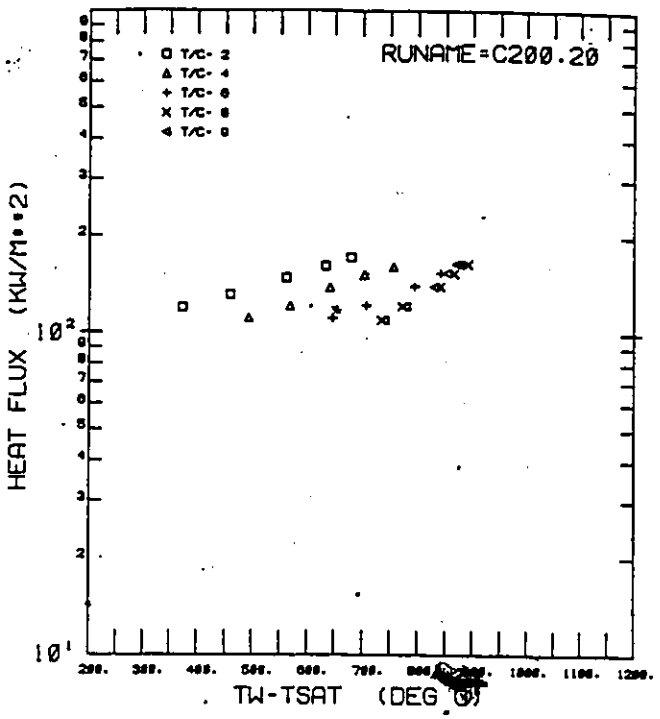
RUNAME=C200.20
T/C- 2
T/C- 4
T/C- 6
T/C- 8
T/C- 9
HEAT FLUX (KW/M**2)
TW-TSAT (DEG C)

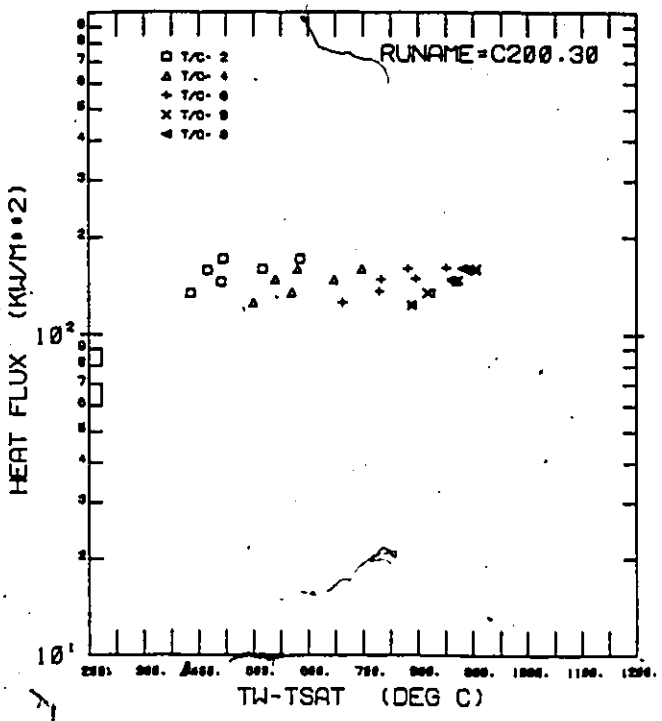
RUNAME=C200.30
T/C- 2
T/C- 4
T/C- 6
T/C- 8
T/C- 9
HEAT FLUX (KW/M**2)
TW-TSAT (DEG C)

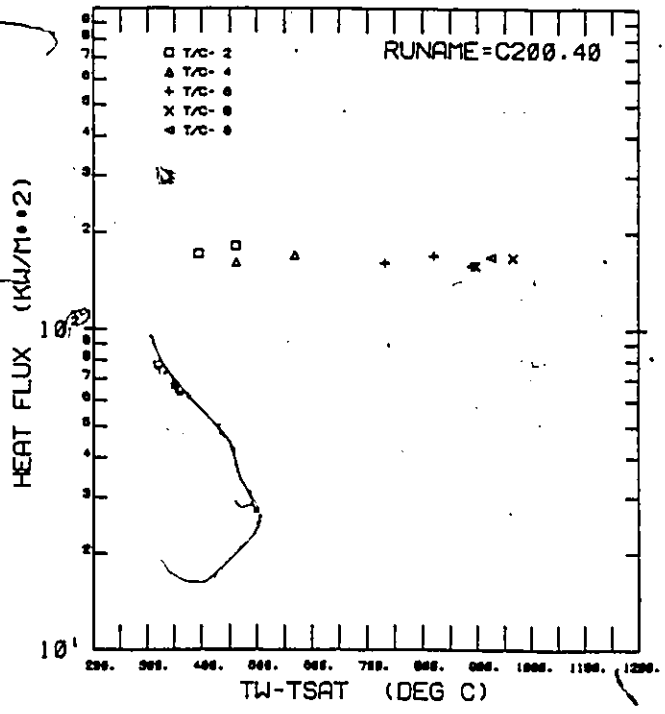
RUNAME=C200.40
T/C- 2
T/C- 4
T/C- 6
T/C- 8
T/C- 9
HEAT FLUX (KW/M**2)
TW-TSAT (DEG C)

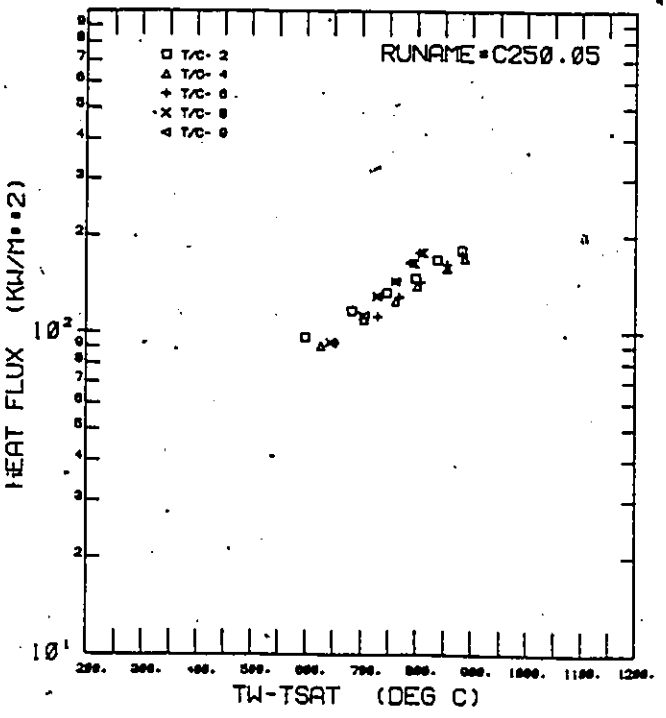
RUNAME=C250.05
T/C- 2
T/C- 4
T/C- 6
T/C- 8
T/C- 9
HEAT FLUX (KW/M**2)
TW-TSAT (DEG C)

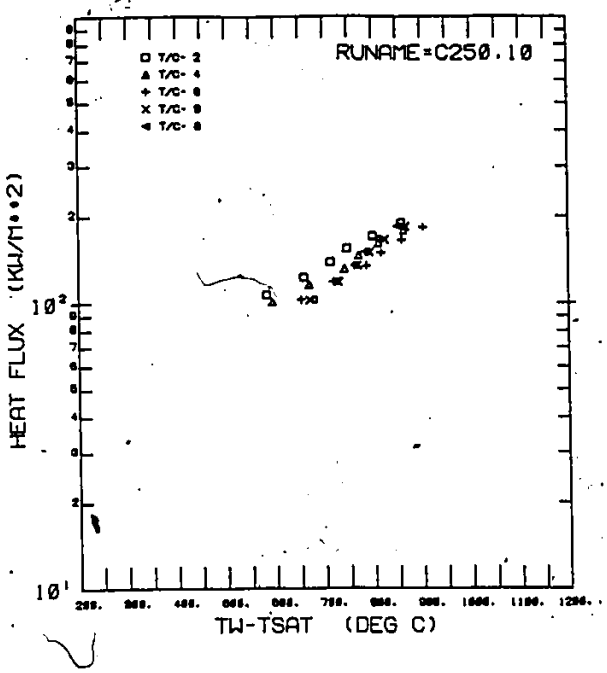
RUNAME=C250.10
HEAT FLUX (KW/M**2)
TW-TSAT (DEG C)

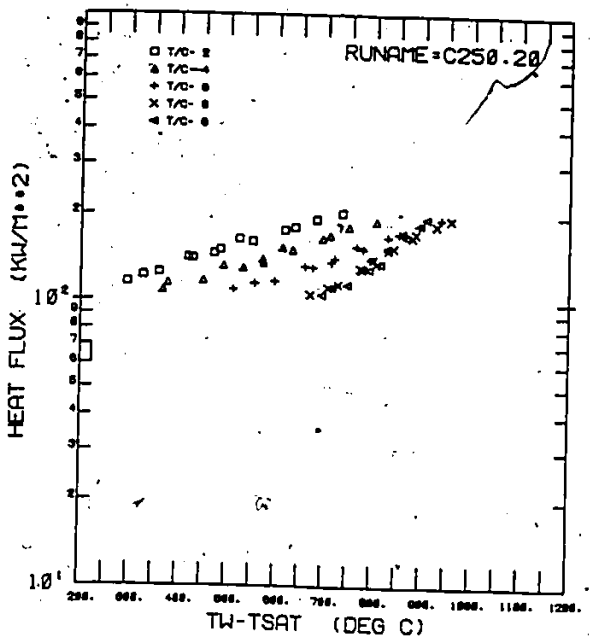
RUNAME=C250.20
HEAT FLUX (KW/M**2)
TW-TSAT (DEG C)

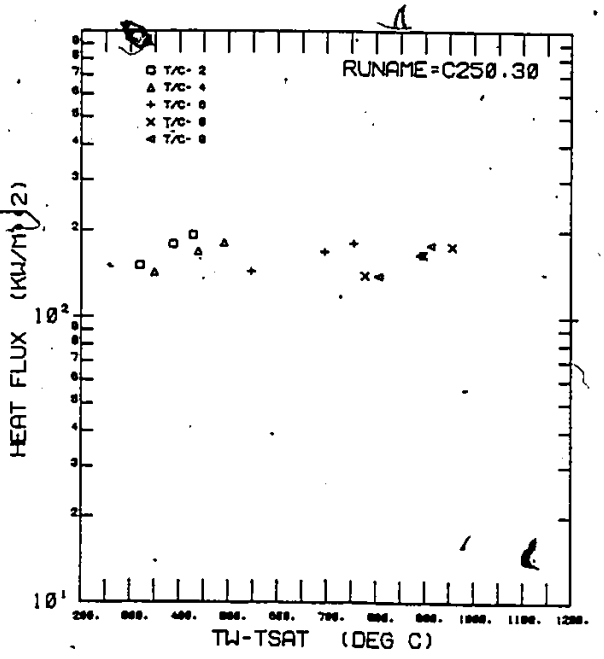
RUNAME=C250.30
HEAT FLUX (KW/M**2)
TW-TSAT (DEG C)

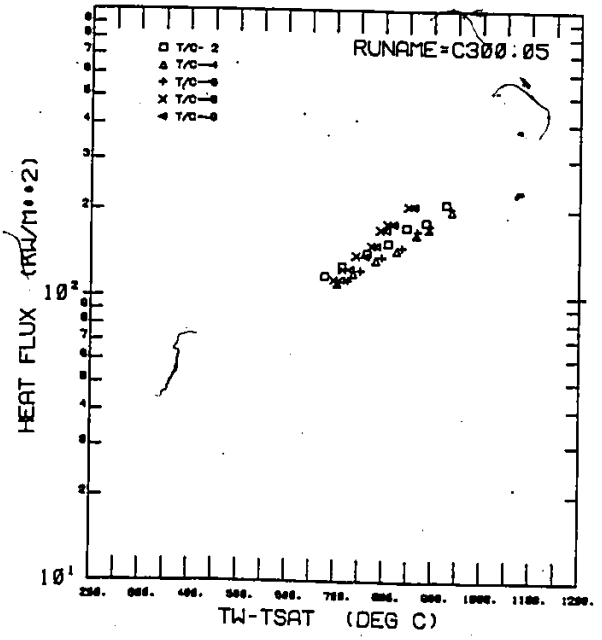
RUNAME=C300.05
HEAT FLUX (KW/M**2)
TW-TSAT (DEG C)

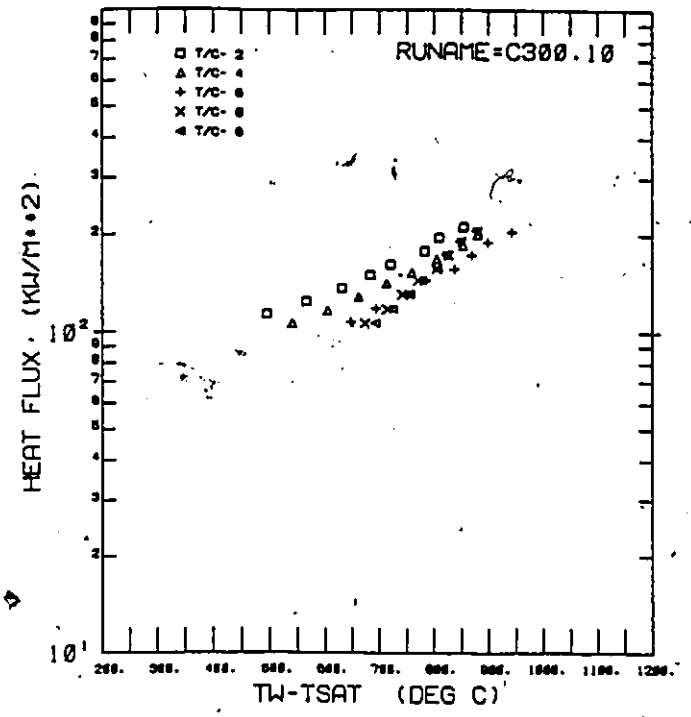
RUNAME=C300.10
HEAT FLUX (KW/M**2)
TW-TSAT (DEG C)

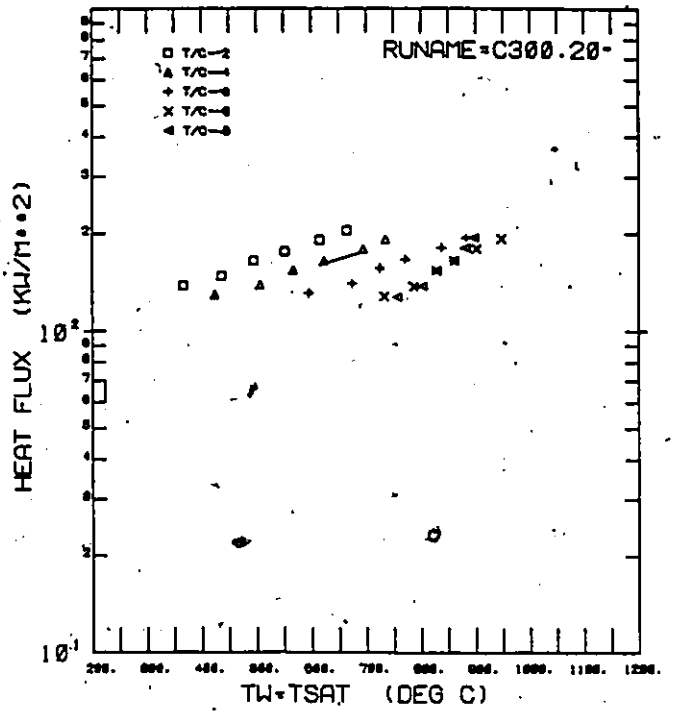
RUNAME=C300.20
HEAT FLUX (KW/M**2)
TW-TSAT (DEG C)

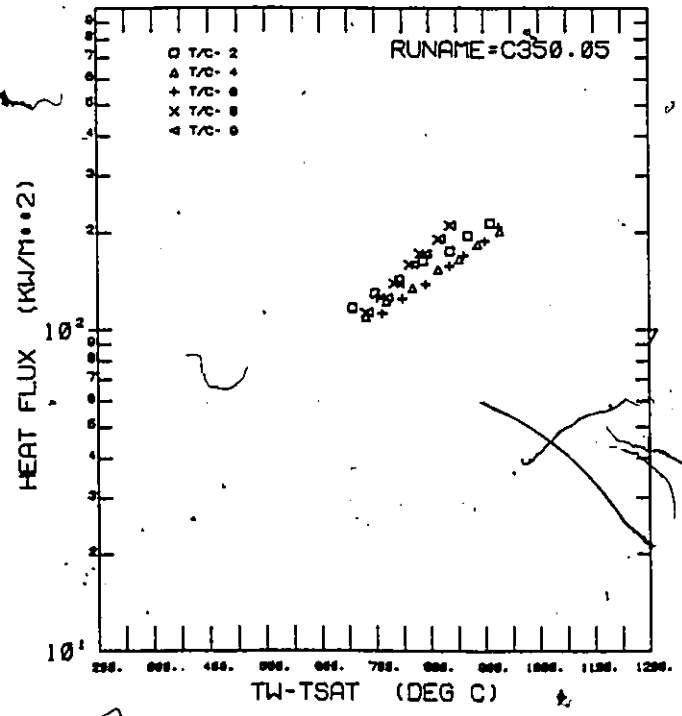
RUNAME=C350.05
HEAT FLUX (KW/M**2)
TW-TSAT (DEG C)

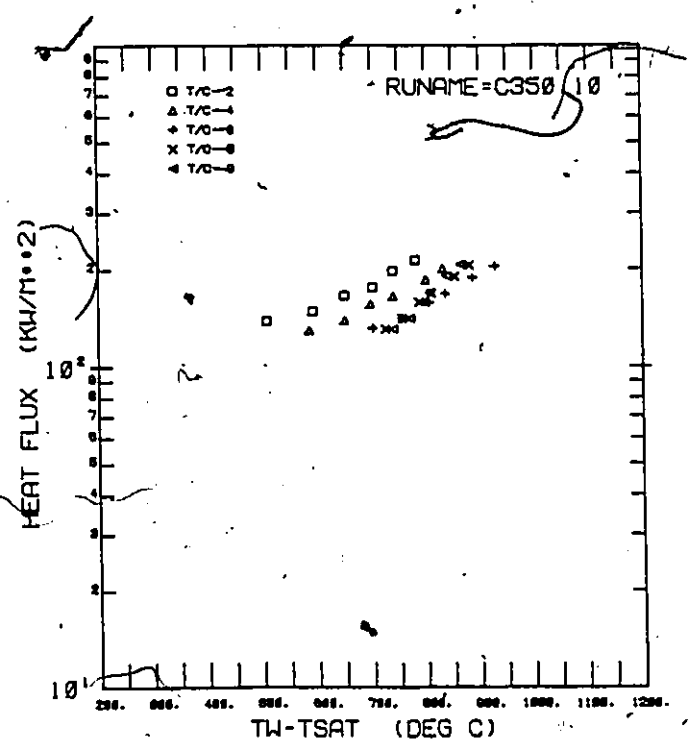
RUNAME=C350.10
HEAT FLUX (KW/M**2)
TW-TSAT (DEG C)

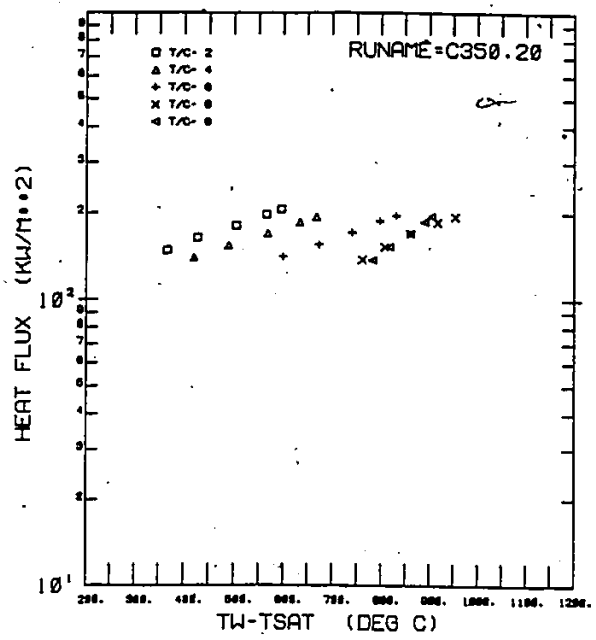
RUNAME=C350.20
HEAT FLUX (KW/M**2)
TW-TSAT (DEG C)

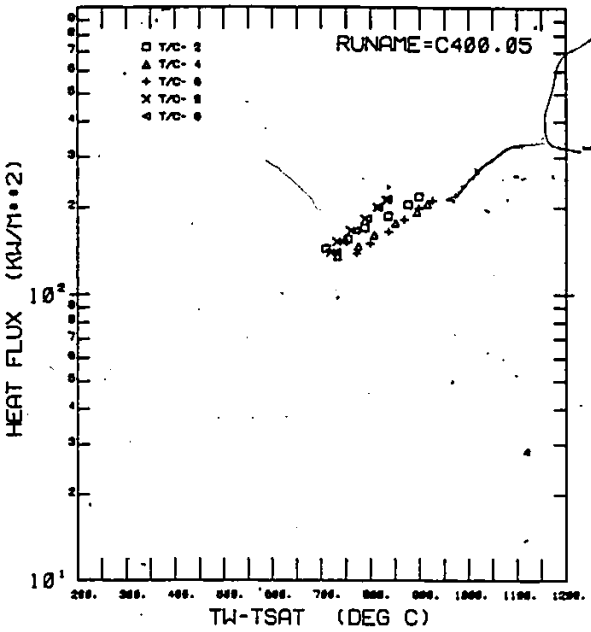
RUNAME=C400.05
HEAT FLUX (KW/M**2)
TW-TSAT (DEG C)

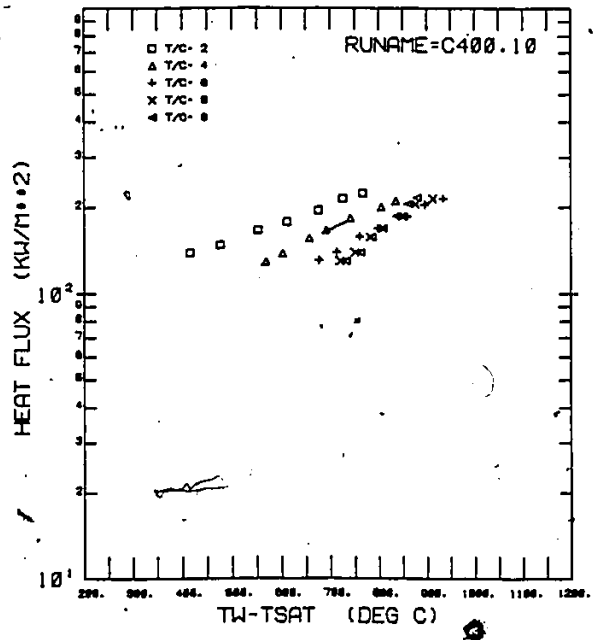
RUNAME=C400.10
HEAT FLUX (KW/M**2)
TW-TSAT (DEG C)

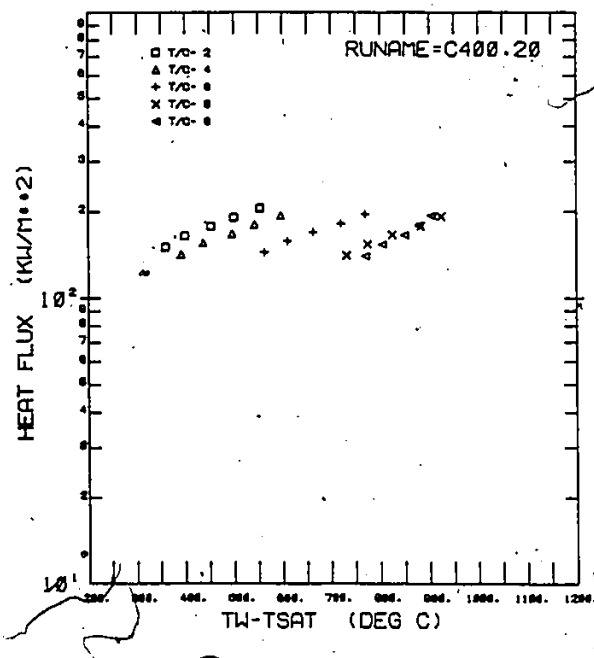
RUNAME=C400.20
HEAT FLUX (KW/M**2)
TW-TSAT (DEG C)

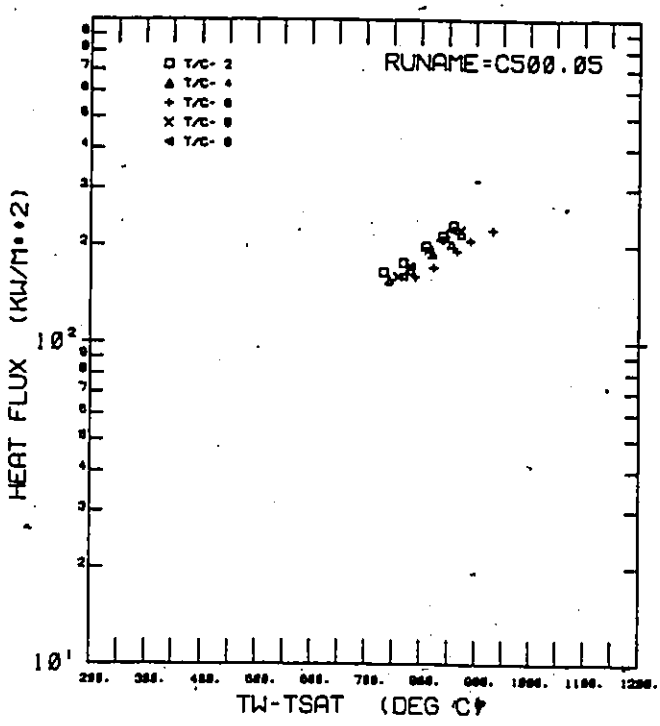
RUNAME=C500.05
T/C- 2
T/C- 4
T/C- 6
T/C- 8
T/C- 8
HEAT FLUX (KW/M**2)
TW-TSAT (DEG C)

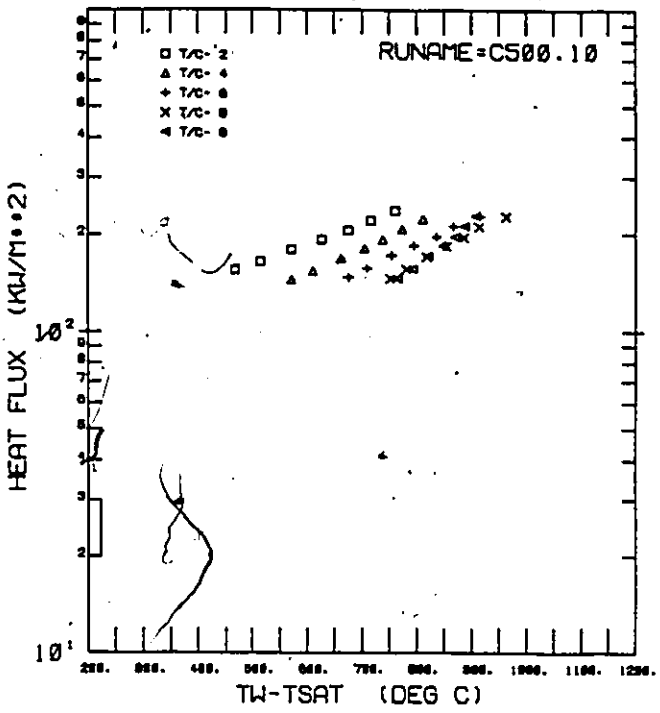
RUNAME=C500.10
T/C- 2
T/C- 4
T/C- 6
T/C- 8
T/C- 8
HEAT FLUX (KW/M**2)
TW-TSAT (DEG C)

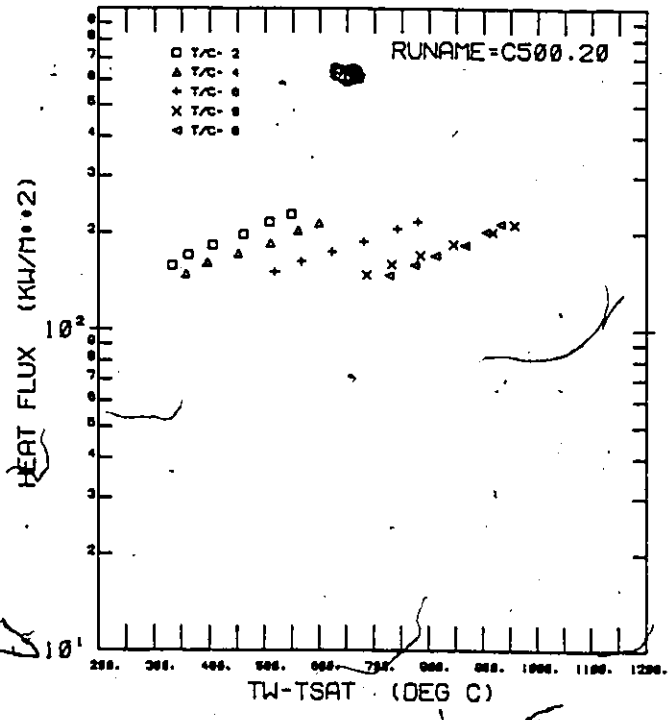
RUNAME=C500.20
T/C- 2
T/C- 4
T/C- 6
T/C- 8
T/C- 8
HEAT FLUX (KW/M**2)
TW-TSAT (DEG C)

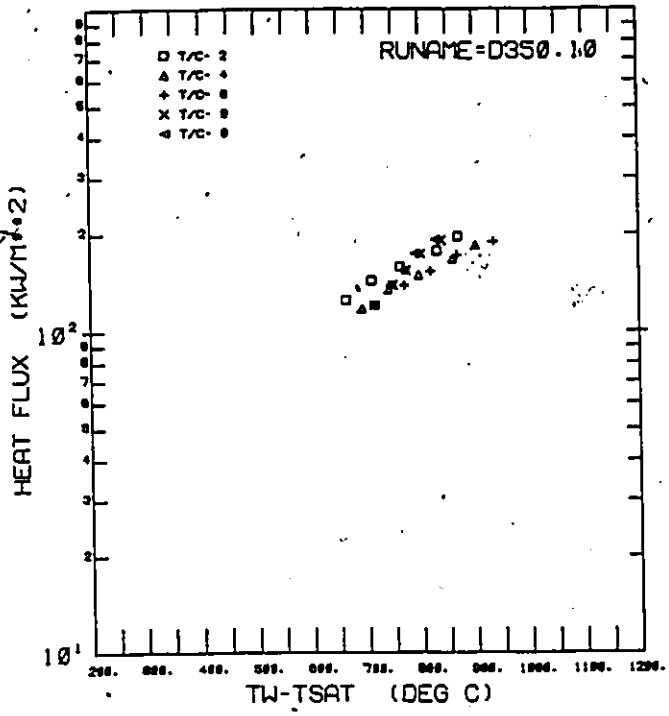
RUNAME=D350.10
T/C- 2
T/C- 4
T/C- 6
T/C- 8
T/C- 9
HEAT FLUX (KW/M**2)
TW-TSAT (DEG C)

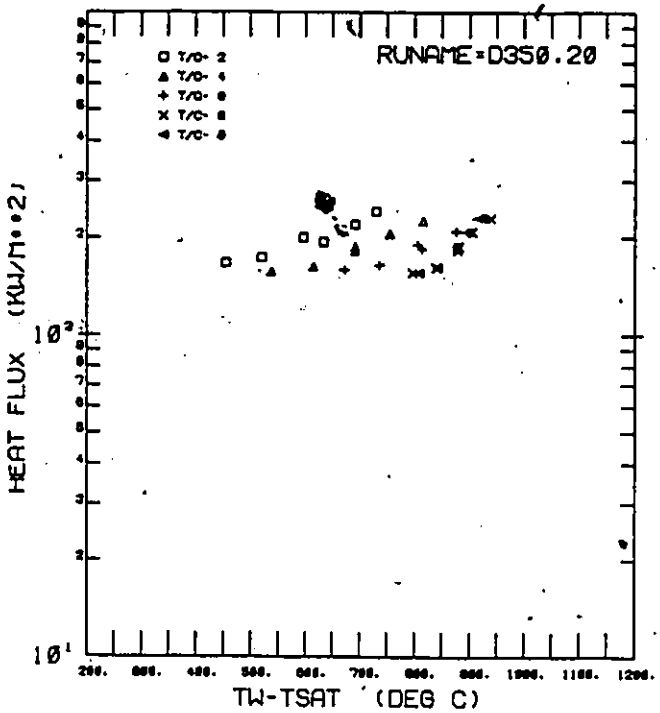
RUNAME=D350.20
T/C- 2
T/C- 4
T/C- 6
T/C- 8
T/C- 9
HEAT FLUX (KW/M**2)
TW-TSAT (DEG C)

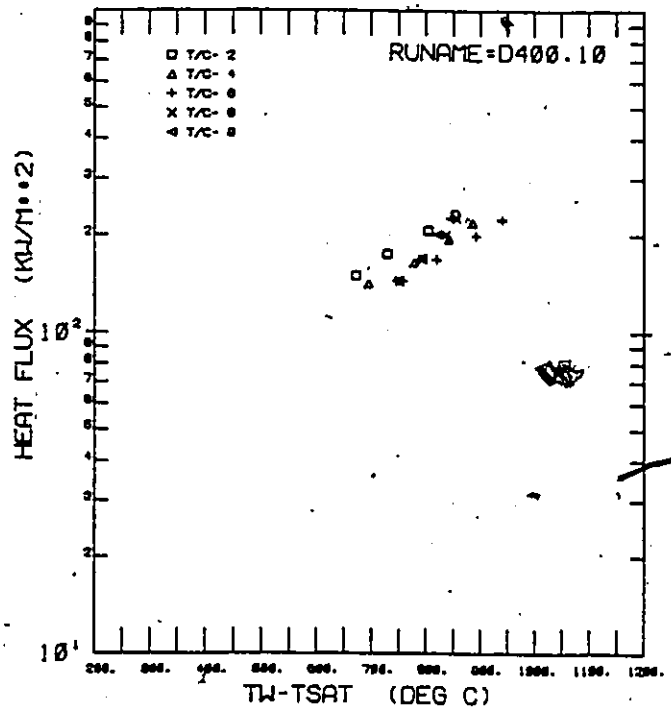
RUNAME=D400.10
T/C- 2
T/C- 4
T/C- 6
T/C- 8
T/C- 9
HEAT FLUX (KW/M**2)
TW-TSAT (DEG C)

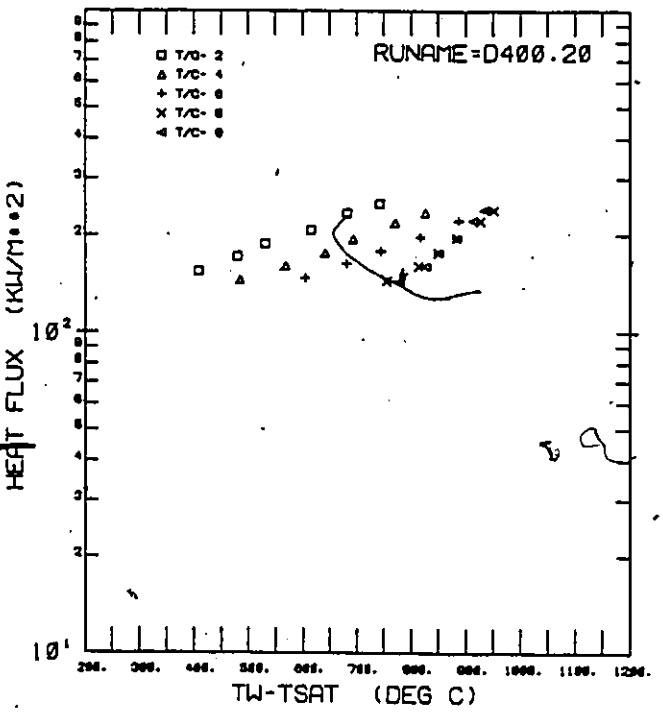
RUNAME=D400.20
T/C- 2
T/C- 4
T/C- 6
T/C- 8
T/C- 9
HEAT FLUX (KW/M**2)
TW-TSAT (DEG C)

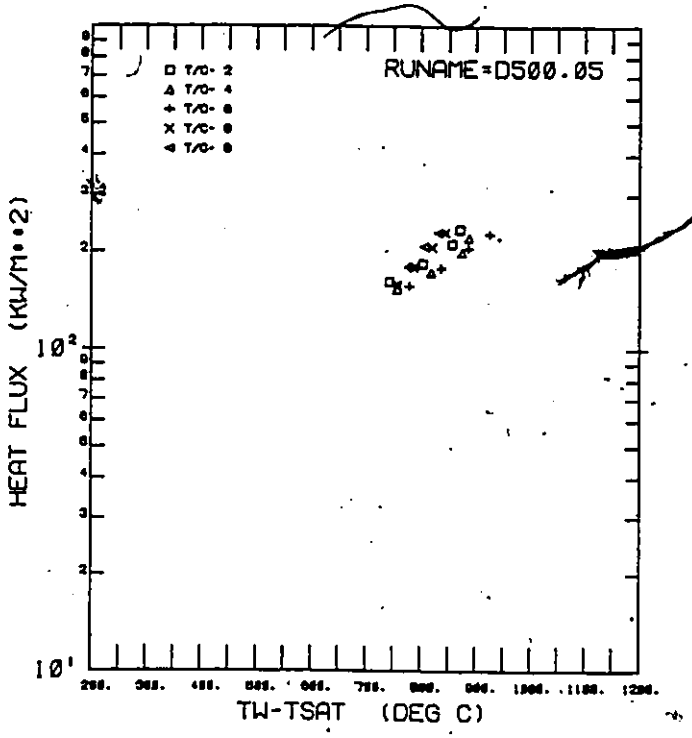
RUNAME=D500.05
T/C- 2
T/C- 4
T/C- 6
T/C- 8
T/C- 8
HEAT FLUX (KW/M**2)
TW-TSAT (DEG C)

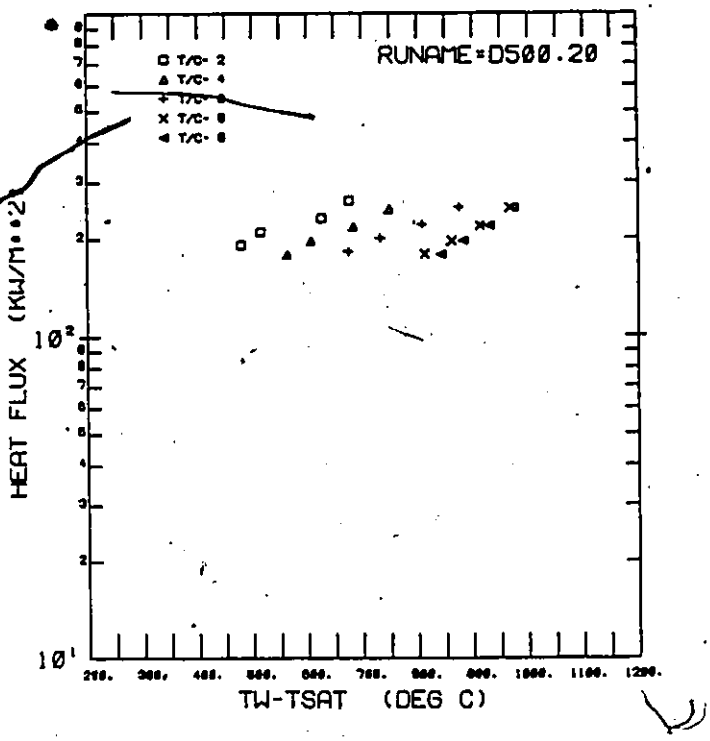
RUNAME=D500.20
T/C- 2
T/C- 4
T/C- 6
T/C- 8
T/C- 8
HEAT FLUX (KW/M**2)
TW-TSAT (DEG C)

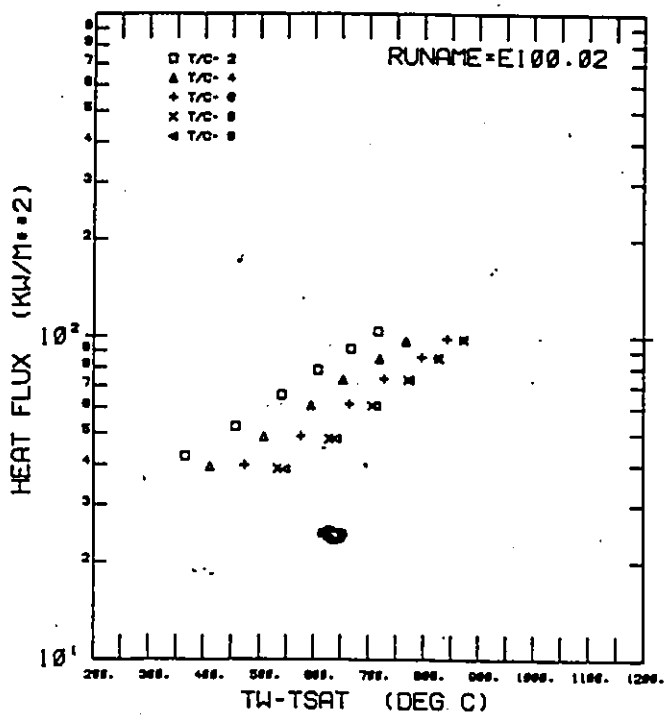
RUNAME=E100.02
T/C- 2
T/C- 4
T/C- 6
T/C- 8
T/C- 9
HEAT FLUX (KW/M**2)
TW-TSAT (DEG C)

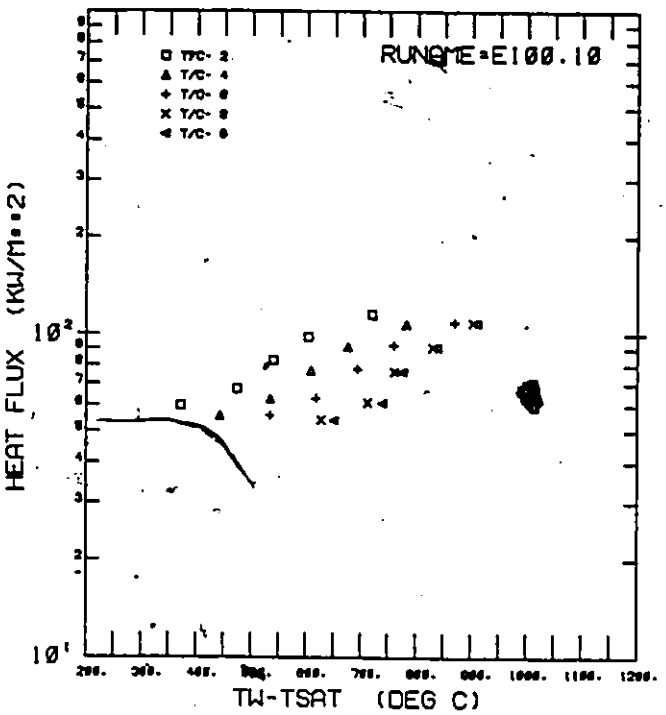
RUNAME=E100.10
T/C- 2
T/C- 4
T/C- 6
T/C- 8
T/C- 9
HEAT FLUX (KW/M**2)
TW-TSAT (DEG C)

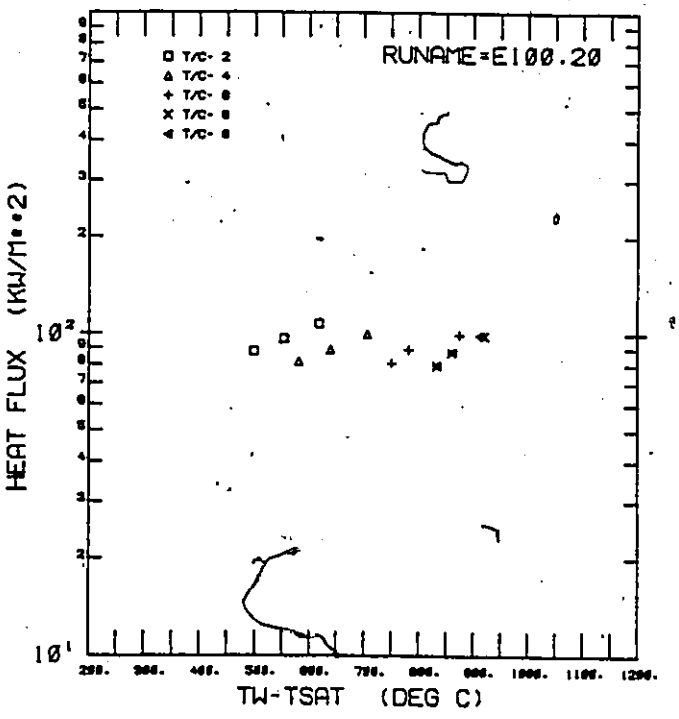
RUNAME=E100.20
T/C- 2
T/C- 4
T/C- 6
T/C- 8
T/C- 9
HEAT FLUX (KW/M**2)
TW-TSAT (DEG C)

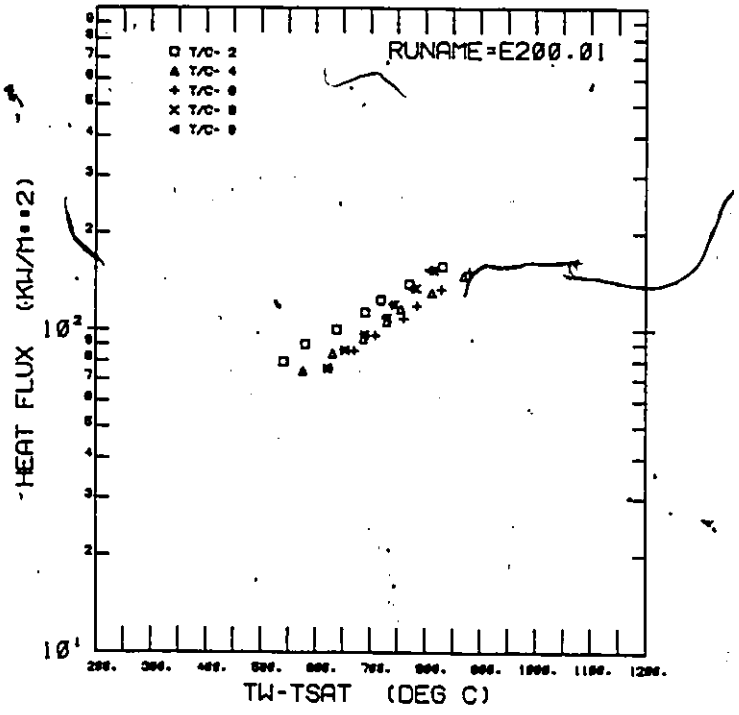
RUNAME=E200.01
T/C- 2
T/C- 4
T/C- 6
T/C- 8
T/C- 9
HEAT FLUX (KW/M**2)
TW-TSAT (DEG C)

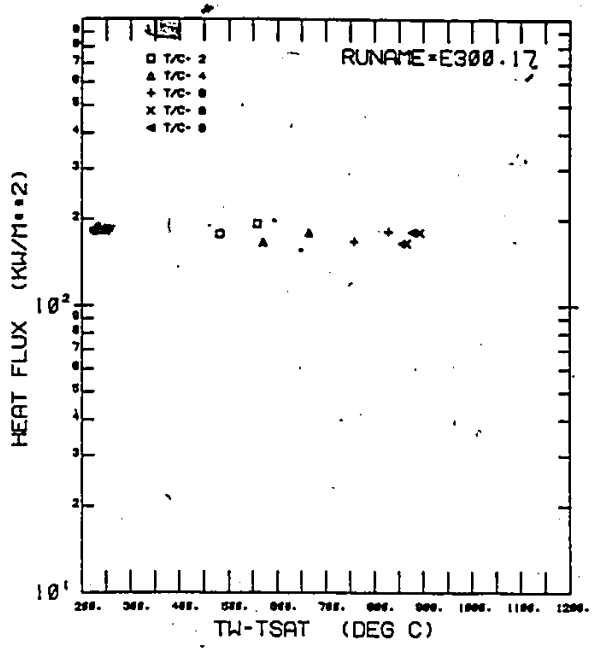
RUNAME=E300.17
T/C- 2
T/C- 4
T/C- 6
T/C- 8
T/C- 9
HEAT FLUX (KW/M**2)
TW-TSAT (DEG C)

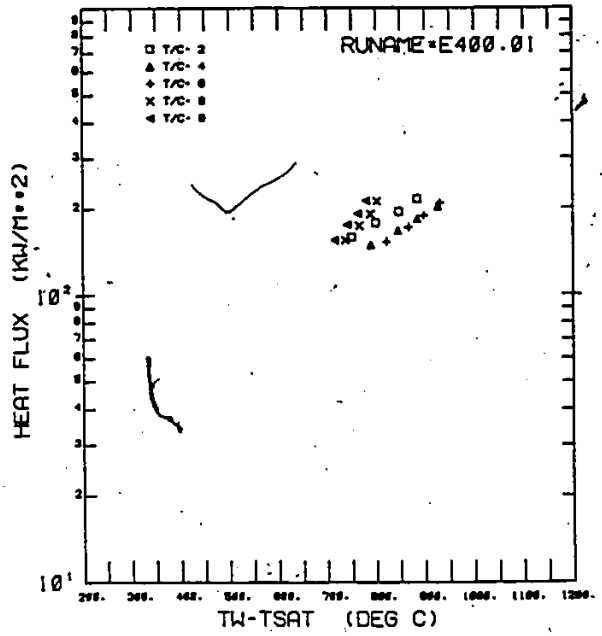
RUNAME=E400.01
T/C- 2
T/C- 4
T/C- 6
T/C- 8
T/C- 9
HEAT FLUX (KW/M**2)
TW-TSAT (DEG C)

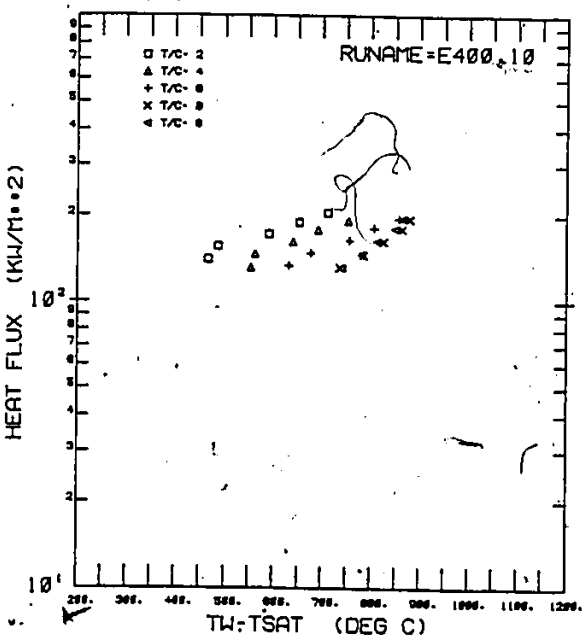
RUNAME=E400.10
T/C- 2
T/C- 4
T/C- 6
T/C- 8
T/C- 9
HEAT FLUX (KW/M**2)
TW-TSAT (DEG C)

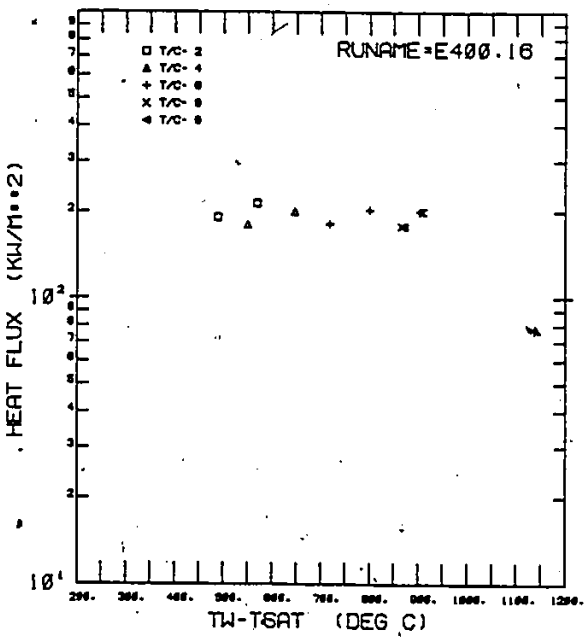
RUNAME=E400.16
T/C- 2
T/C- 4
T/C- 6
T/C- 8
T/C- 9
HEAT FLUX (KW/M**2)
TW-TSAT (DEG C)

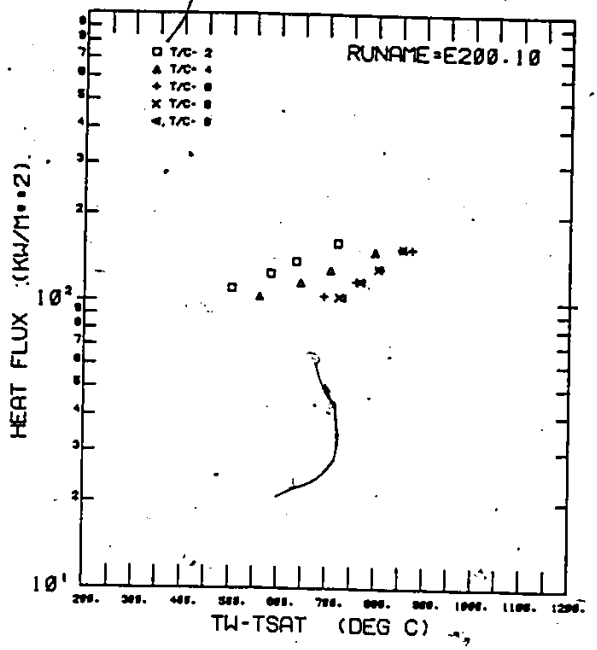
RUNAME=E200.10
T/C- 2
T/C- 4
T/C- 6
T/C- 8
T/C- 9
HEAT FLUX (KW/M**2)
TW-TSAT (DEG C)

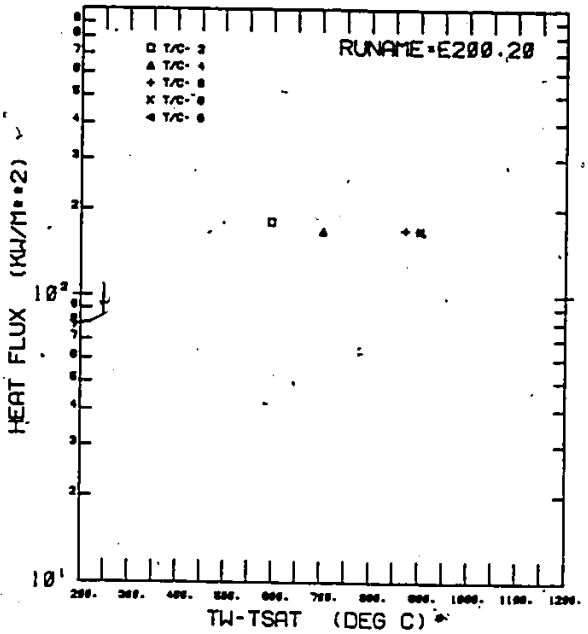
RUNAME=E200.20
T/C- 2
T/C- 4
T/C- 6
T/C- 8
T/C- 9
HEAT FLUX (KW/M**2)
TW-TSAT (DEG C)

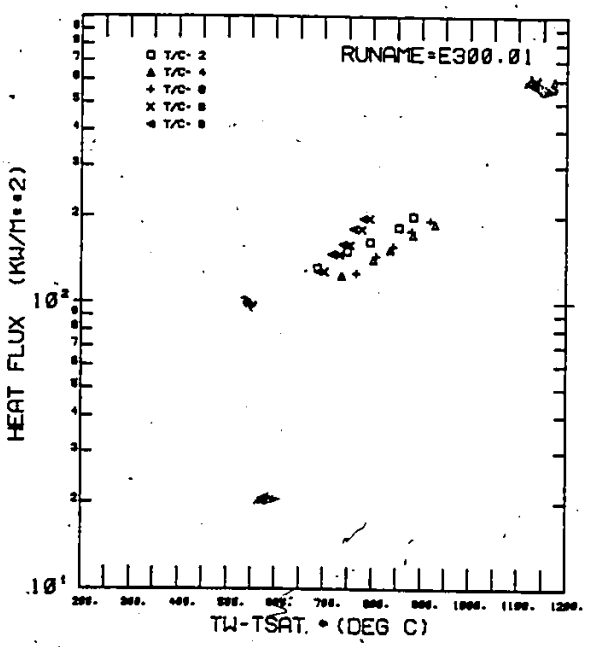
RUNAME=E300.01
T/C- 2
T/C- 4
T/C- 6
T/C- 8
T/C- 9
HEAT FLUX (KW/M**2)
TW-TSAT (DEG C)

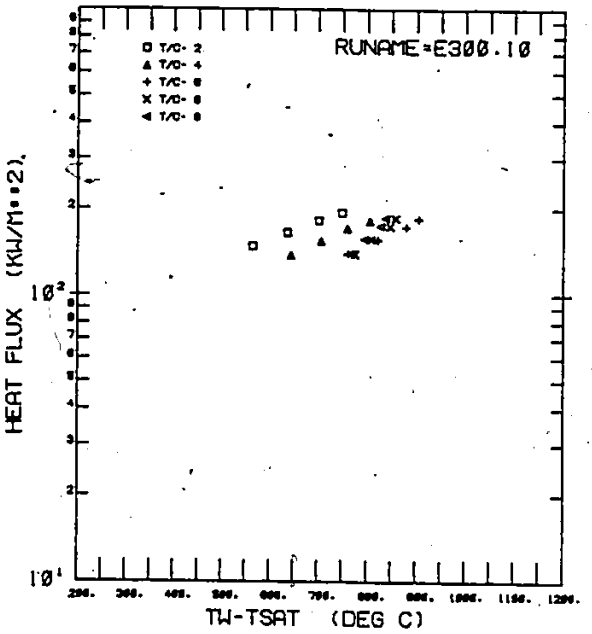
RUNAME=E300.10
T/C- 2
T/C- 4
T/C- 6
T/C- 8
T/C- 9
HEAT FLUX (KW/M**2)
TW-TSAT (DEG C)

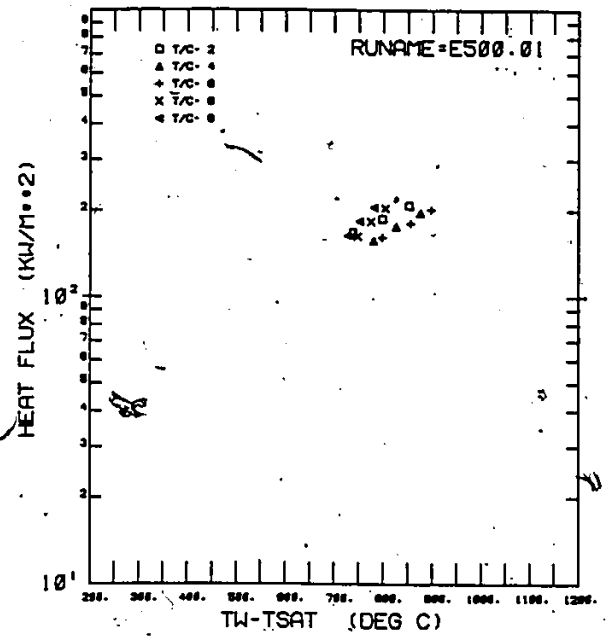
RUNAME=E500.01
T/C- 2
T/C- 4
T/C- 6
T/C- 8
T/C- 8
HEAT FLUX (KW/M**2)
TW-TSAT (DEG C)

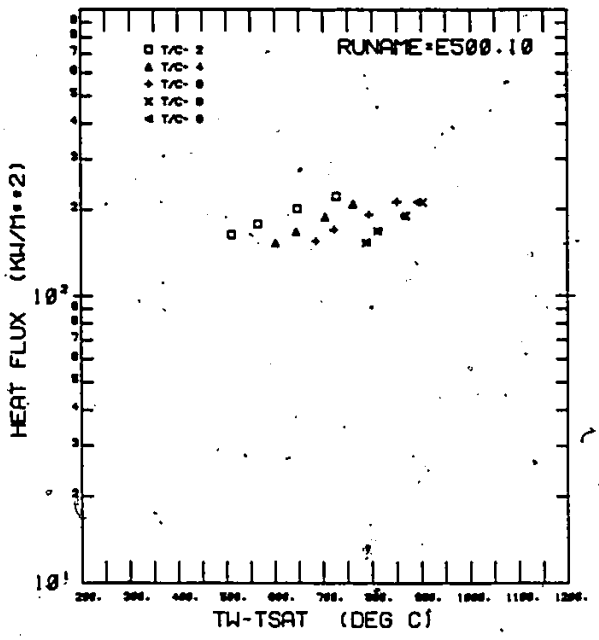
RUNAME=E500.10
T/C- 2
T/C- 4
T/C- 6
T/C- 8
T/C- 8
HEAT FLUX (KW/M**2)
TW-TSAT (DEG C)

APPENDIX E: VOID FRACTION DATA

The void fraction data are tabulated in the following format:

First line

Run name (see Appendix C)

Equilibrium quality at void fraction measurement locations

Second line

Void fraction at five locations

The void fraction measurement locations are at 1.5, 15, 30, 43 and 52 cm downstream from the top of the hot patch. Note that not all five locations were measured. The equilibrium quality is calculated by interpolation between the thermocouple locations (See Appendix C).

The data are shown graphically following the tabulation.

D350.101	-.106E-01	-.380E-02	.394E-02	.107E-01	.155E-01
	58.	59.	76.	83.	92.
D350.102	-.117E-01	-.393E-02	.493E-02	.128E-01	.183E-01
	58.	65.	79.	84.	90.
D350.103	-.118E-01	-.318E-02	.651E-02	.153E-01	.214E-01
	57.	63.	79.	85.	94.
D350.104	-.123E-01	-.272E-02	.791E-02	.178E-01	.247E-01
	58.	68.	81.	89.	92.
D350.105	-.157E-01	-.425E-02	.919E-02	.201E-01	.278E-01
	57.	69.	81.	86.	96.
D350.201	-.214E-01	-.108E-01	.811E-03	.112E-01	.184E-01
	9.	2[illegible]	69.	86.	93.
D350.202	-.231E-01	-.110E-01	.219E-02	.140E-01	.223E-01
	10.	35.	73.	86.	95.
D350.203	-.251E-01	-.118E-01	.279E-02	.158E-01	.249E-01
	10.	38.	74.	90.	96.
D350.204	-.223E-01	-.114E-01	.565E-03	.112E-01	.186E-01
	6.	28.	67.	83.	94.
D350.205	-.202E-01	-.108E-01	-.518E-03	.862E-02	.150E-01
	3.	22.	56.	78.	92.
D350.206	-.202E-01	-.111E-01	-.121E-02	.757E-02	.137E-01
	3.	14.	45.	72.	85.
D400.101	-.157E-01	-.684E-02	.376E-02	.124E-01	.187E-01
	50.	60.	84.	91.	97.
D400.102	-.168E-01	-.626E-02	.566E-02	.162E-01	.236E-01
	47.	61.	88.	93.	98.
D400.103	-.178E-01	-.593E-02	.742E-02		
	45.	64.	91.		
D400.104	-.110E-01	-.353E-02	.225E-02	.102E-01	.155E-01
	48.	57.	79.	87.	96.
D400.201	-.240E-01	-.135E-01	-.199E-02	.821E-02	.154E-01
	10.	29.	68.	86.	93.
D400.202	-.256E-01	-.138E-01	-.733E-03	.108E-01	.189E-01
	11.	36.	75.	89.	93.
D400.203	-.268E-01	-.140E-01	.491E-04	.125E-01	.213E-01
	12.	39.	79.	89.	95.
D400.204	-.222E-01	-.128E-01	-.236E-02	.684E-02	.133E-01
	8.	22.	58.	77.	87.
D400.205	-.216E-01	-.130E-01	-.344E-02	.511E-02	.109E-01
	5.	18.	52.	75.	88.
D400.206	-.184E-01	-.107E-01	-.216E-02	.542E-02	.107E-01
	4.	18.	44.	68.	84.
D500.051	-.142E-01	-.667E-02	.151E-02	.915E-02	.145E-01
	58.	62.	84.	87.	92.
D500.052	-.150E-01	-.637E-02	.260E-02	.115E-01	.177E-01
	51.	65.	83.	93.	97.
D500.053	-.172E-01	-.752E-02	.285E-02	.127E-01	.195E-01
	51.	64.	83.	90.	97.
D500.054	-.131E-01	-.654E-02	.673E-03	.735E-02	.120E-01
	47.	58.	80.	85.	89.
D500.201	-.265E-01	-.171E-01	-.679E-02	.220E-02	.862E-02
	7.	21.	52.	73.	83.
D500.202	-.293E-01	-.186E-01	-.688E-02	.335E-02	.107E-01
	9.	27.	59.	78.	87.
D500.203	-.246E-01	-.161E-01	-.685E-02	.125E-02	.702E-02
	7.	20.	43.	66.	79.
D500.204	-.211E-01	-.134E-01	-.501E-02	.230E-02	.758E-02
	7.	17.	38.	60.	76.

E100.021	.151E-01	.304E-01	.472E-01		
	74.	90.	97.		
E100.022	.154E-01	.334E-01	.531E-01		
	73.	92.	95.		
E100.023	.150E-01	.363E-01	.587E-01		
	74.	93.	95.		
E100.024	.150E-01	.378E-01	.418E-01		
	70.	89.	95.		
E100.025	.143E-01	.245E-01	.355E-01		
	70.	91.	95.		
E100.026	.146E-01	.231E-01	.320E-01		
	70.	87.	94.		
E100.101	-.469E-02	.145E-01	.355E-01	.535E-01	
	42.	80.	95.	97.	
E100.102	-.347E-02	.192E-01	.442E-01	.658E-01	
	46.	83.	91.	98.	
E100.103	-.412E-02	.121E-01	.297E-01	.448E-01	
	40.	78.	92.	94.	
E100.104	-.279E-02	.103E-01	.246E-01	.367E-01	
	37.	73.	90.	95.	
E100.105	-.478E-02	.662E-02	.192E-01	.298E-01	
	30.	66.	87.	93.	
E100.201	-.945E-02	.133E-01	.361E-01	.557E-01	.693E-01
	50.	78.	94.	95.	97.
E100.202	-.732E-02	.112E-01	.315E-01	.489E-01	.609E-01
	45.	79.	92.	94.	95.
E100.203	-.729E-02	.972E-02	.281E-01	.438E-01	.547E-01
	49.	77.	94.	94.	95.
E200.011	.230E-02	.147E-01	.286E-01		
	61.	87.	93.		
E200.012	.202E-02	.160E-01	.316E-01		
	65.	87.	92.		
E200.013	.170E-02	.176E-01	.354E-01		
	62.	87.	93.		
E200.014	.250E-02	.138E-01	.265E-01		
	61.	87.	92.		
E200.015	.309E-02	.131E-01	.243E-01		
	63.	86.	91.		
E200.016	.365E-02	.127E-01	.227E-01		
	64.	86.	90.		
E200.017	.332E-02	.113E-01	.201E-01		
	62.	83.	91.		
E200.101	-.137E-01	-.343E-03	.145E-01	.274E-01	
	20.	57.	83.	92.	
E200.102	-.149E-01	.679E-03	.181E-01	.332E-01	
	18.	63.	85.	98.	
E200.103	-.135E-01	-.147E-02	.119E-01	.235E-01	
	18.	53.	82.	90.	
E200.104	-.134E-01	-.264E-02	.932E-02	.195E-01	
	18.	43.	79.	89.	
E200.201	-.263E-01	-.872E-02	.106E-01	.274E-01	
	7.	34.	78.	96.	
E300.011	-.496E-02	.505E-02	.164E-01	.264E-01	
	43.	82.	89.	95.	
E300.012	-.552E-02	.535E-02	.176E-01	.284E-01	
	54.	81.	87.	94.	
E300.013	-.642E-02	.592E-02	.198E-01	.321E-01	
	50.	81.	89.	97.	
E300.014	-.679E-02	.665E-02	.218E-01	.352E-01	
	52.	79.	89.	96.	
E300.015	-.351E-02	.489E-02	.147E-01	.235E-01	
	50.	80.	87.	92.	
E300.101	-.203E-01	-.732E-02	.721E-02	.199E-01	
	16.	55.	82.	94.	
E300.102	-.200E-01	-.785E-02	.584E-02	.177E-01	
	17.	49.	79.	90.	
E300.103	-.171E-01	-.611E-02	.373E-02	.148E-01	
	16.	42.	78.	87.	
E300.104	-.168E-01	-.704E-02	.309E-02	.127E-01	
	15.	38.	72.	86.	
E300.171	-.275E-01	-.147E-01	-.714E-03	.116E-01	
	9.	24.	67.	84.	
E300.172	-.277E-01	-.159E-01	-.303E-02	.824E-02	
	7.	18.	61.	84.	
E400.011	-.113E-01	-.133E-02	.101E-01	.202E-01	
	46.	72.	85.	94.	
E400.013	-.101E-01	-.975E-03	.943E-02	.186E-01	
	48.	73.	85.	90.	
E400.014	-.919E-02	-.113E-02	.812E-02	.163E-01	
	49.	73.	89.	91.	
E400.101	-.235E-01	-.131E-01	-.170E-02	.843E-02	
	12.	35.	70.	85.	
E400.102	-.230E-01	-.134E-01	-.274E-02	.665E-02	
	11.	33.	66.	82.	
E400.103	-.222E-01	-.135E-01	-.378E-02	.497E-02	
	9.	28.	61.	76.	
E400.104	-.210E-01	-.132E-01	-.474E-02	.258E-02	
	8.	23.	54.	77.	
E400.105	-.179E-01	-.109E-01	-.348E-02	.290E-02	
	12.	19.	53.	72.	
E400.161	-.262E-01	-.186E-01	-.809E-02	.102E-02	
	9.	13.	43.	70.	
E400.162	-.295E-01	-.187E-01	-.695E-02	.326E-02	
	5.	18.	54.	80.	
E500.011	-.117E-01	-.490E-02	.180E-02	.892E-02	.138E-01
	38.	60.	77.	86.	93.
E500.012	-.128E-01	-.519E-02	.215E-02	.102E-01	.157E-01
	41.	60.	78.	87.	93.
E500.013	-.118E-01	-.331E-02	.243E-02	.116E-01	.177E-01
	40.	62.	76.	90.	94.
E500.101	-.237E-01	-.155E-01	-.649E-02	.135E-02	.692E-02
	17.	27.	55.	74.	82.
E500.102	-.259E-01	-.168E-01	-.677E-02	.195E-02	.817E-02
	14.	29.	58.	78.	85.
E500.103	-.218E-01	-.146E-01	-.671E-02	.232E-03	.514E-02
	16.	30.	53.	71.	79.
E500.104	-.205E-01	-.138E-01	-.664E-02	-.255E-03	.423E-02
	21.	31.	47.	68.	75.

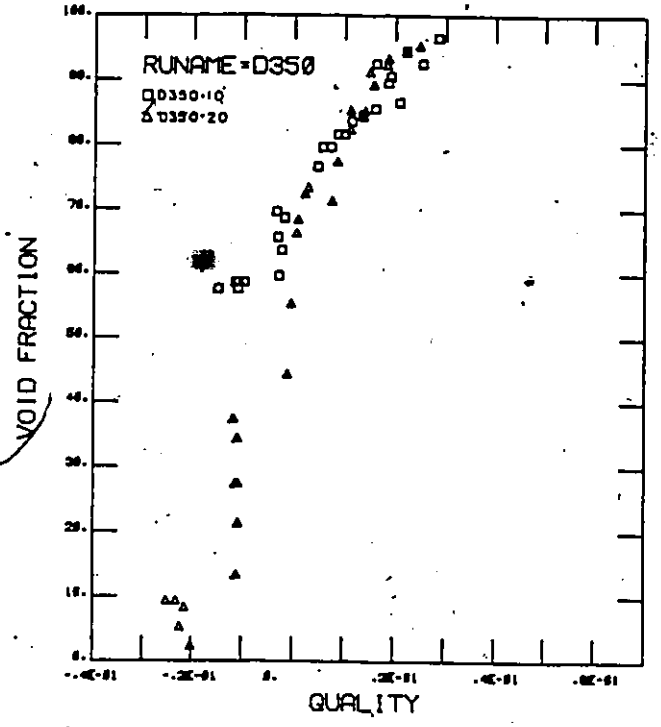
RUNAME=D350
D350-10
D350-20
VOID FRACTION
QUALITY

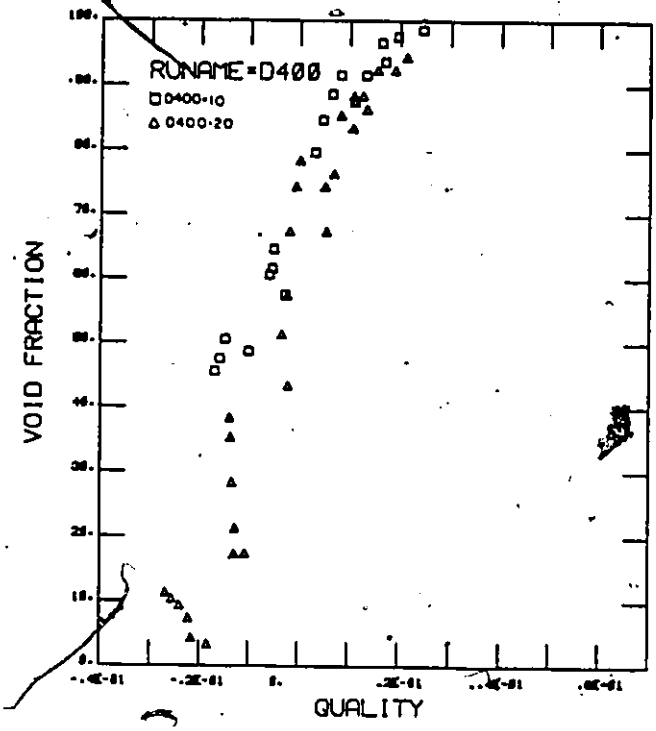
RUNAME=D400
D400-10
D400-20
VOID FRACTION
QUALITY

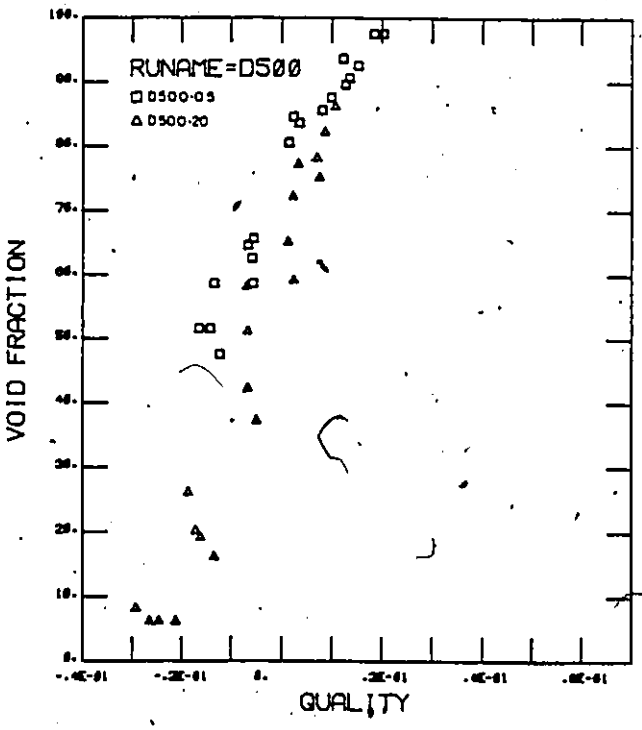
RUNAME=D500
D500-05
D500-20
VOID FRACTION
QUALITY

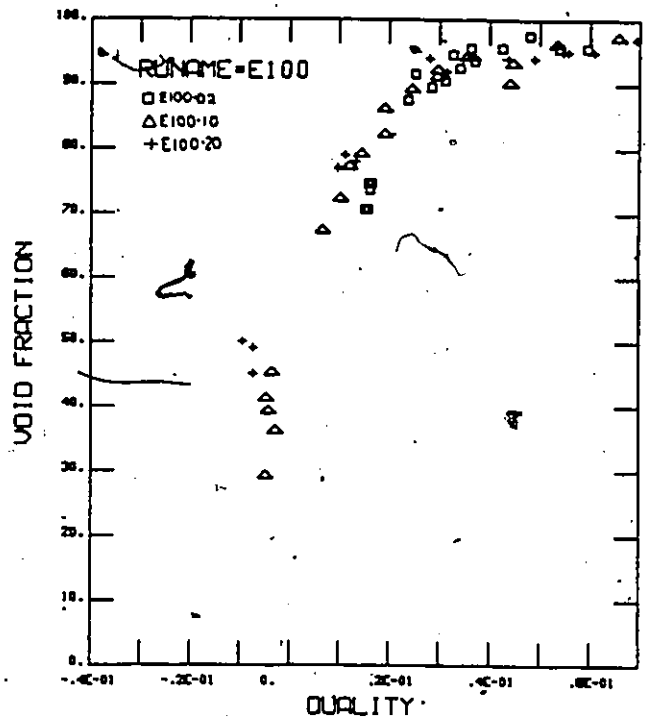
RUNNAME=E100
□ E100-02
△ E100-10
+ E100-20
VOID FRACTION
QUALITY

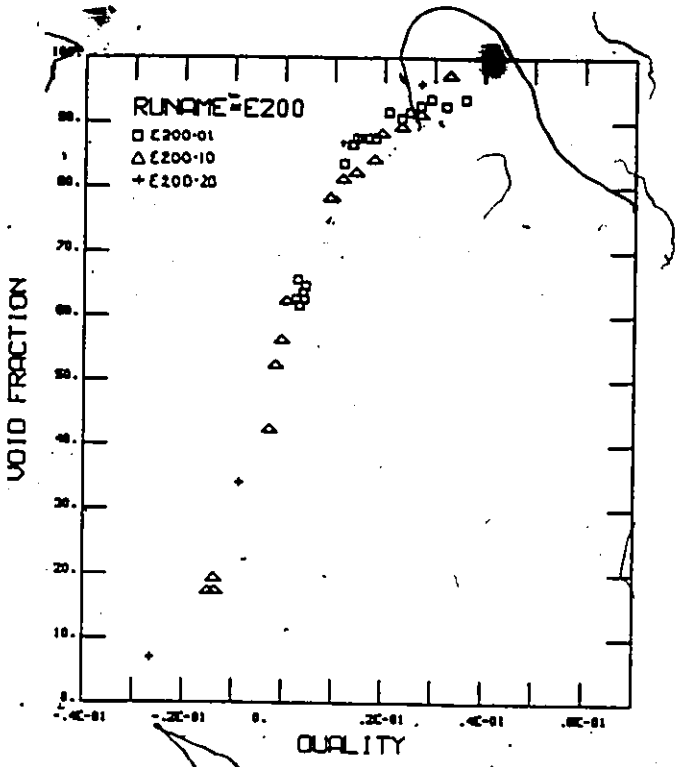
RUNNAME=E200
□ E200-01
△ E200-10
+ E200-20
VOID FRACTION
QUALITY

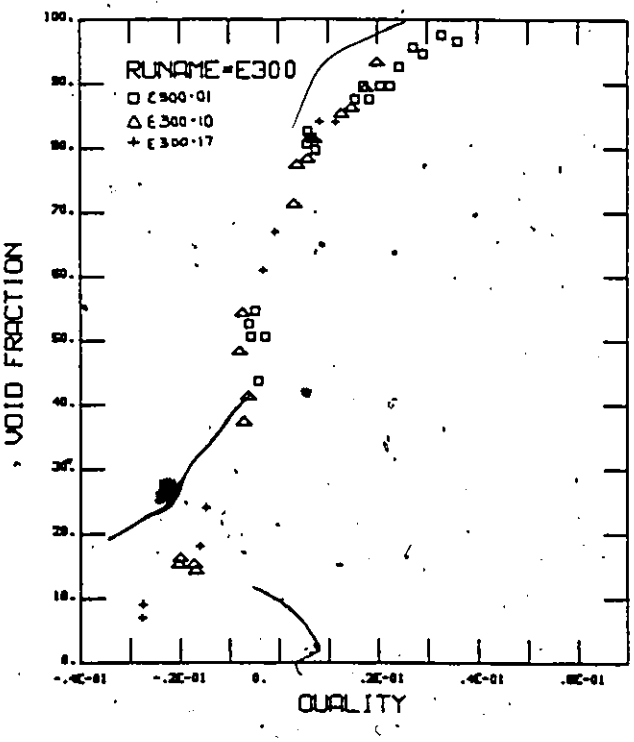
RUNNAME=E300
□ E300-01
△ E300-10
+ E300-17
VOID FRACTION
QUALITY

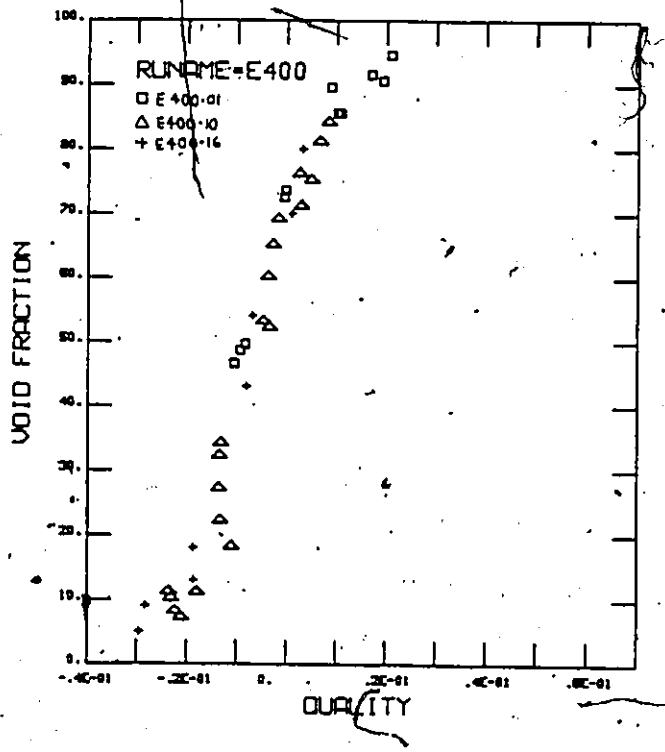
RUNNAME=E400
□ E400-01
△ E400-10
+ E400-16
VOID FRACTION
QUALITY

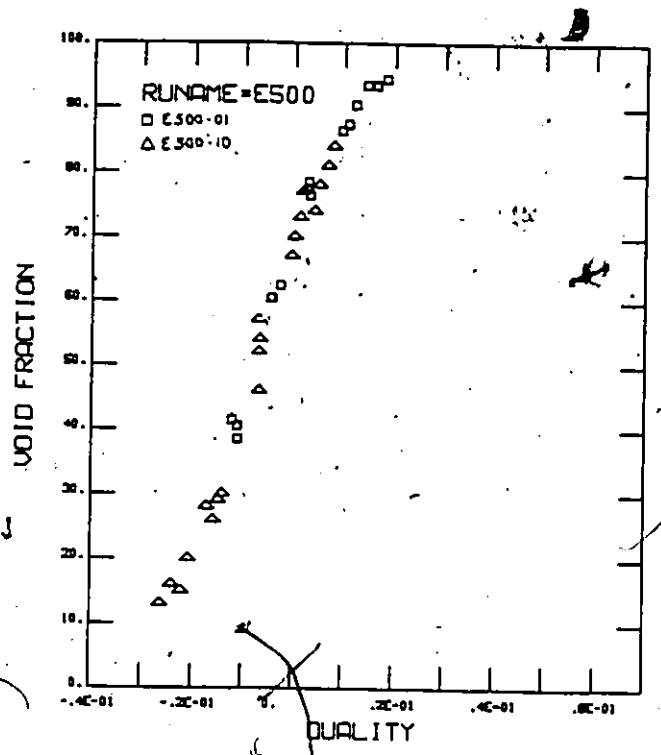
RUNNAME=E500
□ E500-01
△ E500-10
VOID FRACTION
QUALITY

APPENDIX F

CHF CORRELATIONS USED TO COMPARE HOT PATCH POWER

To be applicable to the present situations, the CHF corrections must be based on data at low pressure, low quality and short heated length. The Macbeth correlation chosen is based on the local conditions hypothesis, which has generally been found to be valid at low quality boiling crisis (DNB). The form of the correlation is

$$\phi_{CHF} = A_1 - C_1 * \frac{De \times G \times i_{fg}}{4} X_e$$

$$A_1 = y_o \, De^{y_1} \, (G \times 10^{-6})^{y_2}$$

$$C_1 = y_3 \, De^{y_4} \, (G \times 10^{-6})^{y_5}$$

$y_o = 1.12$

$y_1 = -0.211$

$y_2 = 0.324$

$y_3 = 0.0010$

$y_4 = -1.4$

$y_5 = -1.05$

(ϕ in Btu/ft^{2}h, De in ft., G in lb/ft^{2}h, i_{fg} in Btu/lbm)

The Menegus correlation is

$$\phi = \alpha\left(1 + \beta_o T + \frac{\beta_1 T}{D}\right)\left(1 + \gamma_o V + \frac{\gamma_1 V}{D}\right) \Big/ \left(1 + \frac{\delta_1}{D}\right)$$

(ϕ in MW/ft^2, T in °C, D in ft, V in ft/s)

T is the difference between the saturation temperature and the bulk temperature of the liquid (water).

The Greek letter parameters are all pressure dependent. At 14.7 psia the values are as follows:

$\alpha = 0.1107$

$\beta_o = 21.20 \times 10^{-3}$

$\beta_1 = 1.244 \times 10^{-4}$

$\gamma_o = 1.113 \times 10^{-3}$

$\gamma_1 = 19.542 \times 10^{-4}$

$\delta_1 = 8.04 \times 10^{-3}$

APPENDIX G VOID FRACTION CORRELATION

An empirical correlation is development for the measured void fraction data based on local equilibrium quality and mass flux. The form of the correlation is:

$$Y = \rho_1 * (\frac{G}{100}) + \rho_2$$

$$\alpha = \rho_3 + \frac{2}{\pi} (1-\rho_3)*\tan^{-1} \rho_4*(X_e - Y)$$

Void fraction data measured in test sections D and E are used for the least squares fitting procedure. The estimates for the parameters are:

$\rho_1 = -0.001867$

$\rho_2 = 0.000777$

$\rho_3 = 0.47146$

$\rho_4 = 101.2$

The standard deviation σ is 0.076. The predicted void fraction is plotted against the measured void fraction in Figure G.1. A scatter plot is shown in Figure G.2.

As this empirical vorrelation is based on data at one pressure, extrapolation to other conditions are not recommended.

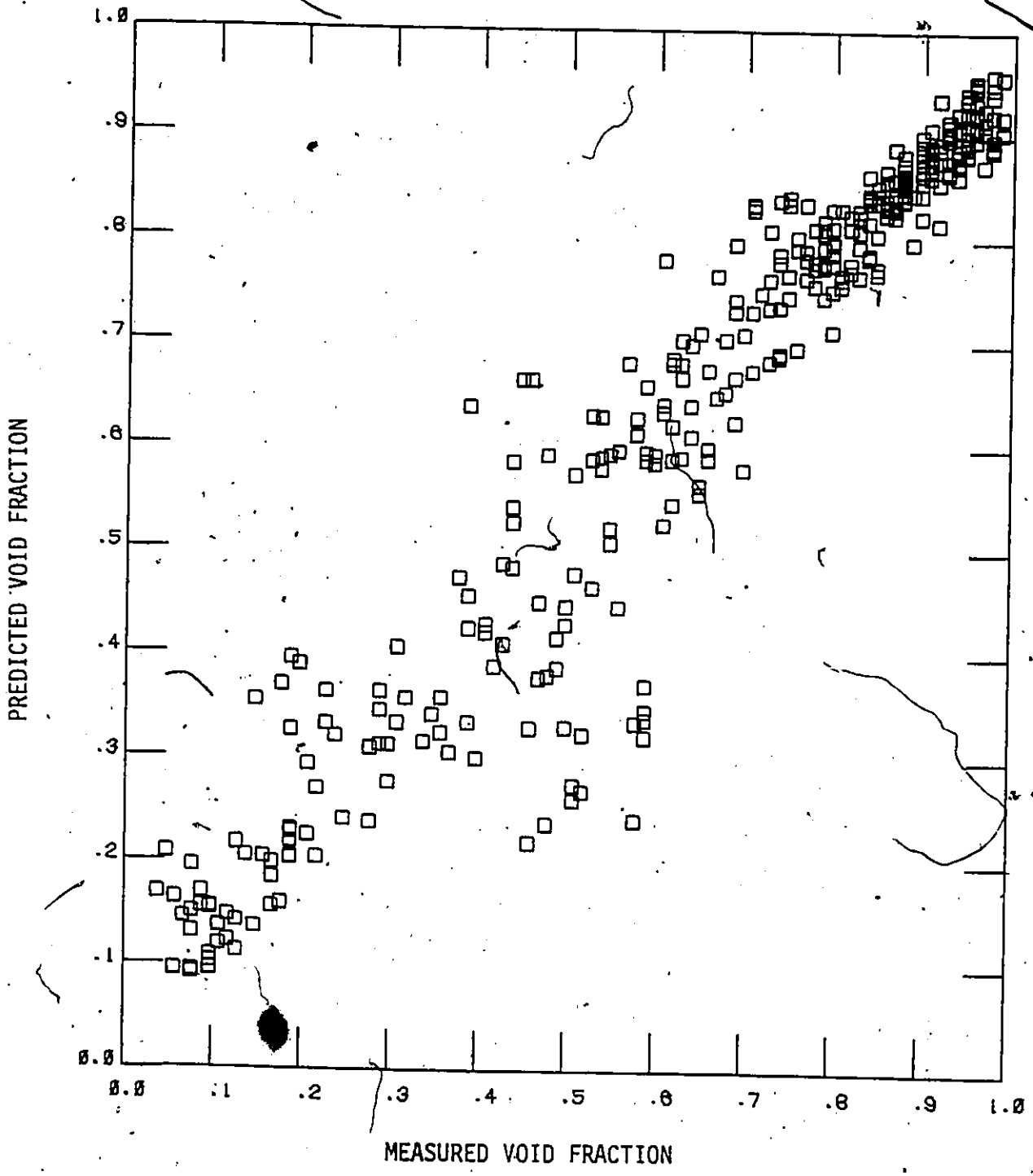

FIGURE G.1 PREDICTED VOID FRACTION

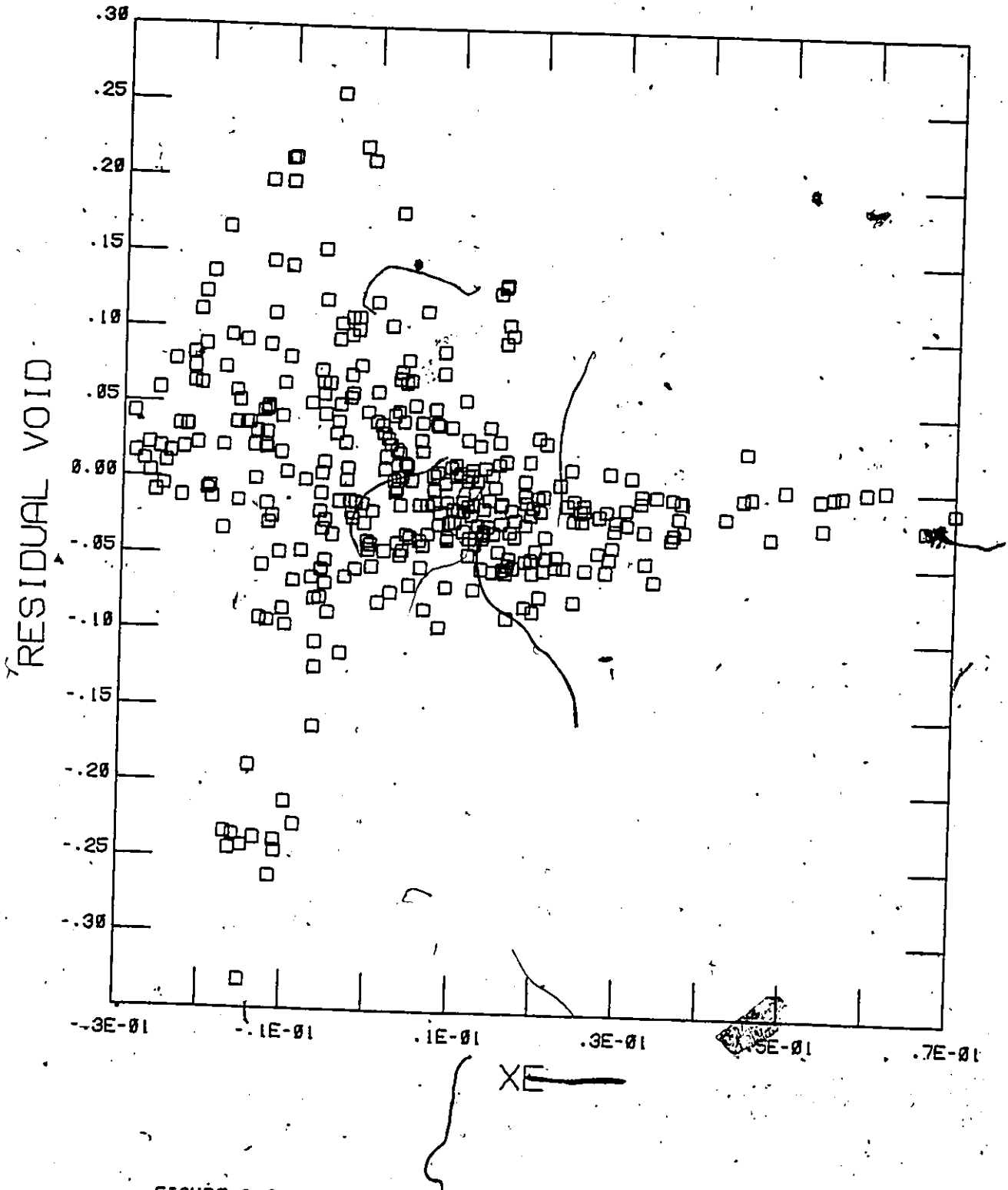

FIGURE G.2 SCATTER PLOT OF PREDICTION ERRORS

APPENDIX H

Radiation Component

H.1 Network Diagram

We assume that all surfaces are gray and that the vapor film is optically thin. The latter assumption will be justified later. This is equivalent to saying that there is no self absorption within the vapor. We can then consider the vapor as a single node in the radiation-network method of estimating the heat transfer between surfaces. We further assume that the liquid core is smooth and concentric with the tube.

Referring to sketch below, the energy leaving surface (1) and arriving at (2) is given by

$$q_{12} = J_1 A_1 F_{12} \tau_v$$

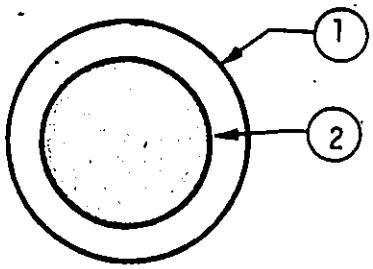

The energy leaving surface (2) and arriving at (1) is given by $q_{21} = J_2 A_2 F_{21} \tau_v$

∴ Net exchange between wall and liquid core

$$= q_{w\ell} = J_1 A_1 F_{12} \tau_v - J_2 A_2 F_{21} \tau_v$$

∵ $A_1 F_{12} = A_2 F_{21}$

$$\therefore q_{w\ell} = (J_1 - J_2) A_1 F_{12} \tau_v = \frac{J_1 - J_2}{\frac{1}{A_1 F_{12} (1-\varepsilon_v)}}$$

Since we consider the vapor film as one single node, the energy leaving the vapor is given by

$$J_v = \varepsilon_v E_{bv}$$

Portion of J_v reaching surface (1) $= A_v F_{v1} J_v$

$$= A_v F_{v1} \varepsilon_v E_{bv}$$

Portion of energy leaving surface (1) and reaching the vapor

$$= J_1 A_1 F_{1v} \alpha_v$$

$$= J_1 A_1 F_{1v} \varepsilon_v$$

$$\therefore q_{wv} = J_1 A_1 F_{1v} \varepsilon_v - A_v F_{v1} \varepsilon_v E_{bv}$$

$$= \frac{(J_1 - E_{bv})}{\frac{1}{A_1 F_{1v} \varepsilon_v}}$$

$$\therefore q_{1net} = q_{w-\ell} + q_{w-v}$$

$$= \frac{J_1 - J_2}{\frac{1}{A_1 F_{12}(1-\varepsilon_v)}} + \frac{J_1 - E_{bv}}{\frac{1}{A_1 F_{1v} \varepsilon_v}}$$

$$\phi_{rad,net} = \frac{J_1 - J_2}{\frac{1}{F_{12}(1-\varepsilon_v)}} + \frac{J_1 - E_{bv}}{\frac{1}{F_{1v}\varepsilon_v}} = \frac{E_{bw} - J_1}{\frac{1}{\frac{\varepsilon_w}{1-\varepsilon_w}}}$$

- - - - - - - - H.1

The network diagram can then be represented by the following sketch.

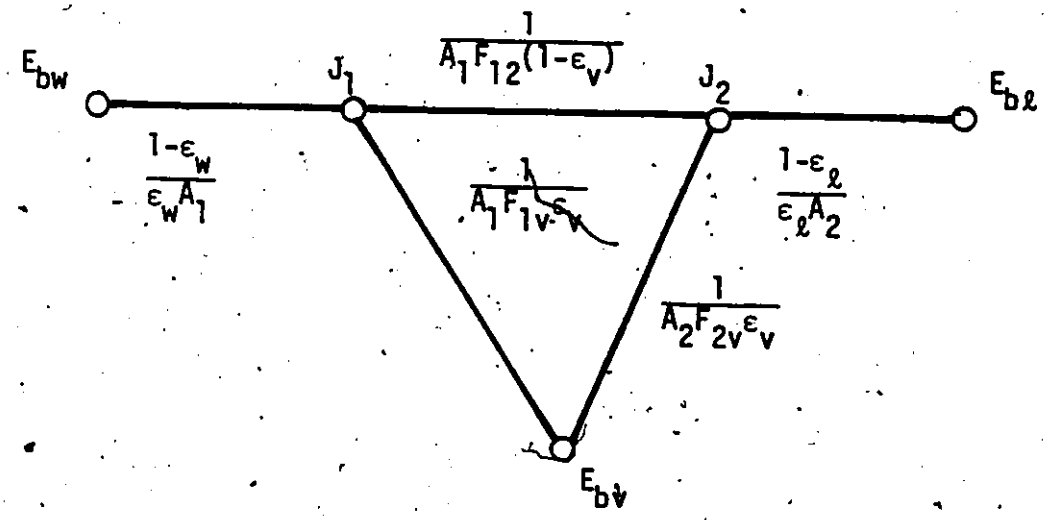

H.2 Vapor Emissivity

The vapor emissivity can be approximated by

$$\varepsilon_v = 1-e^{-a_v L_v}$$

where a_v is the mean absorption coefficient and L_v is the mean path length given by

$$L_v = 4\frac{V}{A} = 4\frac{\alpha A_{tube}}{\pi D+\pi(D-2\delta)} = 4 \times \frac{\frac{\pi}{4}[D^2-(D-\delta)^2]}{2\pi(D-\delta)}$$

$$= \frac{2(D-\delta)2\delta}{2(D-\delta)} = 2\delta$$

To estimate the mean absorption coefficient, we use the Planck mean absorption coefficient K_p for optically thin gas. The functional relationship between K_p and the absolute temperature is shown in Fig. H.1. An approximate fit to the curve is

$$K_p = 5.4e^{-\left(\frac{T-1000}{700}\right)} \qquad T \text{ in } {}^{o}R \text{ and } K_p \text{ in } (\text{atm-ft})^{-1}$$

or $$K_p = 17.72e^{-\left(\frac{1.8T-1000}{700}\right)} \qquad T \text{ in } {}^{o}K \text{ and } K_p \text{ in } (\text{atm-m})^{-1}$$

To simplify the calculation, K_p is evaluated at $\frac{1}{2}(T_w+T_s)$. It is felt that since the method which we have adopted in estimating the radiation component is only approximate, it does not warrant to calculate K_p at some other average temperature.

We can check at this point whether the assumption of optically thin gas is justified. The optical thickness is defined as

$$\tau_o = KL_v$$

where K = extinction coeff.

$\approx$ absorption coeff.

$$\therefore \quad \tau_o = 2\delta(10\ m^{-1}) = 20\delta\ m^{-1}$$

For void fraction $\alpha = 0.3$, $\delta = 9.75 \times 10^{-4}$ m

$$\therefore \quad \tau_o = 0.02 << 1$$

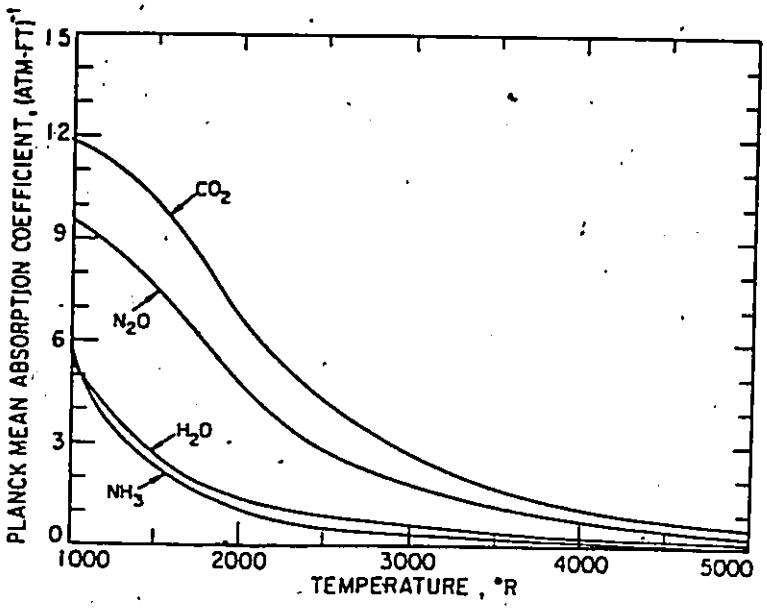

FIG. H.1 PLANCK MEAN ABSORPTION COEFFICIENTS FOR WATER VAPOR (From Tien (1968))

H.3 View Factors

Since surface 2 sees surface 1 only, we have $F_{21} = 1$

$$\therefore \quad A_1 F_{12} = A_2 F_{21} = A_2$$

$$F_{12} = \frac{A_2}{A_1} = \frac{D-2\delta}{D} = (1 - \frac{2\delta}{D})$$

To find F_{1v}, we consider the following:

Energy leaving surface 1 and reaching vapor = $J_1 A_1 F_{1v} \alpha_v$

Energy leaving surface 1 and reaching surface 2 = $J_1 A_1 F_{12} \tau_v$

Energy leaving surface 1 and reaching surface 1 = $J_1 A_1 F_{11} \tau_v$

$\therefore$ Total energy leaving 1 unit area of surface 1

$$= J_1 = J_1(F_{1v}\alpha_v + F_{12}\tau_v + F_{11}\tau_v)$$

$$\therefore \quad F_{1v}\varepsilon_v + F_{12}(1-\varepsilon_v) + F_{11}(1-\varepsilon_v) = 1$$

$$F_{12} = 1 - \frac{2\delta}{D}$$

$$F_{11} = \frac{2\delta}{D}$$

$$\therefore \quad F_{1v}\varepsilon_v + 1 - \varepsilon_v = 1$$

$$F_{1v} = 1$$

Similarly

$$J_2 = J_2(F_{2v}\alpha_v + F_{21}\tau_v)$$

$$\therefore \quad F_{2v}\alpha_v + F_{21}\tau_v = 1$$

Assuming that the vapor is nonreflecting and that Kirchoff's identity applies, then

$$\alpha_v + \tau_v = \varepsilon_v + \tau_v = 1$$

$$F_{2v} = \frac{1 - F_{21}(1-\varepsilon_v)}{\varepsilon_v}$$

H.4 Net Radiation Heat Transfer

Referring to the network diagram, we can calculate J_1 and J_2 as follows:

$$J_1 = \sigma T_w^4 - \phi_r \left(\frac{1-\varepsilon_w}{\varepsilon_w}\right)$$

$$(J_1-J_2)A_1F_{12}(1-\varepsilon_v) + (J_2-E_{bv})A_2F_{2v}\varepsilon_v + (J_2-E_{b\ell})\frac{\varepsilon_\ell A_2}{1-\varepsilon_\ell} = 0$$

$$\therefore J_2\left[A_2F_{2v}\varepsilon_v - A_1F_{12}(1-\varepsilon_v) + \frac{\varepsilon_\ell A_2}{1-\varepsilon_\ell}\right] = \frac{E_{b\ell}\varepsilon_\ell A_2}{1-\varepsilon_\ell} - J_1A_1F_{12}(1-\varepsilon_v) + E_{bv}A_2F_{2v}\varepsilon_v$$

J_1 and J_2 can be substituted into eq. H.1 and ϕ_r can be evaluated. The parametric effect of film thickness and wall temperature is shown in Fig. H.2.

FIG. H.2 - RADIATION COMPONENT

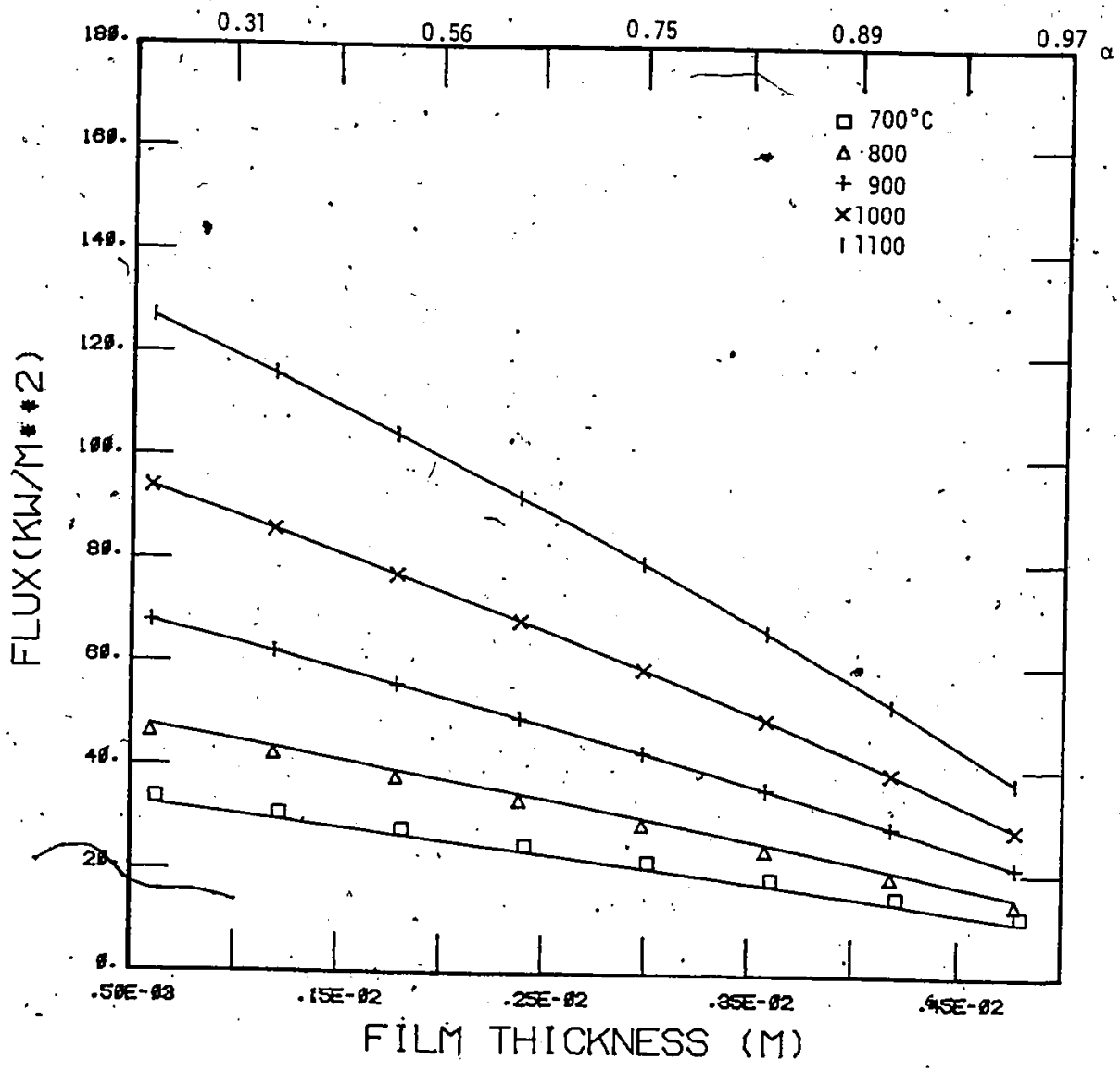

APPENDIX I SOLUTION OF THE MATHEMATICAL MODEL FOR INVERTED ANNULAR FILM BOILING

I.1 LAMINAR VAPOR FILM

Combining eqs. 7.1 and 7.24(a) we obtain

$$\frac{2\rho_v}{R}\left[\frac{g\rho_\ell\delta^2}{4\mu_v}+\frac{U_\ell}{2}\right]\frac{d\delta}{dZ}=\frac{1}{R^2(h_v-h_f)}\times\left[2R\phi_{TOT}-2(R-\delta)\phi_\ell\right]$$

This is the governing equation for the vapor film thickness δ. It is coupled to the liquid core through ϕ_ℓ. The criterion of transition from laminar to turbulent film is the local Reynolds number. For laminar flow, the wall-shear is given by

$$\tau_w=\mu_v\frac{dU_v}{dy}$$

$$=\mu_v\left[\frac{g\rho_\ell\delta}{2\mu_v}+\frac{U_\ell}{\delta}\right]$$

The friction velocity is $\sqrt{\frac{\tau_w}{\rho_v}}$. Therefore, the local Reynolds number is

$$\eta_s=\frac{\delta_{max}\sqrt{\frac{\tau_w}{\rho_v}}}{\nu_v}$$

where δ_{max} is the distance from the wall to the point of maximum velocity in the vapor film. If $\eta_s>\eta^*$, then the flow is turbulent.

I.2 TURBULENT VAPOR FILM

The governing equation for the vapor film is eq. 7.5, which is shown here again for convenience:

$$\frac{dM_v}{dz} - U_\ell \frac{dG_v}{dz} - \frac{\delta(2R-\delta)}{(R-\delta)^2}\frac{dM_\ell}{dz} = -\frac{2\tau_w}{R} - \frac{2\tau_i}{R-\delta} + \frac{g\rho_\ell(2R-\delta)\delta}{R^2} \quad -- \quad I.2$$

Each of the terms in this equation is expressed in terms of δ and η.

From eq. 7.21

$$M_v = \frac{2}{R^2}\rho_v\nu_v^2\left[R\frac{\sqrt{\frac{\tau_w}{\rho_v}}}{\nu_v}\theta_3 - \theta_4\right]$$

$$= \frac{2}{R^2}\rho_v\nu_v^2\eta_s^4\left(\frac{R}{3\delta_s} - \frac{1}{4}\right) + \frac{2}{R^2}\rho_v\nu_v^2(2mc^2)(\eta_T)^{\left(\frac{2+2m}{m}\right)}$$

$$\times\left[\frac{R}{(2+m)\left(\frac{\delta_T}{2}+\delta_s\right)} - \frac{1}{2+2m}\right]$$

$$- \frac{2}{R^2}\rho_v\nu_v^2(2mc^2)\eta_s^{\left(\frac{2+2m}{m}\right)}\left(\frac{R}{\delta_s(2+m)} - \frac{1}{2+2m}\right)$$

$$\frac{dM_v}{dZ} = \frac{-2}{R^2}\rho_v\nu_v^2\eta_s^4\frac{R}{3\delta_s^2}\frac{d\delta_s}{dZ} + \frac{2}{R^2}\rho_v\nu_v^2(2mc^2)\eta_s^{\left(\frac{2+2m}{m}\right)}\frac{R}{(2+m)\delta_s^2}\frac{d\delta_s}{dZ}$$

$$+ \frac{2}{R^2}\rho_v\nu_v^2(2mc^2)\left(\frac{2+2m}{m}\right)(\eta)^{\left(\frac{2+m}{m}\right)}\left[\frac{R}{(2+m)\left(\frac{\delta_T}{2}+\delta_s\right)} - \frac{1}{2+2m}\right]\frac{d\eta}{dZ}$$

$$- \frac{2}{R^2}\rho_v\nu_v^2(2mc^2)(\eta)^{\left(\frac{2+2m}{m}\right)}\left[\frac{R}{(2+m)\left(\frac{\delta_T}{2}+\delta_s\right)^2}\left(\frac{1}{2}\frac{d\delta_T}{dZ} + \frac{d\delta_s}{dZ}\right)\right]$$

$$= \frac{-2}{3R\delta_s^2}\,\rho_v\nu_v^2\,\eta_s^4\,\frac{d\delta_s}{dZ}$$

$$- \frac{4mc^2}{(2+m)R}\,\rho_v\nu_v^2\left[\frac{\frac{2+2m}{m}}{\left(\frac{\delta_T}{2}+\delta_s\right)^2} - \frac{\frac{2+2m}{m}}{\delta_s^2}\right]\frac{d\delta_s}{dZ}$$

$$+ \frac{4mc^2}{R^2}\,\rho_v\nu_v^2\,(\eta)^{\frac{2+m}{m}}\left[\left(\frac{R}{\delta_s(2+m)} - \frac{1}{2+2m}\right)\frac{2+2m}{m}\,\frac{d\eta}{dZ}\right.$$

$$\left. - \frac{\eta}{2}\left(\frac{R}{(2+m)\left(\frac{\delta_T}{2}+\delta_s\right)^2}\right)\frac{d\delta_T}{dZ}\right]$$

From eq. 7.18

$$G_v\,\frac{R^2}{2\mu_v} = R\theta_1 - \frac{\nu_v}{\sqrt{\frac{\tau_w}{\rho_v}}}\,\theta_2$$

$$= R\theta_1 - \frac{\delta_s}{\eta_s}\,\theta_2$$

$$= \eta_s^2\left(\frac{R}{2} - \frac{\delta_s}{3}\right) - 2mc\,\eta_s^{\left(\frac{m+1}{m}\right)}\left(\frac{R}{m+1} - \frac{\delta_s}{2m+1}\right)$$

$$+ 2mc\,\eta^{\left(\frac{m+1}{m}\right)}\left[\frac{R}{m+1} - \frac{\delta_s + \frac{\delta_T}{2}}{2m+1}\right]$$

Assuming that $\delta_s << R$ and $(2m+1)\ R >> (m+1)(\delta_s + \frac{\delta_T}{2})$, the above equation can be simplified to

$$G_v \frac{R^2}{2\mu_v} = \frac{R}{2}\eta_s^2 - \frac{2mc}{(m+1)} R\, \eta_s^{\left(\frac{m+1}{m}\right)} + \frac{2mcR}{(m+1)}\, \eta^{\left(\frac{m+1}{m}\right)}$$

Differentiating with respect to Z we obtain:

$$\frac{R^2}{2\mu_v} \frac{dG_v}{dZ} = 2RC\ \eta^{\frac{1}{m}} \frac{d\eta}{dZ}$$

$$= 2RC\ \eta^{\frac{1}{m}} \frac{d\eta}{dZ}$$

From eq. 7.23

$$M_\ell = \frac{1}{\rho_\ell}\left[\frac{(G-G_v)_R}{R-\delta}\right]^2$$

$$\sqrt{M_\ell} = \frac{1}{\sqrt{\rho_\ell}} \left(\frac{R}{R-\delta}\right) (G-G_v)$$

Differentiating we obtain

$$\frac{1}{2\sqrt{M_\ell}} \frac{dM_\ell}{dZ} = \frac{\sqrt{M_\ell}}{(R-\delta)} \frac{d\delta}{dZ} = \frac{1}{\sqrt{\rho_\ell}} \left(\frac{R}{R-\delta}\right) \frac{dG_v}{dZ}$$

By definition

$$\frac{(\delta-\frac{\delta_T}{2})\sqrt{\frac{\tau_w}{\rho_v}}}{\nu_v} = \eta$$

$$\tau_w = \rho_v \left(\frac{\nu_v \eta}{\delta-\frac{\delta_T}{2}}\right)^2$$

To calculate the interfacial friction, the Reynolds flux ϕ is given by

$$\phi = \frac{R^2}{\rho_v U_v (R-\delta)} \frac{dG_v}{dZ}$$

$$= \frac{R^2}{\rho_v U_v (R-\delta)} \frac{2RC}{R^2} (2\mu_v)\, \eta^{\frac{1}{m}} \frac{d\eta}{dZ}$$

Substituting $\frac{d\eta}{dZ}$ from eq. 7.31, we obtain

$$\phi = \frac{2\mu_v}{(R-\delta)\rho_v U_v} \frac{dQ}{dZ}$$

Finally, $\frac{d\delta_s}{dZ}$ and $\frac{d\delta_T}{dZ}$ can be related to $\frac{d\delta}{dZ}$ and $\frac{d\delta}{dZ}$ as follows:

$$\delta_s = \delta \times \frac{\eta_s}{2\eta-\eta_s} = \frac{\eta_s}{2\eta-\eta_s}\,\delta$$

$$\delta_T = \delta-\delta_s$$

$$\frac{d\delta_s}{dZ} = \frac{d\delta}{dZ}\frac{\eta_s}{2\eta-\eta_s} - \frac{\delta\eta_s}{(2\eta-\eta_s)^2}\left(2\frac{d\eta}{dZ}\right)$$

$$= \frac{\eta_s}{2\eta-\eta_s}\frac{d\delta}{dZ} - \frac{2\delta\eta_s}{(2\eta-\eta_s)^2}\frac{d\eta}{dZ}$$

$$\frac{d\delta_T}{dZ} = \frac{d\delta}{dZ} - \frac{d\delta_s}{dZ}$$

$$= \frac{d\delta}{dZ}\left(1 - \frac{\eta_s}{2\eta-\eta_s}\right) + \frac{2\delta\eta_s}{(2\eta-\eta_s)^2}\frac{d\eta}{dZ}$$

$$= \frac{2(\eta-\eta_s)}{2\eta-\eta_s}\frac{d\delta}{dZ} + \frac{2\delta\eta_s}{(2\eta-\eta_s)^2}\frac{d\eta}{dZ}$$

All the terms in eq. I.2 can now be expressed in the dependent variable $\frac{d\delta}{dZ}$ and the independent variable $\frac{d\eta}{dZ}$ (which in turn is related to $\frac{dQ}{dZ}$). Collecting all terms containing $\frac{d}{dZ}$ to the L.R.S. and all terms containing $\frac{d\eta}{dZ}$ to the R.H.S., the result is eq. 7.32, viz

$$f_1 \frac{d\delta}{dZ} = f_2 \frac{d\eta}{dZ} + f_3 \qquad \text{I.3}$$

I.3 Liquid Core

The governing equation of the liquid core is eq. 7.10, which is

$$U_\ell \frac{\partial\theta}{dZ} = \frac{1}{(R-\delta)^2}\frac{1}{r^*}\frac{\partial}{\partial r^*} r^* (\varepsilon_H + \alpha)\frac{\partial\theta}{\partial r^*} + \frac{r^*}{2}\frac{dU_\ell}{dZ}\frac{\partial\theta}{\partial r^*}$$

This partial differential equation is discretized in space to yield a set of simultaneous equations, which are then coupled to either eq. I.1 or I.3, depending on the flow regime.

I.4 Solution Scheme

The coupled ODE/PDE is solved by using a simulation package FORSIM* on a CDC Cyber 170. A listing of the program FISHY (Film Superheated Hypothesis) is shown on the following pages. An output from a typical run is also included.

* Carver M.B., et al., The Forsim VI Simulation Package for the Automated Solution of Arbitrarily Defined Partial and/or Ordinary Differential Equation Systems, Atomic Energy of Canada Limited report, AECL-5821, 1978.

```
      SUBROUTINE UPDATE
C
CCCCCCCCCCCCCCCCCCCCCCCCCCCCCCCCCCCCCCCCCCCCCCCCCCCCCCCCCCCCCCCC
C
C     FS    LM
C      S    UPERHEATED
C      BY POTHESIS
C
C     THIS PROGRAM CALCULATES THE WALL TEMP OF A HEATED
C     TUBE UNDER FORCED FLOW SUBCOOLED FILM BOILING
C
C
C     THIS SUBROUTINE CONSISTS OF THE FOLLOWING SECTIONS
C  SECTION 0 CONSTANTS AND INITIALIZATION FOR FORSIM
C  SECTION 1 PARAMETERS THAT CAN BE CHANGED FOR SENSITIVITY STUDIES
C  SECTION 2 USER'S SPECIFICATION OF GEOMETRY AND SYSTEM PARAMETERS
C  SECTION 3 SET UP INITIAL AND BOUNDARY CONDITIONS FOR PDE/ODE
C  SECTION 4 CHECK FOR LAMINAR OR TURBULENT VAPOR FILM
C  SECTION 5 SOLUTION OF LAMINAR VAPOR FILM
C  SECTION 6 SOLUTION OF TURBULENT VAPOR FILM
C  SECTION 7 HEAT TRANSFER SECTION
C  SECTION 8 OUTPUT AND TERMINATION HANDLING
C
C     FOR PRODUCTION RUNS,USER ONLY ALTERS SECTION 2
C
C     THE FOLLOWING IS A BRIEF DESCRIPTION OF THE LOGIC.
C     THE COUPLED ODE/PDE'S DEVELOPED IN CHAPTER VII AND APPENDIX I
C     ARE INTEGRATED USING A SIMULATION PACKAGE CALLED FORSIM (SEE
C     ADVERTISEMENT AT THE END OF THIS PROGRAM LISTING).  SECTIONS
C     0 TO 3 ARE EXECUTED ONCE AT THE FIRST CALL TO THIS SUBROUTINE
C     SUBSEQUENT CALLS START IN SECTION 4 AND GO THROUGH EITHER SECTION
C     5 OR 6.  THE LOGIC THEN GOES THROUGH SECTION 7 AND 8 AND RETURN
C     BACK TO THE MASTER CONTROL PROGRAM OF FORSIM
C
C     LABELS 31-41 IN THIS SUBROUTINE ARE SUBJECTS OF GO TO STATEMENTS.
C     THEY APPEAR SEQUENTIALLY.
CCCCCCCCCCCCCCCCCCCCCCCCCCCCCCCCCCCCCCCCCCCCCCCCCCCCCCCCCCCCCCCC
      COMMON/RESERV/Z,DZ,DZOUT,EMAX,ZFIN,METHOD,DZMAX,DZMIN,ICHECK
      COMMON/CNTROL/INOUT,ICONV,IFLAG,NODUMP,NCASE,NTRY,NSTEP,NJAC
      COMMON/INTEGT/U(31),DELE,Q,POWER
      COMMON/DERIVT/UZ(31),DELTAZ,PHIZ,PHITOT
      COMMON/DERVX/UX(31)
      COMMON/DERVXX/UXX(31)
      COMMON/PARTX/NCUP,NPOINT,XL,XU,AUX,AUXX,NBODY,DR,RS(31)
      COMMON/PARTB/BC(4,3,1)
      COMMON/L120/DUMMY(148)
      COMMON/LENGTH/ DE
      REAL RR(13),MOMENL,M,W(31),DW(31)
      REAL STORTW(100),STORKA(100),STORXE(100),STORZ(100),STORAE(100)
     1     ,STORPL(100),STORQN(100),STORAD(100)
      LOGICAL AUXX
C
CCCCCCCCCCCCCCCCCCCCCCCCCCCCCCCCCCCCCCCCCC
C
C     EDDY THERMAL DIFFUSIVITY
C
      AF(DELTA)=TURB*ABS(DELTA)*UL+DIFUSL
```



```
C
CCCCCCCCCCCCCCCCCCCCCCCCCCCCCCCCCCCCCCCCCCCCCCCCCCCCCCCCCCCC
C
C
C  SECTION 0
C
C     CONSTANTS AND INITIALIZATIONS
C
C
C     INITIALIZE ALL CONSTANTS IF THIS IS THE FIRST CALL TO THIS SUBROUTINE
C
      IF(INOUT .EQ. 3) GO TO 41
      IF(INOUT .NE. -1) GO TO 31
C
      WRITE(6,668)
  668 FORMAT(1H0)
C     FORSIM CONTROLS
C
      AUXX=.FALSE.
      ICHECK=1
      NPDE=1
      IT=0
      IS=0
C
C     INITIALIZE OUTPUT VARIABLES
C
      DENOM0=DENOM1=DENOM2=DENOM=0.
      RES1=RES2=RES3=RES4=RES5=RES6=RES7=RES8=0.
      PERAD=0.
      ETAT=0.
      PHICON=0.
C
CCCCCCCCCCCCCCCCCCCCCCCCCCCCCCCCCCCCCCCCCCCCCCCCCCCCCCCCCCCC
C
C  SECTION 1
C
C
C     COMPARE ACCURACY OF VARIOUS INTEGRATION ALGORITHM
C
      METHOD=10
C
C     METHOD 10=GEAR STIFF INTEGRATION ALGORITHM
C
C     NPOINT IS THE NUMBER OF MESH POINTS IN THE LIQUID CORE
C     IF NPOINT IS CHANGED, THE DECLARATION IN THE COMMON BLOCK MUST
C     ALSO BE ALTERED.
C
      EMAX=1.E-4
      NPOINT=31
      NP1=NPOINT-1
      NCUPL=3
C
      NCUP=3
C     VARY THE FOLLOWING FOR SENSITIVITY STUDIES OF MODEL
C     ETAS=TRANSITION POINT BETWEEN LAMINAR AND TURBULENT VAPOR FILM
C     TURB=PROPORTIONALITY  CONSTANT FOR EDDY DIFFUSIVITY
C     CC1=PROPORTIONALITY CONSTANT FOR INTERFACIAL SHEAR
```

```
SUBROUTINE UPDATE     74/74   OPT=1 ROUND=--*/ TRACE        FTN 4.6+433      81-05-27  17.01.24      PAGE     3

      C
            EMITW=0.7
            EMITL=0.96
            STAR=12.0
            TURB=0.08.
          eCC1=1.5
            ETA2=ETAS*ETAS
CCCCCCCCCCCCCCCCCCCCCCCCCCCCCCCCCCCCCCCCCCCCCCCCCCCCCCCCCCCCCCCCCCCCCCC
C
C     SECTION 2
C
C     SPECIFY TUBE ID (M),INLET TEMPERATURE (C),PRESSURE (KPA)
C           MASS FLUX (KG/M**2.S)
C
            DE=0.01194
            TIN=85.
            P=115.
            G=200.
C
            R=0.5*DE
            R2=R*R
C     INTEGRATION TERMINATION CRITERION
C     SPECIFY MAXIMUM FILM THICKNESS,MAX. TUBE LENTH, MAX WALL TEMP
C     OTHER TERMIANTION CRITERION ARE BUILT IN
C
            DELMAX=0.5*R
            XFIN=0.6
C
            TWMAX=1600.
C
C     SPECIFY OUTPUT FREQUENCY, DEFAULT IS EVERY 0.1 M
C
            DXOUT=0.01
C
C     GO TO SUBROUTINE FLUX TO SPECIFY THE HEAT FLUX
CCCCCCCCCCCCCCCCCCCCCCCCCCCCCCCCCCCCCCCCCCCCCCCCCCCCCCCCCCCCCCCCCCCCCCC
C
C     SECTION 3
C     SATURATED LIQUID PROPERTIES
C
            PFPH=P/6.8948
            CALL POLSAN(PFPH,0.,DUMMY,RR,1)
            RHOL=1./RR(1)*16.018
            HL=RR(2)*2326.
            HFG=(RR(6)-RR(2))*2326.
            VISCL=RR(3)*1.4882
            CONDL=RR(4)*1.730
            CPL=RR(5)*4186.8
            PRL=CPL*VISCL/CONDL
            TSAT=(RR(13)-32.)/1.8
            RHOG=1./RR(7)*16.018
            DIFUSL=CONDL/RHOL/CPL
C
C     CALCULAE INLET ENTHALPY


SUBROUTINE UPDATE     74/74   OPT=1 ROUND=--*/ TRACE        FTN 4.6+433      81-05-27  17.01.24      PAGE     4

C
            TINF=TIN*1.8+32.
            CALL POLSAN(0.,TINF,DUMMY,RR,2)
            HIN=RR(2)*2326.
            DTIN=TSAT-TIN
            XIN=(HIN-HL)/HFG
C
C     INITIAL GUESS OF WALL TEMPERATURE
C
            TW=TSAT+10.
C
C     SET UP INITIAL CONDITIONS
C
         31 CONTINUE
            IF (X .GT. 0.) GO TO 32
            DELR=0.
            POWER=0.
            Q=0.
            QV=0.
            DO 11 I=1,NP1
         11 U(I)=1.
            U(NPOINT)=0.
C
C     BOUNDARY CONDITIONS
C     LOWER BOUNDARY
C
            BC(1,1,1)=1.
            BC(2,1,1)=0.
            BC(3,1,1)=0.
            BC(4,1,1)=0.
C
C     UPPER BOUNDARY
C
            BC(1,2,1)=0.
            BC(2,2,1)=1.
            BC(3,2,1)=0.
            BC(4,2,1)=0
CCCCCCCCCCCCCCCCCCCCCCCCCCCCCCCCCCCCCCCCCCCCCCCCCCCCCCCCCCCCCCCCCCCCCCC
C
C     DYNAMIC SECTIONS
C
CCCCCCCCCCCCCCCCCCCCCCCCCCCCCCCCCCCCCCCCCCCCCCCCCCCCCCCCCCCCCCCCCCCCCCC
C
C     SECTION 4
C     CHECK FLOW REGIME
C
         32 CONTINUE
            DELTA=R*DELR
            CALL PARSET(NPDE,NPOINT,U,US,UR,URR)
C     CALCULATE FLUID PROPERTIES
C
C
C     CALCIATE PROPERTIES BASED ON PREVIOUS VALUE OF TW
C     THE LOCATION OF WHICH MAY BE ON EITHER SIDE OF THE CURRENT DISTANCE X
C     THIS WILL FORCE THE INTEGRATING ROUTINE TO TAKE SMALLER STEPS,DEPENDING
C     ON THE TOLERANCE ON (TVAERE-TAB1)
```

```
      SUBROUTINE UPDATE     74/74   OPT=1 ROUND=+-*/ TRACE          FTN 4.6+433        81-05-27  17.01.24        PAGE     5

C
      TF=(TW+TSAT)*0.5
      TFAHRE=TF*1.8+32.
      IF(ISOUT .EQ. -1)GO TO 33
      IF(ABS(TFAHRE-TAH1) .LT.5) GO TO 34
   33 CONTINUE
      TAH1=TFAHRE
      CALL POLSAN(PFPE,TFAHRE,DUMMY,RR,1)
      RHOV=1./RR(1)*16.018
      HV=RR(2)*2326.
      VISCV=RR(3)*1.4882
      CONDV=RR(4)*1.730
      CPV=RR(5)*4186.8
CCCCCCCCCCCCCCCCCCCCCCCCCCCCCCC
C     THE ALGORITHM STARTS IN THE LAMINAR FILM REGION
C     AT EVERY STEP THE LOCAL REYNOLDS NUMBER IS CHECKED
C     IF ETA IS CLOSE TO ETAS, THEN AT THE NEXT CONVERGED STEP
C     CONTROL IS SWITCHED OVER TO THE TURBULENT FILM REGION
C
   34 CONTINUE
      IF (ISOUT .EQ. -1) GO TO 35
      IF(IT .EQ. 1) GO TO 36
      IF(DELTA .LE. 0.) GO TO 35
      FRICTV=SQRT(9.81*RHOL*DELTA/2./RHOV+G/RHOL/DELTA*VISCV/RHOV)
      Y=0.5*(1.+G/RHOL/RHOL*2.*VISCV/9.81/DELTA/DELTA)
      IF (Y .GT. 1.) Y=1.
      ETA=RHOV*DELTA*FRICTV/VISCV*Y
      IF ((ETA-ETAS) .GT. 0. .AND.
     1    ICONV .EQ. 1) GO TO 36
   35 CONTINUE
C
CCCCCCCCCCCCCCCCCCCCCCCCCCCCCCCCCCCCCCCCCCCCCCCCCCCCCCCCCCCCCCCCCCC
C
C  SECTION 5
C
C     LAMINAR FILM REGION

      IT=0

C
C     CALCULATE VAPOR MASS FLUX & LIQUID CORE DISCHARGE VELOCITY

      GV=2./R*RHOV*(9.81*RHOL*DELTA*DELTA/12./VISCV
     1   +G/RHOL/2.)*DELTA
      UL=(G-GV)/RHOL/(R-DELTA)/(R-DELTA)*R2
      IF(GV .GT.1.E-5) GV=GV/RHOV/(1.-(1.-DELTA/R)**2)
C
C     SET UP GOVERNING EQUATION FOR LIQUID CORE

      DULDI=DER(I,UL,0,1)
      DULDI=ALIN(DULDI,-1.,20.)
      IF(DELTA .LE. 0.) Y=1.
      DELTAT=DELTA*(1.-Y)
      DELTAS=DELTA-DELTAT*0.5
      EDDY=AP(DELTAT)
      DO 12 I=1,NPOINT
      W(I)=EDDY*RS(I)*UR(I)


      SUBROUTINE UPDATE     74/74   OPT=1 ROUND=+-*/ TRACE          FTN 4.6+433        81-05-27  17.01.24        PAGE     6

   12 CONTINUE
      CALL PUFX(W,DW,RS,NCUPL,NPOINT,NEQDX)
      DO 13 I=1,NPOINT
      UX(I)=(DW(I)/RS(I)/(R-DELTA)/(R-DELTA)+0.5*RS(I)*DULDI*UR(I))/UL
   13 CONTINUE
      CALL PARFIN (NPDE,NPOINT,U,UX,UR,URR)
C
C
C     CALCULATE HEAT TRANSFER TO LIQUID CORE

      PHIL=-UR(NPOINT)*EDDY*RHOL*CPL*DTIN
      IF(PHIL .LT. 0.)PHIL=0.
      CALL FLUX (PHITOT,I)
C
      PHI=(PHITOT*R-PHIL)/2.
      IF (PHI .LT. 0.) PHI=0.
      PHIX=PHI/2./VISCV/(HV-HL)
      IF (PHIX .LT. 0.) PHIX=0.
      IF(Q .LT. 0.) Q=0.
C
C     CALCULATE TERMS IN DIFFERENTIAL EQUATION FOR VAPOR FILM
      DENOM1=9.81*RHOL*DELTA*DELTA/VISCV/4.
      DENOM2=G/RHOL/2.
      DENOM=2.*R*RHOV*(HV-HL)*(DENOM1+DENOM2)
      RES=PHI
      GO TO 38
   36 CONTINUE
C
CCCCCCCCCCCCCCCCCCCCCCCCCCCCCCCCCCCCCCCCCCCCCCCCCCCCCCCCCCCCCCCCCCC
C
C  SECTION 6
C     TURBULENT FILM

      N=7
      C=8.74
      C1=C*C
      IF(IT .NE. 0) GO TO 37
      EDDY2=EDDY
      WRITE (6,61) Q,PHIX,DELTA,DELTAS,TW,I,DI
   61 FORMAT (//,1X,'AT TRANSITION FROM LAMINAR TO TURBULENT FILM,
     1 THE VALUES OF Q, PHIX, DELTA, DELTAS, TW, I, DI ARE',/
     2 ,5X,8E13.5)
   37 CONTINUE
C
C
C

      ETAT=(Q-ETAS)**R/2.+2**N*C**R/(N+1)*ETAS**((N+1)/N))
     1 /(N*C**DI)*(N+1)
      IF (ETAT .LE. 0.) WRITE (6,62) Q,PHIX,DELTA,DELTAS,ETAT,TW,I,DI
C
   62 FORMAT (//,1X,'ETA IS NEGATIVE. VALUES OF Q,PHIX,DELTA,DELTAS,
     1 ETAT,TW,I,DI ARE',/,1X,8E12.5)
      IF (ETAT .LT. 0.) GO TO 40
      ETA=ETAT**(N/(N+1))
      IF(ETA .LE. ETAS) ETAT=ETAS
C
```

```
      SUBROUTINE UPDATE     74/74   OPT=1 ROUND=+-*/ TRACE          FTN 4.6+433       81-05-27  17.01.24       PAGE     7

                  ETA1=2.*ETA-ETA8
                  ETA2=ETA1*ETA1
      345         C
                  GV=Q*2.*VISCV/R2
                  DELTA8=DELTA*ETA8/ETA1
                  DELTAT=DELTA-DELTA8
      C
      350         UL=(G-GV)/RHOL/(R-DELTA)/(R-DELTA)*R2
                  DULDI=DER(X,UL,0.,1)
                  DULDI=ALIN(DULDI,-1..20.)
                  UV=GV/RHOV/(1.-(1.-DELTA/R)**2)
                  HALF=0.5*DELTAT
      355         EDDY1=AF(HALF)
      C
      C           EDDY DIFUSIVITY IS CHOSEN TO BE THE GREATER OF THE CURRENT
      C           CALCULATED VALUE AND THAT AT TRANSITION FROM LAMINAR TO
      C           TURBULENT
      360         EDDY=AMAX1(EDDY1,EDDY2)
      C
      C           SET UP EQUATIONS FOR LIQUID CORE
      C
                  DO 14 I=1,NPOINT
      365         W(I)=EDDY*RS(I)*UR(I)
                14 CONTINUE
                  CALL FUFX(W,DW,RS,NCUPL,NPOINT,NEQDX)
                  DO 15 I=2,NPOINT
                  US(I)=(DW(I)/RS(I)/(R-DELTA)/(R-DELTA)+0.5*RS(I)*DULDI*UR(I))/UL
      370       15 CONTINUE
                  CALL PARFIN(WPDE,NPOINT,U,US,UR,URS)
      C
                  PHIL=-UR(NPOINT)*EDDY*RHOL*CPL*DTIN
                  IF(PHIL .LT. 0.)PHIL=0.
      375         CALL FLUX(PHITOT,Z)
      C
                  PHI=(PHITOT*R-PHIL)*2.
                  PHIX=PHI/2./VISCV/(HV-HL)
                  IF(PHIX .LT. 0.) PHIX=0.
      380         C
      C
                  MOMENL=1./RHOL*(R/(R-DELTA)*(G-GV))**2
      C
                  DENOM0=VISCV*VISCV/RHOV*2./3./R*ETAS2*ETAS2*ETAS/ETA1
      385       1 /DELTAS/DELTAS
                  DENOM1=2*2*M*C2/R/(M+2)*(((ETA)**((2+2*M)/M))
                1          /(DELTAT/2+DELTAS)/(DELTAT/2+DELTAS)*ETA
                2 -(ETAS**((2+3*M)/M))/DELTAS/DELTAS)
                3 *(VISCV*VISCV/RHOV)/ETA1
      390       C
      C
                  DENOM2=2*(DR-DELTA)*DELTA*MOMENL/((R-DELTA)**3)
      C
      395         C
                  DENOM=-(DENOM0+DENOM1+DENOM2)
      C
      C
      C
```

```
      SUBROUTINE UPDATE     74/74   OPT=1 ROUND=+-*/ TRACE          FTN 4.6+433       81-05-27  17.01.24       PAGE     8

      400         DWDI=((ETA)**(-1/M))/(C*R)*PHIX*0.5
      C
                  RHS1=VISCV*VISCV/RHOV*2./3.*ETAS2*ETAS*ETA2
                1 /R/DELTAS/DELTAS*DELTA*ETAS*2
                  RHS2=8/RHOV*VISCV*VISCV/R*M*C2/(2+M)*
      405       1 ((ETA**((2+2*M)/M))/(((DELTAT/2+DELTAS)**2)
                1 -(ETAS**((2+3*M)/M))/DELTAS/DELTAS)*DELTA*ETAS/ETA2
      C
                  RHS3=4/R2*VISCV*VISCV/RHOV*M*C2*ETA**((2+M)/M)
                1  *(R/DELTAS*(2+2*M)/M/(2+M)-1/M-ETA*ETAS/ETA2
      410       1  *R*DELTA/((DELTAT/2+DELTAS)**2)/(2+M))
      C
      C
                  RHS4=8*SQRT(MOMENL/RHOL)*DELTA*(DR-DELTA)/((R-DELTA)**3)
                1      *VISCV*C*((ETA)**(1/M))
      415       C
                  RHS5=2*(ETA)*(ETA)/R*(VISCV*VISCV/RHOV)
                1 /(((DELTA+DELTAS)*0.5)**2)
                  DG=GV/RHOV/(DR-DELTA)/DELTA-(G-GV)/RHOL/(R-DELTA)/(R-DELTA)
      420         REYFUX=2.*VISCV/(R-DELTA)/RHOV/UV*PHIX
                  FRICTI=0.005*(1.+300.*DELTA/DE)
                  FRICTS=CC1*FRICTI*(EXP(-REYFUX/3/FRICTI)-REYFUX/FRICTI)
                  RHS6=FRICTS*RHOV*R2*R2*DG*ABS(DG)/(R-DELTA)
      C
      425         RHS7=9.81*RHOL*(DR-DELTA)*DELTA/R2
                  RHS8=PHIX**2*VISCV/R2*UL
      C
                  RHS=(-RHS1-RHS2-RHS3-RHS4)*DWDI-RHS5-RHS6+RHS7+RHS8
                  IT=1
      430         C
      CCCCCCCCCCCCCCCCCCCCCCCCCCCCCCCCCCCCCCCCCCCCCCCCCCCCCCCCCCCCCC
      C
                38 CONTINUE
      C
      435         C
                  DIFFERENTIAL EQ FOR DELTA
      C
                  DELTAX=RHS/DENOM/R
                  IF (DELTAX .LT. 0.) DELTAX=0.

      440         C
      CCCCCCCCCCCCCCCCCCCCCCCCCCCCCCCCCCCCCCCCCCCCCCCCCCCCCCCCCCCCCC
      C
      C           SECTION 7
      445         C
      C           HEAT TRANSFER SECTION
      C
                  IF (DELTA .LE. 0.) GO TO 19
      C
      C
      450         C           CONDUCTION COMPONENT
      C
                  PHICON=CONDV/DELTAS*(TW-TSAT)
      C
      C           RADIATION COMPONENT
      455         C
                  TRAD=TSAT+20.
```

```
SUBROUTINE UPDATE     74/74   OPT=1 ROUND=+-*/ TRACE          FTN 4.6+433        81-05-27  17.01.24        PAGE     9

            IF (TW .GT. TRAD)CALL PHIRAD(PHRAD,DELTA,TW,TSAT,EMITW,EMITL,P)
      C
            PHRAD=PHRAD*1.E3
      460   PHICAL=PHICON+PHRAD
      C
      C
      C     ITERATION SECTION
      C
      465   C
      C     COMPARE ACTUAL AND CALCULATED HEAT FLUX
      C
            PHIDIF=PHITOT-PHICAL
            PERDIF=ABS(PHIDIF/PHITOT)
      470   TW=(PHICON+0.5*PHIDIF)*DELTAS/CONDV+TSAT
            IF (TW .LT.TSAT)TW=TSAT+500.
      C
         39 CONTINUE
      C
      475   CCCCCCCCCCCCCCCCCCCCCCCCCCCCCCCCCCCCCCCCCCCCCCCCCCCCCCCCCCCCCCCCCCC
      C
      C     SECTION 8
      C
      C     CHECK CP TIME REMAINING
      480   C
      C
            TLEFT=XTIME(2)
            CALL FINISH (5.,TLEFT,5HTLEFT)
            IF (INOUT .NE. 1) GO TO 40
      485   C
      C     STORE UP INFORMATION
      C
            IS=IS+1
            STORXA(IS)=GV/G
      490   STORAD(IS)=PHRAD/PHITOT
            POW=POWER*3.1416*DE
            STORXE(IS)=XIN+POW/G/3.1416/R2/HFG
            STORAH(IS)=1.-(1.-DELTA/R)**2
            STORTM(IS)=TW
      495   STORPL(IS)=PHIL/(R-DELTA)
            STORZ(IS)=Z
            STORQN(IS)=PHICON/(TW-TSAT)*DE/CONDV
      C
            CALL RITER(RS,10HCOORDINATE)
      500   CALL RITER(U,10HTEMPERATUR)
            CALL RITER(UR,10HGRADIENT     )
            CALL RITE(Z,DELTA,DELTAS,ETA,TW,Q)
            CALL RITE(DENOM0,DENOM1,DENOM2,DENOM,DULDZ,DELTAZ)
            CALL RITE(RHS1,RHS2,RHS3,RHS4,RHS5,RHS6)
      505   CALL RITE (RHS7,RHS8,RHS,UV,UL,PHIL)
         40 CONTINUE
      C
      C     CHECK WHETHER TERMINTION CRITERION HAVE BEEN REACHED
      C
      510   CALL FINISH (-1.E-10,ETAT,4HETAT)
            CALL FINISH(Z,ZFIN,6HLENGTH)
            CALL FINISH(DELTA,DELMAX,5HDELTA)
            CALL FINISH(5.,TLEFT,5HTLEFT)
```

```
SUBROUTINE UPDATE     74/74   OPT=1 ROUND=+-*/ TRACE          FTN 4.6+433        81-05-27  17.01.24        PAGE    10

      515   CALL FINISH (TW ,TWMAX,2HTW)
            RETURN
         41 CONTINUE
      C
      C     END OF PROBLEM SOLUTION
      C     POST-TERMINATION HANDLING
      520   C
            WRITE (6,661) TURB,G,TIN,CC1,PHITOT
            WRITE (6,662) P,TSAT,ETAS
            WRITE(6,663)
            DO 111 J=1,IS
      525   WRITE(6,666)STORZ(J),STORTM(J),STORXE(J),STORXA(J),
           1 STORAH(J),STORQN(J),STORPL(J),STORAD(J)
        111 CONTINUE
        662    FORMAT(1X,"P= ",F7.1,"KPA",5X,"TSAT= ",F7.1,"C    ",
           1  "ETAS= ",F5.2)
      530   661  FORMAT("1",1X,"TURB = ",F6.3,"G = ",F6.0,"TIN = ",F7.2,
           1 "CC1= ",F7.2,1X,"PHITOT=",E9.3)
        666  FORMAT(1X,F4.2,1X,F6.0,1X,2(E9.3,1X),F4.2,1X,F5.0,1X
           1  ,E10.4,1X,F4.2)
        663  FORMAT(1X,"Z",4X,"TW",5X,"XE",8X,"XA",8X,"VOID",1X,"NUSS ",
      535   1 3X,"PHIL ",6X,"PHRAD/PHITOT",/)
            RETURN
            END
```

```
SUBROUTINE FLUX       74/74   OPT=1 ROUND=+-*/ TRACE          FTN 4.6+433       81-05-27  17.01.24       PAGE     1

1               SUBROUTINE FLUX(PHITOT,X)
                C
                C     SPECIFY HEAT FLUX ALONG THE TUBE IN W/M**2
                C
5               PHITOT=146.E3
                RETURN
                END
```

```
SUBROUTINE PHIRAD     74/74   OPT=1 ROUND=+-*/ TRACE          FTN 4.6+433       81-05-27  17.01.24       PAGE     1

1               SUBROUTINE PHIRAD(FLUX,DELTA,TW,TS,EMITW,EMITL,P)
                C
                C     ESTIMATE RADIATION HEAT TRANSFER COMPONENT
                C
5               C     FLUX IN KW/M**2
                C
                      COMMON/LENGTH/DE
                C     CHANGE ALL TEMPERATURES TO ABS TEMP
                C
10              TWK=TW+273.
                TSK=TS+273.
                TVK=0.5*(TWK+TSK)
                C     VIEW FACTORS
                C
15              VF1V=1.
                VF11=2*DELTA/DE
                VF12=1.-VF11
                A1A2=(DE/(DE-2.*DELTA))**2
                C
20              C     VAPOR EMISSIVITY
                C
                PLANCK=17.72*EXP(-(1.8*TVK-1000.)/700.)
                EMITV=1.-EXP(-2.*DELTA*PLANCK*P/100.)
                VF2V=(1-VF12*(1-EMITV))/EMITV
25              C
                C1=VF2V*EMITV-A1A2*VF12*(1-EMITV)+EMITL/(1-EMITL)
                C
                RHS1=(1-A1A2*VF12*(1-EMITV)/C1)*VF12*(1-EMITV)*TWK**4
                RHS2=(EMITV*VF2V*(TVK**4)-EMITL/(1-EMITL)*(TSK**4))
               1  *VF12*(1-EMITV)/C1
30              RHS3=EMITV*VF1V*(TWK**4-TVK**4)
                RHS=(5.669E-11)*(RHS1-RHS2+RHS3)
                DENOM=1+VF1V*EMITV/EMITW*(1-EMITW)+(1-EMITW)/EMITW*(1-
               1  A1A2*VF12*(1.-EMITV)/C1)*VF12*(1-EMITV)
35              FLUX=RHS/DENOM
                RETURN
                END
```

```
**********************************************************
*                  F O R S I M  V I                      *
*  FORTRAN ORIENTED DISTRIBUTED SYSTEM SIMULATION PACKAGE *
*    FOR PARTIAL AND OR ORDINARY DIFFERENTIAL EQUATIONS   *
* USERS MANUAL - ATOMIC ENERGY OF CANADA REPORT AECL 5821 *
* AUTHORS  M B CARVER AND D G STEWART , C.R.N.L./A.E.C.L. *
**********************************************************
FILM BOILING ANALYSIS

   THE FOLLOWING VARIABLES WILL BE OUTPUT AT THE TIME INTERVALS SPECIFIED BY DTOUT
         CHECK THAT THE VARIABLES IN THE CALLS TO  RITE  ARE IN THIS ORDER

Z        DELTA    DELTAS   ETA      TW       Q        DENOM0   DENOM1   DENOM2   DENOM    DULDZ    DELTAZ
RHS1     RHS2     RHS3     RHS4     RHS5     RHS6     RHS7     RHS8     RHS      UV       UL       PHIL

PARTIAL DIFFERENTIAL EQUATION  1 WILL BE DISCRETISED USING  3 POINT FORMULAE AND 31   EQUAL   SPATIAL DIVISIONS

CASE NUMBER  1 USING   GEARS STIFF  (VARIABLE  STEP) INTEGRATION ALGORITHM    WITH    FULL   JACOBIAN ANALYSIS
                                                    INTEGRATING   34 EQUATIONS

     TIME  0.          STEP  .1000E-02    CPTIME  3.477

VARIABLE  --------  S P A T I A L   V A R I A T I O N  --------

COORDINATE  0.       .1000E+00  .2000     .3000     .4000     .5000     .6000     .7000     .8000     .9000     1.000
TEMPERATUR  1.000    1.000      1.000     1.000     1.000     1.000     1.000     1.000     1.000     1.000     0.
GRADIENT    0.       0.         0.        0.        0.        0.        0.        0.        0.        -45.00

  Z      =  0.        DELTA  =  0.        DELTAS =  0.        ETA    =          -R  TW     =  113.6     Q      =  0.
  DENOM0 =  0.        DENOM1 =  0.        DENOM2 =  .1047     DENOM  =  1871.      DULDZ  =  0.        DELTAZ =  53.95
  RHS1   =  0.        RHS2   =  0.        RHS3   =  0.        RHS4   =  0.         RHS5   =  0.        RHS6   =  0.
  RHS7   =  0.        RHS8   =  0.        RHS    =  602.8     UV     =  0.         UL     =  .2093     PHIL   =  570.2

     TIME  .1000E-01   STEP  .5427E-04    CPTIME  12.83

VARIABLE  --------  S P A T I A L   V A R I A T I O N  --------

COORDINATE  0.       .1000E+00  .2000     .3000     .4000     .5000     .6000     .7000     .8000     .9000     1.000
TEMPERATUR  1.000    1.000      1.000     1.000     1.000     1.000     1.000     1.000     .9998     .9777     0.
GRADIENT    0.       0.         0.        0.        -.9592E-12 -.6618E-09 -.2498E-06 -.8964E-04 -.1427E-01 -1.485  -27.27

  Z      =  .1000E-01  DELTA  =  .4532E-04  DELTAS =  .3782E-04  ETA    =  .7696     TW     =  271.9     Q      =  .2327E-02
  DENOM0 =  0.         DENOM1 =  .3098     DENOM2 =  .1047     DENOM  =  6532.      DULDZ  =  .1099     DELTAZ =  .2445
  RHS1   =  0.         RHS2   =  0.        RHS3   =  0.        RHS4   =  0.         RHS5   =  0.        RHS6   =  0.
  RHS7   =  0.         RHS8   =  0.        RHS    =  9.536     UV     =  .2087     UL     =  .2125     PHIL   =  866.9

     TIME  .2000E-01   STEP  .1169E-03    CPTIME  19.27

VARIABLE  --------  S P A T I A L   V A R I A T I O N  --------

COORDINATE  0.       .1000E+00  .2000     .3000     .4000     .5000     .6000     .7000     .8000     .9000     1.000
TEMPERATUR  1.000    1.000      1.000     1.000     1.000     1.000     1.000     .9999     .9968     .9074     0.
GRADIENT    0.       0.         0.        -.1444E-10 -.2433E-08 -.3914E-06 -.3885E-04 -.3247E-02 -.1393  -3.195    -15.62

  Z      =  .2000E-01  DELTA  =  .7443E-04  DELTAS =  .5836E-04  ETA    =  1.126     TW     =  337.2     Q      =  .5853E-02
  DENOM0 =  0.         DENOM1 =  .7691     DENOM2 =  .1047     DENOM  =  .1317E+05  DULDZ  =  .3069     DELTAZ =  .7023
  RHS1   =  0.         RHS2   =  0.        RHS3   =  0.        RHS4   =  0.         RHS5   =  0.        RHS6   =  0.
  RHS7   =  0.         RHS8   =  0.        RHS    =  55.24     UV     =  .3633     UL     =  .2146     PHIL   =  844.0

     TIME  .3000E-01   STEP  .1575E-03    CPTIME  19.87

VARIABLE  --------  S P A T I A L   V A R I A T I O N  --------

COORDINATE  0.       .1000E+00  .2000     .3000     .4000     .5000     .6000     .7000     .8000     .9000     1.000
TEMPERATUR  1.000    1.000      1.000     1.000     1.000     1.000     1.000     .9988     .9767     .7567     0.
GRADIENT    0.       -.2665E-11 -.2193E-09 -.1682E-07 -.9851E-06 -.5018E-04 -.1764E-02 -.4565E-01 -.6803  -4.791    -7.753

  Z      =  .3000E-01  DELTA  =  .1361E-03  DELTAS =  .1036E-03  ETA    =  2.039     TW     =  447.0     Q      =  .2093E-01
  DENOM0 =  0.         DENOM1 =  2.253     DENOM2 =  .1047     DENOM  =  .3323E+05  DULDZ  =  .4276     DELTAZ =  1.134
  RHS1   =  0.         RHS2   =  0.        RHS3   =  0.        RHS4   =  0.         RHS5   =  0.        RHS6   =  0.
  RHS7   =  0.         RHS8   =  0.        RHS    =  225.0     UV     =  .8657     UL     =  .2192     PHIL   =  759.1

     TIME  .4000E-01   STEP  .2290E-03    CPTIME  20.79

VARIABLE  --------  S P A T I A L   V A R I A T I O N  --------

COORDINATE  0.       .1000E+00  .2000     .3000     .4000     .5000     .6000     .7000     .8000     .9000     1.000
TEMPERATUR  1.000    1.000      1.000     1.000     1.000     1.000     .9992     .9902     .9191     .6024     0.
GRADIENT    0.       -.3578E-08 -.1119E-06 -.3363E-05 -.8148E-04 -.1634E-02 -.2389E-01 -.2470  -1.571    -4.970    -5.696

  Z      =  .4000E-01  DELTA  =  .1877E-03  DELTAS =  .1420E-03  ETA    =  2.904     TW     =  519.8     Q      =  .4269E-01
  DENOM0 =  0.         DENOM1 =  4.002     DENOM2 =  .1047     DENOM  =  .5590E+05  DULDZ  =  .3312     DELTAZ =  .6186
  RHS1   =  0.         RHS2   =  0.        RHS3   =  0.        RHS4   =  0.         RHS5   =  0.        RHS6   =  0.
  RHS7   =  0.         RHS8   =  0.        RHS    =  206.5     UV     =  1.462     UL     =  .2231     PHIL   =  768.4
```

TIME .5000E-01 STEP .4809E-03 CPTIME 21.98

VARIABLE		S P A T I A L V A R I A T I O N								
COORDINATE	0.	.1000E+00	.2000	.3000	.4000	.5000	.6000	.7000	.8000	.9000	1.000
TEMPERATUR	1.000	1.000	1.000	1.000	1.000	.9994	.9950	.9666	.8421	.4999	0.
GRADIENT	0.	-.4461E-06	-.7312E-05	-.1087E-03	-.1363E-02	-.1397E-01	-.1085	-.6008	-2.190	-4.536	-4.780

I	= .5000E-01	DELTA	= .2203E-03	DELTAS	= .1663E-03	ETA	= 3.446	TW	= 557.1	Q	= .6112E-01
DENOM0	= 0.	DENOM1	= 5.288	DENOM2	= .1047	DENOM	= .7194E+05	DULDZ	= .2412	DELTAZ	= .5266
RHS1	= 0.	RHS2	= 0.	RHS3	= 0.	RHS4	= 0.	RHS5	= 0.	RHS6	= 0.
RHS7	= 0.	RHS8	= 0.	RHS	= 226.1	UV	= 1.902	UL	= .2256	PHIL	= 758.6

TIME .6000E-01 STEP .6747E-03 CPTIME 22.19

VARIABLE		S P A T I A L V A R I A T I O N								
COORDINATE	0.	.1000E+00	.2000	.3000	.4000	.5000	.6000	.7000	.8000	.9000	1.000
TEMPERATUR	1.000	1.000	1.000	1.000	.9996	.9972	.9839	.9280	.7621	.4243	0.
GRADIENT	0.	-.1196E-04	-.1210E-03	-.1112E-02	-.8656E-02	-.5497E-01	-.2730	-.9853	-2.500	-4.061	-4.010

I	= .6000E-01	DELTA	= .2516E-03	DELTAS	= .1898E-03	ETA	= 4.011	TW	= 590.1	Q	= .8262E-01
DENOM0	= 0.	DENOM1	= 6.707	DENOM2	= .1047	DENOM	= .8960E+05	DULDZ	= .2519	DELTAZ	= .5281
RHS1	= 0.	RHS2	= 0.	RHS3	= 0.	RHS4	= 0.	RHS5	= 0.	RHS6	= 0.
RHS7	= 0.	RHS8	= 0.	RHS	= 282.5	UV	= 2.391	UL	= .2281	PHIL	= 730.4

TIME .7000E-01 STEP .6365E-03 CPTIME 22.35

VARIABLE		S P A T I A L V A R I A T I O N								
COORDINATE	0.	.1000E+00	.2000	.3000	.4000	.5000	.6000	.7000	.8000	.9000	1.000
TEMPERATUR	1.000	1.000	1.000	.9997	.9982	.9911	.9635	.8789	.6871	.3666	0.
GRADIENT	0.	-.1352E-03	-.9455E-03	-.5884E-02	-.3149E-01	-.1386	-.4889	-1.309	-2.598	-3.621	-3.442

I	= .7000E-01	DELTA	= .2627E-03	DELTAS	= .2130E-03	ETA	= 4.554	TW	= 618.2	Q	= .1074
DENOM0	= 0.	DENOM1	= 8.209	DENOM2	= .1047	DENOM	= .1078E+06	DULDZ	= .2367	DELTAZ	= .5095
RHS1	= 0.	RHS2	= 0.	RHS3	= 0.	RHS4	= 0.	RHS5	= 0.	RHS6	= 0.
RHS7	= 0.	RHS8	= 0.	RHS	= 328.0	UV	= 2.910	UL	= .2305	PHIL	= 707.6

TIME .8000E-01 STEP .6832E-03 CPTIME 22.48

VARIABLE		S P A T I A L V A R I A T I O N								
COORDINATE	0.	.1000E+00	.2000	.3000	.4000	.5000	.6000	.7000	.8000	.9000	1.000
TEMPERATUR	1.000	.9999	.9997	.9987	.9946	.9794	.9343	.8250	.6205	.3217	0.
GRADIENT	0.	-.8335E-03	-.4355E-02	-.1986E-01	-.7693E-01	-.2618	-.7142	-1.535	-2.570	-3.239	-3.015

I	= .8000E-01	DELTA	= .3122E-03	DELTAS	= .2350E-03	ETA	= 5.131	TW	= 645.1	Q	= .1347
DENOM0	= 0.	DENOM1	= 9.828	DENOM2	= .1047	DENOM	= .1277E+06	DULDZ	= .2318	DELTAZ	= .4809
RHS1	= 0.	RHS2	= 0.	RHS3	= 0.	RHS4	= 0.	RHS5	= 0.	RHS6	= 0.
RHS7	= 0.	RHS8	= 0.	RHS	= 366.7	UV	= 3.471	UL	= .2329	PHIL	= 688.3

TIME .9000E-01 STEP .1171E-02 CPTIME 22.66

VARIABLE		S P A T I A L V A R I A T I O N								
COORDINATE	0.	.1000E+00	.2000	.3000	.4000	.5000	.6000	.7000	.8000	.9000	1.000
TEMPERATUR	.9999	.9997	.9990	.9963	.9873	.9612	.8984	.7706	.5625	.2860	0.
GRADIENT	0.	-.3306E-02	-.1372E-01	-.4880E-01	-.1529	-.4071	-.9134	-1.671	-2.478	-2.914	-2.679

I	= .9000E-01	DELTA	= .3402E-03	DELTAS	= .2559E-03	ETA	= 5.677	TW	= 667.2	Q	= .1639
DENOM0	= 0.	DENOM1	= 11.47	DENOM2	= .1047	DENOM	= .1476E+06	DULDZ	= .2780	DELTAZ	= .4566
RHS1	= 0.	RHS2	= 0.	RHS3	= 0.	RHS4	= 0.	RHS5	= 0.	RHS6	= 0.
RHS7	= 0.	RHS8	= 0.	RHS	= 402.3	UV	= 4.042	UL	= .2352	PHIL	= 670.5

TIME .1000 STEP .1995E-02 CPTIME 22.95

VARIABLE		S P A T I A L V A R I A T I O N								
COORDINATE	0.	.1000E+00	.2000	.3000	.4000	.5000	.6000	.7000	.8000	.9000	1.000
TEMPERATUR	.9994	.9990	.9971	.9913	.9755	.9372	.8583	.7182	.5123	.2569	0.
GRADIENT	0.	-.9425E-02	-.3268E-01	-.9535E-01	-.2473	-.5544	-1.071	-1.737	-2.357	-2.638	-2.407

I	= .1000	DELTA	= .3669E-03	DELTAS	= .2759E-03	ETA	= 6.173	TW	= 685.6	Q	= .1951
DENOM0	= 0.	DENOM1	= 13.06	DENOM2	= .1047	DENOM	= .1667E+06	DULDZ	= .2127	DELTAZ	= .4379
RHS1	= 0.	RHS2	= 0.	RHS3	= 0.	RHS4	= 0.	RHS5	= 0.	RHS6	= 0.
RHS7	= 0.	RHS8	= 0.	RHS	= 435.8	UV	= 4.606	UL	= .2374	PHIL	= 653.7

TIME .1100 STEP .4082E-03 CPTIME 24.21

VARIABLE		S P A T I A L V A R I A T I O N								
COORDINATE	0.	.1000E+00	.2000	.3000	.4000	.5000	.6000	.7000	.8000	.9000	1.000
TEMPERATUR	.9981	.9971	.9933	.9830	.9589	.9083	.8164	.6690	.4667	.2328	0.
GRADIENT	0.	-.2092E-01	-.6317E-01	-.1576	-.3516	-.6888	-1.184	-1.753	-2.226	-2.403	-2.182

I	= .1100	DELTA	= .3924E-03	DELTAS	= .2950E-03	ETA	= 6.696	TW	= 703.2	Q	= .2279
DENOM0	= 0.	DENOM1	= 14.78	DENOM2	= .1047	DENOM	= .1871E+06	DULDZ	= .2094	DELTAZ	= .4186
RHS1	= 0.	RHS2	= 0.	RHS3	= 0.	RHS4	= 0.	RHS5	= 0.	RHS6	= 0.
RHS7	= 0.	RHS8	= 0.	RHS	= 467.4	UV	= 5.201	UL	= .2395	PHIL	= 637.9

TIME .1200 STEP .1319E-02 CPTIME 26.71

VARIABLE		S P A T I A L V A R I A T I O N								
COORDINATE	0.	.1000E+00	.2000	.3000	.4000	.5000	.6000	.7000	.8000	.9000	1.000
TEMPERATUR	.9952	.9934	.9867	.9708	.9378	.8760	.7742	.6237	.4309	.2125	0.
GRADIENT	0.	-.3842E-01	-.1044	-.2301	-.4552	-.8016	-1.258	-1.734	-2.095	-2.301	-1.993

I	= .1200	DELTA	= .4167E-03	DELTAS	= .3132E-03	ETA	= 7.146	TW	= 716.8	Q	= .2624
DENOM0	= 0.	DENOM1	= 16.39	DENOM2	= .1047	DENOM	= .2058E+06	DULDZ	= .1952	DELTAZ	= .4049
RHS1	= 0.	RHS2	= 0.	RHS3	= 0.	RHS4	= 0.	RHS5	= 0.	RHS6	= 0.
RHS7	= 0.	RHS8	= 0.	RHS	= 497.4	UV	= 5.770	UL	= .2416	PHIL	= 622.9

TIME .1300 STEP .1051E-02 CPTIME 27.85

VARIABLE		SPATIAL VARIATION								
COORDINATE	0.	.1000E+00	.2000	.3000	.4000	.5000	.6000	.7000	.8000	.9000	1.000
TEMPERATUR	.9899	.9870	.9768	.9545	.9129	.8415	.7328	.5820	.3976	.1949	0.
GRADIENT	0.	-.6103E-01	-.1530	-.3062	-.5503	-.8901	-1.299	-1.694	-1.968	-2.025	-1.630

I = .1300	DELTA = .4404E-03	DELTAS = .3309E-03	ETA = 7.630	TW = 731.0	Q = .2982
DENOM0 = 0.	DENOM1 = 18.10	DENOM2 = .1047	DENOM = .2259E+06	DULDI = .1938	DELTAI = .3907
RHS1 = 0.	RHS2 = 0.	RHS3 = 0.	RHS4 = 0.	RHS5 = 0.	RHS6 = 0.
RHS7 = 0.	RHS8 = 0.	RHS = 526.9	UV = 6.373	UL = .2436	PHIL = 608.2

TIME .1400 STEP .1344E-02 CPTIME 27.97

VARIABLE		SPATIAL VARIATION								
COORDINATE	0.	.1000E+00	.2000	.3000	.4000	.5000	.6000	.7000	.8000	.9000	1.000
TEMPERATUR	.9813	.9771	.9631	.9344	.8849	.8058	.6927	.5435	.3679	.1795	0.
GRADIENT	0.	-.8669E-01	-.2046	-.3796	-.6323	-.9554	-1.316	-1.642	-1.848	-1.870	-1.685

I = .1400	DELTA = .4632E-03	DELTAS = .3480E-03	ETA = 8.100	TW = 743.6	Q = .3356
DENOM0 = 0.	DENOM1 = 19.82	DENOM2 = .1047	DENOM = .2460E+06	DULDI = .1895	DELTAI = .3797
RHS1 = 0.	RHS2 = 0.	RHS3 = 0.	RHS4 = 0.	RHS5 = 0.	RHS6 = 0.
RHS7 = 0.	RHS8 = 0.	RHS = 557.6	UV = 6.961	UL = .2456	PHIL = 592.8

TIME .1500 STEP .1344E-02 CPTIME 28.01

VARIABLE		SPATIAL VARIATION								
COORDINATE	0.	.1000E+00	.2000	.3000	.4000	.5000	.6000	.7000	.8000	.9000	1.000
TEMPERATUR	.9688	.9633	.9454	.9108	.8545	.7696	.6542	.5082	.3414	.1660	0.
GRADIENT	0.	-.1129	-.2547	-.4456	-.6985	-.9992	-1.314	-1.581	-1.735	-1.732	-1.558

I = .1500	DELTA = .4854E-03	DELTAS = .3647E-03	ETA = 8.620	TW = 757.2	Q = .3745
DENOM0 = 0.	DENOM1 = 21.65	DENOM2 = .1047	DENOM = .2681E+06	DULDI = .1908	DELTAI = .3666
RHS1 = 0.	RHS2 = 0.	RHS3 = 0.	RHS4 = 0.	RHS5 = 0.	RHS6 = 0.
RHS7 = 0.	RHS8 = 0.	RHS = 586.8	UV = 7.632	UL = .2475	PHIL = 578.2

TIME .1600 STEP .1344E-02 CPTIME 28.06

VARIABLE		SPATIAL VARIATION								
COORDINATE	0.	.1000E+00	.2000	.3000	.4000	.5000	.6000	.7000	.8000	.9000	1.000
TEMPERATUR	.9520	.9453	.9239	.8841	.8223	.7335	.6176	.4757	.3176	.1539	0.
GRADIENT	0.	-.1375	-.2996	-.5010	-.7484	-1.024	-1.297	-1.515	-1.629	-1.609	-1.446

I = .1600	DELTA = .5070E-03	DELTAS = .3808E-03	ETA = 9.072	TW = 767.6	Q = .4148
DENOM0 = 0.	DENOM1 = 23.40	DENOM2 = .1047	DENOM = .2884E+06	DULDI = .1871	DELTAI = .3573
RHS1 = 0.	RHS2 = 0.	RHS3 = 0.	RHS4 = 0.	RHS5 = 0.	RHS6 = 0.
RHS7 = 0.	RHS8 = 0.	RHS = 615.2	UV = 8.255	UL = .2494	PHIL = 564.0

TIME .1700 STEP .1542E-02 CPTIME 28.16

VARIABLE		SPATIAL VARIATION								
COORDINATE	0.	.1000E+00	.2000	.3000	.4000	.5000	.6000	.7000	.8000	.9000	1.000
TEMPERATUR	.9311	.9232	.8988	.8549	.7891	.6979	.5828	.4458	.2961	.1432	0.
GRADIENT	0.	-.1588	-.3372	-.5443	-.7826	-1.034	-1.269	-1.447	-1.531	-1.498	-1.346

I = .1700	DELTA = .5281E-03	DELTAS = .3966E-03	ETA = 9.503	TW = 777.0	Q = .4565
DENOM0 = 0.	DENOM1 = 25.14	DENOM2 = .1047	DENOM = .3064E+06	DULDI = .1824	DELTAI = .3491
RHS1 = 0.	RHS2 = 0.	RHS3 = 0.	RHS4 = 0.	RHS5 = 0.	RHS6 = 0.
RHS7 = 0.	RHS8 = 0.	RHS = 642.7	UV = 8.676	UL = .2513	PHIL = 550.3

TIME .1800 STEP .2309E-02 CPTIME 28.21

VARIABLE		SPATIAL VARIATION								
COORDINATE	0.	.1000E+00	.2000	.3000	.4000	.5000	.6000	.7000	.8000	.9000	1.000
TEMPERATUR	.9061	.8974	.8706	.8236	.7551	.6630	.5498	.4181	.2766	.1335	0.
GRADIENT	0.	-.1759	-.3661	-.5753	-.8024	-1.030	-1.233	-1.379	-1.438	-1.398	-1.256

I = .1800	DELTA = .5486E-03	DELTAS = .4120E-03	ETA = 9.919	TW = 785.1	Q = .4995
DENOM0 = 0.	DENOM1 = 26.87	DENOM2 = .1047	DENOM = .3282E+06	DULDI = .1774	DELTAI = .3422
RHS1 = 0.	RHS2 = 0.	RHS3 = 0.	RHS4 = 0.	RHS5 = 0.	RHS6 = 0.
RHS7 = 0.	RHS8 = 0.	RHS = 670.4	UV = 9.497	UL = .2531	PHIL = 536.4

TIME .1900 STEP .2415E-02 CPTIME 28.32

VARIABLE		SPATIAL VARIATION								
COORDINATE	0.	.1000E+00	.2000	.3000	.4000	.5000	.6000	.7000	.8000	.9000	1.000
TEMPERATUR	.8777	.8683	.8398	.7907	.7208	.6290	.5185	.3924	.2587	.1247	0.
GRADIENT	0.	-.1883	-.3863	-.5944	-.8096	-1.016	-1.191	-1.311	-1.352	-1.306	-1.174

I = .1900	DELTA = .5686E-03	DELTAS = .4270E-03	ETA = 10.37	TW = 794.6	Q = .5439
DENOM0 = 0.	DENOM1 = 28.69	DENOM2 = .1047	DENOM = .3494E+06	DULDI = .1683	DELTAI = .3344
RHS1 = 0.	RHS2 = 0.	RHS3 = 0.	RHS4 = 0.	RHS5 = 0.	RHS6 = 0.
RHS7 = 0.	RHS8 = 0.	RHS = 697.5	UV = 10.15	UL = .2569	PHIL = 522.9

TIME .2000 STEP .1627E-02 CPTIME 28.51

VARIABLE		SPATIAL VARIATION								
COORDINATE	0.	.1000E+00	.2000	.3000	.4000	.5000	.6000	.7000	.8000	.9000	1.000
TEMPERATUR	.8462	.8364	.8069	.7567	.6864	.5959	.4889	.3685	.2422	.1166	0.
GRADIENT	0.	-.1963	-.3982	-.6029	-.8059	-.9928	-1.145	-1.244	-1.271	-1.222	-1.098

I = .2000	DELTA = .5883E-03	DELTAS = .4417E-03	ETA = 10.84	TW = 803.7	Q = .5896
DENOM0 = 0.	DENOM1 = 30.57	DENOM2 = .1047	DENOM = .3714E+06	DULDI = .1784	DELTAI = .3268
RHS1 = 0.	RHS2 = 0.	RHS3 = 0.	RHS4 = 0.	RHS5 = 0.	RHS6 = 0.
RHS7 = 0.	RHS8 = 0.	RHS = 724.7	UV = 10.83	UL = .2567	PHIL = 509.3

TIME .2100 STEP .6424E-03 CPTIME 29.90

VARIABLE	———	S P A T I A L	V A R I A T I O N	———						
COORDINATE	0.	.1000E+00	.2000	.3000	.4000	.5000	.6000	.7000	.8000	.9000	1.000
TEMPERATUR	.8124	.8024	.7724	.7219	.6523	.5639	.4607	.3462	.2270	.1092	0.
GRADIENT	0.	-.2003	-.4027	-.6022	-.7933	-.9631	-1.096	-1.178	-1.195	-1.145	-1.029

X =	.2100	DELTA =	.6076E-03	DELTAS =	.4562E-03	ETA =	11.26	TW =	811.3	Q =	.6366
DENOM0 =	0.	DENOM1 =	32.39	DENOM2 =	.1047	DENOM =	.3924E+06	DULDZ =	.1765	DELTAZ =	.3208
RHS1 =	0.	RHS2 =	0.	RHS3 =	0.	RHS4 =	0.	RHS5 =	0.	RHS6 =	0.
RHS7 =	0.	RHS8 =	0.	RHS =	751.4	UV =	11.49	UL =	.2585	PHIL =	495.9

TIME .2200 STEP .1791E-02 CPTIME 30.02

VARIABLE	———	S P A T I A L	V A R I A T I O N	———						
COORDINATE	0.	.1000E+00	.2000	.3000	.4000	.5000	.6000	.7000	.8000	.9000	1.000
TEMPERATUR	.7769	.7668	.7369	.6868	.6185	.5328	.4339	.3251	.2129	.1023	0.
GRADIENT	0.	-.2007	-.4010	-.5940	-.7736	-.9284	-1.046	-1.114	-1.123	-1.073	-.9646

X =	.2200	DELTA =	.6265E-03	DELTAS =	.4703E-03	ETA =	11.69	TW =	818.4	Q =	.6849
DENOM0 =	0.	DENOM1 =	34.23	DENOM2 =	.1047	DENOM =	.4136E+06	DULDZ =	.1719	DELTAZ =	.3155
RHS1 =	0.	RHS2 =	0.	RHS3 =	0.	RHS4 =	0.	RHS5 =	0.	RHS6 =	0.
RHS7 =	0.	RHS8 =	0.	RHS =	779.0	UV =	12.15	UL =	.2602	PHIL =	482.1

AT TRANSITION FROM LAMINAR TO TURBULENT FILM, THE VALUES OF Q, PHIZ, DELTA, DELTAS, TW, X, DZ ARE
.72260E+00 .49703E+01 .64071E-03 .47801E-03 .82392E+03 .22763E+00 .21536E-02

TIME .2300 STEP .1214E-03 CPTIME 36.64

VARIABLE	———	S P A T I A L	V A R I A T I O N	———						
COORDINATE	0.	.1000E+00	.2000	.3000	.4000	.5000	.6000	.7000	.8000	.9000	1.000
TEMPERATUR	.7403	.7304	.7008	.6517	.5853	.5027	.4082	.3051	.1992	.9510E-01	0.
GRADIENT	0.	-.1985	-.3947	-.5803	-.7491	-.8909	-.9950	-1.053	-1.057	-1.011	-.8553

X =	.2300	DELTA =	.6866E-03	DELTAS =	.5137E-03	ETA =	14.02	TW =	840.3	Q =	.7339
DENOM0 =	.1456E+05	DENOM1 =	.1624E+05	DENOM2 =	5538.	DENOM =	-.3634E+05	DULDZ =	.9803	DELTAZ =	1.654
RHS1 =	1.247	RHS2 =	.2854	RHS3 =	7.866	RHS4 =	.3424E-01	RHS5 =	405.6	RHS6 =	1656.
RHS7 =	2032.	RHS8 =	2.171	RHS =	-358.8	UV =	15.46	UL =	.2658	PHIL =	435.9

TIME .2400 STEP .6169E-04 CPTIME 41.20

VARIABLE	———	S P A T I A L	V A R I A T I O N	———						
COORDINATE	0.	.1000E+00	.2000	.3000	.4000	.5000	.6000	.7000	.8000	.9000	1.000
TEMPERATUR	.7035	.6936	.6640	.6151	.5495	.4686	.3768	.2778	.1776	.8230E-01	0.
GRADIENT	0.	-.1990	-.3940	-.5756	-.7371	-.8689	-.9613	-1.005	-.9882	-.8991	-.7344

X =	.2400	DELTA =	.7703E-03	DELTAS =	.5505E-03	ETA =	14.40	TW =	857.1	Q =	.7913
DENOM0 =	.1260E+05	DENOM1 =	.1673E+05	DENOM2 =	6673.	DENOM =	-.3600E+05	DULDZ =	.9787	DELTAZ =	1.324
RHS1 =	1.156	RHS2 =	.3107	RHS3 =	8.087	RHS4 =	.4133E-01	RHS5 =	367.3	RHS6 =	1807.
RHS7 =	2263.	RHS8 =	2.540	RHS =	-284.6	UV =	15.36	UL =	.2742	PHIL =	374.3

TIME .2500 STEP .1673E-03 CPTIME 45.36

VARIABLE	———	S P A T I A L	V A R I A T I O N	———						
COORDINATE	0.	.1000E+00	.2000	.3000	.4000	.5000	.6000	.7000	.8000	.9000	1.000
TEMPERATUR	.6669	.6570	.6278	.5798	.5156	.4371	.3490	.2550	.1617	.7461E-01	0.
GRADIENT	0.	-.1968	-.3883	-.5744	-.7180	-.8393	-.9183	-.9455	-.9114	-.8160	-.6691

X =	.2500	DELTA =	.8459E-03	DELTAS =	.5768E-03	ETA =	14.80	TW =	869.0	Q =	.8528
DENOM0 =	.1122E+05	DENOM1 =	.1747E+05	DENOM2 =	7822.	DENOM =	-.3651E+05	DULDZ =	.8450	DELTAZ =	1.309
RHS1 =	1.079	RHS2 =	.3352	RHS3 =	8.385	RHS4 =	.4836E-01	RHS5 =	342.7	RHS6 =	2009.
RHS7 =	2468.	RHS8 =	2.778	RHS =	-285.3	UV =	15.42	UL =	.2822	PHIL =	341.0

TIME .2600 STEP .5579E-03 CPTIME 47.21

VARIABLE	———	S P A T I A L	V A R I A T I O N	———						
COORDINATE	0.	.1000E+00	.2000	.3000	.4000	.5000	.6000	.7000	.8000	.9000	1.000
TEMPERATUR	.6307	.6210	.5923	.5454	.4830	.4073	.3231	.2345	.1477	.6772E-01	0.
GRADIENT	0.	-.1935	-.3806	-.5505	-.6956	-.8058	-.8716	-.8855	-.8422	-.7454	-.6019

X =	.2600	DELTA =	.9236E-03	DELTAS =	.6010E-03	ETA =	15.22	TW =	878.3	Q =	.9177
DENOM0 =	.1011E+05	DENOM1 =	.1820E+05	DENOM2 =	9143.	DENOM =	-.3746E+05	DULDZ =	.9019	DELTAZ =	1.462
RHS1 =	1.013	RHS2 =	.3584	RHS3 =	8.741	RHS4 =	.5642E-01	RHS5 =	323.7	RHS6 =	2245.
RHS7 =	2676.	RHS8 =	3.034	RHS =	-326.9	UV =	15.56	UL =	.2908	PHIL =	306.8

TIME .2700 STEP .6446E-03 CPTIME 50.43

VARIABLE -------- S P A T I A L V A R I A T I O N --------

COORDINATE	0.	.1000E+00	.2000	.3000	.4000	.5000	.6000	.7000	.8000	.9000	1.000
TEMPERATUR	.5952	.5857	.5576	.5119	.4514	.3787	.2986	.2152	.1346	.6116E-01	0.
GRADIENT	.1066E-12	-.1895	-.3717	-.5350	-.6713	-.7708	-.8249	-.8282	-.7778	-.6788	-.5382

Z =	.2700	DELTA =	.1010E-02	DELTAS =	.6273E-03	ETA =	15.66	TW =	891.8	Q =	.9856
DENOM0 =	8971.	DENOM1 =	.1844E+05	DENOM2 =	.1080E+05	DENOM =	-.3821E+05	DULDZ =	1.032	DELTAZ =	1.448
RHS1 =	.9379	RHS2 =	.3722	RHS3 =	8.966	RHS4 =	.6611E-01	RHS5 =	300.9	RHS6 =	2471.
RHS7 =	2903.	RHS8 =	3.313	RHS =	-330.3	UV =	15.53	UL =	.3009	PHIL =	274.3

TIME .2800 STEP .6231E-03 CPTIME 54.42

VARIABLE -------- S P A T I A L V A R I A T I O N --------

COORDINATE	0.	.1000E+00	.2000	.3000	.4000	.5000	.6000	.7000	.8000	.9000	1.000
TEMPERATUR	.5604	.5511	.5237	.4792	.4208	.3511	.2750	.1967	.1219	.5484E-01	0.
GRADIENT	0.	-.1853	-.3621	-.5187	-.6463	-.7357	-.7793	-.7733	-.7162	-.6147	-.4768

Z =	.2800	DELTA =	.1105E-02	DELTAS =	.6550E-03	ETA =	16.12	TW =	903.0	Q =	1.056
DENOM0 =	8057.	DENOM1 =	.1871E+05	DENOM2 =	.1288E+05	DENOM =	-.3965E+05	DULDZ =	1.233	DELTAZ =	1.631
RHS1 =	.8795	RHS2 =	.3895	RHS3 =	9.293	RHS4 =	.7835E-01	RHS5 =	283.0	RHS6 =	2759.
RHS7 =	3148.	RHS8 =	3.606	RHS =	-386.1	UV =	15.61	UL =	.3125	PHIL =	243.0

TIME .2900 STEP .6816E-03 CPTIME 59.00

VARIABLE -------- S P A T I A L V A R I A T I O N --------

COORDINATE	0.	.1000E+00	.2000	.3000	.4000	.5000	.6000	.7000	.8000	.9000	1.000
TEMPERATUR	.5263	.5172	.4905	.4474	.3911	.3244	.2523	.1790	.1098	.4884E-01	0.
GRADIENT	0.	-.1806	-.3520	-.5017	-.6209	-.7007	-.7345	-.7198	-.6567	-.5533	-.4197

Z =	.2900	DELTA =	.1210E-02	DELTAS =	.6853E-03	ETA =	16.59	TW =	914.8	Q =	1.190
DENOM0 =	7203.	DENOM1 =	.1871E+05	DENOM2 =	.1356E+05	DENOM =	-.4149E+05	DULDZ =	1.450	DELTAZ =	1.795
RHS1 =	.8227	RHS2 =	.4017	RHS3 =	9.582	RHS4 =	.9383E-01	RHS5 =	264.9	RHS6 =	3081.
RHS7 =	3414.	RHS8 =	3.883	RHS =	-444.8	UV =	15.68	UL =	.3262	PHIL =	220.5

TIME .3000 STEP .5281E-03 CPTIME 62.62

VARIABLE -------- S P A T I A L V A R I A T I O N --------

COORDINATE	0.	.1000E+00	.2000	.3000	.4000	.5000	.6000	.7000	.8000	.9000	1.000
TEMPERATUR	.4888	.4801	.4545	.4133	.3598	.2969	.2296	.1619	.9885E-01	.4391E-01	0.
GRADIENT	0.	-.1736	-.3373	-.4783	-.5877	-.6574	-.6818	-.6602	-.5951	-.4973	-.3790

Z =	.3000	DELTA =	.1325E-02	DELTAS =	.7196E-03	ETA =	17.05	TW =	928.1	Q =	1.202
DENOM0 =	6437.	DENOM1 =	.1851E+05	DENOM2 =	.1905E+05	DENOM =	-.4399E+05	DULDZ =	1.704	DELTAZ =	1.959
RHS1 =	.7721	RHS2 =	.4105	RHS3 =	9.835	RHS4 =	.1137	RHS5 =	247.0	RHS6 =	3469.
RHS7 =	3700.	RHS8 =	3.932	RHS =	-514.6	UV =	15.63	UL =	.3425	PHIL =	240.5

TIME .3100 STEP .7490E-04 CPTIME 66.63

VARIABLE -------- S P A T I A L V A R I A T I O N --------

COORDINATE	0.	.1000E+00	.2000	.3000	.4000	.5000	.6000	.7000	.8000	.9000	1.000
TEMPERATUR	.4457	.4375	.4134	.3749	.3251	.2671	.2056	.1444	.8795E-01	.3909E-01	0.
GRADIENT	0.	-.1635	-.3166	-.4465	-.5446	-.6037	-.6197	-.5939	-.5306	-.4414	-.3404

Z =	.3100	DELTA =	.1449E-02	DELTAS =	.7567E-03	ETA =	17.49	TW =	941.2	Q =	1.271
DENOM0 =	5808.	DENOM1 =	.1823E+05	DENOM2 =	.2353E+05	DENOM =	-.4757E+05	DULDZ =	1.876	DELTAZ =	2.213
RHS1 =	.7325	RHS2 =	.4193	RHS3 =	10.12	RHS4 =	.1390	RHS5 =	231.8	RHS6 =	3911.
RHS7 =	3999.	RHS8 =	3.997	RHS =	-628.3	UV =	15.67	UL =	.3612	PHIL =	259.6

TIME .3200 STEP .3116E-03 CPTIME 70.72

VARIABLE -------- S P A T I A L V A R I A T I O N --------

COORDINATE	0.	.1000E+00	.2000	.3000	.4000	.5000	.6000	.7000	.8000	.9000	1.000
TEMPERATUR	.3979	.3904	.3685	.3336	.2887	.2368	.1822	.1281	.7835E-01	.3509E-01	0.
GRADIENT	0.	-.1489	-.2874	-.4034	-.4890	-.5384	-.5490	-.5238	-.4680	-.3931	-.3080

Z =	.3200	DELTA =	.1580E-02	DELTAS =	.7957E-03	ETA =	17.91	TW =	955.8	Q =	1.337
DENOM0 =	5191.	DENOM1 =	.1760E+05	DENOM2 =	.2927E+05	DENOM =	-.5206E+05	DULDZ =	2.311	DELTAZ =	2.241
RHS1 =	.6884	RHS2 =	.4201	RHS3 =	10.23	RHS4 =	.1700	RHS5 =	214.6	RHS6 =	4322.
RHS7 =	4304.	RHS8 =	4.072	RHS =	-696.6	UV =	15.55	UL =	.3827	PHIL =	280.8

TIME .3300 STEP .5813E-03 CPTIME 74.88

VARIABLE -------- S P A T I A L V A R I A T I O N --------

COORDINATE	0.	.1000E+00	.2000	.3000	.4000	.5000	.6000	.7000	.8000	.9000	1.000
TEMPERATUR	.3467	.3402	.3210	.2904	.2513	.2062	.1588	.1120	.6881E-01	.3101E-01	0.
GRADIENT	0.	-.1307	-.2519	-.3525	-.4257	-.4671	-.4754	-.4538	-.4074	-.3452	-.2744

Z =	.3300	DELTA =	.1715E-02	DELTAS =	.8362E-03	ETA =	18.31	TW =	968.7	Q =	1.399
DENOM0 =	4709.	DENOM1 =	.1710E+05	DENOM2 =	.3665E+05	DENOM =	-.5846E+05	DULDZ =	2.587	DELTAZ =	2.428
RHS1 =	.6563	RHS2 =	.4238	RHS3 =	10.42	RHS4 =	.2096	RHS5 =	201.2	RHS6 =	4810.
RHS7 =	4612.	RHS8 =	4.182	RHS =	-847.3	UV =	15.54	UL =	.4073	PHIL =	297.9

/// THIS RUN TERMINATED BECAUSE THE CURRENT VALUE OF TW IS 1937.9

```
 TURB =   .080G =   200.TIN =   85.00CC1=    1.50 PHITOT= .14[illegible]E+06
P=   115.0KPA     TRAT=   103.6C     ETAS= 12.00
X    TW      XE          XA          VOID MUSS    PHIL        PHIRAD/PHITOT

0.00   114. -.348E-01 0.          0.00    0.   .9552E+05 0.00
 .01   272. -.337E-01  .864E-05   .02   316.  .1463E+06  .03
 .02   337. -.327E-01  .230E-04   .02   205.  .1432E+06  .04
 .03   447. -.316E-01  .888E-04   .05   115.  .1301E+06  .08
 .04   520. -.305E-01  .194E-03   .06    84.  .1329E+06  .11
 .05   557. -.294E-01  .285E-03   .07    72.  .1319E+06  .13
 .06   590. -.283E-01  .398E-03   .08    63.  .1277E+06  .15
 .07   618. -.272E-01  .528E-03   .09    56.  .1244E+06  .17
 .08   649. -.261E-01  .683E-03   .10    51.  .1217E+06  .19
 .09   667. -.250E-01  .851E-03   .11    47.  .1191E+06  .20
 .10   686. -.239E-01  .103E-02   .12    43.  .1167E+06  .22
 .11   703. -.229E-01  .122E-02   .13    40.  .1144E+06  .23
 .12   717. -.218E-01  .142E-02   .13    38.  .1122E+06  .25
 .13   731. -.207E-01  .163E-02   .14    36.  .1100E+06  .26
 .14   744. -.196E-01  .186E-02   .15    35.  .1076E+06  .27
 .15   767. -.185E-01  .212E-02   .16    33.  .1054E+06  .28
 .16   768. -.174E-01  .237E-02   .16    31.  .1032E+06  .30
 .17   777. -.163E-01  .262E-02   .17    30.  .1011E+06  .30
 .18   785. -.152E-01  .288E-02   .18    29.  .9894E+05  .32
 .19   795. -.142E-01  .317E-02   .18    28.  .9681E+05  .32
 .20   804. -.131E-01  .348E-02   .19    27.  .9463E+05  .33
 .21   811. -.120E-01  .378E-02   .19    26.  .9248E+05  .34
 .22   810. -.109E-01  .410E-02   .20    25.  .9022E+05  .35
 .23   840. -.980E-02  .561E-02   .22    23.  .8250E+05  .37
 .24   857. -.871E-02  .613E-02   .24    22.  .7198E+05  .39
 .25   869. -.763E-02  .667E-02   .26    21.  .6655E+05  .40
 .26   878. -.654E-02  .723E-02   .29    20.  .6079E+05  .42
 .27   892. -.545E-02  .780E-02   .31    19.  .5530E+05  .42
 .28   903. -.436E-02  .844E-02   .34    18.  .4995E+05  .44
 .29   915. -.327E-02  .910E-02   .36    17.  .4632E+05  .45
 .30   928. -.219E-02  .977E-02   .39    17.  .3179E+05  .46
 .31   941. -.110E-02  .105E-01   .43    16.  .5743E+05  .47
 .32   956. -.928E-05  .111E-01   .46    15.  .6396E+05  .48
 .33   969.  .108E-02  .118E-01   .49    14.  .7002E+05  .49
```

```
  MFA   NOS/BE 1.3          RELEASE499 81-05-25
17.01.17.FISHYEG   FROM SIO/55
17.01.17.IP   00002624 WORDS - FILE INPUT   , DC 04
17.01.21.FISHY,BJ31-FMX,T200,IO15.
17.01.21.    FUNG  K.K. OR H16E13
17.01.21.LIBRARY(LIB434)
17.01.23.FTN(R=0,T)
17.02.20.      1.178 CP SECONDS COMPILATION TIME
17.02.20.ROUTE,PLOT,TID=AA,DEF.
17.03.18.ATTACH,FORSIM.
17.03.18.PFN IS
17.03.18.FORSIM
17.03.19.PF CYCLE NO. = 008
17.03.19.ATTACH(POLSAM,ID=MORRISON)
17.03.19.PFN IS
17.03.19.POLSAM
17.03.43.GO.
17.26.04.PF CYCLE NO. = 001
17.26.04.COPYN,0,GO,FORSIM,LGO,POLSAM.
17.26.12.RETURN,FORSIM,LGO.
17.26.12.ATTACH,FORSIM,CY=1.
17.26.12.PFN IS
17.26.12.FORSIM
17.26.15.LIBRARY,FORSIM,LIB434.
17.26.17.MAP(OFF)
17.26.18.GO.
17.26.44.      NON-FATAL LOADER ERRORS -
17.26.44.NON-EXISTENT LIBRARY GIVEN -  SYSIO
17.26.49.      NON-FATAL LOADER ERRORS -
17.26.49.TRIED TO LOAD INTO BLOCK BELOW ORIGIN -
17.26.49.GET.RT
17.26.49.LAST PROGRAM READ - W.SQ
17.26.49.LAST FILE ACCESSED- LIB434
17.27.00.      NON-FATAL LOADER ERRORS -
17.27.00.TRIED TO LOAD INTO BLOCK BELOW ORIGIN -
17.27.00.GET.RT
17.27.00.LAST PROGRAM READ - W.SQ
17.27.00.LAST FILE ACCESSED- LIB434
17.35.14.    STOP
17.35.14.    147.607 CP SECONDS EXECUTION TIME
17.35.14.EXIT,S.
17.35.14.OF   00008128 WORDS - FILE OUTPUT , DC 40
17.35.14.MS    21504  WORDS  (  114688 MAX USED)
17.35.15.CPA     151.062 SEC.        83.084 ADJ.
17.35.15.IO       14.456 SEC.          .000 ADJ.
17.35.15.CM    11277.100 KWS.        16.915 ADJ.
17.35.15.SS                         100.000
17.35.15.PP       87.149 SEC.      DATE 81-05-27
17.35.15.EJ   END OF JOB, 55
```

APPENDIX J: SAMPLE CALCULATIONS

The governing equation for the turbulent vapor film is eq. 7.5, which is shown here again for convenience:

$$\underset{(a)}{\frac{dM_v}{dZ}} - \underset{(b)}{U_\ell \frac{dG_v}{dZ}} - \underset{(c)}{\frac{(2R-\delta)}{(R-\delta)^2}\frac{dM_\ell}{dZ}} = \underset{(d)}{-\frac{2\tau_w}{R}} - \underset{(e)}{\frac{2\tau_i}{R-\delta}} + \underset{(f)}{\frac{g\rho_\ell(2R-\delta)\delta}{R^2}}$$

The physical significance of each term is:

(a) rate of change of vapor momentum

(b) rate of increase of vapor momentum due to evaporation

(c) rate of change of liquid momentum

(d) wall friction

(e) interfacial friction

(f) buoyancy force

The magnitude of each of these six terms are evaluated here, using the results from the theoretical solution. The system parameters are:

$G = 200\ kg.m^{-2}.s^{-1}$

$p = 115\ kPa$

$T_{in} = 85^oC$

$\phi = 146\ kW/m^2$

$n^* = 12$

A listing of the theoretical solutions can be found in Appendix I. Immediately after the transition from laminar to turbulent vapor film (at Z = 23 cm), the predicted conditions are:

δ = .6866E-3 m

δ_s = .5137E-3 m

η = 14.02

T_w = 840.3°C

U_v = 15.46 m/s

U_ℓ = .2658 m/s

$\frac{d}{dZ}(\frac{\delta}{R})$ = 1.654 m^{-1}

$\frac{d\eta}{dZ}$ = 35.13 m^{-1}

$\frac{d\delta_s}{dZ}$ = 5.137x10^{-3} m/m

$\frac{d\delta_T}{dZ}$ = 4.737x10^{-3} m/m

Using the equations developed in Appendix I, the value of each of the six terms is (unit in N/m^3):

(a) $\frac{dM_v}{dZ}$ = -116.7 - 26.8 + 17.38

= 30.3

(b) $U_\ell \frac{dG_v}{dZ}$ = 2.17

(c) $\frac{(2R-\delta)}{(R-\delta)^2} \frac{dM_\ell}{dZ}$ = 53.95

(d) $\frac{2\tau_w}{R}$ = 405.6

(e) $\frac{2\tau_i}{R-\delta} = 1656.$

(f) $\frac{g\rho_\ell(2R-\delta)\delta}{R^2} = 2032$

L.H.S. = 30.3 - 2.17 - 53.95 = -25.82

R.H.S. = 405.6 - 1656 + 2032 = -29.6

The difference between the LHS and RHS is due to the slight difference in the fluid properties used in the hand calculations. It can be seen that the rates of change in vapor and liquid momenta are comparable in magnitude.

In the development of the model, it was assumed that the difference between the pressures ρ_v and ρ_ℓ is negligible. The equation for the difference is

$$\rho_v - \rho_\ell = \Delta m_v^2 \left(\frac{1}{\rho_g} - \frac{1}{\rho_\ell}\right)$$

where Δm_v is the rate of evaporation per unit area of interface.

$$\Delta m_v = \pi R^2 \frac{dG_v}{dZ} \times \frac{1}{2\pi(R-\delta)}$$

$$= 2.67\times10^{-2} \text{ kg.m}^{-2}.\text{s}^{-1}$$

$$\rho_v - \rho_\ell = 2.46\times10^{-3} \text{ Pa}$$

The pressure difference across the interface is therefore negligible.

REFERENCES

Anderson, J.G.H. et al., "Low flow film boiling heat transfer on vertical surfaces," Presented at the 16th National Heat Transfer Conference, AIChE-52, St. Louis, 1976.

Barnes, W.P., "Subcooled forced convection film boiling in a verticle annulus," TID - 26335, 1973.

Berenson, P.J., "Film boiling heat transfer from a horizontal surface," Journal of Heat Transfer, Vol. 83, 1961, pp 351-358.

Bromley, L.A., "Heat transfer in stable film boiling," Chem. Eng. Prog., 46, 221-227, 1950.

Bromley, L.A., LeRoy N.R., Robbers, J.A., "Heat transfer in forced convection film boiling," Ind. Eng. Chem., Vol. 45, pp 2639-2646, 1953.

Cadek, E.F., Dominicis, D.P., Leyse, R.H., "PWR FLECHT - Final Report," WCAP - 7665, 1971.

Cess, R.D., Sparrow, E.M., "Subcooled forced - convection film boiling on a flat plate," Journal of Heat Transfer, p 377-379, 1961.

Chan, A.M.C., "Transient Two-Phase Flows: Refilling And Rewetting of Hot Horizontal Systems", PhD Thesis, Department of Nuclear Engineering, McMaster University, 1980.

Cheng, S.C., "Transition boiling heat transfer in forced vertical flow," Progress Report and Research Proposal, Department of Mechanical Engineering, University of Ottawa, April, 1976.

Cheng, S.C., Ng, W.W.L., Heng, K.T., Groeneveld, D.C., "Measurements of transition boiling data for water under forced convective conditions," ASME J. of H.T., (1978).

Collier, J.C., "Post-dryout heat transfer - a review of the current position," AERE-M2723, AERE, Harwell, 1975.

Cohen, L.S., Hanratty, T.J., "Effect of waves at a gas-liquid interface on a turbulent air flow", Journal of Fluid Mechanics, vol. 31, part 3, pp 467-479, 1978.

Dhir, V.K., Purohit, G.P., "Subcooled film-boiling heat transfer from spheres," Nuclear Eng. & Des. 47(1978) 49-66.

Dougall, R.S., Rohsenow, W.M., "Film boiling on the inside of vertical tubes with upward flow of the fluid at low qualities," M.I.T. Technical Report No. 9079-26, 1963.

Ellion, M.E., "A study of the mechanism of boiling heat transfer," California Inst. of Technology report JPL-MEMO-20-88 (1954).

Farahat, M.M., Armstrong, D.R., Eggen, D.T., "Transient heat transfer between hot metal spheres and subcooled water," ATOMKERNERGIE (ATKE) Bd. 29 Lfg. 1, (1977).

Fung, K.K., "Forced convective transition boiling," M.A. Sc. Thesis, U. of Toronto, 1976.

Fung, K.K., "Post-CHF heat transfer during steady-state and transient condition," NUREG/CR-0195, ANL-78-55, 1978.

Groeneveld, D.C., "Forced convective heat transfer to superheated steam in rod bundles," Atomic Energy of Canada Limited Report AECL-4450, 1973.

Groeneveld, D.C., "Effects of a heat flux spike on the downstream dryout behaviour," ASME Journal of Heat Transfer, 96, 121-125 (1974).

Groeneveld, D.C., Cheng, S.C., Stewart, J.C., Snoek, C.W., Wilson, K.E., Shaw, B.P., "Chalk River progress in updating Best-Estimate heat transfer correlations," Paper presented at United States Nuclear Regulatory Commission Workshop on Reviewing heat transfer data and updating Best-Estimate Heat Transfer Package, Washington, D.C., 1981.

Groeneveld, D.C., Fung, K.K., "Forced convective transition boiling: Review of literature and comparison of prediction methods," AECL-5543, 1976.

Groeneveld, D.C., Delorme, G.G.J., "Prediction of thermal non-equilibrium in the post-dryout regime", Nucl. Eng. & Des., Vol. 36, 1976, pp 17-26.

Groeneveld, D.C., Gardiner, S.R.M., "Post-CHF heat transfer under forced convective conditions," Symposium on the Thermal and Hydraulic Aspects of Nuclear Reactor Safety, Vol. 1, Light Water Reactors, ASME, 1977.

Groeneveld, D.C., Gardiner, S.R.M., "A method of obtaining flow film boiling data for subcooled water," Int. J. of Heat & Mass Transfer, 21, 664-665, 1978.

Hein, D., "Heat transfer with subcooled film boiling," Paper presented at the meeting of the European Two Phase Flow Group, Haifa, 1975.

Henry, R.E., "A correlation for the minimum film boiling temperature", AIChE Symposium Series, No. 138, Vol. 70, p. 81-90, 1974.

Hinze, J.O., "Turbulence", McGraw-Hill Book Company, New York, 1975.

Hsu, Y.Y., Westwater, J.W., "Approximate theory for film boiling on vertical surfaces", Chem. Eng. Prog. Symposium Series, No. 30, Vol. 56, 1960.

Hsu, Y.Y., "Proposed heat transfer 'Best Estimate' packages USNRC, November 1977.

Hughes, E.D., Lyczkowski, R.W., McFadden, J.H., "An Evaluation of state-of-the-art two-phase flow models and their applicability to nuclear reactor transient analysis," EPRI Report NP-143, 1976.

Kalinin, E.K. et al., "Heat transfer in tubes with 'Rod' regime in the case of film boiling of a subcooled liquid," Concurrent Gas-Liquid Flow, Plenim, New York, 1969, pp 497-525.

Kalinin, E.K., Balashov, G.I., Berlin, I.I., Liventsov, V.M., "A mathematical model of heat transfer for forced-convective film boiling," J. of Engineering Physics, Vol. 33, 1977.

Kaufman, J.M., "Post critical heat flux heat transfer to water in a vertical tube", M.Sc. thesis, M.I.T., Department of Mechanical Engineering, 1976.

Kays, W.M., "Convective heat and mass transfer," McGraw-Hill Book Company, New York, 1966.

Kordyban, E.S., "Interfacial shear in two-phase wavy flow in closed horizontal channels," Journal of Fluids Engineering, ASME, June 1974.

Lassahn, G.D., Stephens, A.G., Taylor, D.J., Wood, D.B., "X-Ray and Gamma Ray transmission densitometry," EG&G Report, 1979.

Lauer, H., Hufschmidt, W., "Heat transfer and surface rewet during quenching," Proceedings of NATO Advanced Study Institute August 16-27, 1976, Istanbul, Turkey, Vol. III, p 1309-1326.

Macbeth, R.V., "Burnout Analysis, Part 4, Application of a local condition hypothesis to world data for uniformly heated round tubes and rectangular channels," AEEW-R267, 1963.

Mayinger, F., Langner, H., "Post-dryout heat transfer," Keynote paper, Sixth International Heat Transfer Conference, Toronto, Canada, 1978.

Menegus, R.L., "Burnout of heating surfaces in water," TID-4500, 1959.

Mickley, H.S., Ross, R.C., Squires, A.L., Stewart, W.E., NACA-TN-3208, 1954.

Moeck, E.O., "Annular-dispersed two-phase flow and critical heat flux," Atomic Energy of Canada Limited Report, AECL-3656, 1970.

Motte, E.I., Bromley, L.A., "Film boiling of flowing subcooled liquids," Ind. and Eng. Chem., Vol. 49, 1957. pp 1921-1928.

Murphy, C.D., Kermode, R.I., Zakradnik, R.L., "Forced convection film boiling heat transfer," Fourth International Heat Transfer Conference, B4.8, Paris, 1970.

Newbold, F.J., Ralph, J.C., Ward, J.A., "Post dryout heat transfer under low flow and low quality conditions," Paper presented at the European Two Phase Flow Group Meeting, Erlangen, 1976.

Nicholas, L.D., "Temperature profile in the entrance region of an annular passage considering the effects of turbulent convection and radiation," Int. J. Heat Mass Transfer, Vol. 8, pp 589-607, 1965.

Plummer, D.N., Iloeje, O.C., Griffith, P., Rohsenow, W.M., "A study of post critical heat flux heat transfer in a forced convection system," Tech. Report No. 73645-80, M.I.T., 1973.

Rankin, S., "Forced convection film boiling inside of vertical pipes," Ph.D. Thesis, Chemical Engineering, University of Delaware, 1961.

Selander, W.N., Private Communications, 1980.

Silver, R.S., Wallis, G.B., "A simple theory for longitudinal pressure drop in the presence of lateral condensation," Proc. Inst. Mech. Engrs., Vol. 180, part I, pp 36-40, 1965-1966.

Siviour, J.B., Ede, A.J., "Heat transfer in subcooled pool film boiling", Fourth International Heat Transfer Conference, B3.12, Paris, 1970.

Smith, T.A., "Heat transfer and carryover of low pressure water in a heated vertical tube," M. Sc. Thesis, M.I.T., 1976.

Spalding, D.B., "Convective mass transfer," McGraw-Hill Book Company, New York, 1963.

Sparrow, E.M., Cess, R.D., "The effect of subcooled liquid on laminar film boiling," Journal of Heat Transfer, Transaction of the ASME, May 1962, pp 149-156.

Tachibana, F., Fukui, S., "Heat transfer in film boiling to subcooled liquids," Bulletin of the JSME, V16, No. 91, January, 1973.

Tan, H.E., Griffith, P., "A model for quenching with vertical flow boiling", Paper presented at ASME Heat Transfer Conference, St. Louis, IL, 1976.

Tien, C.L., "Thermal radiation properties of gases", Advances in Heat Transfer, Vol. 5, 253-324, Academic Press Inc., New York, 1968.

Tong, L.S., "Two-phase flow and boiling heat transfer", J. Wiley & Sons (1965).

Wallis, G.B., "Annular two-phase flow, Part 1: A simple theory; Part 2: Additional effects", J. of Basic Eng., March, 1970.